Doctoral theses at NTNU, 2022:118

Johannes Georg Brozovsky

The Climate Dimension in the Design of Resilient Urban Neighborhoods in Norway

A study on materials, outdoor thermal comfort, and building energy demand in the context of the urban microclimate

Doctoral thesis

NTNU
Norwegian University of Science and Technology
Thesis for the Degree of
Philosophiae Doctor
Faculty of Architecture and Design
Department of Architecture and Technology

NTNU
Norwegian University of
Science and Technology

Johannes Georg Brozovsky

The Climate Dimension in the Design of Resilient Urban Neighborhoods in Norway

A study on materials, outdoor thermal comfort, and building energy demand in the context of the urban microclimate

Thesis for the Degree of Philosophiae Doctor

Trondheim, May 2022

Norwegian University of Science and Technology
Faculty of Architecture and Design
Department of Architecture and Technology

NTNU
Norwegian University of
Science and Technology

NTNU
Norwegian University of Science and Technology

Thesis for the Degree of Philosophiae Doctor

Faculty of Architecture and Design
Department of Architecture and Technology

ISBN 978-82-326-5192-4 (printed ver.)
ISBN 978-82-326-6886-1 (electronic ver.)
ISSN 1503-8181 (printed ver.)
ISSN 2703-8084 (online ver.)

Doctoral theses at NTNU, 2022:118

Printed by NTNU Grafisk senter

“The roots of education are bitter, but the fruit is sweet”

Aristotle, 384–322 BC

Summary

One of the 17 Sustainable Development Goals proclaimed in the 2030 Agenda for Sustainable Development by the United Nations is *Sustainable Cities and Communities*. In the view of urbanization and a rising world population, the ambition is to create and transform cities into climate-resilient, safe, healthy, climate-friendly, and livable environments for its citizens. This thesis aims to contribute to this goal in the context of Norwegian climate conditions. For that, multiple approaches and methodologies are used.

First, an extensive literature study is conducted to synthesize the characteristics of the urban climate, focus areas, and research gaps from scientific publications addressing cold and polar climate regions. Second, numerical tools including computational fluid dynamics (CFD) and building performance simulation (BPS) are used to create models for studying the effect of different climates and design scenarios particularly with regard to people's outdoor thermal comfort and building energy demand. Field measurements of relevant climate variables from a network of fixed and temporary weather stations are used to provide input and validation data for the numerical models predicting the local climate conditions in an urban neighborhood (microclimate). Finally, a coupling methodology for CFD and BPS is presented that allows investigation of the energy demand of different floors of a high-rise building considering vertical temperature gradients derived from CFD simulations. For most of the thesis work, the *Gløshaugen* campus of the Norwegian University of Science and Technology which is currently under redevelopment served as a case study.

From the literature review, it was found that the urban climate in cold climate regions is strongly affected by the presence of the urban heat island (UHI). Mostly, observational methods were used and only 22 % of the reviewed studies used numerical tools to replicate, predict or investigate different scenarios of the urban climate.

The numerical simulations in this thesis show that solar access is key for improving the outdoor thermal comfort in urban areas during the cool and cold seasons in Norway. Also, wind sheltering proves to be an effective measure, however, only at relatively high wind speeds and on a smaller scale than solar access. Changing the material properties of the urban surface in a dense urban environment only presents a negligible effect on outdoor thermal comfort during cool or cold weather conditions. Moreover, solar access is favorable in buildings, as in Norwegian climate conditions, south-oriented, unshaded windows can lead to more useful solar energy gains than detrimental energy losses, on an annual basis. The benefit of wind sheltering to lower a building's energy demand is found to be small, as new buildings according to the Norwegian building regulations get increasingly airtight.

Furthermore, it is shown that especially during a summerly heat wave in Norway, the cooling energy demand and indoor overheating can be reduced effectively with vast urban greening

compared to a concrete-sealed urban surface. While in summer the effects of different material compositions of the urban surface on the microclimatic conditions are very distinct, they are less pronounced in autumn and marginal in winter during the investigated conditions. Resulting from the proximity to the urban surface, the effect is strongest in the lower floors of a building.

This thesis underlines the importance of including urban microclimate in the planning process of buildings and neighborhoods, as well as giving it a stronger role in study syllabi. It shows that numerical modeling is a valuable resource for the understanding of the urban (micro)climate and gives detailed examples for its application. The results are intended to provide useful knowledge for researchers and practitioners in architecture, building engineering, and urban planning, as well as decision-makers in public authorities.

Acknowledgments

The last three and a half years have been extremely instructive, not only from a professional point of view but also from a personal. Certainly, as also Aristotle implied in the quote from before, there have been moments when endurance and determination were put to the test. But thanks to a lot of wonderful people around me, my time as a PhD candidate was an incredible experience that I will always look back on with joy. I am sure this work would not have been possible without any of them, even if I am not able to mention everyone specifically here.

First of all, I would like to thank Judith Thomsen and Matthias Haase who recruited me for writing my master's thesis at SINTEF Building and Infrastructure at the time, in autumn 2017. It was my first contact with research work, and I got hooked immediately. I would also like to thank all the fantastic people I got to know at SINTEF during that time for the warm welcome and for tolerating my bad Norwegian. A special thanks to Øystein Rønneseth, who immediately became a close friend. Your humorous company made my start in Norway a lot easier and so much fun. I liked it so well in Trondheim that I didn't want to leave again and applied for a PhD position.

This brings me to the next central people of this project, my supervisors Niki Gaitani and Arild Gustavsen. I still cannot believe that I got the position and I remember like it was yesterday when Niki called me on a warm and sunny afternoon in spring (yes, they are rare, but they exist even in Trondheim) to break the good news to me. A big thanks to both of you for putting your trust in me, for discussing my issues, providing invaluable feedback, and allowing me to gain important experience in EU project work. A big thanks also to Are Simonsen from SINTEF Industry who acted as a mentor especially for the CFD simulations and has spent many hours for discussions and solving problems with me.

Equally important were my colleagues and fellow ZEN PhDs who always made it fun going to the office, discussing the recent developments of the COVID-19 pandemic, the US elections or philosophizing about weird conspiracy theories during lunch. It was a pleasure sharing this journey with you!

I would also like to thank Narayan Dungana and Sara Corio whose master's theses I was able to co-supervise. It was fun to work with you and I learned a lot from that.

Back in 2011 when I started studying, I crossed paths with two persons that over the last decade became two of my closest friends, Andreas and Christoph. I cannot thank you enough for the countless hours we spent in lectures, working on study projects, our bachelor's theses and of course also the following festivities. It has always been so much fun spending time with you, and I hope there will be many more occasions for that.

To my dear friends at home whom I have known for the better part of my life, some of them even since before I could think. Thanks to the *Druckis* for the wonderful cabin trips and vacations, as well as Michi, Simon and Flo for many memorable experiences of which are surely many more to come. Chris and Mario, as my oldest and closest friends we've shaped each other's lives probably more than we are aware of. Your friendship during the last three decades has been indispensable for reaching any goal on the way. I couldn't imagine better companions. Not then, and not now.

To my parents and my sister. I feel extremely lucky that I grew up in a home where I never had to worry, where I was always supported and given the right advice when I needed it. It is impossible to list everything you did for me or taught me. The same applies of course to my grandparents, aunts, uncles, and cousins. Thank you for always having my back.

Finally, the biggest thank you goes to my wife Janja. You were not only the one who showed me the announcement of this PhD position but also encouraged me to apply. Having a very similar professional background, I could always count on you discussing my concerns with me, giving your opinions, and listening to (and understanding) my problems. I don't know how many times you calmed me down, cheered me up, or made me take a break to clear my mind. Most of the time, the latter resulted in the solution to the problem I was worried about. Moreover, I could not have wished for a better home office partner during the COVID-19 lockdown. I'm quite sure I wouldn't have made it through that one without you. I cannot thank you enough for putting up with me during these last years, I know it hasn't always been easy.

Table of contents

List of figures

List of tables

List of acronyms and abbreviations

ABL	Atmospheric boundary layer
AP	Air pollution
AUT	Autumn simulation period
BM	Biometeorology
BPS	Building performance simulation
CFD	Computational fluid dynamics
CFN	Climate friendly neighborhood
ES	Energy system
FME ZEN	Research Centre on Zero Emission Neighbourhoods in Smart Cities
FME ZEB	Research Centre on Zero Emission Buildings
HDH	Heating degree hours
HVAC	Heating, ventilation, and air-conditioning
ICT	Information and communication technology
LCA	Life cycle analysis
LCZ	Local climate zone
MC	Microclimate
MRT	Mean radiant temperature
MS	Microclimate scenario
NTNU	Norwegian University of Science and Technology
OTC	Outdoor thermal comfort
OT	Operative temperature
OUMP	Other urban meteorological phenomena
P	Main paper
PED	Positive energy district
PET	Physiological equivalent temperature
PME	Penman-Monteith equation
PMVo	Predicted mean vote for outdoor conditions
POSE	Project organization and stakeholder engagement
RANS	Reynolds-averaged Navier Stokes
RQ	Research question
SA	Social aspects
SUM	Summer simulation period
SP	Supplementary paper
Trans	Transition to climate-friendly neighborhood
TSA	Time series analysis
UBL	Urban boundary layer

UHI	Urban heat island
USA	United States of America
UHI-Mag	Urban heat island magnitude
UHI-Mit	Urban heat island mitigation strategy
UM	Urban morphology
URANS	Unsteady Reynolds-averaged Navier Stokes
VP	Validation period
WIN	Winter simulation period
ZEN	Zero emission neighbourhood
ZEB	Zero emission building

Nomenclature

Latin letters

c_p	Specific heat capacity
C_p	Pressure coefficient
$\vec{f}$	Body force vector
k	Turbulent kinetic energy
N	Number of hours
p	Pressure
p'	Fluctuating pressure component
$\bar{p}$	Mean pressure component
Q_s	Heat storage
Q_H	Turbulent sensible heat flux
Q_F	Anthropogenic heat flux
Q_E	Turbulent latent heat flux
Q_A	Heat advection
Q^*	Surface radiation budget
R_{diff}	Diffuse solar radiation
R_{dir}	Direct solar radiation
RH	Relative humidity
t	Time
T	Temperature
T_a	Air temperature
T_{op}	Operative temperature
u	Longitudinal (x-axis) wind component

u'	Fluctuating velocity component
$\bar{u}$	Mean velocity component
$\vec{u}$	Three-dimensional velocity vector $\vec{u} = (u, v, w)$
U	Wind speed
v	Lateral (y-axis) wind component
w	Vertical (z-axis) wind component
z	Height above the ground

Greek letters

ε	Turbulent dissipation rate
θ	Temperature
$\bar{\theta}$	Mean temperautre component
θ'	Fluctuating temperature component
λ	Thermal conductivity
ν	Kinematic viscosity
ρ	Density
φ	Wind direction
Δ	Difference or net change of a quantity over time or space
ϕ	Viscous dissipation function

Part A

Binding article

1 Introduction

1.1 Motivation

It is one of the most widely discussed topics and one of the greatest threats to humanity of our time: climate change [1,2]. As a result, especially since the 1990s the term and its implications have experienced growing media attention around the world and have thus become increasingly known to a wider public [3]. Simultaneously, the concept of *green building* i.e., a building that minimizes or even eliminates negative environmental impacts, emerged. As one of the main contributors to the global final energy consumption (36 %) and carbon dioxide emissions (39 %), the building sector has long been an inherent part of many countries' efforts to reduce their environmental impact [4,5]. In that context, urban areas are of particular concern as they currently account for around 67 to 76 % of global energy use and between 71 and 76 % of carbon dioxide emissions from global final energy use [6]. But the consumption of energy and the associated emission of greenhouse gases and particulate matter does not only have implications on the large-scale and long-term climate. Especially megacities struggle with air pollution and toxic clouds of smog (see Figure 1) over extended periods of time which make living in these cities increasingly unhealthy. Thus, many governments established regulations to reduce energy use in buildings and increase the share of renewable energy sources in the energy mix.

Figure 1: Smog over Shanghai (Photo: Holger Link).

The focus of these regulations has been mainly to improve the insulating properties of the building envelope, requiring certain levels of insulation and air tightness. Moreover, the efficiency of heating, ventilation, and air-conditioning (HVAC) systems or the share of on-site renewable energy production from e.g., photovoltaics or solar thermal systems are often addressed. On the contrary, comparatively little attention has been given to the space between buildings although scientific evidence has long pointed to its significant impact on microclimatic conditions that in turn strongly affect the energy use in buildings or the health and wellbeing of city dwellers. Significant works forming the basics of today's understanding of the climatic conditions of *modern* urban settlements were published as early as 1927 e.g., by Geiger [7] on the *Climate Near the Ground*[1], in 1937 by Kratzer [8] on *The Climate of Cities*[2], or in 1947 by Balchin and Pye [9] with *A Micro-Climatological Investigation of Bath*.

With the expected rise in the frequency of extreme climate events and the advancements of methodological and technical capabilities, the urban microclimate has been introduced increasingly into the design process of buildings and cities [6]. Many publications stress the necessity of improving the design and the climate resilience[3] of cities and their outdoor environment to provide comfortable spaces that invite people to spend time outdoors or that promote soft mobility, regardless of their climate [11–13]. Primarily, reducing cooling demands during heat waves in temperate or warmer climate zones was targeted in literature. The

[1] Original title "Das Klima der bodennahen Luftschicht". The English translation was published in 1965.
[2] Original title "Das Stadtklima". The English translation was published in 1956.
[3] Resilience: The ability to recover from or adjust easily to misfortune or change [10].

investigation of the urban microclimate in cool or cold weather conditions at high-latitude cities, on the other hand, is scarce in scientific literature. This is where this thesis mainly contributes to the body of knowledge.

1.2 Structure of the thesis

This thesis constitutes a compendium of scientific papers of which most have been published in academic journals or at scientific conferences. Both publication channels were subject to peer review, assuring the scientific relevance and methodological validity of the articles. A binding article (*Norwegian "kappe"*, part A of this thesis) provides an introduction to the topic, summarizes the problems, results, and conclusions presented in the included articles and documents their interrelationship within the thesis.

Consequently, Chapter 2 of this thesis provides the necessary background and theory, namely the urban microclimate, its numerical analysis, and the governing equations of fluid flow. Afterward, in Chapter 3, the objectives, knowledge gap, and research questions that are addressed in this thesis, are presented. Chapter 4 explains the logical development of the thesis and provides overarching information about the applied methodologies in the papers since detailed descriptions of the methodologies are included in the individual articles (part B of this thesis). As the main share of the work was conducted using the *Gløshaugen* campus of the Norwegian University of Science and Technology (NTNU) in Trondheim as a case, Chapter 5 introduces the reader to the climatological and architectural features of the site. Chapter 6 summarizes the included articles and in Chapter 7, the results are discussed in a broader context and the research questions are answered. At last, Chapter 8 concludes the binding article and addresses future research recommendations.

Part B of this thesis contains the scientific papers that provide the basis for the dissertation, either as the published version or as the submitted manuscript. There are two types of papers: (1) the main papers (P) which directly answer the research questions and (2) supplementary papers (SP) which provide supplemental information without answering directly to any of the research questions. The thesis structure is outlined in Figure 2.

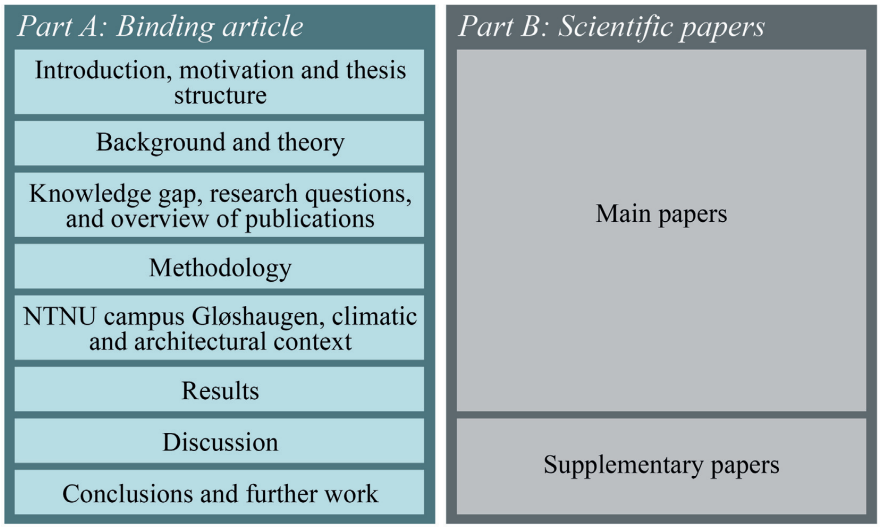

Figure 2: Thesis structure with the main parts and chapters.

2 Background and theory

2.1 The urban surface

Cities, towns, or urban areas distinguish themselves from rural areas primarily in their size and the density of population, and the degree of man-made surface modification. The specific criteria to delimit these regions, however, differ from country to country and are difficult to determine universally valid [14]. Caves [15] defines a city as a *"permanent and densely settled place with administratively defined boundaries whose members work primarily on non-agricultural tasks"*. The last part of his definition already suggests an environment intrinsically different from a natural landscape, as wide, open, and vegetated or forested spaces only play a subordinate role. In contrast to the natural landscape, the *urban landscape* or *cityscape,* as this artificial environment is often called, is characterized by emissions and pollution for instance from motorized vehicles, HVAC systems of buildings, industrial processes, etc. Furthermore, large obstacles to wind and the sun such as buildings, and mostly dark, heavy materials that are impermeable to water are prevailing.

The near-surface meteorological conditions are strongly dependent on the Earth's surface characteristics, as it interacts with radiation (absorption, emission, reflection and its conversion to thermal energy), precipitation (water runoff or retention and snow changing e.g. the optical properties, etc.), and airflow (deflection and slowing of wind). As a result, it is at the surface where most of the energy, mass, and momentum are exchanged, and also where usually the most extreme climates occur [11]. So, in order to assess the near-surface meteorological conditions in cities, namely the *urban climate*, it is critical to have a clear picture of the urban surface and its main climatologically relevant properties (see Table 1).

Table 1: Climatologically most relevant properties of surface fabrics.

Radiative	Thermal	Moisture	Aerodynamic
▪ Geometry	▪ Specific heat	▪ Interception and storage capacity	▪ Roughness
▪ Absorptivity	▪ Heat capacity	▪ Permeability	▪ Zero-plane displacement
▪ Reflectivity	▪ Thermal conductivity	▪ Stomatal characteristics	▪ Porosity
▪ Transmissivity	▪ Thermal diffusivity	▪ Chemical nature	
▪ Emissivity	▪ Thermal admittance		

In Figure 3, the photograph of Oslo's *Rådhusplassen*, taken from *Akershus festningen* near the waterfront of *Pipervika* shows how heterogenic the urban surface can be. There is the old fortification on a small hill which is covered with grass and trees bordering the open water of the inner *Oslofjord* and a large concrete square in front of Oslo's city hall, a large and bulky brick building. In the background, a city of 600,000 which is densely packed with midrise buildings and impervious, dark, and heavy materials in the center and low density, lowrise buildings in the outskirts, sprawls into a hilly and tree-covered Norwegian landscape. All these parts of a city have intrinsically different characteristics and properties that can be classified into different groups and quantify a range of typical parameters which are relevant in urban climatology, as done by Stewart and Oke [16]. They named these different surface groups local climate zones (LCZ, see Figure 4 and Table 2).

Figure 3: Diversity of the urban surface around Oslo's Rådhusplassen as seen from Akershus Festning (Photo: Eirik Skarstein).

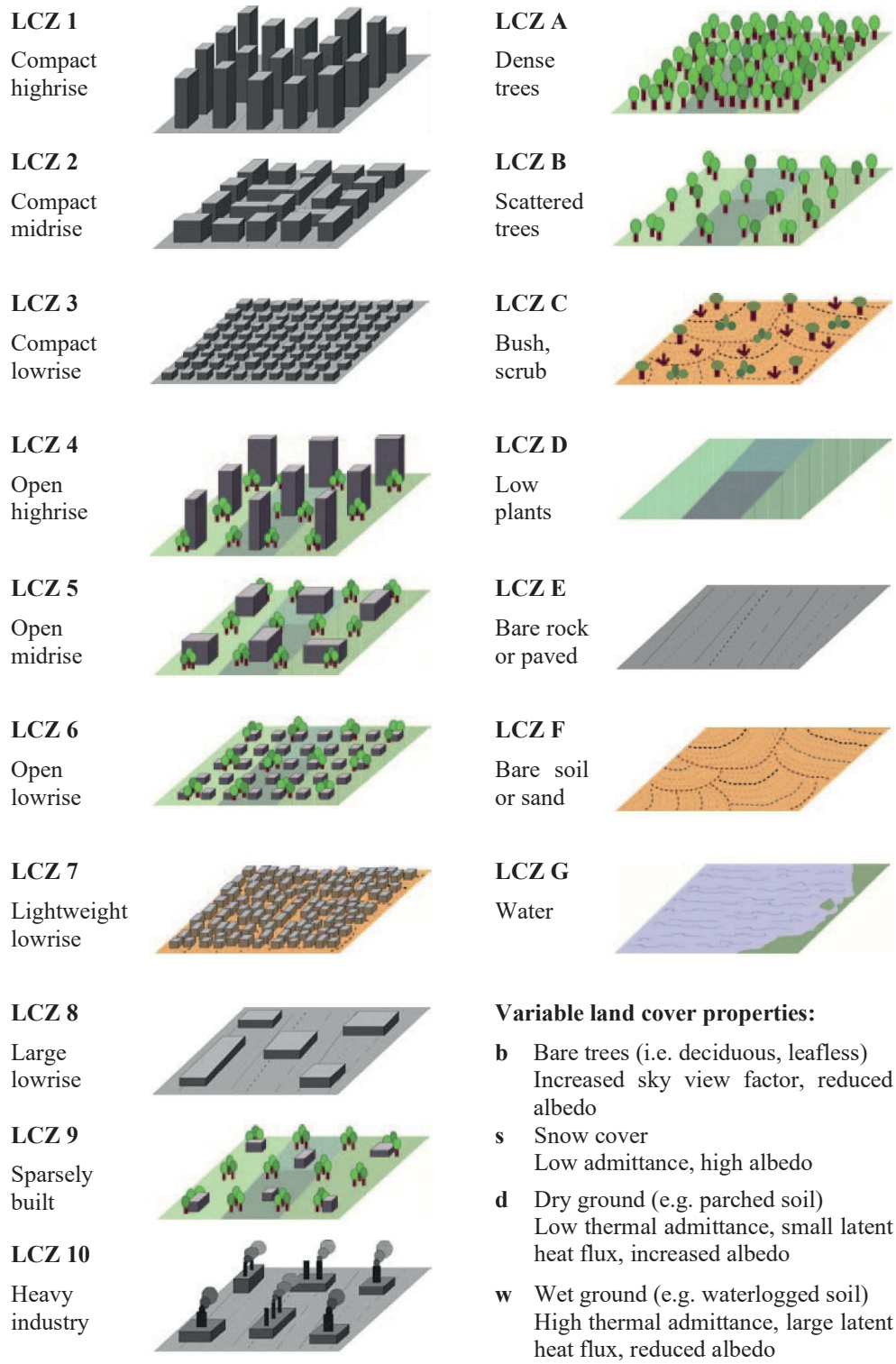

Figure 4: Classification of Local Climate Zones (LCZ) from Stewart and Oke [16]. (Source: © American Meteorological Society, used with permission.)

Table 2: Typical properties of LCZ categories [11,16].

Local Climate Zone	Building plan fraction[a] [%]	Canyon aspect ratio[b] [-]	Sky view factor[c] [-]	Mean height of roughness elements[d] [m]	Aerodynamic roughness length[e] z_0 [m]	Anthropogenic heat flux density[f] [W/m²]	Surface albedo[g] [-]	Surface admittance[h] [J/(m²s$^{1/2}$K)]
LCZ 1	40–60	>2	0.2–0.4	>25	≥2	50–300	0.1–0.2	1,500–1,800
LCZ 2	40–70	0.75–2	0.3–0.6	10–25	0.5–1	<75	0.1–0.2	1,500–2,200
LCZ 3	40–70	0.75–1.5	0.2–0.6	3–10	0.5	<75	0.1–0.2	1,200–1,800
LCZ 4	20–40	0.75–1.25	0.5–0.7	>25	1–2	<50	0.12–0.25	1,400–1,800
LCZ 5	20–40	0.3–0.75	0.5–0.8	10–25	0.25–0.5	<25	0.12–0.25	1,400–2,000
LCZ 6	20–40	0.3–0.75	0.6–0.9	3–10	0.25–0.5	<25	0.12–0.25	1,200–1,800
LCZ 7	60–90	1–2	0.2–0.5	2–4	0.1–0.25	<35	0.15–0.35	800–1,500
LCZ 8	30–50	0.1–0.3	>0.7	3–10	0.25	<50	0.15–0.25	1,200–1,800
LCZ 9	10–20	0.1–0.25	>0.8	3–10	0.25–0.5	<10	0.12–0.25	1,000–1,800
LCZ 10	20–30	0.2–0.5	0.6–0.9	5–15	0.25–0.5	>300	0.12–0.2	1,000–2,500
LCZ A	<10	>1	<0.4	3–30	≥2	0	0.1–0.2	unknown
LCZ B	<10	0.25–0.75	0.5–0.8	3–15	0.25–0.5	0	0.15–0.25	1,000–1,800
LCZ C	<10	0.25–1	0.7–0.9	<2	0.1–0.25	0	0.15–0.3	700–1,500
LCZ D	<10	<0.1	>0.9	<1	0.03–0.1	0	0.15–0.25	1,200–1,600
LCZ E	<10	<0.1	>0.9	<0.25	0.0002–0.005	0	0.15–0.3	1,200–2,500
LCZ F	<10	<0.1	>0.9	<0.25	0.0002–0.005	0	0.2–0.35	600–1,400
LCZ G	<10	<0.1	>0.9	–	0.0002	0	0.02–0.1	1,500

[a] Plan area fraction of ground covered by buildings.

[b] Ratio of the mean height of buildings to the mean street width (LCZ 1–7), the distance between houses and trees (LCZ 8–10), or the tree spacing (LCZ A–G)

[c] Ratio of the amount of sky hemisphere visible from ground level to that of an unobstructed hemisphere.

[d] Geometric average of building heights (LCZ 1–10) and tree/plant heights (LCZ A–F).

[e] Davenport et al.'s [17] classification of effective terrain roughness for city and country landscapes.

[f] Mean annual heat flux density from fuel combustion and human activity (transportation, space heating/cooling), industrial processing, human metabolism). Varies significantly with latitude, season, and population density.

[g] Ratio of the amount of solar radiation reflected by a surface to the amount received by it. Varies with surface color, wetness, and roughness.

[h] Ability of a surface to accept or release heat. Varies with soil wetness and material density. Few estimates of local-scale admittance exist in the literature; values given here are therefore subjective and should be used cautiously. Note that the *surface* in LCZ A is undefined and its admittance is unknown.

2.2 The urban atmosphere

As indicated by the typical categories of LCZ (Table 2) the man-modified surfaces (LCZ 1–10) strongly impact the air flow relative to natural surfaces (LCZ A–G). The highest impact is to be expected in the lower part of the atmosphere which is in direct contact with the Earth's surface. This part of the atmosphere is called the *planetary* or *atmospheric boundary layer* (ABL). It is usually between 100 and 3,000 m deep and is dominated by the roughness, thermal mixing, and introduction of pollutants and moisture from the surface of the Earth [11].

Table 3: Subdivision of the urban boundary layer (UBL) based on typical vertical length scales [11].

Name	Definition	Typical vertical dimension
Urban canopy layer	From ground to the mean height of buildings/trees. It consists of exterior and interior (inside buildings atmosphere).	Tens of meters
Roughness sublayer	From the ground up to two to five times the height of buildings/trees including the urban canopy layer. In the roughness sublayer, flow is affected by individual elements.	Tens of meters
Intertial sublayer	Above the roughness sublayer, where shear-dominated turbulence creates a logarithmic velocity profile and variation of turbulent fluxes with height is small (< 5%).	~25–250 meters
Mixed layer	Above the inertial sublayer, where atmospheric properties are uniformly mixed by thermal turbulence and usually capped by an inversion.	~250–2,500 meters

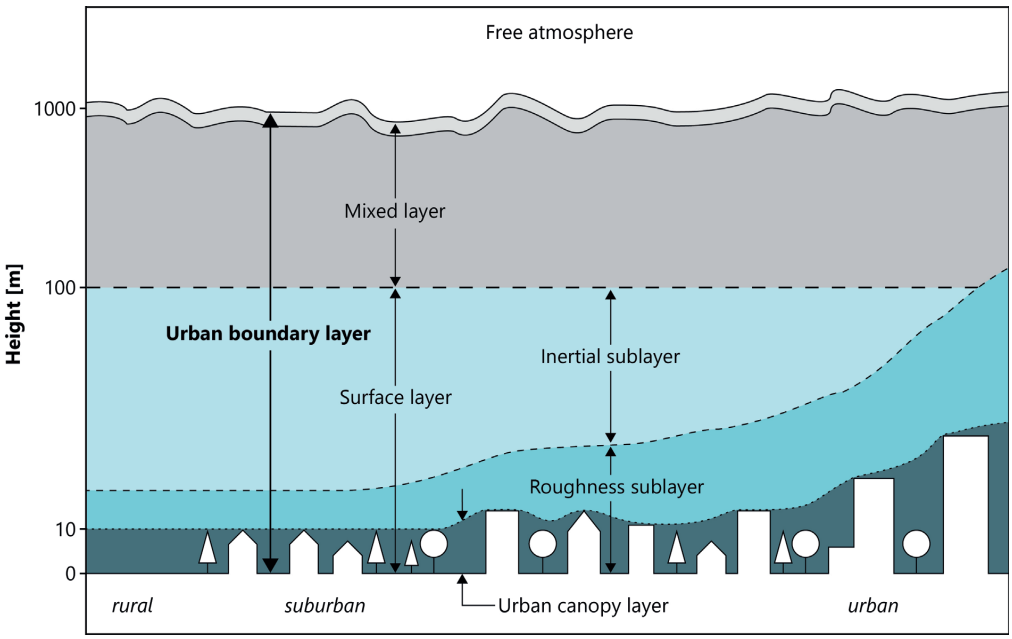

Figure 5: Schematic illustration of the urban boundary layer (UBL) structure by day (modified from [11]).

Over a city, the structure of the ABL is so characteristically altered that it is given a name of its own, the urban boundary layer (UBL). It can be subdivided into the *mixed layer* and the *surface layer*. The latter is again subdivided into the *inertial sublayer*, the *roughness sublayer*, and the *urban canopy layer* (see Table 3 and Figure 5).

As the name states, the surface layer is dominated by thermal and turbulent effects from the urban surface. The heat flux from the ground and the reduction of turbulent heat transfer in cities usually lead to the so-called *urban heat island* (UHI) effect, which is one of the most-researched areas within urban climatology. It describes the distinct warmth of an urban

settlement compared to its rural surroundings and has been reported across all climate zones and settlement sizes [11,16]. The UHI magnitude T_{UHI} is obtained from the difference between the air temperature measured at an urban station T_{urban} and a rural station T_{rural} (see Equation 1).

$$T_{UHI} = T_{urban} - T_{rural} \quad (1)$$

Warmer city centers can furthermore cause the so-called *urban heat island circulation* or *urban breeze* which is a weak flow close to the ground directed towards the warmer areas (usually the city center) [18]. Even though the daytime UHI magnitude is usually lower, the instability of the air during the day makes the vertical movement easier and thus induces more developed horizontal airflows than at night [19–23]. This weak surface flow amounts to around 0.3 m/s [13] and creates a plume over the city center within a moderate regional wind regime but forms a dome when regional winds are nearly calm [11] (see Figure 6). It was reported to develop even at relatively small UHI magnitudes of 1–2 °C [21]. However, urban climatology covers a lot more aspects than the UHI, even though it is the most prominent one. The research field of urban climatology is furthermore not limited to meteorology or climatology only but includes many other disciplines like air pollution science, architecture, building engineering, urban design, biometeorology, wind engineering, etc. [24].

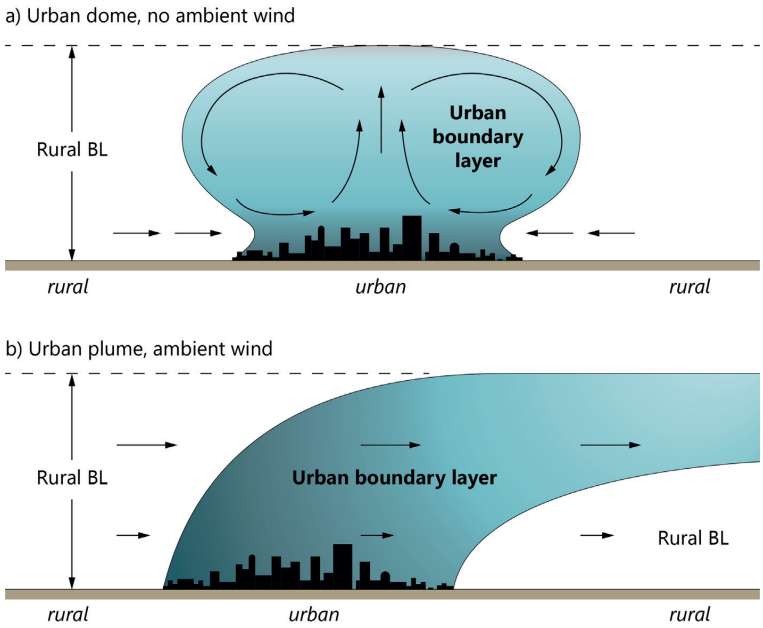

Figure 6: Typical shape of the urban boundary layer above a city: (a) without ambient wind flow and (b) with ambient wind (modified from [11]).

Although the first scientific descriptions of an urban-rural temperature difference date back about two centuries [25,26], the current global developments with regard to population growth [27], ongoing urbanization [14], and climate change [6] bring high relevance to this field of

research. Climate-resilient, sustainable, healthy, and liveable cities, as well as spatial quality, and wellbeing are aspects with increasing importance in urban planning [28]. In 2016, these and many other matters were adopted as the fundamentals of urban development within the United Nation's New Urban Agenda [29].

Many research studies have aimed to mitigate the adverse effects of the UHI. This has been mainly addressed by studying the influence of urban trees and parks [30–36], green roofs and facades [31,37–39], water bodies [40], the albedo of surfaces [37–39,41–43], or smart materials [44,45]. The importance of tackling the risks related to excessive heat was painfully brought to public attention during the 2003 heat wave in Europe that reportedly claimed the lives of about 70,000 people, most of them in Western Europe [46]. But the negative impacts from heat waves on people's health have also been reported in Scandinavia [47–49]. Lower air quality and the UHI make the elderly population in cities particularly vulnerable to heat stress-related health problems [50].

On the other hand, also cold stress increases mortality, especially in cold climate regions. In a study on the connection between temperature and mortality between 1990–1995 in Oslo, Nafstad et al. [51] reported increases in daily mortality for respiratory diseases by 2.1 %, for cardiovascular diseases by 1.7 %, and all other diseases by 1.4 %, for a 1°C fall in average temperature during the previous 7 days. Therefore, higher winter temperatures caused by the UHI might reduce cold stress-related mortality. A similar conclusion was drawn by Lowe [52], who estimated the UHI to lower cold-related deaths by 4 deaths per million people in the United States.

A different aspect that is directly connected to the urban climate is the energy demand in buildings. More frequent heat waves and insufficient aeration strongly increase the energy use for air-conditioning at locations with hot summers [53–56]. Conversely, the UHI was reported to contribute to reducing heating demands in winter [55,56]. In cities located in colder climate regions, the reductions in heating demand from the UHI can be higher than the increased cooling demand, as reported for instance in the United States [52].

2.3 Numerical analysis of the urban microclimate

Until the 1960s, among a variety of methodological approaches, studies in urban climatology focused mainly on the recording and analysis of field measurements. Then, scientists began to focus on the energy balance of cities which laid the foundation for the first computer models [24,57]. In the urban energy balance, the urban surface with its physical characteristics is parameterized, and an equation of fluxes from different energy exchange mechanisms is set up (see Equation 2).

$$Q^* + Q_F = Q_H + Q_E + \Delta Q_S + \Delta Q_A \quad (2)$$

The terms in this equation are the surface radiation budget (or net radiation) Q^*, the anthropogenic heat flux Q_F, the turbulent sensible (Q_H) and latent (Q_E) heat flux, net heat storage ΔQ_S and heat advection ΔQ_A.

Especially since about the year 2000, numerical approaches emerged as a supplement to experimental investigations [24,58]. Increasing computational power allows models to become steadily larger regarding their spatial dimensions and cover more physics. Hence, today, it is possible to perform many numerical studies on ordinary laptops and researchers are no longer entirely reliant on large high-performance computers.

However, resulting from the global population distribution, the majority of numerical urban microclimate studies up to the present day have been carried out in temperate and warm climate zones with many of them being temperature- or UHI-related [58]. Nevertheless, the UHI is not limited to low- and mid-latitude cities. Distinct heat islands were reported in high-latitude settlements in North America [59–62], Siberia [63–66], and Fennoscandia [67–69] as well. Considering that more than 25 million people live above 60° North, research in these high-latitude and cold-climate regions is extremely valuable. It has considerable potential to reduce energy usage, carbon emissions, and to improve the lives of many.

There are many different ways, tools, methodologies, and scales to study the physical processes in urban areas, that ultimately evoke the characteristic urban climates. The horizontal extension of cities typically puts them near the border between the micro- (smaller than 2 km) and the mesoscale (from 2 km to 2,000 km), see Figure 7 [70]. Aiming to capture mesoscale processes and to cover the physics of for instance cloud formation and precipitation, meteorological mesoscale models can cover several hundred square kilometers with grid cell sizes of typically 1–100 km [71]. Representatives of such models are for instance the Naval Research Laboratory's Coupled Ocean/Atmosphere Mesoscale Prediction System [72] or the Fifth-Generation Mesoscale Model developed by the National Center for Atmospheric Research and The Pennsylvania State University [73].

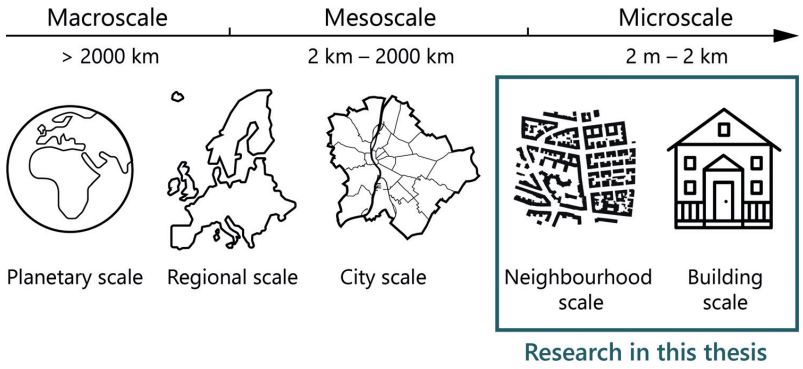

Figure 7: Terminology of climatological scales with their horizontal extension [70].

Generally, meteorological mesoscale models are not suited for microscale analyses like the flow around buildings or resolving the processes of heat and mass transfer and turbulence on a smaller spatial and temporal scale. Typically, microscale models don't include features like cloud formation, precipitation, or atmospheric radiative characteristics and are summarized with the terms computational fluid dynamics (CFD) or computational wind engineering models. Their spatial extents typically range between fractions of a meter up to several square kilometers, discretized in grid cells of a few centimeters or even millimeters up to ca. 100 m [71]. Often, meteorological mesoscale models and CFD or computational wind engineering models are coupled to either include mesoscale effects in the microscale or vice versa. Up-scaling CFD and computational wind engineering to include mesoscale meteorological influences is discussed in a review by Mochida et al. [74], down-scaling meteorological mesoscale models to include CFD and computational wind engineering capabilities is reviewed by Yamada et al. [75]. A thorough overview of numerical approaches in urban physics with a focus on CFD is given by Blocken [71].

Situated at the lower end of the spatial scale illustrated in Figure 7 is the building scale. It is of particular interest from a human point of view as Europeans and Americans spend between on average 85 and 90 % of their time indoors [76,77]. Numerical models at the building scale besides CFD are for example building performance simulation (BPS) models. They are used for modeling the thermal behavior of buildings with regard to their indoor climate and HVAC systems (see for example the following review papers on different modeling approaches to estimate a building's energy consumption [78–81]). However, they are less suited for representing the complex interactions between neighboring buildings, vegetation, and a building's surroundings.

While CFD is particularly well suited for high-resolution modeling in time and space with regard to airflows, temperatures, etc. for comparatively short periods of time (either stationary or a few minutes/hours), long-time CFD calculations over weeks/months with dynamic boundary conditions are computationally extremely expensive. On the other hand, BPS tools are usually applied for annual simulations and can take into account all necessary meteorological conditions relevant for the thermal building performance, as well as internal loads from occupants, electric equipment, HVAC components, lighting, shading, etc. (see Figure 8). Thus, CFD-BPS coupling has received increasing attention for making use of the quite complementary strengths of the two model families [71,82]. CFD-BPS coupling has been applied for example for evaluating the influence of building design on the microclimate [83] or the impact of microclimate on the summertime building cooling demands [84]. More references and a coupling framework are given by Zhang et al. [82].

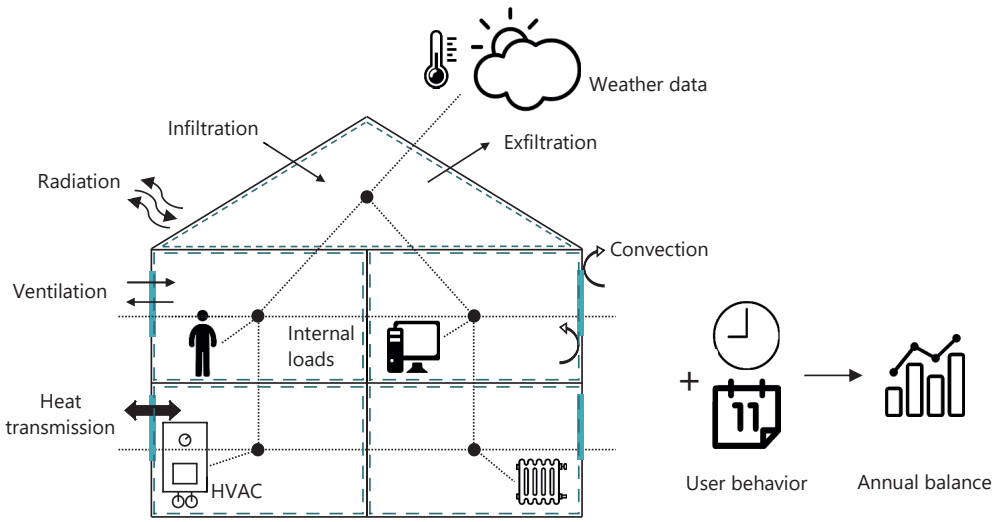

Figure 8: Schematic illustration of a thermal node model in BPS [85].

Having in mind the complexity of using a coupled CFD-BPS approach for the purpose of microclimate-building interactions, its application is largely limited to research. As a result, numerous studies using *ENVI-met* [86] to investigate the urban microclimate have been published. In contrast to CFD programs like *ANSYS Fluent*, *STAR-CCM*, or *OpenFoam*, *ENVI-met* uses simplified correlations of the convective heat-transfer coefficient, and the spatial discretization is structured, uniform, and of comparatively low resolution [87]. On the other hand, the program is relatively easy to handle and pursues a holistic approach to include the flow around buildings, heat and vapor transfer, turbulence, the impact of vegetation, bioclimatology, and pollutant dispersion [86]. According to the developer's webpage, it was used in more than 3,000 independent studies.

2.4 Governing equations in CFD and their approximate forms

At the heart of most CFD codes are the three laws of conservation: (1) conservation of mass, (2) conservation of momentum, and (3) conservation of energy. The Navier-Stokes equations for a confined, incompressible, viscous flow of a Newtonian fluid may be written as follows:

$$\nabla \cdot \vec{u} = 0 \tag{3}$$

$$\frac{\partial \vec{u}}{\partial t} + (\vec{u} \cdot \nabla)\vec{u} = -\frac{1}{\rho}\nabla p + \nu \nabla^2 \vec{u} + \vec{f} \tag{4}$$

$$\frac{\partial \theta}{\partial t} + (\vec{u} \cdot \nabla)\theta = \frac{1}{\rho c_p}(\lambda \nabla^2 \theta + \phi) \tag{5}$$

Equation 3 shows the divergence-free constraint, meaning that the velocity field of an incompressible flow should be divergence-free[4]. It is the continuity equation where the density of the fluid medium is constant (incompressible), where $\vec{u}$ is the velocity vector. The conservation of momentum is given in Equation 4, where t is time, ρ is the density, p is the pressure, ν is the constant kinematic viscosity and $\vec{f}$ is the body force per unit mass. Finally, Equation 5 shows the conservation of energy with temperature θ, specific heat capacity c_p, and thermal conductivity λ. The dissipation function ϕ in the energy equation is a term frequently omitted, as viscous heating effects in urban physics are marginal.

Despite the continually growing computational power, directly solving the Navier-Stokes equations for highly turbulent (meaning high-Reynolds number) flows in the context of urban physics is still unaffordably expensive today. Thus, commonly in this field, only approximate forms of these equations are solved instead of using direct numerical simulation. In the Reynolds-averaged Navier Stokes (RANS) approach, the Navier-Stokes equations are time-averaged to only solve the mean flow. This entails unknown terms for turbulence that have to be modeled (by turbulence models). RANS is the most widely applied approach in CFD in urban physics.

The basis of the RANS approach is the Reynolds-decomposition, where the instantaneous values of the flow properties $\vec{u}$, p, and θ are divided into a mean component ($\bar{u}$, $\bar{p}$, and $\bar{\theta}$) and a fluctuating component (u', p', and θ') as in Equations 6a–c (see also Figure 9).

$$\vec{u} = \bar{u} + u' \tag{6a}$$

$$p = \bar{p} + p' \tag{6b}$$

$$\theta = \bar{\theta} + \theta' \tag{6c}$$

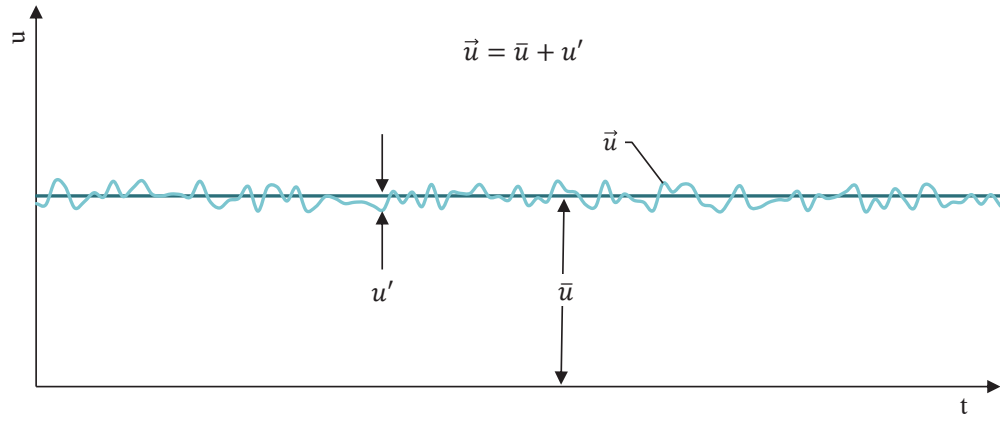

Figure 9: Reynolds decomposition of a fluctuating velocity signal in time.

[4] $\nabla = \frac{\partial}{\partial x} + \frac{\partial}{\partial y} + \frac{\partial}{\partial z}$

After that, the RANS equations read as in the following equations 7–9:

$$\nabla \cdot \bar{u} = 0 \tag{7}$$

$$\frac{\partial \bar{u}}{\partial t} + \nabla \bar{u}^2 = -\frac{1}{\rho}\nabla \bar{p} + \nu \nabla^2 \bar{u} - \nabla \overline{u'^2} \tag{8}$$

$$\frac{\partial \bar{\theta}}{\partial t} + (\bar{u} \cdot \nabla)\bar{\theta} = \frac{1}{\rho c_p}(\lambda \nabla^2 \bar{\theta} - \nabla \overline{u'\theta'}) \tag{9}$$

Note that in Equation 8 the body forces and in Equation 9 the dissipation term were omitted. The previously unknown terms are called Reynolds stresses for momentum ($\nabla \overline{u'^2}$) in Equation 8 and turbulent heat fluxes ($\nabla \overline{u'\theta'}$) in Equation 9, and need to be modeled in order to close the equation set. This is done by using turbulence models, which will not be further discussed in this work. For more information, the reader is referred to Wilcox's book on turbulence modeling [88]. It is important to bear in mind that RANS is a steady description of the turbulent flow. In unsteady RANS (URANS) on the other hand, the unsteady mean-flow structures are resolved, whereas turbulence again is modeled.

Large Eddy Simulation refers to an approach where only small eddies below a chosen threshold (often taken as the mesh size) are modeled. The filtering process produces unknowns that are taken care of by a so-called sub-filter turbulence model. As a result, Large Eddy Simulation usually has better performance than RANS/URANS but also has much higher computational demands. Again, the reader is referred to the literature at this point [89].

3 Knowledge gap, aim and research questions

3.1 Knowledge gap and aim of the thesis

Urban climatology is an evolving research field that is driven by the adverse effects of climate change, urbanization, and ongoing population growth (see also Chapters 1 and 2). All over the world, research in urban climatology is needed to provide resilient, livable, and healthy spaces for city dwellers. Moreover, *Sustainable Cities and Communities* is one of the United Nations' 17 Sustainable Development Goals. However, the focus of research activities in urban climatology is neither geographically, nor thematically equally distributed. The motives calling for this particular PhD thesis are mainly twofold and can be summarized briefly with the following statements:

1. Urban climatology-related research concentrates on the mid-latitudes. Studies in high-latitude locations are largely limited to observational studies of the UHI, including the recording and analysis of temperature series. Numerical studies such as using CFD techniques and the investigation of different scenarios in high-latitude cities are scarce.

2. While the main part of numerical studies in the scientific literature on the urban (micro)climate addresses the mitigation of the adverse effects of heat waves and the UHI, only a relatively small number of scientific publications investigate cool or cold weather conditions.

In Norway, the specific climatic conditions with its long, pronounced winter periods demand particular attention to cool outdoor conditions. In addition, due to its high latitude, the cooler half year in Norway is characterized by low sun angles that drastically limit solar accessibility in densely built-up areas, both for buildings and pedestrians. However, climate change increasingly requires counteracting overheating in urban areas, as heat waves[5] are expected to occur more and more frequently in the future, also in Norway. Therefore, investigating the identified research gap from the two statements above by using a Norwegian case study, can contribute greatly to the understanding of the urban climate. Furthermore, the results from this thesis are expected to be transferable to other countries with similar climatic conditions. Considering that there are more than 25 million people living above 60° N, many of them in urban areas, the findings from this thesis have the potential to positively impact the lives of many.

This thesis aims to provide useful knowledge not only for researchers but primarily for practitioners in architecture, building engineering, and urban planning, as well as decision-makers in public authorities in order to contribute to more livable, sustainable, and resilient cities and communities. Many of them experience severe effects from climate change already today. Accordingly, actions need to be taken immediately to make urban areas and their citizens more resilient to these changes. Therefore, practitioners and public authorities play a key role to act fast and on a large scale. With this in mind, these main objectives were defined:

- Determine the most important characteristics of the urban climate in cold climate regions from the existing body of literature and derive the implications for Norwegian cities.
- Set up and validate numerical simulation models of the microclimate in an urban neighborhood in Norway.
- Perform numerical simulations to investigate how different designs and materials of the urban surface affect the urban microclimate, and how microclimatic parameters can influence the energy balance of buildings and the outdoor thermal comfort (OTC) of humans at the neighborhood scale in Norway during different seasons.
- Evaluate measures for climate adaption to enhance the transition to resilient cities and develop guidelines to support urban planning professionals and public authorities in their decision-making process for improved environmental quality in urban neighborhoods in Norway.

[5] The Norwegian Meteorological Institute defines a heat wave as at least three consecutive days with a mean maximum temperature above 28 °C [90]. Many countries have their own definition of a heat wave and the World Meteorological Organization defines it as five or more consecutive days during which the daily maximum temperature surpasses the average maximum temperature by 5 °C or more [91].

3.2 Research questions

From the knowledge gap, the aim, and the main objectives of the thesis, the following research questions (RQ) were derived:

Research question 1

What are the characteristics of the urban climate in cold climate regions?

What are the main differences to the urban climate in warmer climate regions? What are the most researched topics, where are the research gaps, and what methods were applied most frequently? What implications arise for Norwegian cities?

Research question 2

What is the impact of the urban fabric on the urban microclimate in Norwegian climate conditions with regard to...

1. ***Outdoor thermal comfort?***
2. ***Building energy demand?***

How do the properties and the type and scale of modification of the urban surface including building surfaces, vegetation, and the building energy level affect the microclimate? What consequences for people's outdoor thermal comfort and the energy demand of buildings are to be expected in Norway?

Research question 3

To what extent can numerical tools help analyze the urban microclimate in Norwegian climate conditions?

What are feasible levels of detail regarding the geometrical input and physical models? What are the main limitations of these tools, and which developments are to expect in the future?

Research question 4

What are the benefits of a microclimate-based approach in neighborhood planning and building design?

What are the most important microclimatic aspects to be considered by planning professionals and municipalities in Norway? How to better take the urban (micro)climate into account in the planning and design process?

3.3 List of publications and author contributions

The research questions were answered using the results from five main papers (P I–V) which can be found in their entirety in part B of this thesis. All published articles were subjected to peer review. Three were published in academic journals and P II is a conference article. P V represents the manuscript of a paper submitted for publication in an academic journal. Part B also contains two supplementary papers (SP I–II). One of which was published in conference proceedings, the other one as a journal article. The contribution of the author of this thesis in each of the scientific papers is listed below.

Main papers:

P I: Brozovsky J, Gaitani N, Gustavsen A (2021). A systematic review of urban climate research in cold and polar climate regions. *Renewable and Sustainable Energy Reviews 138*, 110551. https://doi.org/10.1016/j.rser.2020.110551

Contribution: Johannes Brozovsky developed the methodological approach, collected, analyzed, and visualized the data, and wrote the original draft of the article. Editing and revision of the article were done collaboratively by Johannes Brozovsky and all the co-authors.

P II: Brozovsky J, Gaitani N, Gustavsen A (2019). Characterisation of Heat Losses in Zero Emission Buildings (ZEB) in Cold Climate. *Proceedings of the 16th IBPSA Conference, Rome, Italy, Sept 2–4, 2019*, pp. 343–50. https://doi.org/10.26868/25222708.2019.210560.

Contribution: Johannes Brozovsky conceptualized the research for this paper in collaboration with the co-authors, carried out the simulations, and wrote the original draft of the article. Editing and revision of the paper were done together with the co-authors.

P III: Brozovsky J, Corio S, Gaitani N, Gustavsen A (2021). Evaluation of sustainable strategies and design solutions at high-latitude urban settlements to enhance outdoor thermal comfort. *Energy and Buildings 244* (12), 111037. https://doi.org/10.1016/j.enbuild.2021.111037.

Contribution: Johannes Brozovsky conceptualized the research design and methodology together with Niki Gaitani and Arild Gustavsen. The creation of the simulation model, the analysis of simulation results, and the visualizations were done by Johannes Brozovsky in collaboration with Sara Corio. Johannes Brozovsky carried out the simulations and wrote the original draft of the article. Editing and revision were done together with Sara Corio and Niki Gaitani.

P IV: Brozovsky J, Simonsen A, Gaitani N (2021). Validation of a CFD model for the evaluation of urban microclimate at high latitudes: A case study in Trondheim, Norway. *Building and Environment 205*, 108175. https://doi.org/10.1016/j.buildenv.2021.108175.

Contribution: Johannes Brozovsky conceptualized the research together with all co-authors. The simulation model was created by Johannes Brozovsky based on an initial geometrical model provided by Are Simonsen. The analysis of results was done by Johannes Brozovsky in collaboration with Are Simonsen. Johannes Brozovsky wrote the original draft of the article, while editing and revision were done together with all co-authors.

P V: Brozovsky J, Radivojevic J, Simonsen A (2021). Assessing the Impact of Urban Microclimate on Building Energy Demand by Coupling CFD and Building Performance Simulation. *Manuscript submitted for publication*.

Contribution: Johannes Brozovsky conceptualized the research, designed the methodological approach, carried out all simulations, analyzed the results, and wrote the original draft of the article. The BPS modeling work was done together with Janja Radivojevic. Editing and revision of the original draft were done by all co-authors.

Supplementary papers:

SP I: Brozovsky J, Corio S, Gaitani N, Gustavsen A (2019). Microclimate analysis of a university campus in Norway. *IOP Conference Series: Earth and Environmental Science 352* (1), 012015. https://doi.org/10.1088/1755-1315/352/1/012015.

Contribution: Johannes Brozovsky carried out the simulations and field measurements for this article in collaboration with Sara Corio. Conceptualization, editing, and revision were done together with all co-authors. Johannes Brozovsky wrote the original draft of the article.

SP II: Brozovsky J, Gustavsen A, Gaitani N (2021). Zero emission neighbourhoods and positive energy districts – A state-of-the-art review. *Sustainable Cities and Society 72*, 103013. https://doi.org/10.1016/j.scs.2021.103013.

Contribution: The conceptualization of the research was done by Arild Gustavsen and Niki Gaitani. Johannes Brozovsky collected, categorized, and analyzed the reviewed publications and wrote the first draft of the article. Editing and revision of the article were done by Johannes Brozovsky in collaboration with all co-authors.

4 Methodology

As the included research articles in this work already contain a detailed description of the applied methods, they will not be presented specifically at this point. Instead, a more general view of the methods in this thesis will be outlined in this section.

4.1 The research process

Since the field of urban climatology is particularly multidisciplinary, the methodological approaches to study the urban (micro)climate are numerous. Partly, this is reflected in the presented thesis, however, the use of numerical tools and their validation with field measurements are at the core of this work. It can be seen in Figure 10 that in four out of five main papers, numerical tools were used. In P I, a systematic literature review was conducted. The approach of a systematic literature review was chosen in order to provide a fully repeatable procedure and analysis.

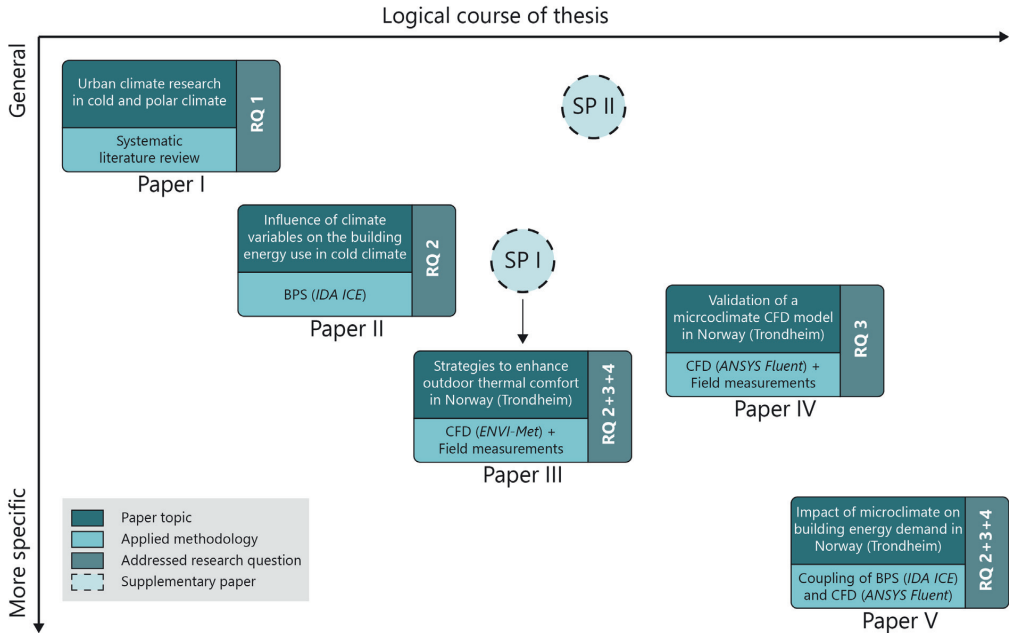

Figure 10: Qualitative overview of the included papers with their research topic, methodology, and the addressed research questions.

In Figure 10, the scientific papers are furthermore arranged qualitatively with respect to the logical course of the thesis and the degree of detail in which the thesis topic was addressed. It can be seen that the articles shifted from more general to more specific research topics with the thesis work progressing. This is indicated through the used methodology (or simulation tool), a more specific problem formulation, or the analysis of a precise location. While in P I, the urban climate research with all its subgenres in all cold and polar climate regions was analyzed generally in the very beginning of the thesis work, a quite specific study using a coupled CFD-BPS approach is presented in P V in order to investigate the impact of different materials on the energy demand of a building in Trondheim, Norway. The reason why P III is seen as less specific than P V is that CFD-BPS coupling (*ANSYS Fluent* and *IDA ICE*) covers more physics than *ENVI-met*. P IV on the other hand is regarded as being more general than P III as it covers solely the validation of a CFD model without addressing a variety of scenarios and their effects on microclimate. Figure 10 also shows the role of the two supplementary papers. SP I has a clear connection to P III as it represents the first version of the later extended and deepened analysis of the journal paper. SP II on the other hand has no direct connection to any of the main papers. However, it provides valuable insights into the research structure of Zero Emission Neighborhoods (ZEN) and Positive Energy Districts (PED) in the microclimate context. This information is regarded as being rather general.

Most of the research in this thesis was carried out on the neighborhood scale which is highly efficient in analyzing the effects of different design strategies, layouts, materials, and scenarios with regard to microclimate, outdoor thermal comfort, and building energy demand. It benefits

from a suitable density and heterogeneity of materials and features without forming too complex settings to fit into numerical models. Furthermore, this scale allows a comparatively detailed validation process in CFD, as already a few measuring locations make up a relatively dense network to capture the flow characteristics.

4.2 Validation and verification

Clearly, when using numerical tools for a study like in BPS or CFD, validation and verification are key to obtaining meaningful and reliable results [92–95]. Verification is necessary to ensure that the applied code is in accordance with the actual physical processes and to minimize errors that result from turning the mathematical model into a numerical model [96]. One might assume that commercial codes have been extensively tested prior to their release in order to produce similar results, but in a paper by Abanto et al. [97] from 2005 on the performance of different CFD tools, significant variations in performance were reported. Furthermore, in many commercially available codes, it is usually not possible to access the program code directly. Quantifying the numerical error in complex cases such as in urban physics is additionally inherently difficult. Highly accurate solutions or benchmarks are either analytical or extremely precise numerical solutions like from direct numerical simulation [95]. However, these only exist for relatively simple cases. Program users are then often left with validating their model against experimental data [98].

The American Institute of Aeronautics and Astronautics defines validation as the *"[…] process of determining the degree to which a model is an accurate representation of the real world from the perspective of the intended uses of the model"* [99]. This can be achieved by using field measurements, or in the case of CFD, also wind tunnel experiments. In a thorough article on verification and validation in CFD, Oberkampf and Trucano [95] write in this context, that the *"[…] fundamental strategy of validation involves identification and quantification of the error and uncertainty in the conceptual and computational models, quantification of the numerical error in the computational solution, estimation of the experimental uncertainty, and finally, comparison between the computational results and the experimental data. That is, accuracy is measured in relation to experimental data, our best measure of reality. This strategy does not assume that the experimental measurements are more accurate than the computational results. The strategy only asserts that experimental measurements are the most faithful reflections of reality for the purposes of validation."*

Besides that, the human factor plays an important role in numerical modeling. The varying experience and expertise of the person using a numerical model can lead to significantly differing results. In CFD, many commercial codes were found to be *"designed to always converge"*, for example by changing the discretization schemes in order to stabilize the solution without the users knowing [98]. The price for this, however, is paid with much lower accuracy which often remains undetected. Likewise, numerical modeling is prone to user errors as

reported for instance by Guyon [100] and Imam et al. [101] in the context of BPS. For this reason, best practice guidelines [93,102] were developed for CFD to avoid common mistakes and minimize the user's input error.

It has been of central importance in this PhD thesis to ensure the quality of the results obtained from numerical models. The sizing of the domain in the *ENVI-met* model which is used in P III and SP I has been designed according to the *ENVI-met* guidelines [103]. Additionally, and more importantly, the model has undergone a validation process in which simulation results from a selected date have been compared to field measurements. In SP I, the simulated surface temperature was compared to measurements taken with an infrared camera at several selected locations. In P III, measurements of wind speed, wind direction, air temperature, and relative humidity from one fixed and four mobile weather stations (Figure 11) within the study area were compared to the simulation results in addition to infrared surface temperature measurements. The accordance between simulation results and field measurements is reported in detail using the coefficient of determination and the coefficient of variance of the root mean square deviation as quality indicators in P III.

For the *ANSYS Fluent* model used in P IV and V a detailed validation process was carried out. First of all, the model's computational grid is based on a sensitivity analysis which included the comparison of three grids of different resolutions. All three grids were created following the best practice guidelines by Franke et al. [93] and Tominaga et al. [102]. Again, simulation results were compared to field measurements at selected dates. Similar to P III, these measurements were obtained from a fixed weather station 10 m above the roof of a building, and five mobile weather stations (Figure 11) at different locations in the study area at 3 m height. The compared weather variables were wind speed, wind direction, and air temperature. The coefficient of determination, the coefficient of variance of the root mean square deviation, and the maximum absolute deviation value were used as quality indicators.

Regarding the BPS model used in P II, the validation was not performed by the author of this thesis, but in a previous study conducted by Clauß et al. [104]. The BPS model from P V did not undergo a validation process. This is mainly because detailed information on the number, power output, and operating times of the electrical appliances and lighting, as well as the number of people and occupancy schedules, are not available for the investigated periods. The building was modeled according to the author's best professional judgment according to the available drawings and information from previous work [105]. However, it needs to be pointed out that with regard to the comparative nature of the study in P V, the impact of using a non-validated BPS model on the study's results is estimated to be negligible (see also Chapter 6.5). For more detailed information, the reader is kindly referred to the full-text versions of the articles in part B of the thesis.

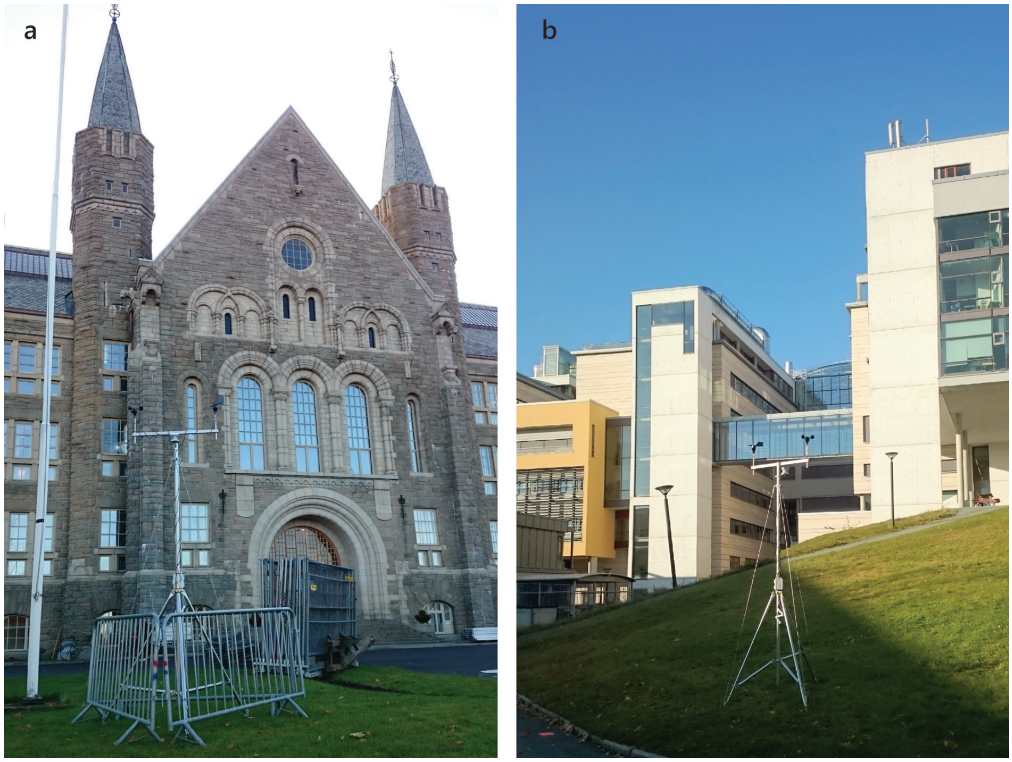

Figure 11: Mobile weather station in front of NTNU's Hovedbygg (a) and behind Realfagbygg (b).

5 NTNU campus Gløshaugen

5.1 Location and climate

The research using NTNU's *Gløshaugen* campus in Trondheim, Norway (see Figure 12) as a case, is at the core of this thesis. Consequently, in this chapter, a brief overview of its location, (meso)climate, layout, characteristics, and buildings will be presented.

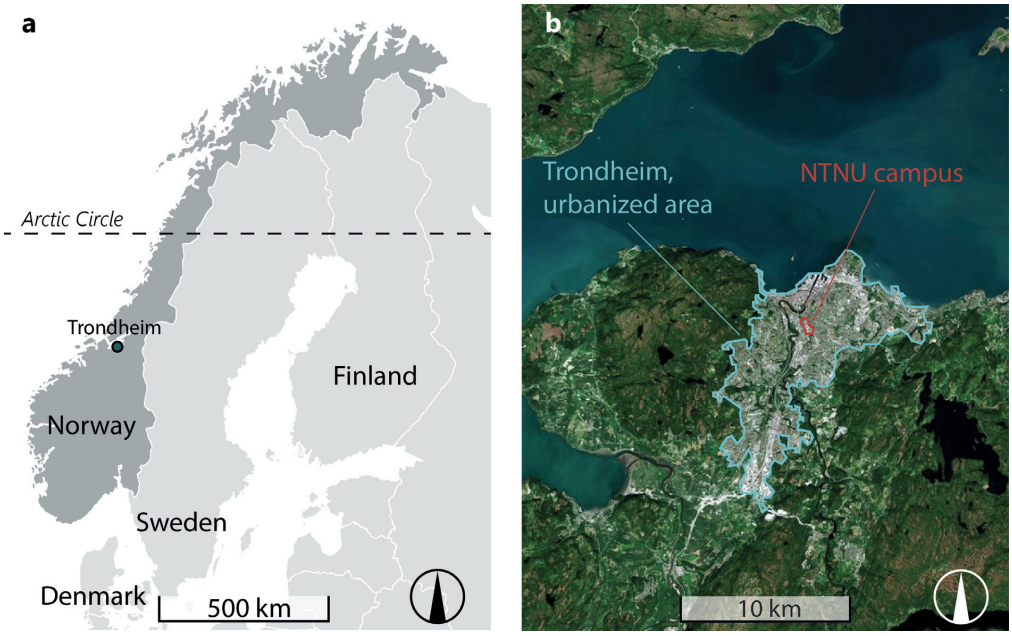

Figure 12: Location of Trondheim within the Nordic countries (a) and of NTNU campus within Trondheim (b).

Trondheim is Norway's third-biggest municipality with about 208,000 inhabitants in 2020 [106] and is located at 63.4° N and 10.4° E at the coast of a large fjord. The climate type according to the Köppen-Geiger classification system [107] is Dfb or oceanic according to the most recent norm period from 1991–2020, but closely borders the subarctic climate (Dfc) [108]. In the previous norm period from 1961–1990, Trondheim's Köppen-Geiger climate type [107] was classified as Dfc as only three months had a mean air temperature above 10 °C. Due to the effects of global warming which lets the arctic regions warm at a much faster pace than the lower latitudes [109,110], air temperature in Norway and consequently Trondheim has been rising significantly during the last decades. At 5.8 °C, the average air temperature in Trondheim in the most recent norm period from 1991–2020 has increased by 1.0 °C compared to 1961–1990 at the reference station in *Voll* (see Figure 13). While it has been observed that the amount of rainfall in Norway has increased by about 15 % since 1900 and is expected to further increase in the near future [111], Trondheim's precipitation levels stayed rather constant and have even decreased slightly by 1.9 % from 855 mm (1961–1990) to 839 mm (1991–2020). The average monthly wind speed during the last 25 years was 2.6 m/s, ranging from 2.1 m/s in August to 3.1 m/s in January with southwest as the predominant direction. The monthly average of relative humidity in Trondheim over the last decade ranges from 68.1 % in May to 78.7 % in October, with a mean value of 74.3 %.

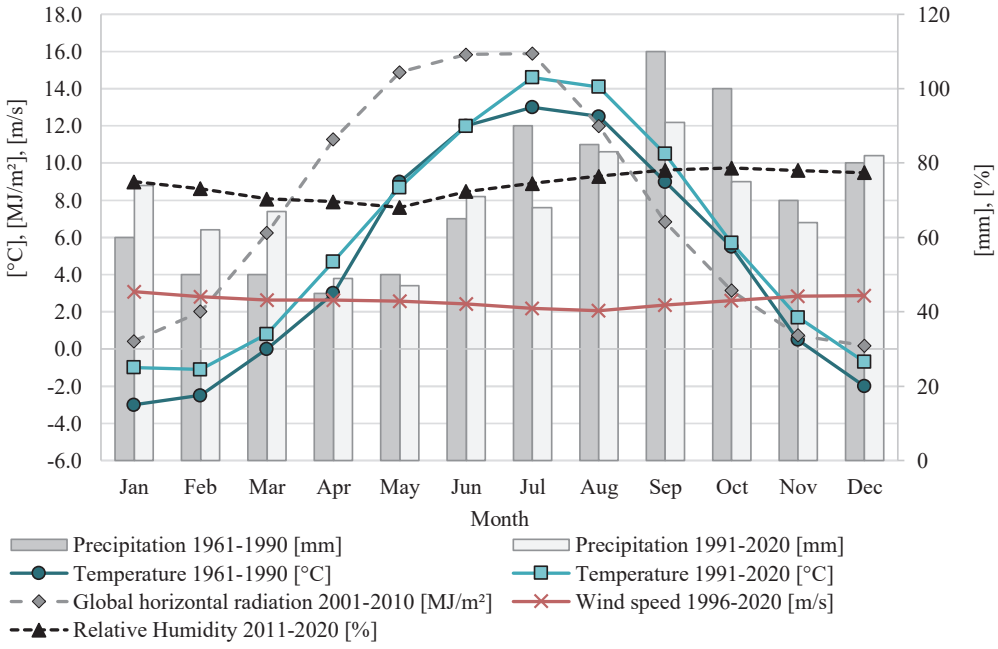

Figure 13: Monthly averages of temperature, precipitation, daily global horizontal radiation, wind speed, and relative humidity for different averaging periods according to data availability at Trondheim's reference station in Voll [112].

Table 4: Maximum sun elevation angles for different dates in Toronto, Canada, and Trondheim, Norway.

Date	Max. sun elevation angle	
	Toronto, Canada (43.6° N)	Trondheim, Norway (63.4° N)
21.03. (vernal equinox)	47.0°	27.1°
21.06. (summer solstice)	69.8°	50.0°
23.09. (autumnal equinox)	45.9°	26.2°
21.12. (winter solstice)	22.9°	3.3°

From about November to March, Trondheim commonly experiences moderate snowfall with periods of milder weather patterns and rain. However, rising temperatures have reduced the number of days with snow cover in the 2000s by 12 days since the 1960s [113]. Moreover, the number of winter days (days with a mean temperature below 0 °C) in Trondheim has decreased by 15 days compared to the norm period from 1961–1990. They are projected to further decrease by about 50 days until 2050 [114]. These developments are mainly associated with climate change but might be also partly caused by ongoing urbanization, higher anthropogenic heat release, and potentially higher UHI magnitudes.

Due to the strong influence of the large water bodies nearby and especially because of the Gulf Stream, Norway's coastal cities experience a much milder climate than their latitude would let assume [115]. Thus, even though Trondheim and Toronto, Canada, are classified with the same Köppen-Geiger climate type, from an urban climatology point of view, they cannot be regarded as equal. This is because the differences in solar access which are key to improving outdoor thermal comfort [116–120] and reducing building energy demands through passive solar gains [121] are significant (see Table 4) The low sun elevation angles during the cold season of the year in connection with complex, mountainous terrain, are a major challenge for sustainable urban development and need to be taken into account. For clarification, the solar irradiance in Trondheim of an average day in December is about 1.1 % of the value in June [112], while the ratio in Toronto is about 25.7 % [122].

5.2 Campus layout and architecture

The core area of *Gløshaugen* campus is approximately 0.26 km^2 in size and is situated ca. 1.5 km south of the city center at an altitude between 38 and 49 m above sea level, embedded into a park-like environment on a hill (see Figure 14). The close surroundings beyond the university park are detached, low-rise residential buildings to the north and east, an industrial area (with football stadium) to the south, and dense urban midrise buildings to the west. Referring to Stewart and Oke's [16] classification of urban landscape types, the city is mainly characterized by a mix of open, lowrise (LCZ 6), and midrise (LCZ 5) built-up areas, as well as park-like areas (LCZ 9/LCZ B). The built-up areas are frequently traversed by patches of forests (LCZ

A) and the meandering *Nidelva* river. The city center can be categorized as compact midrise (LCZ 2). Another essential feature of the city is the large water body of the *Trondheim Fjord* to the north of the city center (LCZ G, Figure 12). The campus itself might be categorized as a mixture of compact and open midrise (LCZ 2/LCZ 5).

The architecture at *Gløshaugen* is dominated by a series of development periods in the long history of the campus. The three oldest buildings in the north of the campus are remnants of a time when *Gløshaugen* was used as a farm and date back to the second half of the 19th century. First, when *Norges tekniske høgskole*, the Norwegian Institute of Technology, was founded in 1910, the characteristic university buildings that now form the *entrance* to the campus were erected. One of these buildings was the Main Building, easily recognizable from its characteristic granite façade and towers, which is the university's trademark ever since (see also Figure 11a). The other buildings' main construction (and façade) material was brick (see Figure 15).

The biggest part of buildings originates from the period between 1950 and 1990 for which concrete was used as the main construction material. Also, the two highest buildings on campus (44.5 m), the Central Buildings (buildings *SB1* and *SB2* in Figure 15) were constructed during this period. Newer concrete buildings were moved to a separate category in Figure 15, as they feature a layer of external insulation which makes them behave in a different way with respect to the urban microclimate (see also Figure 11b).

Figure 14: Aerial view of NTNU Gløshaugen campus from the north (Photo: Lars Strømmen).

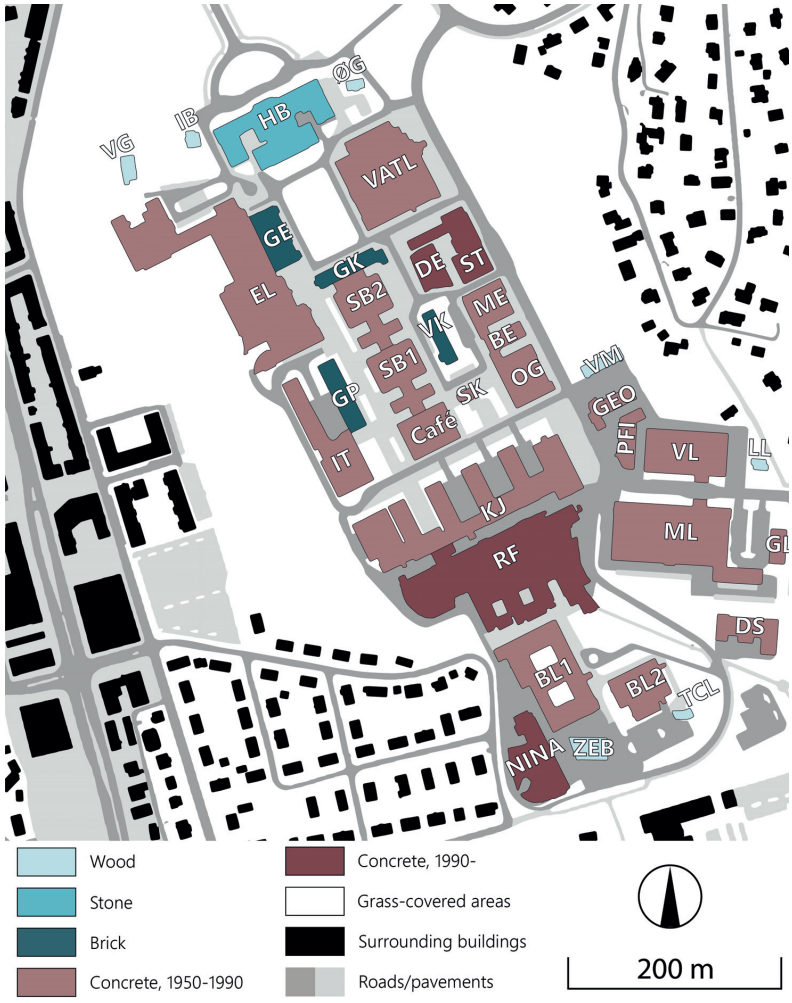

Figure 15: Layout of NTNU's campus at Gløshaugen with categorized main construction materials of the buildings.

During the last decade, the Research Centre on Zero Emission Buildings (FME ZEB) has developed three experimental buildings. The ZEB Living Laboratory (building *LL* in Figure 15) and the ZEB Test Cell Laboratory (building *TCL* in Figure 15) were completed in 2015, and the ZEB Laboratory (building *ZEB* in Figure 15) in 2020. They are high-performance buildings constructed from prefabricated and highly-insulated wood elements.

It needs to be mentioned that the campus is currently undergoing a major redevelopment aiming to increase its density by adding and refurbishing over 130,000 m^2 of gross floor area in the area until the year 2028. Along with this process comes the transition to a ZEN. A ZEN is defined as a group of interconnected buildings (new, existing, retrofitted, or a combination) with associated infrastructure that aims to reduce its direct and indirect greenhouse gas emissions towards zero over the analysis period (usually 60 years for buildings and 100 years for infrastructure). Depending on the ambition level, different life cycle modules and building and infrastructure elements are included in the analysis [123,124]. The concept was developed

by the Research Centre on Zero Emission Neighbourhoods in Smart Cities (FME ZEN) [125–128]. Because during the writing of this thesis the final area concepts have not yet been agreed upon, the reader is referred to *NTNU Campussamling's* webpage (https://www.ntnucampussamling.no/) for the most recent information about the progress.

6 Results

In this chapter, the main results from the research connected to this work are presented. For that, the following sections will briefly summarize and contextualize the included papers of this thesis. Of each paper's content, only the essentials will be shown which mainly consist of the respective methodology and results section. For more detailed information, it is recommended to read through the articles in their entirety (part B of this thesis).

6.1 Summary of P I: Review of urban climate research in cold and polar climate

Paper I presents *A systematic review of urban climate research in cold and polar climate regions* [129]. In the context of this thesis, the aim of this paper was to gain a deep understanding of the research structure in urban climatology and the characteristics and peculiarities of the urban climate in cold and polar climate regions as defined by the Köppen-Geiger climate classification system [107]. For that, a systematic review approach was pursued which included the categorization (see Table 5) and analysis of in total 101 scientific articles according to their publication year, geographical location, climate, topic, method, keywords, citations, and publication channels. These articles were identified by a database search using a structured question formulation and mainly applying the four-phase approach by Moher et al. [130] for structuring literature retrieval and reporting in systematic reviews. Paper I also features a meta-analysis of the included articles, pointing out similarities and differences of articles in the same category.

Table 5: Abbreviations and descriptions of categories (modified from [129]).

Category name	Description
UHI-Mag	Focusing on quantifying the UHI
UHI-Mit	UHI-mitigation strategies
UHI-Other	Other research on the UHI
BM	Biometeorology (health, comfort)
AP	Air pollution
UBL/ABL	Urban and atmospheric boundary layer
TSA	Time series analysis
OUMP	Other urban meteorological phenomena
Other	Research not related to previous categories

The earliest identified study was published in 1975, the newest in early 2019 (as a result of the time the article identification was carried out). Since then, there has been a clear trend towards an accelerating increase of urban climatology-related studies, especially during the last decade (see Figure 16). However, especially in the beginning, there were many years in which no relevant articles were published. Of the 101 articles, 58 addressed the UHI effect which is a common phenomenon also in cold and polar climate cities.

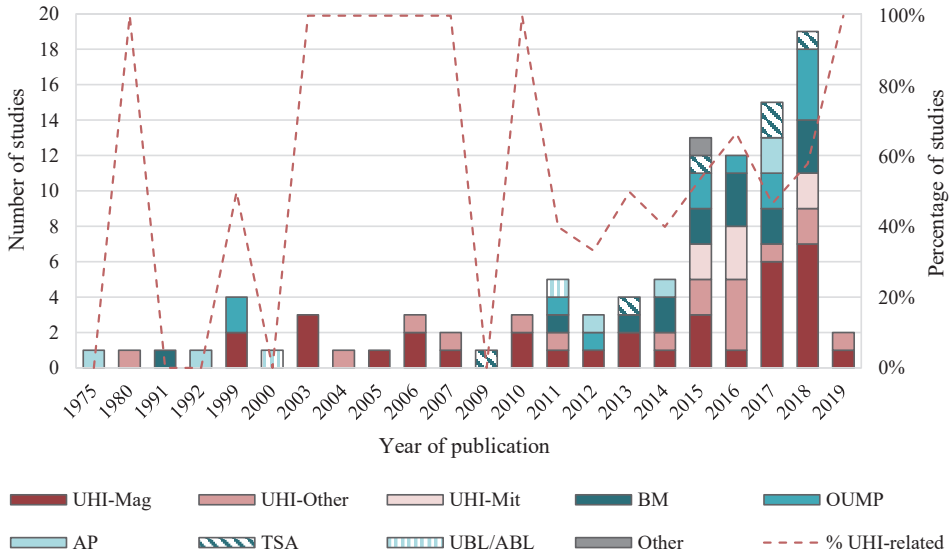

Figure 16: Number and distribution of categories of studies by year. The red dashed line indicates the percentage of studies published within a certain year dedicated to one of the three UHI-related categories. (Original illustration in [129].)

Geographically, the studies were unequally distributed, especially when taking the Köppen-Geiger climate classification system as a reference (see also Figure 17). Certainly, this imbalance is partly attributable to the geographical distribution (size and extent) of the climate

zones and the fact that some climate zones only cover very remote, mountainous areas with harsh conditions where only a few small human settlements exist. By far the most studies were carried out in climate type Dfb (51), followed by Dwa (20), Dfc (15), and Dfa (10), whereas many climate types were not represented by any of the included studies, such as Dsa, Dsc, Dsd, Dwd, Dfd, and EF. Regarding countries, most studies were conducted in the USA (21), followed by China (16), Russia (15), and Poland (12).

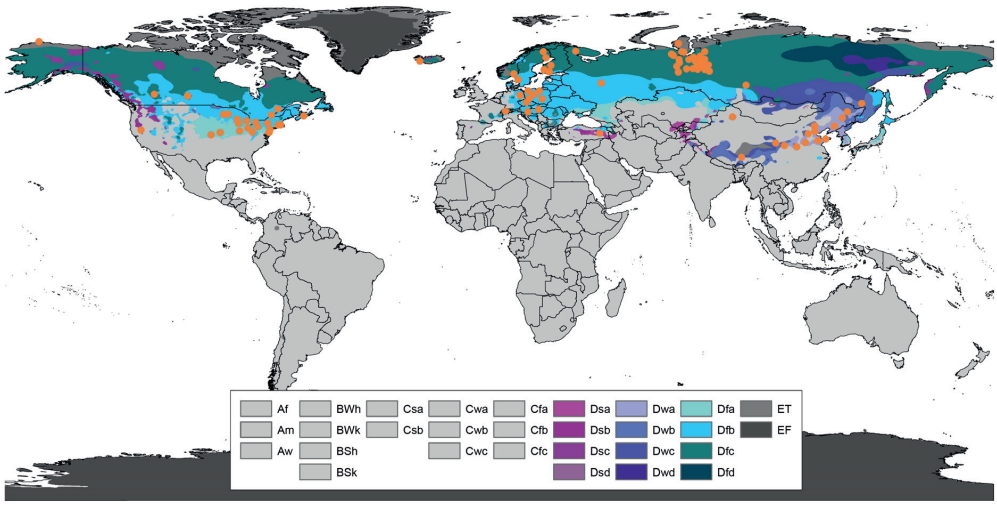

Figure 17: Geographical distribution of investigated locations in the reviewed studies (if specifically indicated) and Köppen-Geiger climate zones. Each of the marked locations (orange dots) represents one city/human settlement. (Original illustration in [129].)

Many of the included studies are based on more than one method, like for example applying a numerical model and conducting on-site or remote sensing measurements. However, the research field is clearly dominated by observational methods. In 81 of the 101 studies, on-site measurements were included. In 22 studies, numerical models were applied, and 20 studies used remote sensing techniques. 4 studies conducted a survey (interview/questionnaire) or review, respectively.

The meta-analysis of the included articles showed that the UHI is a common phenomenon in cold and polar climate regions. Most commonly, the UHI magnitude was reported to be 1–3 K reaching up to 10–12 K during anticyclonic weather. Mostly, the UHI occurred during summer nights, while the winter UHI was less common and weaker. Many articles correlated the highest surface temperatures to densely built-up areas like industrial and commercial areas. In urban parks, forests, and water bodies, on the other hand, the lowest surface temperatures were reported [131–134]. The reviewed studies largely agreed that higher wind speeds weakened the UHI, and numerous studies highlighted the significant contribution of anthropogenic heat release, such as from heating buildings. As opposed to most more temperate and warm climate cities that are characterized by warm summers and due to climate change experience summerly heat waves more and more frequent, cold climate cities from a building energy use perspective

were found to profit from the UHI. It reportedly led to more heating energy savings during winter than cooling energy increase during summer [52,135] and benefitted in mitigating periods of extreme cold [136]. In addition, the urban climate was reported to affect precipitation and vice versa. One of the main findings was the continuous shift to less snow and more rain during the winter months [12,137]. Some studies that analyzed long temperature series highlighted the continuous warming of the investigated cities, like Oslo, Norway [138], Toronto, Canada [139], and Moscow, Russia [140]. Especially winter and daily minimum temperatures were affected strongest by the temperature increase. Regarding the OTC, Polish studies found that during winter, the city centers of Szczecin, Warsaw, and Gdańsk provided more comfortable conditions than the city outskirts. During summer, on the other hand, the opposite is true [141–143].

Other studies that addressed issues not related to the UHI or thermal environment in urban areas often covered very specific topics of research like the statistical analysis of low-level jets [144], associating immunological parameters from blood samples with climatic indicators [145], or the diurnal patterns of gaseous elementary mercury, gaseous oxidized mercury, and particle-bound mercury [146]. Due to their lower relevance in the context of this thesis, these topics will not be presented in detail. The reader is kindly referred to the full-text version of the article in part B of this thesis.

6.2 Summary of P II: Characterization of heat losses in ZEB in cold climate

In the conference article *Characterisation of Heat Losses in Zero Emission Buildings (ZEB) in Cold Climate,* the distribution of heat losses of a validated BPS model (*IDA ICE*) of the ZEB Living Lab is discussed [147]. For that, the model was simulated with eight different cold climate weather files for eight different locations. This was done for two building usages, (1) residential and (2) office building with ventilation rates and operation times according to SN/TS 3031:2016 [148].

The aim of this paper in the context of this thesis was to determine the most important climate variables influencing the building energy demand in cold climate locations. This information is important in order to know if urban areas, districts, or buildings should be designed with a stronger focus on solar accessibility, wind sheltering, or a certain mix of materials in the outdoor areas that might provide better outdoor air temperature conditions (i.e., less temperature variation), etc. The variables of interest were heat losses and solar heat gains, for which a counting methodology was developed and implemented in the simulation tool *IDA ICE*. This methodology distinguishes between *useful* and *detrimental* heat losses and solar heat gains. This is because losing heat in a building during the cooling season for instance is most definitely desirable while solar heat gains are not. The opposite is the case during the heating season. Therefore, heat losses are only counted when indoor air temperatures fall below 21.5 °C (heating threshold temperature is 21.0 °C). At indoor air temperatures above 21.5 °C, heat

losses are not counted, as they are not necessarily considered detrimental. Analogously, (desired) solar heat gains are counted at indoor air temperatures up to 23.5 °C. Above that indoor air temperature, solar heat gains are regarded as detrimental, as they contribute to uncomfortably warm indoor conditions.

The investigated locations were Oslo, Bergen, Trondheim, and Tromsø in Norway, Kiruna in Sweden, Fairbanks and Utqiaġvik (until 2016: Barrow) in the USA, and Vorkuta in Russia. The selection criteria for the locations were a minimum latitude of 60° N and significant population or climate characteristics. Furthermore, the simulation model was analyzed using three different wind profiles and pressure coefficients (1) *open country* and *exposed*, (2) *suburban* and *semi-exposed*, and (3) *city center* and *sheltered*, according to the Air Infiltration and Ventilation Centre's pressure coefficients for wind-induced infiltration [149].

The results showed that compared to wind condition 1, wind sheltering according to wind condition 3 can reduce the heat losses by up to 7.0 % (office) and 8.3 % (residential) in the extremely cold and windy weather conditions of Vorkuta in Russia. In the Norwegian locations, however, savings were between 3.6 % (office and residential) in Oslo and 6.4 % (office) and 7.2 % (residential) in Tromsø. The reason for the lower savings is lower wind speeds and generally milder winters in Norway's coastal cities compared to the Siberian city of Vorkuta. But the main effect of wind sheltering on the heat loss reduction comes from reduced infiltration losses which, in new high-performance buildings such as ZEBs, only account for a relatively small fraction of total losses due to high air tightness levels. It was found that heat losses were strongly correlated with the locations' heating degree hours ($HDH_{21/15}$[6]). In the investigated building, infiltration losses accounted for the smallest share of total heat losses, while walls and doors accounted for the largest in all locations (see Figure 18).

[6] The $HDH_{21/15}$ describe the sum of hourly temperature differences between inside and outside over the year when hourly mean outdoor temperatures drop below 15 °C at a constant indoor temperature of 21 °C. Heating degree hours were used in this study as hourly weather files were used in the simulation tool.

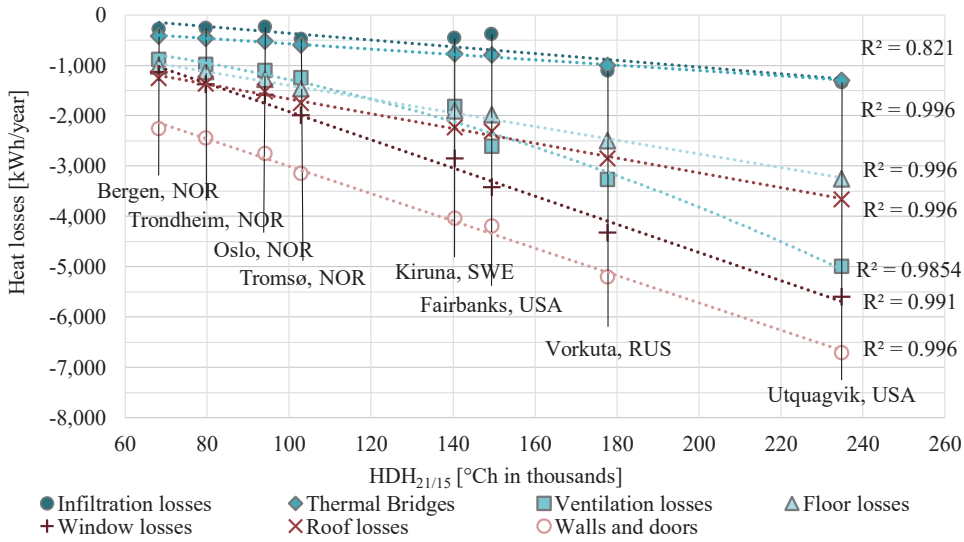

Figure 18: Heat losses through the envelope and ventilation system as a function of $HDH_{21/15}$ of the ZEB Living Lab as a residential building with wind condition 2 (modified from [147]).

In most cases, the heat losses had a distinct linear correlation with the $HDH_{21/15}$. The ventilation losses, on the other hand, presented a nonlinear correlation, resulting from preheating of the air at temperatures below -15 °C to counteract the buildup of ice.

Yet another main finding from the simulations in this paper was the specific role of windows in the energy balance of a building. From Figure 19 it can be seen that especially in the Norwegian cities, with on average 43 % of all windows' annual heat losses in the ZEB Living Lab, *useful* or *desired* solar gains can significantly improve the overall energy balance. Unobstructed, south-oriented windows can even account for more useful solar gains than detrimental heat losses over the year in Norway.

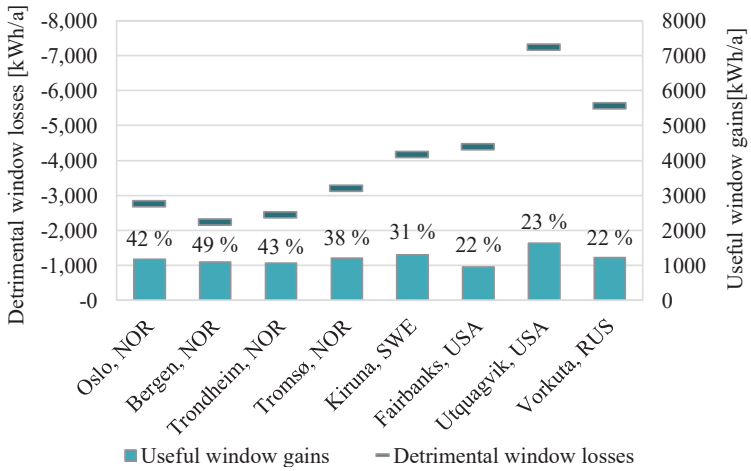

Figure 19: Useful gains and detrimental losses of windows in the ZEB Living Lab as a residential building with wind condition 2 (modified from [147]).

6.3 Summary of P III: Evaluation of design solutions to enhance OTC at high latitudes

The journal article *Evaluation of sustainable strategies and design solutions at high-latitude urban settlements to enhance outdoor thermal comfort* [150] is an improved and extended version of SP I (see Chapter 6.6) and in addition contains a more in-depth validation process, extended analysis of different scenarios and has a focus on OTC. Within the scope of this thesis, the article's aim was to investigate how *typical* microclimatic design strategies can enhance OTC in high-latitude urban settings during autumn. The research was carried out by using the numerical microclimate simulation tool *ENVI-met* and was validated with on-site measurement data of wind speed, wind direction, air temperature, humidity, and surface temperatures taken on October 20, 2019 (average temperature 5.5 °C, average wind speed 2.22 m/s). In total, four scenarios were investigated: a) removing all trees from the study area, closing passages between the existing buildings with b) new buildings and c) trees, and d) changing the surface material of the buildings to a dark charred wood façade with a higher solar absorption value than the present material (see Figure 20).

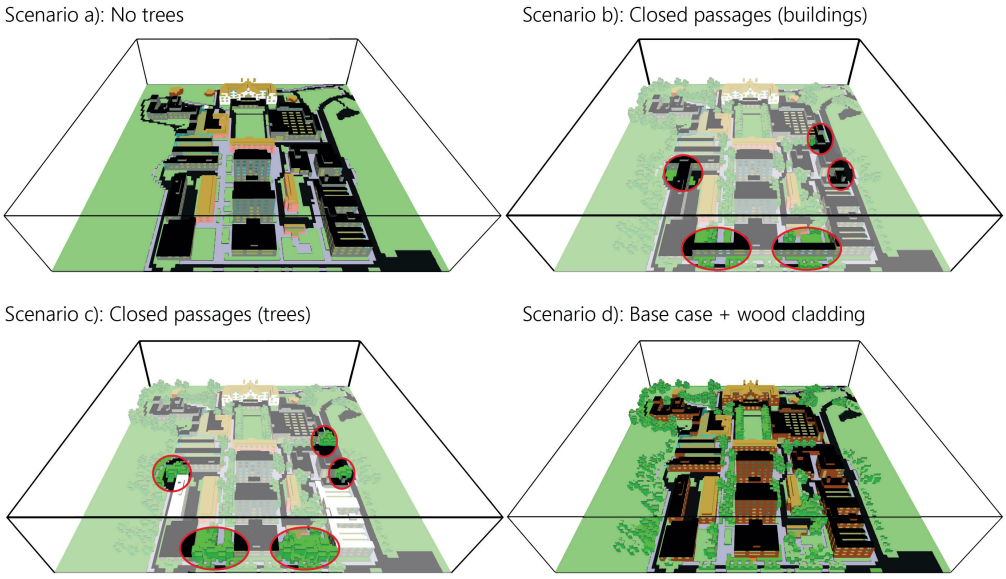

Figure 20: Bird's eye views of investigated scenarios from the southeast. (Original illustration in [150].)

The simulation model features physical models of soil and ground surfaces (bare soil, asphalt road, concrete pavement), vegetation (grass surfaces, trees, hedges), and five building categories (brick, wood, concrete, stone, and glass as façade materials). The computational domain includes a volume of 416 × 400 × 94.5 m³ and was discretized into 104 × 100 × 32 grid cells, resulting in a 4-m grid in the horizontal directions, and a 3-m grid in the vertical. The lowest grid cell is subdivided into five cells with 0.6 m height respectively.

A detailed validation process featured meteorological measurements from four mobile weather stations and one fixed reference weather station 10 m above the roof of a building (28 m above ground). Additionally, infrared thermography was used to obtain surface temperature data of in total 37 locations at the campus, of differently oriented ground and building surface materials. The validation process was carried out in three stages, where a different number of nesting grids (numerical space around the actual study area), and meteorological conditions at the inlets were slightly modified until acceptable accuracy and simulation time were reached[7].

The scenarios were investigated for the main area for an outdoor stay at the campus, *Stripa*, at 12:00 on October 20, and PMVo (Predicted mean vote for outdoor conditions [151–153]) was used as an index for OTC. The results from Figure 21 show that solar access is a key element to provide OTC in autumnal conditions in Norway. Removing the trees in scenario a) led to increased wind speeds on the one hand (on average 10.7 %), but on the other provided excellent access to solar radiation so that the average PMVo in the area increased by 0.33. Wind sheltering was also found to enhance OTC conditions, although not as pronounced as providing solar access. Simulations of the investigated day with a higher inlet wind speed showed that from about 8 m/s, the wind sheltering strategies were more effective in increasing OTC than providing solar access. However, during the actual meteorological conditions, scenarios b) to d) had only a very limited effect on average OTC conditions on *Stripa* (see Figure 22).

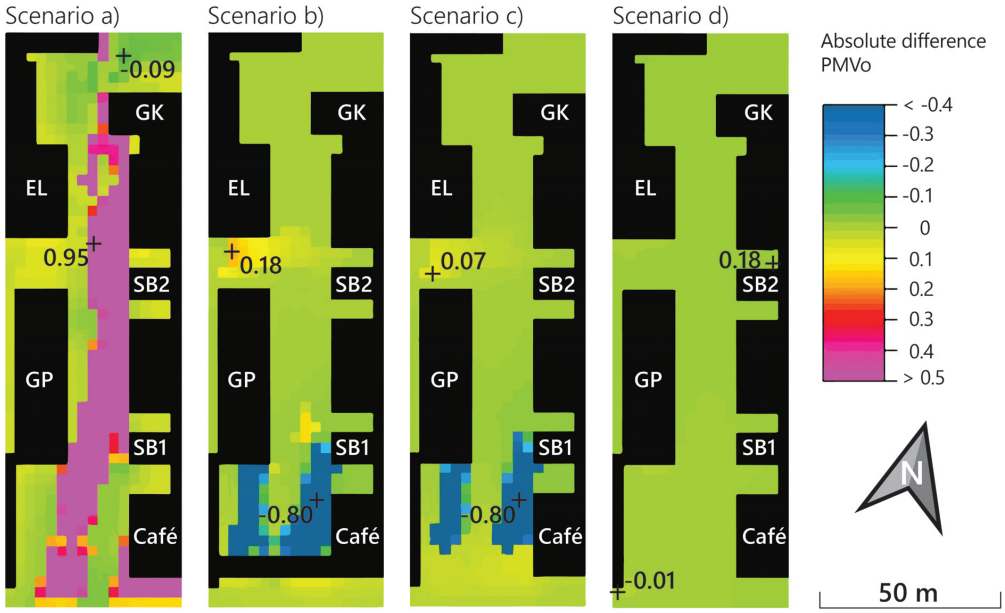

Figure 21: Absolute change of PMVo at Stripa at 12:00 at pedestrian level (1.5 m) of the scenarios a) to d) compared to the base case. The crosses indicate the spots with the highest and lowest value of each scenario. (Original illustration in [150].)

[7] For a detailed description and the results of this validation process, the reader is kindly referred to the full-text version of the article in part B of this thesis.

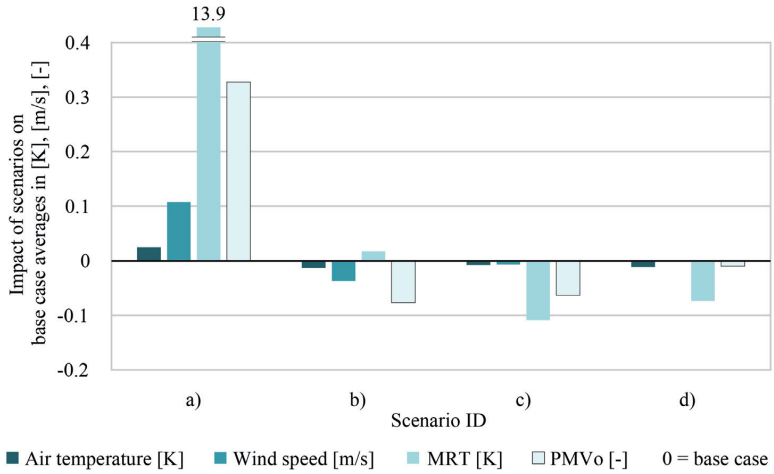

Figure 22: Impact of the investigated microclimatic design scenarios a) through d) on average air temperature, wind speed, mean radiant temperature (MRT) and PMVo when compared to the base case at Stripa (modified from [150]).

6.4 Summary of P IV: Validation of a CFD model for urban microclimate analyses

In P IV [154], the process of developing and validating a CFD model (*ANSYS Fluent*) for the evaluation of the urban microclimate at high-latitude locations is discussed in detail. In the context of this thesis, the article provides important information about the applicability of a commercial CFD tool which in principle is not specifically developed for the investigation of the urban microclimate. Such studies are scarce at high-latitude locations. Again, NTNU's *Gløshaugen* campus was used as a case. Unlike in previous studies of the campus using *ENVI-met*, this time, the whole campus area and surrounding buildings within 250 m of the university, and close to 18 km^2 of surrounding terrain were included. Consequently, the computational domain (4,225 × 4,225 × 1,550 m^3) features an area in the center where the buildings were modeled explicitly, areas further away in which the urban surface is included with roughness parameters, different surface materials like grass, concrete pavement, asphalt, water, brick, stone, wood, and a number of physical models to simulate the urban microclimate. These models include the 3D URANS approach with the realizable k-ε turbulence model, solar irradiation, longwave radiation exchange, heat conduction, heat storage in the urban surface, and the thermal effects from evapotranspiration from trees and grass surfaces. With a height of 1,550 m, the domain includes all relevant layers of the UBL (see Figure 5 and Table 3, Chapter 2.2).

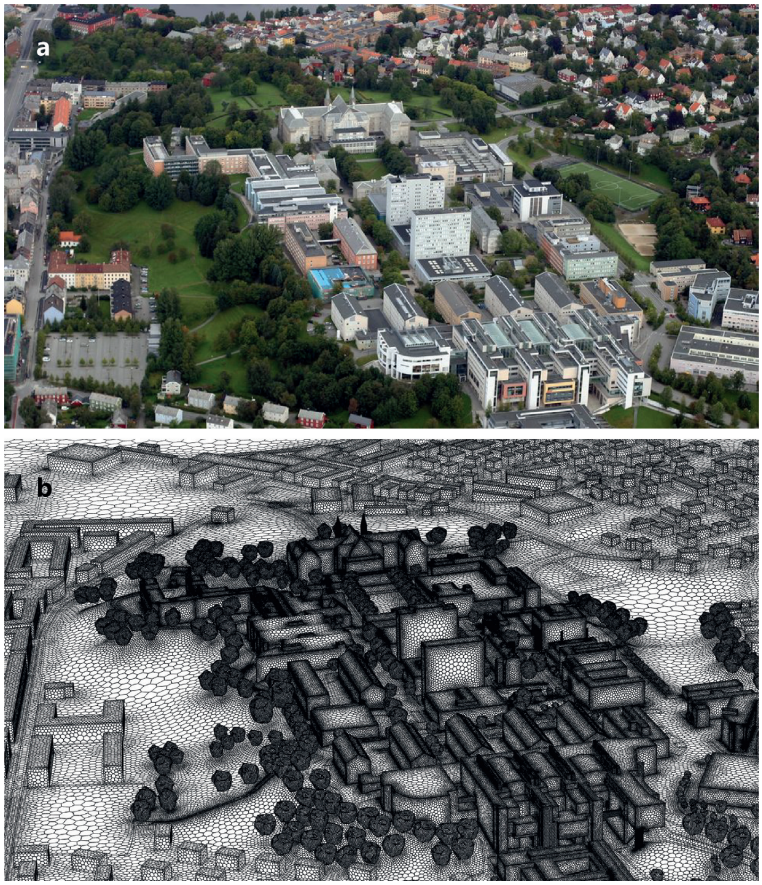

Figure 23: (a) Aerial view of the NTNU campus from the south (Photo: Lars Strømmen); (b) Computational grid with 9,123,834 cells, featuring buildings and trees on the campus. (Original illustration in [154].)

Following the best practice guidelines from literature, the domain was discretized into a polyhedral grid of 9.1 million cells (see Figure 23) and was based on a grid convergence analysis. Certainly, a notable feature of the CFD model is the implementation of the Penman-Monteith equation (PME) [155–157] for the thermal effects from evapotranspiration at grass surfaces, and of the outdoor thermal comfort index PET (physiological equivalent temperature) [153,158–160]. To the best of the authors' knowledge, neither the PME nor the PET have been implemented in *ANSYS Fluent* previously for the purpose of studying the urban microclimate. For more information about the computational settings and boundary conditions, as well as the results from the grid convergence analysis, the reader is kindly referred to the full-text version of the article in part B of this thesis.

The validation process included the comparison of simulated data with on-site measurements at five mobile weather stations 3 m above the ground and one reference weather station, located 28 m above the ground, 10 m above a building on campus. This was done for two 48-hour validation periods (VP) in autumn (VP1: September 27–28 and VP2: October 19–20). Each VP was simulated using hourly time steps and in total 19,600 iterations per VP.

The comparison of simulated and measured climate data at the reference weather station showed an overall acceptable agreement between the two. While in both VP1 and VP2, the air temperature was represented with an R^2 of 0.98 and 0.93, respectively, there were larger deviations regarding wind speed and wind direction between the two periods. In VP1, the wind speed was well represented by the CFD model, while there were larger differences regarding wind direction (see Figure 24). In VP2, the situation was just the opposite. Larger deviations regarding wind speed and a fairly good agreement between simulated and measured wind direction (see Figure 25). This behavior was found to be partly caused by the terrain which deflects the wind when coming from southern directions (see especially the accumulation of data points in Figure 24d and Figure 25d) and partly by the wake created by buildings during westerly and northwesterly winds. Comparing the results between the simulated and measured meteorological variables at the locations of the five mobile weather stations revealed that the PME slightly overestimated the cooling flux from evapotranspiration at grass-covered surfaces. For detailed illustrations and information about the accordance of measured and simulated meteorological variables at these locations, the reader is kindly referred to the full-text version of the article in part B of this thesis.

All in all, the CFD model proved to be well suited for urban microclimate studies in meteorological conditions similar to the investigated. It can be used in studies focusing for instance on the influence of the urban fabric and vegetation on the energy demand in buildings, OTC, pedestrian wind comfort, pollutant dispersion, pressure coefficients on building façades, or urban wind energy potential.

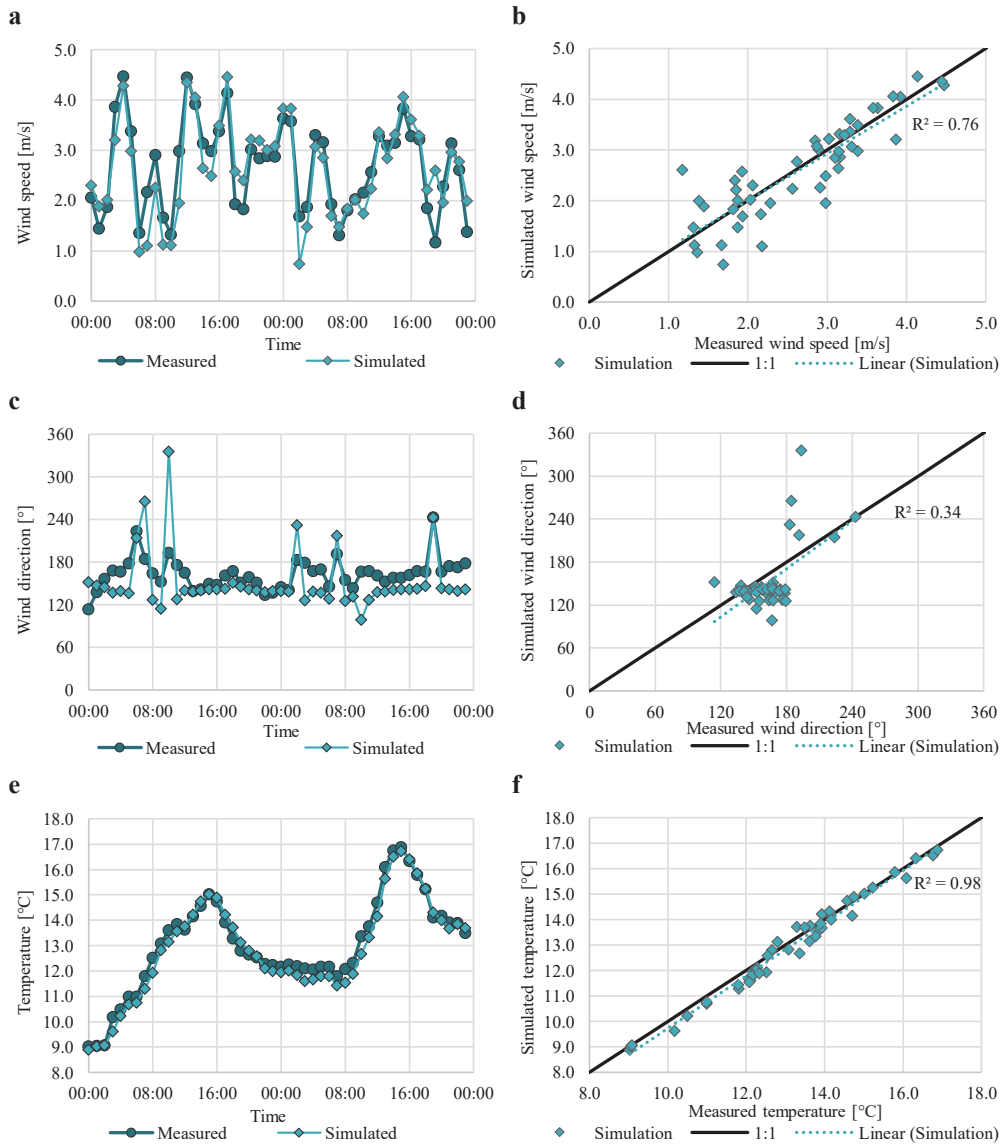

Figure 24: Comparison of simulated and measured wind speed (a and b), wind direction (c and d), and air temperature (e and f) with error bars indicating the range of measurement uncertainty for VP1: September 27–28. Due to the high sensor accuracy, the error bars are hidden behind the data points. (Original illustration in [154].)

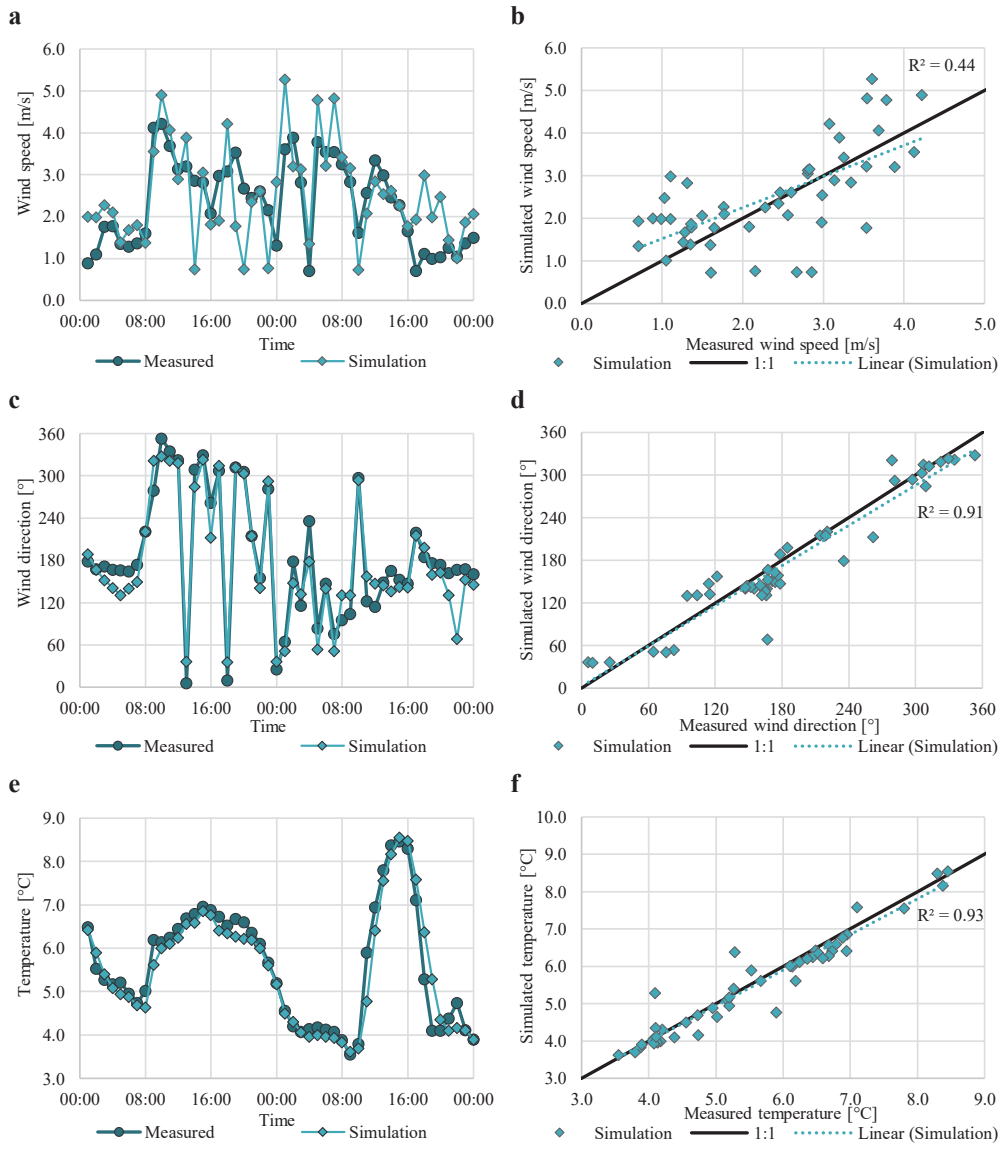

Figure 25: Comparison of simulated and measured wind speed (a and b), wind direction (c and d), and air temperature (e and f) with error bars indicating the range of measurement uncertainty for VP2: October 19–20. Due to the high sensor accuracy, the error bars are hidden behind the data points. (Original illustration in [154].)

6.5 Summary of P V: Impact of urban microclimate on building energy demand

In the study *Assessing the Impact of Urban Microclimate on Building Energy Demand by Coupling CFD and Building Performance Simulation*, four scenarios of different compositions of the urban surface were simulated with the CFD model validated in P IV. The resulting microclimatic conditions were then used as input in BPS of a 13-floor office building (SB1) from the 1960s on the NTNU campus.

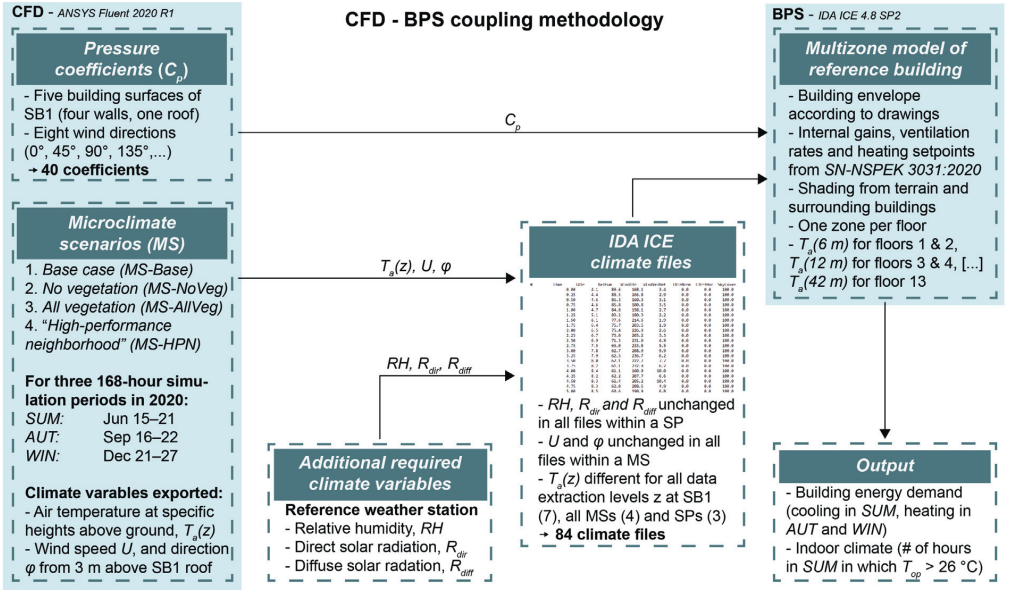

Figure 26: Coupling methodology between CFD and BPS in this study.

The investigated microclimate scenarios (MS) were:

1. *Base case (MS-Base)*: actual situation.
2. *No vegetation (MS-NoVeg)*: no trees, all vegetated ground surfaces substituted with concrete.
3. *All vegetation (MS-AllVeg)*: all ground surfaces substituted with grass.
4. *"High-Performance Neighborhood" (MS-HPN)*: All explicitly modeled buildings surrounding SB1 with high-performance building envelope (0.3 m insulation and exterior charred wood cladding)

Although *MS-HPN* addresses the microclimatic situation with a district-wide high-performance building envelope, the BPS model of the building of interest was not changed to ensure comparability between the scenarios. The four MSs are simulated for three 168-hour (1 week) simulation periods in different seasons of the year. The dates and names of the simulation periods are June 15 00:00:00 – June 21 23:59:59 (SUM), September 16 00:00:00 – September 22 23:59:59 (AUT), and December 21 00:00:00 – December 27 23:59:59 (WIN) for summer, autumn, and winter 2020, respectively. To capture the microclimatic conditions around SB1, a methodology was presented that accounts for a changing air temperature $T_a(z)$ over the height of the building, where z is the height above ground. For that, separate weather files with an air temperature calculated as a mean of all data extraction points with the same z (6 m, 12 m, etc.) were created and assigned to always two building floors at about the same height. The first and second floor have been assigned $T_a(6\ m)$, the third and fourth floor $T_a(12\ m)$ etc. Finally, the thirteenth floor is assigned $T_a(42\ m)$. CFD was also used to determine the pressure coefficients on the façades of SB1, which then served as input in the BPS tool *IDA ICE 4.8 SP2*. The aim of this study was to compare the cooling energy demand and the number of hours in which the

operative temperature (T_{op}) of SB1 indoors exceeds 26 °C ($N_{T_{op}>26\,°C}$) during SUM, and the heating energy demand of SB1 during AUT and WIN, for the previously described MSs. Figure 26 shows the methodology which was followed in this study.

From the CFD simulations, quite pronounced differences between the MSs were observed during SUM, particularly with regard to *MS-NoVeg*. During AUT and WIN, however, the investigated MSs had a fairly small impact on air temperature. This tendency can be explained by the seasonal availability and intensity of solar irradiation onto the urban surface. While during SUM, the solar elevation angle is rather high and days are long, the urban surface can absorb a large amount of solar energy. Towards WIN, the situation reverts. Figure 27 shows the air temperature at SB1 of the different MSs and simulation periods and the differences in air temperature $\Delta T_{MS-Base}$ at SB1 of *MS-NoVeg*, *MS-AllVeg*, and *MS-HPN* compared to the base case *MS-Base*.

In all three simulation periods, *MS-NoVeg* showed the largest variation of microclimatic conditions with an air temperature that almost continuously surpassed that of *MS-Base*. Because of lower solar irradiation levels, this behavior was not observed during AUT and WIN where a smaller elevation angle hides the sun behind the large hill in the west of the computational domain. The simulated average air temperatures at SB1 for *MS-NoVeg* were 1.0 °C, 0.2 °C, and 0.1 °C warmer than in *MS-Base* in SUM, AUT, and WIN, respectively. On the other hand, *MS-AllVeg* was 0.1 °C cooler than *MS-Base* in both SUM and AUT. In WIN, the temperature difference was negligible. While *MS-HPN* was 0.1 °C warmer than *MS-Base* during SUM, there was only a marginal influence on air temperature at SB1 during AUT and WIN on average. In *MS-NoVeg*, up to 2.4 °C higher air temperatures were obtained in SUM, 0.4 °C in AUT and 0.3 °C in WIN. In *MS-AllVeg*, the additional greening led to a maximum decrease in air temperature of 0.6 °C during SUM, 0.3 °C during AUT, and 0.1 °C in WIN. *MS-HPN* on the one hand led to relatively large reductions of air temperature at certain points in time with a maximum of 0.6 °C during SUM and AUT, and 0.2 °C during WIN, but also caused significant air temperature increases at other times. These maximum increases were 1.0 °C and 0.6 °C during SUM and AUT, respectively.

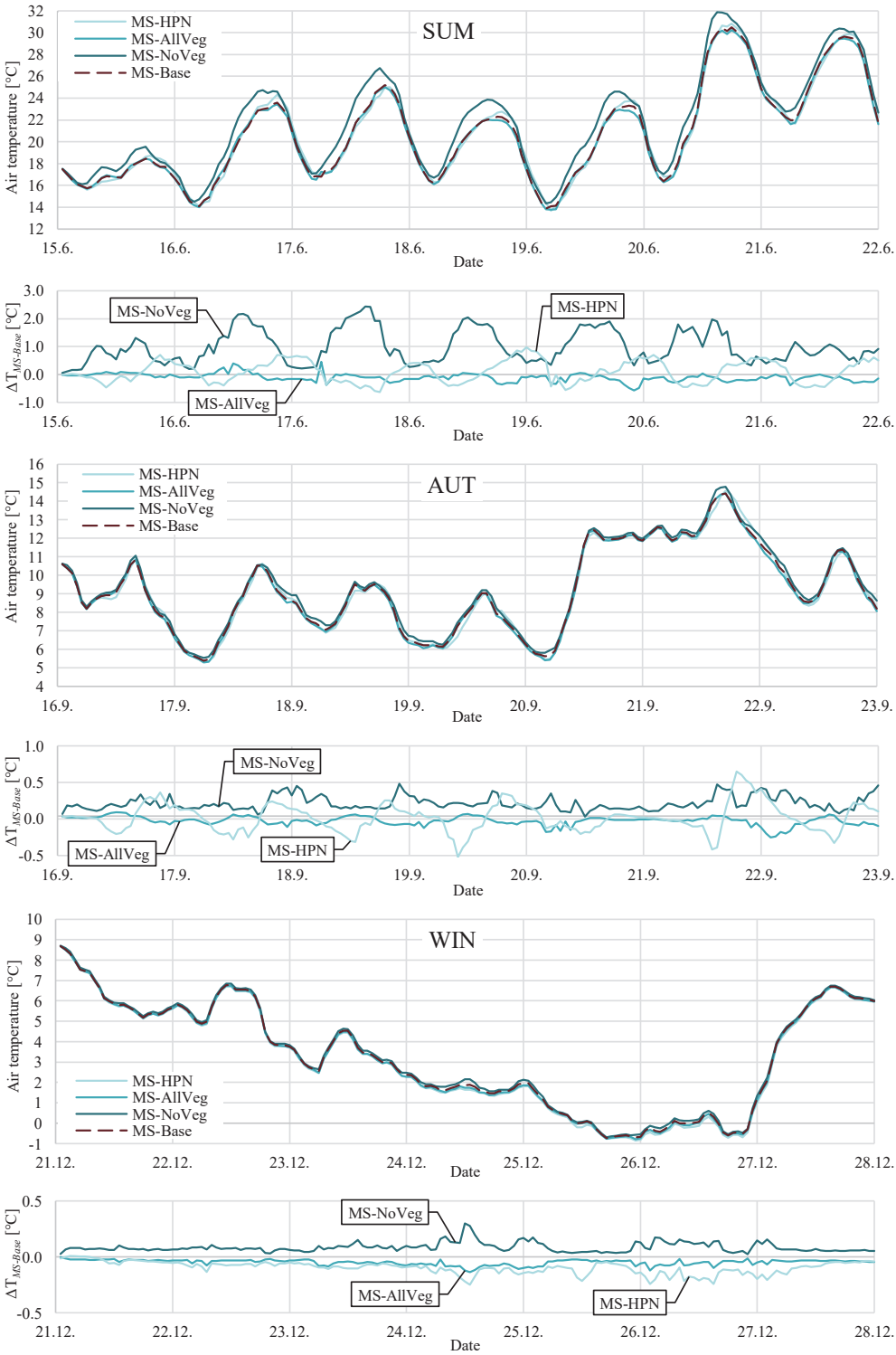

Figure 27: Air temperature of the different MSs and air temperature difference MS-NoVeg, MS-AllVeg, and MS-HPN compared to MS-Base during SUM, AUT, and WIN around the building of interest (SB1).

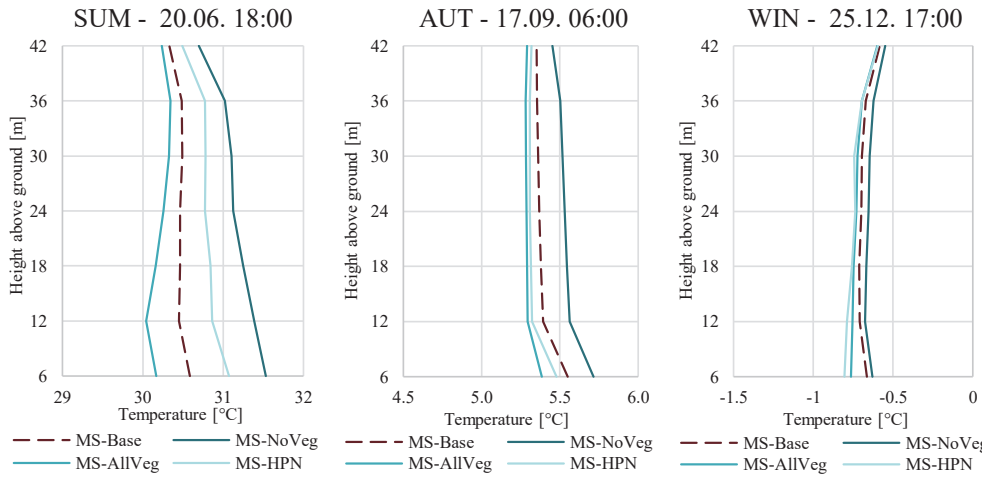

Figure 28: Average air temperature of the 42 logging points around SB1 for all MSs at selected times of the day during SUM (20.06. at 18:00), AUT (17.09. at 06:00), and WIN (25.12. at 17:00).

Figure 28 presents the air temperature around SB1 for the different MSs at selected points in time, averaged and plotted with respect to the height above the ground. It can be seen that the differences between the temperature profiles were larger close to the ground and that they converged with increasing height. It is also noticeable that with the transition from summer to winter, the differences between the MSs of a simulation period got smaller.

The influence of the local microclimate conditions on building energy demand is strongly in line with the results from the CFD simulations where the differences were largest in SUM and smallest in WIN. Figure 29 shows the total heating/cooling energy demand of the four MSs in every simulation period. Resulting from the large temperature differences between *MS-NoVeg* and *MS-Base* in the CFD simulations during SUM, the absence of green infrastructure as in *MS-NoVeg* in Trondheim during the simulated week in June 2020 would have increased the cooling energy demand in SB1 by 26.6 %. At the same time, an entirely greened urban surface as in *MS-AllVeg* would have reduced the cooling energy demand by 1.5 % compared to the situation as it is. As Trondheim is a city that already features considerable amounts of green spaces in the *MS-Base* scenario, the difference to *MS-AllVeg* is rather small. Changing the properties of the building façades in *MS-HPN* led to an increase of cooling energy demand by 0.8 %. In this scenario, a lower albedo of the building envelopes led to more radiation being absorbed which causes higher outdoor air temperatures.

On the other hand, in both AUT and WIN, *MS-NoVeg* represented the scenario with the lowest energy demand. As in both simulation periods, outdoor temperatures required the building to be actively heated, slightly higher outdoor temperatures from an urban surface without greening resulted in reduced heating demands. These reductions added up to 2.5 % and 0.5 % in AUT and WIN, respectively. Conversely, as more vegetation led to lower outdoor temperatures, heating energy demands are slightly higher than in the base case. Accordingly, *MS-AllVeg*

caused increases in heating energy demands by 1.0 % and 0.4 % in AUT and WIN, respectively. In *MS-HPN*, however, the tendency of the summer simulation period also persisted in AUT and WIN, showing slight increases in heating energy demand with 0.9 % and 0.8 %, respectively. An explanation for that are the better insulation levels of the buildings' envelopes which led to less *urban self-heating* and consequently slightly lower air temperatures [161].

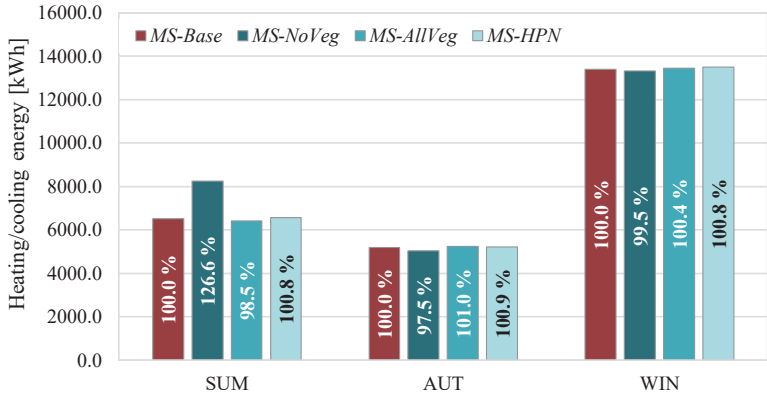

Figure 29: Total heating (AUT and WIN) and cooling (SUM) energy demand of SB1 during the investigated simulation periods.

When looking at the simulated energy demands per floor, large differences can be noticed (see Figure 30). From Figure 30a, especially the differences between the lower two floors to the upper nine are apparent in SUM. Floors 5–13 had an energy demand significantly higher than floors 1 and 2. As the lower floors (1–4) had adjacent buildings on the northwest and southeast façade, the area exposed to the ambient conditions became lower. While the lower floors benefited strongly from the smaller surface area and higher shading levels from surrounding buildings during SUM, floor 13 was adversely affected by a higher surface area to ambient conditions because of the roof. However, resulting from the more uniform air temperature profile over the height of SB1, the differences between the MSs in AUT and WIN (Figure 30b and c) were relatively small among the floors. During SUM on the other hand, especially the two lower floors benefited from close-by green spaces in *MS-AllVeg*, reducing the energy demand needed for cooling by about 50 % compared to *MS-NoVeg*. When simulating SB1 in SUM without an active cooling system, the investigated scenarios can be compared in terms of $N_{T_{op}>26\,°C}$ (Figure 31). Across all floors and scenarios, values ranged from 6.8 h on the first floor in *MS-AllVeg*, to 48.8 h on floor 10 in *MS-NoVeg*. While the differences among the investigated scenarios were rather small from floors 5–13 (from 17 % to 40 % between the highest and lowest value on each floor), especially on the first four floors, *MS-NoVeg* exceeded *MS-AllVeg* by 160 % to 171 %, respectively. Floor 13 benefited from the additional envelope area from the roof to cool down during the night which also had a positive effect on the floor below. On both floors, the thermal inertia of the building delayed re-exceeding 26 °C during the day when they were effectively cooled down the night before. The mean values of $N_{T_{op}>26\,°C}$

across all floors were 31.5 h, 41.6 h, 29.7 h, and 30.8 h for *MS-Base*, *MS-NoVeg*, *MS-AllVeg*, and *MS-HPN*, respectively.

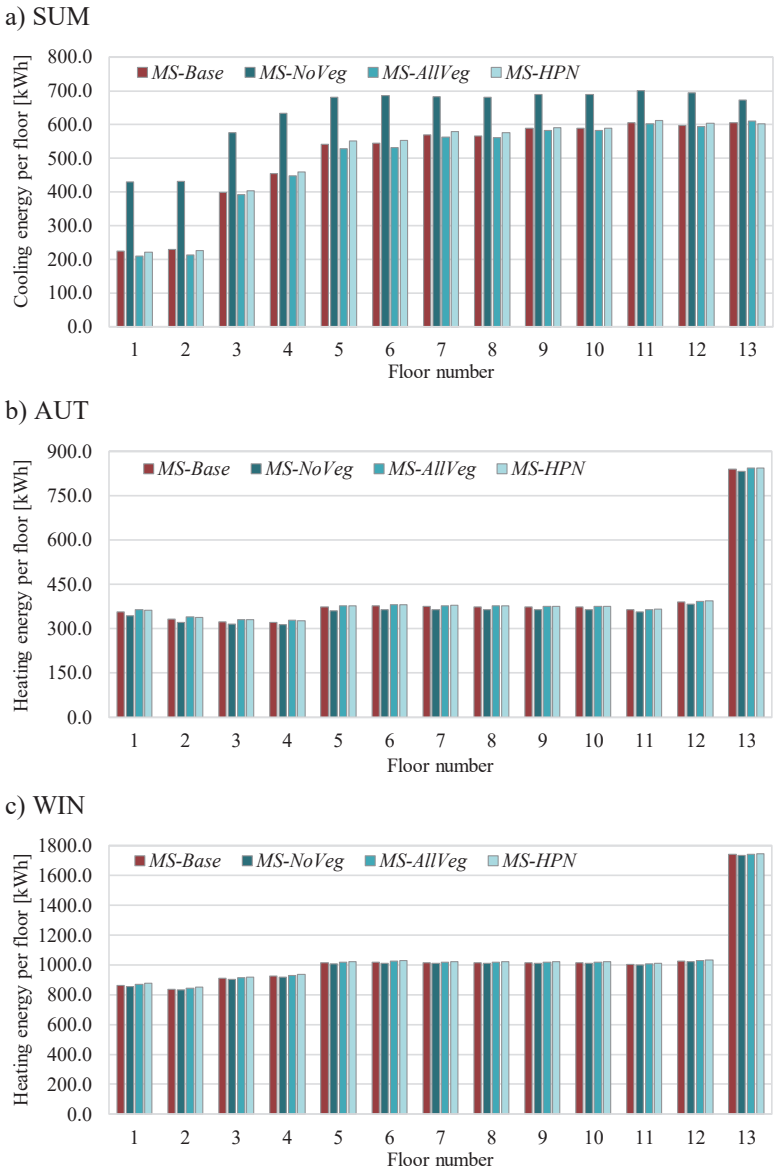

Figure 30: Energy demands of the simulated scenarios in the simulation periods per floor. a) cooling energy demand in SUM; b) heating energy demand in AUT; c) heating energy demand in WIN.

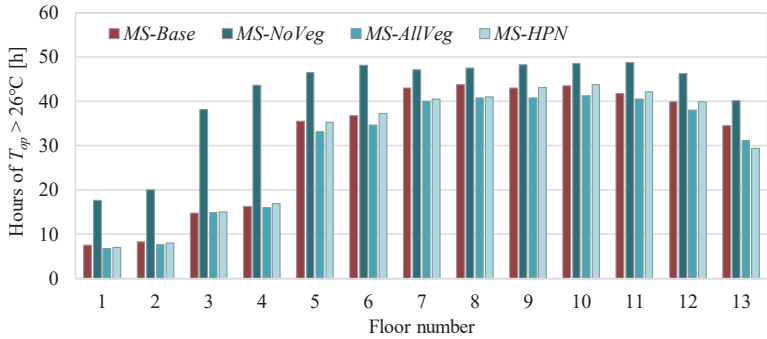

Figure 31: Number of hours with the indoor operative temperature above 26 °C for each floor during SUM, when SB1 is simulated without active cooling elements in the zones.

6.6 Summary of SP I: Microclimate analysis of a university campus in Norway

Microclimate analysis of a university campus in Norway [162] is a conference paper that discusses the microclimatic conditions of NTNU's *Gløshaugen* campus in its present form. For that, a numerical model was used after validating it with surface temperature measurements. The purpose of this paper in the context of this thesis was to investigate the capabilities of the applied simulation tool (*ENVI-met*) and to investigate the microclimatic characteristics on the campus, including the identification of areas with critical conditions. This article represents an early version of P III (see section 6.3). Like in P III, only the northern part of the campus was investigated. The simulation model features physical models of soil and ground surfaces (bare soil, asphalt road, concrete pavement), vegetation (grass surfaces, trees, hedges), and five building categories (brick, wood, concrete, stone, and glass as façade materials).

The comparison of preliminary simulations for the validation showed an acceptable accuracy of the simulation model with an average deviation from the measurements (infrared thermography) of 4.9 K. It was found that *ENVI-met* tended to overestimate surface temperature values where measurements were close or below 0 °C.

The simulation results of four dates (21.03., 21.06., 23.09., and 21.12.) showed that especially the areas in front of south-facing and sunlit surfaces presented elevated temperature values. On June 21, the temperature variation on campus was highest with 3.4 K between the warmest and coolest point in the domain, while on December 21, it was lowest with 1.2 K. The analysis of the wind field showed especially the east-west passages on campus to be problematic. There, local air velocities surpassed the inlet wind speed by up to 57.1 %. The lowest wind speeds occurred in the wakes of the larger buildings. In Figure 32, the air temperature and wind field at 12:00 for the simulated days are shown.

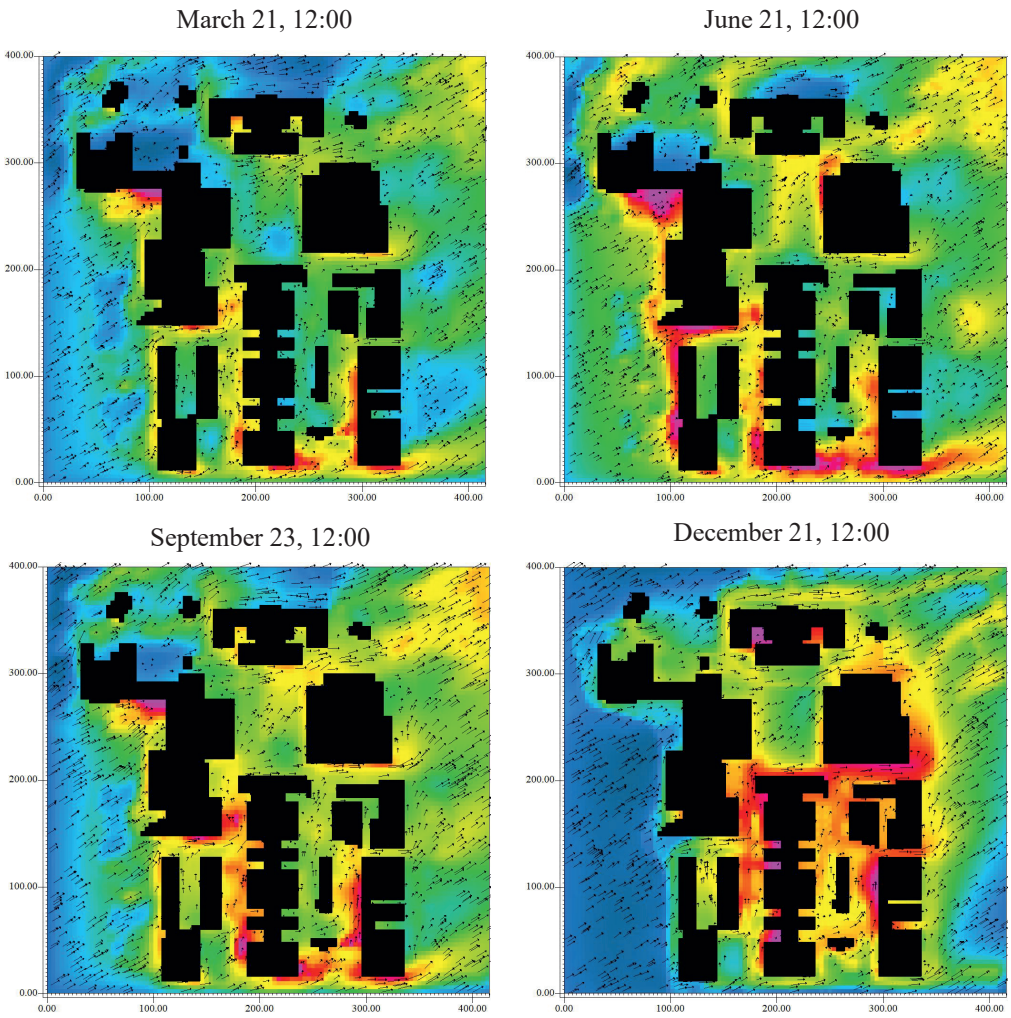

Figure 32: Air temperature and wind field at 12:00 at pedestrian level (1.5 m above ground) for the four simulated days. (Original illustration in [162].)

6.7 Summary of SP II: State-of-the-art and systematic review of ZEN and PED

In this article [163], research on ZENs, PEDs, and different concepts of climate-friendly neighborhoods (CFN) is reviewed in two parts. In the first part of the paper, a systematic review is presented, while the second lists and discusses a selection of CFN definitions of public initiatives and research projects. The objective of the article was to identify focus areas, research gaps, and future research possibilities connected to CFNs. A total of 144 elements were included in the categorization (see Table 6) and analysis based on the included articles' nomenclature, usage and location of case studies, the main topic of the articles, the methodological approaches, the publication channels, years, and citations, and author keywords. In the following, only a short extract of the results that are relevant for this thesis is shown.

Table 6: Abbreviations and descriptions of categories (modified from [163]).

Category name	Description
ES	Energy system
Trans	Transition to CFN
ICT	Information and communication technology
POSE	Project organization and stakeholder engagement
UM	Urban morphology
LCA	Life cycle assessment
SA	Social aspects
MC	Microclimate
Other	Research not captured by previous categories

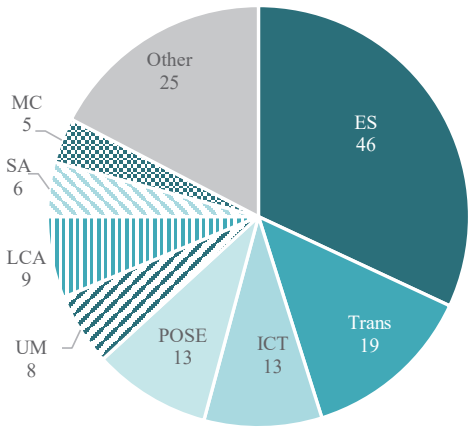

Figure 33: Distribution of the topics of the included articles. (Original illustration in [163].)

It was found that only 5 out of 144 papers (3.5 %) addressed issues connected to the microclimate in CFNs (see Figure 33). The largest part of the studies (46 or 31.9 %) focused on the energy system, followed by articles that addressed the transition of an existing neighborhood to a CFN (19 or 13.2 %). In the second part of the article which lists and discusses different CFN definitions, microclimate is largely left out. The term does not appear in any of the available definitions. Microclimatic conditions are included only indirectly, through *spatial qualities*, in a wider sense in the ZEN definition [124].

7 Discussion

In this section, the results from the individual papers are interrelated and the research questions from Chapter 3.2 are answered.

7.1 RQ 1: Main characteristics of urban climate in cold climate regions

Research question 1

What are the characteristics of the urban climate in cold climate regions?

What are the main differences to the urban climate in warmer climate regions? What are the most researched topics, where are the research gaps, and what methods were applied most frequently? What implications arise for Norwegian cities?

This research question is mainly answered by the systematic review in P I. From its most relevant results for this thesis, the main characteristics of the urban climate in cold climate regions can be summarized in the following statements:

- The urban climate in cold climate regions is dominated by the presence of the UHI
- Coastal cities experience a distinct cooling (warming) effect of large water bodies in spring and summer (autumn and winter).
- There is a pronounced UHI with a typical UHI magnitude of about 1–3 K and reaching up to 10–12 K during anticyclonic weather (often come along with clear and dry conditions).

- Most commonly, the UHI occurs during summer nights, while the winter UHI is usually weaker and less common.
- The highest surface temperatures occur in densely built-up areas where impervious materials dominate (industrial and commercial areas) while parks, forests, and water bodies are coolest.
- Higher wind speeds weaken the UHI.
- Anthropogenic heat release contributes significantly to the UHI.
- The UHI leads to more heating energy savings during winter than cooling energy increase during summer.
- More precipitation in the form of rain than snow.
- Increased (decreased) OTC during winter (summer) in the city centers compared to the outskirts.
- In the long term, cities keep getting warmer due to ongoing urbanization and increased anthropogenic heat release. Especially winter temperatures rise faster than summer temperatures.

Generally, the governing source of energy to the urban surface is solar radiation [11]. Its uneven incidence is the main cause of the macroclimates (tropical, temperate, polar, etc.). As an example, in a tropical location, the seasonality of average monthly solar irradiance[8] might be as low as 12 % [11] while in the high-latitude city of Trondheim it is about 80 % [112]. Anthropogenic heat flux Q_F (see also Eq. 2 in Chapter 2.3) compensates for a lower solar radiation load onto the urban surface during the winter months in colder climates, while Q_F is significantly less relevant for the urban energy balance in warmer climates. This is reported to be one of the main causes for the reduction of maximum UHI magnitudes moving from higher to lower latitudes [164].

It is important to have in mind that the urban climate is not dependent on city characteristics only, but to a large degree on the properties of its surrounding as well. Orographic features, for instance, can cause wind patterns that lead to recirculation in the city provoking higher air pollution levels due to a lack of aeration [11]. Depending on the surrounding land use type and especially the biome[9], UHI magnitudes can be significantly different despite similar city characteristics. In this connection, a study in the USA showed that cities in the *temperate forest* biome displayed the highest surface UHI magnitudes during daytime in summer. During winter, on the other hand, when the vegetation in the *temperate forest* biome is physiologically less active, cities in the studied *Mediterranean* and *(sub)tropical* biomes showed higher surface UHI magnitudes [166].

[8] Expressed as the ratio of standard deviation of monthly average irradiance to annual average irradiance [%].
[9] A biome is a large area characterized by its vegetation, soil, climate, and wildlife. There are five major types of biomes: aquatic, grassland, forest, desert, and tundra [165].

Along with two of the most-cited scientific articles on the UHI [167,168], literature in general reports a rather strong positive correlation between city size/population/population density and UHI intensity across various climate zones [169–172]. One of the reviewed articles from P I reported a similar relationship [63]. However, studies that due to their later publication date were not included in the review reported a weak correlation between city size or population and UHI intensity in 57 cities across Fennoscandia [69] and 118 high-latitude circum-Arctic cities [173]. Ultimately, it is concluded that the presence of a UHI in Norwegian towns and cities is very likely, yet its average magnitude is estimated to be stronger influenced by other factors than city size or population (i.e. influence of large water bodies, terrain, etc.).

Another purpose of P I was to identify research gaps and the most researched topics which were also outlined in the published paper. More than half of the reviewed articles addressed the UHI (57 %) while the second most studied topic was found to be biometeorological research (15 %). The most relevant research gap in the context of this thesis was that the use of numerical tools is underrepresented. As P I showed, the field of urban climatology in the cold climate regions is still to a great extent dominated by observational methods, especially of the UHI. The use of numerical tools to replicate, predict or investigate different scenarios of the urban climate conditions accounted for a relatively small share (22 %) of the reviewed articles. Especially at high-latitude locations, such studies are scarce [58,174] which is supported by the literature reviews in the introduction sections of P IV and P V. Furthermore, the few articles addressing numerical tools in high-latitude cold climate locations are predominantly focused on the summer conditions of the investigated areas and how to mitigate the adverse effects of summerly overheating. Therefore, a clear research gap regarding the investigation of the urban microclimate by the means of CFD and other numerical tools during cool or cold weather conditions in cold-climate and high-latitude locations was identified.

Additionally, it was found in SP II that microclimatic aspects are rarely accounted for when research is carried out in CFNs. The definitions of various CFN concepts neglect the effect of the urban microclimate on the energy and environmental performance of buildings or OTC entirely. Only the ZEN definition [124] mentions *spatial qualities* which in a broader context also includes the microclimatic conditions, although not explicitly referring to the term *microclimate*.

But as P V showed, the building insulation level can affect the microclimate conditions due to lower rates of anthropogenic heat release. Especially OTC is expected to be negatively influenced by less anthropogenic heat release and consequently slightly lower air temperatures during winter. Researchers, practitioners, and authorities need to be aware of this connection, allocate more resources to its investigation, and include gained knowledge in their work.

Based on the results from the body of literature and the main conclusions drawn from the authors of extensive literature reviews and meta-analyses [164,175,176] including P I, the

scientific evidence does not allow for simply transferring the characteristics from one city to another. The system of influencing meteorological, geographical, topographical, anthropogenic, and physical features, as well as their interactions on the micro- and macroscale are far too complex to allow for that. Even though there are some quite recent studies of for instance the UHI [69,173] or temperature series analyses [138] in Norwegian cities, more studies that involve measurements and numerical models are needed for a conclusive answer to this research question. Of central importance in the Norwegian context is for instance the influence of large water bodies on the urban climate, since about 80 % of the Norwegians live within 10 km distance to the sea [177]. Similarly, the significant influence of the Gulf Stream [115] needs to be investigated more deeply in connection to the urban climate in Norwegian cities.

As mentioned in P I [129] "*[...] it needs to be pointed out that the results and especially the UHI-magnitudes of the reviewed studies are not directly comparable with one another. This is because methodologies, season, time of the day, measurement periods and equipment, elevations of (and differences in elevation between) the city weather station and its "non-urban" counterpart in the studies varied significantly. Those "non-urban" stations were sometimes parks, airports, suburbs, intraurban (within urban areas) locations of different typology or rural areas located outside the city. Even more importantly, every city is different from each other. They differ with respect to population, extension and density, amount of green spaces, building density and typologies, height profile, centrality (what can be actually characterized as a city center) and furthermore building standards.*"

7.2 RQ 2: Impact of the urban fabric on OTC and building energy demand

Research question 2

What is the impact of the urban fabric on the urban microclimate in Norwegian climate conditions with regard to...

1. Outdoor thermal comfort?
2. Building energy demand?

How do the properties and the type and scale of modification of the urban surface including building surfaces, vegetation, and the building energy level affect the micro-climate? What consequences for people's outdoor thermal comfort and the energy demand of buildings are to be expected in Norway?

The answer to RQ 2 is mainly given in P II, P III, and P V. Regarding OTC, P III showed that providing solar access is the most effective way to improve OTC conditions during autumn in Norway. Also, wind sheltering proved to be an effective measure to increase OTC conditions

in cool or cold conditions, however, only at relatively high wind speeds and on a much smaller scale than solar access which is broadly supported by the literature [116–120]. But especially on cloudy and windy days, wind sheltering is the only available passive strategy to improve OTC. Therefore, a combination of both, providing solar access and wind sheltering is recommended particularly for outdoor sitting areas like cafés, etc. Similar considerations were also found in the literature [178–180]. Although not specifically investigated, the situation in spring is assumed to be similar to the studied autumn conditions.

Unlike in more southern locations where the modification of the urban surface albedo resulted in significant changes of the microclimate during warm or hot summer conditions [39,181–183], the effect in the investigated conditions of P III was small. A probable explanation for that is the low solar elevation angle during the cold season at high latitudes. At this time of the year, only a very small amount of solar radiation reaches the ground or pedestrian level. Consequently, changing a material property dependent on solar radiation (e.g., albedo) in these locations will only have a small effect on OTC unless the area is particularly exposed to the sun.

The effect of different climate variables on building energy demand was investigated in P II and P V. Similar to OTC, P II showed that solar access is a key variable in reducing heating energy demands in a ZEB. In Norwegian climate conditions, south-oriented, unshaded windows can lead to more useful solar energy gains than energy losses which supports the findings from Grynning et al. [184]. Consequently, promoting solar access when designing buildings and especially neighborhoods can effectively lower the buildings' energy demand. Wind sheltering had a positive effect on reducing the building heating energy demand, but only in particularly windy conditions. In the investigated Norwegian locations, it led to about 5.3 % reductions in heating energy demand on average. Savings of this magnitude were reached by comparing simulation results using two strongly opposing wind profiles: (1) *open country, exposed*, and (2) *city center, sheltered* [149]. In reality, improving the wind sheltering of a building in such an order of magnitude is only achievable if entire city districts are built around an already existing and exposed, rather small building. Thus, the saving potential for new neighborhood developments is estimated to be relatively small. As shown in P II, the outdoor air temperature has the largest influence on a building's energy demand.

The results from P V show the impact of the urban surface on urban microclimatic conditions and consequently on building energy demands. This effect, however, is inherently linked to the seasonal cycle of macroclimatic conditions that are mainly caused by the globally uneven receipt of solar radiation. In Trondheim, it was shown that during a heat wave in summer, cooling energy demands or the number of hours in which the operative temperature indoors exceeds 26 °C can be reduced effectively with vast urban greening compared to a concrete-sealed urban surface. On the other hand, due to the significantly lower solar heat flux to the urban surface during autumn and winter, different material compositions of the urban surface

had considerably less influence on microclimatic conditions and building energy demands. Resulting from the proximity to the urban surface, the effect was observed to be largest in the lower floors of the investigated office building. During the heat wave scenario in summer, the use of concrete instead of green spaces led to a doubling of cooling energy demands and a 147 % increase of hours in which the operative temperature indoors exceeds 26 °C in the building's lowest floor. In autumn and winter, on the other hand, respectively 3.5 % and 0.9 % reductions in heating demand were achieved by an entirely concrete-sealed urban surface compared to vast urban greening.

Although the cool and cold seasons will dominate Norway's climate in the future as well, the Norwegian Center for Climate Services projects a significant rise in air temperature. Depending on the emission scenario, the median increment of the annual mean temperature is expected to be between 1.5 °C and 4.5 °C until the end of the century [111]. Additionally, summerly heat waves have been occurring more often during the last decades (see Figure 34) and are expected to become more common and more pronounced in the future. It is important to counteract these developments in order to protect vulnerable population groups and minimize the need for active cooling in buildings. Unlike in countries with warmer climates, neither the people nor buildings in Norway are adequately prepared for such a development. It is long-known that well-insulated office buildings tend to experience increased cooling demands as the dissipation of heat from internal sources is hindered [84,185]. Furthermore, due to noise pollution from traffic or other sources, opening the windows for natural ventilation is often not possible. The generally well-insulated building stock in Norway is therefore particularly prone to overheating. Additionally, it needs to be kept in mind that the simulations in P V were carried out for a rather poorly insulated building. For better-insulated buildings, even higher cooling energy demands and a more distinct increase of $N_{T_{op}>26\,°C}$ can be expected [186]. At the same time, well-insulated buildings will generally have less benefit from slightly warmer temperatures during the heating season [187].

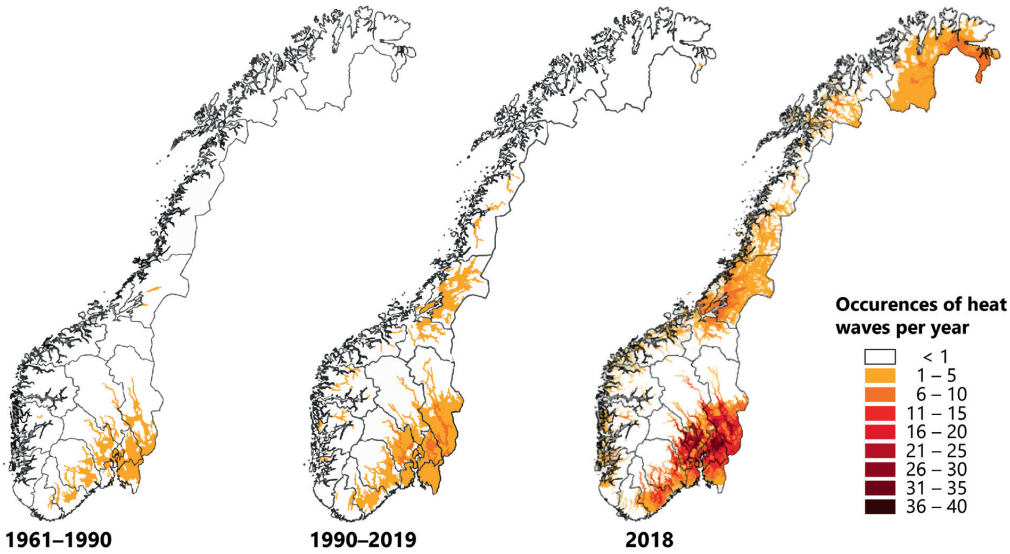

Figure 34: Heat wave occurrences per year in Norway for the previous norm period of 1961–1990, the years 1990–2019, and 2018 (modified from [188]).

Other positive aspects of urban greening that are often overlooked are its benefits on mental health and the reduction of stress which has been reported in many studies [189–192]. Even from within buildings, viewing natural features like green spaces, trees, birds, etc. briefly through the windows allow people opportunities for so-called *micro-restorative* experiences [193]. Furthermore, the steadily progressing sealing of the urban surface puts increasing pressure on the public sewage system as water runoff increases [194,195]. In Norway, not only temperatures are expected to rise due to climate change, but also precipitation levels by about 18 % [111]. Several studies underlined the efficacy of urban green to reduce peak runoff levels in urban environments [196,197]. Even the trees themselves contribute to stormwater retention by temporarily withholding a portion of the rainfall in the crowns and directing it down the trunk into the soil and their root network [198,199].

Even though not specifically investigated, the results from P V are also relevant for OTC, particularly during a heat wave scenario. As the concrete-sealed urban surface evoked on average 2.0 °C higher air temperatures at the ground level compared to the scenario with vast urban greening, with maximum differences up to 6.3 °C, especially pedestrians would benefit greatly from more urban green spaces.

7.3 RQ 3: Features and benefits of numerical tools to analyze the microclimate

Research question 3

To what extent can numerical tools help analyze the urban microclimate in Norwegian climate conditions?

What are feasible levels of detail regarding the geometrical input and physical models? What are the main limitations of these tools, and which developments are to expect in the future?

In general, numerical modeling can significantly contribute to our understanding of the urban (micro)climate and the possibilities for application are diverse [200–202]. Compared to field or wind tunnel measurements, there are several benefits when using numerical models, such as [203]:

- Almost no constraints regarding the geometry as opposed to a wind tunnel
- High spatial resolution of the flow field that allows for non-invasive extraction of results
- No scaling problems
- Surface- or volume-averaged flow variables and scalar quantities are easily obtained

In many cases, numerical modeling represents the only effective way to investigate different design scenarios or different design options, e.g., of building projects in the planning phase. However, despite the increasing computational power, the complexity of urban areas and relevant physical processes often require the implementation of parameterizations or physical models, such as turbulence models, evaporation models, etc, as well as spatial and temporal discretization. Therefore, it is essential to validate numerical models ahead of their application (see Chapter 4.2).

For the work in this thesis, two different numerical tools were used that allow for analyzing the urban microclimate: (1) *ENVI-met* and (2) *ANSYS Fluent*. Besides studying the urban microclimate, both tools can also be used to evaluate OTC, as shown in P III and P IV. At the same time, there are significant differences between these tools, which will be outlined in brief and their applicability for investigating the urban microclimate in Norway will be discussed.

ENVI-met was developed specifically for the purpose of microclimatic investigations of the urban environment and already contains many relevant modules and functions, such as the most common OTC indices, vegetation, and soil models, and large databases of different materials of the urban surface, tree, and plant species, etc. The geometry of the study area (and if applicable, the terrain) is created directly inside *ENVI-met* for which the domain is discretized into a regular grid with a user-selected cell size of usually around 2–6 m, depending on the study area's spatial extent. Deviating from this regular, orthogonal grid is not possible. The

shapes of objects smaller or close to the grid cell size, as well as skewed, sloped, or curved geometries need to be approximated by the grid points. In the case of NTNU's *Gløshaugen* campus, difficulties emerged in this context, as the building sizes vary in the range of a small one-story timber cottage to large, 13-story office towers (see P III and SP I). Regarding the output, the typical time interval is one hour but can be reduced down to 10 minutes.

Significantly more flexibility is granted in the CFD tool *ANSYS Fluent* where the computational grid can be refined, coarsened, and modified almost arbitrarily. Even moving grids are possible. Usually, 3D geometries from external software, such as *Rhinoceros*, etc. are imported and successively cleaned up and meshed. Commonly, for studies like the ones presented in this thesis, a finer grid resolution ($\sim 10^{-1}$ m) is chosen in the center of the computational domain and close to the buildings or ground surfaces than in the outskirts (up to $\sim 10^{2}$ m), close to the domain boundaries[10]. The user can also set the output time intervals freely. While *ANSYS Fluent*, in contrast to *ENVI-met*, also offers great flexibility regarding the selection and fine-tuning of for instance turbulence models or discretization schemes, it requires much more hands-on work in order to implement physical models for the effects of vegetation on the urban microclimate or the evaluation of OTC (as outlined in P IV). These models need to be programmed manually. Although this process is extremely time-consuming, it also offers great flexibility and above all full control over all included parameters and computations. In theory, *ANSYS Fluent* can be almost freely customized and extended with self-programmed modules. This is especially advantageous, as *ENVI-met* is a dry model that cannot deal with precipitation or the freezing and thawing of water. Due to time constraints not directly applied in this thesis, *ANSYS Fluent* already provides built-in models, e.g., for multiphase flows, and can be expanded arbitrarily with additional, self-programmed models to be able to include these effects. However, not including the effect of humidity in studies of OTC is expected to introduce only a minor error to the calculations, as humans usually feel comfortable in a broad humidity range. At this point, it needs to be added that every additional physical model increases the simulation time of computationally already very heavy numerical models.

Ultimately, a compromise between computational expense, the number and complexity of included models, and degree of detail regarding temporal and spatial discretization needs to be made, in order to keep simulation times within a reasonable timeframe. As a benchmark, the simulation time for the model presented in P III *(ENVI-Met)* was about 5.7 hours in real-time per simulated hour on an Intel® Core™ i7-8650U @ 1.90GHz for the central processing unit using one core, as the purchased license did not allow for parallel computing. On the other hand, the computations from P IV and PV took about 1.5 hours in real-time per simulated hour, however on a high-performance computer using five nodes of 30 Intel® Xeon® E5-2683 v4 central processing units @ 2.10GHz each. Considering, that the reported simulation time in

[10] Rough indication of scales for studies of a neighborhood or urban district as presented in this thesis.

ENVI-Met only used one core while the *ANSYS Fluent* simulation used 150, significantly faster simulation times are expected if *ENVI-Met* is run on multiple cores in parallel.

Table 7: Comparison of the two numerical tools for the investigation of the urban microclimate used in this thesis: ENVI-met and ANSYS Fluent. The statements in this table represent the author's personal opinion and assessment.

	ENVI-met	ANSYS Fluent
Required pre-knowledge (for microclimate simulations like in this thesis)	Medium knowledge of urban physics sufficient	Expert knowledge in urban physics and additional qualifications in fluid dynamics (or similar) and programming needed
Applicability for urban microclimate simulations	Built-in modules and data for: - Effect of vegetation on microclimate - OTC indices - Pollutant dispersion - Databases for different materials of the urban surface, soil types, trees, and plants, etc.	Applicable only with additional efforts. Modules for the effect of vegetation on the urban microclimate or OTC indices etc. need to be programmed and included manually
Flexibility	Limited flexibility, especially regarding the geometry, computational grid, and numerical schemes	High flexibility and full control of all flow-specific variables and settings, the geometry and computational grid, numerical schemes, and physical models
Expandability	Rather limited	Enables customization, extension and enhancement of the standard features
Complexity of microclimate simulations (like in this thesis)	Low to medium complex	Highly complex
Computational cost of microclimate simulations (like in this thesis)	Medium for typical studies (runs on standard computers) up to very high for large study areas and fine grid resolution	Generally very high (use of high-performance computing recommended)
Recommended target groups	Architecture and building engineering students; planning offices and planning departments of authorities; researchers	Mainly researchers and large building projects

When it comes to the influence of microclimatic conditions on the building energy demand, *ENVI-met* is able to run a building energy simulation for the individual buildings in parallel to the simulation of microclimatic conditions. The developer, however, writes on its website that it is not recommended to be used as a BPS tool as only some building-related variables are calculated, but it can be used to support BPS [204]. For a detailed analysis of advanced control

strategies, detailed geometries, user schedules, etc., it is necessary to couple both *ENVI-met* and *ANSYS Fluent* with a BPS [205] tool such as *IDA ICE* (see P V). Table 7 summarizes and compares the capabilities of *ENVI-met* and *ANSYS Fluent* point by point. Independently, similar observations about the two software tools have been made by Stavrakakis et al. [206] who collected and assessed the most common computational tools, their capabilities, strengths, weaknesses, etc. in the context of urban microclimate and building energy simulations in an extensive review.

All things considered, *ENVI-met* is a powerful tool for practitioners in urban planning and architecture, students, and non-experts to compare different design strategies in the early stages of a project. Using this tool is comparatively easy and does not require extensive previous knowledge. Moreover, the first results can be obtained relatively fast. However, depending on the level of detail of the input, the selected accuracy, and time resolution, advanced simulations can be carried out. On the other hand, the tool has clear limitations when it comes to certain physical processes (like freezing and thawing), geometry (no deviation from a pre-defined, regular grid), or the possibility of extending it with user-defined models. In theory, none of these limitations apply to *ANSYS Fluent*, and merely available computational resources, time, and the user's expertise restrict its utilization. The tool requires expert knowledge in CFD, urban physics, and programming, in order to be able to make use of all of the program's functions. In terms of microclimate simulations, it is assumed that only a few companies and projects manage to take on such large expenditures of time and labor. Therefore, CFD tools like *ANSYS Fluent* are more likely to be applied in research when used in the context of the urban microclimate. There, access to the necessary computational resources is easier, and time, as well as financial restrictions for carrying out such studies, are less crucial.

As written in Chapter 2.3, the progress in developing tools for advanced physical modeling has been immense, especially during the last two decades [24,58,206]. The steadily increasing computational power and cloud computing services make it possible to run more and more complex models even on standard laptops, providing access to an ever-growing audience. Following this trend, the new releases of simulation tools usually tend to cover more physics and apply more holistic approaches. Therefore, the development of suitable physical models for complex processes such as water vapor transfer processes for implementation into CFD microclimate models or built-in two-way coupling mechanisms between CFD and BPS in standard software packages is only a question of time. A good example of more holistic approaches is the *Ladybug Tools* suite [207,208] which is a collection of open-source plugins for *Grasshopper* and *Rhinoceros* that support the design and simulation of the environmental performance of buildings. It connects computer-aided design tools to open-source simulation engines like the BPS tool *EnergyPlus*, the CFD tool *OpenFOAM*, the lighting simulation engine *Radiance*, and the heat transfer modeling tool *Therm*. The tool suite allows the user to analyze and visualize climate data, run daylight simulations, simplified indoor and outdoor CFD and

urban climate simulations like for instance of the UHI. However, especially the functionality of the CFD and urban climate modules *Butterfly* and *Dragonfly* of the *Ladybug Tools* is still quite limited (e.g. no transient simulations possible) compared to the tools used in this PhD thesis. The developer's community, on the other hand, is very active, and significant improvements can be expected in the next few years.

While numerical tools steadily get more powerful and offer a growing range of possibilities for their application, they are often considered to be *"[…] strange, uncomfortable, and challenging to learn"*, as found in a study on BPS tools by Fernandez-Antolin et al. [209]. In another study, the authors report a worrying lack of knowledge of BPS tools among recent graduate architects in Spain that often have never heard of BPS tools before [210]. In both studies, the authors call for bringing such simulation tools to the attention of architecture students early on in the university syllabus to justify design decisions already in the conceptual stage of the design process. These findings can be transferred without further ado from the BPS to the CFD and urban microclimate modeling dimension. Only by spreading knowledge among the future architects, designers, and city planners, and allowing them to gain experience with these methods, a fast and sustainable transition to a built environment with minimal ecological impact is possible.

7.4 RQ 4: Benefits of microclimate-based design

Research question 4

What are the benefits of a microclimate-based approach in neighborhood planning and building design?

What are the most important microclimatic aspects to be considered by planning professionals and municipalities in Norway? How to better take the urban (micro)climate into account in the planning and design process?

This section outlines the implications and most of all the benefits of following a more microclimate-based design approach at the neighborhood and the building level (see Figure 35).

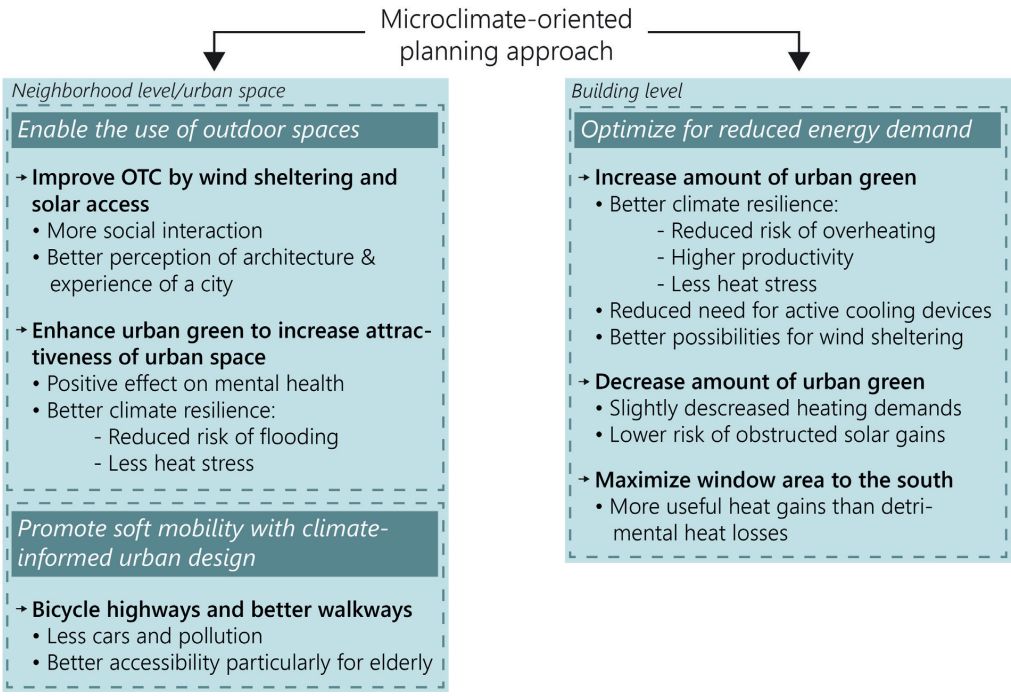

Figure 35: The microclimate-oriented planning approach at the neighborhood level and urban space, as well as the building level with aims in italics, possible strategies in bold, and achievable benefits as bullet points.

Improving OTC in general means increasing the attractiveness of public urban spaces, and most importantly, promoting people to spend more time outdoors. A major benefit of that is related to the inherently social aspect of public urban space [211]. Urban areas and neighborhoods are complex environments and are central to many aspects of people's day-to-day lives. Hallman [212] particularly highlights the social component in his definition of a neighborhood, describing it as *"[…] a limited territory within a larger urban context, where people inhabit dwellings and interact socially"*. It is an area where the majority of people have their homes, where they go to school or work, go shopping, relax in the park, or pursue other free-time activities. If designed appropriately, urban spaces can play an important role in hosting social activities [213].

As the results from P II and P III showed, solar access needs to be given top priority in order to improve OTC. In many cases, solar access and urban green conflict as particularly trees cast long shadows during the winter half-year when the solar elevation angles are low. Therefore, public sitting areas, playgrounds, etc., should be located at an adequate distance to possible sun-obstructing structures to the south. In that way, maximized solar irradiance will not only actively contribute to increased OTC but also accelerate the melting of snow and ice in spring, facilitating the access and use of such areas. Because playgrounds in urban residential areas are often embedded between tall multi-family apartment blocks (e.g.,Figure 36), the use of this important hub for social interaction among children as well as their parents [214] might be restricted in many cases.

Figure 36: Playground embedded between tall residential apartment blocks in Norway (Photo: Morten Antonsen, from [214]).

Another effective strategy to increase OTC during the cool and cold seasons of the year is wind sheltering. Even though from the findings in P III, it turned out to be less effective than providing solar access on sunny days, it is the only effective way to improve OTC in windy and cloudy conditions. The main considerations when planning for high OTC in cold conditions should, therefore, include wind sheltering while at the same time enabling maximum solar access. Trees can partly take over this function. Evergreen trees with canopies reaching almost all the way down to the ground are well suited for protecting from winds but block solar radiation year-round. Deciduous trees with higher crowns may be also used in the south of outdoor areas in certain situations. They can give access to the lower winter sun while providing shade during the summer.

The second benefit of increased microclimatic quality, OTC, and people enjoying being outdoors is related to the perception of architecture and urban planning. In his book about the *Life Between Buildings* [213], Jan Gehl emphasizes that it is a dimension of architecture that should be given more attention. Not only is it the place where much of a city dweller's social interaction takes place, but also where the sensory experience of a city happens, from where architecture is perceived, and where architectural context is created. Consequently, urban planning and design should promote people staying outdoors also from an architectural point of view. Also in research, urban spaces and their important function as platforms for social interaction and supporting sustainable behavior are not sufficiently addressed, although social aspects represent one of the three pillars of sustainability [215]. As found in SP II, most definitions among the increasing variety of CFN concepts fail to address the space between buildings adequately. Only the definition by FME ZEN [124] includes spatial qualities as a category for its assessment criteria and key performance indicators. Thus, it is vital that more

research projects exploring the urban districts and neighborhoods of tomorrow recognize the importance of attractive urban spaces for architecture and city residents.

As a way to increase the attractiveness of the urban environment, green spaces have often been reported to be positive assets, resulting for instance in the more frequent use of outdoor spaces [216] and improved mental health of citizens nearby [189–192]. Other benefits are e.g., their stormwater retention potential [196,197] and a mitigating effect on summerly overheating during heat waves as reported in P V (see Chapter 6.5 and 7.2). The growing need to counteract summerly heat waves in the future to protect vulnerable population groups in Scandinavia was highlighted in several studies [47–49].

Another aim of climate-oriented urban design, which in a wider sense is also linked to people spending more time outdoors, is to facilitate soft mobility. As the results from the meta-analysis in P I have shown (see Chapter 7.1), warming city environments in the cold climate region leads to more and more precipitation in the form of rain than snow in winter. According to a study by Chapman et al. in Sweden [12], icy surfaces and rain are the main barriers to soft mobility like walking and cycling during winter. Especially for the elderly population, accessibility to their neighborhood must be facilitated to enable them to go for walks in order to support their health [217] and maintain their social contacts. Municipalities need to be prepared to diligently clear pedestrian and bicycle paths from ice during winter and provide enough sheltered parking facilities for bikes. This is particularly important, as Norway's larger municipalities increasingly aim to reduce the number of private cars in the city centers and promote soft mobility instead. New city districts or redevelopment projects should additionally consider so-called *bicycle highways* that do not feature traffic lights, steep climbs, or interaction with any motorized or pedestrian traffic, and thus reduce commuting time [218]. Measures to decrease the exposure to wind and regular winter service, as well as lighting are important in the long, dark, snowy, and especially icy winters in Norway. Consequently, adverse weather might not be regarded as much of a barrier after all if less time is spent in such conditions. The same concept applies to pedestrian paths.

At the building level, considering the urban microclimate in the neighborhood and building design has the potential to positively affect the building energy demand and indoor environmental conditions. With the expected worldwide rise in building cooling energy demands as a result of climate change, the strongest percentage increase is estimated to occur in cold-climate regions [219]. A benefit of lower cooling energy demands as a result of proactive microclimatic design solutions (see Chapters 6.5 and 7.2) is for instance to limit the need for active cooling systems. However, large-scale changes of the urban environment such as those described and analyzed in P V to yield the desired and necessary improvements are often not possible. As heat waves are usually quite short for most parts of Norway, architects and building engineers should implement appropriate passive strategies such as improving night-time cooling, reducing solar heat gains during the long summer days, or increasing the

thermal mass of a building to buffer the hottest hours of the day. An increasingly popular strategy is for instance to use phase change materials[11], i.e., either in building construction components [220–222] or as heat storage in the HVAC system [223]. Moreover, heat pumps that can be used for both heating and cooling purposes are a meaningful alternative where passive measures do not suffice. In buildings that do not have active cooling systems, passive measures and especially increased urban green infrastructure can result in significantly improved indoor environmental quality during summer. As shown in P V, the number of hours in which the indoor temperature exceeds 26 °C was significantly reduced by vast urban greening. This leads to less heat stress and thus increased productivity at the workplace [224,225]. On the other hand, extensive urban greening leads to slightly higher heating demands during winter due to a small decrease in air temperature. For well-insulated buildings, however, the benefits from slightly higher outdoor air temperatures are estimated to be rather small [187] while the risk of overheating in summer increases [84,185,186] (see also Chapters 6.5 and 7.2).

In the cold season, similar to the strategy to increase OTC, buildings should make use of solar gains by increasing the window areas to the south. If unshaded, more useful energy gains than losses can be generated in Scandinavian locations as shown in P II (see Chapters 6.2 and 7.2). At the same time, provisions must be made to limit excessive solar heat gains during summer, for instance through external shading devices. Therefore, urban green must be placed strategically, as close as possible to residents and city dwellers, but at the same time minimizing its shading effect during the cold season in public spaces and on buildings. Furthermore, wind sheltering can reduce the energy demand in buildings, e.g., by strategically placed vegetation or a proficient layout of buildings in a neighborhood (see Chapters 6.2 and 7.2).

As Erell et al. [13] accurately write in their book on the urban microclimate and designing the spaces between buildings, *"[r]ecommendations must be based on analysis of all factors influencing the urban microclimate. Conclusions based upon the study of one or even several factors in conjunction may be misleading if they fail to take into account the effect of other, significant processes."* Giving general advice is difficult and, in many cases, might not consider location-specific characteristics that demand conflicting actions, e.g. when the prevailing wind direction in winter is from the south at a certain location in Norway. Providing shelter from the wind with trees would significantly limit solar access and, thus, might not lead to the desired improvement of microclimatic conditions. Therefore, it is important to highlight that every situation requires an individual solution that involves a multitude of interacting aspects to be considered.

It is stressed to raise awareness in relevant fields such as urban planning, architecture, and building engineering to adopt a more microclimate-oriented approach in building projects. The

[11] Phase change materials can absorb and release heat by changing their physical state from solid to liquid and vice versa. This phase change absorbs or releases large amounts of thermal energy without changing the temperature of the material (latent heat).

first step towards this aim would be to provide better education around the theory of the urban (micro)climate and training in suitable numerical tools in building-related study syllabi. In this context, also the developers of relevant tools should improve the user-friendliness of their tools and facilitate their use by professionals outside of meteorology, climatology, urban physics, or fluid dynamics (see Chapter 7.3). Lastly, municipalities should implement regulations that require a stronger focus on microclimatic conditions.

7.5 Limitations

All the included articles in this thesis contain a section or paragraph that discusses the limitations of the respective study. Therefore, this section lists merely the main, overarching limitation of this thesis. For the study-specific limitations, the reader is kindly referred to the full-text versions of the articles in part B of this thesis.

Neither of the two numerical tools used to study the urban microclimate in this thesis considers all relevant physical processes for the Norwegian climate conditions. In the case of *ENVI-met*, the current version does not support the freezing and thawing of water. In *ANSYS Fluent* on the other hand, including the phase behavior of water is generally possible, but due to lack of time could not be realized within this thesis. As Norway's cold season is quite pronounced and characterized by a significant amount of snow and ice, the inclusion of these processes is important for a holistic representation and study of the urban microclimate in Norway. During the investigated conditions in this thesis, however, good agreement between simulation results and measurements was found. Furthermore, anthropogenic heat sources apart from heat transmission losses through the building envelope, such as motorized vehicles or exhaust vents of ventilation systems were not modeled.

A major part of the presented investigations was carried out having as a study area the NTNU *Gløshaugen* campus in Trondheim. Therefore, the presented results cannot be regarded as universally valid in Norway, as there are major differences in local climates, topography, and city characteristics. However, the methodological approach and the results are well transferable to other urban areas in Norway or the cold climate region in general that experience climatic conditions similar to Trondheim, if relevant differences between the respective urban spaces are considered appropriately.

Moreover, there are most commonly several other limiting factors that prohibit a pure OTC or building energy demand-oriented design of an urban district or neighborhood. These might be local zoning maps, urban development plans, building regulations, specific requirements regarding the usage of a building or urban area, to name a few. Like with all complex decision-making processes that involve numerous different stakeholders and interests, a case-by-case evaluation needs to be carried out to obtain the best compromise.

8 Conclusions and further work

8.1 Summary of work

The research in this thesis discusses the urban microclimate from multiple perspectives and by applying different methodologies and tools. Moreover, its importance for the transition to a resilient, sustainable, and liveable urban environment in the Norwegian context is illustrated.

First, a systematic review and meta-analysis of existing literature on the urban climate in cold and polar climate regions revealed important focus areas, research gaps, and most of all, characteristics of the urban climate in these regions. In total, 101 papers were included in the review. They were categorized and analyzed according to their publication year, country, climate, topic, method, keywords, citations, and publication channels. The results showed a strong dominance of urban heat island (UHI) related research topics in urban climate research (57 %) and that the UHI effect is a common phenomenon. Moreover, of particular importance in the Norwegian context, coastal cities experience a distinct cooling (warming) effect of large water bodies in spring and summer (autumn and winter), and especially inner-city air temperatures in winter continue to rise in the long term.

Considering the distribution of the global population in cold and polar climate areas, specific climate types according to Köppen-Geiger classification have been the subject of research more often than others. Most articles covered locations in Dfb-climate (50 %), mainly from studies in North America and Europe, followed by Dwa (20 %), predominantly from studies in China and South Korea. Dfc (15 %) was the third most often used climate type, mainly from studies in Russia. Several climate types were not represented by any study included in the review and

should be subject to future research. The outweighing part of studies used on-site measurements as a method for obtaining data (80 %), while 20 % used remote sensing data. In 22 of 101 studies, numerical models have been validated with measurements and used to predict the outcomes of urban redevelopments.

Then, different numerical models, using building performance simulation (BPS) and computational fluid dynamics (CFD) tools were created to study the urban microclimate with regard to different materials of the urban surface, the energy demand in buildings, and outdoor thermal comfort (OTC). It was shown which climate variables affect the heating energy demand in high-performance buildings the most, and which parts of a building and its technical systems to focus on in order to reduce the heating energy demand. The air temperature was found to be the most important variable in BPS. Furthermore, south-oriented, unshaded windows can generate more useful energy gains than detrimental energy losses over the year in Scandinavia. Therefore, solar access plays an important role in reducing building heating energy demands. Additionally, if neighborhoods are designed appropriately, wind sheltering can lead to considerable reductions in building heating energy demands (5.3 % on average in the investigated locations).

ENVI-Met and *ANSYS Fluent* were used to create numerical models in order to investigate the urban microclimate at NTNU's *Gløshaugen* campus. Both models were designed according to existing guidelines and validated using a network of on-site weather stations. A detailed comparison and evaluation of measured and simulated data ensured their applicability. The CFD model created in *ANSYS Fluent* applied the 3D URANS approach with the realizable k-ε turbulence model. It featured a polyhedral grid of a highly complex urban environment, including explicitly modeled buildings of a whole city district, trees, short- and longwave radiation exchange, anthropogenic heat from the buildings, and heat storage in the urban surface. Furthermore, it was extended with self-programmed functions to account for the thermal effects from evapotranspiration at grass surfaces with the Penman-Monteith equation (PME) and the Physiological Equivalent Temperature (PET) OTC index. To the best of the author's knowledge, no previous scientific publication featured an *ANSYS Fluent* CFD model using the PME or PET. The detailed validation process presented in this thesis showed good agreement between simulated and measured microclimatic conditions.

The results from the microclimate model created in the software environment *ENVI-Met* showed that during cool weather conditions, providing better solar access is the most effective measure to improve OTC. Wind sheltering was found to be less effective but often represents the only available passive strategy to improve OTC during the typically windy and cloudy Scandinavian autumns. In outdoor sitting areas, pedestrian zones, playgrounds, and other areas of outdoor stay, both strategies should be applied. Buildings, vegetation, and urban furniture at the site should be designed taking low solar elevation angles and the prevailing wind field into account.

This thesis also presented a one-way coupling methodology between CFD (*ANSYS Fluent*) and BPS software (*IDA ICE*) to account for the vertical temperature gradient around a 13-floor office building from the 1960s. Different material compositions of the urban surface and their impact on the urban microclimate at the NTNU *Gløshaugen* campus were simulated using CFD. From three simulation periods of each 7 days in summer, autumn, and winter, weather files for BPS were generated. With these weather files, the impact of the microclimate at the campus on building energy demand and indoor thermal conditions of the office high-rise was investigated. The results showed that the effect of different materials at the urban surface on the microclimatic conditions is strongest during a heat wave scenario. During autumn and winter, on the other hand, little solar irradiation on the urban surface due to low solar elevation angles led to significantly lower influence on the microclimatic conditions. Resulting from the proximity to the urban surface, the lower floors of a building were affected the most by different surface materials. During the heat wave scenario in summer, the use of concrete instead of green spaces led to a doubling of cooling energy demands and a 147 % increase of hours in which the operative temperature indoors exceeds 26 °C in the building's lowest floor. During autumn and winter, on the other hand, a concrete-sealed urban surface reduced the building's heating energy demands by 2.5 % and 0.5 %, respectively. While the cool and cold seasons will continue to dominate the climate in Norway, climate change demands increasing attention to heat waves and overheating in cities in the future, especially as well-insulated buildings are more prone to overheating.

It was pointed out in this thesis, how numerical modeling can contribute to the understanding of the urban (micro)climate, and extensive descriptions of possibilities for application were shown. While such numerical tools get steadily more holistic, cover more physics, and computational power continues to increase, specific attention must be given to the new generations of architects, building engineers, city planners, etc., to keep pace with these developments. Generally, the current rather subordinate role of microclimate issues in study syllabi does not meet the importance it has for city dwellers and the built environment.

Finally, the benefits of following a more microclimate-oriented approach in the planning process of urban neighborhoods were presented. Facilitating the use of outdoor spaces by improving OTC and a more climate-informed design and planning approach in urban areas is associated with several benefits. These are, for instance, increased social interaction, better perception of architectural design, and more soft mobility. At the same time, microclimatic considerations can contribute to reducing the energy demand in buildings. The most important design strategies in the context of the urban (micro)climate in Norwegian climate conditions can be summarized in short as:

- Maximize solar access in areas of outdoor stay by carefully designing buildings, vegetation, and urban furniture according to the low solar elevation angles and the prevailing wind field especially during the cool and cold seasons.

- Facilitate commuting using soft transport. Adverse weather might not be regarded as much of a barrier after all if less time is spent in such conditions.
- Urban greening is an effective way to lower the risk of overheating in cities. Additionally, it contributes to water retention during heavy rain events and has a positive psychological effect on humans.
- Counteract the need for active cooling systems in buildings by planning for passive measures such as more urban greening, night-time cooling, external shading devices, or increasing the thermal mass of a building to buffer the hottest hours of the day.
- The window area of buildings should be mainly towards the south, as from an energy balance point of view, they can outperform opaque wall elements.
- In wind-exposed buildings, energy losses due to infiltration can be reduced by providing shelter from wind, for instance by vegetation and appropriate neighborhood design. This should be done in a way that does not compromise solar access.
- Every situation requires an individual solution that usually involves a variety of interacting aspects to be considered. The final design must be based on all relevant factors that influence the microclimate.

8.2 Further work

The work and findings presented in this thesis contribute to the advancement of our understanding of the urban (micro)climate in cold climate locations such as in Norway. However, it can only be regarded as the first step of many. Like in this thesis, future work should focus on multimethod research, involving e.g., measurements and numerical studies of the urban climate. Measurements and observations of this extremely complex system are particularly important to obtain better input data for the numerical models and can cover for instance location-specific inlet profiles for air temperature, wind speed, and the turbulence variables, the spatial distribution of anthropogenic heat sources, or the implementation of a denser network of fixed weather stations for long-term recordings and their analysis. Additionally, further studies should explore the impact of microclimate on a larger variety of building types regarding size, usage, energy performance, and main construction material.

Since it allows more flexibility and accuracy than *ENVI-met*, especially the presented *ANSYS Fluent* CFD model can be improved and extended with additional physical models or model parametrizations. These should include a more precise representation of a plant's metabolic processes instead of the PME, the consideration of soil moisture, the phase behavior of water, and additional sources of anthropogenic heat. Additionally, a sensitivity analysis should be carried out to find an optimal balance between accuracy and computational cost. This analysis should address the flow-related methods such as the chosen turbulence model, and the URANS approach in general. Furthermore, the degree of detail regarding the geometrical input and discretization can be analyzed, such as the extent and detail of explicitly modeled roughness

elements, type of mesh elements, or necessity to include windows on building surfaces as reflecting elements for solar radiation.

Again, as opposed to *ENVI-met*, the flexibility and features in *ANSYS Fluent* can be used for many other purposes than the presented microclimate studies focusing on OTC and building energy demand. These can be used for instance to explore the natural ventilation potential in buildings by combining indoor and outdoor CFD, urban wind energy potential, wind-driven rain and snow accumulation, or more in general, the investigation of airflow and its statistics in, above, and around urban areas. Especially with the ongoing pandemic in mind, studying the aeration and pollutant dispersion in urban areas and buildings with a coupled indoor-outdoor CFD approach can contribute to a healthier city population.

Given these points, the work presented in this thesis opens up a great range of research possibilities particularly for the case of Trondheim and the NTNU *Gløshaugen* campus. Considering that the design phase of redeveloping and densifying the campus is still in progress, continuing the work from this thesis has the potential to contribute substantially to a better outcome of this major project. This PhD thesis underlines the importance of a multi-perspective and interdisciplinary approach in city planning which is necessary to meet the complex requirements that city dwellers inherently pose to an urban environment.

Finally, from a personal point of view, the most important outcome of this thesis is that I was able to acquire important knowledge and experience throughout my time as a PhD candidate. I am determined to use these skills to contribute to better cities, a more sustainable society, and to counteract climate change as much as I can.

Bibliography

[1] World Economic Forum. The Global Risks Report 2019: 14th Edition. 14th ed. Geneva: World Economic Forum; 2019.

[2] World Health Organization. Ten threats to global health in 2019. [Accessed April 28, 2020]; Available from: https://www.who.int/news-room/feature-stories/ten-threats-to-global-health-in-2019.

[3] Schmidt A, Ivanova A, Schäfer MS. Media attention for climate change around the world: A comparative analysis of newspaper coverage in 27 countries. Glob Environ Chang 2013;23(5):1233–48. https://doi.org/10.1016/j.gloenvcha.2013.07.020.

[4] UN Environment, International Energy Agency. Towards a zero-emission, efficient, and resilient buildings and construction sector: Global Status Report 2017; 2017.

[5] Yudelson J. The green building revolution. Washington: Island Press; 2008.

[6] Edenhofer O (ed.). Climate Change 2014: Contribution of Working Group III to the Fifth Assessment Report of the Intergovernmental Panel on Climate Change: Mitigation of climate change. New York: Cambridge Univ. Pr; 2014.

[7] Geiger R. Das Klima der bodennahen Luftschicht; 1927.

[8] Kratzer A. Das Stadtklima. Braunschweig: Vieweg; 1937.

[9] Balchin W, Pye N. A micro-climatological investigation of Bath and the surrounding district. Q J Roy Meteorol Soc 1947;73(317-318):297–323.

[10] Merriam-Webster.com Dictionary. Resilience. [Accessed December 17, 2021]; Available from: https://www.merriam-webster.com/dictionary/resilience.

[11] Oke TR, Mills G, Christen A, Voogt JA. Urban climates. Cambridge: Cambridge University Press; 2017.

[12] Chapman D, Nilsson K, Larsson A, Rizzo A. Climatic barriers to soft-mobility in winter: Luleå, Sweden as case study. Sustain Cities Soc 2017;35:574–80. https://doi.org/10.1016/j.scs.2017.09.003.

[13] Erell E, Pearlmutter D, Williamson T. Urban microclimate: Designing the spaces between buildings. London: Earthscan; 2011.

[14] United Nations, Department of Economic and Social Affairs, Population Division. World Urbanization Prospects: The 2018 Revision. Online Edition. New York, USA; 2018.

[15] Caves RW. Encyclopedia of the city. Abingdon, Oxon, OX, New York, NY: Routledge; 2005.

[16] Stewart ID, Oke TR. Local Climate Zones for Urban Temperature Studies. Bull Amer Meteor Soc 2012;93(12):1879–900. https://doi.org/10.1175/BAMS-D-11-00019.1.

[17] Wieringa J. Updating the Davenport roughness classification. J Wind Eng Ind Aerodyn 1992;41(1-3):357–68. https://doi.org/10.1016/0167-6105(92)90434-C.

[18] Eliasson I, Holmer B. Urban Heat Island Circulation in Göteborg, Sweden. Theor Appl Climatol 1990;42(3):187–96. https://doi.org/10.1007/BF00866874.

[19] Shreffler JH. Detection of centripetal heat-island circulations from tower data in St. Louis. Bound-Layer Meteorol. 1978;15(2):229–42.

[20] Wong KK, Dirks RA. Mesoscale Perturbations on Airflow in the Urban Mixing Layer. J Appl Meteorol 1978;17:677–88.

[21] Vukovich FM, King WJ, Dunn JW, Worth JJB. Observations and Simulations of the Diurnal Variation of the Urban Heat Island Circulation and Associated Variations of the Ozone Distribution: A Case Study. J Appl Meteorol 1979;18(7):836–54. https://doi.org/10.1175/1520-0450(1979)018<0836:OASOTD>2.0.CO;2.

[22] Hidalgo J, Masson V, Gimeno L. Scaling the Daytime Urban Heat Island and Urban-Breeze Circulation. J Appl Meteorol Climatol 2010;49(5):889–901. https://doi.org/10.1175/2009JAMC2195.1.

[23] Ryu Y-H, Baik J-J, Han J-Y. Daytime urban breeze circulation and its interaction with convective cells. Q J Roy Meteorol Soc 2013;139(671):401–13. https://doi.org/10.1002/qj.1973.

[24] Mills G. Urban climatology: History, status and prospects. Urban Clim 2014;10:479–89. https://doi.org/10.1016/j.uclim.2014.06.004.

[25] Howard L. The climate of London deduced from meteorological observations made in the metropolis and at various places around it. 2nd ed. London: Harvey and Darton; J. Rickerby; 1833.

[26] Webster N. A brief history of epidemic and pestilential diseases: With the principal phenomena of the physical world, which precede and accompany them, and observations deduced from the facts stated. In two volumes. By Noah Webster, author of Dissertations on the English language and several other works--member of the Connecticut Academy of Arts and Sciences--of the Society for the Promotion of Agriculture, Arts and Manufactures, in the state of New-York--of the American Academy of Arts and Sciences, and corresponding member of the Historical Society in Massachusetts. Vol. I[-II. Hartford: Printed by Hudson & Goodwin; 1799.

[27] United Nations, Department of Economic and Social Affairs, Population Division. World Population Prospects 2019: Volume I: Comprehensive Tables. New York, USA; 2019.

[28] Wu J. Urban ecology and sustainability: The state-of-the-science and future directions. Landsc Urban Plan 2014;125:209–21. https://doi.org/10.1016/j.landurbplan.2014.01.018.

[29] New urban agenda: H III: Habitat III: Quito 17-20 October 2016. Nairobi: United Nations; 2017.

[30] Akbari H. Shade trees reduce building energy use and CO2 emissions from power plants. Environ Pollut 2002;116:S119-S126. https://doi.org/10.1016/S0269-7491(01)00264-0.

[31] Bowler DE, Buyung-Ali L, Knight TM, Pullin AS. Urban greening to cool towns and cities: A systematic review of the empirical evidence. Landsc Urban Plan 2010;97(3):147–55. https://doi.org/10.1016/j.landurbplan.2010.05.006.

[32] Chang C-R, Li M-H. Effects of urban parks on the local urban thermal environment. Urban For Urban Green 2014;13(4):672–81. https://doi.org/10.1016/j.ufug.2014.08.001.

[33] Georgi NJ, Zafiriadis K. The impact of park trees on microclimate in urban areas. Urban Ecosyst 2006;9(3):195–209. https://doi.org/10.1007/s11252-006-8590-9.

[34] Hsieh C-M, Li J-J, Zhang L, Schwegler B. Effects of tree shading and transpiration on building cooling energy use. Energy Build 2018;159:382–97. https://doi.org/10.1016/j.enbuild.2017.10.045.

[35] Yan H, Wu F, Dong L. Influence of a large urban park on the local urban thermal environment. Sci Total Environ 2018;622-623:882–91. https://doi.org/10.1016/j.scitotenv.2017.11.327.

[36] McPherson EG, Simpson JR. Potential energy savings in buildings by an urban tree planting programme in California. Urban For Urban Green 2003;2(2):73–86. https://doi.org/10.1078/1618-8667-00025.

[37] Akbari H, Menon S, Rosenfeld A. Global cooling: increasing world-wide urban albedos to offset CO2. Clim Change 2009;94(3-4):275–86. https://doi.org/10.1007/s10584-008-9515-9.

[38] Akbari H, Pomerantz M, Taha H. Cool surfaces and shade trees to reduce energy use and improve air quality in urban areas. Sol Energy 2001;70(3):295–310. https://doi.org/10.1016/S0038-092X(00)00089-X.

[39] Doulos L, Santamouris M, Livada I. Passive cooling of outdoor urban spaces. The role of materials. Sol Energy 2004;77(2):231–49. https://doi.org/10.1016/j.solener.2004.04.005.

[40] Jin H, Shao T, Zhang R. Effect of water body forms on microclimate of residential district. Energy Proc 2017;134:256–65. https://doi.org/10.1016/j.egypro.2017.09.615.

[41] Mohajerani A, Bakaric J, Jeffrey-Bailey T. The urban heat island effect, its causes, and mitigation, with reference to the thermal properties of asphalt concrete. J Environ Manage 2017;197:522–38. https://doi.org/10.1016/j.jenvman.2017.03.095.

[42] Savio P, Rosenzweig C, Solecki WD, Slosberg RB. Mitigating New York City's Heat Island with Urban Forestry, Living Roofs, and Light Surfaces: New York City Regional Heat Island Initiative; 2006.

[43] Jacobson MZ, Hoeve JE ten. Effects of Urban Surfaces and White Roofs on Global and Regional Climate. J Clim 2012;25(3):1028–44. https://doi.org/10.1175/JCLI-D-11-00032.1.

[44] Wang Y, Akbari H. Analysis of urban heat island phenomenon and mitigation solutions evaluation for Montreal. Sustain Cities Soc 2016;26:438–46. https://doi.org/10.1016/j.scs.2016.04.015.

[45] Touchaei AG, Akbari H. Evaluation of the seasonal effect of increasing albedo on urban climate and energy consumption of buildings in Montreal. Urban Clim 2015;14:278–89. https://doi.org/10.1016/j.uclim.2015.09.007.

[46] Robine J-M, Cheung SLK, Le Roy S, van Oyen H, Griffiths C, Michel J-P et al. Death toll exceeded 70,000 in Europe during the summer of 2003. C R Biol 2008;331(2):171–8. https://doi.org/10.1016/j.crvi.2007.12.001.

[47] Oudin Åström D, Åström C, Forsberg B, Vicedo-Cabrera AM, Gasparrini A, Oudin A et al. Heat wave-related mortality in Sweden: A case-crossover study investigating effect modification by neighbourhood deprivation. Scand J Public Health 2020;48(4):428–35. https://doi.org/10.1177/1403494818801615.

[48] Venter ZS, Krog NH, Barton DN. Linking green infrastructure to urban heat and human health risk mitigation in Oslo, Norway. Sci Total Environ 2020;709:136193. https://doi.org/10.1016/j.scitotenv.2019.136193.

[49] Vicedo-Cabrera AM, Scovronick N, Sera F, Royé D, Schneider R, Tobias A et al. The burden of heat-related mortality attributable to recent human-induced climate change. Nat Clim Chang 2021;11(6):492–500. https://doi.org/10.1038/s41558-021-01058-x.

[50] D'Ippoliti D, Michelozzi P, Marino C, de'Donato F, Menne B, Katsouyanni K et al. The impact of heat waves on mortality in 9 European cities: results from the EuroHEAT project. Environ Health 2010;9:37. https://doi.org/10.1186/1476-069X-9-37.

[51] Nafstad P, Skrondal, Anders, Bjertness, Espen. Mortality and temperature in Oslo, Norway, 1990-1995. Eur J Epidemiol 2001;17(7):621–7.

[52] Lowe SA. An energy and mortality impact assessment of the urban heat island in the US. Environ Impact Assess Rev 2016;56:139–44. https://doi.org/10.1016/j.eiar.2015.10.004.

[53] Kolokotroni M, Giannitsaris I, Watkins R. The effect of the London urban heat island on building summer cooling demand and night ventilation strategies. Sol Energy 2006;80(4):383–92. https://doi.org/10.1016/j.solener.2005.03.010.

[54] Santamouris M, Cartalis C, Synnefa A, Kolokotsa D. On the impact of urban heat island and global warming on the power demand and electricity consumption of buildings—A review. Energy Build 2015;98:119–24. https://doi.org/10.1016/j.enbuild.2014.09.052.

[55] Santamouris M. On the energy impact of urban heat island and global warming on buildings. Energy Build 2014;82:100–13. https://doi.org/10.1016/j.enbuild.2014.07.022.

[56] Vardoulakis E, Karamanis D, Fotiadi A, Mihalakakou G. The urban heat island effect in a small Mediterranean city of high summer temperatures and cooling energy demands. Solar Energy 2013;94:128–44. https://doi.org/10.1016/j.solener.2013.04.016.

[57] Oke TR. The urban energy balance. Prog Phys Geogr 1988;12(4):471–508.

[58] Toparlar Y, Blocken B, Maiheu B, van Heijst G. A review on the CFD analysis of urban microclimate. Renew Sustain Energy Rev 2017;80:1613–40. https://doi.org/10.1016/j.rser.2017.05.248.

[59] Bowling SA, Benson CS. Study of the Subarctic Heat Island at Fairbanks, Alaska; 1978.

[60] Magee N, Wendler G, Curtis J. The Urban Heat Island Effect at Fairbanks, Alaska. Theor Appl Climatol 1999;64(1-2):39–47. https://doi.org/10.1007/s007040050109.

[61] Hinkel KM, Nelson FE, Klene AE, Bell JH. The urban heat island in winter at Barrow, Alaska. Int J Climatol 2003;23(15):1889–905. https://doi.org/10.1002/joc.971.

[62] Klene AE, Hinkel KM, Nelson FE. The Barrow Urban Heat Island Study: soil temperatures and active-layer thickness. Int Conf Permafrost Proc 2003:555–60.

[63] Miles V, Esau I. Seasonal and Spatial Characteristics of Urban Heat Islands (UHIs) in Northern West Siberian Cities. Remote Sens 2017;9(10):989. https://doi.org/10.3390/rs9100989.

[64] Konstantinov P, Varentsov M, Esau I. A high density urban temperature network deployed in several cities of Eurasian Arctic. Environ Res Lett 2018;13(7):75007. https://doi.org/10.1088/1748-9326/aacb84.

[65] Esau I, Miles V. Warmer Urban Climates For Development Of Green Spaces In Northern Siberian Cities. Geogr Environ Sustain 2016;9(4):48–62. https://doi.org/10.24057/2071-9388-2016-9-4-48-62.

[66] Esau I, Miles V, Varentsov M, Konstantinov P, Melnikov V. Spatial structure and temporal variability of a surface urban heat island in cold continental climate. Theor Appl Climatol 2019;31(12):1990. https://doi.org/10.1007/s00704-018-02754-z.

[67] Varentsov M, Konstantinov P, Baklanov A, Esau I, Miles V, Davy R. Anthropogenic and natural drivers of a strong winter urban heat island in a typical Arctic city. Atmos Chem Phys Discuss 2018:1–28. https://doi.org/10.5194/acp-2018-569.

[68] Konstantinov P, Grishchenko MY, Varentsov M. Mapping urban heat islands of arctic cities using combined data on field measurements and satellite images based on the example of the city of Apatity (Murmansk Oblast). Izv Atmos Ocean Phys 2015;51(9):992–8. https://doi.org/10.1134/S000143381509011X.

[69] Miles V, Esau I. Surface urban heat islands in 57 cities across different climates in northern Fennoscandia. Urban Clim 2020;31:100575. https://doi.org/10.1016/j.uclim.2019.100575.

[70] Orlanski I. A Rational Subdivision of Scales for Atmospheric Processes. Bull Amer Meteor Soc 1975;56(5):527–30.

[71] Blocken B. Computational Fluid Dynamics for urban physics: Importance, scales, possibilities, limitations and ten tips and tricks towards accurate and reliable simulations. Build Environ 2015;91:219–45. https://doi.org/10.1016/j.buildenv.2015.02.015.

[72] Hodur RM. The Naval Research Laboratory's Coupled Ocean/Atmosphere Mesoscale Prediction System (COAMPS). Mon Wea Rev 1997;125:1414–30.

[73] Grell G, Dudhia J, Stauffer D. A description of the fifth-generation Penn State/NCAR Mesoscale Model (MM5). UCAR/NCAR; 1994.

[74] Mochida A, Iizuka S, Tominaga Y, Lun IY-F. Up-scaling CWE models to include mesoscale meteorological influences. J Wind Eng Ind Aerodyn 2011;99(4):187–98. https://doi.org/10.1016/j.jweia.2011.01.012.

[75] Yamada T, Koike K. Downscaling mesoscale meteorological models for computational wind engineering applications. J Wind Eng Ind Aerodyn 2011;99(4):199–216. https://doi.org/10.1016/j.jweia.2011.01.024.

[76] European Commission. Indoor air pollution: new EU research reveals higher risks than previously thought. Brussels; 2003.

[77] Klepeis NE, Nelson WC, Ott WR, Robinson JP, Tsang AM, Switzer P et al. The National Human Activity Pattern Survey (NHAPS): a resource for assessing exposure to environmental pollutants. J Expo Anal Environ Epidemiol 2001;11:231–52.

[78] Fumo N. A review on the basics of building energy estimation. Renew Sustain Energy Rev 2014;31:53–60. https://doi.org/10.1016/j.rser.2013.11.040.

[79] Li X, Wen J. Review of building energy modeling for control and operation. Renew Sustain Energy Rev 2014;37:517–37. https://doi.org/10.1016/j.rser.2014.05.056.

[80] Zhao H, Magoulès F. A review on the prediction of building energy consumption. Renew Sustain Energy Rev 2012;16(6):3586–92. https://doi.org/10.1016/j.rser.2012.02.049.

[81] Harish V, Kumar A. A review on modeling and simulation of building energy systems. Renew Sustain Energy Rev 2016;56:1272–92. https://doi.org/10.1016/j.rser.2015.12.040.

[82] Zhang R, Mirzaei PA, Jones B. Development of a dynamic external CFD and BES coupling framework for application of urban neighbourhoods energy modelling. Build Environ 2018;146:37–49. https://doi.org/10.1016/j.buildenv.2018.09.006.

[83] Allegrini J, Carmeliet J. Simulations of local heat islands in Zürich with coupled CFD and building energy models. Urban Clim 2018;24:340–59. https://doi.org/10.1016/j.uclim.2017.02.003.

[84] Toparlar Y, Blocken B, Maiheu B, van Heijst G. Impact of urban microclimate on summertime building cooling demand: A parametric analysis for Antwerp, Belgium. Appl Energy 2018;228:852–72. https://doi.org/10.1016/j.apenergy.2018.06.110.

[85] Brozovsky J. Study of a Digital Twin for a Test Cell Laboratory: Set Up and Calibration of a Simulation Model of the Test Cell Laboratory in Trondheim, Norway, with Particular Regard to Air Flows through an Opened Window [Masterthesis]: Technical University Munich; 2018.

[86] Bruse M, Fleer H. Simulating surface–plant–air interactions inside urban environments with a three dimensional numerical model. Environ Model Softw 1998;13(3-4):373–84. https://doi.org/10.1016/S1364-8152(98)00042-5.

[87] Allegrini J, Dorer V, Carmeliet J. Influence of morphologies on the microclimate in urban neighbourhoods. J Wind Eng Ind Aerodyn 2015;144:108–17. https://doi.org/10.1016/j.jweia.2015.03.024.

[88] Wilcox DC. Turbulence modeling for CFD. 3rd ed. La Cañada, Calif.: DCW Industries; 2010.

[89] Sagaut P. Large Eddy Simulation for Incompressible Flows: An Introduction. Berlin, Heidelberg: Springer-Verlag Berlin Heidelberg; 2006.

[90] Sivle AD. hetebølge. [Accessed December 09, 2021]; Available from: https://snl.no/heteb%C3%B8lge.

[91] Rafferty JP. heat wave. Encyclopedia Britannica, 5 December 2018; Available from: https://www.britannica.com/science/heat-wave-meteorology. [Accessed December 10, 2021].

[92] Zikanov O. Essential computational fluid dynamics. Hoboken, NJ: John Wiley & Sons, Inc; 2019.

[93] Franke J, Hirsch C, Jensen AG, Krüs HW, Schatzmann M, Westbury PS et al. Recommendations on the Use of CFD in Wind Engineering. Proc. Int. Conf. Urban Wind Engineering and Building Aerodynamics. COST Action C14, Impact of Wind and Storm on City Life Built Environment, von Karman Institute, Sint-Genesius-Rode, Belgium May 5-7 2004.

[94] Roache PJ. Verification and validation in computational science and engineering. Albuquerque, NM: Hermosa; 1998.

[95] Oberkampf WL, Trucano TG. Verification and validation in computational fluid dynamics. Prog Aerosp Sci 2002;38:209–72.

[96] Schatzmann M, Leitl B. Issues with validation of urban flow and dispersion CFD models. J Wind Eng Ind Aerodyn 2011;99(4):169–86. https://doi.org/10.1016/j.jweia.2011.01.005.

[97] Abanto J, Pelletier D, Garon A, Trepanier J-Y, Reggio M. Verification of some Commercial CFD Codes on Atypical CFD Problems. In: 43rd AIAA Aerospace Sciences Meeting.

[98] Timchenko V, Reizes JA. Validation Problems in Computational Modelling of Natural Convection. In: Runchal A, editor. 50 Years of CFD in Engineering Sciences: A Commemorative Volume in Memory of D. Brian Spalding, 1st ed; 2020, p. 689–718.

[99] American Institute of Aeronautics and Astronautics. AIAA guide for the verification and validation of computational fluid dynamics simulations. Reston, VA: American Institute of Aeronautics and Astronautics; 1998.

[100] Guyon G. Role of the Model User in Results obtained from Simulation Software Program. Proc. 5th Int. Build. Perform. Simul. Assoc. Conf. (Prague, Czech Republic) 1997.

[101] Imam S, Coley DA, Walker I. The building performance gap: Are modellers literate? Build Serv Eng Res T 2017;38(3):351–75. https://doi.org/10.1177/0143624416684641.

[102] Tominaga Y, Mochida A, Yoshie R, Kataoka H, Nozu T, Yoshikawa M et al. AIJ guidelines for practical applications of CFD to pedestrian wind environment around buildings. J Wind Eng Ind Aerodyn 2008;96(10-11):1749–61. https://doi.org/10.1016/j.jweia.2008.02.058.

[103] ENVI-met GmbH. ENVI-Met Knowledgebase Overview. [Accessed December 15, 2021]; Available from: https://envi-met.info/doku.php?id=kb:start.

[104] Clauß J, Vogler-Finck P, Georges L. Calibration of a High-Resolution Dynamic Model for Detailed Investigation of the Energy Flexibility of a Zero Emission Residential Building. In: Johansson D, Bagge H, Wahlström Å, editors. Cold Climate HVAC 2018: Sustainable Buildings in Cold Climates. Cham: Springer International Publishing; 2019, p. 725–736.

[105] Skeie K. Sustainable Facade Renovation [Master's thesis]: Norwegian University of Science and Technology (NTNU); 2013.

[106] Statistisk sentralbyrå. Kommunefakta Trondheim; Available from: https://www.ssb.no/kommunefakta/trondheim.

[107] Peel MC, Finlayson BL, McMahon TA. Updated world map of the Köppen-Geiger climate classification. Hydrol Earth Syst Sci Discuss 2007;4(2):439–73. https://doi.org/10.5194/hessd-4-439-2007.

[108] Lundstad E, Tveito OE. Homogenization of daily mean temperature in Norway; 2016.

[109] Dicks L. Arctic climate issues 2011: Changes in Arctic snow, water, ice and permafrost. Oslo, Norway, Ottawa, Ontario: Arctic Monitoring and Assessment Programme; Canadian Electronic Library; 2013.

[110] Thoman RL, Richter-Menge J, Druckenmiller ML. Arctic Report Card 2020. Alaska Center for Climate Assessment and Policy (U.S.) International Arctic Research Center University of Alaska Fairbanks National Snow and Ice Data Center (U.S.) University of Colorado Boulder United States. National Oceanic and Atmospheric Administration. Office of Oceanic and Atmospheric Research Global Ocean Observing System Geophysical Fluid Dynamics Laboratory (U.S.) Pacific Marine Environmental Laboratory (U.S.) Cooperative Institute for Research in the Atmosphere (Fort Collins, Colo.); 2020.

[111] Norsk Klima Service Senter. Klima i Norge 2100 [Climate in Norway 2100]; 2016.

[112] Meteorologisk Institutt. eKlima [meanwhile shut down]: Free access to weather- and climate data from Norwegian Meteorological Institute from historical data to real time observations. Normals. [Accessed March 11, 2021]; Available from: http://sharki.oslo.dnmi.no/portal/page?_pageid=73,39035,73_39049&_dad=portal&_schema=PORTAL.

[113] Less and less snow in January (in Norwegian). Aftenposten, 16 January 2009; Available from: https://www.aftenposten.no/norge/i/5nBKz/stadig-mindre-snoe-i-januar.

[114] Bergskaug E. Winters get shorter and will have less days with skiing conditions (in Norwegian). abc nyheter, 7 January 2020; Available from: https://www.abcnyheter.no/nyheter/norge/2020/01/07/195639534/vinteren-blir-kortere-og-antall-dager-med-skifore-blir-faerre.

[115] Palter JB. The role of the Gulf Stream in European climate. Ann Rev Mar Sci 2015;7:113–37. https://doi.org/10.1146/annurev-marine-010814-015656.

[116] Xu M, Hong B, Mi J, Yan S. Outdoor thermal comfort in an urban park during winter in cold regions of China. Sustain Cities Soc 2018;43:208–20. https://doi.org/10.1016/j.scs.2018.08.034.

[117] Liu W, Zhang Y, Deng Q. The effects of urban microclimate on outdoor thermal sensation and neutral temperature in hot-summer and cold-winter climate. Energy Build 2016;128:190–7. https://doi.org/10.1016/j.enbuild.2016.06.086.

[118] Nikolopoulou M, Lykoudis S. Thermal comfort in outdoor urban spaces: Analysis across different European countries. Build Environ 2006;41(11):1455–70. https://doi.org/10.1016/j.buildenv.2005.05.031.

[119] Yang B, Olofsson T, Nair G, Kabanshi A. Outdoor thermal comfort under subarctic climate of north Sweden – A pilot study in Umeå. Sustain Cities Soc 2017;28:387–97. https://doi.org/10.1016/j.scs.2016.10.011.

[120] Chen X, Gao L, Xue P, Du J, Liu J. Investigation of outdoor thermal sensation and comfort evaluation methods in severe cold area. Sci Total Environ 2020;749:141520. https://doi.org/10.1016/j.scitotenv.2020.141520.

[121] Strømann-Andersen J, Sattrup PA. The urban canyon and building energy use: Urban density versus daylight and passive solar gains. Energy Build 2011;43(8):2011–20. https://doi.org/10.1016/j.enbuild.2011.04.007.

[122] Government of Canada. Canadian Climate Normals 1981-2010 Station Data: Toronto, Ontario. [Accessed December 06, 2021]; Available from: https://climate.weather.gc.ca/climate_normals/results_1981_2010_e.html?stnID=5051&autofwd=1.

[123] Wiik MK, Fufa SM, Baer D, Sartori I, Andresen I. The ZEN Definition - A Guideline for the ZEN Pilot Areas: Version 1.0; 2018.

[124] Wiik MK, Fufa SM, Fjellheim K, Krekling SL, Krogstie J, Ahlers D et al. Zero Emission Neighbourhoods in Smart Cities: Definition, key performance indicators and assessment criteria: Version 2.0 Bilingual version; 2021.

[125] Kvellheim AK, Danielsen SM, Hestnes AG, Gustavsen A. ZEN Research Centre on Zero Emission Neighbourhoods in Smart Cities: Annual Report 2020. Trondheim, Norway; 2021.

[126] Bremvåg A, Hestnes AG, Gustavsen A (eds.). ZEN Research Centre on Zero Emission Neighbourhoods in Smart Cities: Annual Report 2019. Trondheim, Norway; 2020.

[127] Woods R, Sætersdal Remøe K, Hestnes AG, Gustavsen A. ZEN Research Centre on Zero Emission Neighbourhoods in Smart Cities: Annual Report 2018. Trondheim, Norway; 2019.

[128] Bremvåg A, Gustavsen A, Hestnes AG. ZEN Research Centre on Zero Emission Neighbourhoods in Smart Cities: Annual Report 2017. Trondheim, Norway; 2018.

[129] Brozovsky J, Gaitani N, Gustavsen A. A systematic review of urban microclimate in cold and polar climate regions. Renew Sustain Energy Rev 2021;138. https://doi.org/10.1016/j.rser.2020.110551.

[130] Moher D, Liberati A, Tetzlaff J, Altman DG. Preferred reporting items for systematic reviews and meta-analyses: the PRISMA statement. Int J Surg 2010;8(5):336–41. https://doi.org/10.1016/j.ijsu.2010.02.007.

[131] Lu D, Weng Q. Spectral mixture analysis of ASTER images for examining the relationship between urban thermal features and biophysical descriptors in Indianapolis,

Indiana, USA. Remote Sens Environ 2006;104(2):157–67. https://doi.org/10.1016/j.rse.2005.11.015.

[132] Walawender JP, Szymanowski M, Hajto MJ, Bokwa A. Land Surface Temperature Patterns in the Urban Agglomeration of Krakow (Poland) Derived from Landsat-7/ETM+ Data. Pure Appl Geophys 2014;171(6):913–40. https://doi.org/10.1007/s00024-013-0685-7.

[133] Schatz J, Kucharik CJ. Seasonality of the Urban Heat Island Effect in Madison, Wisconsin. J Appl Meteorol Climatol 2014;53(10):2371–86. https://doi.org/10.1175/JAMC-D-14-0107.1.

[134] Matuzko AK, Yakubailik OE. Urban heat island effects over Krasnoyarsk obtained on the basis of Landsat 8 remote sensing data. IOP Conf Ser Earth Environ Sci 2018;211:12010. https://doi.org/10.1088/1755-1315/211/1/012010.

[135] Klimenko VV, Ginzburg AS, Demchenko PF, Tereshin AG, Belova IN, Kasilova EV. Impact of urbanization and climate warming on energy consumption in large cities. Dokl Phys 2016;61(10):521–5. https://doi.org/10.1134/S1028335816100050.

[136] Yang J, Bou-Zeid E. Should Cities Embrace Their Heat Islands as Shields from Extreme Cold? J Appl Meteorol Climatol 2018;57(6):1309–20. https://doi.org/10.1175/JAMC-D-17-0265.1.

[137] Johnson B, Shepherd JM. An urban-based climatology of winter precipitation in the northeast United States. Urban Clim 2018;24:205–20. https://doi.org/10.1016/j.uclim.2018.03.003.

[138] Nordli Ø, Hestmark G, Benestad RE, Isaksen K. The Oslo temperature series 1837-2012: homogeneity testing and temperature analysis. Int J Climatol 2015;35(12):3486–504. https://doi.org/10.1002/joc.4223.

[139] Anderson CI, Gough WA. Evolution of Winter Temperature in Toronto, Ontario, Canada: A Case Study of Winters 2013/14 and 2014/15. J Clim 2017;30(14):5361–76. https://doi.org/10.1175/JCLI-D-16-0562.1.

[140] Lokoshchenko MA, Korneva IA, Kochin AV, Dubovetsky AZ, Novitsky MA, Razin PY. Current changes of the lower troposphere temperature in the Moscow region. Izv Atmos Ocean Phys 2017;53(4):392–401. https://doi.org/10.1134/S0001433817040089.

[141] Czarnecka M, Mąkosza A, Nidzgorska-Lencewicz J. Variability of meteorological elements shaping biometeorological conditions in Szczecin, Poland. Theor Appl Climatol 2011;104(1-2):101–10. https://doi.org/10.1007/s00704-010-0326-3.

[142] Majewski G, Przewoźniczuk W, Kleniewska M. The effect of urban conurbation on the modification of human thermal perception, as illustrated by the example of Warsaw (Poland). Theor Appl Climatol 2014;116(1-2):147–54. https://doi.org/10.1007/s00704-013-0939-4.

[143] Nidzgorska-Lencewicz J. Variability of Human-Biometeorological Conditions in Gdańsk. Pol J Environ Stud 2015;24:215–26. https://doi.org/10.15244/pjoes/26116.

[144] Kallistratova MA, Kouznetsov RD. Low-Level Jets in the Moscow Region in Summer and Winter Observed with a Sodar Network. Bound-Layer Meteorol. 2012;143(1):159–75. https://doi.org/10.1007/s10546-011-9639-8.

[145] Petrov S, Mamaeva N, Narushko M. Urban development of heat island territories and the health of the northern indigenous population. MATEC Web Conf. 2017;106(1-3):1035. https://doi.org/10.1051/matecconf/201710601035.

[146] Cheng I, Zhang L, Mao H, Blanchard P, Tordon R, Dalziel J. Seasonal and diurnal patterns of speciated atmospheric mercury at a coastal-rural and a coastal-urban site. Atmos Environ 2014;82:193–205. https://doi.org/10.1016/j.atmosenv.2013.10.016.

[147] Brozovsky J, Gaitani N, Gustavsen A. Characterisation of Heat Losses in Zero Emission Buildings (ZEB) in Cold Climate. Proc. 16th Int. Build. Perform. Simul. Assoc. Conf. (Rome, Italy) 2019:343–50. https://doi.org/10.26868/25222708.2019.210560.

[148] SN/TS 3031:2016. Energy performance of buildings: Calculation of energy needs and energy supply (in Norwegian);01.040.91; 91.120.10: Standard Norge.

[149] Liddament MW. Air Infiltration Calculation Techniques - An application guide. Coventry (UK); 1986.

[150] Brozovsky J, Corio S, Gaitani N, Gustavsen A. Evaluation of sustainable strategies and design solutions at high-latitude urban settlements to enhance outdoor thermal comfort. Energy Build 2021;244(12):111037. https://doi.org/10.1016/j.enbuild.2021.111037.

[151] Fanger PO. Thermal comfort: Analysis and applications in environmental engineering. Copenhagen: Danish Technical Pr; 1970.

[152] Jendritzky G, Nübler W. A Model Analysing the Urban Thermal Environment in Physiologically Significant Terms. Arch Met Geoph Biokl B 1981;29(4):313–26.

[153] Verein Deutscher Ingenieure. VDI 3787 Blatt 2 - Environmental meteorology: Methods for the human biometeorological evaluation of climate and air quality for urban and regional planning at regional level - Part I: Climate; 2008.

[154] Brozovsky J, Simonsen A, Gaitani N. Validation of a CFD model for the evaluation of urban microclimate at high latitudes: A case study in Trondheim, Norway. Build Environ 2021;205:108175. https://doi.org/10.1016/j.buildenv.2021.108175.

[155] Jones HG. Plants and Microclimate: A Quantitative Approach to Environmental Plant Physiology. 3rd ed. Cambridge: Cambridge University Press; 2013.

[156] Monteith JL. Evaporation and environment. Symp Soc Exp Biol 1965;19:205–34.

[157] Penman HL. The Physical Bases of Irrigation Control. Report of the 13th International Horticultural Congress 1953:1–13.

[158] Mayer H, Höppe P. Thermal comfort of man in different urban environments. Theor Appl Climatol 1987;38:43–9.

[159] Höppe P. The physiological equivalent temperature - a universal index for the biometeorological assessment of the thermal environment. Int J Biometeorol 1999;43(2):71–5. https://doi.org/10.1007/s004840050118.

[160] Walther E, Goestchel Q. The P.E.T. comfort index: Questioning the model. Build Environ 2018;137(no. 2):1–10. https://doi.org/10.1016/j.buildenv.2018.03.054.

[161] Yang J, Tham KW, Lee SE, Santamouris M, Sekhar C, Cheong DKW. Anthropogenic heat reduction through retrofitting strategies of campus buildings. Energy Build 2017;152:813–22. https://doi.org/10.1016/j.enbuild.2016.11.051.

[162] Brozovsky J, Corio S, Gaitani N, Gustavsen A. Microclimate Analysis of a University Campus in Norway. IOP Conf Ser Earth Environ Sci 2019;352(1). https://doi.org/10.1088/1755-1315/352/1/012015.

[163] Brozovsky J, Gustavsen A, Gaitani N. Zero emission neighbourhoods and positive energy Districts – A state-of-the-art review. Sustain Cities Soc 2021;72:103013. https://doi.org/10.1016/j.scs.2021.103013.

[164] Wienert U, Kuttler W. The dependence of the urban heat island intensity on latitude - A statistical approach. Metereol Z 2005;14(5):677–86.

[165] National Geographic. The Five Major Types of Biomes. [Accessed December 06, 2021]; Available from: https://www.nationalgeographic.org/article/five-major-types-biomes/.

[166] Imhoff ML, Zhang P, Wolfe RE, Bounoua L. Remote sensing of the urban heat island effect across biomes in the continental USA. Remote Sens Environ 2010;114(3):504–13. https://doi.org/10.1016/j.rse.2009.10.008.

[167] Oke TR. City size and the urban heat island. Atmos Environ 1973;7(8):769–79. https://doi.org/10.1016/0004-6981(73)90140-6.

[168] Oke TR. The energetic basis of the urban heat island. Q J Roy Meteorol Soc 1982;108(455):1–24. https://doi.org/10.1002/qj.49710845502.

[169] Zhou B, Rybski D, Kropp JP. The role of city size and urban form in the surface urban heat island. Sci Rep 2017;7(1):4791. https://doi.org/10.1038/s41598-017-04242-2.

[170] Ramírez-Aguilar EA, Lucas Souza LC. Urban form and population density: Influences on Urban Heat Island intensities in Bogotá, Colombia. Urban Clim 2019;29:100497. https://doi.org/10.1016/j.uclim.2019.100497.

[171] Zhou B, Rybski D, Kropp JP. On the statistics of urban heat island intensity. Geophys. Res. Lett. 2013;40(20):5486–91. https://doi.org/10.1002/2013GL057320.

[172] Zhao L, Lee X, Smith RB, Oleson K. Strong contributions of local background climate to urban heat islands. Nature 2014;511(7508):216–9. https://doi.org/10.1038/nature13462.

[173] Esau I, Miles V, Soromotin A, Sizov O, Varentsov M, Konstantinov P. Urban heat islands in the Arctic cities: an updated compilation of in situ and remote-sensing estimations. Adv. Sci. Res. 2021;18:51–7. https://doi.org/10.5194/asr-18-51-2021.

[174] Ebrahimabadi S, Nilsson KL, Johansson C. The Problems of Addressing Microclimate Factors in Urban Planning of the Subarctic Regions. Environ Plann B 2015;42(3):415–30. https://doi.org/10.1068/b130117p.

[175] Roth M. Review of urban climate research in (sub)tropical regions. Int J Climatol 2007;27(14):1859–73. https://doi.org/10.1002/joc.1591.

[176] Stewart ID. A systematic review and scientific critique of methodology in modern urban heat island literature. Int J Climatol 2011;31(2):200–17. https://doi.org/10.1002/joc.2141.

[177] Miljødirektoratet. Kysten [The coast]. [Accessed July 11, 2018]; Available from: http://www.miljostatus.no/Tema/Hav-og-kyst/Kysten/.

[178] Leng H, Liang S, Yuan Q. Outdoor thermal comfort and adaptive behaviors in the residential public open spaces of winter cities during the marginal season. Int J Biometeorol 2020;64(2):217–29. https://doi.org/10.1007/s00484-019-01709-x.

[179] Westerberg U. Climatic Planning - Physics or Symbolism? Arch & Behav 1994;10(1):49–71.

[180] Eliasson I, Knez I, Westerberg U, Thorsson S, Lindberg F. Climate and behaviour in a Nordic city. Landsc Urban Plan 2007;82(1-2):72–84. https://doi.org/10.1016/j.landurbplan.2007.01.020.

[181] Taleghani M, Berardi U. The effect of pavement characteristics on pedestrians' thermal comfort in Toronto. Urban Clim 2018;24:449–59. https://doi.org/10.1016/j.uclim.2017.05.007.

[182] Santamouris M, Gaitani N, Spanou A, Saliari M, Giannopoulou K, Vasilakopoulou K et al. Using cool paving materials to improve microclimate of urban areas – Design realization and results of the flisvos project. Build Environ 2012;53(14):128–36. https://doi.org/10.1016/j.buildenv.2012.01.022.

[183] Fintikakis N, Gaitani N, Santamouris M, Assimakopoulos M, Assimakopoulos DN, Fintikaki M et al. Bioclimatic design of open public spaces in the historic centre of Tirana, Albania. Sustain Cities Soc 2011;1(1):54–62. https://doi.org/10.1016/j.scs.2010.12.001.

[184] Grynning S, Gustavsen A, Time B, Jelle BP. Windows in the buildings of tomorrow: Energy losers or energy gainers? Energy Build 2013;61:185–92. https://doi.org/10.1016/j.enbuild.2013.02.029.

[185] Boyano A, Hernandez P, Wolf O. Energy demands and potential savings in European office buildings: Case studies based on EnergyPlus simulations. Energy Build 2013;65:19–28. https://doi.org/10.1016/j.enbuild.2013.05.039.

[186] Ihara T, Gustavsen A, Jelle BP. Effect of facade components on energy efficiency in office buildings. Appl Energy 2015;158:422–32. https://doi.org/10.1016/j.apenergy.2015.08.074.

[187] Wang R, Lu S, Zhai X, Feng W. The energy performance and passive survivability of high thermal insulation buildings in future climate scenarios. Build. Simul. 2021. https://doi.org/10.1007/s12273-021-0818-3.

[188] Tilley Tajet HT. Hetebølger i Norge fra 1957 - 2019 [Heat waves in Norway from 1957 - 2019]; 2020.

[189] Grahn P, Stigsdotter UA. Landscape planning and stress. Urban For Urban Green 2003;2(1):1–18. https://doi.org/10.1078/1618-8667-00019.

[190] O'Brien L, Williams K, Stewart A. Urban health and health inequalities and the role of urban forestry in Britain: A review; 2010.

[191] Barton J, Rogerson M. The importance of greenspace for mental health. Br J Psychiatry Int 2017;14(4):79–81.

[192] Alcock I, White MP, Wheeler BW, Fleming LE, Depledge MH. Longitudinal effects on mental health of moving to greener and less green urban areas. Environ Sci Technol 2014;48(2):1247–55. https://doi.org/10.1021/es403688w.

[193] Kaplan R. The role of nature in the context of the workplace. Landsc Urban Plan 1993;26(1-4):193–201. https://doi.org/10.1016/0169-2046(93)90016-7.

[194] Galderisi A, Treccozzi E. Green Strategies for Flood Resilient Cities: The Benevento Case Study. Proc Environ Sci 2017;37:655–66. https://doi.org/10.1016/j.proenv.2017.03.052.

[195] Pistocchi A, Calzolari C, Malucelli F, Ungaro F. Soil sealing and flood risks in the plains of Emilia-Romagna, Italy. J Hydrol Reg Stud 2015;4:398–409. https://doi.org/10.1016/j.ejrh.2015.06.021.

[196] Thorolfsson ST. A new direction in the urban runoff and pollution management in the city of Bergen, Norway. Water Sci Tech 1998;38(10):123–30.

[197] Bai T, Mayer AL, Shuster WD, Tian G. The Hydrologic Role of Urban Green Space in Mitigating Flooding (Luohe, China). Sustainability 2018;10(10):1–3584. https://doi.org/10.3390/su10103584.

[198] Xiao Q, McPherson EG. Rainfall interception by Santa Monica's municipal urban forest. Urban Ecosyst 2002;6(4):291–302. https://doi.org/10.1023/B:UECO.0000004828.05143.67.

[199] Xiao Q, McPherson EG, Ustin SL, Grismer ME, Simpson JR. Winter rainfall interception by two mature open-grown trees in Davis, California. Hydrol. Process. 2000;14(4):763–84. https://doi.org/10.1002/(SICI)1099-1085(200003)14:4<763:AID-HYP971>3.0.CO;2-7.

[200] Singh M, Laefer DF. Recent Trends and Remaining Limitations in Urban Microclimate Models. OUSDJ 2015;1(1):1–12. https://doi.org/10.2174/2352631901401010001.

[201] Palme M, Salvati A. Urban Microclimate Modelling for Comfort and Energy Studies. Cham: Springer International Publishing; 2021.

[202] Jänicke B, Milošević D, Manavvi S. Review of User-Friendly Models to Improve the Urban Micro-Climate. Atmosphere 2021;12(10):1291. https://doi.org/10.3390/atmos12101291.

[203] Moonen P, Defraeye T, Dorer V, Blocken B, Carmeliet J. Urban Physics: Effect of the micro-climate on comfort, health and energy demand. Front Archit Res 2012;1(3):197–228. https://doi.org/10.1016/j.foar.2012.05.002.

[204] ENVI-met GmbH. Software: FAQ. [Accessed December 09, 2021]; Available from: https://www.envi-met.com/software/.

[205] Clarke JA, Hensen J. Integrated building performance simulation: Progress, prospects and requirements. Build Environ 2015;91:294–306. https://doi.org/10.1016/j.buildenv.2015.04.002.

[206] Stavrakakis GM, Katsaprakakis DA, Damasiotis M. Basic Principles, Most Common Computational Tools, and Capabilities for Building Energy and Urban Microclimate Simulations. Energies 2021;14(20):6707. https://doi.org/10.3390/en14206707.

[207] Sadeghipour Roudsari M, Pak M, Smith A. Ladybug: A Parametric Environmental Plugin for Grasshopper to Help Designers Create an Environmentally-Conscious Design. Proc. 13th Int. Build. Perform. Simul. Assoc. Conf. (Chambéry, France) 2013:3128–35.

[208] Mackey C, Glanos T, Norford LK, Sadeghipour Roudsari M. Wind, Sun, Surface Temperature, and Heat Island: Critical Variables for High-Resolution Outdoor Thermal Comfort. Proc. 15th Int. Build. Perform. Simul. Assoc. Conf. (San Francisco, CA, USA) 2017:985–93. https://doi.org/10.26868/25222708.2017.260.

[209] Fernandez-Antolin M-M, del-Río J-M, Del Ama Gonzalo F, Gonzalez-Lezcano R-A. The Relationship between the Use of Building Performance Simulation Tools by Recent Graduate Architects and the Deficiencies in Architectural Education. Energies 2020;13(5):1134. https://doi.org/10.3390/en13051134.

[210] Fernandez-Antolin M-M, Del Río JM, Gonzalez-Lezcano R-A. Building performance simulation tools as part of architectural design: breaking the gap through software simulation. Int J Technol Des Educ 2021. https://doi.org/10.1007/s10798-020-09641-7.

[211] Wheeler JO. Social Interaction and Urban Space. J Geogr 1971;70(4):200–3. https://doi.org/10.1080/00221347108981620.

[212] Hallman HW. Neighborhoods [Neighbourhoods]: Their place in urban life. Beverly Hills: Sage Publications; 1984.

[213] Gehl J. Life between buildings: Using public space. Washington DC: Island Press; 2011.

[214] Bennet SA, Yiannakoulias N, Williams AM, Kitchen P. Playground Accessibility and Neighbourhood Social Interaction Among Parents. Soc Indic Res 2012;108(2):199–213. https://doi.org/10.1007/s11205-012-0062-4.

[215] Purvis B, Mao Y, Robinson D. Three pillars of sustainability: in search of conceptual origins. Sustain Sci 2019;14(3):681–95. https://doi.org/10.1007/s11625-018-0627-5.

[216] Sullivan WC, Kuo FE, Depooter SF. The Fruit of Urban Nature. Environ Behav 2004;36(5):678–700. https://doi.org/10.1177/0193841X04264945.

[217] Sugiyama T, Ward Thompson C. Older people's health, outdoor activity and supportiveness of neighbourhood environments. Landsc Urban Plan 2007;83(2-3):168–75. https://doi.org/10.1016/j.landurbplan.2007.04.002.

[218] Rayaprolu HS, Llorca C, Moeckel R. Impact of bicycle highways on commuter mode choice: A scenario analysis. Eviron Plann B 2020;47(4):662–77. https://doi.org/10.1177/2399808318797334.

[219] Isaac M, van Vuuren DP. Modeling global residential sector energy demand for heating and air conditioning in the context of climate change. Energy Policy 2009;37(2):507–21. https://doi.org/10.1016/j.enpol.2008.09.051.

[220] Kuznik F, David D, Johannes K, Roux J-J. A review on phase change materials integrated in building walls. Renew Sustain Energy Rev 2011;15(1):379–91. https://doi.org/10.1016/j.rser.2010.08.019.

[221] Lizana J, de-Borja-Torrejon M, Barrios-Padura A, Auer T, Chacartegui R. Passive cooling through phase change materials in buildings. A critical study of implementation alternatives. Appl Energy 2019;254:113658. https://doi.org/10.1016/j.apenergy.2019.113658.

[222] Baetens R, Jelle BP, Gustavsen A. Phase change materials for building applications: A state-of-the-art review. Energy Build 2010;42(9):1361–8. https://doi.org/10.1016/j.enbuild.2010.03.026.

[223] Li Y, Zhang N, Ding Z. Investigation on the energy performance of using air-source heat pump to charge PCM storage tank. J Energy Storage 2020;28:101270. https://doi.org/10.1016/j.est.2020.101270.

[224] Seppanen O, Fisk WJ, Lei QH. Room temperature and productivity in office work; 2006.

[225] Wargocki P, Wyon D. The Effects of Moderately Raised Classroom Temperatures and Classroom Ventilation Rate on the Performance of Schoolwork by Children (RP-1257). HVAC&R Res. 2007;13(2):193–220. https://doi.org/10.1080/10789669.2007.10390951.

Part B

Scientific papers

—

Main papers

Paper I

A systematic review of urban climate research in cold and polar climate regions

J. Brozovsky, N. Gaitani, A. Gustavsen

Published in *Renewable and Sustainable Energy Reviews 136* (2021), 110551

https://doi.org/10.1016/j.rser.2020.110551

Renewable and Sustainable Energy Reviews 138 (2021) 110551

Contents lists available at ScienceDirect

Renewable and Sustainable Energy Reviews

journal homepage: http://www.elsevier.com/locate/rser

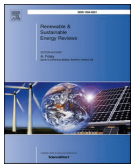

A systematic review of urban climate research in cold and polar climate regions

J. Brozovsky *, N. Gaitani, A. Gustavsen

Department of Architecture and Technology, Faculty for Architecture and Design, NTNU – Norwegian University of Science and Technology, Høgskoleringen 1, 7491, Trondheim, Norway

ARTICLE INFO

Keywords:
Urban climate
Cold and polar climate
Microclimate
Urban heat island
Climate adaptation
Mitigation

ABSTRACT

Cities are at the forefront of the climate change issue and are responsible for about 39% of global carbon dioxide emissions. They can form their own climate which is often characterized by higher temperatures and pollution levels, less wind, and solar access compared to their surroundings. This paper presents a systematic review of publications on cities in cold and polar climate regions as defined by the Köppen-Geiger climate classification to determine the most-researched topics, identify sparsely incorporated research areas, synthesize research evidence and summarize the most important results. In total, 101 papers have been included, categorized, and analyzed according to their publication year, country, climate, topic, method, keywords, citations, and publication channels. The articles were classified into nine main topics: urban heat island (UHI) magnitude, UHI mitigation, other UHI related, biometeorology, air pollution, urban boundary layer and atmospheric boundary layer, time series analysis, other urban meteorological phenomena, and research not falling under the previous eight categories. The most-covered topic was the UHI effect. The outweighing part of studies used on-site measurements for obtaining data, while some studies were dedicated to understanding the structure, or the temporal and spatial variability of the UHI, often by using numerical tools. The review reveals significant gaps in the research of microclimatic characteristics and physical properties of the materials in urban design. Ongoing climate change and the particular vulnerability of cold and polar climate regions makes it especially important to review, develop, and adopt climate adaption and mitigation strategies for sustainable urban development.

1. Introduction

1.1. Global situation

The buildings and construction sector amounts to about 36% of global final energy consumption and 39% of energy-related carbon dioxide emissions globally [1]. Reducing the adverse environmental impact of it is hence undoubtedly one of the key aspects to keep global temperature rise within 1.5 °C above pre-industrial levels. Of particular concern are cities which currently account for around 67–76% of global energy use and between 71 and 76% of CO_2 emissions from global final energy use [2].

Since 1950, the number of people living in cities has rapidly grown from 751 million (30% of the world's population) to 4.2 billion (55%) in 2018 [3]. By 2050, 68% of the projected global population of 9.7 billion is expected to live in urban settlements [3,4]. With the ongoing growth of the global economy and population, which are the most important drivers in CO_2 emissions from fossil fuel consumption, the situation aggravates [2]. These numbers, in particular, express the need for sustainable concepts and solutions to address the risks and problems connected to health, the environment and the consumption ofvd energy and resources in urban environments.

1.2. Urban climate characteristics

Urban spaces differ from rural areas primarily by the materials of the built environment and the high density of people. As a consequence, the consumption of resources, the use of energy, and the production of waste concentrate in densely populated areas. Differences in the physical properties of the surface covers, topography and anthropogenic impacts (such as increased anthropogenic heat, lack of green spaces, increased air pollution etc.) can influence the weather variables at the meteorological microscale, as for instance temperature, rainfall, wind or humidity [5]. Commonly, *microscale* is used as a term for horizontal extents smaller than 1 km. In the definition by the American Meteorological

* Corresponding author.
E-mail addresses: johannes.brozovsky@ntnu.no (J. Brozovsky), niki.gaitani@ntnu.no (N. Gaitani).

https://doi.org/10.1016/j.rser.2020.110551
Received 22 August 2019; Received in revised form 4 October 2020; Accepted 2 November 2020
Available online 12 November 2020

Abbreviations

ABL	Atmospheric boundary layer
AP	Air pollution
BM	Biometeorology
BVOC	Biogenic volatile organic compounds
CFD	Computational Fluid Dynamics
CLHI	Canopy layer heat island
CW	Comfort and wellbeing
GEM	Gaseous elementary mercury
GIS	Geographical Information System
GOM	Gaseous oxidized mercury
HVAC	Heating, ventilation and air-conditioning
LST	Land surface temperature (°C)
LULC	Land use/land cover
MODIS	Moderate-Resolution Imaging Spectroradiometer
M-OS	On-site measurements
M-RS	Remote sensing measurements
NMV	Numerical models with validation
OUMP	Other urban meteorological phenomena
PBM	Particle-bound mercury
PET	Physiological equivalent temperature (°C)
PM	Particulate matter
Rev	Review
RMUHI	Relief-modified urban heat island
S	Survey
SLHI	Surface layer heat island
SVF	Sky view factor (-)
TEB	Town Energy Balance
TSA	Time series analysis
UBL	Urban boundary layer
UCL	Urban canopy layer
UHI	Urban heat island
UHI-Mag	Urban heat island magnitude
UHI-Mit	Urban heat island mitigation strategy
UHI-Other	Other research on the urban heat island
UTCI	Universal Thermal Climate Index (°C)

Society, the upper limit is taken as 2 km [6,7]. The distinctive climate of such a small-scale area that differs from the surrounding area is then called microclimate. The climate for a city is, therefore, to be regarded as a mixture of many slightly different microclimates [5].

Numerous publications – the first pioneering work was published in three volumes in 1833 by Luke Howard on *The Climate of London* [8] – have shown that urbanization changes the characteristics of surface and atmospheric properties of a region significantly, e.g. Ref. [9–11]. These changes include thermal, moisture and aerodynamic properties. Those then again affect natural solar and hydrological balances, as well as air flow patterns, heat fluxes etc. [9] (see also Table 1).

One of the most-investigated phenomena is the so-called urban heat island (UHI). The term came up in the 1940s, for example in Balchin and Pye's study on Bath, UK [13], and describes the warmth of a settlement compared with its rural surroundings [14]. It is reported to occur in almost all urban areas, of every size and disregarding warm or cold climate conditions [15]. According to a study from Oke in 1973, almost half a century ago, it was *"one of the most widely documented climatological effects of man's modification of the atmospheric environment"* [16]. As early as in 1970, Chandler [17] prepared a selected bibliography on urban climate, a first draft of which already contained more than 2000 references.

Table 1
Causes for the urban heat island (not rank-ordered) [12].

Altered energy balance terms	Underlying features of urbanization
Canopy layer	
1. Increased absorption of short-wave radiation	Street canyon geometry – increased surface area and multiple reflection
2. Increased long-wave radiation from the sky	Air pollution – greater absorption and re-emission
3. Decreased long-wave radiation loss	Street canyon geometry – reduction of sky view factor
4. Anthropogenic heat source	Building, traffic and people heat loss
5. Increased sensible heat storage	Construction materials – increased thermal admittance
6. Decreased evapotranspiration	Construction materials – increased 'water proofing'
7. Decreased total turbulent heat transport	Street canyon geometry – reduction of wind speed
Boundary layer	
1. Increased absorption of short-wave radiation	Air pollution – increased aerosol absorption
2. Anthropogenic heat source	Chimney and stack heat losses
3. Increased sensible heat input-entrainment from below	Canopy heat island – increased heat flux from canopy layer and roofs
4. Increased sensible heat input-entrainment from above	Heat island, roughness – increased turbulent entrainment

In 1976, Oke [18] concluded that there is not one but at least two heat islands produced by urbanization, and he proposed to divide the urban atmosphere into two layers. The urban canopy layer (UCL) is made up of the air spaces between a city's "roughness elements" (mainly between buildings up to their rooftops) and is governed by the processes at the microscale. The urban boundary layer (UBL) is directly adjoining the UCL above. The UBL is governed by the processes at mesoscale and defined as *"that part of the planetary boundary layer whose characteristics are affected by the presence of an urban area at its lower boundary"* [18]. It extends from roof level to a few kilometers above it. Both layers interact strongly. While the UCL affects the UBL through heating, cooling and evaporation, the UBL contributes greater mesoscale weather conditions to the UCL [12]. Most studies refer to atmospheric heat islands that can be determined by higher air temperatures, like the urban canopy layer heat island (CLHI). With the increasing availability of remote sensing techniques and resources, surface layer heat islands (SLHI) get evermore attention. Unlike the atmospheric heat islands before, it is determined by a higher surface temperature of an area [9,10].

Warmer temperatures in the inner city can furthermore cause the so-called urban heat island circulation or urban breeze – a weak flow close to the ground directed towards the city's center [19]. Even though the daytime UHI is usually weaker, the instability of the air during the day makes the vertical movement easier and thus induces more developed horizontal airflows, than at night [20–24]. This weak surface flow amounts to around 0.3 m/s [10] and creates a plume over the city center [9]. It was reported to develop even at relatively small heat island intensities of 1–2 °C [22]. However, the term *urban climatology* incorporates a lot more aspects than the UHI, even though it is the most prominent one. It is furthermore not limited to meteorology or climatology only but includes many other disciplines like air pollution science, architecture, building engineering, urban design, biometeorology etc. [25].

Traditionally, data was obtained experimentally, before increasing computing power led to several arithmetic codes, calculation methodologies and publications in urban physics, especially during the last two decades [26]. Most commonly, computational fluid dynamics (CFD) tools or large-scale energy balance models like the Town Energy Balance (TEB) scheme [27,28] are used. Namely, the tool ENVI-met [29] has gained particular popularity since it had been available freely for a long time [26] and has, therefore, been used extensively over the years, e.g. Refs. [30–38]. Due to the high complexity of these models, a careful

validation process is imperative when using them. Moonen et al. [39] discussed five major problems connected with urbanization in their review and provided examples, how numerical approaches can help to address them: pedestrian wind comfort, pedestrian thermal comfort, building energy demand, pollutant dispersion and wind-driven rain.

1.3. Cold and polar climate classification

According to the widely used Köppen-Geiger climate classification, updated by Peel et al. [40], *cold climate* encompasses 12 subtypes, beginning with a *D* in Table 2. Those beginning with an *E* are subtypes of *polar climate*. Fig. 1 shows the location of climate zones based on a 0.1° × 0.1° grid resolution and the cities where the research of the reviewed articles was carried out.

Due to the distribution of landmass, the cold and polar climate zones are mostly situated on the northern hemisphere (with exception of Antarctica, where no permanent settlements with significant population are present). Subclimate "Dfc" extends over large parts of the Russian Federation, Canada and Northern Europe, as well as several smaller mountainous areas e.g. in the US and Europe and represents the most common type of cold climate (again with exception of climate type "ET" in Antarctica).

In this paper, studies on the urban microclimate in cold and polar climate (14 climate types) according to the Köppen-Geiger climate classification are reviewed. Numerical studies were only considered when sufficient validation, for instance with experimental data, was provided. The aim is to determine the most researched topics, identify sparsely incorporated research areas and summarize the most important results. The outcomes of this review and meta-analysis will help researchers to grasp the structure of published research and identify future research possibilities. They will also facilitate comparing obtained results with previously published studies with the same (sub)climate, location, research topic, or method, as the reviewed literature will be listed in comprehensive tables, providing all necessary information. To the best of our knowledge, no systematic review focusing on urban climate research in the cold and polar climate regions has been published yet. This systematic review will therefore fill this gap and provide a statistical analysis of included articles and summarize their main results.

Section 2 of this study will describe the applied methodology for obtaining the reviewed articles. Section 3 gives a statistical evaluation of different characteristics of the included articles and lists them according to their categories. It furthermore summarizes the main outcomes of the reviewed articles. Sections 4 and 5 discuss and conclude the findings from this paper, respectively.

Table 2
Description of Köppen climate symbols and defining criteria for cold and polar climate from Peel et al. [40].

1st	2nd	3rd	Description	Criteria
D			Cold	$T_{hot} > 10$ & $T_{cold} \leq 0$
	s		- Dry Summer	$P_{sdry} < 40$ & $P_{sdry} < P_{wwet}/3$
	w		- Dry Winter	$P_{wdry} < P_{swet}/10$
	f		- Without Dry Season	Not (Ds) or (Dw)
		a	- Hot Summer	$T_{hot} \geq 22$
		b	- Warm Summer	Not (a) & $T_{mon10} \geq 4$
		c	- Cold Summer	Not (a, b or d)
		d	- Very Cold Winter	Not (a or b) & $T_{cold} < -38$
E			Polar	$T_{hot} < 10$
	T		- Tundra	$T_{hot} > 0$
	F		- Frost	$T_{hot} \leq 0$

T_{hot} = temperature of the hottest month [°C], T_{cold} = temperature of the coldest month [°C], T_{mon10} = number of months where the temperature is above 10 °C, P_{dry} = precipitation of the driest month [mm], P_{sdry} = precipitation of the driest month in summer [mm], P_{wdry} = precipitation of the driest month in winter [mm], P_{swet} = precipitation of the wettest month in summer [mm], P_{wwet} = precipitation of the wettest month in winter [mm]. Summer (winter) is defined as the warmer (cooler) six month period of ONDJFM and AMJJAS.

2. Method

To identify relevant literature, a systematic review approach was pursued. A systematic literature review is mainly characterized by a structured question formulation, the use of methodological filters for retrieving a subset of literature and the specification of a reproducible search procedure [41]. With employing the term "subset", this definition already implies that retrieving every relevant article with this approach is rather unlikely. The extent of search results is strongly dependent on the search terms and databases used. However, using too many terms and key phrases may result in an unnecessarily high number of database hits, more irrelevant literature and thus disproportionally high demand for screening.

This study applies the four-phase approach described by Moher et al. [42] as part of the PRISMA (Preferred Reporting Items for Systematic Reviews and Meta-Analyses) statement for structuring literature retrieval and reporting in systematic reviews. In each of the four phases, articles that do not fit into the scope of this review or have been identified twice were removed as illustrated in the flow chart in Fig. 2. This methodological approach has been widely applied, mainly in health care and medicine. Using this approach benefits this systematic review as it presents a repeatable and well-defined in-depth procedure for including literature which not only facilitates the reader to follow but also other researchers to conduct a similar review.

Following the practice in other studies, e.g. Ref. [43,44], the indexed electronic databases Scopus and Web of Science were used. In Scopus, the search was conducted within the search fields *Article Title, Abstract and Keywords*. Analogously, in Web of Science, the search field was chosen to be *Topic*, which means *Title, Abstract, Author keywords* and *Keywords Plus®*. The search was conducted in March 2019. Due to different requirements for the search syntax in the two databases, the entered query was slightly different from one another. For Scopus it was: *((microclimate W/5 urban) OR "anthropogenic heat" OR "heat island" OR "UHI") AND (cold OR arctic)*. In Web of Science, the corresponding query was: *((microclimate NEAR/5 urban) OR "anthropogenic heat" OR "heat island" OR "UHI") AND (cold OR arctic)*. *W/5* and *NEAR/5* indicate that the search should only identify articles where the words *microclimate* and *urban* appear within a range of 5 words in the selected search fields.

Numerical studies which do not include validation were removed since validation usually comprises three parts: (1) a thorough model description, (2) model verification, and (3) model validation. While model description and model verification is usually done by the developer when using a commercial tool (comprehensive description of the model content, assumptions, parametrizations, quality control etc.), model validation is an imperative step that has to be done by the user [45]. This is because in practice the quality of model outputs depend not only on the accuracy of the model itself or its input but also on the qualification of the person running a model as a numerical simulation is a knowledge-based activity [46]. Therefore, it is considered vital for reliable research results to present sufficient validation documentation in numerical studies.

2.1. Classification

The included articles were then grouped according to their main topic (category) and the methods used for evaluation. Sometimes, articles were devoted to more than one topic. They were then placed into a category according to their focus of research. The categories were:

1. *UHI magnitude:* Articles that mainly address the urban-rural temperature difference, either in air temperatures or land surface temperatures. Furthermore, studies on the spatial and temporal variability of those temperature differences are included.

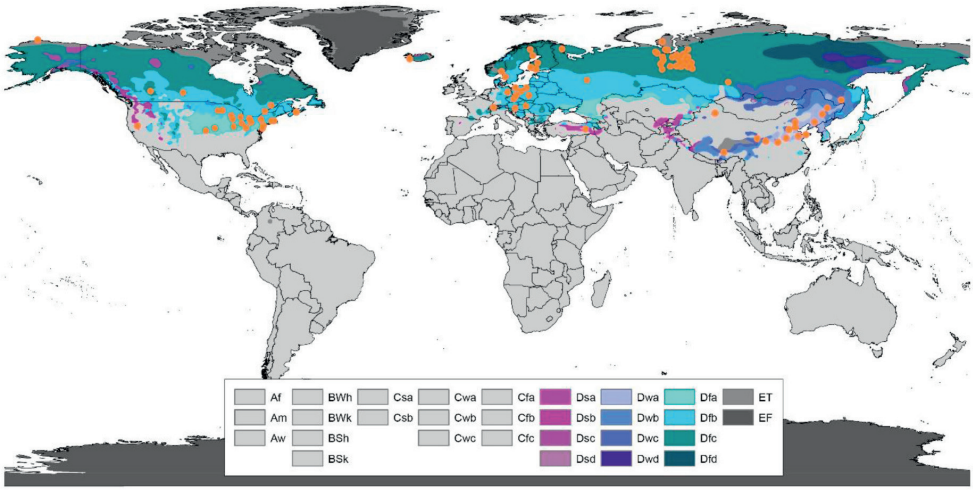

Fig. 1. Cold and polar climate regions according to the data from Peel et al. [40] and locations of studies included in the review, if specifically indicated. Each of the orange dots represents one city. (For interpretation of the references to color in this figure legend, the reader is referred to the Web version of this article.)

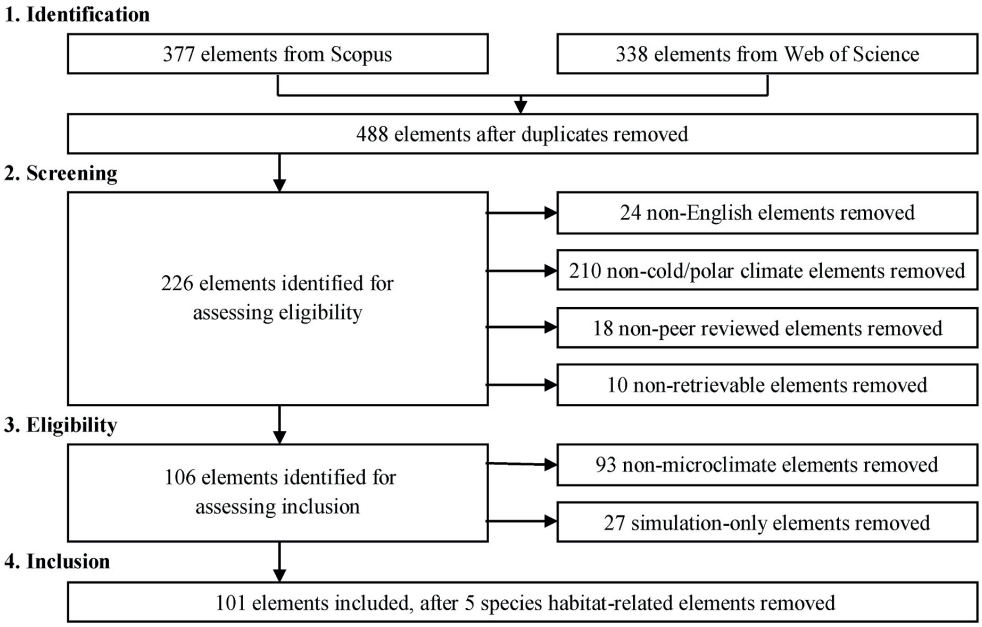

Fig. 2. Flow chart of the applied model for article inclusion (modified from Moher et al. [42]).

2. *UHI mitigation:* Research mainly investigating techniques to mitigate the UHI. This category includes the influence of vegetation, the urban fabric, urban geometry etc.
3. *Other UHI related:* Remaining studies addressing other aspects of the UHI effect.
4. *Biometeorology:* Investigating the impact of meteorological aspects on humans. This can be thermal comfort, health and social studies like behavioral investigations.
5. *Air pollution:* Research focusing on pollutant and aerosol concentrations etc.
6. *UBL and ABL:* Studies on the properties and characteristics of the urban and atmospheric boundary layer.
7. *Time series analyses:* Statistical investigations of long-term temperature measurements without focusing specifically on the UHI etc.
8. *Other urban meteorological phenomena:* All remaining studies satisfying the above-mentioned criteria for inclusion.
9. *Other:* Research not falling under the previous eight categories.

In addition, the articles were classified according to the methods used. The included articles often used more than one method. Following

methods were assigned: *On-site measurements*, *remote-sensed measurements*, *numerical studies with validation*, *survey/interview/questionnaire*, and *review*. Table 3 gives an overview of categories and methods with their abbreviations.

3. Results

In total, 715 studies were identified from the two databases. However, not all of the studies were eligible for inclusion in this study. Only 101 fulfilled the criteria and were thus included in this systematic review. Note that the articles presented in this section are the result of applying the above-described methodology. Characteristics like the global distribution of city locations, research topics etc. are purely influenced by the search terms and the content of the databases. The authors did neither include additional sources nor remove any of the identified articles from the literature search in the following analysis.

3.1. Publication analysis

3.1.1. Publication history

Fig. 3 shows a timeline and the number of articles in each year together with the main topic covered in the studies. The red dashed line indicates the percentage of papers in each year dedicated to one of the three UHI-related categories. In total, more than half of the included studies (58 out of 101) address the UHI effect (see also Fig. 4). There is a clear tendency towards more recent publication years. While of the included studies, the first was published in 1975 on the pollution concentration and stratification in the Calgary UHI [47], only 8 of the included studies have been published before the year 2000. However, searching for studies in scientific databases often misses reports issued by public or other research institutions that were not published in the form of a peer-reviewed article but still are of high quality. Especially those public institutions started researching the urban microclimate quite early, e.g. a report on the UHI in Fairbanks, Alaska by the United States Environmental Protection Agency in 1978 [48]. Furthermore, many relevant publications and reports were missed as they did not explicitly mention any of the search terms in their title or abstract. Regarding Norway for instance, missed but very relevant studies covered (among others) the vertical temperature profile [49,50], a statistical analysis of air quality observations [51] in Bergen, or snow mapping in Longyearbyen, Svalbard to improve forecasting of avalanches [52]. Moreover, it needs to be pointed out that many relevant publications have not been published in English and are thus not as accessible to international researchers. It can hence be reasonably assumed that the literature included in this article is only a part of all relevant studies.

Table 3
Abbreviations and descriptions of categories and methods.

Category		Method	
Abbreviation	Description	Abbreviation	Description
UHI-Mag	Focusing on quantifying the UHI	M-OS	On-site measurements
UHI-Mit	UHI-mitigation strategies	M-RS	Remote sensing measurements
UHI-Other	Other research on the UHI	NMV	Numerical models with validation
BM	Biometeorology (health, comfort)	S	Survey (interviews, questionnaires)
AP	Air pollution	Rev	Review
UBL/ABL	Urban and atmospheric boundary layer		
TSA	Time series analysis		
OUMP	Other urban meteorological phenomena		
Other	Research not related to previous categories		

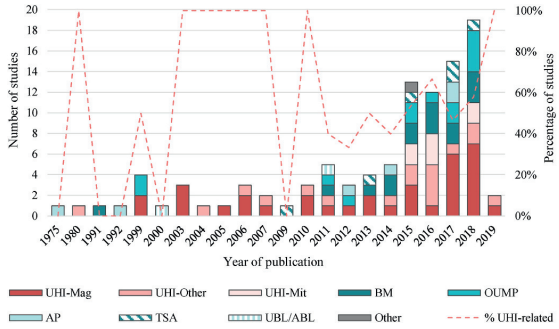

Fig. 3. Number and distribution of categories of studies by year. The dashed line indicates the percentage of studies dedicated to one of the three UHI-related categories.

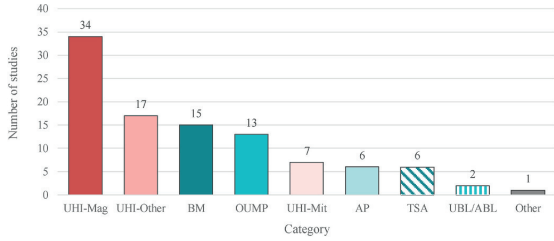

Fig. 4. Number of publications within each category.

3.1.2. Keywords

The dominance of UHI-related research was confirmed by the analysis of used keywords. Table 4 shows the 10 most utilized keywords, where *urban heat island* clearly takes the first rank with 23 times used. *Urban climate* is ranked second (9 times) and *urban microclimate, urbanization/urbanisation*, *land surface temperature,* and *climate change* share the third place (6 times). However, about one-third of the included articles (34 out of 101) had no keywords indicated.

3.1.3. Journals published and citations

In total, the included articles were published in 53 different peer-reviewed journals. Three studies were conference articles, published in indexed conference proceedings. The journals' thematic background covered atmospheric sciences and climatology, engineering, biometeorology, geography, and health and medicine among others. Fig. 5 illustrates the five most popular journals among the included studies, together with the number of published articles.

Most frequently, they were published in *Theoretical and Applied Climatology* with a count of 13. Following behind, 6 were published in the *Journal of Applied Meteorology and Climatology*, 5 in *Atmospheric*

Table 4
10 most used keywords in the included studies.

Rank	Keyword	No. of times used
1	Urban heat island	23
2	Urban climate	9
3	Urban microclimate	6
3	Urbanization/Urbanisation	6
3	Land surface temperature	6
3	Climate change	6
7	Air temperature	5
8	Finland	3
8	MODIS (imagery)	3
8	Surface Energy balance	3

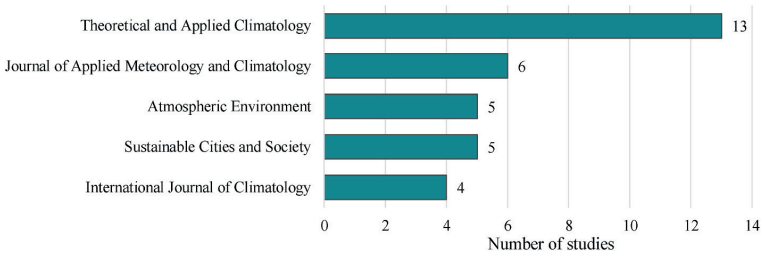

Fig. 5. Most popular journals among the included studies for publication on urban microclimate in cold and polar climate.

environment and *Sustainable Cities and Society*, and 4 in the *International Journal of Climatology*. The overwhelming part of journals was used for one article only.

According to the Scopus database as of March 2019, the study on the *Temporal and spatial characteristics of the urban heat island of Łódź, Poland* by Kłysik and Fortuniak [53] is the most cited article that was included in this study (see Table 5). All but one of the 10 most cited studies covered a UHI-related topic.

3.1.4. Location and climate

Research on urban microclimate in cold and polar climate regions (according to the Köppen-Geiger classification) was carried out in 16 different countries (see Fig. 6). In 6 of those, only one study was conducted. Three of the included studies were review papers that did not focus on specific locations. Most frequently, research was carried out on locations in the USA (21), China (16) and Russia (15). Only a few articles took Scandinavian cities as case studies (11 in total), most of them in Finland (6).

In a similar way, Fig. 7 shows the number of studies according to the climate type of their locations.

A climate type received a count only if an article used at least one location from the respective climate type. Several locations from one climate type in the same study only result in one count. Most frequently, Dfb-locations (Warm summer humid continental climate) were object of investigation (51), mainly in North America and Europe, followed by Dwa (20) (Monsoon-influenced hot-summer humid continental climate) mainly from studies in China and South Korea, and Dfc (15) (Subarctic climate) which is by far the most common subarctic type primarily from

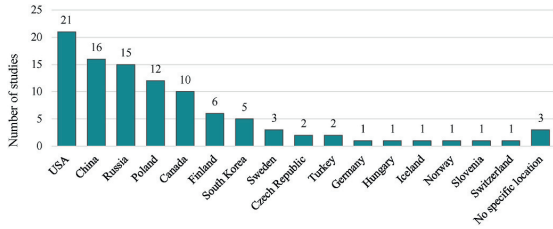

Fig. 6. Number of studies covering research on a location in the respective countries.

studies in Russia. Only few studies covered Dfa (Hot summer humid continental), ET (Tundra climate), Dwd (Monsoon-influenced extremely cold subarctic climate), Dsb (Mediterranean-influenced warm-summer humid continental climate) and Dwc (Moonsoon-influenced subarctic climate) regions.

Several climate types were not represented by any of the included studies, such as Dsa (Mediterranean-influenced hot summer humid continental climate), Dsc (Mediterranean influenced subarctic climate), Dsd (Mediterranean-influenced extremely cold subarctic climate), Dwd (Monsoon-influenced subarctic climate), Dfd (extremely cold subarctic climate), and EF (Ice cap climate).

3.1.5. Research methods

The following Fig. 8 illustrates the number of studies applying each

Table 5
Top 10 most cited articles of included studies according to Scopus.

Rank	Times cited	Title	Authors	Year	Journal	Category
1	195	Temporal and spatial characteristics of the urban heat island of Łódź, Poland	Kłysik and Fortuniak [53]	1999	Atmospheric Environment	UHI-Mag
2	148	Spatial and Temporal Structure of the Urban Heat Island in Seoul	Kim and Baik [54]	2005	Journal of Applied Meteorology	UHI-Mag
3	144	Mesoscale aspects of the Urban Heat Island around New York City	Gedzelman et al. [55]	2003	Theoretical and Applied Climatology	UHI-Mag
4	81	Urban Canopy Modeling of the New York City Metropolitan Area: A Comparison and Validation of Single- and Multilayer Parameterizations	Holt and Pullen [56]	2007	Monthly Weather Review	UHI-Other
5	80	The Urban Heat Island in Winter at Barrow, Alaska	Hinkel et al. [57]	2003	International Journal of Climatology	UHI-Mag
6	78	Comparing the effects of urban heat island mitigation strategies for Toronto, Canada	Wang et al. [58]	2016	Energy & Buildings	UHI-Mit
7	48	Influence of geographical factors and meteorological variables on nocturnal urban-park temperature differences - a case study of summer 1995 in Göteborg, Sweden	Upmanis and Chen [59]	1999	Climate Research	OUMP
8	47	Urban climatological studies in the Reykjavik subarctic environment, Iceland	Steinecke [60]	1999	Atmospheric Environment	UHI-Mag
9	42	Analysis of observations on the urban surface energy balance in Beijing	Miao et al. [61]	2012	Science China Earth Sciences	UHI-Other
10	41	Statistical and dynamical characteristics of the urban heat island intensity in Seoul	Lee and Baik [62]	2010	Theoretical and Applied Climatology	UHI-Mag

Abbreviations: Magnitude of the UHI (UHI-Mag); Other research on the UHI effect (UHI-Other); Mitigation strategies of the UHI (UHI-Mit); Other urban meteorological phenomena (OUMP).

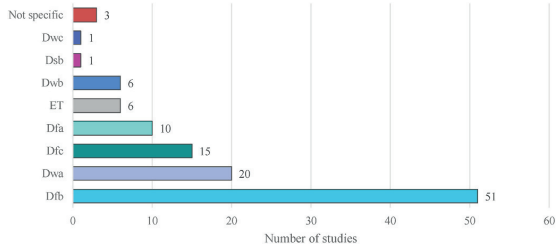

Fig. 7. Number of studies covering a specific climate type according to the Köppen-Geiger classification. The colors of the bars represent the same colors as used in Fig. 1 and thus the study by Peel et al. [40]. (For interpretation of the references to color in this figure legend, the reader is referred to the Web version of this article.)

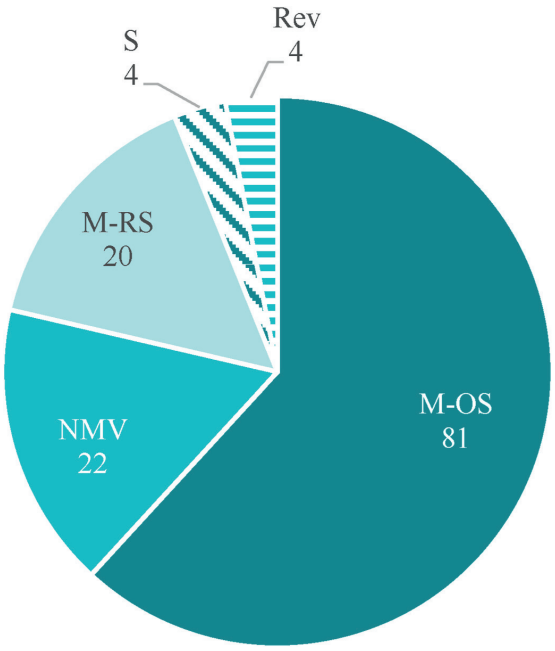

Fig. 8. Number of studies using each research method. M-OS: On-site measurement; NMV: Numerical model with validation; M-RS: Remote sensing measurement; S: Survey; Rev: Review.

of the research methods.

Many of the included studies based on more than one method, combining a numerical model for example with on-site or remote sensing measurements etc. However, direct measurements on site were the predominantly used method with 81 out the 101 included studies, followed by validated numerical models (22) and remote sensing measurements (20). Since one of the eligibility criteria was to not include numerical studies without validation, NMV has exclusively been applied in combination with M – OS and M-RS for validation purposes. Only 4 of the included articles conducted a survey (interview/questionnaire) and a review, respectively.

3.2. Research evaluation

The following sections discuss the main findings of research carried

Table 6
Overview of studies in the category "UHI-magnitude".

No.	Authors	Year	Location, Country	Climate	Method
1	Klysik and Fortuniak [53]	1999	Łódź, Poland	Dfb	M-OS
2	Steinecke [60]	1999	Reykjavik, Iceland	Dfc	M-OS
3	Gedzelman et al. [55]	2003	New York, USA	Dfa	M-OS
4	Hinkel et al. [57]	2003	Barrow, USA	ET	M-OS
5	Klene et al. [63]	2003	Barrow, USA	ET	M-OS
6	Kim and Baik [54]	2005	Seoul, South Korea	Dwa	M-OS
7	Khaikine et al. [64]	2006	Moscow, Russia	Dfb	M-RS
8	Lu and Weng [65]	2006	Indianapolis, USA	Dfa	M-RS
9	Hinkel and Nelson [66]	2007	Barrow, USA	ET	M-OS
10	Lee and Baik [62]	2010	Seoul, South Korea	Dwa	M-OS
11	Stopa-Boryczka et al. [67]	2010	Warsaw, Poland	Dfb	M-OS
12	Malevich and Klink [68]	2011	Minneapolis, USA	Dfb	M – OS, NMV
13	Suomi and Käyhkö [69]	2012	Turku, Finland	Dfb	M-OS
14	Klene et al. [70]	2013	Barrow, USA	ET	M-OS
15	Walawender et al. [71]	2013	Kraków, Poland	Dfb	M-RS
16	Schatz and Kucharik [72]	2014	Madison, USA	Dfb	M-OS
17	Konstantinov et al. [73]	2015	Apatity, Russia	Dfc	M – OS, M-RS
18	Schatz and Kucharik [74]	2015	Madison, USA	Dfb	M-OS
19	Sun et al. [75]	2015	Beijing, China	Dwa	M-RS
20	Ramamurthy and Sangobanwo [76]	2016	several in Northern USA	Dfa/Dfb	M-OS
21	Huang et al. [77]	2017	several in China	Dwa/ Dwb/ Dwc	M – OS, M-RS
22	Kuznetsova et al. [78]	2017	Moscow, Russia	Dfb	M-OS
23	Miles and Esau [79]	2017	Northern West Siberia	Dfc	M-RS
24	Półrolniczak et al. [80]	2017	Poznań, Poland	Dfb	M-OS
25	Przybylak et al. [81]	2017	Toruń, Poland	Dfb	M-OS
26	Shumilov et al. [82]	2017	Kirovsk and Apatity, Russia	Dfc	M-OS
27	Konstantinov et al. [83]	2018	Russian Arctic	Dfc	M-OS
28	Marzban et al. [84]	2018	Berlin, Germany	Dfb	M – OS, M-RS
29	Matuzko and Yakubailik [85]	2018	Krasnoyarsk, Russia	Dfc	M – OS, M-RS
30	Suomi [86]	2018	Lahti, Finland	Dfc	M-OS
31	Varentsov et al. [87]	2018	Apatity, Russia	Dfc	M – OS, NMV, M-RS
32	Yang and Bou-Zeid [88]	2018	12 cities in the US	Dfa/Dfb	M – OS, NMV
33	Yao et al. [89]	2018	Northern China	Dwa/ Dwb	M-RS
34	Esau et al. [90]	2019	Nefteyugansk, Russia	Dfc	M-RS

Abbreviations: On-site measurements (M – OS); Remote-sensed measurements (M-RS); Numerical models with validation (NMV).

out in each of the categories and summarizes some of the main publications shortly.

3.2.1. UHI-magnitude

With almost one-third of all studies dealing with the UHI-magnitude, which are summarized in Table 6, it was the most-covered research topic of all included articles.

Typically, direct M − OS was used to identify the magnitude, spatial and temporal structure of the UHI. A smaller number of studies used M-RS or satellite images, like Moderate-Resolution Imaging Spectroradiometer (MODIS) [75,79], Landsat-8 [71,90], or both [89] for obtaining data, sometimes also in addition to M − OS [73,77,84,85,87]. One study on the UHI in Moscow, Russia used microwave temperature profilers (MTP-5) to obtain a temperature profile of the lower 600-m layer of the atmosphere [64].

Generally, magnitude and temporal appearance of the UHI differed significantly between the reviewed studies. Almost all of them observed a seasonal variation of the UHI, although quite varied and with highest intensities in different seasons: summer [53,67,69,72,81,86], summer and autumn [55], autumn [62], and winter [54,57,66,76,79]. In the majority of cases, highest UHI-intensities were reported during nights [62,64,67,76,80,81] or nights with clear skies [53–55,72,78]. The studies largely agreed that higher wind speeds weakened the intensity of the UHI [53–55,57,60,66,67,72,76,78,81,83,86,87]. Highest UHI-intensities frequently occurred during anticyclonic weather conditions as they often come along with clear and dry weather [80,83,87].

Several studies reported the distinct cooling influence of large water bodies on the spring and summer UHI in coastal cities [55,60,69,76]. Equally, they contribute to the UHI in autumn [62,86], which frequently evoked a cool island during the day [60,69]. Even without the influence of large water bodies, a cool island during daytime was observed in two studies [53,62]. Arguably, even though not specifically mentioned in the study by Lee and Baik [62], the daytime cool island in spring in Seoul, South Korea may be evoked by the close-by and cooler sea in a similar way, as it is supposed to contribute to the UHI in autumn because of higher water temperatures and frequent westerly winds [91].

The studies in this category largely agree upon the significant influence of anthropogenic heat release [62,66,76,78,83,87,88,90]. One article, on the contrary, suspected meteorological and topographical factors to be more important than anthropogenic in Apatity and Kirovsk in the Russian Arctic [82].

Studies focusing on the land surface temperature (LST) agreed that highest temperature anomalies generally occur within industrial and commercial areas like shopping centers where vegetation is scarce. Forests, larger urban parks, and water bodies were always coolest [65,71,74,85]. Not surprisingly, due to increased heat storage capacity and shadowing, urban areas were often reported to have slower warming and cooling pace [60,67,69]. In Minneapolis, USA, a snow cover of 5 cm or more was reported to increase the UHI by about 1 °C due to a higher albedo during the day and 0.5 °C at night because of enhanced insulation properties, compared to same weather conditions, just without snow [68,72]. Moderate snowfall decreased the magnitude of the UHI by up to 2 °C [68].

A considerable amount of research has been conducted in Barrow in Northern Alaska, USA (now Utqiaġvik), one of the few locations in climate type ET. Despite the small size of the settlement (around 4.500 inhabitants), a distinct winter-UHI has been measured, amounting to 2.2 °C on average and reaching up to 6 °C [57]. A strong correlation between the UHI-intensity and anthropogenic heat release (consumption of natural gas) was reported [66]. Both studies mention a reduction in freezing degree days [57,66]. Furthermore, summer soil-surface temperatures were reported to be between 0.3 and 2.3 °C higher in the city. This caused the active layer (the near-surface layer of the soil that freezes and thaws annually) to be 15–40 cm thicker in urban than in rural locations [70]. Similar results were obtained in an earlier study, where the active layer was indicated even 25–55 cm thicker [63].

Some of the largest settlements by population above the Arctic Circle are situated in Russia. In Apatity, Konstantinov et al. [73] made use of MODIS satellite images and field measurements to quantify the urban-rural temperature differences. The mean UHI magnitude of a three-day period in January 2014 was 2.7 °C from the satellite images and 1.6 °C from the field measurements. Differences got as high as 4–5 °C. Other studies in Apatity [87], and Apatity and Kirovsk [82] reported similar results.

In a comprehensive study, the UHI characteristics of 28 cities in northern West Siberia were analyzed from MODIS imagery [79]. All cities are located above 60° N with populations from just a few in Bovanenkovskiy in the very North of the region, up to around 330 000 in Surgut in the South. Despite the very low mean annual surface air temperatures of between −2 and −9 °C and permafrost soil [92], the mean summer UHI was 0.5–2.5 °C. Only in the three northernmost (and quite small) towns Yar-Sale, Bovanenkovskiy, and Tazovskiy, a cool island of −0.5 to −1.7 °C was detected. In winter, the UHI ranges from around 0.2 to 3.1 °C. Only in the city of Surgut, where a huge gas-fired power plant changes LST significantly, the UHI reaches 8 °C on average in winter. A study using on-site measurements in a smaller subset of cities in the same region reports a UHI intensity in a similar magnitude [83]. In this category's most recent study, a similar UHI intensity was reported in the city of Nefteyugansk, near Surgut (2.4 °C in summer and 2.1 °C in winter) [90].

Sun et al. [75] compared the CLHI and the remotely measured SLHI in Beijing, China. They report greater differences during the daytime than during the nighttime. The daytime difference had a noticeable seasonal variation that was small and negative in cold seasons but large and positive in warm seasons. The night-time difference was not subjected to significant seasonal variation. A similar study in Berlin, focusing on the differences between remotely measured LST and air temperature in 2 m height, found a quite opposing relationship. The correlation was reported higher during cold seasons than in warm seasons, and higher during daytime than during night-time [84].

3.2.2. UHI-other

In this category, articles of several different research areas around the UHI that are not primarily focusing on its intensity or mitigation strategies are collected (see Table 7). However, there are partly overlaps to other categories, especially when it comes to the categories *UHI-Mag* and *UHI-Mit*.

Some of the studies used NMV to investigate how new construction will affect the UHI or the microclimate in urban areas [34,100]. Using single- and multilayer parametrizations, two studies conducted simulations with the coupled *Ocean-Atmosphere Mesoscale Prediction System* and different urban canopy parametrizations to assess their impact in a mesoscale model of New York in the USA [56,95].

Another two studies were dedicated to predicting urban-rural temperature differences. While one study in Turku, Finland used variables from Geographical Information System (GIS) databases [97], a study in Ljutomer, Slovenia, used a geospatially weighted regression model to predict the urban-rural temperature differences in different weather patterns [107]. Similar to other studies mentioned before, e.g. Ref. [80,83,87], they found the UHI intensity was highest during anticyclonic weather patterns. However, predictions were most accurate during cyclonic weather patterns [107]. Lemonsu et al. [96] used the TEB and the *Interactions between Soil, Biosphere, and Atmosphere parametrization* to simulate surface radiation and energy exchanges in Montreal, Canada. Simulations showed good performance when the roads were snow-covered. Snowmelt and anthropogenic heat fluxes were reasonably well represented, whereas storage heat flux was underestimated.

Bokwa et al. [99] proposed a relief-modified UHI (RMUHI) approach since in cities that are located in concave landforms, the impact of land use and relief on air temperature cannot be separated from one another. Their RMUHI approach consists of two steps: (1) recognition of the areal thermal structure taking into consideration the city center as a reference

Table 7
Overview of studies in the category "UHI-Other"

No.	Authors	Year	Location, Country	Climate	Method
1	Nkemdirim [93]	1980	Calgary, Canada	Dfb	M-OS
2	Hinkel et al. [94]	2004	Barrow, USA	ET	M-OS
3	Pullen et al. [95]	2006	New York/New Jersey, USA	Dfa	M – OS, NMV
4	Holt and Pullen [56]	2007	New York, USA	Dfa	M – OS, NMV
5	Lemonsu et al. [96]	2010	Montreal, Canada	Dfb	M – OS, NMV
6	Hjort et al. [97]	2011	Turku, Finland	Dfb	M-OS
7	Arola and Korkka-Niemi [98]	2014	Turku, Lohja, and Lahti, Finland	Dfb/Dfc	M-OS
8	Bokwa et al. [99]	2015	Kraków, Poland	Dfb	M-OS
9	Fang et al. [100]	2015	Beijing, China	Dwa	M – OS, NMV, M-RS
10	Berardi et Wang [101]	2016	Toronto, Canada	Dfb	M – OS, NMV
11	Hatchett et al. [102]	2016	Reno, USA	Dsb	M-OS
12	Klimenko et al. [103]	2016	Large cities in Russia, Poland and Germany	Dfb	M-OS
13	Lokoshchenko et al. [104]	2016	Moscow, Russia	Dfb	M-OS
14	Wicki and Parlow [105]	2017	Basel, Switzerland	Dfb	M-RS
15	Fu and Weng [106]	2018	Numerous cities in the US	Dwb/ Dfa/Dfb/ Dfc	M-RS
16	Ivajnšič and Žiberna [107]	2018	Ljutomer, Slovenia	Dfb	M – OS, NMV
17	He et al. [108]	2019	Shenyang, China	Dwa	M-RS

Abbreviations: On-site measurements (M – OS); Remote-sensed measurements (M-RS); Numerical models with validation (NMV).

point and (2) calculation of RMUHI intensity separately for each vertical zone. Using helicopter transacts in Calgary, Canada, it was found that the influence of relief, or more precisely of cold air drainage from the surrounding hills reduced the magnitude of the UHI by about 40% of its potential value [93].

Arola and Korkka-Niemi [98] investigated groundwater temperature differences in southern Finland. They found that the average temperature below the zone of seasonal temperature fluctuations (from around 8 m depth) was 1.3–2.0 °C higher in the urban area and 3–4 °C higher in the city centers than in the rural areas. They estimate that 50–60% more peak heating power could be utilized from a groundwater-based heat pump in populated areas. Simultaneously 40–50% peak cooling power is lost through the higher temperatures.

Two studies were dedicated to the relationships between LST and land use/land cover (LULC). He et al. [108] investigated the impact of background temperature on the performances of cool/hot sources in either enhancing or mitigating the LST. Wicki and Parlow [105] analyzed the dependence of LST on LULC and found a stronger correlation during warmer summer months and the increasing influence of the topography and albedo during colder seasons. Both studies confirmed the frequently reported positive relationship between higher LST in industrially and commercially dominated surface patches and the negative relationship between forests or highly vegetated surface patches [65,71,74,85].

3.2.3. UHI-mitigation

Despite the cold or polar climate classification, several cities face pronounced heat waves and thus overheating during summer. In this category, those dedicated to mitigating the adverse effects of the UHI are collected (see Table 8).

Two Canadian studies used the numerical micro-scale climate model

Table 8
Overview of studies in the category "UHI-Mit"

No.	Authors	Year	Location, Country	Climate	Method
1	Jianying et al. [109]	2015	Cleveland, USA	Dfb	M-OS
2	Touchaei and Akbari [110]	2015	Montreal, Canada	Dfb	M – OS, NMV
3	Kim et al. [111]	2016	Seoul, South Korea	Dwa	M – OS, NMV
4	Wang and Akbari [112]	2016	Montreal, Canada	Dfb	M – OS, NMV
5	Wang et al. [58]	2016	Toronto, Canada	Dfb	M – OS, NMV
6	Chun and Guldmann [113]	2018	Columbus, USA	Dfa	M-RS
7	Jiang et al. [114]	2018	Xi'an, China	Dwa	M-OS

Abbreviations: On-site measurements (M – OS); Remote-sensed measurements (M-RS); Numerical models with validation (NMV).

ENVI-met to analyze different UHI mitigation strategies in Montreal and Toronto. In Montreal, vegetation planting and an increased urban albedo can reduce the UHI effect during the day, while urban sky view factor (SVF) control can reduce the UHI effect at nighttime [112]. Urban typology and urban vegetation shading affected solar radiation storage during the summer day in Toronto and contributed to the UHI mitigation. By adding 10% of urban vegetation, the outdoor air temperature could be reduced by 0.5–0.8 °C in the day time [58]. The positive effects of urban greenery were furthermore emphasized in a study in Seoul, South Korea [111] and Columbus, Ohio, USA [113]. However, in an article investigating the cooling potential of an increased albedo in Montreal and the impact on annual energy demands of heating, ventilation and air-conditioning (HVAC) systems found only a minor financial saving potential of around 1 $/100 m^2 urban area [110].

Two studies dealt with experimental investigations on asphalt composition since their impervious and dark surfaces contribute strongly to the UHI. It was found that thermoelectric asphalt pavements can reduce the surface temperature by 8–9 °C in hot seasons by simultaneously generating electricity. The output of a 1 km long and 10 m wide surface was quantified with 33 kWh on a single day in summer [114]. The other article studied the asphalt's optical properties when thermochromic powder is added to a conventional asphalt binder. They report that a thermochromic asphalt binder can reduce the surface temperature during summer and increase it during winter. This way, it contributes to the asphalt's durability and mitigates the adverse effects of the UHI in summer [109].

3.2.4. Other urban meteorological phenomena

This section collects articles on different other urban meteorological phenomena (see Table 9).

Some articles were dedicated for example to the urban-rural humidity difference [115], the statistical properties of low-level jets [116], or low-level temperature inversions [117]. Other addressed the magnitude of nighttime air temperature differences between an urban park and a built-up area [59], the simulation of nighttime cold airflow from near-by mountains [123], or the occurrence of cold days and cold waves [124].

The urban energy balance was the object of investigation in three articles. In particular, one study focused on the area-averaged sensible heat flux [125], another used measurements on a 325-m tower in downtown Beijing to quantify the energy balance of the urban surface [61]. The third study investigated the performance of three urban land-surface models for two distinctly different sites in Helsinki. They suggested that improvements are needed in the parametrization of anthropogenic heat flux, thermal parameters in winter, snow cover in spring, and evapotranspiration [119]. Generally, all models had the most difficulties in simulating the latent heat flux.

Multiple studies confirmed the significant influence of cities on

Table 9
Overview of studies in the category "OUMP"

No.	Authors	Year	Location, Country	Climate	Method
1	Unger [115]	1999	Szeged, Hungary	Dfb	M-OS
2	Upmanis and Chen [59]	1999	Gothenburg, Sweden	Dfb	M-OS
3	Kallistratova and Kouznetsov [116]	2011	Moscow, Russia	Dfb	M-OS
4	Miao et al. [61]	2012	Beijing, China	Dwa	M-OS
5	Stryhal et al. [117]	2015	Prague, Czech Republic	Dfb	M-RS
6	Zhong and Yang [118]	2015	Beijing, China	Dwa	M – OS, NMV
7	Karsisto et al. [119]	2016	Helsinki, Finland	Dfb	M – OS, NMV
8	Li et al. [120]	2017	Beijing, China	Dwa	M – OS, NMV
9	Li et al. [121]	2017	Beijing, China	Dwa	M – OS, NMV
10	Johnson and Shepherd [122]	2018	Northeastern US	Dfa/ Dfb	M-OS
11	Son et al. [123]	2018	Gwangju, South Korea	Dfb	M – OS, NMV, M-RS
12	Tomczyk et al. [124]	2018	Poznań, Poland	Dfb	M-OS
13	Zieliński et al. [125]	2018	Łódź, Poland	Dfb	M-OS

Abbreviations: On-site measurements (M – OS); Remote-sensed measurements (M-RS); Numerical models with validation (NMV).

precipitation events [118,120–122]. Johnson and Shepherd [122] concluded that in the northeastern USA, the boundary layer UHI may play an important role in increasing the melting of hydrometeors. Proximity to urban centers plays a role in the surface observation of mixed precipitation events.

3.2.5. Biometeorology

The term biometeorology comprises the interactions between atmospheric processes and living organisms, i.e. plants, animals and humans [126]. Due to the focus of this systematic review on climate-human interactions, studies addressing plants and animal species have been excluded. Most of the studies that used a survey (S) as research method (3 out of 4) are embodied in this category. Comfort and wellbeing were the most frequently covered topics in this category. The studies in this category are summarized in Table 10.

A survey in the subarctic Finnish town of Kuopio reported that green spaces and time spent in nature were associated with high levels of comfort and wellbeing (CW) while cold housing and poor indoor air quality were related with low levels of CW [137]. An experiment in an urban park in Xi'an, China indicated that CW and thermal sensation closely correlated. In winter, most important factors affecting CW were global radiation, followed by air temperature and relative humidity. Wind speed was found to be least important [141].

Three articles studied the meteorological factors influencing comfort in the Polish cities Szczecin, Warsaw and Gdańsk. Generally, the studies agree that close to the city center "hot" conditions appear more and "cold" less often than in the outskirts. Therefore, the outskirts provide a more favorable microclimate during summer but the city during winter [128,130,132]. Dursun and Yavaş [140] used simulations with ENVI-Met and measurements in Erzurum, Turkey, to investigate the relationship between microclimate and urban planning, specifically in terms of CW. Results indicated that irregular building plots and heights led to more favorable microclimatic conditions than regular ones. Targhi and van Dessel [133] studied the summer conditions in Worcester, Massachusetts USA. They found considerable differences in heat stress for pedestrians between street canyons of different orientations in July. Especially at around noon, the East-West configuration led to extreme values of the Physiological Equivalent Temperature (PET) [142] of around 50 °C, while maximum values of a North-South oriented canyon in the afternoon hours led to a PET of only around 30–40 °C [133].

Table 10
Overview of studies in the category "BM"

No.	Authors	Year	Location, Country	Climate	Method
1	Taesler [127]	1991	–	–	Rev
2	Czarnecka et al. [128]	2011	Szczecin, Poland	Dfb	M-OS
3	Bauche et al. [129]	2013	Birobidzhan, Russia	Dwb	M-OS
4	Majewski et al. [130]	2014	Warsaw, Poland	Dfb	M-OS
5	Urban et al. [131]	2014	Prague and Bohemia, Czech Republic	Dfb	M-OS
6	Nidzgorska-Lencewicz [132]	2015	Gdańsk, Poland	Dfb	M-OS
7	Targhi and van Dessel [133]	2015	Worcester, USA	Dfb	M – OS, NMV
8	Coccolo et al. [134]	2016	–	D/E	Rev
9	Lowe [135]	2016	Several in Northern USA	Dfa/Dfb	M-RS
10	Chapman et al. [136]	2017	Luleå, Sweden	Dfc	S
11	Hiscock et al. [137]	2017	Kuopio, Finland	Dfc	S
12	Petrov et al. [138]	2017	Samburg, Russia	Dfc	M-OS
13	Chi et al. [139]	2018	Several Cities in China	Dwa/ Dwb	M-OS
14	Dursun and Yavaş [140]	2018	Erzurum, Turkey	Dsa	M – OS, NMV
15	Xu et al. [141]	2018	Xi'an, China	Dwa	M – OS, S

Abbreviations: On-site measurements (M – OS); Remote-sensed measurements (M-RS); Numerical models with validation (NMV); Review (Rev); Survey (S).

Another component of biometeorology is the impact of meteorological factors on people's health. Bauche et al. [129] investigated the effect of urban structures on human thermal comfort indices in the extreme climate of Birobidzhan in the Russian Far East, where the annual temperature can range from around −30 °C to +30 °C. The winter conditions lead to extreme cold stress with a PET below −20 °C in about 70% of the time in January. Urban et al. [131] examined the heat- and cold-stress related cardiovascular morbidity and possible regional differences in the Czech Republic, namely the city of Prague and the rural region of southern Bohemia from 1994 to 2009. They reported a generally higher relative cardiovascular excess mortality on warm compared to cold days. The results furthermore indicated slight differences in population vulnerability between the two regions, due to environmental and socioeconomic factors. Petrov et al. [138] considered the impact of urbanization and climatic conditions on the health status of the indigenous Nenets people in Samburg, Russia, by taking blood samples and correlating immunological parameters with climatic indicators. Lowe [135] analyzed the impact of the UHI on energy and mortality. He found that in the north of the US, energy use decreased from the UHI as heating energy reductions were larger than cooling energy increase. At the same time, cold-related deaths were estimated with a decrease of 4 deaths per million people. Hypothermia-related death rates were three times higher in rural areas than in urban areas. A surprising result, considering that homeless people that predominantly live in urban areas are usually considered the most at risk.

Teasler [127] collected research and elaborated on the processes of the urban atmosphere in temperate and high-latitude locations. He stressed the need for relevant bioclimatic design tools. Certainly, regarding the almost three-decade spanning period of time in between his study and today, a great amount of computational progress has been made and a variety of tools and models have been developed to assess and quantify thermal comfort in outdoor spaces. The Universal Thermal

Climate Index (UTCI) [143] or the PET, for instance, can be obtained spatially resolved from several numerical tools. Another review of tools for modelling outdoor human comfort and thermal stress was conducted by Coccolo et al. [134].

3.2.6. Air pollution

Anthropogenic pollution is considered to be one of the main threats to physiological systems and the environment [144]. Especially urban air is frequently linked to medical risks. Several studies were thus dedicated to air pollution, e.g. the variation of toxicants and the coefficient of haze [47], the air pollution concentration of particulate matter (PM) [145] or air pollution levels an ancient city U-type street canyon in China [146] (see Table 11).

Leahey and Hansen [147] presented a method for estimating the CO_2 flux from Calgary, Canada, during nocturnal periods characterized by stable air. Cheng et al. [148] studied the seasonal and diurnal patterns of gaseous elementary mercury (GEM), gaseous oxidized mercury (GOM) and particle-bound mercury (PBM) in Dartmouth, Canada.

Because trees can contribute actively to air pollution through the emission of Biogenic Volatile Organic Compounds (BVOC) in particular conditions, Fierravanti et al. [149] gave an overview of reference cities for expanding research on this issue. However, several publications that were not identified by the search methodology indicated that urban trees are able to reduce the concentration of pollutants like traffic emissions in the air [150–155]. On the other hand, some studies point to the diminished ventilation ability in urban tree canopies and thus locally higher pollutant concentrations, e.g. Ref. [156].

3.2.7. Time series analysis

A time series is defined as a collection of observations taken sequentially in time [157]. In the case of meteorological observations, those are often long-time records over several years, decades or even centuries. They are usually analyzed to extract statistically relevant information or correlations to other covariates or trends. Table 12 summarizes the studies in this category.

The articles in this category frequently reported increasing temperatures during the times of observation. In the 175-year temperature records of Oslo, Norway, Nordli et al. [160] found a significant increase of annual mean temperature (1.5 °C), which mainly occurred during the last 50 years and in the early 20th century. Especially cold seasons were affected the most by the changes, as temperatures in winter and spring increased more than twice as much as in summer.

Anderson and Gough [161] contextualized the pronounced cold-anomaly winters of 2013/14 and 2014/15 in Toronto, Canada within historical weather observations. Toronto winter temperatures have warmed significantly during the history of the weather records since 1840, especially the December temperatures. Urbanization and the UHI are supposed to contribute considerably to the local conditions since Toronto's weather station is situated in the very center of the city.

Lokoshchenko et al. [162] used long-term radiosonde measurements and sensors installed on a television tower in Moscow, Russia from 1991 to 2013 to investigate the lower 4-km layer of the atmosphere. During this period, the mean annual temperature at all heights from 2 to 4000 m increased by an average of 0.1 °C per year, with the warming slowing down in the more recent years.

In the Huang-Huai-Hai river basin in China, the daily maximum temperature increased with a magnitude of 0.15 °C per decade on the regional scale from 1961 to 2014. The increase of daily minimum temperatures was even more pronounced with 0.49 °C per decade. Due to rapid urbanization, the UHI is assumed to have an impact on the amplitude of variations in extreme temperatures [163].

In Erzurum in Turkey, population growth, the number of vehicles, buildings and green area amount in the city had no significant effect on mean air temperatures from 1950 to 2005. However, the relationships partly between population growth and maximum temperature and partly between the number of vehicles and minimum temperature were found to be statistically significant [158].

Wang et al. [159] quantified the impact of urbanization on changes in observed surface air temperatures and temperature extremes in Beijing, China, between 1978 and 2008. They found that at urbanized sites an added warming trend in annual mean temperature occurred. Urbanization has furthermore increased the amount of extremely warm nights and decreased the amount of extremely cold nights at the urbanized sites.

3.2.8. Urban and atmospheric boundary layer

Only two articles specifically focused on the structure of the urban boundary layer (UBL) or the atmospheric boundary layer (ABL) (see Table 13).

Sang et al. [164] studied the characteristics of the winter UBL in Shenyang, China. Observations showed that with light winds the ground inversion at nighttime was around 200 m deep and that anthropogenic heating caused a heat island circulation that induced reverse flow at the downwind part of the city. Lee and Baik [165] compared simulation results from coupling the Vegetated Urban Canopy Model with the Regional Atmospheric Modeling System with meteorological observations in Seoul, South Korea. The results indicate a similar size of the nighttime UBL of about 100–200 m, as in Shenyang [164].

3.2.9. Other

One included paper could not be categorized by one of the previously presented categories, as it addresses a quite different perspective of

Table 11
Overview of studies in the category "AP"

No.	Authors	Year	Location, Country	Climate	Method
1	Nkemdirim et al. [47]	1975	Calgary, Canada	Dfb	M-OS
2	Leahey and Hansen [147]	1992	Calgary, Canada	Dfb	M-OS
3	Górka-Kostrubiec et al. [145]	2012	Warsaw, Poland	Dfb	M-OS
4	Cheng et al. [148]	2014	Dartmouth, Canada	Dfb	M-OS
5	Cui et al. [146]	2017	Xi'an, China	Dwa	M-OS
6	Fierravanti [149]	2017	–	various	Rev

Abbreviations: On-site measurements (M – OS); Review (Rev).

Table 12
Overview of studies in the category "TSA"

No.	Authors	Year	Location, Country	Climate	Method
1	Yilmaz et al. [158]	2009	Erzurum, Turkey	Dsa	M-OS
2	Wang et al. [159]	2013	Beijing, China	Dwa	M-OS
3	Nordli et al. [160]	2015	Oslo, Norway	Dfb	M-OS
4	Anderson and Gough [161]	2017	Toronto, Canada	Dfb	M-OS
5	Lokoshchenko et al. [162]	2017	Moscow, Russia	Dfb	M-OS
6	Wang et al. [163]	2018	Huang-Huai-Hai River Basin, China	Dwa/ Dwb	M-OS

Abbreviations: On-site measurements (M – OS).

Table 13
Overview of studies in the category "UBL/ABL"

No.	Authors	Year	Location, Country	Climate	Method
1	Sang et al. [164]	2000	Shenyang, China	Dwa	M – OS, NMV
2	Lee and Baik [165]	2011	Seoul, South Korea	Dwa	M – OS, NMV

Abbreviations: On-site measurements (M – OS); Numerical models with validation (NMV).

microclimate. This article by Ebrahimabadi et al. [166] focused specifically on the problems of incorporating microclimatic factors into urban planning practices in subarctic northern Sweden (climate type Dfc). They conducted a literature study and interviewed planning practitioners. Some of the major problems identified are the lack of design knowledge relevant to cold climate, lack of user-friendly tools to analyze microclimate, overlooking the potential uses of local climate, and lack of support from politicians.

4. Discussion

Most of the studies in this systematic review addressed the UHI effect as a primary topic (58 out of 101). The reviewed studies indicate that the UHI is a common phenomenon in cold polar climate locations with UHI intensities of up to 10–12 °C being reported (e.g. Refs. [53,87]). While commonly, the UHI is most pronounced during summer nights, winter heat islands are usually weaker and occur less often. Despite the cold or polar climate conditions, the UHI can lead to excessive heat during summer. Some of the articles, therefore, focused on mitigation strategies (e.g. Refs. [58,110,112]). However, the UHI was reported to lead to greater heating energy savings than cooling energy increases on an annual basis in two studies [103,135]. Many studies were furthermore dedicated to understanding the structure and the temporal and spatial variability of the UHI, often by using numerical tools [95,97].

However, it needs to be pointed out that the results and especially the UHI-magnitudes of the reviewed studies are not directly comparable with one another. This is because methodologies, season, time of the day, measurement periods and equipment, elevations of (and differences in elevation between) the city weather station and its "non-urban" counterpart in the studies varied significantly. Those "non-urban" stations were sometimes parks, airports, suburbs, intraurban (within urban areas) locations of different typology or rural areas located outside the city.

Even more importantly, every city is different from each other. They differ with respect to population, extension and density, amount of green spaces, building density and typologies, height profile, centrality (what can be actually characterized as a city center) and furthermore building standards. Due to the typically longer absence of the sun in cold and polar climate during winter, the heat islands are often substantially supported by urban self-heating, mainly as a result of anthropogenic heat release and the urban fabric's increased heat storage capacity [66,87]. The anthropogenic heat flux is mainly caused by building energy use and heat from vehicle transport. With a higher energy standard in buildings, it is a reasonable assumption that the anthropogenic impact is smaller in areas like Zero or Plus Energy Neighborhoods and will generally decrease in the future. Changes in urban mobility like increased use of electric vehicles is expected to further reduce anthropogenic heat emissions.

Urban microclimate also affects precipitation and vice versa [118,120–122]. These increasingly observable changes in precipitation behavior (less snow, more rain [122,136]) might furthermore influence people's mobility habits and outdoor free time activities in cold and polar climate cities more than low temperatures do. Especially in high-latitude cities, where daylight in winter is scarce, snow cover is substantially increasing outdoor lighting levels in winter [136]. And as long-time meteorological records have shown in many cities, especially winter temperatures have been rising distinctly [160,161]. Considering higher air pollution and heat stress from elevated temperatures, even cold and polar climate cities increasingly pose a risk to human health. Given that city planners might often lack relevant design knowledge for cold and polar climate conditions and even are not aware of the problems [166], the situation could aggravate.

Vegetation is a commonly used intervention in warmer climate regions to mitigate the adverse effects of the UHI. However, greenery spaces were also reported to increase the temperature in winter [113]. Considering the many other reported advantages of vegetation like pollution dispersion and removal [153–155,167], decreasing wind speeds in winter [168], and the positive effects of urban greenspaces on human health [169–174] and relaxation [175,176], it might be a key element to achieve climate-adapted cold and polar climate cities with high environmental quality and livability.

5. Conclusion

The trend towards population growth, urbanization and increasing awareness of the health issues that are connected to life in cities are expected to further increase popularity and attention on urban microclimate in the future. While there has been a considerable amount of publications in the field of urban microclimate, to the best of our knowledge, there has been no review article focusing on cold and/or polar climate locations yet.

This paper presented a systematic literature review of urban microclimate relevant publications, identified from the scientific databases Scopus and Web of Science by using a reproducible search query and eligibility criteria. In total, 101 papers have been identified for inclusion, categorized, and analyzed according to their publication year, country, climate, topic, method, keywords, citations, and publication channels. The oldest study identified was published in 1975, the most recent one in early 2019. For every category, the studies were listed in tables according to their publication year, location, climate, and method. The main findings of this review can be summarized as follows:

- The most-covered topic of the included studies in this review is the UHI. 58 of 101 studies were categorized in one of the three UHI-related categories *UHI-Mag* (34), *UHI-Mit* (7), and *UHI-Other* (17). This was also visible from the keyword analysis, where *Urban heat island* was by far the most used keyword (23) before *Urban climate* (9) and *Urban microclimate* (6). Behind *UHI-Mag* and *UHI-Other, BM* (15) is the third most researched topic.
- Considering the global population distribution in cold and polar climate areas, some climate types have been subject of research more often than others. Most articles covered locations in Dfb-climate (51), mainly from studies in North America and Europe, followed by Dwa (20), predominately from studies in China and South Korea. Dfc (15) was the third most often used climate type, mainly in studies from Russia.
- The outweighing part of studies used on-site measurements as a method for obtaining data (81), 20 used remote sensed data. In 22 studies, numerical models have been validated with measurements and used to predict the outcomes of urban redevelopments. Only 4 studies used a survey to collect data, another 4 conducted a review.

With the ongoing climate change and urbanization, UHI-related research is expected to stay dominant among publications about the urban microclimate in cold and polar climate regions. However, there is a lack of studies investigating the microclimatic characteristics and physical properties of the materials in urban design. Moreover, future research should focus more on the interactions between humans and urban climate, for instance in order to promote outdoor activities, soft mobility and comfort in cold and polar climate regions. This is seen as an aspect of major importance in sustainable urban development.

Many of the included studies used numerical tools to evaluate different design interventions or to model meteorological processes. However, during the eligibility phase of article-inclusion methodology, many simulation-only studies that did not provide sufficient validation with experimental data had to be removed. Further validation studies should be made in order to improve the reliability and user-friendliness of numerical models and tools to make them also useable for planning professionals and not limit them to research applications only.

Several climate types were not represented by any study included in the review, such as Dsa, Dsc, Dsd, Dwd, Dfd, and EF and should, therefore, be subject to future research. Even though most of these

climate regions are sparsely populated, research on those remote locations can enhance the understanding of the urban microclimate.

The outcomes of this systematic review and meta-analysis will help researchers to grasp the structure of published research and facilitate comparing obtained results with previously published studies. The statistical analysis and overview of studies provided in this article revealed core areas and side issues of current urban climate research in cold and polar climate regions. Researchers can use this information to quickly find published articles covering their topic of interest and identify gaps for future research possibilities.

Ongoing climate change and the particular vulnerability of cold and polar climate regions make it especially important to disseminate knowledge among planning professionals to adopt climate adaption strategies for sustainable urban development. Therefore, studies focusing specifically on measures for improving urban microclimatic conditions in cold and polar climate regions are needed to advise planners and municipalities.

Declaration of competing interest

The authors declare that they have no known competing financial interests or personal relationships that could have appeared to influence the work reported in this paper.

Acknowledgements

This paper has been written within the Research Centre on Zero Emission Neighbourhoods in Smart Cities (FME ZEN). The authors gratefully acknowledge the support from the ZEN partners and the Research Council of Norway.

References

[1] UN Environment, International Energy Agency. Towards a zero-emission, efficient, and resilient buildings and construction sector: global Status Report 2017. 2017.
[2] Edenhofer O, editor. Climate change 2014: contribution of working group III to the fifth assessment report of the intergovernmental panel on climate change: mitigation of climate change. New York (USA): Cambridge Univ. Pr; 2014.
[3] United Nations, Department of Economic, Affairs Social, Division Population. World population prospects: key findings and advance tables. 2017.
[4] United Nations, Department of Economic, Affairs Social, Division Population. World urbanization prospects: the 2018 revision. New York, USA: Online Edition; 2018.
[5] UK: Met Office. Microclimates. Devon; 2011.
[6] American Meteorological Society. Glossary of Meteorology. [September 21, 2020]; Available from: http://glossary.ametsoc.org/wiki/Microscale.
[7] Orlanski I. A rational subdivision of scales for atmospheric processes. Bull Am Meteorol Soc 1975;56(5):527–30.
[8] Howard L. The climate of London deduced from meteorological observations made in the metropolis and at various places around it. second ed. London: Harvey and Darton; J. Rickerby; 1833.
[9] Oke TR, Mills G, Christen A, Voogt JA. Urban climates. Cambridge: Cambridge University Press; 2017.
[10] Erell E, Pearlmutter D, Williamson T. Urban microclimate: designing the spaces between buildings. London: Earthscan; 2011.
[11] Kratzer A. The climate of cities (Das Stadtklima). In: Bedford mass. second ed. Air Force Cambridge Research Laboratories; 1956.
[12] Oke TR. The energetic basis of the urban heat island. Q J Roy Meteorol Soc 1982; 108(455):1–24. https://doi.org/10.1002/qj.49710845502.
[13] Balchin WGV, Pye N. A micro-climatological investigation of Bath and the surrounding district. Q J Roy Meteorol Soc 1947;73(317–318):297–323.
[14] Oke TR. Urban heat islands. In: Douglas I, Goode D, Houck M, Maddox D, editors. The routledge handbook of urban ecology. first ed. London: Routledge; 2011. p. 120–31.
[15] Stewart ID, Oke TR. Local climate zones for urban temperature studies. Bull Am Meteorol Soc 2012;93(12):1879–900. https://doi.org/10.1175/BAMS-D-11-00019.1.
[16] Oke TR. City size and the urban heat island. Atmos Environ 1973;7(8):769–79. https://doi.org/10.1016/0004-6981(73)90140-6.
[17] Chandler TJ. Selected bibliography on urban climate. 1970. Geneva, Switzerland.
[18] Oke TR. The distinction between canopy and boundary-layer urban heat islands. Atmosphere 1976;14(4):268–77.
[19] Eliasson I, Holmer B. Urban heat island circulation in Göteborg, Sweden. Theor Appl Climatol 1990;42(3):187–96. https://doi.org/10.1007/BF00866874.
[20] Shreffler JH. Detection of centripetal heat-island circulations from tower data in St. Louis. Bound-Layer Meteorol 1978;15(2):229–42.
[21] Wong KK, Dirks RA. Mesoscale perturbations on airflow in the urban mixing layer. J Appl Meteorol 1978;17:677–88.
[22] Vukovich FM, King WJ, Dunn JW, JJB Worth. Observations and simulations of the diurnal variation of the urban heat island circulation and associated variations of the ozone distribution: a case study. J Appl Meteorol 1979;18(7): 836–54. https://doi.org/10.1175/1520-0450(1979)018<0836:OASOTD>2.0.CO;2.
[23] Hidalgo J, Masson V, Gimeno L. Scaling the daytime urban heat island and urban-breeze circulation. J Appl Meteorol Climatol 2010;49(5):889–901. https://doi.org/10.1175/2009JAMC2195.1.
[24] Ryu Y-H, Baik J-J, Han J-Y. Daytime urban breeze circulation and its interaction with convective cells. Q J Roy Meteorol Soc 2013;139(671):401–13. https://doi.org/10.1002/qj.1973.
[25] Mills G. Urban climatology: history, status and prospects. Urban Clim 2014;10: 479–89. https://doi.org/10.1016/j.uclim.2014.06.004.
[26] Toparlar Y, Blocken B, Vos PEJ, van Heijst GJF, Janssen WD, van Hooff T, et al. CFD simulation and validation of urban microclimate: a case study for Bergpolder Zuid, Rotterdam. Build Environ 2015;83:79–90. https://doi.org/10.1016/j.buildenv.2014.08.004.
[27] Masson V. A physically-based scheme for the urban energy budget in atmospheric models. Bound-Layer Meteorol 2000;94(3):357–97.
[28] Masson V, Grimmond CSB, Oke TR. Evaluation of the town energy balance (TEB) scheme with direct measurements from dry districts in two cities. J Appl Meteorol 2002;41(10):1011–26.
[29] Bruse M, Fleer H. Simulating surface–plant–air interactions inside urban environments with a three dimensional numerical model. Environ Model Software 1998;13(3–4):373–84. https://doi.org/10.1016/S1364-8152(98)00042-5.
[30] Shahidan MF, Jones PJ, Gwilliam J, Salleh E. An evaluation of outdoor and building environment cooling achieved through combination modification of trees with ground materials. Build Environ 2012;58:245–57. https://doi.org/10.1016/j.buildenv.2012.07.012.
[31] Simon H, Lindén J, Hoffmann D, Braun P, Bruse M, Esper J. Modeling transpiration and leaf temperature of urban trees – a case study evaluating the microclimate model ENVI-met against measurement data. Landsc Urban Plann 2018;174:33–40. https://doi.org/10.1016/j.landurbplan.2018.03.003.
[32] Zhang H, Gao Z, Ding W, Zhang W. Numerical study of the impact of green space layout on microclimate. Process Eng 2017;205:1762–8. https://doi.org/10.1016/j.proeng.2017.10.027.
[33] Chokhachian A, Santucci D, Auer T. A human-centered approach to enhance urban resilience, implications and application to improve outdoor comfort in dense urban spaces. Buildings 2017;7(4):113. https://doi.org/10.3390/buildings7040113.
[34] Berardi U. The outdoor microclimate benefits and energy saving resulting from green roofs retrofits. Energy Build 2016;121:217–29. https://doi.org/10.1016/j.enbuild.2016.03.021.
[35] Castaldo VL, Pisello AL, Piselli C, Fabiani C, Cotana F, Santamouris M. How outdoor microclimate mitigation affects building thermal-energy performance: a new design-stage method for energy saving in residential near-zero energy settlements in Italy. Renew Energy 2018;127:920–35. https://doi.org/10.1016/j.renene.2018.04.090.
[36] Deng J-Y, Wong NH, Zheng X. The study of the effects of building arrangement on microclimate and energy demand of CBD in Nanjing, China. Process Eng 2016; 169:44–54. https://doi.org/10.1016/j.proeng.2016.10.006.
[37] Jin H, Shao T, Zhang R. Effect of water body forms on microclimate of residential district. Energy Proc 2017;134:256–65. https://doi.org/10.1016/j.egypro.2017.09.615.
[38] Wei R, Song D, Wong NH, Martin M. Impact of urban morphology parameters on microclimate. Process Eng 2016;169:142–9. https://doi.org/10.1016/j.proeng.2016.10.017.
[39] Moonen P, Defraeye T, Dorer V, Blocken B, Carmeliet J. Urban Physics: effect of the micro-climate on comfort, health and energy demand. Front Archit Res 2012; 1(3):197–228. https://doi.org/10.1016/j.foar.2012.05.002.
[40] Peel MC, Finlayson BL, McMahon TA. Updated world map of the Köppen-Geiger climate classification. Hydrol Earth Syst Sci Discuss 2007;4(2):439–73. https://doi.org/10.5194/hessd-4-439-2007.
[41] Booth A, Carroll C. Systematic searching for theory to inform systematic reviews: is it feasible? Is it desirable? Health Inf Libr J 2015;32(3):220–35. https://doi.org/10.1111/hir.12108.
[42] Moher D, Liberati A, Tetzlaff J, Altman DG. Preferred reporting items for systematic reviews and meta-analyses: the PRISMA statement. Int J Surg 2010;8 (5):336–41. https://doi.org/10.1016/j.ijsu.2010.02.007.
[43] Bustami RA, Belusko M, Ward J, Beecham S. Vertical greenery systems: a systematic review of research trends. Build Environ 2018;146:226–37. https://doi.org/10.1016/j.buildenv.2018.09.045.
[44] Mavrigiannaki A, Ampatzi E. Latent heat storage in building elements: a systematic review on properties and contextual performance factors. Renew Sustain Energy Rev 2016;60:852–66. https://doi.org/10.1016/j.rser.2016.01.115.
[45] Schatzmann M, Rafailidis S, Pavageau M. Some remarks on the validation of small-scale dispersion models with field and laboratory data. J Wind Eng Ind Aerod 1997;67–68:885–93. https://doi.org/10.1016/S0167-6105(97)00126-8.

[46] Schatzmann M, Leitl B. Issues with validation of urban flow and dispersion CFD models. J Wind Eng Ind Aerod 2011;99(4):169–86. https://doi.org/10.1016/j.jweia.2011.01.005.
[47] Nkemdirim LC, Lunn GR, Rowe RD. Pollutant concentration and stratification in urban heat island. Water Air Soil Pollut 1975;4(1):99–112.
[48] Bowling SA, Benson CS. Study of the subarctic heat Island at Fairbanks. 1978. Alaska.
[49] Wolf T, Esau I, Reuder J. Analysis of the vertical temperature structure in the Bergen valley, Norway, and its connection to pollution episodes. J Geophys Res Atmos 2014;119(18):10,645–10,662. https://doi.org/10.1002/2014JD022085.
[50] Ezau IN, Wolf T, Miller EA, Repina IA, Troitskaya YI, Zilitinkevich SS. The analysis of results of remote sensing monitoring of the temperature profile in lower atmosphere in Bergen (Norway). Russ Metorol Hydrol 2013;38(10):715–22. https://doi.org/10.3103/S1068373913100099.
[51] Wolf T, Esau I. A proxy for air quality hazards under present and future climate conditions in Bergen, Norway. Urban Clim 2014;10:801–14. https://doi.org/10.1016/j.uclim.2014.10.006.
[52] Hancock H, Prokop A, Eckerstorfer M, Hendrikx J. Combining high spatial resolution snow mapping and meteorological analyses to improve forecasting of destructive avalanches in Longyearbyen, Svalbard. Cold Reg Sci Technol 2018;154:120–32. https://doi.org/10.1016/j.coldregions.2018.05.011.
[53] Kłysik K, Fortuniak K. Temporal and spatial characteristics of the urban heat island of Łódź, Poland. Atmos Environ 1999;33(24–25):3885–95. https://doi.org/10.1016/S1352-2310(99)00131-4.
[54] Kim Y-H, Baik J-J. Spatial and temporal structure of the urban heat island in Seoul. J Appl Meteorol 2005;44:591–605.
[55] Gedzelman SD, Austin S, Cermak R, Stefano N, Partridge S, Quesenberry S, et al. Mesoscale Aspects of the urban heat island around New York city. Theor Appl Climatol 2003;75(1–2):29–42. https://doi.org/10.1007/s00704-002-0724-2.
[56] Holt T, Pullen J. Urban canopy modeling of the New York city metropolitan area: a comparison and validation of single- and multilayer parameterizations. Mon Weather Rev 2007;135(5):1906–30. https://doi.org/10.1175/MWR3372.1.
[57] Hinkel KM, Nelson FE, Klene AE, Bell JH. The urban heat island in winter at Barrow, Alaska. Int J Climatol 2003;23(15):1889–905. https://doi.org/10.1002/joc.971.
[58] Wang Y, Berardi U, Akbari H. Comparing the effects of urban heat island mitigation strategies for Toronto, Canada. Energy Build 2016;114:2–19. https://doi.org/10.1016/j.enbuild.2015.06.046.
[59] Upmanis H, Chen D. Influence of geographical factors and meteorological variables on nocturnal urban-park temperature differences - a case study of summer 1995 in Göteborg, Sweden. Clim Res 1999;13(2):125–39.
[60] Steinecke K. Urban climatological studies in the Reykjavík subarctic environment, Iceland. Atmos Environ 1999;33(24–25):4157–62.
[61] Miao S, Dou J, Chen F, Li J, Li A. Analysis of observations on the urban surface energy balance in Beijing. Sci China Earth Sci 2012;55(11):1881–90. https://doi.org/10.1007/s11430-012-4411-6.
[62] Lee S-H, Baik J-J. Statistical and dynamical characteristics of the urban heat island intensity in Seoul. Theor Appl Climatol 2010;100(1–2):227–37. https://doi.org/10.1007/s00704-009-0247-1.
[63] Klene AE, Hinkel KM, Nelson FE. The Barrow urban heat island study: soil temperatures and active-layer thickness. Int Conf Permafrost Proc 2003:555–60.
[64] Khaikine MN, Kuznetsova IN, Kadygrov EN, Miller EA. Investigation of temporal-spatial parameters of an urban heat island on the basis of passive microwave remote sensing. Theor Appl Climatol 2006;84(1–3):161–9. https://doi.org/10.1007/s00704-005-0154-z.
[65] Lu D, Weng Q. Spectral mixture analysis of ASTER images for examining the relationship between urban thermal features and biophysical descriptors in Indianapolis, Indiana, USA. Remote Sens Environ 2006;104(2):157–67. https://doi.org/10.1016/j.rse.2005.11.015.
[66] Hinkel KM, Nelson FE. Anthropogenic heat island at Barrow, Alaska, during winter: 2001–2005. J Geophys Res 2007;112(D6):1. https://doi.org/10.1029/2006JD007837.
[67] Stopa-Boryczka M, Boryzka J, Wawer J. Impact of build-up areas and housing estate vegetation on diversity of the local climate in Warsaw. Misc Geogr 2010;14(1):121–34. https://doi.org/10.2478/mgrsd-2010-0012.
[68] Malevich SB, Klink K. Relationships between snow and the wintertime Minneapolis urban heat island. J Appl Meteorol Climatol 2011;50(9):1884–94. https://doi.org/10.1175/JAMC-D-11-05.1.
[69] Suomi J, Käyhkö J. The impact of environmental factors on urban temperature variability in the coastal city of Turku, SW Finland. Int J Climatol 2012;32(3):451–63. https://doi.org/10.1002/joc.2277.
[70] Klene AE, Nelson FE, Hinkel KM. Urban–rural contrasts in summer soil-surface temperature and active-layer thickness, Barrow, Alaska, USA. Polar Geogr 2013;36(3):183–201. https://doi.org/10.1080/1088937X.2012.706756.
[71] Walawender JP, Szymanowski M, Hajto MJ, Bokwa A. Land surface temperature patterns in the urban agglomeration of Krakow (Poland) derived from landsat-7/ETM+ data. Pure Appl Geophys 2014;171(6):913–40. https://doi.org/10.1007/s00024-013-0685-7.
[72] Schatz J, Kucharik CJ. Seasonality of the urban heat island effect in Madison, Wisconsin. J Appl Meteorol Climatol 2014;53(10):2371–86. https://doi.org/10.1175/JAMC-D-14-0107.1.
[73] Konstantinov P, Grishchenko MY, Varentsov M. Mapping urban heat islands of arctic cities using combined data on field measurements and satellite images based on the example of the city of Apatity (Murmansk Oblast). Izvestiya Atmos Ocean Phys 2015;51(9):992–8. https://doi.org/10.1134/S000143381509011X.
[74] Schatz J, Kucharik CJ. Urban climate effects on extreme temperatures in Madison, Wisconsin, USA. Environ Res Lett 2015;10(9):94024. https://doi.org/10.1088/1748-9326/10/9/094024.
[75] Sun H, Chen Y, Zhan W. Comparing surface- and canopy-layer urban heat islands over Beijing using MODIS data. Int J Rem Sens 2015;36(21):5448–65. https://doi.org/10.1080/01431161.2015.1101504.
[76] Ramamurthy P, Sangobanwo M. Inter-annual variability in urban heat island intensity over 10 major cities in the United States. Sustain Cities Soc 2016;26:65–75. https://doi.org/10.1016/j.scs.2016.05.012.
[77] Huang F, Zhan W, Wang Z, Wang K, Chen JM, Liu Y, et al. Positive or negative? Urbanization-induced variations in diurnal skin-surface temperature range detected using satellite data. J Geophys Res Atmos 2017;122(24):13,229–13,244. https://doi.org/10.1002/2017JD027021.
[78] Kuznetsova IN, Brusova NE, Nakhaev MI. Moscow urban heat island: detection, boundaries, and variability. Russ Metorol Hydrol 2017;42(5):305–13. https://doi.org/10.3103/S1068373917050053.
[79] Miles V, Esau I. Seasonal and spatial characteristics of urban heat islands (UHIs) in northern West siberian cities. Rem Sens 2017;9(10):989. https://doi.org/10.3390/rs9100989.
[80] Półrolniczak M, Kolendowicz L, Majkowska A, Czernecki B. The influence of atmospheric circulation on the intensity of urban heat island and urban cold island in Poznań, Poland. Theor Appl Climatol 2017;127(3–4):611–25. https://doi.org/10.1007/s00704-015-1654-0.
[81] Przybylak R, Uscka-Kowalkowska J, Araźny A, Kejna M, Kunz M, Maszewski R. Spatial distribution of air temperature in Toruń (Central Poland) and its causes. Theor Appl Climatol 2017;127(1–2):441–63. https://doi.org/10.1007/s00704-015-1644-2.
[82] Shumilov OI, Kasatkina EA, Kanatjev AG. Urban heat island investigations in Arctic cities of northwestern Russia. J Meteorol Res 2017;31(6):1161–6. https://doi.org/10.1007/s13351-017-7048-8.
[83] Konstantinov P, Varentsov M, Esau I. A high density urban temperature network deployed in several cities of Eurasian Arctic. Environ Res Lett 2018;13(7):75007. https://doi.org/10.1088/1748-9326/aacb84.
[84] Marzban F, Sodoudi S, Preusker R. The influence of land-cover type on the relationship between NDVI–LST and LST- Tair. Int J Rem Sens 2018;39(5):1377–98. https://doi.org/10.1080/01431161.2017.1402386.
[85] Matuzko AK, Yakubailik OE. Urban heat island effects over Krasnoyarsk obtained on the basis of Landsat 8 remote sensing data. IOP Conf Ser Earth Environ Sci 2018;211:12010. https://doi.org/10.1088/1755-1315/211/1/012010.
[86] Suomi J. Extreme temperature differences in the city of Lahti, southern Finland: intensity, seasonality and environmental drivers. Weather Clim Extrem 2018;19:20–8. https://doi.org/10.1016/j.wace.2017.12.001.
[87] Varentsov M, Konstantinov P, Baklanov A, Esau I, Miles V, Davy R. Anthropogenic and natural drivers of a strong winter urban heat island in a typical Arctic city. Atmos Chem Phys Discuss 2018;1–28. https://doi.org/10.5194/acp-2018-569.
[88] Yang J, Bou-Zeid E. Should cities embrace their heat islands as shields from extreme cold? J Appl Meteorol Climatol 2018;57(6):1309–20. https://doi.org/10.1175/JAMC-D-17-0265.1.
[89] Yao R, Wang L, Huang X, Chen J, Li J, Niu Z. Less sensitive of urban surface to climate variability than rural in Northern China. Sci Total Environ 2018;628–629:650–60. https://doi.org/10.1016/j.scitotenv.2018.02.087.
[90] Esau I, Miles V, Varentsov M, Konstantinov P, Melnikov V. Spatial structure and temporal variability of a surface urban heat island in cold continental climate. Theor Appl Climatol 2019;31(12):1990. https://doi.org/10.1007/s00704-018-02754-z.
[91] Kim Y, Guldmann J-M. Impact of traffic flows and wind directions on air pollution concentrations in Seoul, Korea. Atmos Environ 2011;45(16):2803–10. https://doi.org/10.1016/j.atmosenv.2011.02.050.
[92] International Permafrost Association. What is Permafrost? [October 18, 2018]; Available from: https://ipa.arcticportal.org/publications/occasional-publications/what-is-permafrost.
[93] Nkemdirim LC. Cold air drainage and temperature fields in an urban environment: a case study of topographical influence on climate. Atmos Environ 1980;14(3):375–81.
[94] Hinkel KM, Klene AE, Nelson FE. The summer climate of an arctic coastal village: preliminary observations from the Barrow urban heat-island study. Polar Geogr 2004;28(3):197–221. https://doi.org/10.1080/789610187.
[95] Pullen J, Holt T, Blumberg AF, Bornstein RD. Atmospheric response to local upwelling in the vicinity of New York–New Jersey harbor. J Appl Meteorol Climatol 2007;46(7):1031–52. https://doi.org/10.1175/JAM2511.1.
[96] Lemonsu A, Bélair S, Mailhot J, Leroyer S. Evaluation of the town energy balance model in cold and snowy conditions during the Montreal urban snow experiment 2005. J Appl Meteorol Climatol 2010;49(3):346–62. https://doi.org/10.1175/2009JAMC2131.1.
[97] Hjort J, Suomi J, Käyhkö J. Spatial prediction of urban–rural temperatures using statistical methods. Theor Appl Climatol 2011;106(1–2):139–52. https://doi.org/10.1007/s00704-011-0425-9.
[98] Arola T, Korkka-Niemi K. The effect of urban heat islands on geothermal potential: examples from Quaternary aquifers in Finland. Hydrogeol J 2014;22(8):1953–67. https://doi.org/10.1007/s10040-014-1174-5.
[99] Bokwa A, Hajto MJ, Walawender JP, Szymanowski M. Influence of diversified relief on the urban heat island in the city of Kraków, Poland. Theor Appl Climatol 2015;122(1–2):365–82. https://doi.org/10.1007/s00704-015-1577-9.
[100] Fang X-Y, Cheng C, Liu Y-H, Du W-P, Xiao X-J, Dang B. A climatic environmental performance assessment method for ecological city construction: application to

Beijing Yanqi Lake. Adv Clim Change Res 2015;6(1):23–35. https://doi.org/10.1016/j.accre.2015.08.001.
[101] Berardi U, Wang Y. The effect of a denser city over the urban microclimate: the case of Toronto. Sustainability 2016;8(8):822. https://doi.org/10.3390/su8080822.
[102] Hatchett BJ, Koračin D, Mejía JF, Boyle DP. Assimilating urban heat island effects into climate projections. J Arid Environ 2016;128:59–64. https://doi.org/10.1016/j.jaridenv.2016.01.007.
[103] Klimenko VV, Ginzburg AS, Demchenko PF, Tereshin AG, Belova IN, Kasilova EV. Impact of urbanization and climate warming on energy consumption in large cities. Dokl Phys 2016;61(10):521–5. https://doi.org/10.1134/S1028335816100050.
[104] Lokoshchenko MA, Korneva IA, Kochin AV, Dubovetsky AZ, Novitsky MA, Razin PY. Vertical extension of the urban heat island above Moscow. Dokl Earth Sci 2016;466(1):70–4. https://doi.org/10.1134/S1028334X16010128.
[105] Wicki A, Parlow E. Multiple regression analysis for unmixing of surface temperature data in an urban environment. Rem Sens 2017;9(7):684. https://doi.org/10.3390/rs9070684.
[106] Fu P, Weng Q. Variability in annual temperature cycle in the urban areas of the United States as revealed by MODIS imagery. ISPRS J Photogrammetry Remote Sens 2018;146:65–73. https://doi.org/10.1016/j.isprsjprs.2018.09.003.
[107] Ivajnšič D, Žiberna I. The effect of weather patterns on winter small city urban heat islands. Meteorol Appl 2018;16(3):275. https://doi.org/10.1002/met.1752.
[108] He B-J, Zhao Z-Q, Shen L-D, Wang H-B, Li L-G. An approach to examining performances of cool/hot sources in mitigating/enhancing land surface temperature under different temperature backgrounds based on landsat 8 image. Sustain Cities Soc 2019;44:416–27. https://doi.org/10.1016/j.scs.2018.10.049.
[109] Jianying Hu, S.M.ASCE1, Quan Gao, S.M.ASCE2, and Xiong Yu, M. ASCE31Graduate Research Assistant et al. Characterization of the optical and mechanical properties of innovative multifunctional thermochromic asphalt binders.
[110] Touchaei AG, Akbari H. Evaluation of the seasonal effect of increasing albedo on urban climate and energy consumption of buildings in Montreal. Urban Clim 2015;14:278–89. https://doi.org/10.1016/j.uclim.2015.09.007.
[111] Kim Y, An S, Eum J-H, Woo J-H. Analysis of thermal environment over a small-scale landscape in a densely built-up asian megacity. Sustainability 2016;8(4):358. https://doi.org/10.3390/su8040358.
[112] Wang Y, Akbari H. Analysis of urban heat island phenomenon and mitigation solutions evaluation for Montreal. Sustain Cities Soc 2016;26:438–46. https://doi.org/10.1016/j.scs.2016.04.015.
[113] Chun B, Guldmann J-M. Impact of greening on the urban heat island: seasonal variations and mitigation strategies. Comput Environ Urban 2018;71:165–76. https://doi.org/10.1016/j.compenvurbsys.2018.05.006.
[114] Jiang W, Xiao J, Yuan D, Lu H, Xu S, Huang Y. Design and experiment of thermoelectric asphalt pavements with power-generation and temperature-reduction functions. Energy Build 2018;169:39–47. https://doi.org/10.1016/j.enbuild.2018.03.049.
[115] Unger J. Urban-rural air humidity differences in Szeged, Hungary. Int J Climatol 1999;19(13):1509–15.
[116] Kallistratova MA, Kouznetsov RD. Low-level jets in the Moscow region in summer and winter observed with a sodar network. Bound-Layer Meteorol 2012;143(1):159–75. https://doi.org/10.1007/s10546-011-9639-8.
[117] Stryhal J, Huth R, Sládek I. Climatology of low-level temperature inversions at the Prague-Libuš aerological station. Theor Appl Climatol 2017;127(1–2):409–20. https://doi.org/10.1007/s00704-015-1639-z.
[118] Zhong S, Yang X-Q. Ensemble simulations of the urban effect on a summer rainfall event in the Great Beijing Metropolitan Area. Atmos Res 2015;153:318–34. https://doi.org/10.1016/j.atmosres.2014.09.005.
[119] Karsisto P, Fortelius C, Demuzere M, Grimmond CSB, Oleson KW, Kouznetsov R, et al. Seasonal surface urban energy balance and wintertime stability simulated using three land-surface models in the high-latitude city Helsinki. Q J Roy Meteorol Soc 2016;142(694):401–17. https://doi.org/10.1002/qj.2659.
[120] Li H, Cui X, Zhang D-L. On the initiation of an isolated heavy-rain-producing storm near the central urban area of beijing metropolitan region. Mon Weather Rev 2017;145(1):181–97. https://doi.org/10.1175/MWR-D-16-0115.1.
[121] Li H, Cui X, Zhang D-L. Sensitivity of the initiation of an isolated thunderstorm over the Beijing metropolitan region to urbanization, terrain morphology and cold outflows. Q J Roy Meteorol Soc 2017;143(709):3153–64. https://doi.org/10.1002/qj.3169.
[122] Johnson B, Shepherd JM. An urban-based climatology of winter precipitation in the northeast United States. Urban Clim 2018;24:205–20. https://doi.org/10.1016/j.uclim.2018.03.003.
[123] Son J-M, Eum J-H, Kim D-P, Kwon J. Management strategies of thermal environment in urban area using the cooling function of the mountains: a case study of the honam Jeongmaek areas in South Korea. Sustainability 2018;10(12):4691. https://doi.org/10.3390/su10124691.
[124] Tomczyk A, Półrolniczak M, Kolendowicz L. Cold waves in poznań (Poland) and thermal conditions in the city during selected cold waves. Atmosphere 2018;9(6):208. https://doi.org/10.3390/atmos9060208.
[125] Zieliński M, Fortuniak K, Pawlak W, Siedlecki M. Long-term turbulent sensible-heat-flux measurements with a large-aperture scintillometer in the Centre of Łódź, Central Poland. Bound-Layer Meteorol 2018;167(3):469–92. https://doi.org/10.1007/s10546-017-0331-5.
[126] International Society of Biometeorology. What is Biometeorology? [May 12, 2019]; Available from: https://uwm.edu/biometeorology/what-is-biometeorology/.
[127] Taesler R. The bioclimate in temperate and northern cities. Int J Biometeorol 1991;35(3):161–8.
[128] Czarnecka M, Mąkosza A, Nidzgorska-Lencewicz J. Variability of meteorological elements shaping biometeorological conditions in Szczecin, Poland. Theor Appl Climatol 2011;104(1–2). https://doi.org/10.1007/s00704-010-0326-3. 101–10.
[129] Bauche JP, Grigorieva EA, Matzarakis A. Human-Biometeorological assessment of urban structures in extreme climate conditions: the example of birobidzhan, Russian Far East. Adv Meteorol 2013;2013(2):1–10. https://doi.org/10.1155/2013/749270.
[130] Majewski G, Przewoźniczuk W, Kleniewska M. The effect of urban conurbation on the modification of human thermal perception, as illustrated by the example of Warsaw (Poland). Theor Appl Climatol 2014;116(1–2):147–54. https://doi.org/10.1007/s00704-013-0939-4.
[131] Urban A, Davídkovová H, Kyselý J. Heat- and cold-stress effects on cardiovascular mortality and morbidity among urban and rural populations in the Czech Republic. Int J Biometeorol 2014;58(6):1057–68. https://doi.org/10.1007/s00484-013-0693-4.
[132] Nidzgorska-Lencewicz J. Variability of human-biometeorological conditions in Gdańsk. Pol J Environ Stud 2015;24:215–26. https://doi.org/10.15244/pjoes/26116.
[133] Targhi MZ, van Dessel S. Potential contribution of urban developments to outdoor thermal comfort conditions: the influence of urban geometry and form in worcester, Massachusetts, USA. Process Eng 2015;118:1153–61. https://doi.org/10.1016/j.proeng.2015.08.457.
[134] Coccolo S, Kämpf J, Scartezzini J-L, Pearlmutter D. Outdoor human comfort and thermal stress: a comprehensive review on models and standards. Urban Clim 2016;18:33–57. https://doi.org/10.1016/j.uclim.2016.08.004.
[135] Lowe SA. An energy and mortality impact assessment of the urban heat island in the US. Environ Impact Assess Rev 2016;56:139–44. https://doi.org/10.1016/j.eiar.2015.10.004.
[136] Chapman D, Nilsson K, Larsson A, Rizzo A. Climatic barriers to soft-mobility in winter: luleå, Sweden as case study. Sustain Cities Soc 2017;35:574–80. https://doi.org/10.1016/j.scs.2017.09.003.
[137] Hiscock R, Asikainen A, Tuomisto J, Jantunen M, Pärjälä E, Sabel CE. City scale climate change policies: do they matter for wellbeing? Prev Med Rep 2017;6:265–70. https://doi.org/10.1016/j.pmedr.2017.03.019.
[138] Petrov S, Mamaeva N, Narushko M. Urban development of heat island territories and the health of the northern indigenous population. MATEC Web Conf 2017;106(1–3):1035. https://doi.org/10.1051/matecconf/201710601035.
[139] Chi X, Li R, Cubasch U, Cao W. The thermal comfort and its changes in the 31 provincial capital cities of mainland China in the past 30 years. Theor Appl Climatol 2018;132(1–2):599–619. https://doi.org/10.1007/s00704-017-2099-4.
[140] Dursun D, Yavaş M. Microclimate analysis of different urban forms in cold climates and the effect of thermal comfort. Int Arch Photogram Rem Sens Spatial Inf Sci 2018;XLII-4:155–60. https://doi.org/10.5194/isprs-archives-XLII-4-155-2018.
[141] Xu M, Hong B, Mi J, Yan S. Outdoor thermal comfort in an urban park during winter in cold regions of China. Sustain Cities Soc 2018;43:208–20. https://doi.org/10.1016/j.scs.2018.08.034.
[142] Höppe P. The physiological equivalent temperature - a universal index for the biometeorological assessment of the thermal environment. Int J Biometeorol 1999;43(2):71–5. https://doi.org/10.1007/s004840050118.
[143] Jendritzky G, Maarouf A, Fiala D, Staiger H. An update on the development of a universal thermal climate index. 15th Conf. on Biometeorology/Aerobiology and 16th International Congress of Biometeorology 2002:129–33.
[144] Rhind SM. Anthropogenic pollutants: a threat to ecosystem sustainability? Philos Trans R Soc Lond B Biol Sci 2009;364(1534):3391–401. https://doi.org/10.1098/rstb.2009.0122.
[145] Górka-Kostrubiec B, Król E, Jeleńska M. Dependence of air pollution on meteorological conditions based on magnetic susceptibility measurements: a case study from Warsaw. Studia Geophys Geod 2012;56(3):861–77. https://doi.org/10.1007/s11200-010-9094-x.
[146] Cui DJ, Mak CM, Ai ZT, Kwok KCS, Meng XZ, Niu JL. On-site evaluation of pedestrian-level air quality at a U-type street canyon in an ancient city. J Wind Eng Ind Aerod 2017;168:322–33. https://doi.org/10.1016/j.jweia.2017.06.014.
[147] Leahey DM, Hansen MC. Estimates of dark ecosystem respiration of CO2 from the city of calgary, alberta. Atmos Environ 1992;26(9):1725–33.
[148] Cheng I, Zhang L, Mao H, Blanchard P, Tordon R, Dalziel J. Seasonal and diurnal patterns of speciated atmospheric mercury at a coastal-rural and a coastal-urban site. Atmos Environ 2014;82:193–205. https://doi.org/10.1016/j.atmosenv.2013.10.016.
[149] Fierravanti A, Fierravanti E, Cocozza C, Tognetti R, Rossi S. Eligible reference cities in relation to BVOC-derived O 3 pollution. Urban For Urban Green 2017;28:73–80. https://doi.org/10.1016/j.ufug.2017.09.012.
[150] Akbari H, Pomerantz M, Taha H. Cool surfaces and shade trees to reduce energy use and improve air quality in urban areas. Sol Energy 2001;70(3):295–310. https://doi.org/10.1016/S0038-092X(00)00089-X.
[151] Janhäll S. Review on urban vegetation and particle air pollution – deposition and dispersion. Atmos Environ 2015;105:130–7. https://doi.org/10.1016/j.atmosenv.2015.01.052.
[152] Litschke T, Kuttler W. On the reduction of urban particle concentration by vegetation a review. Metereol Z 2008;17(3):229–40. https://doi.org/10.1127/0941-2948/2008/0284.
[153] Nowak DJ, Crane DE, Stevens JC. Air pollution removal by urban trees and shrubs in the United States. Urban For Urban Green 2006;4(3–4):115–23. https://doi.org/10.1016/j.ufug.2006.01.007.

[154] Selmi W, Weber C, Rivière E, Blond N, Mehdi L, Nowak DJ. Air pollution removal by trees in public green spaces in Strasbourg city, France. Urban For Urban Green 2016;17:192–201. https://doi.org/10.1016/j.ufug.2016.04.010.
[155] Tallis M, Taylor G, Sinnett D, Freer-Smith P. Estimating the removal of atmospheric particulate pollution by the urban tree canopy of London, under current and future environments. Landsc Urban Plann 2011;103(2):129–38. https://doi.org/10.1016/j.landurbplan.2011.07.003.
[156] Vos PEJ, Maiheu B, Vankerkom J, Janssen S. Improving local air quality in cities: to tree or not to tree? Environ Pollut 2013;183:113–22. https://doi.org/10.1016/j.envpol.2012.10.021.
[157] Palma W. Time series analysis. Hoboken, NY: Wiley; 2016.
[158] Yilmaz S, Toy S, Demircioglu Yildiz N, Yilmaz H. Human population growth and temperature increase along with the increase in urbanisation, motor vehicle numbers and green area amount in the sample of Erzurum city, Turkey. Environ Monit Assess 2009;148(1–4):205–13. https://doi.org/10.1007/s10661-007-0151-z.
[159] Wang J, Yan Z, Li Z, Liu W, Wang Y. Impact of urbanization on changes in temperature extremes in Beijing during 1978–2008. Chin Sci Buill 2013;58(36):4679–86. https://doi.org/10.1007/s11434-013-5976-y.
[160] Ø Nordli, Hestmark G, Benestad RE, Isaksen K. The Oslo temperature series 1837-2012: homogeneity testing and temperature analysis. Int J Climatol 2015;35(12):3486–504. https://doi.org/10.1002/joc.4223.
[161] Anderson CI, Gough WA. Evolution of winter temperature in Toronto, ontario, Canada: a case study of winters 2013/14 and 2014/15. J Clim 2017;30(14):5361–76. https://doi.org/10.1175/JCLI-D-16-0562.1.
[162] Lokoshchenko MA, Korneva IA, Kochin AV, Dubovetsky AZ, Novitsky MA, Razin PY. Current changes of the lower troposphere temperature in the Moscow region. Izvestiya Atmos Ocean Phys 2017;53(4):392–401. https://doi.org/10.1134/S0001433817040089.
[163] Wang G, Yan D, He X, Liu S, Zhang C, Xing Z, et al. Trends in extreme temperature indices in huang-huai-Hai river basin of China during 1961–2014. Theor Appl Climatol 2018;134(1–2):51–65. https://doi.org/10.1007/s00704-017-2252-0.
[164] Sang J, Liu H, Liu H, Zhang Z. Observational and numerical studies of wintertime urban boundary layer. J Wind Eng Ind Aerod 2000;87(2–3):243–58.
[165] Lee S-H, Baik J-J. Evaluation of the vegetated urban canopy model (VUCM) and its impacts on urban boundary layer simulation. Asia-Pacific J Atmos Sci 2011;47(2):151–65. https://doi.org/10.1007/s13143-011-0005-z.
[166] Ebrahimabadi S, Nilsson KL, Johansson C. The problems of addressing microclimate factors in urban planning of the subarctic regions. Environ Plann B 2015;42(3):415–30. https://doi.org/10.1068/b130117p.
[167] Setälä H, Viippola V, Rantalainen A-L, Pennanen A, Yli-Pelkonen V. Does urban vegetation mitigate air pollution in northern conditions? Environ Pollut 2013;183:104–12. https://doi.org/10.1016/j.envpol.2012.11.010.
[168] McPherson EG, Herrington LP, Heisler GM. Impacts of vegetation on residential heating and cooling. Energy Build 1988;12(1):41–51. https://doi.org/10.1016/0378-7788(88)90054-0.
[169] Grahn P, Stigsdotter UA. Landscape planning and stress. Urban For Urban Green 2003;2(1):1–18. https://doi.org/10.1078/1618-8667-00019.
[170] Alcock I, White MP, Wheeler BW, Fleming LE, Depledge MH. Longitudinal effects on mental health of moving to greener and less green urban areas. Environ Sci Technol 2014;48(2):1247–55. https://doi.org/10.1021/es403688w.
[171] Mitchell R, Popham F. Greenspace, urbanity and health: relationships in England. J Epidemiol Community Health 2007;61(8):681–3. https://doi.org/10.1136/jech.2006.053553.
[172] Mitchell R, Popham F. Effect of exposure to natural environment on health inequalities: an observational population study. Lancet 2008;372(9650):1655–60.
[173] Maas J, Verheij RA, Vries S de, Spreeuwenberg P, Schellevis FG, Groenewegen PP. Morbidity is related to a green living environment. J Epidemiol Community Health 2009;63(12):967–73. https://doi.org/10.1136/jech.2008.079038.
[174] Maas J, Verheij RA, Groenewegen PP, Vries S de, Spreeuwenberg P. Green space, urbanity, and health: how strong is the relation? J Epidemiol Community Health 2006;60(7):587–92. https://doi.org/10.1136/jech.2005.043125.
[175] Kaplan R. The role of nature in the context of the workplace. Landsc Urban Plann 1993;26(1–4):193–201. https://doi.org/10.1016/0169-2046(93)90016-7.
[176] Park BJ, Tsunetsugu Y, Kasetani T, Kagawa T, Miyazaki Y. The physiological effects of Shinrin-yoku (taking in the forest atmosphere or forest bathing): evidence from field experiments in 24 forests across Japan. Environ Health Prev Med 2010;15(1):18–26. https://doi.org/10.1007/s12199-009-0086-9.

Paper II

Characterisation of Heat Losses in Zero Emission Buildings (ZEB) in Cold Climate

J. Brozovsky, N. Gaitani, A. Gustavsen

Published in *Proceedings of the 16th IBPSA Conference, Rome, Italy, Sept. 2–4, 2019, pp. 343–350*

https://doi.org/10.26868/25222708.2019.210560

Characterisation of Heat Losses in Zero Emission Buildings (ZEB) in Cold Climate

Johannes Brozovsky*, Niki Gaitani, Arild Gustavsen
Department of Architecture and Technology, NTNU, Trondheim, Norway

*Corresponding e-mail: johannes.brozovsky@ntnu.no

Abstract

It is well known that urban districts and neighbourhoods can form their own microclimate that can affect the energy balances of buildings significantly. In order to assess the effects of climatic parameters on a building's performance, detailed knowledge about the energy balance of buildings is essential. In this study, the distribution of heat losses in a validated simulation model of a Zero Emission Building (ZEB) was analysed. The model was set to eight different cold climate locations and climate datasets to investigate the influence of wind and the building usage (residential and office building).

The results show that in residential buildings envelope transmission, especially through windows and walls, dominate a typical ZEB's energy losses. In office buildings, ventilation losses gain relevance due to more stringent requirements for ventilation rates. Wind sheltering can lower heat losses by 1.9 % to 8.3 %, depending on location and weather data.

Introduction

Climate and the environment where buildings are located determine their thermal behaviour and final energy use. Thus, it affects the selection of materials, technologies, concepts, or techniques in order to guarantee the buildings' energy efficiency. Energy uses that are influenced by climate are primarily space heating and cooling. Space heating is responsible for around 70 % of final energy use (Building Performance Institute Europe, 2011).

It is widely accepted that urban microclimate and in particular the urban heat island (UHI), have a large influence on a building's energy balance (Oke et al., 2017). Mainly, the UHI effect is described as a phenomenon to be mitigated, as it is regarded to obstruct the effectiveness of natural ventilation and to cause outdoor discomfort, higher need for cooling, or even higher mortality rates during summertime (Moonen et al., 2012). But the UHI is not necessarily detrimental but can be favourable especially in cold climate conditions, where heating energy use typically accounts for the largest fraction of a building's energy demand over the year. Warmer night-time and winter temperatures can thus lead to lower heating demands and increased outdoor thermal comfort (Watkins et al., 2007). Most energy efficiency measures, such as the Energy Performance of Buildings Directive in the European Union (EU), focus on the building scale, demanding for example nearly zero energy buildings. The Research Centre on Zero Emission Neighbourhoods in Smart Cities (FME ZEN) however, pursues a different goal. Founded by the Norwegian University of Science and Technology (NTNU) and SINTEF, it aims to reach an overall zero emission balance over a neighbourhood's life cycle (ZEN). Hence, ZENs and ZEBs are of particular importance for reaching the EU's climate goals.

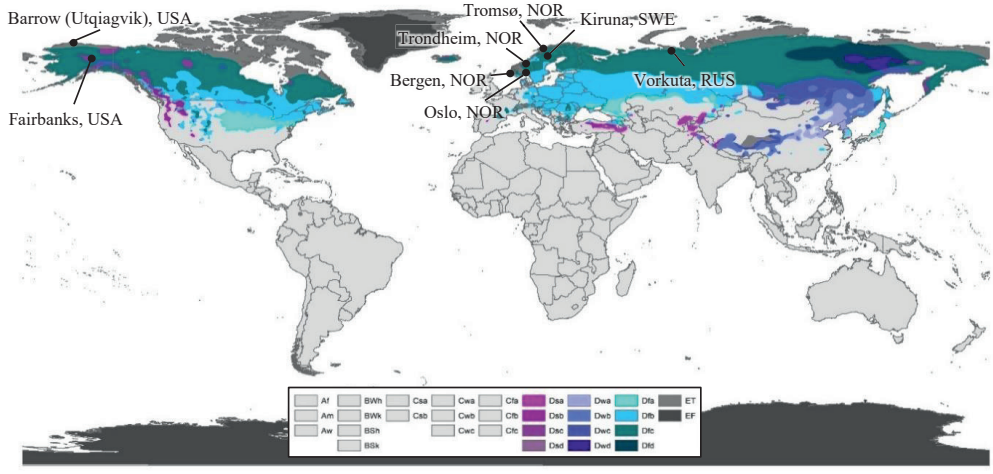

Figure 1: Polar and cold climate regions according to the data from Peel et al. (2007).

https://doi.org/10.26868/25222708.2019.210560

Therefore, characterizing the distribution of heat losses in a ZEB and their dependency on climate data will indicate, which microclimatic parameters are the most critical to address in the ZEN context. It can furthermore help architects and planners in the design of ZEBs with respect to different climate parameters.

Commonly, the heat losses of a building are categorized as follows:

- *Building envelope losses*
  are defined as the heat flux from inside to outside over the floor, roof, external walls, doors, windows, and thermal bridges. The losses are caused by heat transfer via conduction through the building parts, and convection as well as longwave radiation exchange on their inner and outer surfaces.
- *Infiltration losses*
  are unwanted flows of air through cracks and other passages in the building envelope. They cause additional energy use for heating the incoming outdoor air
- *Ventilation losses*
  occur when outdoor air is supplied either via natural ventilation or a mechanical ventilation system (MVS) into the building. In order to keep losses as low as possible, often a heat recovery unit (HRU) is used.

ZEB Living Laboratory

The ZEB Living Living Laboratory (LL) is a 100 m² detached house test facility on the NTNU campus in Trondheim, Norway (see Figure 2 and Figure 3). As the name implies, zero emission buildings (ZEB) are not targeting energy use as a criterion, at least not primarily, but focus on the reduction of GHG-emissions, which are first and foremost responsible for climate change (Edenhofer, 2014). A ZEB aims to produce enough renewable energy to compensate for the building's greenhouse gas emissions over its life span (Hestnes and Eik-Nes, 2017). This does not only demand the use of renewable energy on site but also promotes energy efficiency measures and the choice of building materials and products according to a life cycle assessment.

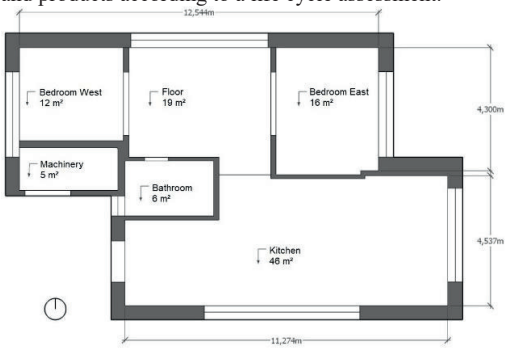

Figure 2: Floor plan of the ZEB Living Laboratory.

Figure 3: The ZEB LL from outside (photo by Katrine Peck Sze Lim).

The LL was designed to host people for behavioural studies in interaction with zero emission technology. In several experiments, the building has been home for families, couples and single persons of different age and over different periods of time. The building is equipped with a heat pump, several smart home appliances, a PV system on the roof and several sensors to monitor the building's energy consumption and production, and local weather conditions. The building envelope is well insulated and airtight. A double skin window with a ventilated gap is installed on the south façade (Goia et al., 2015). Table 1 shows the building-physical properties of the LL's envelope.

Table 1: Building-physical properties of the ZEB LL.

	Value	Unit
Wall U-value	0.16	[W/(m²K)]
Floor U-value	0.11	[W/(m²K)]
Roof U-value	0.11	[W/(m²K)]
Windows (south) U-values	0.65/0.69	[W/(m²K)]
Windows (north) U-values	0.97	[W/(m²K)]
Windows (east/west) U-values	0.80	[W/(m²K)]
g-value	0.5	[-]
Infiltration n_{50}	0.7	[ACH]
Normalized thermal bridge	0.03	[W/m²K]

Because in the following simulation results, heating demands will not be looked into, but only the heat balance of gains and losses, a detailed description of internal loads and occupancy is not necessary. To shorten the duration of the simulations, the existing heat pump model with its complex control strategies was replaced by a much faster simulating basic heating system, as this does not affect the distribution of the heat losses.

With regard to the MVS, the operation times and ventilation rates are of particular importance, as those will influence the ventilation losses. As a basis for the model, the Norwegian Standard SN/TS 3031:2016 has been used (see Table 2). The standard is the basis for calculating a building's energy demand in a transient simulation program. On the one hand, by not adjusting the simulation model to the country-specific requirements, the distribution of heat losses is not fully realistic for the locations (except for Norway in this case). On the other hand, by using the same input data for the building, it is possible to highlight the effects of the locations' climatic differences, on which this paper is focusing on.

Table 2: Ventilation rates and times of operation according to SN/TS 3031:2016.

	Residential	Office*
Operation	Mon–Sun, 0:00–24:00	Mon–Fri, 7:00–19:00
Ventilation rate during operation	Bedroom: 26 m³/h per sleeping place** Else: 1.2 m³/(hm²)	7 m³/(hm²)
Ventilation rate outside operation	-	2 m³/(hm²)

* For the office, a constant air volume (CAV) system was modelled with a time control
** Requirement by the Norwegian Building Authority (2017)

Method

In this study, the energy losses of a ZEB, located in Trondheim, Norway, are analysed for selected cold climate conditions with the use of building energy performance simulation (BEPS). For that, a simulation model of the investigated building is set to eight different cold climate locations (Oslo, Bergen, Trondheim and Tromsø in Norway, Kiruna in Sweden, Fairbanks and Barrow in Alaska and Vorkuta in Russia; see Figure 1) in the BEPS program IDA Indoor Climate and Energy (IDA ICE) (Bring et al., 1999).

Most commonly, simulation studies use generic building models. In this study, the simulation model of the LL has been mainly developed, updated and calibrated by doctoral and master students at the NTNU in Trondheim in their theses and is used for several research purposes. It is already validated for Trondheim weather conditions. Compared to using an invalidated, generic building model, this study is expected to deliver more reliable results on heat losses in a ZEB. However, using a model outside of its validated domain of application can still induce errors (Sargent, 2013).

The output from IDA ICE v. 4.8 will be used to categorise heat losses, evaluate their magnitudes and dependencies on the locations' climate and to investigate energy balances of building parts. It is furthermore used to investigate the influence of different wind conditions according to ASHRAE wind profiles (American Society of Heating, Refrigerating and Air-Conditioning Engineers, 2009) and wind-induced infiltration according to the AIVC database (Liddament, 1986).

In this study, both heat gains and losses are considered. Particular attention has to be given to the windows as they are able to let solar radiation pass through the building envelope and thus to "generate" energy gains. With the definitions from above, heat losses occur all year round, even in summer, when they may be considered *favourable*. This can be the case for example during nighttime-ventilation when the cooler outdoor temperatures are used to cool the warmer indoor air to its set point temperature. In the same way, as those losses should not be considered *detrimental*, not all gains can be considered *useful*. In summer, when indoor temperatures are generally higher, heat gains from solar irradiation contribute to overheating and are thus classified as *detrimental* in this specific case. But especially in the transitional seasons, solar gains can reduce a building's heating demand significantly. Therefore, a rule based on the zone's indoor air temperature indicates when heat gains and losses are counted. There are two indoor temperature thresholds from where losses or gains are metered. The threshold temperature for heat losses was determined to be 21.5 °C and for gains 23.5 °C (see Figure 4).

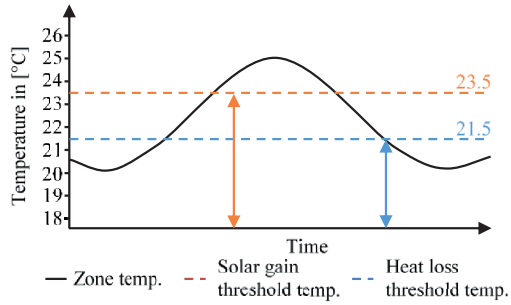

Figure 4: Heat gain and loss threshold temperatures.

With 21.5 °C, the heat loss threshold (HLT) temperature is 0.5 K higher than the heating setpoint temperature (HST) of 21.0 °C which is the HST according to SN/TS 3031:2016. Heat losses above this value are not regarded to be generally detrimental, as they commonly do not induce the use of energy for heating. In analogy with the HLT, the solar gain threshold (SGT) temperature is 0.5 K below the cooling setpoint temperature (CST) of 24.0 °C (which is the CST according to SN/TS 3031:2016), as there is usually no need for cooling below this temperature, even though the building does not have a cooling unit. The offset of 0.5 K to HST and CST are necessary to avoid the heating system to be active during times, in which no losses are counted. Due to control behaviour, the HST will never be kept precisely at 21.0 °C but sway around it within a certain range (ca. ±0.1 K) and the heating system in the zones is active below 21.5 °C.

To keep indoor conditions within the desired limits, energy in the same magnitude as the losses has to be supplied to the building. Generally, in ZEBs, a large fraction of this energy comes from electrical appliances, lighting, persons or solar gains. Therefore, the amount of heat losses is not to be equated with the heating energy demand. For the calculation of heating energy to be supplied in addition, e.g. over radiators or surface heating, SN/TS 3031:2016 gives internal loads as high as 42 kWh/m²a for residential buildings and 72 kWh/m²a for office buildings. In the case of ZEBs, internal loads contribute significantly to covering the heating demand.

For selecting the locations, available weather data of selected high latitude cities were analysed according to temperature variation, heating degree hours ($HDH_{21/15}$, since hourly weather data are used), annual global horizontal radiation and mean wind speed (see Figure 5).

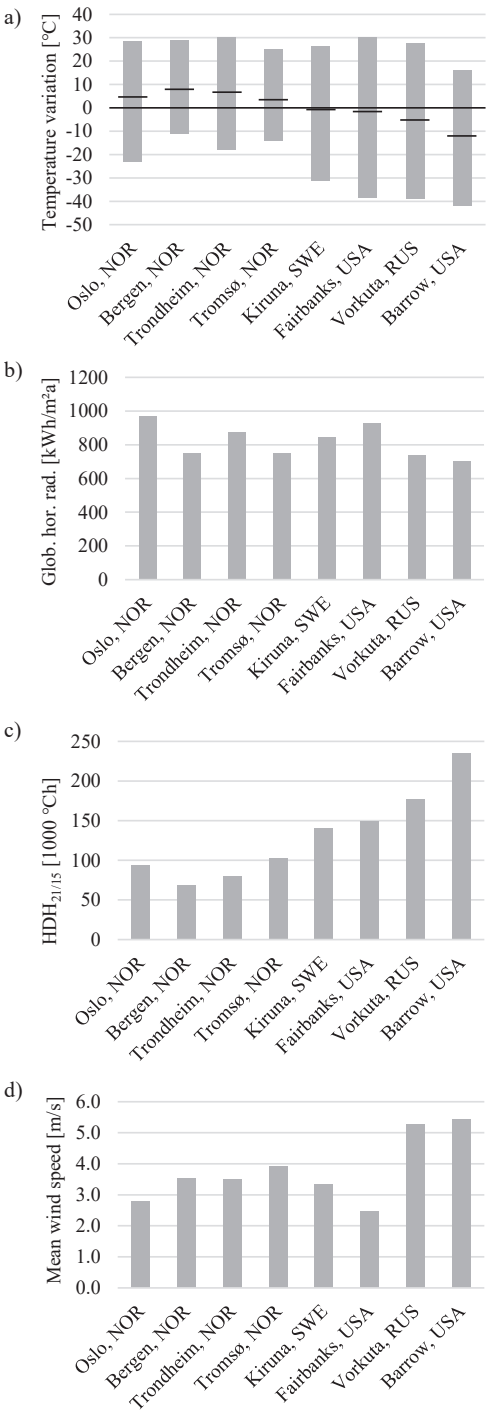

Figure 5: Comparison of locations with regard to a) temperature range and average; b) annual global horizontal radiation; c) $HDH_{21/15}$; d) mean wind speed.

$HDH_{21/15}$ describe the sum of hourly temperature differences between inside and outside over the year when hourly mean outdoor temperatures drop below 15 °C at an indoor temperature of 21 °C.

The study aims to evaluate heat losses in buildings for typical weather conditions in high latitude cold climate regions. Due to the distribution of landmass, these regions are mostly located on the northern hemisphere, except for Antarctica. The locations were selected according to the following two criteria:

- Latitude of at least 60° N
- Significant population or climate

The city of Oslo, however, located at 59.9° N was also included, as parts of the urban agglomeration and the site of the weather station at Oslo airport are located over 60° N. Apart from Barrow, which was included due to its harsh and severe climate conditions, all cities have rather large populations (from 1.7×10^4 in Kiruna to over 1.0×10^6 for the agglomeration of Oslo). Other large cities over 60° N like for example Reykjavik in Iceland, Helsinki in Finland, Murmansk in Russia or the large cities in North America have not been included since their climate was too similar to the already selected locations.

This study evaluates where heat losses in ZEBs in cold climate occur, how they are distributed, and which climatic parameters influence them the most. The results will then deliver valuable information, which measures in terms of a neighbourhood setting may be most effective concerning its energy use. This study's outcome will then be used for further, more detailed investigations on the most important microclimatic parameters.

Simulation cases

As mentioned before, a central part of this study is the analysis of the influence of different wind conditions on the building's energy balance. This will be done for the LL as a residential (R) and an office building (O). The basis for this investigation is the wind speed and direction from the weather file. The wind speed at the building site (roof height, V_{loc}) is then calculated by the IDA ICE with the reference wind speed from the climate data set (V_{ref}) the coefficients a_0 and a_{exp}, and the quotient of building height h_{b} to the reference height h_{ref} of the wind measurement, as in Eq. 1 (Bring et al., 1999). The coefficients a_0 and a_{exp} can be chosen from a database, as listed in Table 3, but can also be defined individually. Furthermore, pressure coefficients according to AIVC (sheltered, semi exposed, exposed) can be used. In the following simulations, three cases will be analysed:

1. "Open country" wind profile with "exposed" pressure coefficients (OC/E),
2. "Suburban" wind profile with "semi-exposed" pressure coefficients (SU/SE), and
3. "City centre" wind profile with "sheltered" pressure coefficients (CC/S)

$$V_{\mathrm{loc}} = V_{\mathrm{ref}} \cdot a_0 \cdot \left(\frac{h_{\mathrm{b}}}{h_{\mathrm{ref}}}\right)^{a_{\mathrm{exp}}} \quad (1)$$

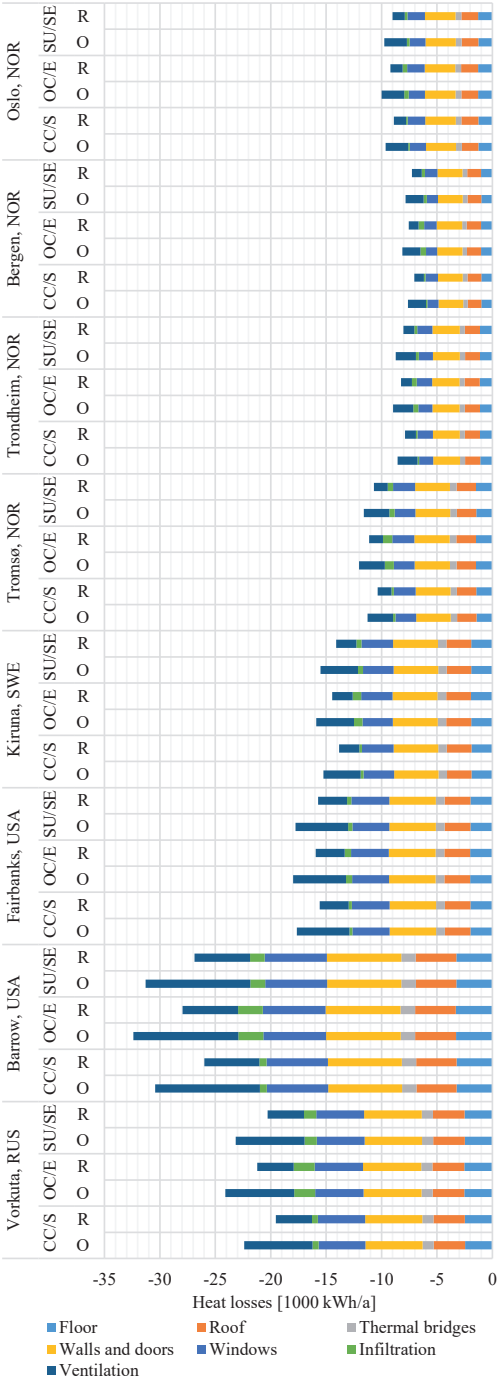

Figure 6: Distribution of heat losses for the residential building (R) and office building (O) for different locations and wind conditions: suburban/semi-exposed (SU/SE), open country/exposed (OC/E) and city centre/sheltered (CC/S).

Table 3: IDA ICE wind profile database according to ASHRAE 1993.

	a_0	a_{exp}
Ocean	1.30	0.10
Airport	1.00	0.15
Open country	0.85	0.20
Suburban	0.67	0.25
City centre	0.47	0.35

Results

Figure 6 displays the heat balance of the ZEB LL for the investigated cases in the eight selected locations. While in Bergen comparably little heat is lost, the extreme winter conditions in Barrow result in more than three times the energy losses in the residential (R) case and four times as much in the office (O) case. The results show that the different wind conditions (OC/E, SU/SE, CC/S) influence a ZEB's energy balance in cold climate mostly relatively little (see Table 4).

Table 4: Maximum reduction of heat losses through wind sheltering (OC/E compared to CC/S)

Location	Residential	Office
Oslo, NOR	−3.6%	−3.6%
Bergen, NOR	−6.8%	−6.3%
Trondheim, NOR	−4.8%	−4.6%
Tromsø, NOR	−7.2%	−6.4%
Kiruna, SWE	−4.4%	−4.1%
Fairbanks, USA	−2.3%	−1.9%
Barrow, USA	−7.3%	−6.0%
Vorkuta, RUS	−8.3%	−7.0%

Compared to the OC/E case, wind sheltering (CC/S) reduces energy losses only by 1.9 % (O) to 2.3 % (R) in Fairbanks, since its winter climate is characterized by low wind speeds. In contrast to that, even though mean wind speed in Barrow is even higher, savings of 7.0 % (O) to 8.3 % (R) can be obtained from proper wind sheltering in Vorkuta, because high wind speeds predominantly coincide with low outdoor temperatures.

Unsurprisingly infiltration losses are largely influenced by wind conditions. Compared to CC/S, wind-induced infiltration in OC/E-conditions doubled in Fairbanks and quadrupled in Bergen with an average increase of 222.6 % (see Figure 7). There were no notable differences between the LL as a residential or an office building.

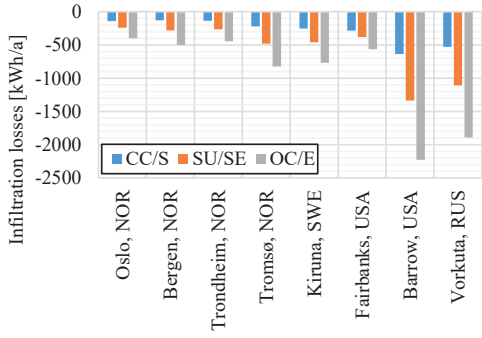

Figure 7: Infiltration losses of the ZEB LL as a residential building for different wind conditions

Building envelope and ventilation losses remained relatively stable (changes below 2 %), even though wind speed is considered by the BEPS tool for the calculation of convective heat transfer coefficients. Figure 8 shows the envelope and infiltration heat losses as a function of the $HDH_{21/15}$. The losses caused by the thermal bridges, floor, roof, walls and doors and windows show a strong dependency on $HDH_{21/15}$ with R^2 close to 1. Infiltration losses correlate with $HDH_{21/15}$ with an R^2 of 0.821 as they partly also correlate with wind speed. From the slope of the linear regression line in Figure 8, it is visible that the losses from windows and walls and doors are stronger influenced by outdoor temperature.

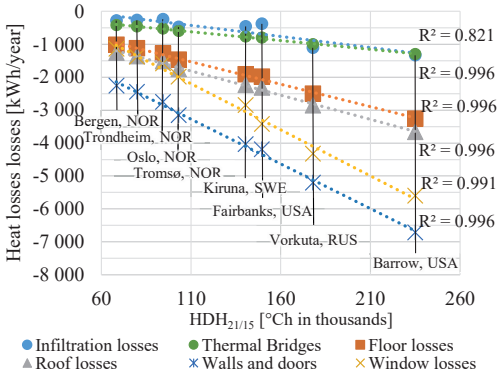

Figure 8: Envelope and infiltration losses as a function of $HDH_{21/15}$ of the ZEB LL as a residential building with SU/SE wind conditions

When looking at the ventilation losses, the relationship to $HDH_{21/15}$ is not linear but exponential (see Figure 9). Whereas in Barrow, losses through the roof and the wall are about three times higher than in Bergen, ventilation losses differ with the factor 5.

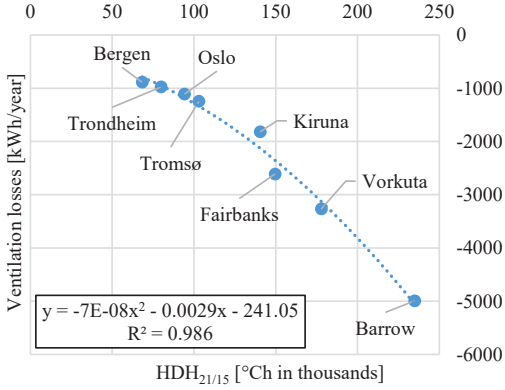

Figure 9: Ventilation losses of the ZEB LL as a residential building as a function of $HDH_{21/15}$

It is visible as well in Figure 6 that ventilation losses in office buildings are approximately twice as high compared to residential buildings, resulting from more stringent requirements for ventilation rates in Norway. The differences between residential and office buildings are listed in Table 5.

Table 5: Overview of total heat losses of the ZEB LL in different locations as residential and office buildings in SU/SE wind conditions.

Location	Residential [kWh/a]	Office [kWh/a]	Difference [-]
Oslo, NOR	−9 011	−9 756	−8.3 %
Bergen, NOR	−7 265	−7 837	−7.9 %
Trondheim, NOR	−8 025	−8 725	−8.7 %
Tromsø, NOR	−10 695	−11 607	−8.5 %
Kiruna, SWE	−14 091	−15 498	−10.0 %
Fairbanks, USA	−15 715	−17 757	−13.0 %
Barrow, USA	−26 865	−31 297	−16.5 %
Vorkuta, RUS	−20 271	−23 147	−14.2 %

Windows take a special role in the energy balance of a building, as they can account for significant amounts of solar energy gains. Figure 10 illustrates the proportion of gains and losses in the respective locations. Especially in the Norwegian cities with around 40 % of the total heat losses, useful solar gains significantly enhance the windows' overall energy balance. In Barrow, the highest amount of useful gains can be obtained, but losses overweigh the gains by the factor 5.5.

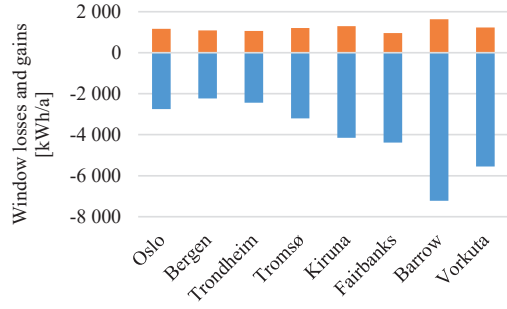

Figure 10: Unwanted losses and useful solar gains of windows in the ZEB LL as a residential building with SU/SE wind conditions.

Discussion

The IDA ICE simulations show a considerable variation of the distribution of heat losses, depending on the location's climate and the building's usage. Extremely low outdoor air temperatures affect ventilation losses stronger than e.g. envelope losses. The MVS and the HRU in particular face the problem of building up ice at very low temperatures and/or high moisture loads (Justo Alonso et al., 2015). In case of the ZEB LL, the HRU can operate until ca. −15 °C at full efficiency without building up ice. Below this temperature, preheating the air clearly deteriorates the overall efficiency and leads to a nonlinear correlation. While in the oceanic dominated climates of coastal Scandinavia, those extreme conditions occur only at rare intervals, the continental climate of its inland, central Alaska, or Siberia results in longer periods of extreme frost with temperatures dropping to −30 or even −40°C. Because of higher requirements for ventilation rates in office spaces from the Norwegian building code (NBC), ventilation losses are considerably higher. In all locations, windows account for a large fraction of heat

losses, when only losses from conduction and longwave radiation are considered. The useful solar gains of west and east-oriented windows compensate for around 50 % of unwanted losses over the year in the Norwegian cities. South-oriented windows can even have a positive energy balance with over 20 % more useful energy gains than unwanted losses. These results support the findings by Grynning et al. (2013) that a window can outperform opaque building parts even in high-latitude locations when window properties, orientation etc. are chosen appropriately. Unwanted solar gains during summertime, on the other hand, increase the risk of overheating. This issue has not been considered in this study, though it generally should not be disregarded. In the non-Norwegian locations, none of the ZEB LL's windows came close to a positive annual energy balance.

Floor and roof of the LL account for large fractions of total the total envelope area, as it only consists of one storey (building envelope area A to volume V ratio A/V = 1.1 m^{-1}). Therefore, these building parts also account for a high share of the building's total heat losses. In larger multi-storey residential or office buildings, the envelope losses will account for a lower fraction of total heat losses (with A/V as low as 0.2 m^{-1}), which puts more importance on ventilation losses as they are a function of a building's floor area. The distribution of heat losses for the ZEB LL in the different locations can be seen in Figure 11 and Figure 12.

It is worth noting that floor losses in IDA ICE are calculated according to ISO 13370 (International Standard Organisation, 2017). The program determines the heat resistance of the ground layer based on the geometry of the building and the heat conductivity of the ground material (kept at its default values with thermal conductivity λ = 2.0 W/(mK), density ρ = 2000 kg/m³, and heat storage capacity c = 1000 kJ/kg). According to ISO 13370, the ground temperature is calculated as a weighted average value of the annual and the monthly mean air temperatures, including a given time lag.

However, the study is limited by the fact that the ZEB LL cannot be regarded as a typical office building. In addition, the results are not generalisable for single-family homes in the selected locations either, apart from the Norwegian ones because input parameters for the simulations are based on the NBC. Country-specific regulations in the non-Norwegian locations would certainly lead to different results. However, because the focus in this study was put on the influence of climate, results are only comparable when using an identical input.

Other limiting aspects are the weather data. Mostly, they have been recorded at the locations' airports, often more than 20 km away. The wind situations there may be entirely different from what an average building in the cities might experience. The same limitation applies to solar irradiation, as no mutual shadowing was accounted for in this study. Beyond, especially when it comes to the influence of wind, BEPS programs are not very well suited for meaningful quantitative analyses. For that, computational fluid dynamics (CFD) programs should be used to evaluate reasonable boundary conditions. Moreover, this study is based on self-defined thresholds as there are no official definitions of *useful* gains and *unwanted* or *detrimental* losses. Different definitions may, therefore, lead to different results.

Conclusion

In this study, a validated model of the ZEB Living Laboratory, located on the campus of the Norwegian University of Science and Technology in Trondheim, Norway, was simulated at different locations in cold climate to analyse the distribution of heat losses. While envelope and infiltration losses were found to be linearly dependent on the number of heating degree hours, ventilation losses revealed to have an exponential relationship. When using the Norwegian building code for the input parameters, the main difference between residential (R) and office (O) building was found to be the ventilation losses due to more stringent requirements for ventilation rates in offices.

Whereas the presented results might seem rather self-evident, such quantitative analysis of heat losses in a ZEB in cold climate conditions can be regarded as the first step towards a comprehensive analysis of microclimatic effects on ZEBs and delivers useful information on how heat losses are distributed. The setting of a Zero Emission Neighbourhood not only impacts the wind sheltering situation which is able to reduce heat losses by 1.9 % (O) to 2.3 % (R) in Fairbanks and 7.0 % (O) to 8.3 % (R) in Vorkuta.

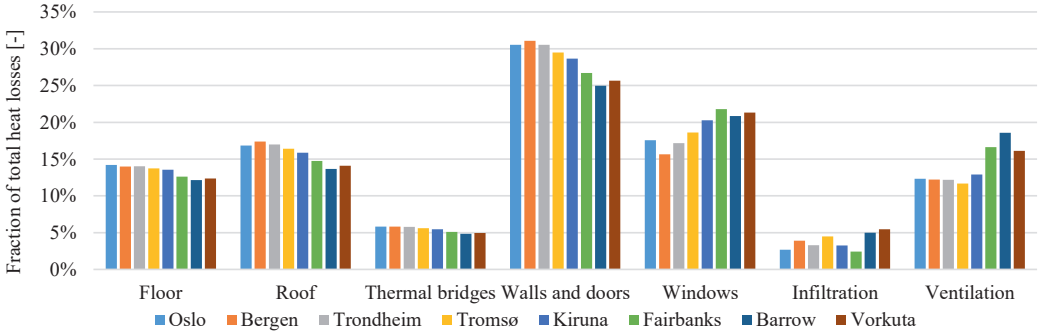

Figure 11: Distribution of heat losses for the ZEB LL as a residential building for SU/SE wind conditions.

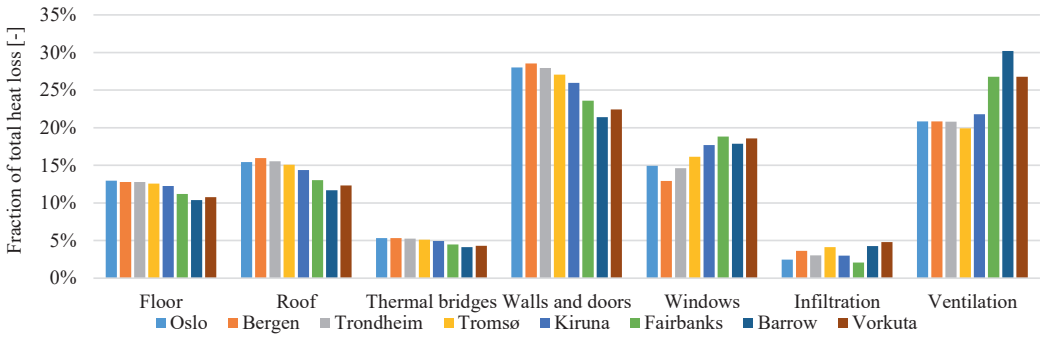

Figure 12: Distribution of heat losses for the ZEB LL as an office building for SU/SE wind conditions.

It also influences solar accessibility, which was found to account for significant amounts of solar gains. Windows can, in fact, outperform opaque building parts, even in high-latitude locations.

Additional investigations of different kinds of buildings, regarding their shape, usage and material properties need to be carried out to further quantify the impact of microclimatic aspects on a ZEB's energy balance. For that, measurements and simulations are currently carried out on FME ZEN's pilot projects as case studies.

Acknowledgements

This paper has been written within the Research Centre on Zero Emission Neighbourhoods in Smart Cities (FME ZEN). The authors gratefully acknowledge the support from the ZEN partners and the Research Council of Norway.

References

American Society of Heating, Refrigerating and Air-Conditioning Engineers (2009): 2009 ASHRAE handbook. *Fundamentals*. SI ed. Atlanta GA: American Society of Heating Refrigeration and Air-Conditioning Engineers.

Bring, A.; Sahlin, P.; Vuolle, M. (1999): Models for Building Indoor Climate and Energy Simulation. *A Report of IEA SHC Task 22: Building Energy Analysis Tools, Subtask B: Model Documentation*. Edited by KTH Stockholm.

Building Performance Institute Europe (2011): Europe's buildings under the microscope. *A country-by-country review of the energy performance in buildings*. Edited by Building Performance Institute Europe (BPIE), checked on 1/3/2019.

Edenhofer, O. (Ed.) (2014): Climate Change 2014: Contribution of Working Group III to the Fifth Assessment Report of the Intergovernmental Panel on Climate Change. *Mitigation of climate change*. IPCC. New York (USA): Cambridge Univ. Pr.

Goia, F.; Finocchiaro, L.; Gustavsen, A. (2015): The ZEB Living Laboratory at the Norwegian University of Science and Technology: a zero emission house for engineering and social science experiments. In *7th Passivhus Norden - Conference Proceedings*.

Grynning, S.; Gustavsen, A.; Time, B.; Jelle, B. P. (2013): Windows in the buildings of tomorrow: Energy losers or energy gainers? In *Energy and Buildings 61*, 185–192.

Hestnes, A. G.; Eik-Nes, N. L. (Eds.) (2017): Zero emission buildings. Bergen (Norway): Fagbokforlaget.

International Standard Organisation (2017): Thermal performance of buildings - Heat transfer via the ground - Calculation methods (ISO 13370).

Justo Alonso, M.; Liu, P.; Mathisen, H. M.; Ge, G.; Simonson, C. (2015): Review of heat/energy recovery exchangers for use in ZEBs in cold climate countries. In *Building and Environment 84*, 228–237.

Liddament, M. W. (1986): Air Infiltration Calculation Techniques - An application guide. Edited by The Air Infiltration and Ventilation Centre. Coventry (UK).

Moonen, P.; Defraeye, T.; Dorer, V.; Blocken, B.; Carmeliet, J. (2012): Urban Physics: Effect of the micro-climate on comfort, health and energy demand. In *Frontiers of Architectural Research 1* (3), 197–228.

Norwegian Building Authority (2017): Regulations on technical requirements for construction works.

Oke, T. R.; Mills, G.; Christen, A.; Voogt, J. A. (2017): Urban climates. Cambridge: Cambridge University Press.

Peel, M. C.; Finlayson, B. L.; McMahon, T. A. (2007): Updated world map of the Köppen-Geiger climate classification. In *Hydrology and Earth System Sciences Discussions 4* (2), 439–473.

Sargent, R. G. (2013): Verification and validation of simulation models. In *Journal of Simulation 7* (1), 12–24.

Watkins, R.; Palmer, J.; Kolokotroni, M. (2007): Increased Temperature and Intensification of the Urban Heat Island: Implications for Human Comfort and Urban Design. In *Built Environment 33* (1), 85–96.

Paper III

Evaluation of sustainable strategies and design solutions at high-latitude urban settlements to enhance outdoor thermal comfort

J. Brozovsky, S. Corio, N. Gaitani, A. Gustavsen

Published in *Energy and Buildings 244* (2021), 111037

https://doi.org/10.1016/j.enbuild.2021.111037

Energy & Buildings 244 (2021) 111037

Contents lists available at ScienceDirect

Energy & Buildings

journal homepage: www.elsevier.com/locate/enb

Evaluation of sustainable strategies and design solutions at high-latitude urban settlements to enhance outdoor thermal comfort

J. Brozovsky [a,*], S. Corio [b], N. Gaitani [a], A. Gustavsen [a]

[a] Department of Architecture and Technology, Faculty for Architecture and Design, NTNU – Norwegian University of Science and Technology, Høgskoleringen 1, 7491 Trondheim, Norway
[b] Department of Civil, Chemical and Environmental Engineering (DICCA), University of Genoa, 16145 Genoa, Italy

ARTICLE INFO

Article history:
Received 10 April 2020
Revised 21 March 2021
Accepted 15 April 2021
Available online 22 April 2021

Keywords:
Urban microclimate
Cold climate
Outdoor thermal comfort
Numerical analysis
Validation study

ABSTRACT

Driven by the necessity to design resilient and prosperous cities and to counteract the impacts of climate change, this study aims to shed light on the interactions between microclimate, urban built environment, and the outdoor thermal comfort (OTC) conditions at a university campus in Trondheim, Norway. This paper calls into question up to which degree four typical microclimatic design solutions can enhance OTC in high-latitude areas which are generally characterized by strong seasonal variability in meteorological conditions, particularly in solar radiation. An on-site measurement campaign in autumn 2019 for the validation of numerical simulations with ENVI-met were carried out. Solar access proved to be the key parameter to improve OTC by a Predicted Mean Vote of up to 1.0 in the investigated climatic situation. Moreover, wind sheltering resulted in an increase of OTC, although not as pronounced and on a smaller spatial scale. Changing the buildings' surface material resulted in no significant changes in microclimatic conditionsAt a higher wind speed (8 m/s), wind sheltering becomes more effective in improving OTC than solar access. This study underlines the importance of microclimatic assessments in order to understand the effect of different interventions with the urban environment on OTC at high-latitude urban settlements.

1. Introduction

Already in the 1830s, it was discovered that a city – London in this case – had a distinctly different climate than its rural surroundings [1]. Driven by the necessity for designing better cities and, especially nowadays, to counteract the observed and projected impacts of climate change and rapidly growing city populations worldwide [2,3], a great number of publications on urban climatology (UC) have been published since then. UC brings together many different disciplines such as meteorology, climatology, air pollution science, architecture, building engineering, physics, urban design, biometeorology, social sciences, etc. [4].

Undoubtedly, one of the most documented topics in urban climate research is the urban heat island (UHI) effect which describes the observed higher temperatures in urban areas by several degrees compared to the surrounding rural areas [5]. The UHI phenomenon has been reported to occur in urban areas of nearly any size and across all climate zones [6]. As the overheating of cities pose a serious threat to people's health [7–10] while at the same time increasing the cooling energy demand in buildings [11], research studies have primarily been aiming to mitigate the adverse effects of the UHI. This has been mainly addressed by studying the influence of urban trees and parks, e.g. [12–18], green roofs and facades, e.g. [13,19–22], water bodies, e.g. [19], the albedo of surfaces, e.g. [20–26], or smart materials, e.g. [27,28].

Even in cold-climate cities as defined by the Köppen-Geiger climate classification system, measures need to be taken to shield the urban areas from elevated temperatures. This was highlighted for example in Montreal [27,28] and Toronto [29] in Canada, as well as in Columbus in Ohio, USA [30]. However, the overall effect of the UHI on a city's energy use was found to be positive in some cases, e.g. in the North of the USA [31] or large Russian cities [32], meaning that the heating energy savings in winter surpass the cooling energy increase during the summer months.

The most commonly reported differences in air temperature between a city and its rural surroundings (the UHI-magnitude) over time are about 1–3 K in cold climate locations. The highest magnitudes were frequently reported during anticyclonic and calm weather conditions [33–35], mostly during the night [36–38] and

* Corresponding author.
E-mail address: johannes.brozovsky@ntnu.no (J. Brozovsky).

https://doi.org/10.1016/j.enbuild.2021.111037
0378-7788/

either in winter [39–41] or summer [38,42,43]. High-latitude areas experience a more pronounced seasonal variability in meteorological conditions compared to mid- or low-latitude areas [44]. In winter and spring, snow on the ground reflects most of the incident solar radiation during the short days due to a higher surface albedo [45]. In these regions, the anthropogenic heat release, related to space-heating and vehicle traffic, was identified as a major contributor to the UHI. Thus, the so-called urban self-heating is strongly linked to fuel use [36,46–49].

In the history of UC, among a variety of methodological approaches, the focus has been mainly in the careful recording and analysis of observations and field measurements until the 1960 s [4]. Nevertheless, over the last two decades, numerical analyses as a method to supplement the experimental investigations in urban studies have received a lot of attention [4,50]. However, they have primarily been carried out in warm and temperate climate regions [50]. Considering that there are more than 25 million people living above 60° N, research carried out in the high-latitude and cold-climate regions are extremely valuable. Local factors like an increasing population and ongoing urbanization [51–53] put increasing pressure on the circumpolar region as well as global ones like the increasing exploitation of resources in the more and more ice- and permafrost-free and thus accessible North [54]. This contributes to the steadily increasing global greenhouse gas emissions [55]. Having in mind that the arctic region is particularly vulnerable to the effects of climate change as it warms more rapidly than the global mean, research in these regions is much-needed [56].

Many publications stress the necessity of improving the design and the climate resilience of cities and their outdoor environment to provide comfortable spaces that invite people to spend time outdoors or that promote soft mobility, regardless of their climate, e.g. [11,57,58]. Human comfort (“the pleasant feeling of being physically or mentally free from pain or suffering” [59]) and well-being (“feeling healthy and happy” [59]) are terms frequently used when investigating the environmental quality in cities and the people’s perception. An experiment in an urban park in Xi’an, China by Xu et al. [60] suggests that human comfort and thermal sensation are strongly connected. In winter conditions, they identified solar radiation as the most important aspect, followed by air temperature and relative humidity. Wind was reported to be the least important aspect. The authors also highlighted that human perception of the environment was affected by psychological factors, supporting the physical and mental characteristics of comfort and well-being. Another survey by Liu et al. [61] underlined that air temperature is the most important microclimatic parameter in public urban squares. Thermal radiation was identified as the second most important one. In winter, however, when temperatures are always low, the authors observed the relative importance of solar radiation to increase and that of air temperature to decrease. In other words, solar radiation contributed more to outdoor thermal comfort than the air temperature. An increment in wind speed was reported to cause the outdoor neutral air temperature (i.e. the temperature at which the thermal sensation vote would be neutral) to increase, while thermal radiation had the opposite effect. An increase in humidity elevated the outdoor neutral air temperature in spring and autumn while showing contrary behavior in summer and winter. Similar results were obtained by Chen et al. [62] who investigated thermal sensation and comfort evaluation methods in Harbin, China. There, air temperature and solar radiation were found to be most influential for the thermal sensation in Harbin.

Nikolopoulou and Lykoudis [63] analyzed the data obtained from microclimatic and human monitoring of about 10.000 interviews across five different countries in Europe. They proved the strong relationship between microclimatic and human comfort conditions with air temperature and solar radiation as the most important parameters. High wind speeds furthermore amplified the feeling of discomfort. Only at high temperatures, the elevated wind speed was identified as desired. The authors attributed minor importance to relative humidity as people cannot judge these changes unless the humidity is particularly high or low. Their analysis revealed that people tend to adapt more easily to heat than to cold and that both physical and psychological adaptation is taking place.

Yang et al. [64] performed a field survey with structured interviews and microclimatic measurements in an urban park in the subarctic city of Umeå in Sweden. About half of the interviewed people expressed their preference to higher solar radiation even at a thermal sensation of “slightly warm”. Since lower wind speeds together with exposure to sunshine can improve the thermal sensation of people, they suggested a curved terrain to decrease wind without providing shade in urban outdoor environments, such as parks in the subarctic or arctic climate.

A questionnaire survey at public spaces in Montreal, Canada was analyzed by Stathopoulos et al. [65] for the development of an overall comfort index. The study revealed that Montreal’s citizens desire higher air temperatures and solar radiation but lower wind speed and relative humidity during spring and autumn, regardless of the actual weather conditions.

Lai et al. [66] conducted a survey in the city of Tianjin in northern China. Along with the previously mentioned studies, people preferred lower wind speed and higher solar radiation at low air temperatures and vice versa at high air temperatures. People were able to adapt to warm temperatures by changing their clothing and activity levels. At temperatures above 30 °C, people were not able to further adapt to the environment.

In their review of outdoor thermal comfort (OTC) and outdoor activities, Chen and Ng [67] stressed the importance of outdoor spaces in promoting the quality of life and livability in cities. As people most commonly interact with each other and the physical amenities in urban spaces, like street furniture, kiosk stands, etc., the use and the quality of outdoor spaces is not only determined by the “state of body” but also by the “state of mind”. Therefore, they suggested that the perception of thermal comfort should be assessed on four different levels; physical, physiological, psychological and social/behavioral.

ENVI-met is a frequently used tool to assess thermal comfort in outdoor spaces [68–71] and has also been used to assess OTC in cold climate conditions, e.g. Toronto, Canada [72,73]. Most commonly, however, the summerly OTC and mitigation strategies in the context of heatwaves and the UHI are investigated. Numerical studies dealing with OTC in the transitional seasons or winter in high-latitude locations, are scarce. In a paper by Gatto et al. [74], the impact of urban vegetation on OTC was investigated in winter conditions in Lahti, Finland by using ENVI-Met. They found that urban vegetation generally decreases the mean radiant temperature in a neighbourhood, not only close to the vegetation. On the other hand, local improvements of OTC were reported from urban vegetation through lower wind velocities, although very close to the trees, shading led to strongly decreased OTC.

To form a better view of the microclimatic considerations for outdoor spaces in cold climate regions and to assess how different strategies may improve OTC conditions in autumn conditions, four alternative design strategies for the thermal comfort improvement of NTNU campus in Norway were considered, simulated and evaluated. The paper is divided into five sections. The second section provides the geographic and climatic context of the study area. In the third section, the applied methodology and the validation process are presented along with the investigated solution strategies. The results and the discussion follow in Section 4. The conclusions are drawn in Section 5.

2. Study area and climatic context

This study was carried out at the Norwegian University of Science and Technology (NTNU) which is located on a hill near the city center of Trondheim (63.4° N, 10.4° E). Trondheim is Norway's third-largest city with close to 200.000 inhabitants and is situated at a large fjord in Central Norway. NTNU's campus (called Gløshaugen) is 0.23 km^2 and lies at an altitude between 38 and 49 m above sea level (see Fig. 1). Due to the integration of another separated campus to Gløshaugen, the study area is undergoing a large redevelopment process until 2027. Step-by-step, 90.000 m^2 of buildings will be added to the area, and about 45.000 m^2 of existing buildings are to be refurbished.

According to the Köppen-Geiger climate classification system Trondheim's climate is oceanic (Dfb), but closely borders continental, subpolar and subarctic climates [75]. From November to March, moderate snowfall mixed with milder weather patterns and rain is common. The annual mean temperature is 4.8 °C (1961–1990), summers are relatively short, and winters are long and cool (see Fig. 2). However, due to climate change, temperatures in the arctic and subarctic regions have been rising, so that the Norwegian average annual temperature of the last 10 years from 2009 to 2018 has been 1.1 °C higher than the long-term mean from 1900 to 2018 [76]. In Trondheim, the mean annual temperature from 2009 to 2018 was 6.0 °C which is 1.2 °C above the average temperature of the norm period from 1961 to 1990 [76]. The monthly average of relative humidity in the period from 2009 to 2018 is highest in September with 78.2%, while in May, it is lowest with 67.6%. It can be also seen in Fig. 2 that the windiest month is March with 3.0 m/s, while July and August both show the lowest average wind speed of 2.1 m/s for the period from 2009 to 2018. Considering the monthly averages of global horizontal radiation, the differences are much more pronounced on a monthly basis. While in July 17.5 MJ/m^2 have been recorded on average, in December it is only 0.2 MJ/m^2 [76].

These relatively pronounced differences are caused by the proximity to the Arctic Circle that leads to quite short days in winter (sunrise at 10:01 and sunset at 14:31 local time on 21st December) and relatively long days in summer (sunrise at 03:02 and sunset at 23:37 local time on 21st June). Consequently, the sun elevation angles throughout the year are relatively low, reaching 50.0° at the summer solstice and only 3.3° at the winter solstice (see Table 1). For comparison, the sun elevation angles of Toronto, Canada, a city located in the same Köppen-Geiger climate region (Dfb) are 69.8° and 22.9° at the solstices, respectively. Such low elevations, like in the case of Trondheim, impact the solar access in street canyons of urban areas significantly.

To the North and Northwest, the campus is embedded into a park-like surrounding. To the East, South, and Southwest, the campus borders suburban residential areas with predominately single-family homes. Due to computational limitations in the numerical model size, which will be explained in the next chapter, only the northern part of the campus is used for the investigation. It was selected as it is the busiest and most vibrant outdoor space on campus.

The main connection route between the buildings, and a space frequently used for activities of any kind, is "Stripa", a North-South oriented pedestrian zone, lined by trees and largely surrounded by buildings in the West, North and East, and open to the South (see also Fig. 3). There are three entrances to Stripa, one in the North, one in the West and one in the South. This area represents the most-frequented on campus. Here, students and staff tend to eat their lunch outside during nice weather, change classrooms or just go out to get some fresh air at around 12:00 local time. The results of our study should help to determine how thermal comfort at this time of the day can be enhanced, in order to promote these activities and extend the periods in which acceptable outdoor conditions allow for them.

3. Methodology

The methodology used in this study is twofold: (i) field measurements and (ii) numerical simulations. Punctual field measurements of microclimatic parameters in the area of interest provided the necessary data to validate the numerical simulation model of the campus. That was an imperative step to confirm that the accuracy of the model is sufficient for the intended use [77,78]. The numerical simulations were carried out with ENVI-met v. 4.4, a three-dimensional non-hydrostatic software model for the surface-plant-air interaction [79] that is broadly used for the analysis of design impacts on the local environment, the specification of materials, and the usage of vegetation in a different configuration.

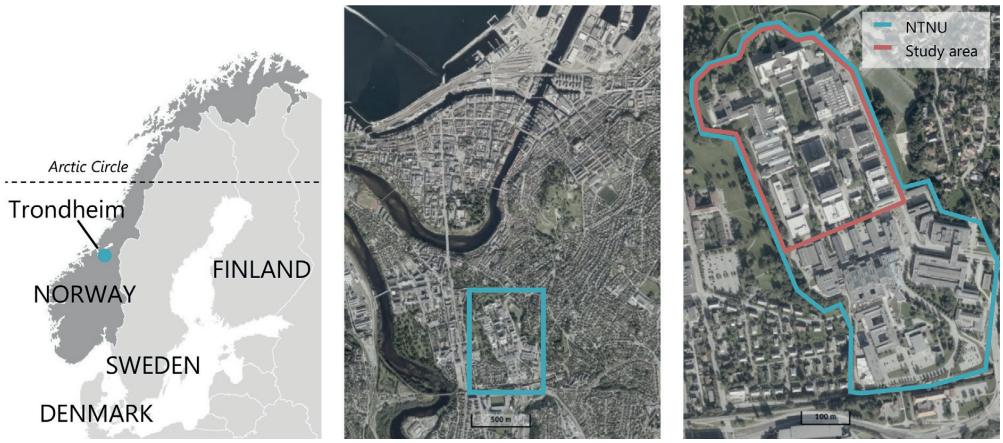

Fig. 1. Location of the study area and NTNU within Norway and Trondheim (aerial photographs from the Norwegian Mapping Authority www.kartverket.no).

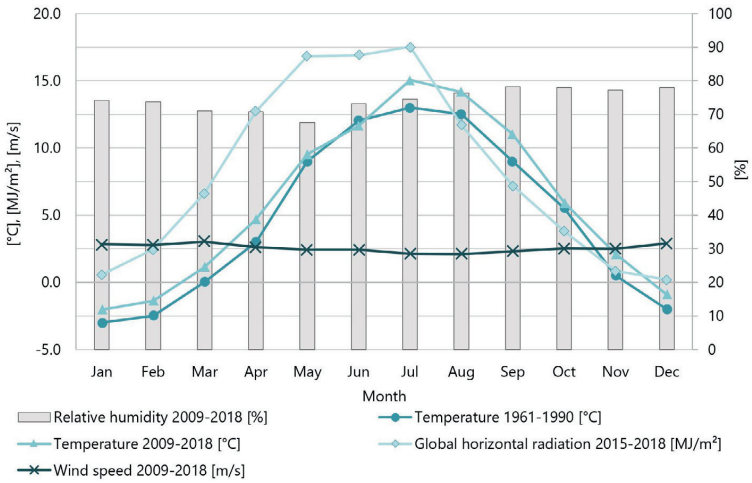

Fig. 2. Monthly averages of temperature, humidity and wind speed for Trondheim's weather station in Voll and average daily global horizontal radiation for each month for Gløshaugen campus [76].

Table 1
Sun elevation angles for different dates in Toronto, Canada and Trondheim, Norway.

Date	Max. sun elevation angle	
	Toronto, Canada (43.6° N)	Trondheim, Norway (63.4° N)
21.03. (vernal equinox)	47.0°	27.1°
21.06. (summer solstice)	69.8°	50.0°
23.09. (autumnal equinox)	45.9°	26.2°
20.10. (investigated day in this study)	35.7°	16.0°
21.12. (winter solstice)	22.9°	3.3°

Fig. 3. Stripa, seen from the South, during a sunny morning in autumn.

3.1. Measurement campaign

This study contains data collected from two different kinds of field measurements: (i) meteorological recordings and (ii) infrared (IR) thermography. For this study, measurements of one fixed weather station and four mobile weather stations were used (see Fig. 4). Fig. 5 shows photos of buildings in the different building categories on site. The fixed weather station of the campus, operated by the Dept. of Energy and Process Engineering, is located 10 m above the roof of the Varmeteknisk Laboratorium (VATL), 28 m above ground level. In this article, it will be further referred to as the reference weather station (RWS). The experimental data were obtained during a 4-week measurement campaign in autumn 2019 (from 27th September to 25th October) from four new on-site weather stations, mounted on tripods in 3 m height at different locations around the campus (see Fig. 6). A description of the used measurement equipment is given in Table 2. Furthermore, an H21-USB data logger was used to record data at a frequency of 0.1 Hz.

The conditions for the validation process were obtained on October 20th, 2019. On this day, a light breeze and clear sky conditions prevailed, with an average wind speed of 2.22 m/s, measured at the reference weather station on the VATL building. This day can be regarded as a typical, sunny autumn day in Trondheim. As mentioned earlier, IR thermography was used to obtain surface temperatures in addition to the meteorological measurements. Thermal images were taken for selected building surfaces. At designated locations, ground measurements were taken that include asphalted, paved and vegetated (grass) surfaces (see Fig. 4 and Fig. 5).

ENVI-met v. 4.4.2 was used to create a numerical model of the study area. ENVI-met simulation software incorporates the interactions between the atmosphere, materials, vegetation, radiation and the buildings to assess the urban environment [79]. This software was chosen because it is the most widely evaluated microclimate model available at present. Even though it is mostly used in temperate or warm climate conditions to evaluate measures for counteracting the UHI, e.g. [26,80–85], it can handle lower and below-zero temperature values as well. However, the used version did not permit to include snow on the ground and building surfaces which was found to affect the microclimate in cities [43,86], nor any form of precipitation. Within this limitation, simulations were performed only for dry weather conditions.

3.1.1. Computational domain geometry

For determining the positions of the different surface and vegetation cover types in the 3D model (Fig. 7), maps and aerial photographs provided by the Norwegian Mapping Authority (www.kartverket.no) from 2018 were used. On-site inspections provided

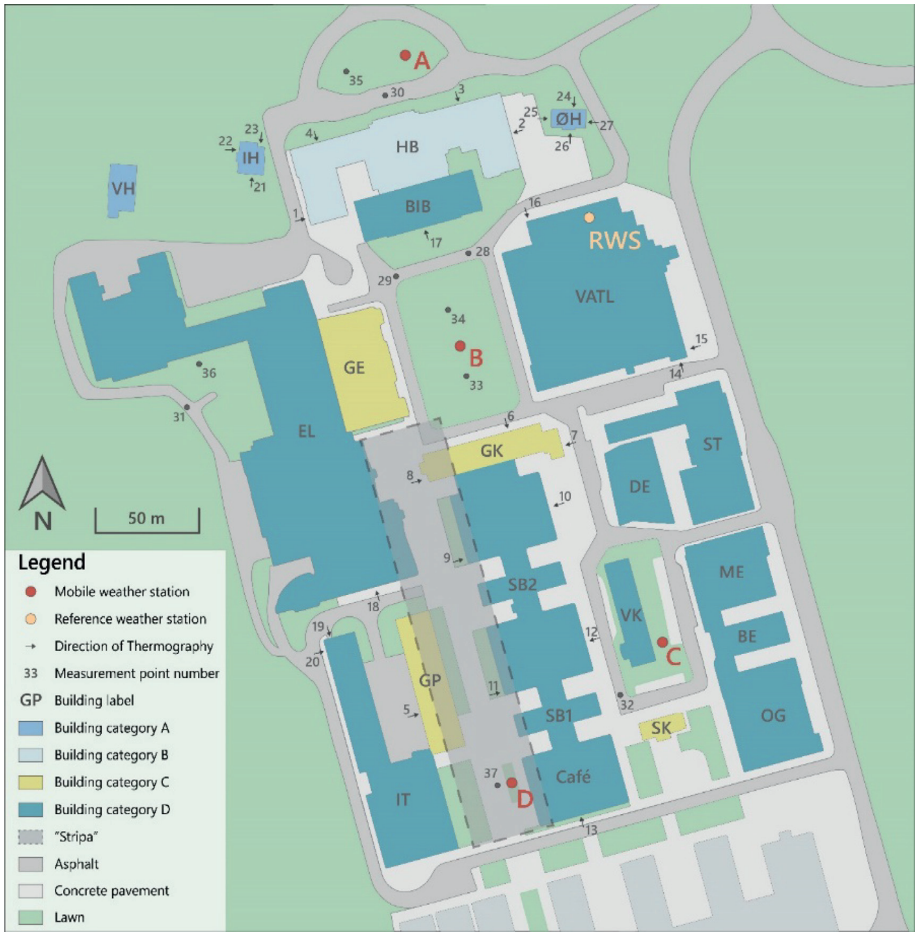

Fig. 4. Schematic site plan of the study area.

Fig. 5. Examples of the different building categories in the study area.

specific characteristics of the buildings, materials, and vegetation, including size and species. The created computational domain has the dimensions of 416 × 400 × 94.5 m^3 and was discretized into 104 × 100 × 32 grid cells, resulting in a 4-m grid in the horizontal directions, and a 3-m grid in the vertical. The lowest grid cell is subdivided into five cells with 0.6 m height respectively. According to the ENVI-met guidelines, the domain was modeled to be more than twice the height of the highest building (SB towers' height: 46 m, or 13 floors) and the horizontal distance to the model boundaries was larger than the closest building's height.

Fig. 6. Weather station B on a grass patch.Numerical model.

Initially, no computational nesting grids were added around the "normal" (visible) domain.

3.1.2. Materials and vegetation

In the area of interest, the ground surface types can be expressed by three main types: (i) grass, (ii) asphalt, and (iii) concrete pavement. Soil maps [87] of the region indicated a distinct clay content in the modeled area which matched the default soil profile (*sandy loam*) in ENVI-met. This profile was used below the buildings and the vegetative elements like grass, hedges, and trees. For the impermeable surfaces (ii) and (iii), the ENVI-met library entries *Asphalt Road* and *Pavement (Concrete), used/dirty* were employed [88].

Resulting from the park-like environment in which NTNU campus is embedded, green spaces, trees, shrubs, and hedges are common features in the study area. The amount of different sizes, species, individual peculiarities and the large number of elements necessitated a simplification of the model. Hence, the model was limited to three tree species, two hedge types and one grass type. The selected tree species were the most common tree types at the study site: (i) *Norway Maple* (modeled 10, 15 and 20 m tall), *Larch* (20 m) and *Scots Pine* (5 and 10 m). The seasonality of the foliation was considered by adapting the leaf area density (LAD) of the trees with a scaling factor. As the trees already started to defoliate, the scaling factor of 0.6 was used (see trees in Fig. 6). The two hedge-types were modeled as 1 m tall, one as conifer, one as deciduous and the height of the grass was set to 0.1 m.

Several construction phases during the long history of the campus resulted in several different building typologies (see Fig. 5). Table 3 shows the four building categories that were used to group the buildings according to their construction type and the specifications of wall and roof construction. In Table 4, the physical properties of the used materials are listed. The most common building type on campus is that of category D (11 buildings), followed by C (4 buildings), B (3 buildings) and A (1 building). Dating back to a time before the foundation of a university in Gløshaugen, the wooden buildings are rather small and not typical institutional buildings, so that wood is the least used façade material on campus. In all the other buildings, the building facades are characterized by heavy materials.

3.2. Validation

Validation is the process of determining how well the computerized model within its domain of applicability represents the real world with a satisfactory range of accuracy, by using physical observations. In other words, it makes sure that a numerical model within a certain range of acceptability is accurate enough for its intended use [77,78]. In practice, the quality of the results not only depends on the accuracy of the model itself but to a considerable degree also on the input provided by the users [91]. Consequently, the user's decisions regarding simplifications and experience in using the software can lead to substantial discrepancies, as found for instance in the case of building performance simulation (BPS) by Imam et al. [92].

The numerical model that was used in this study was created following the design-framework in Fig. 8. The model input for the meteorological boundary conditions was supplied by using the *intermediate* and *full forcing* option in ENVI-met.

The *full forcing* option facilitates variable meteorological boundary conditions (30-min intervals) for air temperature, relative humidity, solar radiation, as well as wind speed and direction. These input boundary conditions were generated from the measured meteorological data retrieved from the reference weather station on the VATL building. To split the measured global horizontal radiation into its direct and diffuse components as required for the input file in ENVI-met, the model by Skartveit and Olseth [93] was applied. Specifically developed for average snow-free conditions close to sea level in Norway, it was assumed to represent a suitable approximation.

The validation process consisted of three stages in which a different number of nesting grids were used, and adjustments of the meteorological boundary conditions were made in order to fit the measurements of the fixed and the four mobile weather stations as well as the IR thermography. An overview of the different calibration stages and their average R^2 and coefficient of variation of the root mean square error, the CV(RMSD), can be seen in Table 5. The equation for determining the CV(RMSD) can be seen in Eq. 1, where s_i and m_i are the simulated and measured value of time step i, respectively, n is the total number of time steps and $\bar{m}$ is the mean value of measurements.

Table 2
Measurement equipment used in the mobile weather stations.

Type of measurement	Measurand	Sensor	Accuracy
In-situ measurements	Wind direction	S-WDA-M003	±5° at 1.4° resolution
	Wind speed	S-WSB-M003	±1.1 m/s or ±4% of reading
	Air temperature	S-THB-M002	±0.21 °C from 0 °C to 50 °C
	RH of air	S-THB-M002	±2.5% from 10% to 90%
IR thermography	Surface temperature	AC080V	±2 °C or ±2% from –20 °C to +350 °C

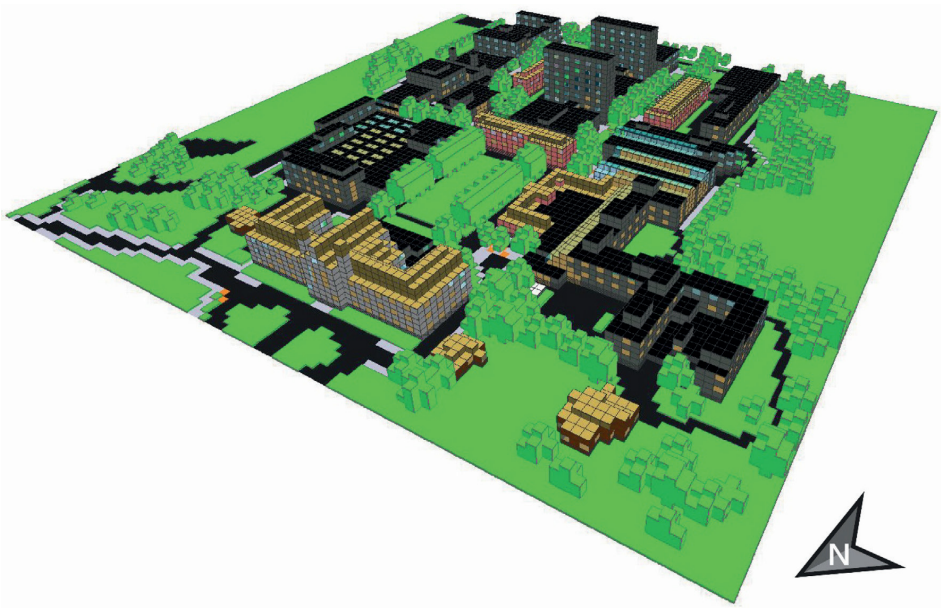

Fig. 7. 3D bird's eye view of the numerical model. Perspective from the northwest (NW).

Table 3
Building categories according to construction type and specifications of walls and roofs.

Category	Year of construction	Type	Layer 1 (outside)		Layer 2		Layer 3 (inside)	
			Material	d [m]	Material	d [m]	Material	d [m]
A	1850–1900	Wall	Wood: spruce	0.06	Insulation	0.08	Wood: spruce	0.06
		Roof	Roofing: tiles	0.03	Wood	0.04	Insulation	0.2
B	1910	Wall	Granite	0.3	–	–	–	–
		Roof	Roofing: tiles	0.03	Wood	0.04	Insulation	0.2
C	1910–1924	Wall	Solid brick	0.3	–	–	–	–
		Roof	Roofing: tiles	0.03	Wood	0.04	Insulation	0.2
D	1951–2002	Wall	Filled concrete blocks	0.3	–	–	–	–
		Roof	Bitumen	0.02	Insulation	0.2	Concrete	0.3

Table 4
Selected physical properties of the building surface materials on campus [88–90].

Surface	α [–]	ω [–]	ε [–]	c [kJ/(kgK)]	δ [kg/m^3]	λ [W/(mK)]
Wood: spruce	0.6	0.4	0.9	1600.0	450.0	0.12
Concrete	0.7	0.3	0.9	840.0	1260.0	0.85
Insulation	–	–	–	1030.0	50.0	0.045
Granite	0.8	0.2	0.9	1000.0	2600.0	2.8
Bitumen	0.92	0.08	0.9	1000.0	1050.0	0.17
Solid brick	0.6	0.4	0.9	1000.0	2400	1.4
Glass: clear float	0.05	0.05	0.9	750.0	2500.0	1.05

Absorptivity (α), reflectivity (ω), emissivity (ε), heat capacity (c), density (δ), thermal conductivity (λ)

A previous investigation of different grid spacing showed disproportionally long simulation times for finer grids than the used one. The discretization in a $4 \times 4 \times 3$ m^3, therefore, represents the finest, computationally still acceptable grid. Coarser grids were omitted as they are not able to sufficiently catch the geometrical features of the study area. The initial ENVI-Met model constitutes stage 1. In stages 2 and 3, the inlet air temperature $T_{a,in}$ and the inlet wind speed $u_{w,in}$ from the forcing file were reduced by 0.5 °C and 25%, respectively. Also, the number of nesting grids was increased from 0 in the initial model to 6 in stage 2, and 15 in stage 3.

$$CV(RMSD) = \frac{RMSD}{\bar{m}} \times 100\% = \frac{\sqrt{\sum_{i=1}^{n}(s_i - m_i)/n}}{\bar{m}} \times 100\,\% \qquad (1)$$

As can be seen from the calibration results, increasing the number of nesting grids did only marginally affect the accordance of simulated meteorological values with the measured ones. Fig. 9

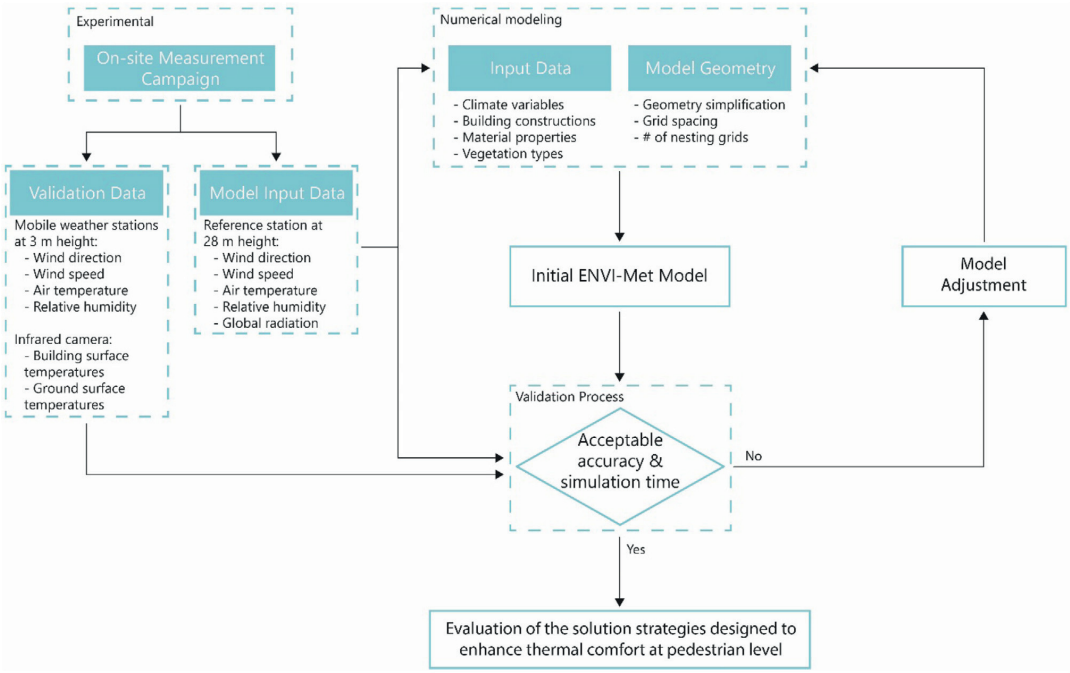

Fig. 8. Applied design framework for creating the ENVI-Met model, modified from [80].

Table 5
Overview of calibration stages and quality measures to compare simulated and measured data.

	Number of nesting grids	Adjustments of meteorological conditions	Mean R^2 of climate variables	Mean CV (RMSD) of climate variables	Mean absolute difference of surface temperatures
Stage 1 (initial model)	0	–	0.55	101.2%	4.58 °C
Stage 2 (selected)	6	$T_{a,in}$ reduced by 0.5 °C $u_{w,in}$ reduced by 25%	0.56	75.4%	2.86 °C
Stage 3	15	$T_{a,in}$ reduced by 0.5 °C $u_{w,in}$ reduced by 25%	0.54	76.5%	4.02 °C

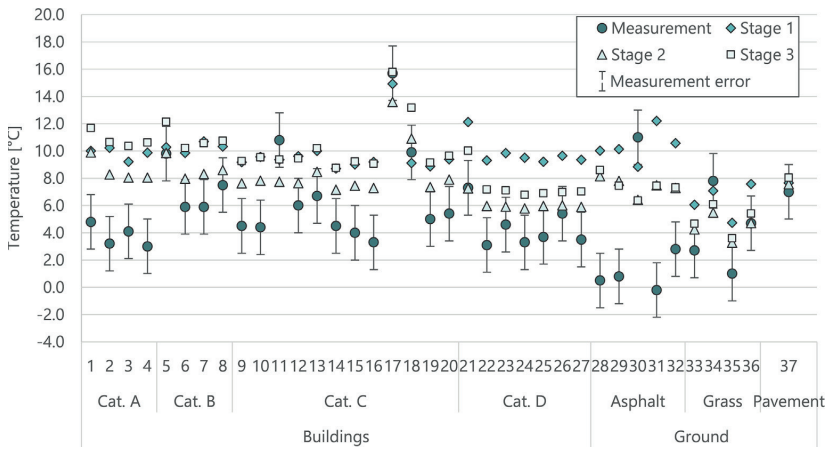

Fig. 9. Measured and simulated surface temperatures of the calibration stages at the 37 measurement spots. The bars above and below the measurement values indicate the measurement errors associated with the accuracy of the IR camera.

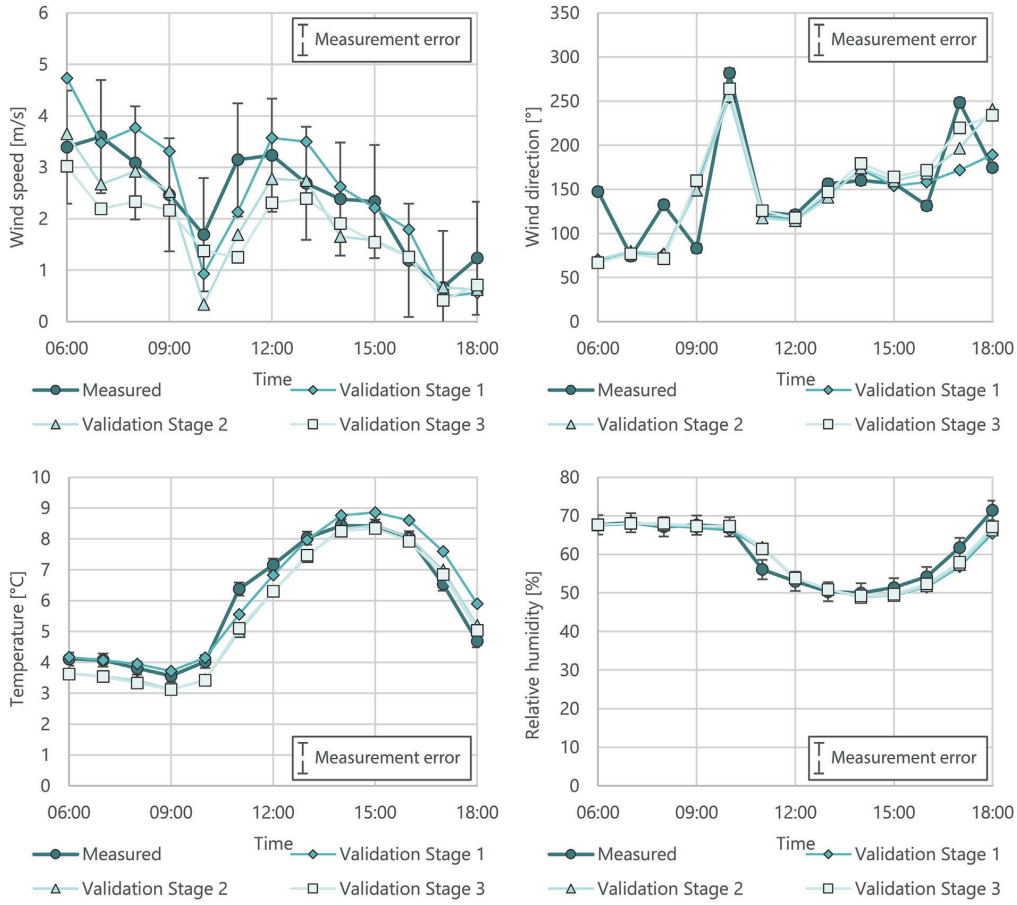

Fig. 10. Measured and simulated climate variables of the calibration stages at the VATL reference weather station. The bars above and below the measurement values indicate the measurement errors associated with the accuracy of the sensors.

and Fig. 10 show the measured and simulated climate variables including the measurement error resulting from the sensor accuracy. On the contrary, the mean absolute difference of simulated and measured surface temperatures was subject to a noticeable variation. The simulations largely overestimate the measured surface temperatures. Especially in building category A and the ground surfaces of type *asphalt*, the simulation results significantly surpass the measurements.

In Fig. 10, the measured and simulated climate variables at the reference weather station on the VATL building are plotted. As visible from the graphs, the course of the measured values is followed by the simulations to a large extent. The validation assessment shows overall good results (see Table 6). Especially stage 2 shows a good correlation (average $R^2 = 0.85$) on modeled air temperature, a moderate correlation (average $R^2 = 0.40$) on modeled wind speed and a good correlation (average $R^2 = 0.80$) on modeled relative humidity. The CV(RMSD) of modeled air temperature and relative humidity in this stage was 9.3% and 7.7%, respectively. The model of stage 2 was considered valid for the set of experimental conditions, as its accuracy is within an acceptable range. Therefore, the model of stage 2 was used in the simulations for the analysis of this study.

However, the model results do not provide adequate accuracy on wind direction data. This may be caused by placing the weather stations close to buildings where turbulence is usually very high. Using a wind vane to capture the direction of the flow will inevitably lead to high uncertainty of the measurement compared to an undisturbed, open setting. Furthermore, it can be noticed that the CV(RMSD) of the wind speed and wind direction in particular are very high. This can be partly explained, as the used measurement equipment to capture wind speed and direction has a relatively high sensitivity threshold of 1 m/s. The measured wind speeds were, therefore, often 0 m/s, while in the simulations, also wind speeds below this threshold occurred. As there are many 0-measuements, calculating the CV(RMSD) of these climate variables results in very high values. Analogously, at wind speeds below 1 m/s, the wind vane of the wind direction sensor will not move to the respective wind direction, while in ENVI-Met such a sensitivity threshold does not exist and every air movement, no matter how small, is captured with its velocity and direction.

3.3. Design strategies for improving urban microclimate and outdoor thermal comfort

As shown in chapter 2, summers in Trondheim are relatively short and mild. With an average monthly temperature of about 12–15 °C and generally less windy conditions, the summer months

Table 6
R^2 and CV(RSMD) of all the validation data. The values with the best accordance with the measurements of each category are highlighted in bold.

Weather station	Climate variable	Stage 1		Stage 2		Stage 3	
		R^2	CV (RMSD)	R^2	CV (RMSD)	R^2	CV (RMSD)
VATL	Wind speed	0.85	**27.6%**	0.74	31.2%	**0.92**	37.2%
	Wind direction	0.02	**27.0%**	**0.05**	27.6%	**0.05**	27.5%
	Air temperature	**0.93**	**9.2%**	0.91	10.2%	0.89	9.7%
	Relative humidity	**0.91**	4.5%	**0.91**	4.2%	0.88	**3.7%**
Station A	Wind speed	0.42	172.3%	0.36	95.9%	**0.45**	**63.8%**
	Wind direction	0.01	**40.1%**	**0.16**	109.9%	0.00	102.1%
	Air temperature	**0.85**	15.0%	0.81	**9.5%**	0.83	10.0%
	Relative humidity	**0.78**	10.2%	0.73	9.2%	0.76	**9.1%**
Station B	Wind speed	**0.38**	1018.3%	**0.38**	**672.1%**	**0.38**	713.0%
	Wind direction	0.15	**74.9%**	**0.22**	79.3%	0.13	75.0%
	Air temperature	**0.82**	16.6%	**0.82**	10.2%	0.79	**8.8%**
	Relative humidity	**0.76**	10.9%	**0.76**	**9.8%**	0.73	**9.8%**
Station C	Wind speed	0.39	250.6%	0.39	**160.9%**	**0.40**	166.6%
	Wind direction	0.27	**41.9%**	**0.40**	52.6%	0.27	58.3%
	Air temperature	**0.86**	11.2%	**0.86**	8.1%	0.81	**6.4%**
	Relative humidity	**0.80**	8.1%	**0.80**	**6.7%**	0.75	**6.7%**
Station D	Wind speed	0.16	218.7%	0.18	**158.2%**	**0.29**	160.0%
	Wind direction	0.00	44.5%	0.00	**35.8%**	0.00	47.3%
	Air temperature	**0.88**	12.0%	0.87	8.8%	0.82	**7.8%**
	Relative humidity	**0.80**	9.6%	0.79	8.3%	0.70	**8.1%**
Average		0.55	101.2%	**0.56**	**75.4%**	0.54	76.5%

from June to August, in general, provide good conditions for spending time outdoors, apart from the many showers of rain that frequently occur throughout the year in the area [75]. Regarding OTC research in this kind of climate, the focus should be put on winter and the transitional seasons rather than summer. Thus, the aim of this study is to promote outdoor activities and extend the period in which people feel comfortable being outside at the university campus during the transitional season of autumn.

The weather conditions of the day that was used for the validation (October 20th, 2019) can be regarded as a typical, sunny autumn day, as its mean temperature (5.5 °C) and wind speed (2.22 m/s) were in close vicinity to the average values for Trondheim for the period from September to November (6.3 °C and 2.45 m/s for the years 2009–2018). Hence, the following solution strategies were simulated using the same weather conditions as for the validation except for the wind direction. Since there were strong fluctuations in wind direction on the validation day, the prevailing wind direction for Trondheim during autumn, which is 225° from North (SW), was used. SW is the prevailing wind direction throughout the whole year.

The frequently used Predicted Mean Vote for outdoor conditions (PMVo), originally developed by Fanger [94] for indoor conditions (PMV) and adapted for outdoor by Jendritzky and Nübler [95], served as an indicator of OTC in this study. The software ENVI-Met applies the PMVo equations on a 9-point scale (−4 very cold, −3 cold, −2 cool, −1 slightly cool, 0 neutral, 1 slightly warm, 2 warm, 3 hot, 4 very hot) as described in the German VDI 3787 Part 2 [96]. Although originally developed for the application indoors, the PMV was chosen as it represents the most renowned comfort index and is expected to deliver meaningful results as it has been adapted to the use for outdoor spaces. The PMVo has been applied in many other studies of OTC using ENVI-met and can therefore be considered as a reliable indicator for this study's purpose [26,68,69,97].

As outlined in the introduction, people in cool or wintry conditions prefer higher air temperatures and solar radiation, as well as lower wind speeds. These variables are key parameters in evaluating thermal comfort in a comfort index like the PMVo. Hence, solution strategies in the built environment need to take them into consideration in order to improve OTC. The recognized measures to counteract overheating in cities and tackle people's heat stress in regions with hot summers provide useful guidance for this study's purpose, as the exact opposite is supposed to lead to suitable solutions. Thus, decreasing the surface albedo to increase solar absorption and thus surface temperatures and the emittance of longwave radiation may have a favorable effect on OTC. Additionally, the decrease of the wind speed through vegetation or constructive elements like buildings or walls, wind shelter, etc. may locally improve OTC conditions. Finally, increasing solar access in frequently-occupied spaces, for example by removing redundant vegetation, etc. may have a beneficial impact.

With this in mind, four scenarios have been developed and investigated (see Fig. 11) to improve OTC at 12:00 local time in the most-occupied outdoor space on campus, "Stripa" (see Fig. 3 and Fig. 4). 12:00 was selected because people use to spend their lunch break outside near the Café on sunny days or change buildings for lectures, using Stripa as the main connection.

The scenarios build upon the current situation which represents the base case of this study (see Fig. 7). In its current form, greenery covers about 48% of the area at ground surface level (3% trees and hedges, 45% grass). The remaining area is covered by buildings (26%), asphalt (16%), and pavement (10%). The surface materials of the buildings are defined by their building category and their respective wall constructions which can be seen in Fig. 4, Table 3 and Table 4.

In scenario a) all the trees have been removed from the study area. The next two scenarios aim to reduce the wind speed by "closing" the entrances in the East, West and South of the campus with building structures (b) and trees (c). In scenario b), the inserted buildings were modelled to be of the same height as the structures on each side of the passages that they close. In the case of the two passages in the east, the inserted buildings were 12 m, in the two southern passages they were 14 m, and in the western passage, the building was 16 m high. In scenario c), the passages were closed with one row of 20 m high trees (Norway Maple). Scenario d) addresses the building surfaces by adding a dark façade cladding in the form of charred wood panels to the base case. The darker color at the surfaces generally leads to higher surface temperatures and thus a higher mean radiant temperature (MRT).

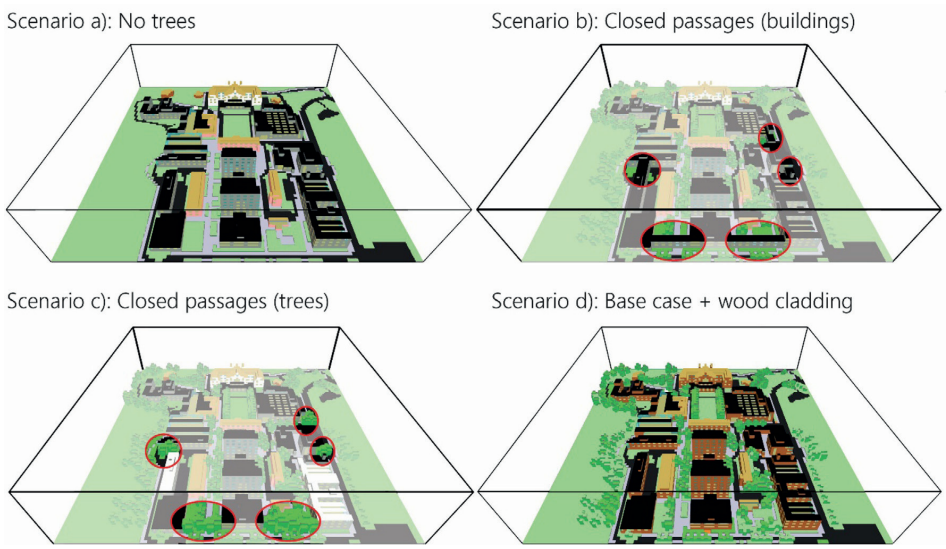

Fig. 11. Bird's eye views of scenarios a) to d).

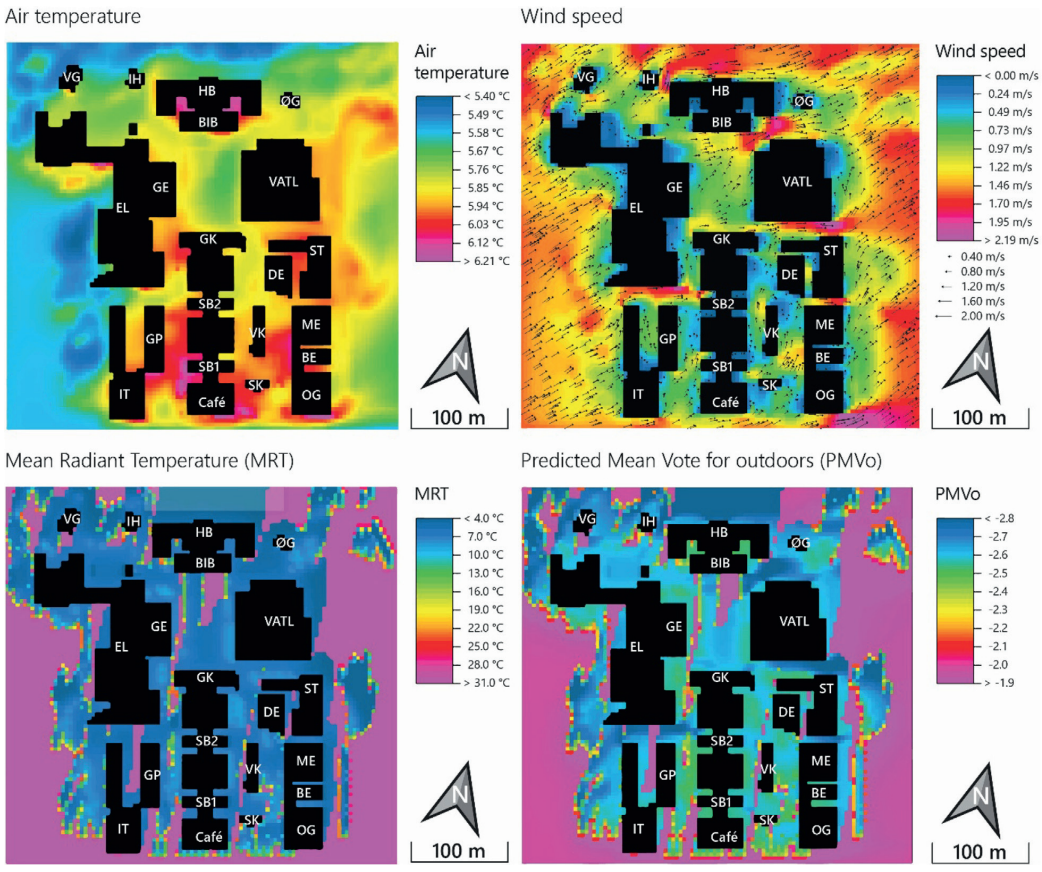

Fig. 12. The simulated spatial distribution of the air temperature, wind speed, MRT and PMVo for the campus in its current situation (base case).

4. Results

4.1. Base case

Fig. 12 shows the air temperature, the wind speed, the MRT, and PMVo of the campus in its current situation (base case). The PMVo was calculated at the pedestrian level (1.5 m) for an average 22-year-old person (male) with 75 kg, a metabolic rate of 1.52 met (activity: walking at 1.2 m/s) and a clothing level of 1.2 clo (regarded as typical for autumn). The spatial data visualization was performed with LEONARDO, ENVI-met's module for visualizing and analyzing the performance of the model environment.

The PMVo values for a typical day in October in the study area were between −2.8 (cold) and −1.9 (cool), with the highest values occurring in areas where unobstructed solar radiation is available. The lowest values were reached in shaded areas where additionally high wind speeds occur which was mostly the case in narrow passages between buildings. There, channeling effects accelerated the air from the inlet wind speed of 2.2 m/s to a top speed of up to 2.5 m/s. At Stripa, the average values for air temperature, wind speed, MRT and PMVo were calculated as 6.54 °C, 0.78 m/s, 12.45 °C and −2.72 respectively.

4.2. Strategy evaluation

The simulated results (for a typical autumn day at 12:00) show that the suggested strategies have a small effect on OTC. The examined solutions aimed at improving the thermal sensation of the humans and thus increasing the PMVo (through addressing different microclimatic parameters such as the solar radiation, the air temperature, the MRT and the wind speed). The simulated scenarios indicate that significant improvements in terms of the PMVo (up to 1.1 higher) at the pedestrian level were only possible if the solar access was maximized (see Fig. 13).

4.2.1. Air temperature

In scenario a), where all trees were removed from the study area, the largest improvement of air temperature at Stripa was registered with 0.37 K in front of the EL building (see Fig. 13). Where trees in the base case obstructed the sun, it now warms up the ground and building surfaces, causing the air temperature closeby to rise.

In scenario b), changes in air temperature of this magnitude only occurred directly in front of the south façade of the inserted building west of the Café at Stripa's southern entrance. There, unobstructed solar radiation reaches the south-facing building surface all the way down to the pedestrian level and thus causes air temperatures to rise. However, at Stripa, shadowing from buildings and trees largely prohibit positive changes in air temperature at the pedestrian level, as the obstructed sun cannot warm up the building surfaces close to the ground. For that reason, the air temperature at the pedestrian level remains close to unchanged in scenario d). On the contrary, the newly inserted building in scenario b) which is meant to provide protection from wind, obstructs incoming solar radiation and therefore causes the air temperature to decrease by up to 0.31 K near the SB1 building and the Café. The same is visible in scenario c) where additional trees at Stripa's southern entrance cast more shadow and thus prevent surfaces nearby to warm up. On average, however, the change in air temperature was negligible in all the investigated scenarios (see Fig. 17).

4.2.2. Wind speed

Removing the trees in scenario a) had an amplifying effect on wind speed as visible from Fig. 14. Almost throughout the entire extent of Stripa, the wind speed increased with reaching values up to 26.3% higher than in the base case. Only in the wake of the GP building at the northern end of the examined area, wind speed slightly decreased by up to 9.4%. On average, values increased by 10.7% in scenario a). Conversely, inserting buildings to close the southern and western entrances to Stripa contributed to a lower wind speed in scenario b) where the average values went down by 3.7%. Maximum reductions reached 46%. In scenario c), adding more trees to the entrance areas in the West and South resulted in only 0.6% lower average values where the largest decrements reached 13.7%. In the scenarios b) and c), significant increases in wind speed occurred only in the very south of Stripa with 14.1% and 10.3%, respectively. Naturally, the change of the surface materials as in scenario d) did not have a noteworthy impact on the

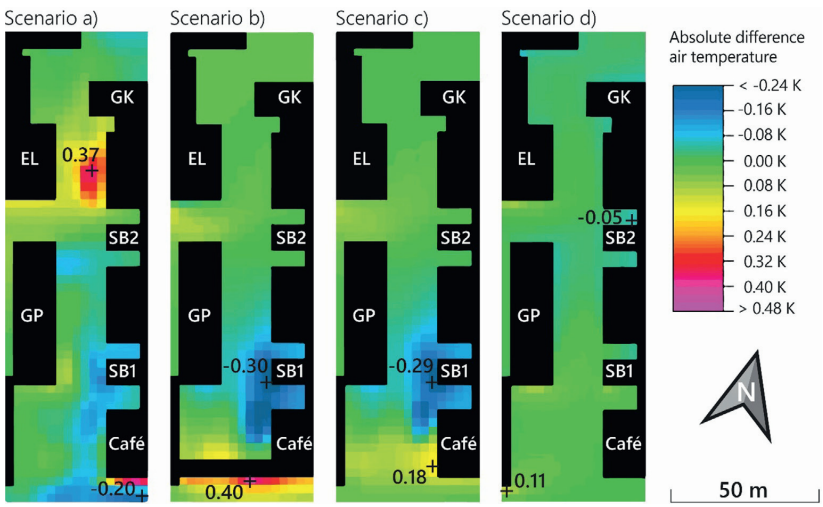

Fig. 13. Absolute change in air temperature in the examined area Stripa at 12:00 at pedestrian level (1.5 m) of the scenarios a) to d) compared to the base case. The crosses indicate the spots with the highest and lowest value of each scenario.

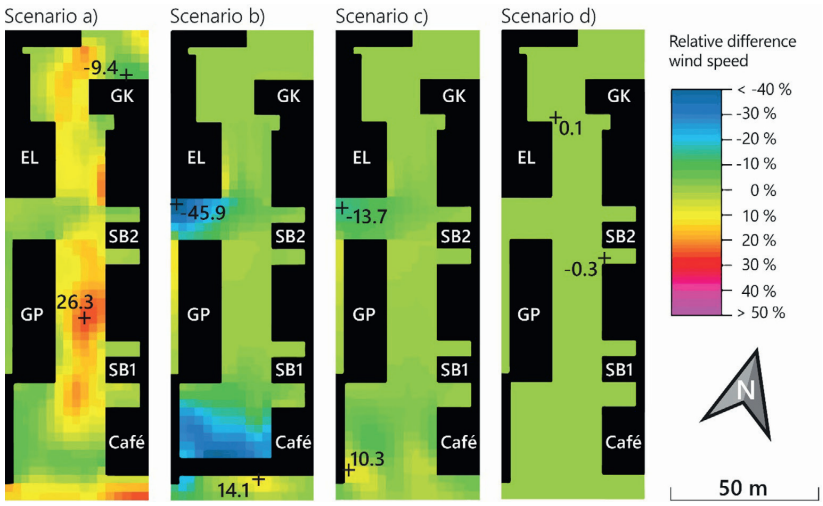

Fig. 14. Relative difference of wind speed at Stripa at 12:00 at pedestrian level (1.5 m) of the scenarios a) to d) compared to the base case. The crosses indicate the spots with the highest and lowest value of each scenario.

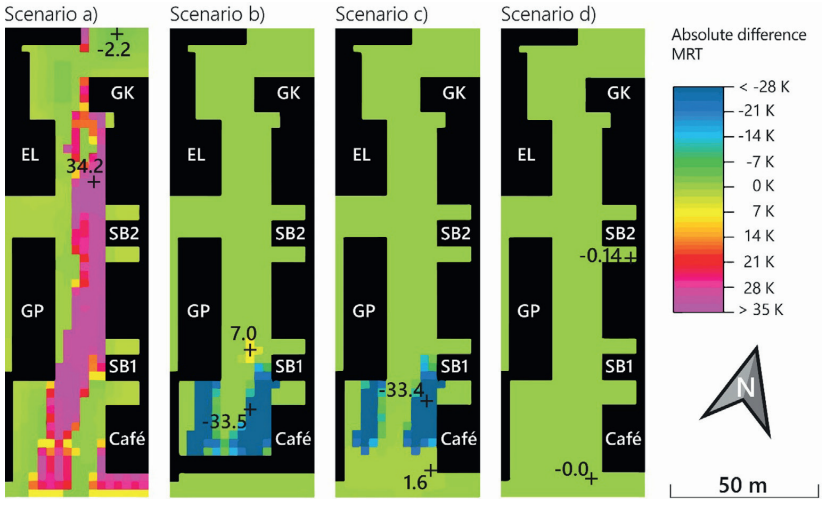

Fig. 15. Absolute change of MRT at Stripa at 12:00 at pedestrian level (1.5 m) of the scenarios a) to d) compared to the base case. The crosses indicate the spots with the highest and lowest value of each scenario.

wind field. The average value at Stripa for the wind speed remained unchanged.

4.2.3. Mean radiant temperature and PMVo

Fig. 15 and Fig. 16 show the change of MRT and PMVo for the scenarios a) to d) compared to the base case. The visual similarity of both parameters' colormaps illustrates the strong correlation between the MRT and PMVo. Consequently, in areas of an increased MRT compared to the base case, also the PMVo values were improved. Especially in scenario a), where removing the trees resulted in maximized solar access, the change in MRT and PMVo reached top values of 34.2 K and 0.95, respectively. There, the points in which the maximum and minimum values almost match. In scenario b, the average MRT and PMVo at Stripa improved by 13.9 K and 0.33, respectively.

Similarly, in scenarios b) and c) the largest decreases of MRT and PMVo roughly coincide in the same points. This is because the added building and trees in the south of Stripa obstruct the sun, causing the MRT and the PMVo to drop by up to 33.5 K or 0.80, respectively. While in the scenario b), the average MRT, compared to the base case, slightly improved by 0.02 K, the PMVo dropped by 0.08 at Stripa.

In scenario c), the effect of additional trees resulted in both, a lower average MRT (−0.11 K) and PMVo (−0.06) compared to the base case at Stripa. In scenario d) however, where a lower surface albedo was expected to result in higher surface temperatures and

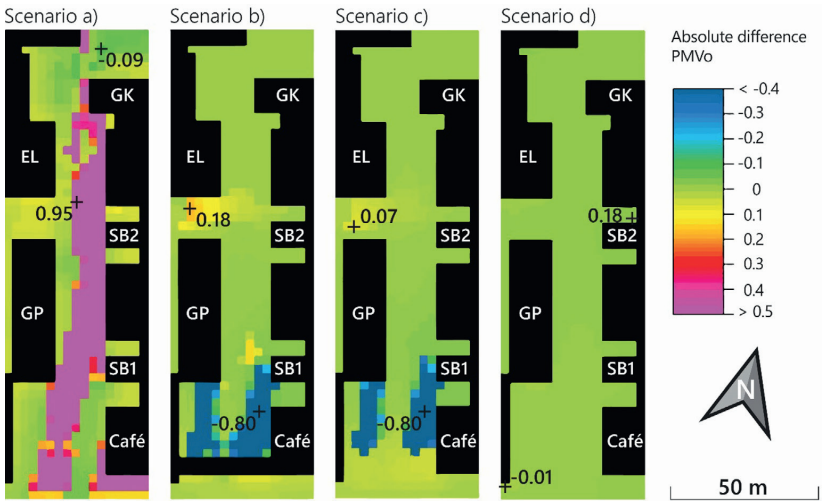

Fig. 16. Absolute change of PMVo at Stripa at 12:00 at pedestrian level (1.5 m) of the scenarios a) to d) compared to the base case. The crosses indicate the spots with the highest and lowest value of each scenario.

thus higher MRT and PMVo, the exact opposite effect was identified. The average MRT and PMVo both slightly decreased at Stripa. This is because, during the cold season in a high-latitude location as Trondheim, only little solar radiation reaches building surfaces at the pedestrian level due to low solar angles. Shadowing from buildings and trees in this scenario does not allow to make use of the new façade properties. Consequently, a different surface material will generally have a rather small effect on the MRT and hence the PMVo. The largest improvements in PMVo in the scenarios b) and c) are attributable to reduced wind speed near the closed western entrance to Stripa. There, maximum improvements were 0.18, 0.07 and 0.18, respectively. Again, in scenario d), changes were negligible.

5. Discussion

In summary, most pronounced improvements were achieved with maximizing solar access. The difference between shaded and unshaded areas with otherwise equal conditions on the simulated day can be quantified with a PMVo of ca. 1.0. Having in mind the variability in meteorological conditions, particularly in solar radiation, wind sheltering can be an effective measure to increase OTC, especially on windy days. This is particularly the case when days get even shorter and sun angles lower in winter. The effect of wind-sheltering, however, was found to be quite local. Considerable reductions of the wind speed occurred only within a range of 1.0–2.5 times the height of the inserted buildings and 0–1.5 times the height of the inserted trees. However, only one row of 20 m high Norway Maple trees was placed in the passages. Inserting a mix of small and high conifers in addition in two or more rows might reduce the wind speed more effectively [98]. Additionally, the sheltering elements may provide additional shade which leads to an overall negative effect on sunny days when sun angles are not too low.

On the simulated, typical and sunny autumn day in Trondheim with a comparatively low wind speed of 2.2 m/s as an inlet condition, access to solar radiation turned out to be significantly more effective than wind protection. The former was able to increase local PMVo values by up to 1.0 compared to shaded areas while the latter accounted for improvements not exceeding 0.6 on the campus. At Stripa on the other hand, the effects of increased solar access and wind sheltering were lower, as it improved local PMVo values by 0.95 and 0.18 respectively. These results corroborate the findings from other studies that solar radiation is one of the most important factors for OTC and that it is more important than wind sheltering [60,61,63,64].

As the resulting changes in PMVo are comparatively small, wind sheltering in locations with rather low average wind speeds cannot be regarded as a suitable strategy to improve outdoor thermal comfort on a larger scale. This especially applies to areas, where people tend to move around such as pedestrian zones. In areas, however, where people tend to stay in one area, like seating areas in cafés for instance, wind sheltering can be used to improve outdoor thermal comfort. More customized design solutions than the ones investigated in this study are necessary in order to achieve larger improvements of OTC. Similar design considerations were given by Leng et al. [99] who stress the consideration of solar access in the design of public spaces, as people in winter cities, during the transional seasons, tend to seek sunlight. They also refer to sheltered sitting areas and heated seats.

Simulations with a higher wind speed showed that wind sheltering can become more effective in increasing the PMVo than solar access. From about 8 m/s imposed at the inlet, both measures became equally effective in increasing OTC. As a solution, transparent wind sheltering elements e.g. around outdoor sitting areas (for instance from glass) may be able to provide near unobstructed solar access and protection from the wind at the same time. Introducing darker surface materials to building façades in order to increase the MRT had a negligible effect on the microclimate and thus OTC, as low solar angles during the cold seasons prevent solar radiation to warm up the surfaces. As Jamei et al. [100] concluded in their review on the impact of urban geometry and pedestrian level greening on OTC, a larger distance between buildings is necessary in high-latitude locations to avoid overshadowing and thus increase solar access. It can be seen in Fig. 7 and Fig. 11 that Stripa is shaded during the morning hours by numerous trees and the two large buildings (SB1 and SB2) in the east. At lunch time, the sun reaches a sufficient elevation and azimuth to finally reach pedestrian level surfaces. However, without solar access over a

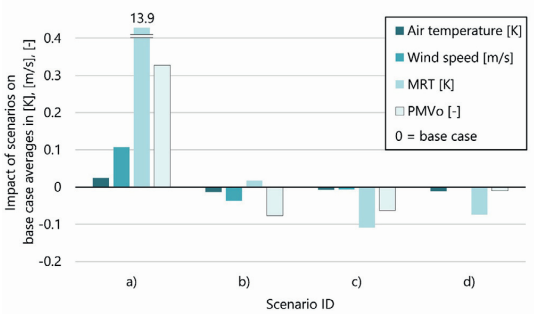

Fig. 17. Impact of the investigated microclimatic design scenarios a) through d) on average air temperature, wind speed, MRT and PMVo when compared to the base case at Stripa.

sufficient time span, changing the surface materials consequently has a negligible influence on OTC at the investigated location and time. Fig. 17 sums up the changes in the investigated scenarios at Stripa and shows the direction and magnitude of change of the different variables of the four scenarios compared to the base case averages. Fig. 18 visualizes the resulting predicted percentage of dissatisfied (PPD) for all investigated scenarios as well as the base case. Only scenario a) noticeably improved the situation, while the scenarios b) and c) affected the OTC slightly negative at Stripa. Scenario d) resulted only in marginal changes.

With regard to the software ENVI-Met which was used to create the numerical model, some limitations apply in this study as well. First of all, ENVI-Met does not allow to depart from a fixed, structured grid when setting up the geometry of the model area. Curved and sloped surfaces need to be approximated with square blocks, which not only influences their orientation and aerodynamics but also increases the surface area of these elements. For this study, a 4-m grid was chosen to ensure acceptable simulation times and accuracy, as it was not possible refining the grid in the areas of interest while coarsening it at the boundaries. Furthermore, the program's output is time- (hourly) and space-averaged (per grid cell). Especially in the validation of the model these limitations might explain part of the deviations between measurements and simulations. However, the investigated climate variables were represented reasonably well by the numerical model.

6. Conclusion

In this study, numerical simulations of the urban microclimate of a university campus in Trondheim, Norway were carried out with ENVI-met. The numerical model was validated with on-site measurements of wind speed, wind direction, air temperature, humidity, and surface temperatures taken in autumn 2019. The validated model was used to investigate four scenarios: (a) removing all trees from the study area, (b) closing the passages with buildings and (c) trees, and (d) changing the surface material of the buildings.

When designing public spaces in a cold climate like in Norway, the access to solar radiation proved to be a key element to provide OTC. Wind sheltering also enhanced OTC conditions, although not quite as sharply outlined as solar access. However, on particularly windy and cloudy days, wind sheltering is the only effective way to increase OTC. Thus, a combination of both, increased access to solar

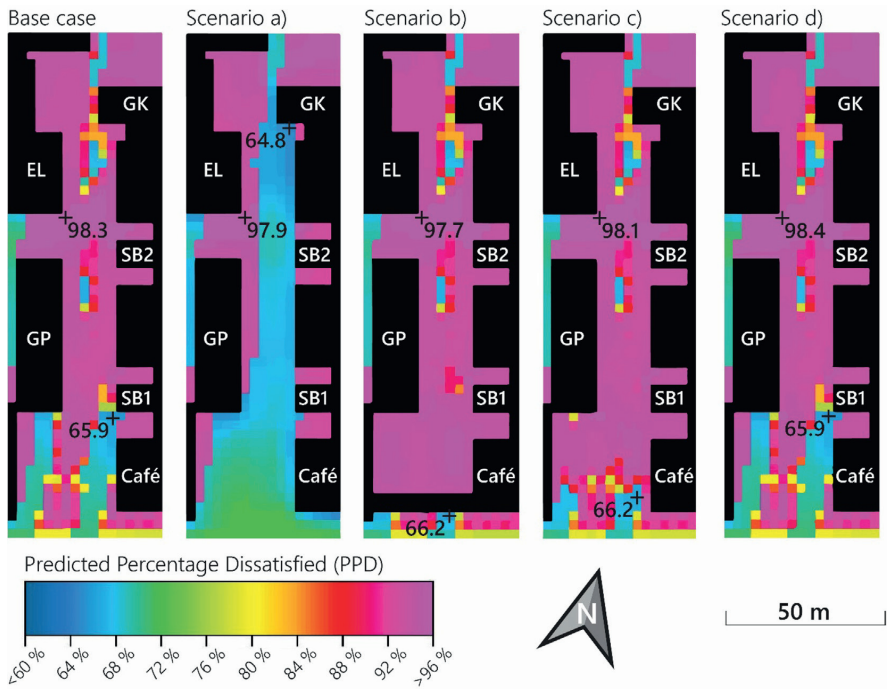

Fig. 18. PPD at Stripa at 12:00 at pedestrian level (1.5 m) of the base case and scenarios a) to d). The crosses indicate the spots with the highest and lowest value of each scenario.

radiation and protection from elevated wind speed can effectively increase OTC and consequently promote outdoor activities and make people stay outdoors longer. Increasing the albedo of the building surface materials had an insignificant effect on OTC as the solar angles during the cool and cold seasons in a city with typical building-height-to-street-width ratio at this latitude are too low to significantly increase surface temperatures and thus the MRT and PMVo at pedestrian level.

This study has gone some way towards enhancing our understanding of the design of open spaces in high-latitude urban settlements. We have obtained comprehensive results showing the effect of solar access and wind sheltering to enable thermal comfortable environments in outdoor areas. Furthermore, this study has shown that reversing design interventions which proved to be effective and are typically used in warmer climates to mitigate the UHI like changing the albedo of surface materials, are not as effective in high-latitude locations due to less solar incidence and lower sun angles during the cold season.

This study helped to understand the effect of different interventions with the urban environment on OTC. It confirms that of the microclimatic parameters that affect people's comfort only solar radiation and wind can be favorably modified by the surrounding. Further research is needed to mitigate adverse effects and maximize the climate-resilience of high-latitude cities. Studies that also consider the morphology of urban districts or neighborhoods like building-height-to-street-width ratios, building patterns, shapes, and orientation should be conducted.

CRediT authorship contribution statement

J. Brozovsky: Conceptualization, Data curation, Investigation, Methodology, Formal analysis, Software, Validation, Project administration, Writing - original draft, Writing - review & editing. **S. Corio:** Formal analysis, Investigation, Software, Validation, Visualization, Writing - review & editing. **N. Gaitani:** Conceptualization, Methodology, Writing - review & editing. **A. Gustavsen:** Conceptualization, Methodology, Supervision.

Declaration of Competing Interest

The authors declare that they have no known competing financial interests or personal relationships that could have appeared to influence the work reported in this paper.

Acknowledgments

This paper has been written within the Research Centre on Zero Emission Neighbourhoods in Smart Cities (FME ZEN). The authors gratefully acknowledge the support from the ZEN partners and the Research Council of Norway.

References

[1] L. Howard, The Climate of London Deduced From Meteorological Observations Made in the Metropolis and at Various Places Around It, 2nd ed., Harvey and Darton; J. Rickerby, London, 1833.
[2] United Nations, Department of Economic and Social Affairs, Population Division. World Urbanization Prospects: The 2018 Revision. Online Edition. New York, USA; 2018.
[3] O. Edenhofer (Ed.), Climate change 2014: Mitigation of climate change Working Group III contribution to the Fifth Assessment Report of the Intergovernmental Panel on Climate Change, Cambridge University Press, New York (USA), 2014.
[4] G. Mills, Urban climatology: history, status and prospects, Urban Clim. 10 (2014) 479–489, https://doi.org/10.1016/j.uclim.2014.06.004.
[5] T.R. Oke, Urban heat islands, in: I. Douglas, D. Goode, M. Houck, D. Maddox (Eds.), The Routledge Handbook of Urban Ecology, 1st ed., Routledge, London, 2011, pp. 120–131.
[6] I.D. Stewart, T.R. Oke, Local climate zones for urban temperature studies, Bull. Am. Meteor. Soc. 93 (12) (2012) 1879–1900, https://doi.org/10.1175/BAMS-D-11-00019.1.
[7] J. Berko, D.D. Ingram, S. Saha, J.D. Parker, Deaths Attributed to Heat, Cold and Other Weather Events in the United States, 2006–2010, Hyattsville, MD, USA, 2014.
[8] A. Fouillet, G. Rey, F. Laurent, G. Pavillon, S. Bellec, C. Guihenneuc-Jouyaux, et al., Excess mortality related to the August 2003 heat wave in France, Int. Arch. Occup. Environ. Health 80 (1) (2006) 16–24, https://doi.org/10.1007/s00420-006-0089-4.
[9] D. Shaposhnikov, B. Revich, T. Bellander, G.B. Bedada, M. Bottai, T. Kharkova, et al., Mortality related to air pollution with the moscow heat wave and wildfire of 2010, Epidemiology (Cambridge, Mass.) 25 (3) (2014) 359–364, https://doi.org/10.1097/EDE.0s000000000000090.
[10] M.S. O'Neill, K.L. Ebi, Temperature extremes and health: impacts of climate variability and change in the United States, J. Occup. Environ. Med. 51 (1) (2009) 13–25, https://doi.org/10.1097/JOM.0b013e318173e122.
[11] T.R. Oke, G. Mills, A. Christen, J.A. Voogt, Urban Climates, Cambridge University Press, Cambridge, 2017.
[12] H. Akbari, Shade trees reduce building energy use and CO2 emissions from power plants, Environ. Pollut. 116 (2002) S119–S126, https://doi.org/10.1016/S0269-7491(01)00264-0.
[13] D.E. Bowler, L. Buyung-Ali, T.M. Knight, A.S. Pullin, Urban greening to cool towns and cities: a systematic review of the empirical evidence, Landsc Urban Plan 97 (3) (2010) 147–155, https://doi.org/10.1016/j.landurbplan.2010.05.006.
[14] C.-R. Chang, M.-H. Li, Effects of urban parks on the local urban thermal environment, Urban Urban Green 13 (4) (2014) 672–681, https://doi.org/10.1016/j.ufug.2014.08.001.
[15] N.J. Georgi, K. Zafiriadis, The impact of park trees on microclimate in urban areas, Urban Ecosyst. 9 (3) (2006) 195–209, https://doi.org/10.1007/s11252-006-8590-9.
[16] C.-M. Hsieh, J.-J. Li, L. Zhang, B. Schwegler, Effects of tree shading and transpiration on building cooling energy use, Energy Build. 159 (2018) 382–397, https://doi.org/10.1016/j.enbuild.2017.10.045.
[17] H. Yan, F. Wu, L. Dong, Influence of a large urban park on the local urban thermal environment, Sci. Total Environ. 622–623 (2018) 882–891, https://doi.org/10.1016/j.scitotenv.2017.11.327.
[18] E.G. McPherson, J.R. Simpson, Potential energy savings in buildings by an urban tree planting programme in California, Urban Urban Green 2 (2) (2003) 73–86, https://doi.org/10.1078/1618-8667-00025.
[19] H. Jin, T. Shao, R. Zhang, Effect of water body forms on microclimate of residential district, Energy Proc. 134 (2017) 256–265, https://doi.org/10.1016/j.egypro.2017.09.615.
[20] H. Akbari, S. Menon, A. Rosenfeld, Global cooling: increasing world-wide urban albedos to offset CO2, Clim. Change 94 (3–4) (2009) 275–286, https://doi.org/10.1007/s10584-008-9515-9.
[21] H. Akbari, M. Pomerantz, H. Taha, Cool surfaces and shade trees to reduce energy use and improve air quality in urban areas, Sol Energy 70 (3) (2001) 295–310, https://doi.org/10.1016/S0038-092X(00)00089-X.
[22] L. Doulos, M. Santamouris, I. Livada, Passive cooling of outdoor urban spaces. The role of materials, Sol. Energy 77 (2) (2004) 231–249, https://doi.org/10.1016/j.solener.2004.04.005.
[23] A. Mohajerani, J. Bakaric, T. Jeffrey-Bailey, The urban heat island effect, its causes, and mitigation, with reference to the thermal properties of asphalt concrete, J. Environ. Manage. 197 (2017) 522–538, https://doi.org/10.1016/j.jenvman.2017.03.095.
[24] P. Savio, C. Rosenzweig, W.D. Solecki, R.B. Slosberg. Mitigating New York City's Heat Island with Urban Forestry, Living Roofs, and Light Surfaces: New York City Regional Heat Island Initiative; 2006.
[25] M.Z. Jacobson, J.E. ten Hoeve, Effects of urban surfaces and white roofs on global and regional climate, J. Clim. 25 (3) (2012) 1028–1044, https://doi.org/10.1175/JCLI-D-11-00032.1.
[26] F. Salata, I. Golasi, Ad.L. Vollaro, Rd.L. Vollaro, How high albedo and traditional buildings' materials and vegetation affect the quality of urban microclimate. A case study, Energy Build. 99 (2015) 32–49, https://doi.org/10.1016/j.enbuild.2015.04.010.
[27] Y. Wang, H. Akbari, Analysis of urban heat island phenomenon and mitigation solutions evaluation for Montreal, Sustain. Cities Soc. 26 (2016) 438–446, https://doi.org/10.1016/j.scs.2016.04.015.
[28] A.G. Touchaei, H. Akbari, Evaluation of the seasonal effect of increasing albedo on urban climate and energy consumption of buildings in Montreal, Urban Clim. 14 (2015) 278–289, https://doi.org/10.1016/j.uclim.2015.09.007.
[29] Y. Wang, U. Berardi, H. Akbari, Comparing the effects of urban heat island mitigation strategies for Toronto, Canada, Energy Build. 114 (2016) 2–19, https://doi.org/10.1016/j.enbuild.2015.06.046.
[30] B. Chun, J.-M. Guldmann, Impact of greening on the urban heat island: seasonal variations and mitigation strategies, Comput. Environ. Urban 71 (2018) 165–176, https://doi.org/10.1016/j.compenvurbsys.2018.05.006.
[31] S.A. Lowe, An energy and mortality impact assessment of the urban heat island in the US, Environ. Impact Assess Rev. 56 (2016) 139–144, https://doi.org/10.1016/j.eiar.2015.10.004.
[32] V.V. Klimenko, A.S. Ginzburg, P.F. Demchenko, A.G. Tereshin, I.N. Belova, E.V. Kasilova, Impact of urbanization and climate warming on energy consumption in large cities, Dokl Phys. 61 (10) (2016) 521–525, https://doi.org/10.1134/S1028335816100050.

[33] M. Varentsov, P. Konstantinov, A. Baklanov, I. Esau, V. Miles, R. Davy, Anthropogenic and natural drivers of a strong winter urban heat island in a typical Arctic city, Atmos. Chem. Phys. Discuss. (2018) 1–28, https://doi.org/10.5194/acp-2018-569.
[34] M. Półrolniczak, L. Kolendowicz, A. Majkowska, B. Czernecki, The influence of atmospheric circulation on the intensity of urban heat island and urban cold island in Poznań, Poland, Theor. Appl. Climatol. 127 (3–4) (2017) 611–625, https://doi.org/10.1007/s00704-015-1654-0.
[35] P. Konstantinov, M. Varentsov, I. Esau, A high density urban temperature network deployed in several cities of Eurasian Arctic, Environ. Res. Lett. 13 (7) (2018) 75007, https://doi.org/10.1088/1748-9326/aacb84.
[36] S.-H. Lee, J.-J. Baik, Statistical and dynamical characteristics of the urban heat island intensity in Seoul, Theor. Appl. Climatol. 100 (1–2) (2010) 227–237, https://doi.org/10.1007/s00704-009-0247-1.
[37] M.N. Khaikine, I.N. Kuznetsova, E.N. Kadygrov, E.A. Miller, Investigation of temporal-spatial parameters of an urban heat island on the basis of passive microwave remote sensing, Theor. Appl. Climatol. 84 (1–3) (2006) 161–169, https://doi.org/10.1007/s00704-005-0154-z.
[38] M. Stopa-Boryczka, J. Boryczka, J. Wawer, Impact of build-up areas and housing estate vegetation on diversity of the local climate in Warsaw, Misc. Geogr. 14 (1) (2010) 121–134, https://doi.org/10.2478/mgrsd-2010-0012.
[39] Y.-H. Kim, J.-J. Baik, Spatial and temporal structure of the urban heat island in Seoul, J. Appl. Meteorol. 44 (2005) 591–605.
[40] K.M. Hinkel, F.E. Nelson, A.E. Klene, J.H. Bell, The urban heat island in winter at Barrow, Alaska, Int. J. Climatol. 23 (15) (2003) 1889–1905, https://doi.org/10.1002/joc.971.
[41] V. Miles, I. Esau, Seasonal and spatial characteristics of Urban Heat Islands (UHIs) in Northern West Siberian Cities, Remote Sens. 9 (10) (2017) 989, https://doi.org/10.3390/rs9100989.
[42] J. Suomi, J. Käyhkö, The impact of environmental factors on urban temperature variability in the coastal city of Turku, SW Finland, Int. J. Climatol. 32 (3) (2012) 451–463, https://doi.org/10.1002/joc.2277.
[43] J. Schatz, C.J. Kucharik, Seasonality of the Urban Heat Island Effect in Madison, Wisconsin, J. Appl. Meteorol. Climatol. 53 (10) (2014) 2371–2386, https://doi.org/10.1175/JAMC-D-14-0107.1.
[44] P. Karsisto, C. Fortelius, M. Demuzere, C.S.B. Grimmond, K.W. Oleson, R. Kouznetsov, et al., Seasonal surface urban energy balance and wintertime stability simulated using three land-surface models in the high-latitude city Helsinki, Q. J. Roy Meteorol. Soc. 142 (694) (2016) 401–417, https://doi.org/10.1002/qj.2659.
[45] A. Semádeni-Davies, L. Bengtsson, Snowmelt sensitivity to radiation in the urban environment, Hydrol. Sci. J. 43 (1) (1998) 67–89, https://doi.org/10.1080/02626669809492103.
[46] S.A. Bowling, C.S. Benson, Study of the subarctic heat island at fairbanks, Alaska (1978).
[47] G.G. Aleksandrov, I.N. Belova, A.S. Ginzburg, Anthropogenic heat flows in the capital agglomerations of Russia and China, Dokl Earth Sci. 457 (1) (2014) 850–854, https://doi.org/10.1134/S1028334X14070010.
[48] I. Esau, V. Miles, M. Varentsov, P. Konstantinov, V. Melnikov, Spatial structure and temporal variability of a surface urban heat island in cold continental climate, Theor. Appl. Climatol. 31 (12) (2019) 1990, https://doi.org/10.1007/s00704-018-02754-z.
[49] K.M. Hinkel, F.E. Nelson, Anthropogenic heat island at Barrow, Alaska, during winter: 2001–2005, J. Geophys. Res. 112 (D6) (2007) 1, https://doi.org/10.1029/2006JD007837.
[50] Y. Toparlar, B. Blocken, B. Maiheu, G.J.F. van Heijst, A review on the CFD analysis of urban microclimate, Renew Sustain. Energy Rev. 80 (2017) 1613–1640, https://doi.org/10.1016/j.rser.2017.05.248.
[51] T. Heleniak, The future of the Arctic populations, Polar Geogr. (2020) 1–17, https://doi.org/10.1080/1088937X.2019.1707316.
[52] T. Heleniak, S. Wang, E. Turunen. Cities on Ice: Population change in the Arctic; Available from: http://www.nordregio.org/nordregio-magazine/issues/arctic-changes-and-challenges/cities-on-ice-population-change-in-the-arctic/.
[53] K.G. Hansen, R.O. Rasmussen, R. Weber. Proceedings from the First International Conference on Urbanisation in the Arctic; 2013.
[54] L. Dicks, Arctic climate issues 2011: Changes in Arctic snow, water, ice and permafrost, Arctic Monitoring and Assessment Programme; Canadian Electronic Library, Oslo, Norway, Ottawa, Ontario, 2013.
[55] R.B. Jackson, P. Friedlingstein, R.M. Andrew, J.G. Canadell, C. Le Quéré, G.P. Peters, Persistent fossil fuel growth threatens the Paris Agreement and planetary health, Environ. Res. Lett. 14 (12) (2019), https://doi.org/10.1088/1748-9326/ab57b3 121001.
[56] R.K. Pachauri, L. Mayer (eds.). Climate change 2014: Synthesis report. Geneva, Switzerland: Intergovernmental Panel on Climate Change; 2015.
[57] D. Chapman, K. Nilsson, A. Larsson, A. Rizzo, Climatic barriers to soft-mobility in winter: Luleå, Sweden as case study, Sustain. Cities Soc. 35 (2017) 574–580, https://doi.org/10.1016/j.scs.2017.09.003.
[58] E. Erell, D. Pearlmutter, T. Williamson, Urban Microclimate: Designing the Spaces Between Buildings, Earthscan, London, 2011.
[59] Cambridge University Press. Cambridge Dictionary: English Dictionary. [April 23, 2020]; Available from: https://dictionary.cambridge.org/dictionary/english/.
[60] M. Xu, B. Hong, J. Mi, S. Yan, Outdoor thermal comfort in an urban park during winter in cold regions of China, Sustain. Cities Soc. 43 (2018) 208–220, https://doi.org/10.1016/j.scs.2018.08.034.
[61] W. Liu, Y. Zhang, Q. Deng, The effects of urban microclimate on outdoor thermal sensation and neutral temperature in hot-summer and cold-winter climate, Energy Build. 128 (2016) 190–197, https://doi.org/10.1016/j.enbuild.2016.06.086.
[62] X. Chen, L. Gao, P. Xue, J. Du, J. Liu, Investigation of outdoor thermal sensation and comfort evaluation methods in severe cold area, Sci. Total Environ. 749 (2020), https://doi.org/10.1016/j.scitotenv.2020.141520 141520.
[63] M. Nikolopoulou, S. Lykoudis, Thermal comfort in outdoor urban spaces: analysis across different European countries, Build. Environ. 41 (11) (2006) 1455–1470, https://doi.org/10.1016/j.buildenv.2005.05.031.
[64] B. Yang, T. Olofsson, G. Nair, A. Kabanshi, Outdoor thermal comfort under subarctic climate of north Sweden – A pilot study in Umeå, Sustain. Cities Soc. 28 (2017) 387–397, https://doi.org/10.1016/j.scs.2016.10.011.
[65] T. Stathopoulos, H. Wu, J. Zacharias, Outdoor human comfort in an urban climate, Build. Environ. 39 (3) (2004) 297–305, https://doi.org/10.1016/j.buildenv.2003.09.001.
[66] D. Lai, D. Guo, Y. Hou, C. Lin, Q. Chen, Studies of outdoor thermal comfort in northern China, Build. Environ. 77 (2014) 110–118, https://doi.org/10.1016/j.buildenv.2014.03.026.
[67] L. Chen, E. Ng, Outdoor thermal comfort and outdoor activities: A review of research in the past decade, Cities 29 (2) (2012) 118–125, https://doi.org/10.1016/j.cities.2011.08.006.
[68] L. Rui, R. Buccolieri, Z. Gao, E. Gatto, W. Ding, Study of the effect of green quantity and structure on thermal comfort and air quality in an urban-like residential district by ENVI-met modelling, Build. Simul. 12 (2) (2019) 183–194, https://doi.org/10.1007/s12273-018-0498-9.
[69] I. Karakounos, A. Dimoudi, S. Zoras, The influence of bioclimatic urban redevelopment on outdoor thermal comfort, Energy Build. 158 (2018) 1266–1274, https://doi.org/10.1016/j.enbuild.2017.11.035.
[70] A. Qaid, H. Bin Lamit, D.R. Ossen, R.N. Raja Shahminan, Urban heat island and thermal comfort conditions at micro-climate scale in a tropical planned city, Energy Build. 133 (2016) 577–595, https://doi.org/10.1016/j.enbuild.2016.10.006.
[71] M. Taleghani, L. Kleerekoper, M. Tenpierik, A. van den Dobbelsteen, Outdoor thermal comfort within five different urban forms in the Netherlands, Build. Environ. 83 (2015) 65–78, https://doi.org/10.1016/j.buildenv.2014.03.014.
[72] M. Taleghani, U. Berardi, The effect of pavement characteristics on pedestrians' thermal comfort in Toronto, Urban Clim. 24 (2018) 449–459, https://doi.org/10.1016/j.uclim.2017.05.007.
[73] U. Berardi, Y. Wang, The effect of a denser city over the urban microclimate: the case of toronto, Sustainability 8 (8) (2016) 822, https://doi.org/10.3390/su8080822.
[74] E. Gatto, R. Buccolieri, E. Aarrevaara, F. Ippolito, R. Emmanuel, L. Perronace, et al., Impact of urban vegetation on outdoor thermal comfort: comparison between a Mediterranean City (Lecce, Italy) and a Northern European City (Lahti, Finland), Forests 11 (2) (2020) 228, https://doi.org/10.3390/f11020228.
[75] E. Lundstad, O.E. Tveito. Homogenization of daily mean temperature in Norway; 2016.
[76] Meteorologisk Institutt. eKlima: Free access to weather- and climate data from Norwegian Meteorological Institute from historical data to real time observations. Normals; Available from: http://sharki.oslo.dnmi.no/portal/page?_pageid=73,39035,73_39049&_dad=portal&_schema=PORTAL.
[77] W.L. Oberkampf, T.G. Trucano, Verification and validation in computational fluid dynamics, Prog. Aerosp. Sci. 38 (2002) 209–272.
[78] American Institute of Aeronautics and Astronautics (ed.). 43rd AIAA Aerospace Sciences Meeting and Exhibit. Reston, Virigina: American Institute of Aeronautics and Astronautics; 2005.
[79] M. Bruse, H. Fleer, Simulating surface–plant–air interactions inside urban environments with a three dimensional numerical model, Environ. Model Softw. 13 (3–4) (1998) 373–384, https://doi.org/10.1016/S1364-8152(98)00042-5.
[80] M. Srivanit, K. Hokao, Evaluating the cooling effects of greening for improving the outdoor thermal environment at an institutional campus in the summer, Build. Environ. 66 (2013) 158–172, https://doi.org/10.1016/j.buildenv.2013.04.012.
[81] M.F. Shahidan, P.J. Jones, J. Gwilliam, E. Salleh, An evaluation of outdoor and building environment cooling achieved through combination modification of trees with ground materials, Build. Environ. 58 (2012) 245–257, https://doi.org/10.1016/j.buildenv.2012.07.012.
[82] W.T.L. Chow, A.J. Brazel, Assessing xeriscaping as a sustainable heat island mitigation approach for a desert city, Build. Environ. 47 (2012) 170–181, https://doi.org/10.1016/j.buildenv.2011.07.027.
[83] E. Carnielo, M. Zinzi, Optical and thermal characterisation of cool asphalts to mitigate urban temperatures and building cooling demand, Build. Environ. 60 (2013) 56–65, https://doi.org/10.1016/j.buildenv.2012.11.004.
[84] H. Lee, H. Mayer, L. Chen, Contribution of trees and grasslands to the mitigation of human heat stress in a residential district of Freiburg, Southwest Germany, Landsc Urban Plan 148 (2016) 37–50, https://doi.org/10.1016/j.landurbplan.2015.12.004.
[85] M. Taleghani, D.J. Sailor, M. Tenpierik, A. van den Dobbelsteen, Thermal assessment of heat mitigation strategies: the case of Portland State University, Oregon, USA, Build. Environ. 73 (2014) 138–150, https://doi.org/10.1016/j.buildenv.2013.12.006.

[86] S.B. Malevich, K. Klink, Relationships between Snow and the Wintertime Minneapolis Urban Heat Island, J. Appl. Meteorol. Climatol. 50 (9) (2011) 1884–1894, https://doi.org/10.1175/JAMC-D-11-05.1.
[87] E.M.O. Sigmond, Nasjonalatlas for Norge: National atlas of Norway, Statens kartverk, Oslo, 1985.
[88] ENVI_MET GmbH. ENVI_MET V4.4.2: Winter1819. Essen, Germany; 2019.
[89] M. Santamouris (Ed.), Environmental design of urban buildings: An integrated approach, Earthscan, London, 2006.
[90] A. Goris, K.-J. Schneider, A. Albert (Eds.), Bautabellen für Ingenieure: Mit Berechnungshinweisen und Beispielen, 19th ed., Neuwied, Köln, Werner; Wolters Kluwer, 2010.
[91] M. Schatzmann, B. Leitl, Issues with validation of urban flow and dispersion CFD models, J. Wind Eng. Ind. Aerodyn. 99 (4) (2011) 169–186, https://doi.org/10.1016/j.jweia.2011.01.005.
[92] S. Imam, D.A. Coley, I. Walker, The building performance gap: are modellers literate?, Build Serv. Eng. Res. T 38 (3) (2017) 351–375, https://doi.org/10.1177/0143624416684641.
[93] A. Skartveit, J.A. Olseth, A model for the diffuse fraction of hourly global radiation, Sol Energy 38 (4) (1987) 271–274.
[94] P.O. Fanger, Thermal Comfort: Analysis and Applications in Environmental Engineering, Danish Technical Pr, Copenhagen, 1970.
[95] G. Jendritzky, W. Nübler, A model analysing the urban thermal environment in physiologically significant terms, Arch. Met. Geoph. Biokl. B 29 (4) (1981) 313–326.
[96] Association of German Engineers. VDI 3787 Part 2: Environmental meteorology - Methods for the human biometeorological evaluation of climate and air quality for urban and regional planning at regional level; 2008.
[97] F. Salata, I. Golasi, R. de Lieto Vollaro, Lieto Vollaro A de. Urban microclimate and outdoor thermal comfort. A proper procedure to fit ENVI-met simulation outputs to experimental data, Sustain. Cities Soc. 26 (2016) 318–343, https://doi.org/10.1016/j.scs.2016.07.005.
[98] Alemu M. Mekonnen, Ecological benefits of trees as Windbreaks, Int. J. Ecosyst. 6 (1) (2016) 10–13.
[99] H. Leng, S. Liang, Q. Yuan, Outdoor thermal comfort and adaptive behaviors in the residential public open spaces of winter cities during the marginal season, Int. J. Biometeorol. 64 (2) (2020) 217–229, https://doi.org/10.1007/s00484-019-01709-x.
[100] E. Jamei, P. Rajagopalan, M. Seyedmahmoudian, Y. Jamei, Review on the impact of urban geometry and pedestrian level greening on outdoor thermal comfort, Renew. Sustain. Energy Rev. 54 (2016) 1002–1017, https://doi.org/10.1016/j.rser.2015.10.104.

Paper IV

Validation of a CFD model for the evaluation of urban microclimate at high latitudes: A case study in Trondheim, Norway

J. Brozovsky, A. Simonsen, N. Gaitani

Published in *Building and Environment 205* (2021), 108175

https://doi.org/10.1016/j.buildenv.2021.108175

Building and Environment 205 (2021) 108175

Contents lists available at ScienceDirect

Building and Environment

journal homepage: www.elsevier.com/locate/buildenv

Validation of a CFD model for the evaluation of urban microclimate at high latitudes: A case study in Trondheim, Norway

Johannes Brozovsky [a,*], Are Simonsen [b], Niki Gaitani [a]

[a] Department of Architecture and Technology, Faculty for Architecture and Design, NTNU – Norwegian University of Science and Technology, 7491, Trondheim, Norway
[b] Process Technology, SINTEF Industry, S.P. Andersens Veg 15B, 7031, Trondheim, Norway

ARTICLE INFO

Keywords:
Urban microclimate
Computational fluid dynamics
Validation study
Cold climate
Materials

ABSTRACT

The urban microclimate is a rapidly evolving field of research gaining increasing interest from public authorities and researchers. However, studies at high-latitude cities are scarce and researchers primarily focus on summerly overheating. This study focuses on the validation process of a CFD model that applies the 3D URANS approach with the realisable k-ε turbulence model at a highly complex urban area in Trondheim, Norway (63.4° N) during autumn. The CFD model features a polyhedral grid of the urban environment, including geometrically explicitly modelled buildings and trees in the area of interest. Furthermore, solar radiation, longwave radiation exchange, heat transfer from the buildings, heat storage in the urban surface, and the thermal effects of evapotranspiration from trees and grass surfaces are considered. The CFD model is validated with experimental results from a network of five mobile and one reference weather stations in the study area, providing hourly-averaged measurements for wind speed, wind direction (only reference weather station) and air temperature for two 48-h periods from September 27–28 and October 19–20. The results show that the CFD model is well able to reproduce the measured conditions at the area of interest with a mean R^2 of 0.60, 0.63, and 0.96 for wind speed, wind direction and air temperature, respectively, at the reference weather station. It will be used in future studies, including the analysis of the impact of urban microclimate on buildings' energy performance, outdoor thermal and pedestrian wind comfort.

1. Introduction

Urban climatology (UC) is a much-discussed field of research, driven by ongoing global urbanisation, population growth and climate change [1,2]. Urban areas account for around 67–76% of global energy use and between 71 and 76% of CO_2 emissions from global final energy use [1]. Considering these significant shares, solutions are urgently needed to reduce the negative impact of cities on the environment while ensuring a healthy and habitable space for humans. UC combines a variety of different disciplines to deepen the knowledge in how to address these issues, such as meteorology, climatology, air pollution science, architecture, building engineering, physics, urban design, biometeorology, social sciences etc. [3]. While at the beginning of UC research, studies involving the thorough analysis of field observations dominated the methodological approaches, numerical studies gained increasing attention, especially during the last two decades [3–5]. There are several advantages arising from the utilisation of computer simulations, like for instance a weather forecasting model, compared to observational approaches. For instance, different scenarios and strategies can be easily investigated and assessed, and the variables of interest are available for every location in the computational domain and not only for a few measurement points.

In UC, the focus lies generally on the lower part of the troposphere (up to about 1 km). In the horizontal extension, cities are typically located near the border between the meteorological micro- (smaller than 2 km) and the mesoscale (from 2 km to 2000 km), see also Fig. 1 [6]. Therefore, UC is mostly influenced by physical processes at both these scales which impact the so-called microclimate (MC). As human activity primarily takes place within these scales, the MC is of significant importance for people's daily lives.

It is well known that urban areas can have significantly different climatic conditions than their rural surroundings [7]. Most commonly, these differences get apparent as an urban heat island (UHI) which refers to the fact that temperatures in cities are usually higher than their surroundings. Oke [8] gives seven main reasons for that:

1. Increased absorption of short-wave radiation,

* Corresponding author.
E-mail address: johannes.brozovsky@ntnu.no (J. Brozovsky).

https://doi.org/10.1016/j.buildenv.2021.108175
Received 3 May 2021; Received in revised form 6 July 2021; Accepted 18 July 2021
Available online 21 July 2021

Abbreviations

AT	Air temperature
BPG	Best practice guidelines
CFD	Computational fluid dynamics
CO_2	Carbon dioxide
CV_{RMSD}	Coefficient of variance of the root mean square deviation
D_{max}	Maximum deviation
DO	Discrete ordinates
H	Humidity
HF	Heat flux
LAD	Leaf area density
LAI	Leaf area index
LiDAR	Light detection and ranging
MC	Microclimate
MRT	Mean radiant temperature
NTNU	Norwegian University of Science and Technology
ORM	Obstacle resolving meteorological models
OSM	On-site measurements
PET	Physiological equivalent temperature
PME	Penman-Monteith equation
R^2	Coefficient of determination
RANS	Reynolds averaged Navier-Stokes
RS	Remote sensing
SET	Standard effective temperature
SOT	Soil temperature
SR	Solar radiation
ST	Surface temperature
SVF	Sky view factor
UC	Urban climate
UDF	User defined function
URANS	Unsteady Reynolds averaged Navier-Stokes
VP	Validation period
WD	Wind direction
WS	Wind speed
WT	Wind tunnel

2. Increased long-wave radiation from the sky,
3. Decreased long-wave radiation loss,
4. Anthropogenic heat sources,
5. Increased sensible heat storage,
6. Decreased evapotranspiration,
7. Decreased total turbulent heat transport.

Especially during heat waves, these causes can negatively impact the urban environment and lead to unfavourable conditions [9,10], excess mortality [11–13] and increased building cooling demands [13–15]. However, in cold climate regions, it was reported that savings from the heating energy demand during winter were larger than increases in cooling energy demand during summer [16,17]. With the expected rise in the frequency of extreme climate events and the advancements of methodological and technical capabilities, the urban MC has therefore been introduced increasingly into the design process of buildings and cities. Many publications stress the necessity of improving the design and the climate resilience of cities and their outdoor environment to provide comfortable spaces that invite people to spend time outdoors or that promote soft mobility, regardless of their climate [18–20].

At the microscale, especially Computational Fluid Dynamics (CFD) has emerged as a method to study different aspects of the MC such as wind flow, heat convection, conductivity and storage, short and long wave radiation exchange, natural convection, water vapour transfer, pollutant/particle dispersion etc. Although mesoscale processes like the Coriolis effect, atmospheric vertical mixing or cloud formation are usually not considered in microscale CFD modelling, the computational cost of transient simulations that cover more physics than just fluid flow is generally very high. Therefore, the size of the computational domain of such studies is typically limited to a couple of blocks within a city that are explicitly modelled, while the larger surroundings are included implicitly, for example with an imposed roughness index [21].

Besides for instance pedestrian wind comfort [22–26], pollutant dispersal [27–30] or wind-driven rain [31–33], CFD has been used extensively to investigate the thermal conditions in real urban areas (see Table 1). Many of these studies focused on topics such as cooling strategies [34–52] or outdoor thermal comfort [53–62]. About half of the studies (51.1%) were conducted with ENVI-Met [63], a three-dimensional non-hydrostatic tool for the surface-plant-air interaction that is increasingly used to evaluate different scenarios like the effect of different greening strategies, surface characteristics and urban morphology on the MC or outdoor thermal comfort. In 77.8% of the studies, the effects of vegetation on the local climatic conditions were considered.

Table 1 also shows that the majority (75.6%) of the listed publications provided a validation process, even though the degree of detail and number of climate variables in the validation varied significantly. The most frequently used climate variable for validation was the air

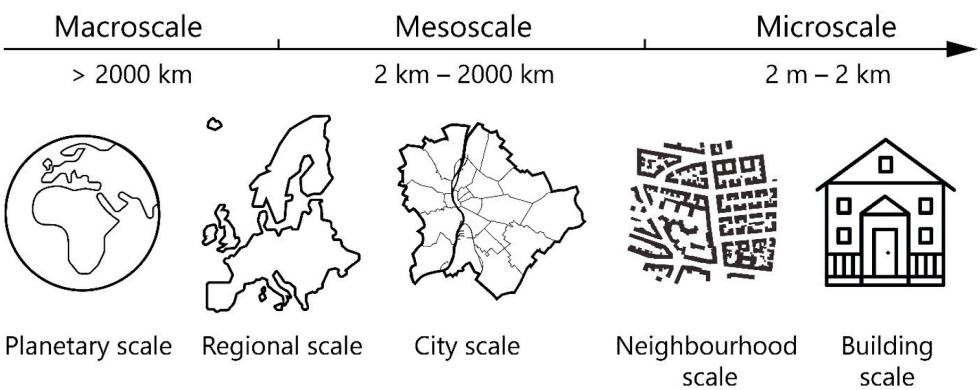

Fig. 1. Terminology of climatological scales with their horizontal extension from Ref. [6].

Table 1
Overview of published articles on the thermal conditions in real urban areas. The column "Validation variables" lists the variables that were compared to experimental data: Air temperature (AT); humidity (H); heat flux (HF); mean radiant temperature (MRT); Physiological Equivalent Temperature (PET); Standard Effective Temperature (SET); soil temperature (SOT); solar radiation (SR); surface temperature (ST); sky view factor (SVF); wind direction (WD); wind speed (WS). The column "Validation data" refers to the data acquisition method: On-site measurements (OSM); wind tunnel (WT); remote sensing (RS).

Authors	Year	Reference	City, country	Research focus	Validation variables	Validation data	Vegetation considered	ENVI-Met
Chen et al.	2004	[53]	Shenzhen, China	Pedestrian level comfort at an apartment block	AT, ST, WS, H, MRT, SET	OSM	Yes	No
Takahashi et al.	2004	[72]	Kyoto, Japan	Measurement and CFD prediction of the thermal environment	AT, HF	OSM	Yes	No
Huang et al.	2005	[59]	Tokyo, Japan	Simulation and measurement of urban thermal environment	AT, WS, H	OSM	No	No
Priyadarsini et al.	2008	[66]	Singapore	Key factors of the UHI	AT, WS	OSM, WT	No	No
Chen et al.	2009	[34]	Tokyo, Japan	Different mitigation scenarios for the UHI	–	–	Yes	No
Hsieh et al.	2010	[35]	Tokyo, Japan	Site design and layout planning to mitigate the thermal environment	–	–	Yes	No
Chow et al.	2011	[73]	Tempe, AZ, USA	Horizontal and vertical nocturnal cooling influence of a small park	AT	OSM	Yes	Yes
Fintikakis et al.	2011	[48]	Tirana, Albania	Improving the urban microclimatic and thermal comfort conditions	AT, ST, WS, WD	OSM	Yes	No
Gaitani et al.	2011	[49]	Athens, Greece	Improve thermal comfort conditions in open spaces	AT, ST, WS, WD	OSM	Yes	No
Kaoru et al.	2011	[74]	Osaka, Japan	Solar and longwave radiation model to simulate air flow and temperature	–	–	No	No
Synnefa et al.	2011	[52]	Athens, Greece	UHI mitigation potential of cool asphalt	–	–	No	No
Chow et al.	2012	[36]	Phoenix, AZ, USA	Xerophytic trees in residential yards as UHI mitigation approach	AT	OSM	Yes	Yes
Ma et al.	2012	[54]	Beijing, China	Method to predict outdoor thermal environment in a residential district	AT, WS	OSM	Yes	No
Santamouris et al.	2012	[51]	Athens, Greece	Design of a rehabilitation plan for an urban area to improve the microclimate	AT, ST, WS, WD	OSM	Yes	No
Santamouris et al.	2012	[50]	Athens, Greece	Using cool pavements to improve the urban microclimate	AT, ST	OSM	Not indicated	No
Shahidan et al.	2012	[37]	Putrajaya, Malaysia	Impact of materials and trees on mitigating the UHI and reducing building cooling demands	AT, ST	OSM	Yes	Yes
Carnielo and Zinzi	2013	[38]	Rome, Italy	Effect of cool materials on the microclimate of an urban neighbourhood	ST	OSM	Yes	Yes
Srivanit et al.	2013	[39]	Saga, Japan	Cooling effect of different greening strategies at a university campus	AT, H, WS, SR	OSM	Yes	Yes
Yang et al.	2013	[75]	Guangzhou, China	Evaluation of a microclimate model to predict the thermal behaviour of surfaces	AT, ST, HF, H, SOT	OSM	Yes	Yes
Maragkogiannis et al.	2014	[76]	Chania, Greece	Terrestrial laser scanning and CFD to study urban thermal environment	–	–	No	No
Su et al.	2014	[40]	Nanjing, China	Impact of greenspace patterns on land surface temperature	ST	OSM	Yes	Yes
Taleghani et al.	2014	[41]	Portland, OR, USA	Courtyard vegetation, ponds, and high albedo surfaces as UHI mitigation strategies	AT	OSM	Yes	Yes
Salata et al.	2015	[62]	Rome, Italy	Impact of material albedo and vegetation on urban microclimate	AT, MRT, H, SR	OSM	Yes	Yes
Targhi and Van Dessel	2015	[55]	Worcester, MA, USA	Influence of urban geometry on outdoor thermal comfort conditions	–	–	Yes	Yes
Tominaga et al.	2015	[42]	Hadano, Japan	Evaporative cooling effect from water bodies	AT, H	OSM	No	No
Toparlar et al.	2015	[65]	Rotterdam, Netherlands	Validation of a CFD simulation model of urban microclimate	ST	RS	No	No
Wang and Akbari	2015	[43]	Montreal, Canada	Different UHI mitigation strategies	AT	OSM	Yes	Yes
Berardi	2016	[44]	Toronto, Canada	Energy savings and outdoor microclimate benefits from green roof retrofits	SVF, AT	OSM	Yes	Yes
Berardi and Wang	2016	[77]	Toronto, Canada	Microclimatic effect of city densification	AT	OSM	Yes	Yes
Kim et al.	2016	[45]	Seoul, Korea	Cooling effect of different land cover on surface and air temperatures	ST	OSM	Yes	Yes
Lee et al.	2016	[60]	Freiburg, Germany	Reduce human heat stress through trees and grasslands	AT, MRT, PET	OSM	Yes	Yes
Quaid et al.	2016	[61]	Putrajaya, Malaysia	UHI and thermal comfort conditions	AT	OSM	Yes	Yes
Wang et al.	2016	[46]	Toronto, Canada	Different UHI mitigation strategies	AT	OSM	Yes	Yes
Allegrini and Carmeliet	2017	[78]	Zürich, Switzerland	Effect of new buildings on the local urban microclimate	–	–	No	No
Park et al.	2017	[79]	Jeonju, Korea	Microclimate of urban infrastructure regeneration programs	–	–	Yes	No
Karakounos et al.	2018	[56]	Serres, Greece	Different scenarios for improving outdoor thermal comfort	–	–	Yes	Yes
Kyrakodis and Santamouris	2018	[47]	Athens, Greece	Mitigation of the UHI using reflective pavements	AT, ST	OSM	Yes	Yes

(*continued on next page*)

Table 1 (*continued*)

Authors	Year	Reference	City, country	Research focus	Validation variables	Validation data	Vegetation considered	ENVI-Met
Taleghani and Berardi	2018	[57]	Toronto, Canada	Effect of pavement characteristics on outdoor thermal comfort	–	–	Yes	Yes
Toparlar et al.	2018	[80]	Antwerp, Belgium	Effect of an urban park on microclimate in its vicinity	AT	OSM	Yes	No
Toparlar et al.	2018	[81]	Antwerp, Belgium	Impact of urban microclimate on summertime building cooling demand	AT	OSM	Yes	No
Antoniou et al.	2019	[71]	Nicosia, Cyprus	Validation of a CFD simulation model of urban microclimate	AT, ST, WS	OSM	No	No
Brozovsky et al.	2019	[82]	Trondheim, Norway	Microclimatic conditions at a university campus	ST	OSM	Yes	Yes
Ghaffarianhoseini et al.	2019	[58]	Kuala Lumpur, Malaysia	Thermal comfort conditions at a university campus	AT	OSM	Yes	Yes
Yang and Li	2020	[83]	Xiantao, China	Urban thermal environment of an urban area within a network of water channels	–	–	Yes	No
Brozovsky et al.	2021	[64]	Trondheim, Norway	Influence of different design strategies and the urban fabric on outdoor thermal comfort conditions	AT, ST, H, WS, WD	OSM	Yes	Yes
This study	–	–	Trondheim, Norway	Validation of a CFD model for urban microclimate evaluation	AT, WS, WD	OSM	Yes	No

temperature (85.3% of validation studies). Surprisingly, only few studies validated wind speed (29.4% of validation studies) while wind direction has been validated only in four (11.8 %) studies [48,49,51,64]. However, in three of these publications [48,49,51], only the wind direction patterns were compared, and no quantitative analysis of accordance was presented. In all except for one publication by Toparlar et al. [65] where remote sensing (RS) was used to get surface temperatures from satellite imagery, on-site measurements (OSM) provided the validation data. In one case, wind tunnel measurements were carried out to obtain validation data in addition to OSM [66].

Most commonly, CFD MC studies were carried out for locations in temperate and warm climate zones during summer conditions, while there is a clear lack of urban MC studies in climatic regions close to or above the Arctic Circle, as pointed out e.g. in a review by Toparlar et al. [4] or in a research paper by Ebrahimabadi et al. [67]. Considering that more than 25 million people live above 60° N, UC and MC research in the cold-climate and high-latitude regions of the world can contribute to resilient and sustainable urban (re)development and improve the living quality of many. Additionally, a large number of cities in temperate climate experience pronounced cold periods for significant parts of the year and would benefit from research in cold climate non-summer conditions.

Numerical models are often used without sufficient proof of their accuracy. In fact, validation is an essential part of applying a numerical model and is defined as the process of determining how well simulations represent the real world by using physical observations as a reference [68]. Moreover, in practice, the quality of the results are not only dependent on the capabilities of the used software, but to a considerable degree also on the input of the user, as human errors cannot be eliminated entirely [69]. It is therefore indispensable to ensure that a numerical model meets the requirements specified for its planned purpose [68,70].

Similar to previous studies [65,71], this article presents the validation of a CFD model to investigate the urban MC in the software ANSYS Fluent 2020.R1 by using field measurements. Unlike the vast majority of published articles (as indicated in Table 1), this work addresses the MC at an urban high-latitude and cold-climate location at the campus of the Norwegian University of Science and Technology (NTNU) in Trondheim, Norway. The aim of this study is to investigate the applicability of a CFD model for the analysis of the MC in a complex, high-latitude urban setting during autumn. In this article, the inclusion of the Penman-Monteith equation (PME) to account for evapotranspirational cooling from grass-covered surfaces is described. Furthermore, the outdoor thermal comfort index Physiological Equivalent Temperature (PET) has been implemented in the CFD model. To the best of our knowledge, neither the PME nor the PET has been implemented in ANSYS Fluent in a previously published article for studying the urban MC. The range of applications for CFD models such as the one in this study are many as it can be used not only for evaluating the thermal environment, like studying the outdoor thermal comfort or the influence of MC on building energy demand, but also to evaluate the local wind conditions for urban wind energy generation, pollutant dispersion, or determining pressure coefficients for natural ventilation potential.

In section 2, the study area, on-site measurements, computational settings, structure and grid of the CFD model are described. Section 3 presents the results of a grid-convergence analysis and the validation of the CFD model for two 48-h periods in autumn 2019. The paper concludes with section 4 (discussion) and 5 (conclusions).

2. Methodology

2.1. Study area and local climate

This study was carried out at the NTNU campus in Trondheim, Norway. The city lies at a latitude of 63.4° N, has 200,000 inhabitants, and is located at the coast of a large fjord. NTNU's campus *(Gløshaugen)* is approximately 0.26 km^2 in size and is situated ca. 1.5 km south of the city centre at an altitude between 38 and 49 m a.s.l. Trondheim is embedded in complex terrain and mainly characterized by a mix of dense, but low-rise built-up and open, park-like areas, frequently traversed by patches of forests (see Fig. 2).

The Köppen-Geiger climate type for Trondheim is oceanic (Dfb), but closely borders continental, subpolar and subarctic climates [85]. From November to March, moderate snowfall with periods of milder weather patterns and rain are common. With 4.8 °C (1961–1990), the annual mean temperature is quite cool, including relatively short and mild summers, and long and cool winters. Due to climate change, temperatures in the arctic and subarctic regions have been rising over the last decades. In Trondheim, the mean annual temperature from 1991 to 2020 was 1.0 °C higher (5.8 °C) than in the norm period from 1961 to 1990 [86].

Due to the significant warming effect of the Gulf Stream, Norway's coastal cities have a rather mild climate considering their comparatively high latitudes [87]. Thus, even though Trondheim and Toronto, Canada, being classified by the same Köppen-Geiger climate type, from a UC point of view, they cannot be treated climatologically as equivalent. Not only are the two cities different in terms of their size, topography, morphology etc., but also with regard to the availability of solar radiation. The access to which is considered to be key to human outdoor thermal comfort [88–91] and to reduce building energy demands [92]

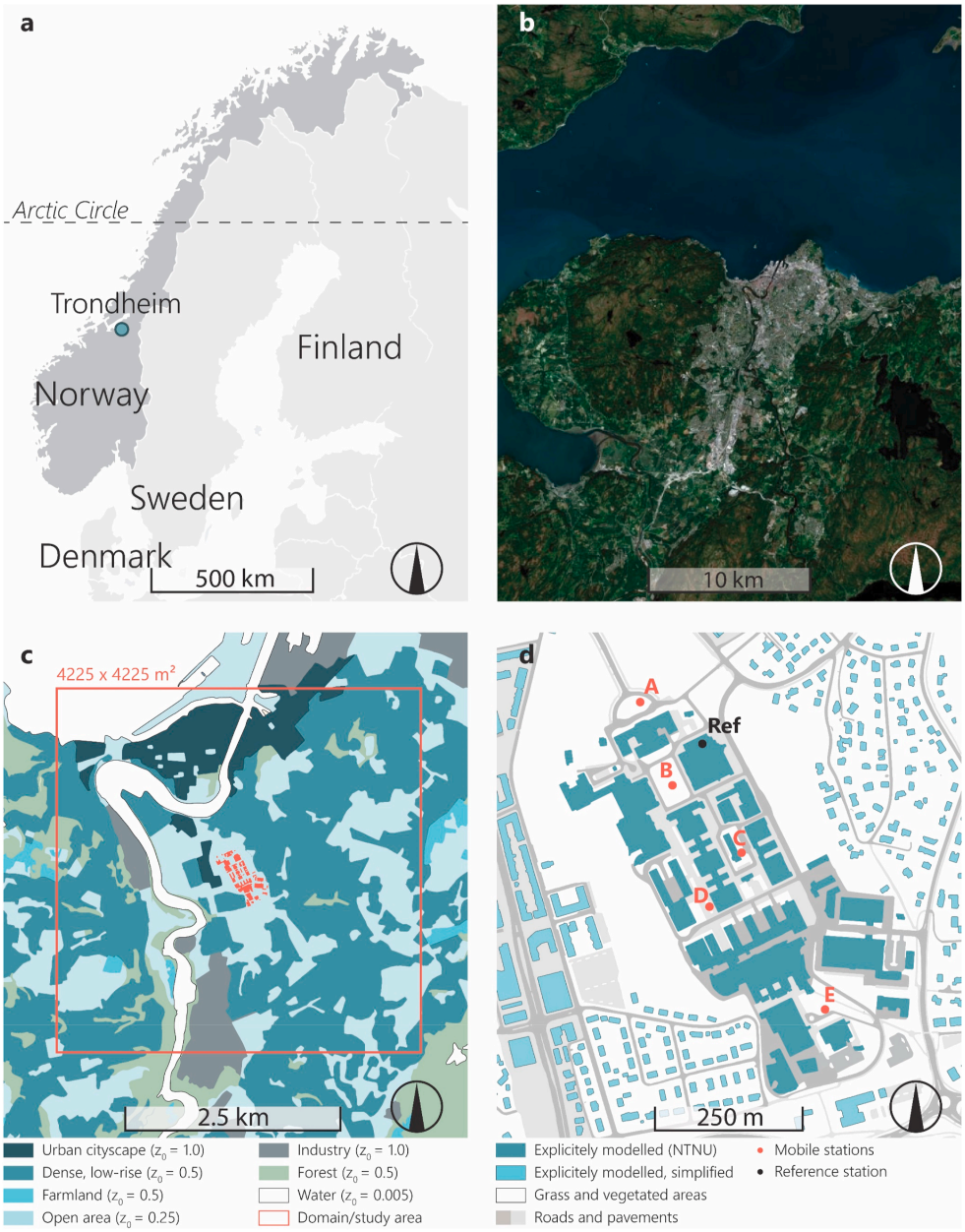

Fig. 2. (a) Location of Trondheim within Norway and Fennoscandia. (b) Aerial photograph of Trondheim's built-up area (from the Norwegian Mapping Authority, www.kartverket.no). (c) Surrounding of the NTNU campus with aerodynamic roughness length z_0 indicated according to the updated Davenport roughness classification [84] (data from the Norwegian Mapping Authority). (d) Site plan of the NTNU campus with indication of geometrical building modelling degree, surface types, and location of mobile and reference weather stations.

(e.g. passive solar gains, solar thermal or photovoltaics production). These differences in solar access are caused by the location of the two cities in terms of latitude (see Table 2). The almost 20° lower sun elevation angles in Trondheim, together with complex, mountainous terrain and an urban landscape result in high shading levels and short days during the cold season. Therefore, at this particular time of the year, low sun angles need to be taken into consideration in high-latitude cities as they can be detrimental to sustainable urban development.

2.2. Measurement campaign

In order to capture the microclimatic conditions on-site, a mea-

Table 2
Sun elevation angles for different dates in Toronto, Canada and Trondheim, Norway.

Date	Max. sun elevation angle	
	Toronto, Canada (43.6° N)	Trondheim, Norway (63.4° N)
21.03. (vernal equinox)	47.0°	27.1°
21.06. (summer solstice)	69.8°	50.0°
23.09. (autumnal equinox)	45.9°	26.2°
21.12. (winter solstice)	22.9°	3.3°

surement campaign was conducted from September 23 to October 21, 2019. Fig. 2 shows the fixed location of five mobile weather stations (see also Fig. 3) that recorded air temperature ($T_{a,C}$) [°C], relative humidity (*RH*) [%], wind speed (*WS*) [m s^{-1}] and direction (*WD*) [°] in 0.1 Hz intervals in a height of 3 m. A fixed weather station, 10 m above the roof of the VATL building (28 m above the ground) is used as a reference station for calibration. At the reference weather station, also global horizontal radiation (S_g) was measured. The recorded climate variables from the reference weather station served as a basis for the input at the domain boundaries in the simulations. Fig. 4 shows the data flow of the climate variables in this study. The accuracies of the sensors are listed in Table 3.

For validation purposes, two distinct 48-h validation periods (VP) during the measurement campaign are selected that contain at least one very sunny day, relatively strong fluctuations and a relatively high average of wind speed, a pronounced diurnal temperature variation and preferably a large variation of wind direction. These criteria are established to verify the CFD model's performance under demanding and large variety of conditions. The selected days are September 27–28 (VP1) and October 19–20 (VP2). During both periods, a pronounced variability in wind speed occurred at the reference weather station, ranging between 1.2 and 4.5 m s^{-1} in VP1 and between 0.7 and 4.2 m s^{-1} in VP2. In VP2 strong fluctuations in wind direction were observed, while VP1 contained only minor changes in wind direction (south-east to south-west). The air temperature ranged from 9.0 to 16.9 °C in VP1 and 3.6–8.5 °C in VP2. The hourly global horizontal radiation reached 400 W m^{-2} in VP1 and 200 W m^{-2} in VP2. Graphs of the climate variables used for validation during both VPs are presented in the results section.

2.3. Computational domain

The computational domain of the study area features regions of three different types of geometrical modelling: (a) where buildings and trees are represented explicitly with a rather high degree of details (NTNU

Fig. 3. Weather station B on a lawn behind the main building (HB) in mid-October 2019.

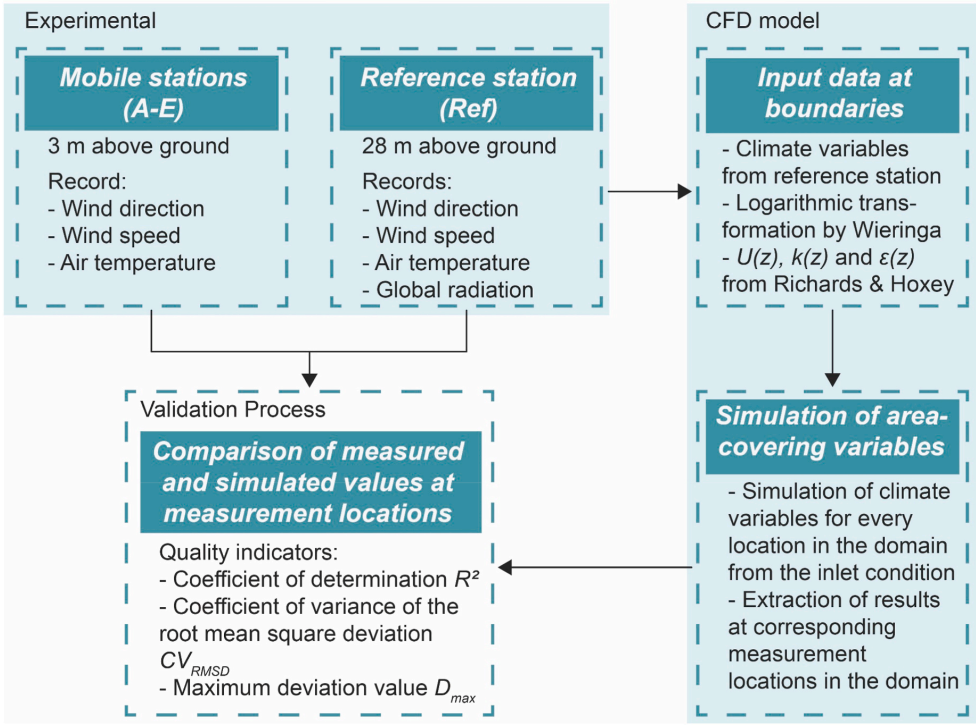

Fig. 4. Schematic illustration of the data flow of climate variables in this study.

Table 3
Accuracy of the sensors mounted on the mobile and the reference weather stations.

Weather station	*WD*	*WS*	$T_{a,C}$	S_g
Mobile stations	±5° at 1.4° resolution	±1.1 m s^{-1} or ±4% of reading at 0.5 m s^{-1} resolution	±0.21 °C from 0 °C to 50 °C	–
Reference station	±2° RMSE at 0.1° resolution	±0.2 m s^{-1} or ±2% of reading at 0.01 m s^{-1} resolution	±0.15 °C or ±0.1% of reading	2nd class pyranometer at 1 W m^{-2} resolution

campus), (b) the area around the NTNU campus, where only buildings and no vegetation are represented explicitly yet with a lower degree of details (representation of buildings as simple boxes), and (c) the wider area surroundings of (a) and (b) which are only represented implicitly by assigning an aerodynamic roughness length z_0 according to the Davenport-Wieringa roughness classification [84].

There are two main sources of geometrical data in this study. (1) A freely available 3D geometrical city model from Trondheim Municipality and (2) Light detection and ranging (LiDAR) data created at NTNU. The data from Trondheim Municipality contains detailed geometrical information of the terrain and the position of buildings at the location of the computational domain. However, it does not contain elements like street signs, bus stops, lamp posts, curbs, vehicles, statues or small monuments and public artwork. Furthermore, the building geometries are not watertight and often show a deficient geometrical representation of complex roof shapes for instance. Thus, the buildings surrounding NTNU campus (see Figs. 2 and 5) were simplified into box-like geometries, omitting details like balconies, protrusions, oriels etc. These simplifications conserved the footprint but changed the height of the building which was taken as the mean height of the building's eaves and ridge for pitched roofs. Furthermore, smaller elements like garden sheds, dog houses etc. were omitted. Rhino 5 was used for these modifications.

The LiDAR-based data provides higher accuracy and geometrical quality of the building on campus and was provided in form of a Trimble SketchUp file. Nevertheless, most of the buildings were geometrically remodelled as also the LiDAR data exhibited some geometrical deficiencies such as distorted faces, holes etc. Three newer buildings (ZEB, TCL and LL, see Fig. 5) on campus that are not included in this data were then designed in Trimble SketchUp according to their technical drawings.

Both, the Rhino file containing the modified data from Trondheim Municipality and the SketchUp file of the campus buildings were imported into ANSYS SpaceClaim 2020.R1 and merged. In SpaceClaim, the dimensioning of the domain, positioning of the tree geometries according to on-site visits and satellite images was performed.

Satisfying the suggestion from the CFD best practice guidelines (BPG) by Franke et al. [93] and Tominaga et al. [94], all buildings within a distance of at least 250 m (at least one street block) around the campus buildings are included to act as a direct obstacle to the wind flow. The height of the highest building in the area of interest (on the campus) is 44.5 m, the highest geometrically explicitly modelled building is 73 m and is located about 300 m south-west of the campus. The surrounding terrain is quite complex and ranges in elevation from 0 to 172 m a.s.l., causing obstructions to the wind flow much higher than the modelled buildings. Therefore, the domain's bottom boundary was copied to the top, so that they largely have the same shape (the only difference is the lower grid resolution at the top) and all lateral

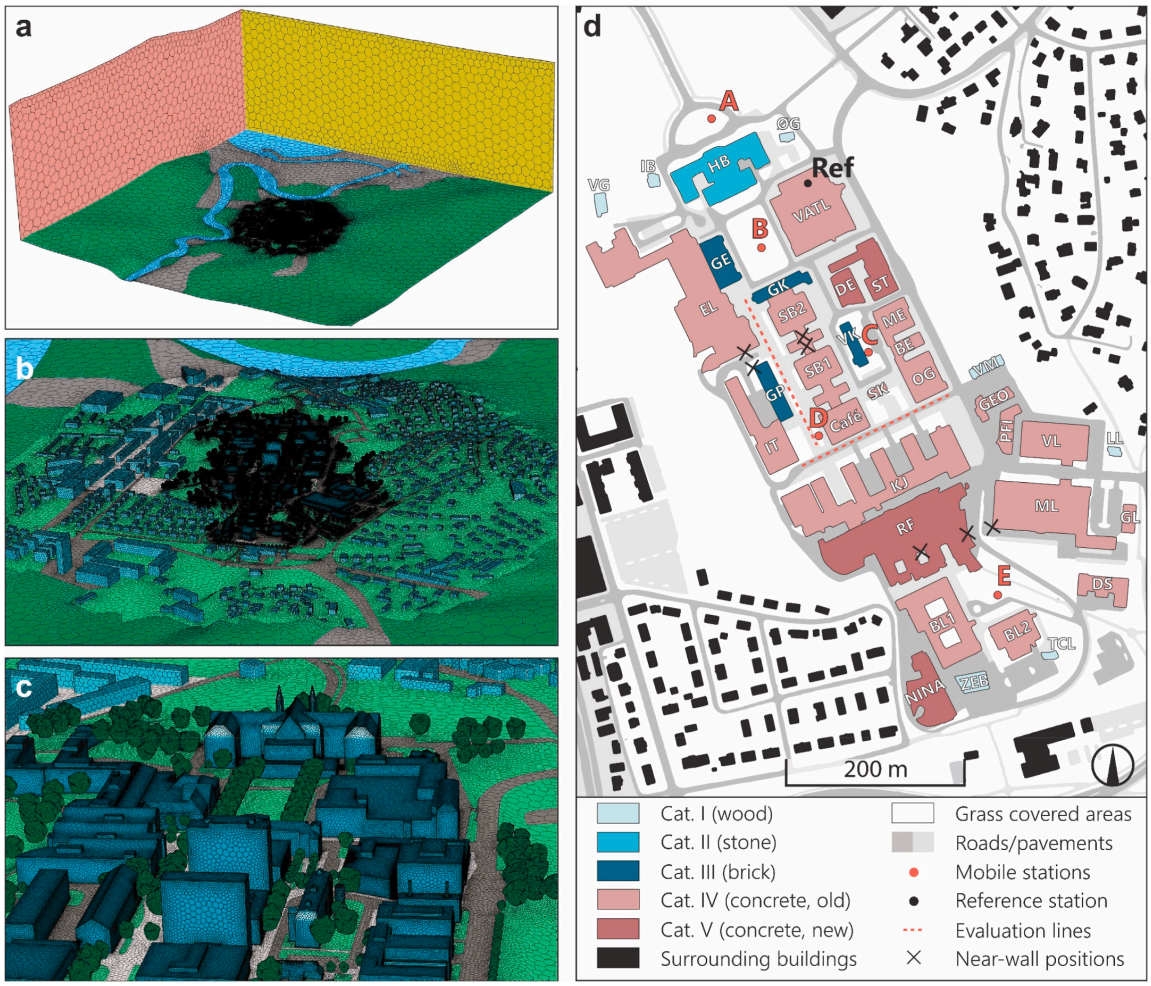

Fig. 5. Computational domain (4225 × 4225 × 1550 m^3) with 9,123,834 cells; (a) View from south-east with different surface types: water (blue), primarily green spaces (green), densely built-up or industrial areas (grey), northern (yellow) and western (red) boundary; (b) View of the geometrically explicitly modelled area with different surface types: asphalt (dark grey), concrete/pavement (light grey) and green spaces (green); (c) Close-up view of the NTNU campus buildings and trees; (d) Building categories, surface types, positions of the mobile and reference weather stations, the evaluation lines, and near-wall positions for the grid-convergence analysis. (For interpretation of the references to colour in this figure legend, the reader is referred to the Web version of this article.)

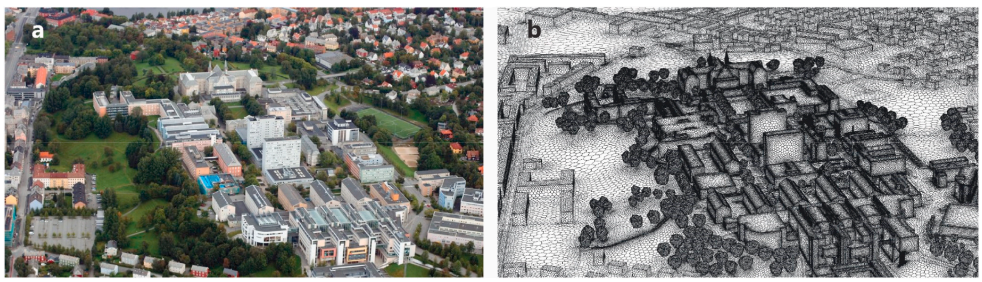

Fig. 6. (a) Aerial view of the NTNU campus from south (photo: Lars Strømmen); (b) Computational grid with 9,123,834 cells, featuring buildings and trees on the campus.

boundaries have the same surface area (see Fig. 5). This way, instead of having a flat top boundary surface, the terrain leads to less constriction in the domain. Only relying on the BPG which do not consider complex terrain would have led to a much smaller domain and a too high blockage ratio. Due to the hourly changing wind direction, always two of the lateral boundaries are set as inlets and two as outlets at a time. The maximum blockage ratio of all buildings and trees is 1.1% which satisfies the BPG [93,94] to keep the blockage ratio below 3%. The resulting domain size is 4225 × 4225 × 1550 m^3.

The domain is discretised into a poly-hexcore grid that consists of 9,123,834 cells (see Fig. 6) with ANSYS Fluent 2020.R1 in meshing mode. The grid is based on a grid-convergence analysis where three meshes of different resolutions were checked for their impact on the solution. For that, wind speed ratios at different locations in the area of interest were compared for a coarse grid with 4,371,409 cells, a basic grid with 9,123,834 cells, and a fine grid with 23, 566, 616 cells. These locations include the five mobile weather stations, the reference weather station, two horizontal lines at 3 m height, and selected near-wall positions as illustrated in Fig. 5. The main difference between the three grids was the sizing of the surface mesh in the area of interest, mainly consisting of the geometrically explicitly modelled buildings and trees (see Table 4). The grid sizing settings near the top and lateral boundaries of the domain were kept the same in the three grids. For all grids, the simulations are carried out using steady-state Reynolds Averaged Navier Stokes (RANS), using the same inlet conditions as described in section 2.3, but with a constant southern wind direction and wind speed of 3 m s^{-1} at 28 m height (the reference weather station). All three grids were created following the BPG [93,94].

In the ultimately selected basic grid, a cell expansion rate of 1.2 ensures a smooth transition of cell sizes between a fine resolution in the area of interest to a coarse mesh in the regions further away. The smallest resulting cell in the domain has a volume of 8.8 cm^3 whereas the largest has 2.3 × 10^6 m^3. As recommended in the BPG [93,94], at least 10 cells are kept between buildings and the evaluation height (1.75 m in this case, as the climate variables at the pedestrian level are of interest) coincides with at least the third cell above ground in the area of interest. Furthermore, inflation layers ensure vertical grid lines on the building walls and the ground surface in the study area.

2.4. Boundary conditions

In order to account for surface roughness elements in the areas of the domain where buildings and other obstacles have not been modelled explicitly, surface roughness parameters are used. Fluent does not allow for the direct input of the aerodynamic roughness length z_0 as given by Wieringa [84], but requires a sand-grain roughness height k_s. For that, the correlation $k_s = 9.793\, z_0\, C_s^{-1}$, where C_s is a roughness constant [−] was used [95]. In Fluent 2020.R1, C_s is limited to a range between 0 and 1. In this study, the default value of 0.5 was kept for all surface types. Asphalt, concrete and pavement surfaces for the geometrical modelling types *a* and *b* were assigned a sand-grain roughness height $k_s = 0.05$ m, while for grass and building surfaces, k_s was set to 0.1 m to account for irregularities and protrusions. Table 5 shows the surface roughness parameters for all rough walls in the domain. For the geometrically explicitly modelled surfaces, the sand-grain roughness was entered directly. Only for the geometrically implicitly modelled surfaces, a conversion from z_0 to k_s was made. Note that the surface roughness of the geometrically implicitly modelled parts of the domain was not calculated but based on the authors' estimations. Fluid-wall interactions are treated with the standard wall functions by Launder and Spalding [96].

To account for the influence of thermal mass, the urban surface and all buildings are modelled according to their construction type, using shell conduction in Fluent. For that, the buildings at the campus are grouped into five categories, see Fig. 5 and Table 6. For simplification, it was not distinguished between the wall and the roof structures. I.e. the constructions listed in Table 6 are used for both, walls and roofs. Windows, doors, balconies and small chimneys were omitted. All geometrically explicitly modelled buildings are assigned a constant indoor temperature of 21 °C. For the surrounding buildings, 0.3 m brick is used for the wall and roof construction. The ground surface has a thickness of 10 m and a constant temperature of 5 °C at the exterior surface (not facing the fluid cells). This temperature boundary condition is based on groundwater temperature measurements near the study site. The water-covered areas, namely the river Nidelva and Trondheim Fjord are not modelled as a fluid but as a "thin wall" with temperatures recorded at ships traversing the Norwegian coastline and Trondheim Fjord at the simulated dates [97]. The temperatures used as boundary conditions were 15 °C in VP1 and 9 °C in VP2. The grass surfaces are divided into three layers of earth with a top layer thickness of only 0.01 m as there, the evapotranspirational cooling flux from the grass is applied (see section 2.5). As this heat flux is applied in the centre of the respective layer, a thickness of 0.01 m ensures this cooling flux is close to the surface facing the fluid cells. Table 7 lists the optical and thermal properties of the surface materials that were used in the model.

For the simulation, it is specified that always two of the lateral domain boundaries are set as inlets and the other two as outlets, depending on the wind direction. At the inlets, a logarithmic profile of the air velocity $U(z)$ [m s^{-1}] (see Eq. (1)) is imposed. Depending on the wind direction, different surface roughness lengths $z_{0,b}$ [m] at the inlet boundaries are used to determine the shape of the profile. Due to the coastal location of Trondheim, the northern boundary is bordering the sea, for which a different $z_{0,b}$ was used than for the other three boundaries that are located on land (see Fig. 2). Therefore, it is estimated that $z_{0,b} = 0.25$ m, based on the terrain, farmland, patches of forests and the built-up areas upwind of the study area between 65 and 310° from north. For the remaining directions, $z_{0,b}$ is set to a lower value of 0.1 m. Although, according to the surface type categories from Wieringa [84] a roughness length of 0.002 m should be chosen for the ocean, it was

Table 4
Surface grid sizing settings of the three investigated computational grids in the grid-convergence analysis.

	Element in domain	Coarse grid (4.4 M cells)	Basic grid (9.1 M cells)	Fine grid (23.6 M cells)
Node distance at edges [m]	Cat. I	0.35	0.25	0.2
	Cat II–V	1.0	0.75	0.6
	Trees	0.8	0.6	0.45
Max. node distance [m]	Cat. I	2.5	2.0	1.6
	Cat II–V	5.0	4.0	3.2
	Trees	0.8	0.6	0.45
Expansion rate [−]		1.3	1.2	1.1
Number of prism layers [−]	Buildings	2	3	4
	Ground	2	3	4
Thickness of 1st prism layer [m]	Buildings	0.4	0.15	0.1
	Ground	0.6	0.4	0.3
Min. number of cells between buildings		10	10	10

Table 5
Surface roughness settings in the computational domain.

Modelling type	Surface	z_0 [m]	k_s [m]	C_s [−]
Explicit	Building surfaces	–	0.10	0.5
	Asphalt	–	0.05	0.5
	Concrete	–	0.05	0.5
	Grass-covered earth	–	0.10	0.5
Implicit	Urban cityscape	1.0	19.59	0.5
	Industry	1.0	19.59	0.5
	Other[a]	0.5	9.79	0.5

[a] Combining the surface types *Dense low-rise*, *Farmland*, *Open area*, and *Forest* (see Fig. 2) into one boundary condition type.

Table 6
Wall structure of buildings and the urban surface.

Building categories/ Urban surface	Layer 1 (adjacent to fluid cells)		Layer 2		Layer 3 (domain's exterior)	
	Material	d [m]	Material	d [m]	Material	d [m]
I (Wood)	Wood: spruce	0.05	Insulation	0.25	Wood: spruce	0.05
II (Stone)	Granite	0.2	Brick	0.2	–	–
III (Brick)	Brick	0.36	–	–	–	–
IV (Concrete, old)	Concrete	0.36	–	–	–	–
V (Concrete, new)	Plaster	0.02	Insulation	0.2	Concrete	0.2
Surrounding buildings	Brick	0.3	–	–	–	–
Roads	Asphalt	0.3	Granite	1.0	Earth	8.7
Pavement	Concrete	0.3	Granite	1.0	Earth	8.7
Grass	Earth	0.01	Earth	0.49	Earth	9.5

Table 7
Selected optical and thermal properties of the surface materials on campus [18, 98–100].

Surface	α [−]	ε [−]	c [kJ kg^{-1} K^{-1}]	δ [kg m^{-3}]	λ [W m^{-1} K^{-1}]
Wood: spruce	0.75	0.90	2310	700	0.17
Asphalt	0.70	0.95	800	2400	0.75
Concrete	0.66	0.95	1000	2300	1.60
Plaster	0.66	0.95	1000	1800	1.00
Insulation (not a surface material)	–	–	840	50	0.05
Granite	0.70	0.95	790	2800	3.00
Earth (covered with grass)	0.77	0.95	1000	1400	1.80
Brick	0.66	0.95	900	2050	0.80

Absorptivity (α), emissivity (ε), heat capacity (c), density (δ), thermal conductivity (λ).

found that $z_{0,b} = 0.1$ m results in a better fit of simulations and measurements which can be partially attributed to the complex terrain around the area of interest that is strongly influencing the vertical wind profile.

Reference wind speed and direction are taken from the reference weather station at $h_{ref} = 28$ m height (10 m above the VATL building, see Fig. 5). The formulations of inlet profiles for air velocity $U(z)$ [m s^{-1}] (Eq. (1)), turbulent kinetic energy $k(z)$ [m^2 s^{-2}] (Eq. (2)), and turbulence dissipation rate $\varepsilon(z)$ [m^2 s^{-3}] (Eq. (3)) are taken from the frequently used conditions provided by Richards and Hoxey [101]. In these relationships, u^*_{ABL} [m s^{-1}] (Eq. (4)) is the Atmospheric Boundary Layer friction velocity [m s^{-1}], κ is the von Karman constant [−] (= 0.42), z is the height coordinate [m], and C_μ is a constant [−] (= 0.09). For determining u^*_{ABL} the wind speed at the boundaries u_b [m s^{-1}] is needed, for which no measurements are available during VP1 and VP2. Therefore, Wieringa's [102] logarithmic transformation equation (Eq. (5)) is used to determine u_b based on the wind speed measured at the reference station u_{ref} [m s^{-1}], the surface roughness at the reference station $z_{0,ref}$ [m], the target height of the transformation h_b [m] and a blending height h_{bh} [m]. In this study, only a transformation due to different roughness lengths is needed, thus h_b is set equal to h_{ref}. The blending height h_{bh} defines the height at which the influence of the ground gets negligible. In Wieringa's work it is taken as 60 m based on a study by Munn and Reimer [103] in Pinawa, Canada. However, in contrast to Trondheim's surrounding, the terrain in both Wieringa's (the Netherlands) and Munn and Reimer's (south-east Manitoba, Canada) studies can be considered as rather flat. There are no measurements of h_{bh} available in Trondheim, but it can be reasonably assumed to be significantly higher than 60 m. It was therefore set to 200 m due to the complex terrain in the area of the computational domain.

$$U(z) = \frac{u^*_{ABL}}{\kappa} \ln\left(\frac{z + z_{0,b}}{z_{0,b}}\right) \tag{1}$$

$$k(z) = \frac{u^{*\,2}_{ABL}}{\sqrt{C_\mu}} \tag{2}$$

$$\varepsilon(z) = \frac{u^{*\,3}_{ABL}}{\kappa\,(z + z_{0,b})} \tag{3}$$

$$u^*_{ABL} = \frac{\kappa\, u_b}{\ln\left(\frac{h_b + z_{0,b}}{z_{0,b}}\right)} \tag{4}$$

$$u_b = u_{ref}\left[\frac{\ln\left(\frac{h_{bh}}{z_{0,ref}}\right)\ln\left(\frac{h_b}{z_{0,b}}\right)}{\ln\left(\frac{h_{ref}}{z_{0,ref}}\right)\ln\left(\frac{h_{bh}}{z_{0,b}}\right)}\right] \tag{5}$$

The shear condition at the domain top is set to a free-slip condition, assuming zero normal gradients for all the flow variables. To account for longwave radiation losses to the sky, the domain's inlets, outlets and top boundary are assigned a temperature T_{sky} according to Swinbank's [105] simplified correlation (Eq. (6)). As a basis, the air temperature measured at the reference weather station $T_{a,C,ref}$ [°C] is used.

$$T_{sky} = 0.0552\, T^{1.5}_{a,C,ref} \tag{6}$$

2.5. Other computational settings

For the CFD simulations, 3D unsteady Reynolds Averaged Navier Stokes (URANS) equations are applied for which the realisable k-ε turbulence model [106] provides closure. This turbulence model has been used successfully in other validated CFD studies of the urban MC, e.g. Refs. [71,78,80,81,107] and is recommended to use by Franke et al. [93] over the standard k-ε model. Furthermore, it was attributed a generally good performance for wind flow around buildings [24,108,109]. Natural convection is included by using the Boussinesq approximation. The trees are modelled as volumetric porous zones in a spherical shape. This spherical, not perfectly round but to a certain degree irregular shape was created to resemble a "standard" tree crown and was used for all trees in the study area according to their approximate size. For the cells of these porous zones, source/sink terms for the momentum S_{u_i} [Pa m^{-1}] for each velocity component $u_i$with $i = x, y, z$ (Eq. (7), from Refs. [110, 111]), turbulent kinetic energy S_k [kg m^{-1} s^{-3}] (Eq. (8), from Ref. [111]), turbulent dissipation rate S_ε [kg m^{-1} s^{-4}] (Eq. (9), from Ref. [112]) and volumetric heat transfer from evaporation P_c [W m^{-3}] (Eq. (10), from Refs. [80,113,114]) are added:

$$S_{u_i} = -\,\rho\, LAD\, C_d\, U\, u_i \tag{7}$$

$$S_k = \rho\, LAD\, C_d\, \left(\beta_p\, U^3 - \beta_d\, U\, k\right) \tag{8}$$

$$S_\varepsilon = \rho\, LAD\, C_d \left(C_{\varepsilon 4}\, \beta_p \frac{\varepsilon}{k} U^3 - C_{\varepsilon 5}\, \beta_d\, U\, \varepsilon\right) \tag{9}$$

$$P_{c,trees} = (0.0252\, T_a - 0.078)\, R_h\, LAD \tag{10}$$

In equations (7)–(10), ρ is the density of air [kg m^{-3}], LAD the Leaf Area Density [m^{-1}], C_d the sectional drag for vegetation [−], $(\beta_p, \beta_d, C_{\varepsilon 4}, C_{\varepsilon 5}) = (1.0, 4.0, 0.9, 0.9)$ are model coefficients [−], U the wind speed (across all directions) [m s^{-1}], T_a the air temperature [K], R_h the incoming global solar radiation [W m^{-2}] [115]. The LAD of the trees is selected based on a study by Klingberg et al. [116], who mapped the leaf area of urban greenery using aerial LiDAR (light detection and ranging) and ground-based measurements in Gothenburg, Sweden. The reported LADs for Maples and Chestnuts, very common tree species for the area of interest, were between around 0.6 and 2.1 m^{-1}. Since there are only few

coniferous trees in the explicitly modelled area of the domain, only deciduous trees are used as a simplification. With 1.0 m^{-1}, a slightly lower LAD than the average from Klingberg et al.'s study [116] is applied, as the trees already started to defoliate in the VPs (see Fig. 3).

Many other urban MC CFD studies addressed dense and concrete-dominated city environments [65,71,80,81] and therefore either only included the tree crowns or fully omitted the microclimatic impact of vegetation. Since the NTNU campus is embedded within a park and is surrounded predominantly by single-family homes with gardens (see also Fig. 2), not only the trees but also the evaporative cooling effect from grass-covered soil is expected to significantly impact the microclimatic conditions close to the ground surface. As a consequence, the evapotranspirational cooling effect from short grass canopies was included in the CFD model. For that, the PME is implemented as a user-defined function (UDF) to compute the heat flux from evapotranspiration E [W m^{-2}] which is shown in Eq. (11) [100,117,118].

$$E = \frac{\Delta \ (R_n - G) + \rho \ c_p \frac{D}{r_a}}{\Delta + \gamma \left(1 + \frac{r_s}{r_a}\right)} \tag{11}$$

The PME takes into account the available energy $(R_n - G)$ where R_n is the net radiation [W m^{-2}], G is the soil heat flux [W m^{-2}], D is the vapour pressure deficit of the air [Pa], r_s and r_a are the (bulk) surface and the aerodynamic resistances [s m^{-1}], λ is the latent heat of water vaporization [J kg^{-1}] as calculated from Eq. (12) [119], and γ is the psychrometric constant [Pa K^{-1}], calculated from $P_{atm}\ c_p\ (0.622\ \lambda)^{-1}$, where P_{atm} is the atmospheric pressure [Pa] and c_p is the specific heat capacity of air [J kg^{-1} K^{-1}]. The (bulk) surface resistance r_s and the aerodynamic resistance r_a can be obtained from Eqs. (13) and (14), respectively, where h_{grass} is the height of the grass [m], taken as 0.1 m and r_i is the bulk stomatal resistance of the leaf, taken as $r_i = 100\ s\ m^{-1}$ [120]. The Leaf Area Index (LAI) [−], similar to the volumetric LAD, indicates the available leaf surface area per m^2 vegetated surface, whereas the active Leaf Area Index LAI_{active} [−] takes into consideration that only the upper half of dense clipped grass is actively contributing to the surface heat and vapour transfer. In Eq. (14), $z_{ref.u}$ and $z_{ref.h}$ (both in [m]) are the heights of the wind and humidity measurements, respectively, and u_{ref} is the measured wind speed [m s^{-1}] (in this case at the reference weather station). Although the application of Eq. (14) is restricted to neutral stability conditions where temperature, pressure, and wind velocity follow near adiabatic conditions, it is considered a suitable method for the rough estimation of the cooling flux from evapotranspiration at grass-covered surfaces [120].

$$\lambda = 1.91846 \ \times 10^6 \left[\frac{T_{a,C,ref} + 273.15}{T_{a,C,ref} + 239.24}\right]^2 \tag{12}$$

$$r_s = \frac{r_i}{LAI_{active}} = \frac{r_i}{0.5\ LAI} = \frac{r_i}{12\ h_{grass}} \tag{13}$$

$$r_a = \frac{\ln\left[\frac{z_{ref.u} - \frac{2}{3}h_{grass}}{0.123\ h_{grass}}\right] \ln\left[\frac{z_{ref.h} - \frac{2}{3}h_{grass}}{0.0123\ h_{grass}}\right]}{\kappa^2 u_{ref}} \tag{14}$$

The evaporative cooling flux is significantly influenced by the prevailing humidity regime, expressed in Eq. (11) through the slope of the vapour pressure curve Δ [Pa K^{-1}] and the atmospheric vapour pressure deficit D [Pa], calculated from Eqs. (15) and (16), respectively. There, e_{act} is the actual vapour pressure [Pa] and e_{sat} the saturation water pressure [Pa] (see Eq. (17)) for the air temperature $T_{a,C,ref}$ [°C] and relative humidity RH_{ref} [%], as measured from the reference weather station.

$$\Delta = \frac{4098\left[610.8\ exp\left(\frac{17.27\ T_{a,C,ref}}{T_{a,C,ref} + 237.3}\right)\right]}{\left(T_{a,C,ref} + 237.3\right)^2} \tag{15}$$

$$D = e_{sat} - e_{act} = \left(1 - RH_{ref}\right)\ e_{sat} \tag{16}$$

$$e_{sat} = \left(1.0007 + 3.46 \times 10^{-8}\ P_{atm}\right)\ 611.21\ exp\left(\frac{\left(18.678 - \frac{T_{a,C,ref}}{234.5}\right) T_{a,C,ref}}{257.14 + T_{a,C,ref}}\right) \tag{17}$$

To facilitate the application of the PME, some simplifications were made. First, the presented CFD model only considers one single phase (only air as a fluid medium) and therefore does not include vapour species transport or evaporation directly. Therefore, the atmospheric vapour pressure deficit D and the slope of the vapour pressure curve δ are calculated as an overall value from the relative humidity RH_{ref} and air temperature $T_{a,C,ref}$ which are recorded at the reference weather station (Eq. (15)–(17)). The same applies to the wind speed u_{ref} in Eq. (14). Therefore, $z_{ref.u}$ and $z_{ref.h}$ are both taken as the height of the reference weather station, which is 28 m above the ground. Second, the available energy for evaporation $(R_n - G)$ is defined as the difference between the net gain from shortwave and longwave radiation R_n and the heat flux into the soil G. For this study, G is neglected in this equation, as for dense canopies such as lawns in a park, its value is relatively small compared to R_n [100]. Third, the atmospheric pressure P_{atm} and the specific heat capacity of air c_p are assumed to be constant and are taken as 101325 Pa and 1008 J kg^{-1} K^{-1}, respectively. The resulting evaporation heat flux is implemented in the CFD model as an internal heat generation rate in the top 1 cm layer of earth at the grass-covered surfaces.

As mentioned before, CFD models can be used to investigate outdoor thermal comfort conditions. For that reason, the standard functionality of ANSYS Fluent is extended with a UDF for calculating the PET [121,122]. According to Fischereit and Schlünzen [123], the PET index is the most frequently used comfort index in obstacle-resolving meteorology models (ORM) such as CFD. They found that it was one among only four out of 165 indices that fulfilled all criteria posed to be applicable in ORMs. To include the PET comfort index in the presented CFD model, the corrected PET equations of the German VDI 3787 [124] from Walther and Goestchel's Python code [125] were translated into C language to make them useable as a UDF in ANSYS Fluent.

The Solar Calculator in ANSYS Fluent was used to determine the sun's position for each time step. Measured values of global horizontal radiation on-site (reference station), divided into direct and diffuse fractions using the approach by Skartveit and Olseth [126] provide the input for the instantaneous solar intensities which are updated once every hour for each time step. Long-wave radiation exchange is incorporated with the discrete ordinates (DO) radiation model [127,128]. For the angular discretization of the DO model, the standard settings for the number of theta and phi divisions are kept at 2, and the number of theta and phi pixels at 1. Pressure-velocity coupling is provided by the SIMPLEC [129] algorithm and schemes of second-order only are used for the spatial discretization.

In this study, two 48-h periods are simulated with 1-h time steps and 400 iterations per time step except for the first one, for which 800 iterations were performed to provide better convergence. As a consequence, in total 48 time steps with 19,600 iterations were carried out for each of the two 48-h periods. On average, the following scaled residuals were reached at the end of each time step in VP1: 6.6×10^{-6} for continuity, 4.0×10^{-5} for x-velocity, 1.6×10^{-5} for y-velocity, 3.6×10^{-5} for z-velocity, 3.8×10^{-4} for k, 9.2×10^{-4} for ε, 2.8×10^{-8} for energy, and 8.0×10^{-7} for radiation. In VP2, the average scaled residuals at the end of each time step were: 3.7×10^{-5} for continuity, 2.2×10^{-4} for x-

velocity, 2.3×10^{-4} for y-velocity, 1.9×10^{-4} for z-velocity, 5.7×10^{-4} for k, 3.6×10^{-3} for ε, 5.0×10^{-8} for energy, and 1.1×10^{-6} for radiation. For comparing simulated with measured values, the simulation results are extracted at the corresponding points of the measurement locations in the domain (see Fig. 5).

3. Results

3.1. Grid-convergence analysis

In this section, the results of the grid-convergence analysis are shown. The grid sizing and computational settings are presented in chapter 2.3. From Fig. 7, it can be seen that the differences between the medium-sized grid, hereafter referred to as the basic grid (9,123,834 cells), and the coarse grid (4,371,409 cells) are relatively small for the measurement points at the weather stations and the additional evaluation lines. Larger grid cells on the walls of the coarser grid, however, resulted in large deviations at the near-wall positions (0.15–0.5 m from the walls).

The differences between the basic and the fine grid (23, 566, 616 cells) on the other hand are so small that a further refinement of the grid would only marginally change the numerical result. The basic grid can be regarded as a good compromise between computational cost and accuracy. Therefore, it was selected for the validation process.

3.2. Simulation results

For evaluating the accordance of the simulation with the measurements, three quality indicators are used: (1) the coefficient of determination (R^2, see Eqs. (18) and (2)) the coefficient of variance of the root mean square deviation (CV_{RMSD}, see Eqs. 19), and (3) the maximum deviation value (D_{max}, see Eq. (20)). In Eqs. (18) and (19), s_i and m_i are the simulated and measured value of time step i, respectively, n is the total number of time steps and $\overline{m}$ is the mean value of measurements.

$$R^2 = 1 - \frac{\sum_{i=0}^{n}(m_i - s_i)^2}{\sum_{i=0}^{n}(m_i - \overline{m})^2} \tag{18}$$

$$CV_{RMSD} = \frac{RMSD}{\overline{m}} \times 100\% = \frac{\sqrt{\sum_{i=1}^{n}(s_i - m_i)/n}}{\overline{m}} \times 100\% \tag{19}$$

$$D_{max} = \max_{i \in \{1,\cdots,n\}}(|s_i - m_i|) \tag{20}$$

In both of the investigated 48-h periods VP1 (September 27–28) and VP2 (October 19–20), the CFD model was able to reproduce the measured conditions at the reference weather station with acceptable accuracy (see Fig. 8 and Fig. 9). Overall, the air temperature is best represented with an R^2 of 0.98 and 0.93, and a CV_{RMSD} of 2.5% and 6.5% for VP1 and VP2 respectively. D_{max} amounted to 0.7 °C in VP1 (28.09. 11:00) and 1.2 °C in VP2 (20.10. 19:00). Both, in VP1 and VP2, the air temperature is slightly underestimated in the simulations.

Simulated wind speed and wind direction also show a satisfactory correlation with the measurements at the reference weather station. In VP1, an R^2 of 0.76 and 0.34 as well as a CV_{RMSD} of 17.3% and 21.9% is obtained for wind speed and direction, respectively. D_{max} is 1.4 m s^{-1} (28.09. 20:00) for the wind speed and 143° (27.09. 11:00) for the wind direction. In VP2, the quality indicators for wind speed and wind direction are 0.44 and 0.91, 38.8% and 14.5%, and 2.1 m s^{-1} (19.10. 14:00) and 99° (20.10. 22:00) for R^2, CV_{RMSD}, and D_{max}, respectively.

The quite large starting threshold of 1 m s^{-1} for both the wind speed and wind direction sensor of the mobile weather stations A–E resulted in a large amount of data falling within the measurement inaccuracy of the sensors. In fact, the measured wind speed at the mobile weather stations was below the sensors' starting threshold 95% and 98% of the time in VP1 and VP2, respectively. For these times, the recorded values are not necessarily zero, but most certainly lower than the actual wind speed at the mobile weather stations A–E. The measured and simulated wind speeds of VP1 and VP2 are shown in Fig. 10. It shows that the measured values are mostly lower than the simulated ones. With exception of only a few data points, the simulated wind speeds lie within the measurement inaccuracy of the sensors.

Comparing measured and simulated wind direction with another was not regarded as meaningful, as low wind speeds will keep the wind direction sensor (a wind vane) for a long time in a steady position that might not be representative of the actual wind direction. During the hourly averaging, these measurements of unrepresentative wind directions then result in unrepresentative values for the respective hours. Other than for the wind speed, the obtained data was not regarded as meaningful for comparison.

Fig. 11 shows the comparison between temperature measurements and simulations at the locations of the mobile weather stations A–E. Similar to the reference weather station, the simulated temperatures show an acceptable agreement with the measurements. The quality indicators of the simulated air temperatures and wind speeds at the locations of the mobile weather stations are summarized in Table 8. Overall, the accordance with the measured values is lower than at the

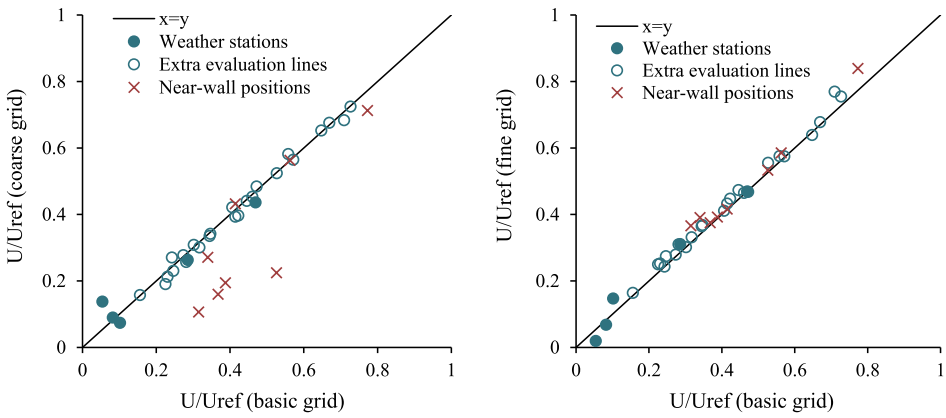

Fig. 7. Comparison of wind speed ratios for the coarse and the basic grid (left) and the fine and the basic grid (right) at the measurement points, the extra evaluation lines, and the near-wall positions.

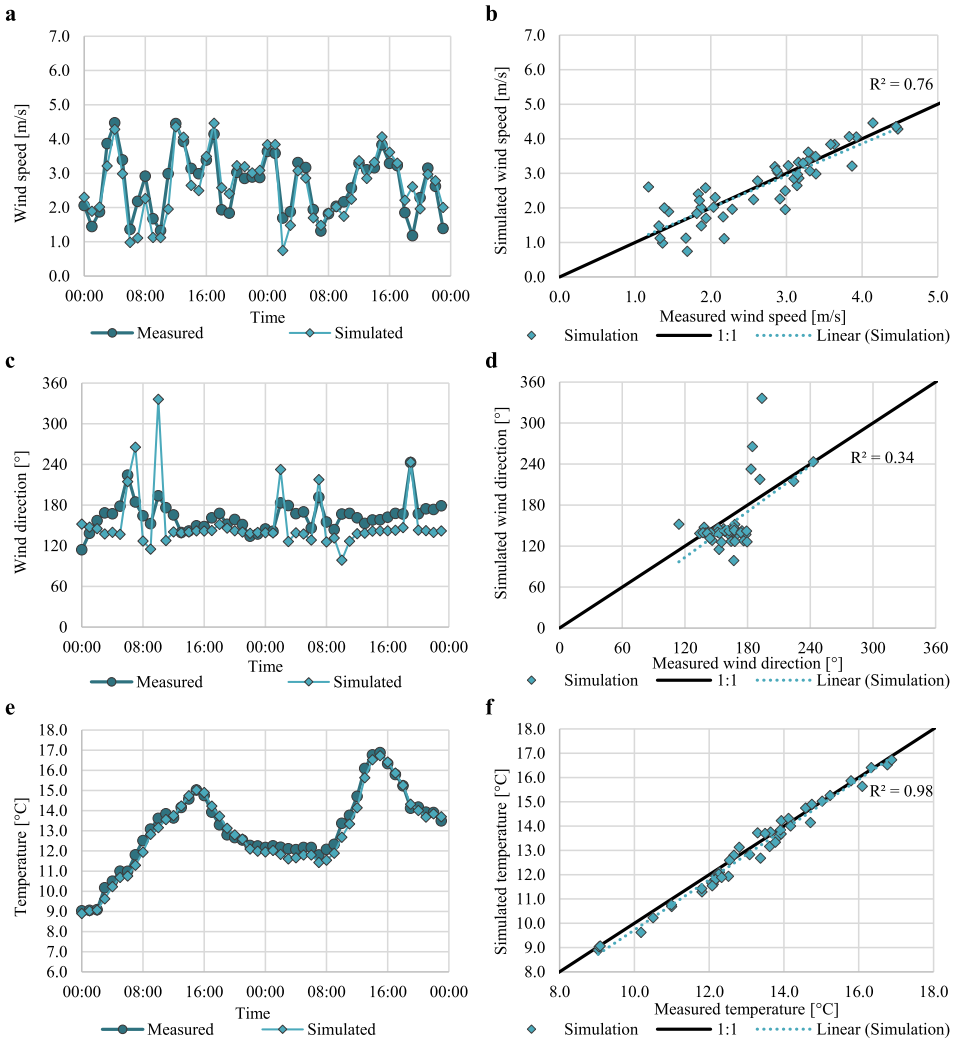

Fig. 8. Comparison of simulated and measured wind speed (a1 and a2), wind direction (c and d) and air temperature (e and f) with error bars indicating the range of measurement uncertainty for September 27–28. Due to the high sensor accuracy, the error bars are hidden behind the data points.

reference weather station. Regarding air temperature, a more pronounced underestimation of the simulated values is noticeable at the mobile weather stations compared to the reference weather station. This is especially the case during the second day of VP1 (high amount of solar irradiation) at station B which is located between trees and on a large lawn. At weather station D, the accordance with measured air temperature is best, both for VP1 and VP2. Note that station D is the only weather station which is not placed on grass but on concrete pavement. Although the quality indicators of the simulated wind speed in Fig. 10 give the impression of a poor fit, it needs to be taken into consideration that the simulated values are almost always within the sensors' uncertainty of measurement.

4. Discussion

4.1. Interpretation of results

When looking at the simulation results and the quality indicators at the reference weather station, especially the differences of wind speed and direction between VP1 and VP2 stand out. In VP1, the wind speed ($R^2 = 0.76$, $CV_{RMSD} = 17.3\%$, $D_{max} = 1.4\ m\ s^{-1}$) is much better represented than wind direction ($R^2 = 0.34$, $CV_{RMSD} = 21.9\%$, $D_{max} = 143°$). In VP2 on the other hand, the correlation between simulated and measured wind speed ($R^2 = 0.44$, $CV_{RMSD} = 38.8\%$, $D_{max} = 2.1\ m\ s^{-1}$) is significantly lower than the correlation between simulated and measured wind direction ($R^2 = 0.91$, $CV_{RMSD} = 14.5\%$, $D_{max} = 98°$).

These differences can be partly explained by the influence of the hilly terrain which is higher towards the east and lower towards the west of the campus. With a prevailing southern wind direction, the air flow is deflected to a more south-eastern wind direction by the higher terrain to

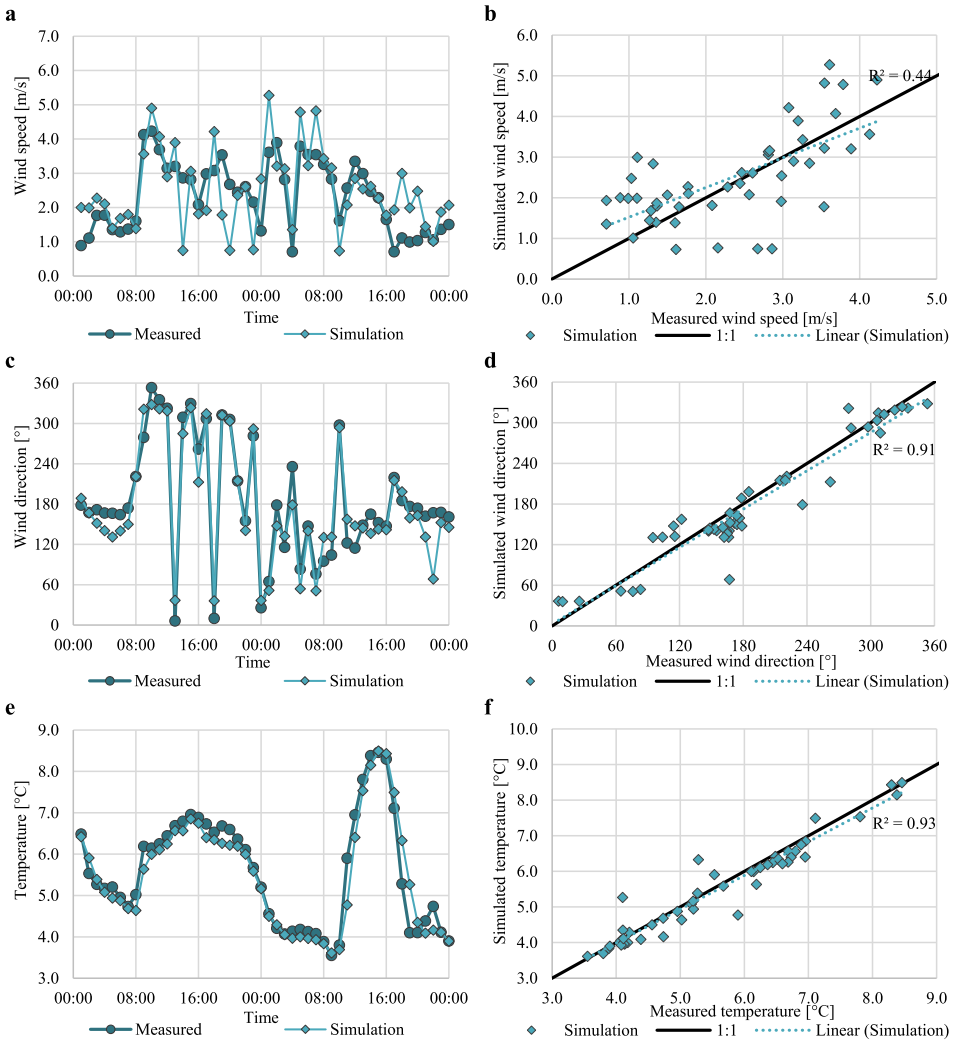

Fig. 9. Comparison of simulated and measured wind speed (a and b), wind direction (c and d) and air temperature (e and f) with error bars indicating the range of measurement uncertainty for October 19–20. Due to the high sensor accuracy, the error bars are hidden behind the data points.

the east (represented in grey in Fig. 12). This effect can be seen throughout VP1 where simulated wind directions are constantly below the recorded (input) values at measured wind directions from 150° to 180° (see the accumulation of datapoints below the 1:1 line between 150° and 180° in Fig. 8d). The same applies to the respective times in VP2, as indicated for instance at the first seven and last six time steps of the simulation (see Fig. 9c and the accumulation of datapoints below the 1:1 line between 150° and 180° in Fig. 9d). Moreover, it cannot be ruled out that the inlet reference measurement data from these angles were influenced by this phenomenon and that the true wind directions at the domain inlet, located about 2 km south of the campus, were at slightly higher angles than the ones used.

However, the CFD model proved to be able to represent the wind direction adequately over the whole spectrum of the wind directions, especially during VP2. There, the wind was blowing less often from these wind directions between 150° and 180° and more from directions that are generally better represented. Therefore, the quality indicators and overall accordance between simulated and measured values are much better.

Analogously, using the recorded wind speed from the reference weather station as a basis for the inlet profiles in the CFD simulations certainly introduces an error to the simulations. Even though the reference weather station is located 10 m above the roof of a large building, it is still about 20 m below the roof height of the two central buildings to the south (building SB1 and SB2) and 4 m below the roof height of the much closer main building to the north-west (building HB). These buildings create significant turbulences and have large wakes that most likely impact the measurements at the reference weather station (see Fig. 12).

There are several points in time when the reference weather station is in the wake of building HB during westerly and north-westerly winds (VP2 19.10 at 14:00, 17:00, 19:00, 20:00, 23:00 and 20.10 at 10:00). It is likely that the measurements are taken within the wake of this building and are thus lower than the actual free-stream air velocities.

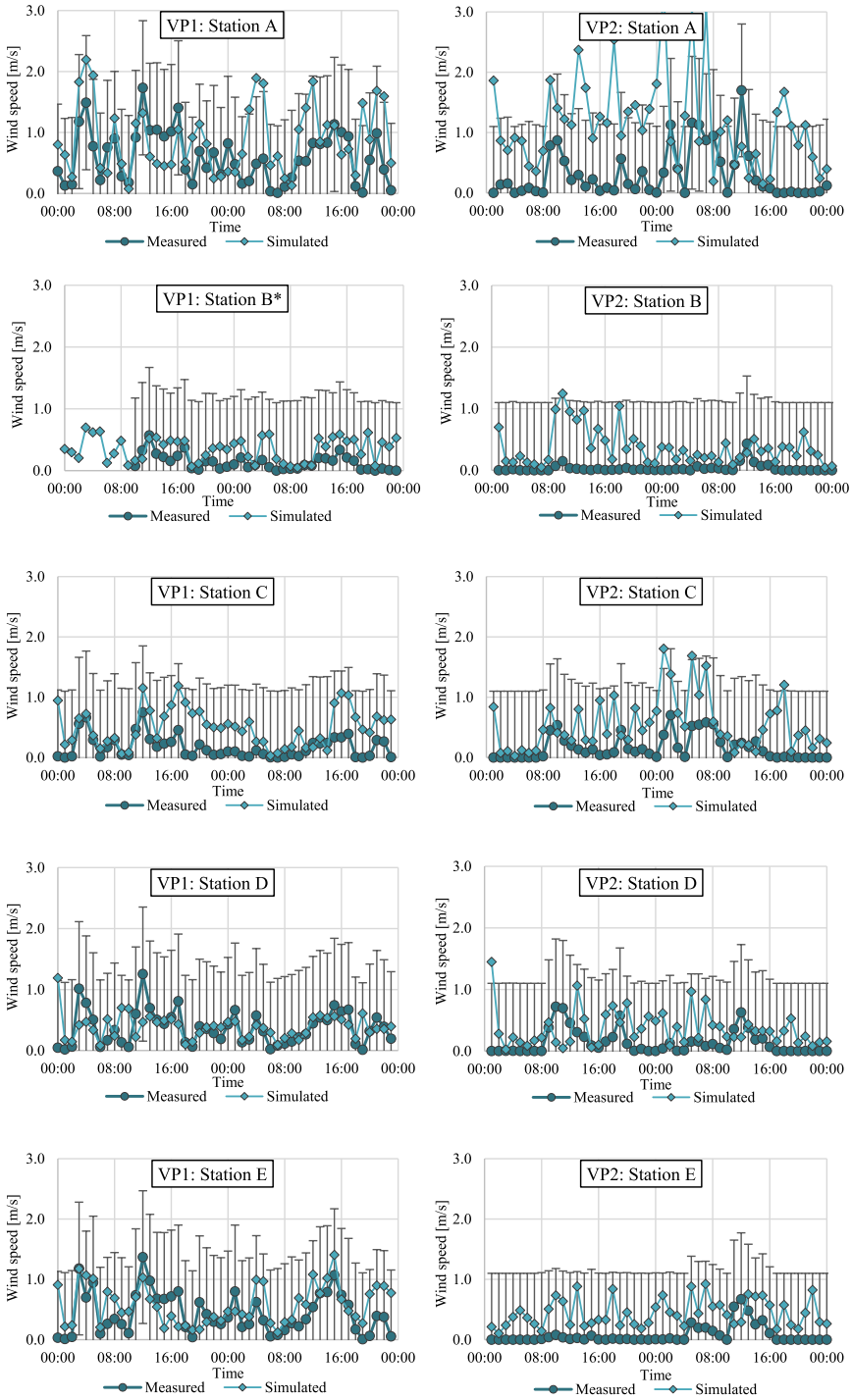

Fig. 10. Comparison of simulated and measured wind speed with error bars indicating the range of measurement uncertainty at the mobile weather stations for VP1 (left) and VP2 (right). *Because of a sensor failure during VP1, the records of the first 9 h of Station B are missing.

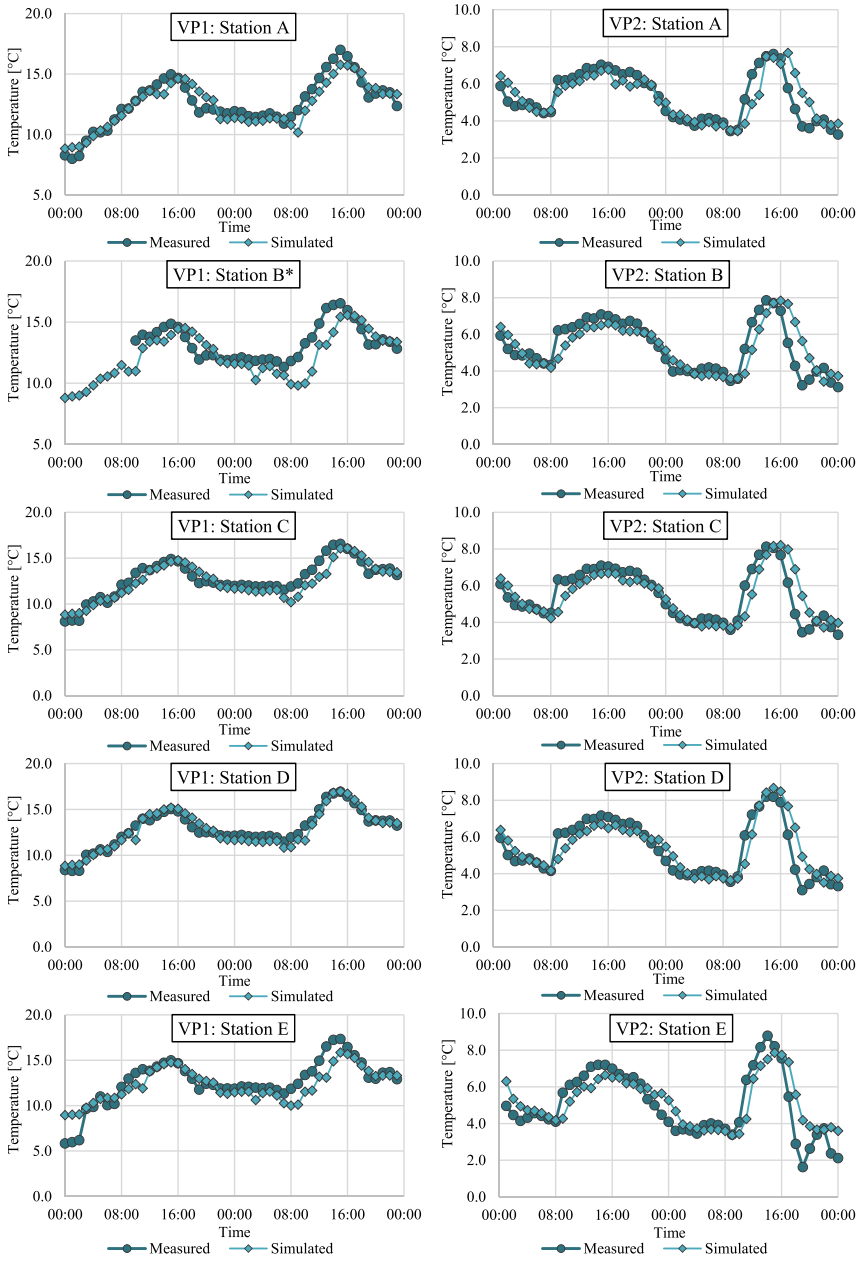

Fig. 11. Comparison of simulated and measured air temperature with error bars indicating the range of measurement uncertainty at the mobile weather stations for VP1 (left) and VP2 (right). Due to the high sensor accuracy, the error bars are hidden behind the data points. *Because of a sensor failure during VP1, the records of the first 9 h of Station B are missing.

Using such measurements as a basis for determining the inlet profiles in the CFD simulations, where data is again extracted within the wake of the building, can lead to significantly lower wind speeds than measured. However, despite wind coming from a similar wind direction, at other time steps the agreement is quite fair (VP2 19.10. at 11:00, 12:00, 15:00). A possible reason for that might be the choice of turbulence model that has a significant impact on the flow variables in wakes behind obstacles, as they determine the wakes' size and extent [109]. Even a slightly different shape of the wake can lead to significant discrepancies between simulation results and measurements as the gradients of the flow variables are usually very high at such locations [130]. In the context of this study, however, no comparison of different turbulence models was made.

As in the simulations, data can be extracted without significant

Table 8
Quality indicators R^2, CV_{RMSD} and D_{max} of the simulated air temperatures and wind speeds at the locations of the mobile weather stations. The best-obtained correlation to measured values in the respective validation periods (VP) and the respective quality indicators are marked in bold.

	Validation Period	Quality indicator	Station A	Station B	Station C	Station D	Station E
Wind Speed	VP1	R^2	0.16	0.20	0.26	0.06	**0.29**
		CV_{RMSD}	102.4%	210.4%	244.3%	82.3%	**80.0%**
		D_{max}	1.5 m s^{-1}	**0.6 m s^{-1}**	0.9 m s^{-1}	1.1 m s^{-1}	0.9 m s^{-1}
	VP2	R^2	0.01	0.02	**0.25**	0.00	0.07
		CV_{RMSD}	383.3%	1388.7%	335.6%	**300.7%**	571.8%
		D_{max}	3.0 m s^{-1}	1.1 m s^{-1}	1.4 m s^{-1}	1.4 m s^{-1}	**0.9 m s^{-1}**
Temperature	VP1	R^2	0.86	0.49	0.83	**0.93**	0.75
		CV_{RMSD}	6.3%	10.2%	6.8%	**4.5%**	10.5%
		D_{max}	1.8 °C	3.3 °C	2.5 °C	**1.6 °C**	3.4 °C
	VP2	R^2	0.68	0.64	0.69	**0.76**	0.69
		CV_{RMSD}	14.0%	15.7%	14.1%	**13.5%**	19.5%
		D_{max}	1.9 °C	2.4 °C	2.4 °C	2.3 °C	2.7 °C

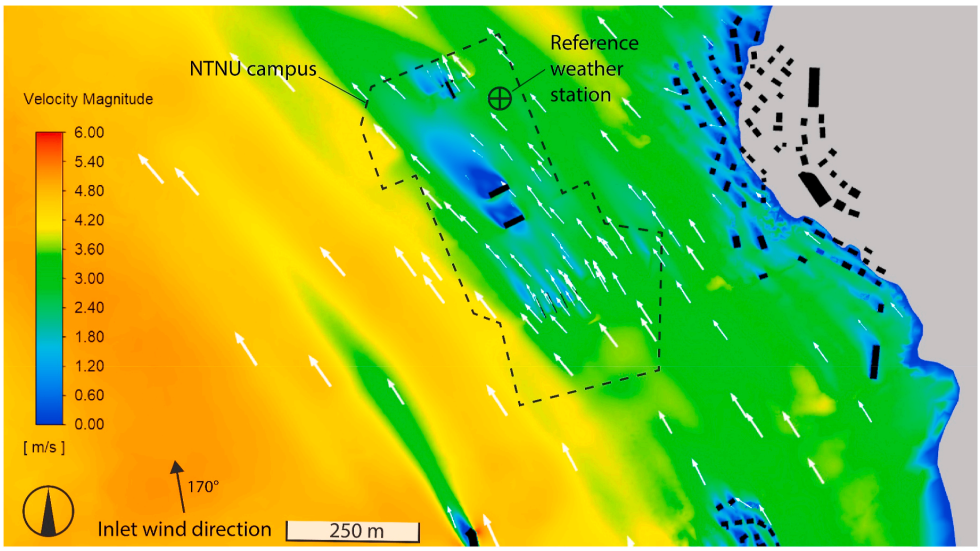

Fig. 12. View from the top at a horizontal cut through the domain at 73.66 m (height of the reference weather station above sea level) showing the velocity magnitude on September 28, at 05:00. The terrain above the cutting plane is visualized in grey.

limitations regarding sensitivity at the control points, simulated wind speeds at the locations of the mobile weather stations A–E are mostly higher than the measurements (see Fig. 10). It must be noted that the simulated values are almost always within the sensors' measurement uncertainty and follow largely the same course as the measurements, particularly at stations B–E in VP1. Hence, considering the large uncertainty of measurements especially below 1 m s^{-1}, the CFD model can be regarded as suitable to predict the wind speeds at the low-level atmospheric boundary layer with acceptable accuracy.

The best-represented climate variable in the simulations is the air temperature with overall good accordance of simulated and measured values at all locations. However, the underestimation of air temperatures is more pronounced closer to the ground at the mobile weather stations compared to the reference weather station. This is especially visible during times of high solar irradiation like on the second day of VP1 (28.09.) It is also noticeable that weather station D, the only mobile station that is not standing on a patch of grass, shows the best accordance with measurements during VP1 and VP2 among the mobile stations. This supports the assumption that the way the Penman-Monteith equation was applied in this research is overestimating the cooling flux from evapotranspiration from the grass surfaces and that adjustment is necessary.

Aside from the CFD model-specific causes for deviations between simulation results and measurements, several factors are generally introducing errors to the simulations. These are for instance geometrical inaccuracies [131] and discretization errors [93,132], the choice of materials and their properties, and the omission of water vapour transfer. Furthermore, inaccuracies related to the choice of inlet profiles for U, k, and ε, or the major detriments that come along with using URANS and a 2-equation turbulence model in the first place are generally considerable sources of errors.

As mentioned before, the underlying geometry of the CFD model is based on a large urban 3D geometrical city model from Trondheim municipality and LiDAR data, containing the terrain and buildings of the area. However, the data did not contain relatively small elements like bus stops, street poles and signs, small garden sheds etc. Furthermore, the surrounding buildings' geometries were simplified by the authors into boxes, omitting complex roof structures, balconies, oriels, and protrusions etc. to limit the computational cost. Their influence on the flow regime was estimated to be negligible based on the work by Ricci et al. [131]. Only when located directly on campus, trees and larger vegetation was included in the geometry.

In this research, the urban surface was grouped into categories of dominant materials (see Fig. 5), in order to limit the time needed for

creating the CFD model and still keep it relatively easy to use. The real urban surface on the other hand is extremely complex and usually composed of a large variety of different materials, colours, and a mix of different plants, each having an individual and heterogenic shape, aerodynamic properties and stomatal characteristics. Additionally, water vapour transfer was only indirectly considered in this work. While water runoff or retention properties of the urban surface and multiphase models were not incorporated in this simulation model, solely the thermal effect of evapotranspiration from the trees and grass were included according to Eq. (10) and Eq. (11).

Richards' and Hoxey's [101] profile for U, k and ε were used in this work, following the practice of many other CFD studies in the urban environment [65,71,78,80,81,133]. These inlet profiles were originally derived for the neutrally stratified atmospheric boundary layer for a uniform fetch of at least 5 km and their applicability in complex terrains like the study area in this research can be questioned. However, as no

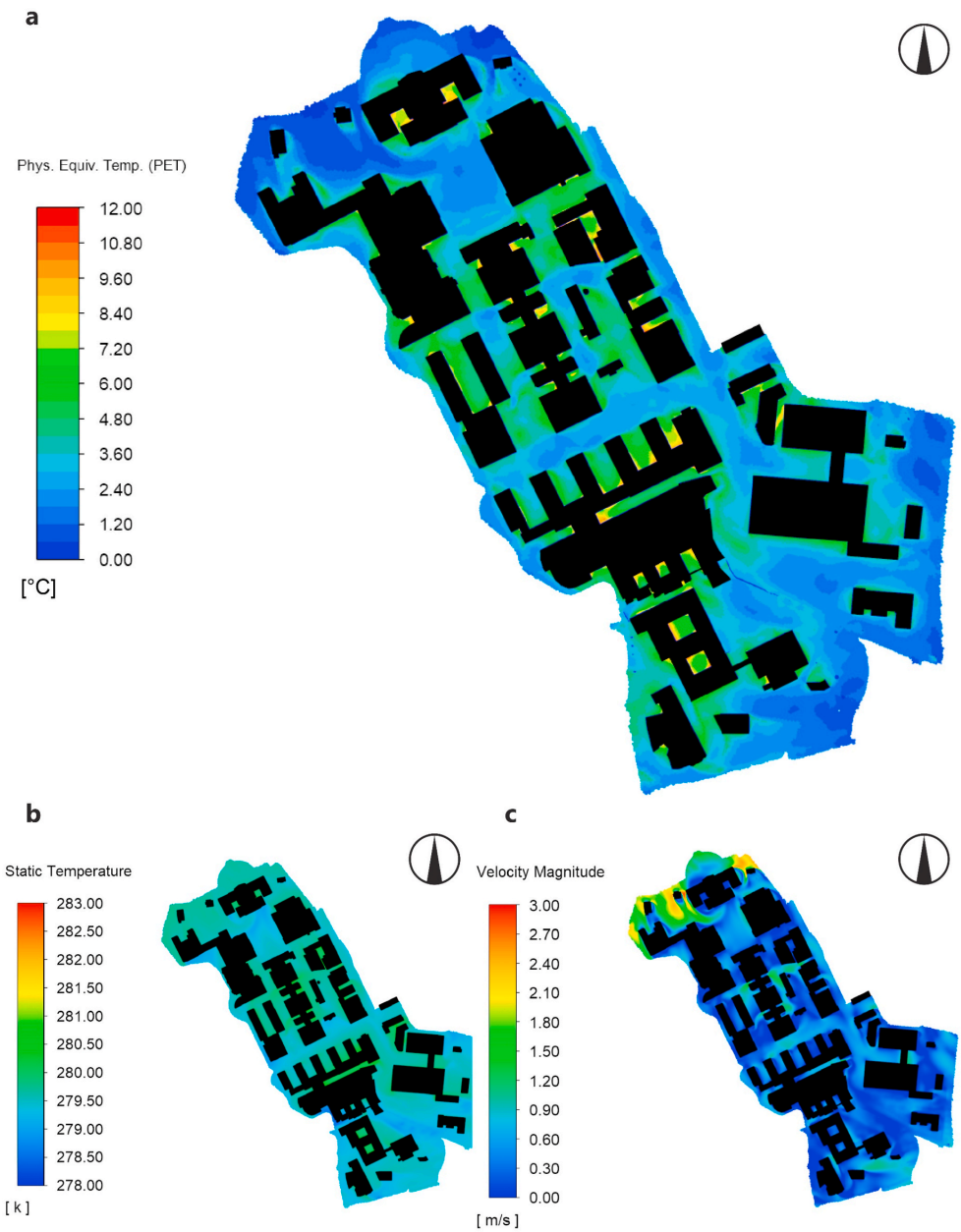

Fig. 13. Simulation results for: a) Physiological Equivalent Temperature (PET), b) air temperature and c) wind speed at 1.75 m height above ground in the study area at 19.10. at 15:00.

measurements near the four lateral domain boundaries were available, the commonly used profiles from Richards and Hoxey [101] represented the best assumption for the inlet profiles in this study. Yet in summary, the presented validation results and overall good fit of measured and simulated values clearly indicate that the benefits from using this CFD model overweigh the uncertainties connected to the input.

4.2. Applicability of the CFD model

Despite the limitations and uncertainties related to the input that can hardly be eliminated completely, the presented CFD model is well suited to be used for predicting the urban microclimatic conditions in the study area. One of the possible applications can be the evaluation of outdoor thermal comfort. Fig. 13 shows the PET, air temperature and wind speed at 1.75 m height on October 19 at 15:00 in the study area. It is noticeable that areas with a low PET coincide with areas of high wind speed, especially in the north/north-west of the campus. In the central part of the study area, however, the PET is higher on average. The highest values are computed close to the buildings and in their inside corners. There, particularly low air velocity combined with heat transfer from the buildings result in better outdoor thermal comfort conditions. Moreover, a clear correlation between the surface material and the PET can be seen. Particularly the grass patches on which the mobile weather stations B and E are located, exhibit a quite low PET.

Fig. 14 shows the solar irradiation on 19.10. at 15:00 in the central, explicitly modelled area of the domain, as viewed from the south. The shadow cast from the hill on which the campus is located is clearly visible on the north-eastern side of the campus. The slope of the hill facing south-west, on the other hand, receives almost twice as much solar radiation. Furthermore, the shadows from the geometrically explicitly modelled trees are clearly visible as blue dots on this slope. The highest solar heat flux is received on building façades facing south-west at the illustrated point in time.

5. Conclusion

In this study, the validation process of a CFD model, applying the 3D URANS approach with the realisable k-ε turbulence model of a highly complex urban area around the NTNU campus in Trondheim, Norway, was presented. The CFD model features a polyhedral grid of the urban environment, including geometrically explicitly modelled buildings and trees within the area of interest, solar and longwave radiation exchange, heat transfer from the buildings, heat storage, and the thermal effects of evapotranspiration from the trees and grass.

To validate the CFD model, a network of six weather stations, of which five were mobile, provided hourly-averaged measurements for wind speed, wind direction and air temperature. Two 48-h validation periods (VP1 and VP2) during the measurement campaign were selected that contained one sunny day, with relatively strong fluctuations and a high average of wind speed, a pronounced diurnal temperature variation and a large variation of wind direction. These criteria were established to test the CFD model's performance under demanding and a large variety of conditions.

Hourly-averaged measurements from the reference weather station were used as a reference for the empirical inlet profiles fed into the CFD model and always two of the lateral boundaries were set as inlets and outlets according to the wind direction. Overall, the CFD model was capable of reproducing the measured conditions at the location of the reference weather station with acceptable accuracy.

As the measured wind direction data was strongly affected by measurement uncertainty due to the sensor threshold of the five mobile weather stations, only temperature and wind speed data from the mobile stations was used in the validation assessment. Yet, all three climate variables served as validation variables at the reference weather station. Overall, the air temperature at the reference weather station was best represented with an R^2 of 0.98 and 0.93, and a CV_{RMSD} of 2.5% and 6.5% for VP1 and VP2 respectively. D_{max} amounted to 0.4 °C in VP1 and 1.2 °C in VP2. Also, at the mobile weather stations, air temperature was well represented during both VPs with an R^2, CV_{RMSD}, and D_{max} of 0.49–0.93, 4.5–19.5% and 1.6–3.4 °C, respectively.

Simulated wind speed and wind direction also showed a satisfactory correlation with the measurements at the reference weather station. In VP1, an R^2 of 0.76 and 0.34 as well as a CV_{RMSD} of 17.3% and 21.9% were obtained for wind speed and direction, respectively. D_{max} was 1.4 m s^{-1} for the wind speed and 143° for the wind direction. In VP2, the quality indicators for wind speed and wind direction were 0.44 and 0.91, 38.8% and 14.5%, and 2.1 m s^{-1} and 98° for R^2, CV_{RMSD}, and D_{max}, respectively. At the mobile weather stations, only the simulated wind speeds were compared to the measurements. Even though the quality metrics did not indicate an acceptable fit, the simulation results were almost entirely within the wind sensors' measurement uncertainty. From that, it can be concluded that the low-level atmospheric boundary layer wind speeds are represented by the CFD model with sufficient accuracy. Hence, the presented CFD model can be used for its intended purpose of evaluating the urban MC in the study area in future studies.

It was observed that the PME slightly overestimated the cooling flux from evapotranspiration at grass-covered surfaces, as the comparison between simulated and measured air temperatures indicated and underestimation of the temperature at the mobile weather stations (3.0 m above ground) compared to the reference weather station (28 m above

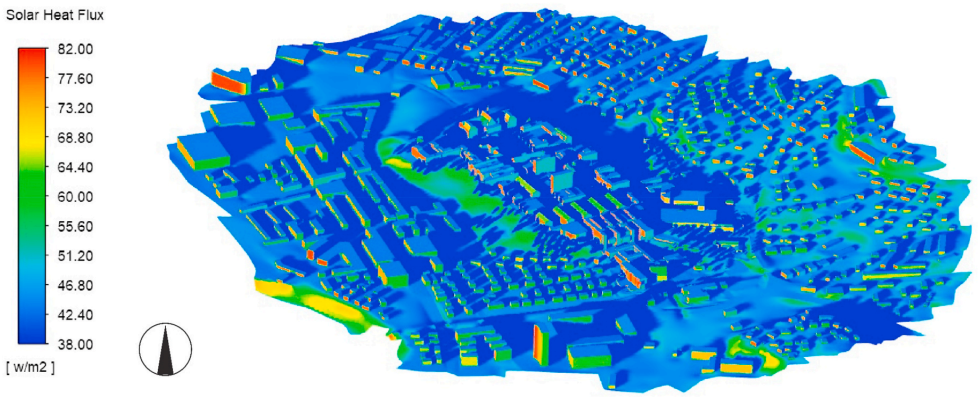

Fig. 14. Solar heat flux in the central, explicitly modelled part of the domain for 19.10. at 15:00 with view from south.

ground). Furthermore, the mobile weather stations standing on patches of grass gave the largest underestimation.

It can be concluded that the presented CFD model has the potential to predict urban microclimatic conditions in the study area with acceptable accuracy. It can be utilized in future studies focusing for instance on the influence of the urban fabric and vegetation on the energy use in buildings, outdoor thermal comfort, pedestrian wind comfort, pollutant dispersion, pressure coefficients on building façades for the natural ventilation potential, or urban wind energy potential. At the same time, more studies focusing on the wind regime in and around Trondheim need to be carried out in order to derive location-specific profiles for CFD inlet conditions. Future studies should also evaluate the impact of different turbulence models on the CFD model's ability to predict the airflow at the NTNU campus.

Declaration of competing interest

The authors declare that they have no known competing financial interests or personal relationships that could have appeared to influence the work reported in this paper.

Acknowledgements

This paper has been written within the Research Centre on Zero Emission Neighbourhoods in Smart Cities (FME ZEN). The authors gratefully acknowledge the support from the ZEN partners and the Research Council of Norway. The simulations were performed on resources provided by UNINETT Sigma2 - the National Infrastructure for High Performance Computing and Data Storage in Norway.

References

[1] O. Edenhofer (Ed.), Climate Change 2014: Mitigation of Climate Change Working Group III Contribution to the Fifth Assessment Report of the Intergovernmental Panel on Climate Change, Cambridge University Press, New York (USA), 2014.
[2] United Nations, Department of Economic, Social Affairs, Population Division, World Urbanization Prospects: the 2018 Revision, Online Edition, New York, USA, 2018.
[3] G. Mills, Urban climatology: history, status and prospects, Urban Clim. 10 (2014) 479–489, https://doi.org/10.1016/j.uclim.2014.06.004.
[4] Y. Toparlar, B. Blocken, B. Maiheu, G. van Heijst, A review on the CFD analysis of urban microclimate, Renew. Sustain. Energy Rev. 80 (2017) 1613–1640, https://doi.org/10.1016/j.rser.2017.05.248.
[5] P.A. Mirzaei, F. Haghighat, Approaches to study urban heat island – abilities and limitations, Build. Environ. 45 (10) (2010) 2192–2201, https://doi.org/10.1016/j.buildenv.2010.04.001.
[6] I. Orlanski, A rational subdivision of scales for atmospheric processes, Bull. Am. Meteorol. Soc. 56 (5) (1975) 527–530.
[7] T.R. Oke, Urban heat islands, in: I. Douglas, D. Goode, M. Houck, D. Maddox (Eds.), The Routledge Handbook of Urban Ecology, first ed., Routledge, London, 2011, pp. 120–131.
[8] T.R. Oke, The energetic basis of the urban heat island, Q. J. Roy. Meteorol. Soc. 108 (455) (1982) 1–24, https://doi.org/10.1002/qj.49710845502.
[9] G.J. Steeneveld, S. Koopmans, B.G. Heusinkveld, L.W.A. van Hove, A.A. M. Holtslag, Quantifying urban heat island effects and human comfort for cities of variable size and urban morphology in The Netherlands, J. Geophys. Res. 116 (D20) (2011) 94, https://doi.org/10.1029/2011JD015988.
[10] R. Watkins, J. Palmer, M. Kolokotroni, Increased temperature and intensification of the urban heat island: implications for human comfort and urban design, Built. Environ. 33 (1) (2007) 85–96, https://doi.org/10.2148/benv.33.1.85.
[11] A. Urban, H. Davídkovová, J. Kyselý, Heat- and cold-stress effects on cardiovascular mortality and morbidity among urban and rural populations in the Czech Republic, Int. J. Biometeorol. 58 (6) (2014) 1057–1068, https://doi.org/10.1007/s00484-013-0693-4.
[12] D. D'Ippoliti, P. Michelozzi, C. Marino, F. de'Donato, B. Menne, K. Katsouyanni, et al., The impact of heat waves on mortality in 9 European cities: results from the EuroHEAT project, Environ. Health 9 (2010) 37, https://doi.org/10.1186/1476-069X-9-37.
[13] M. Davies, P. Steadman, T. Oreszczyn, Strategies for the modification of the urban climate and the consequent impact on building energy use, Energy Pol. 36 (12) (2008) 4548–4551, https://doi.org/10.1016/j.enpol.2008.09.013.
[14] M. Kolokotroni, I. Giannitsaris, R. Watkins, The effect of the London urban heat island on building summer cooling demand and night ventilation strategies, Sol. Energy 80 (4) (2006) 383–392, https://doi.org/10.1016/j.solener.2005.03.010.
[15] E. Vardoulakis, D. Karamanis, A. Fotiadi, G. Mihalakakou, The urban heat island effect in a small Mediterranean city of high summer temperatures and cooling energy demands, Sol. Energy 94 (2013) 128–144, https://doi.org/10.1016/j.solener.2013.04.016.
[16] S.A. Lowe, An energy and mortality impact assessment of the urban heat island in the US, Environ. Impact Assess. Rev. 56 (2016) 139–144, https://doi.org/10.1016/j.eiar.2015.10.004.
[17] V.V. Klimenko, A.S. Ginzburg, P.F. Demchenko, A.G. Tereshin, I.N. Belova, E. V. Kasilova, Impact of urbanization and climate warming on energy consumption in large cities, Dokl. Phys. 61 (10) (2016) 521–525, https://doi.org/10.1134/S1028335816100050.
[18] T.R. Oke, G. Mills, A. Christen, J.A. Voogt, Urban Climates, Cambridge University Press, Cambridge, 2017.
[19] D. Chapman, K. Nilsson, A. Larsson, A. Rizzo, Climatic barriers to soft-mobility in winter: luleå, Sweden as case study, Sustain. Cities Soc. 35 (2017) 574–580, https://doi.org/10.1016/j.scs.2017.09.003.
[20] E. Erell, D. Pearlmutter, T. Williamson, Urban Microclimate: Designing the Spaces between Buildings, Earthscan, London, 2011.
[21] B. Blocken, Computational Fluid Dynamics for urban physics: importance, scales, possibilities, limitations and ten tips and tricks towards accurate and reliable simulations, Build. Environ. 91 (2015) 219–245, https://doi.org/10.1016/j.buildenv.2015.02.015.
[22] B. Blocken, W.D. Janssen, T. van Hooff, CFD simulation for pedestrian wind comfort and wind safety in urban areas: general decision framework and case study for the Eindhoven University campus, Environ. Model. Software 30 (2012) 15–34, https://doi.org/10.1016/j.envsoft.2011.11.009.
[23] B. Blocken, J. Persoon, Pedestrian wind comfort around a large football stadium in an urban environment: CFD simulation, validation and application of the new Dutch wind nuisance standard, J. Wind Eng. Ind. Aerod. 97 (5–6) (2009) 255–270, https://doi.org/10.1016/j.jweia.2009.06.007.
[24] B. Blocken, S. Roels, J. Carmeliet, Modification of pedestrian wind comfort in the Silvertop Tower passages by an automatic control system, J. Wind Eng. Ind. Aerod. 92 (10) (2004) 849–873, https://doi.org/10.1016/j.jweia.2004.04.004.
[25] W.D. Janssen, B. Blocken, T. van Hooff, Pedestrian wind comfort around buildings: comparison of wind comfort criteria based on whole-flow field data for a complex case study, Build. Environ. 59 (2013) 547–562, https://doi.org/10.1016/j.buildenv.2012.10.012.
[26] M.S. Fadl, J. Karadelis, CFD simulation for wind comfort and safety in urban area: a case study of coventry university central campus, Int. J. Archit. Eng. Constr. 2 (2) (2013) 131–143, https://doi.org/10.7492/IJAEC.2013.013.
[27] C. Gromke, B. Blocken, Influence of avenue-trees on air quality at the urban neighborhood scale. Part I: quality assurance studies and turbulent Schmidt number analysis for RANS CFD simulations, Environ. Pollut. 196 (2015) 214–223, https://doi.org/10.1016/j.envpol.2014.10.016.
[28] C. Gromke, B. Blocken, Influence of avenue-trees on air quality at the urban neighborhood scale. Part II: traffic pollutant concentrations at pedestrian level, Environ. Pollut. 196 (2015) 176–184, https://doi.org/10.1016/j.envpol.2014.10.015.
[29] J.H. Amorim, V. Rodrigues, R. Tavares, J. Valente, C. Borrego, CFD modelling of the aerodynamic effect of trees on urban air pollution dispersion, Sci. Total Environ. 461–462 (2013) 541–551, https://doi.org/10.1016/j.scitotenv.2013.05.031.
[30] P. Gousseau, B. Blocken, T. Stathopoulos, G. van Heijst, CFD simulation of near-field pollutant dispersion on a high-resolution grid: a case study by LES and RANS for a building group in downtown Montreal, Atmos. Environ. 45 (2) (2011) 428–438, https://doi.org/10.1016/j.atmosenv.2010.09.065.
[31] B. Blocken, J. Carmeliet, The influence of the wind-blocking effect by a building on its wind-driven rain exposure, J. Wind Eng. Ind. Aerod. 94 (2) (2006) 101–127, https://doi.org/10.1016/j.jweia.2005.11.001.
[32] B. Blocken, J. Carmeliet, Validation of CFD simulations of wind-driven rain on a low-rise building facade, Build. Environ. 42 (7) (2007) 2530–2548, https://doi.org/10.1016/j.buildenv.2006.07.032.
[33] T. van Hooff, B. Blocken, M. van Harten, 3D CFD simulations of wind flow and wind-driven rain shelter in sports stadia: influence of stadium geometry, Build. Environ. 46 (1) (2011) 22–37, https://doi.org/10.1016/j.buildenv.2010.06.013.
[34] H. Chen, R. Ooka, H. Huang, T. Tsuchiya, Study on mitigation measures for outdoor thermal environment on present urban blocks in Tokyo using coupled simulation, Build. Environ. 44 (11) (2009) 2290–2299, https://doi.org/10.1016/j.buildenv.2009.03.012.
[35] C.-M. Hsieh, H. Chen, R. Ooka, J. Yoon, S. Kato, K. Miisho, Simulation analysis of site design and layout planning to mitigate thermal environment of riverside residential development, Build. Simul. 3 (1) (2010) 51–61, https://doi.org/10.1007/s12273-010-0306-7.
[36] W.T. Chow, A.J. Brazel, Assessing xeriscaping as a sustainable heat island mitigation approach for a desert city, Build. Environ. 47 (2012) 170–181, https://doi.org/10.1016/j.buildenv.2011.07.027.
[37] M.F. Shahidan, P.J. Jones, J. Gwilliam, E. Salleh, An evaluation of outdoor and building environment cooling achieved through combination modification of trees with ground materials, Build. Environ. 58 (2012) 245–257, https://doi.org/10.1016/j.buildenv.2012.07.012.
[38] E. Carnielo, M. Zinzi, Optical and thermal characterisation of cool asphalts to mitigate urban temperatures and building cooling demand, Build. Environ. 60 (2013) 56–65, https://doi.org/10.1016/j.buildenv.2012.11.004.
[39] M. Srivanit, K. Hokao, Evaluating the cooling effects of greening for improving the outdoor thermal environment at an institutional campus in the summer, Build. Environ. 66 (2013) 158–172, https://doi.org/10.1016/j.buildenv.2013.04.012.

[40] W. Su, Y. Zhang, Y. Yang, G. Ye, Examining the impact of greenspace patterns on land surface temperature by coupling LiDAR data with a CFD model, Sustainability 6 (10) (2014) 6799–6814, https://doi.org/10.3390/su6106799.

[41] M. Taleghani, D.J. Sailor, M. Tenpierik, A. van den Dobbelsteen, Thermal assessment of heat mitigation strategies: the case of Portland State University, Oregon, USA, Build. Environ. 73 (2014) 138–150, https://doi.org/10.1016/j.buildenv.2013.12.006.

[42] Y. Tominaga, Y. Sato, S. Sadohara, CFD simulations of the effect of evaporative cooling from water bodies in a micro-scale urban environment: validation and application studies, Sustain. Cities Soc. 19 (2015) 259–270, https://doi.org/10.1016/j.scs.2015.03.011.

[43] Y. Wang, H. Akbari, Analysis of urban heat island phenomenon and mitigation solutions evaluation for Montreal, Sustain. Cities Soc. 26 (2016) 438–446, https://doi.org/10.1016/j.scs.2016.04.015.

[44] U. Berardi, The outdoor microclimate benefits and energy saving resulting from green roofs retrofits, Energy Build. 121 (2016) 217–229, https://doi.org/10.1016/j.enbuild.2016.03.021.

[45] Y. Kim, S. An, J.-H. Eum, J.-H. Woo, Analysis of thermal environment over a small-scale landscape in a densely built-up asian megacity, Sustainability 8 (4) (2016) 358, https://doi.org/10.3390/su8040358.

[46] Y. Wang, U. Berardi, H. Akbari, Comparing the effects of urban heat island mitigation strategies for Toronto, Canada, Energy Build. 114 (2016) 2–19, https://doi.org/10.1016/j.enbuild.2015.06.046.

[47] G.-E. Kyriakodis, M. Santamouris, Using reflective pavements to mitigate urban heat island in warm climates - results from a large scale urban mitigation project, Urban Clim. 24 (1) (2018) 326–339, https://doi.org/10.1016/j.uclim.2017.02.002.

[48] N. Fintikakis, N. Gaitani, M. Santamouris, M. Assimakopoulos, D. N. Assimakopoulos, M. Fintikaki, et al., Bioclimatic design of open public spaces in the historic centre of Tirana, Albania, Sustain. Cities Soc. 1 (1) (2011) 54–62, https://doi.org/10.1016/j.scs.2010.12.001.

[49] N. Gaitani, A. Spanou, M. Saliari, A. Synnefa, K. Vassilakopoulou, K. Papadopoulou, et al., Improving the microclimate in urban areas: a case study in the centre of Athens, Build. Serv. Eng. Technol. 32 (1) (2011) 53–71, https://doi.org/10.1177/0143624410394518.

[50] M. Santamouris, N. Gaitani, A. Spanou, M. Saliari, K. Giannopoulou, K. Vasilakopoulou, et al., Using cool paving materials to improve microclimate of urban areas – design realization and results of the flisvos project, Build. Environ. 53 (14) (2012) 128–136, https://doi.org/10.1016/j.buildenv.2012.01.022.

[51] M. Santamouris, F. Xirafi, N. Gaitani, A. Spanou, M. Saliari, K. Vassilakopoulou, Improving the microclimate in a dense urban area using experimental and theoretical techniques - the case of marousi, athens, Int. J. Vent. 11 (1) (2012) 1–16, https://doi.org/10.1080/14733315.2012.11683966.

[52] A. Synnefa, T. Karlessi, N. Gaitani, M. Santamouris, D.N. Assimakopoulos, C. Papakatsikas, Experimental testing of cool colored thin layer asphalt and estimation of its potential to improve the urban microclimate, Build. Environ. 46 (1) (2011) 38–44, https://doi.org/10.1016/j.buildenv.2010.06.014.

[53] H. Chen, R. Ooka, K. Harayama, S. Kato, X. Li, Study on outdoor thermal environment of apartment block in Shenzhen, China with coupled simulation of convection, radiation and conduction, Energy Build. 36 (12) (2004) 1247–1258, https://doi.org/10.1016/j.enbuild.2003.07.003.

[54] J. Ma, X. Li, Y. Zhu, A simplified method to predict the outdoor thermal environment in residential district, Build. Simul. 5 (2) (2012) 157–167, https://doi.org/10.1007/s12273-012-0079-2.

[55] M.Z. Targhi, S. van Dessel, Potential contribution of urban developments to outdoor thermal comfort conditions: the influence of urban geometry and form in worcester, Massachusetts, USA, Process Eng. 118 (2015) 1153–1161, https://doi.org/10.1016/j.proeng.2015.08.457.

[56] I. Karakounos, A. Dimoudi, S. Zoras, The influence of bioclimatic urban redevelopment on outdoor thermal comfort, Energy Build. 158 (2018) 1266–1274, https://doi.org/10.1016/j.enbuild.2017.11.035.

[57] M. Taleghani, U. Berardi, The effect of pavement characteristics on pedestrians' thermal comfort in Toronto, Urban Clim. 24 (2018) 449–459, https://doi.org/10.1016/j.uclim.2017.05.007.

[58] A. Ghaffarianhoseini, U. Berardi, A. Ghaffarianhoseini, K. Al-Obaidi, Analyzing the thermal comfort conditions of outdoor spaces in a university campus in Kuala Lumpur, Malaysia, Sci. Total Environ. 666 (2019) 1327–1345, https://doi.org/10.1016/j.scitotenv.2019.01.284.

[59] H. Huang, R. Ooka, S. Kato, Urban thermal environment measurements and numerical simulation for an actual complex urban area covering a large district heating and cooling system in summer, Atmos. Environ. 39 (34) (2005) 6362–6375, https://doi.org/10.1016/j.atmosenv.2005.07.018.

[60] H. Lee, H. Mayer, L. Chen, Contribution of trees and grasslands to the mitigation of human heat stress in a residential district of Freiburg, Southwest Germany, Landsc. Urban Plann. 148 (2016) 37–50, https://doi.org/10.1016/j.landurbplan.2015.12.004.

[61] A. Qaid, H. Bin Lamit, D.R. Ossen, R.N. Raja Shahminan, Urban heat island and thermal comfort conditions at micro-climate scale in a tropical planned city, Energy Build. 133 (2016) 577–595, https://doi.org/10.1016/j.enbuild.2016.10.006.

[62] F. Salata, I. Golasi, AdL. Vollaro, RdL. Vollaro, How high albedo and traditional buildings' materials and vegetation affect the quality of urban microclimate. A case study, Energy Build. 99 (2015) 32–49, https://doi.org/10.1016/j.enbuild.2015.04.010.

[63] M. Bruse, H. Fleer, Simulating surface–plant–air interactions inside urban environments with a three dimensional numerical model, Environ. Model. Software 13 (3–4) (1998) 373–384, https://doi.org/10.1016/S1364-8152(98)00042-5.

[64] J. Brozovsky, S. Corio, N. Gaitani, A. Gustavsen, Evaluation of sustainable strategies and design solutions at high-latitude urban settlements to enhance outdoor thermal comfort, Energy Build. 244 (12) (2021) 111037, https://doi.org/10.1016/j.enbuild.2021.111037.

[65] Y. Toparlar, B. Blocken, P.E.J. Vos, G. van Heijst, W.D. Janssen, T. van Hooff, et al., CFD simulation and validation of urban microclimate: a case study for Bergpolder Zuid, Rotterdam. Build Environ. 83 (2015) 79–90, https://doi.org/10.1016/j.buildenv.2014.08.004.

[66] R. Priyadarsini, W.N. Hien, C.K. Wai David, Microclimatic modeling of the urban thermal environment of Singapore to mitigate urban heat island, Sol. Energy 82 (8) (2008) 727–745, https://doi.org/10.1016/j.solener.2008.02.008.

[67] S. Ebrahimabadi, K.L. Nilsson, C. Johansson, The problems of addressing microclimate factors in urban planning of the subarctic regions, Environ. Plann. B 42 (3) (2015) 415–430, https://doi.org/10.1068/b130117p.

[68] W.L. Oberkampf, T.G. Trucano, Verification and validation in computational fluid dynamics, Prog. Aero. Sci. 38 (2002) 209–272.

[69] M. Schatzmann, B. Leitl, Issues with validation of urban flow and dispersion CFD models, J. Wind Eng. Ind. Aerod. 99 (4) (2011) 169–186, https://doi.org/10.1016/j.jweia.2011.01.005.

[70] American Institute of Aeronautics and Astronautics, AIAA Guide for the Verification and Validation of Computational Fluid Dynamics Simulations, American Institute of Aeronautics and Astronautics, Reston, VA, 1998.

[71] N. Antoniou, H. Montazeri, M. Neophytou, B. Blocken, CFD simulation of urban microclimate: validation using high-resolution field measurements, Sci. Total Environ. 695 (2019) 133743, https://doi.org/10.1016/j.scitotenv.2019.133743.

[72] K. Takahashi, H. Yoshida, Y. Tanaka, N. Aotake, F. Wang, Measurement of thermal environment in Kyoto city and its prediction by CFD simulation, Energy Build. 36 (8) (2004) 771–779, https://doi.org/10.1016/j.enbuild.2004.01.033.

[73] W.T.L. Chow, R.L. Pope, C.A. Martin, A.J. Brazel, Observing and modeling the nocturnal park cool island of an arid city: horizontal and vertical impacts, Theor. Appl. Climatol. 103 (1–2) (2011) 197–211, https://doi.org/10.1007/s00704-010-0293-8.

[74] I. Kaoru, K. Akira, K. Akikazu, The 24-h unsteady analysis of air flow and temperature in a real city by high-speed radiation calculation method, Build. Environ. 46 (8) (2011) 1632–1638, https://doi.org/10.1016/j.buildenv.2011.01.029.

[75] X. Yang, L. Zhao, M. Bruse, Q. Meng, Evaluation of a microclimate model for predicting the thermal behavior of different ground surfaces, Build. Environ. 60 (2013) 93–104, https://doi.org/10.1016/j.buildenv.2012.11.008.

[76] K. Maragkogiannis, D. Kolokotsa, E. Maravelakis, A. Konstantaras, Combining terrestrial laser scanning and computational fluid dynamics for the study of the urban thermal environment, Sustain. Cities Soc. 13 (2014) 207–216, https://doi.org/10.1016/j.scs.2013.12.002.

[77] U. Berardi, Y. Wang, The effect of a denser city over the urban microclimate: the case of Toronto, Sustainability 8 (8) (2016) 822, https://doi.org/10.3390/su8080822.

[78] J. Allegrini, J. Carmeliet, Simulations of local heat islands in Zürich with coupled CFD and building energy models, Urban Clim. 24 (2018) 340–359, https://doi.org/10.1016/j.uclim.2017.02.003.

[79] K. Park, Analysis of micro-climate on the programs of urban infrastructure regeneration in J city, Republic of Korea, Urban For. Urban Green. 27 (2017) 43–49.

[80] Y. Toparlar, B. Blocken, B. Maiheu, G.J.F. van Heijst, The effect of an urban park on the microclimate in its vicinity: a case study for Antwerp, Belgium, Int. J. Climatol. 38 (2) (2018) e303–e322, https://doi.org/10.1002/joc.5371.

[81] Y. Toparlar, B. Blocken, B. Maiheu, G. van Heijst, Impact of urban microclimate on summertime building cooling demand: a parametric analysis for Antwerp, Belgium, Appl. Energy 228 (2018) 852–872, https://doi.org/10.1016/j.apenergy.2018.06.110.

[82] J. Brozovsky, S. Corio, N. Gaitani, A. Gustavsen, Microclimate analysis of a university campus in Norway, IOP Conf. Ser. Earth Environ. Sci. 352 (1) (2019), https://doi.org/10.1088/1755-1315/352/1/012015.

[83] Y. Yang, J. Li, Study on urban thermal environmental factors in a water network area based on CFD simulation, Environ. Technol. Innov. 20 (2020) 101086, https://doi.org/10.1016/j.eti.2020.101086.

[84] J. Wieringa, Updating the Davenport roughness classification, J. Wind Eng. Ind. Aerod. 41 (1–3) (1992) 357–368, https://doi.org/10.1016/0167-6105(92)90434-C.

[85] E. Lundstad, O.E. Tveito, Homogenization of Daily Mean Temperature in Norway, 2016.

[86] Meteorologisk Institutt, eKlima: free access to weather- and climate data from Norwegian Meteorological Institute from historical data to real time observations. Normals, Available from: http://sharki.oslo.dnmi.no/portal/page?_pageid=73,39035,73_39049&_dad=portal&_schema=PORTAL.

[87] J.B. Palter, The role of the Gulf Stream in European climate, Ann. Rev. Mar. Sci. 7 (2015) 113–137, https://doi.org/10.1146/annurev-marine-010814-015656.

[88] M. Xu, B. Hong, J. Mi, S. Yan, Outdoor thermal comfort in an urban park during winter in cold regions of China, Sustain. Cities Soc. 43 (2018) 208–220, https://doi.org/10.1016/j.scs.2018.08.034.

[89] W. Liu, Y. Zhang, Q. Deng, The effects of urban microclimate on outdoor thermal sensation and neutral temperature in hot-summer and cold-winter climate, Energy Build. 128 (2016) 190–197, https://doi.org/10.1016/j.enbuild.2016.06.086.

[90] M. Nikolopoulou, S. Lykoudis, Thermal comfort in outdoor urban spaces: analysis across different European countries, Build. Environ. 41 (11) (2006) 1455–1470, https://doi.org/10.1016/j.buildenv.2005.05.031.

[91] B. Yang, T. Olofsson, G. Nair, A. Kabanshi, Outdoor thermal comfort under subarctic climate of north Sweden – a pilot study in Umeå, Sustain. Cities Soc. 28 (2017) 387–397, https://doi.org/10.1016/j.scs.2016.10.011.

[92] J. Strømann-Andersen, P.A. Sattrup, The urban canyon and building energy use: urban density versus daylight and passive solar gains, Energy Build. 43 (8) (2011) 2011–2020, https://doi.org/10.1016/j.enbuild.2011.04.007.

[93] Franke J, Hirsch C, Jensen AG, Krüs HW, Schatzmann M, Westbury PS et al. Recommendations on the use of CFD in wind engineering. Proc. Int. Conf. Urban Wind Engineering and Building Aerodynamics. COST Action C14, Impact of Wind and Storm on City Life Built Environment, von Karman Institute, Sint-Genesius-Rode, Belgium May 5-7 2004.

[94] Y. Tominaga, A. Mochida, R. Yoshie, H. Kataoka, T. Nozu, M. Yoshikawa, et al., AIJ guidelines for practical applications of CFD to pedestrian wind environment around buildings, J. Wind Eng. Ind. Aerod. 96 (10–11) (2008) 1749–1761, https://doi.org/10.1016/j.jweia.2008.02.058.

[95] B. Blocken, T. Stathopoulos, J. Carmeliet, CFD simulation of the atmospheric boundary layer: wall function problems, Atmos. Environ. 41 (2) (2007) 238–252, https://doi.org/10.1016/j.atmosenv.2006.08.019.

[96] B.E. Launder, D.B. Spalding, The numerical computation of turbulent flows, Comput. Methods Appl. Mech. Eng. 3 (2) (1974) 269–289, https://doi.org/10.1016/0045-7825(74)90029-2.

[97] W. Petersen, FerryBox systems: state-of-the-art in Europe and future development, J. Mar. Syst. 140 (2014) 4–12, https://doi.org/10.1016/j.jmarsys.2014.07.003.

[98] M. Santamouris (Ed.), Environmental Design of Urban Buildings: an Integrated Approach, Earthscan, London, 2006.

[99] A. Goris, K.-J. Schneider, A. Albert (Eds.), Bautabellen für Ingenieure: Mit Berechnungshinweisen und Beispielen, nineteenth ed.Neuwied, Köln: Werner, Wolters Kluwer, 2010.

[100] H.G. Jones, Plants and Microclimate: A Quantitative Approach to Environmental Plant Physiology, third ed., Cambridge University Press, Cambridge, 2013.

[101] P.J. Richards, R.P. Hoxey, Appropriate boundary conditions for computational wind engineering models using the k-ε turbulence model, J. Wind Eng. Ind. Aerod. 46 & 47 (1993) 145–153.

[102] J. Wieringa, Roughness-dependent geographical interpolation of surface wind speed averages, Q. J. Roy. Meteorol. Soc. 112 (1986) 867–889.

[103] R.E. Munn, A. Reimer, Turbulence statistics at 30 and 200 feet at Pinawa, Manitoba, Atmos. Environ. 2 (4) (1968) 409–417, https://doi.org/10.1016/0004-6981(68)90010-3.

[105] W.C. Swinbank, Long-wave radiation from clear skies, Q. J. Roy. Meteorol. Soc. 89 (381) (1963) 339–348.

[106] T.-H. Shih, W.W. Liou, A. Shabbir, Z. Yang, J. Zhu, A new k-ε viscosity model for high Reynolds number turbulent flows, Comput. Fluids 24 (3) (1995) 227–238, https://doi.org/10.1016/0045-7930(94)00032-T.

[107] J. Allegrini, J. Carmeliet, Coupled CFD and building energy simulations for studying the impacts of building height topology and buoyancy on local urban microclimates, Urban Climate 21 (2) (2017) 278–305, https://doi.org/10.1016/j.uclim.2017.07.005.

[108] B. Blocken, P. Moonen, T. Stathopoulos, J. Carmeliet, Numerical study on the existence of the venturi effect in passages between perpendicular buildings, J. Eng. Mech. 134 (12) (2008) 1021–1028.

[109] G.K. Ntinas, X. Shen, Y. Wang, G. Zhang, Evaluation of CFD turbulence models for simulating external airflow around varied building roof with wind tunnel experiment, Build. Simul. 11 (1) (2018) 115–123, https://doi.org/10.1007/s12273-017-0369-9.

[110] S.R. Green, Modelling turbulent air flow in stand of widely-spaced trees, Phoenics J. 5 (1992) 294–312.

[111] J. Liu, J. Chen, T.A. Black, M.D. Novak, E-ε modelling of turbulent air flow downwind of a model forest edge, Bound-Layer Meteorol 77 (1) (1996) 21–44.

[112] C. Sanz, A note on k-ε modelling of vegetation canopy air-flows, Bound-Layer Meteorol 108 (2003) 191–197, https://doi.org/10.1023/A:1023066012766.

[113] M.E. Jensen, H.R. Haise, Estimating evapotranspiration from solar radiation, Proceedings of the American Society of Civil Engineers, Journal of the Irrigation and Drainage Division 89 (1963) 15–41.

[114] Y.J. Huang, H. Akbari, H. Taha, A. Rosenfeld, The potential of vegetation in reducing summer cooling loads in residential buildings, J. Clim. Adv. Meteorol. 26 (9) (1987) 1103–1116, https://doi.org/10.1175/1520-0450(1987)026<1103:TPOVIR>2.0.CO;2.

[115] R. Buccolieri, J.-L. Santiago, E. Rivas, B. Sanchez, Review on urban tree modelling in CFD simulations: aerodynamic, deposition and thermal effects, Urban For. Urban Green. 31 (2018) 212–220, https://doi.org/10.1016/j.ufug.2018.03.003.

[116] J. Klingberg, J. Konarska, F. Lindberg, L. Johansson, S. Thorsson, Mapping leaf area of urban greenery using aerial LiDAR and ground-based measurements in Gothenburg, Sweden, Urban For. Urban Green. 26 (2017) 31–40, https://doi.org/10.1016/j.ufug.2017.05.011.

[117] J.L. Monteith, Evaporation and environment, Symp. Soc. Exp. Biol. 19 (1965) 205–234.

[118] H.L. Penman, The physical bases of irrigation control, Report of the 13th International Horticultural Congress 1–13 (1953).

[119] B. Henderson-Sellers, A new formula for latent heat of vaporization of water as a function of temperature, Q. J. Roy. Meteorol. Soc. 110 (1984) 1186–1190.

[120] Food and Agriculture Organisation of the United Nations, Crop evapotranspiration: guidelines for computing crop water requirements. FAO Irrigation and drainage paper 56 [December 10, 2020]; Available from: http://www.fao.org/3/X0490E/x0490e00.htm#Contents.

[121] H. Mayer, P. Höppe, Thermal comfort of man in different urban environments, Theor. Appl. Climatol. 38 (1987) 43–49.

[122] P. Höppe, The physiological equivalent temperature - a universal index for the biometeorological assessment of the thermal environment, Int. J. Biometeorol. 43 (2) (1999) 71–75, https://doi.org/10.1007/s004840050118.

[123] J. Fischereit, K.H. Schlünzen, Evaluation of thermal indices for their applicability in obstacle-resolving meteorology models, Int. J. Biometeorol. 62 (10) (2018) 1887–1900, https://doi.org/10.1007/s00484-018-1591-6.

[124] Verein Deutscher Ingenieure, VDI 3787 Blatt 2 - Environmental Meteorology: Methods for the Human Beiometeorological Evaluation of Climate and Air Quality for Urban and Regional Planning at Regional Level - Part I: Climate, 2008.

[125] E. Walther, Q. Goestchel, The P.E.T. comfort index: questioning the model, Build. Environ. 137 (2) (2018) 1–10, https://doi.org/10.1016/j.buildenv.2018.03.054.

[126] A. Skartveit, J.A. Olseth, A model for the diffuse fraction of hourly global radiation, Sol. Energy 38 (4) (1987) 271–274.

[127] ANSYS Inc, ANSYS Fluent Theory Guide: Release 2020 R1 January 2020, 2020. Canonsburg, PA.

[128] ANSYS Inc, Fluent User's Guide: Release 2020 R1 January 2020, 2020. Canonsburg, PA.

[129] J.P. van Doormaal, G.D. Raithby, Enhancements of the SIMPLE method for predicting incompressible fluid flows, Numer. Heat Tran. 7 (2) (1984) 147–163, https://doi.org/10.1080/01495728408961817.

[130] K.B. Rajasekarababu, G. Vinayagamurthy, S. Selvi Rajan, Experimental and computational investigation of outdoor wind flow around a setback building, Build. Simul. 12 (5) (2019) 891–904, https://doi.org/10.1007/s12273-019-0514-8.

[131] A. Ricci, I. Kalkman, B. Blocken, M. Burlando, A. Freda, M.P. Repetto, Local-scale forcing effects on wind flows in an urban environment: impact of geometrical simplifications, J. Wind Eng. Ind. Aerod. 170 (2017) 238–255, https://doi.org/10.1016/j.jweia.2017.08.001.

[132] J. Franke, A. Hellsten, H. Schlünzen, B. Carissimo (Eds.), Best Practice Guideline for the CFD Simulation of Flows in Th Urban Environment: COST Action 732 Quality Assurance and Improvement of Microscale Meteorological Models, Univ. of Hamburg Meteorological Inst, Hamburg, 2007.

[133] J. Allegrini, V. Dorer, J. Carmeliet, Influence of morphologies on the microclimate in urban neighbourhoods, J. Wind Eng. Ind. Aerod. 144 (2015) 108–117, https://doi.org/10.1016/j.jweia.2015.03.024.

Paper V

Assessing the Impact of Urban Microclimate on Building Energy Demand by Coupling CFD and Building Performance Simulation

J. Brozovsky, J. Radivojevic, A. Simonsen

Manuscript submitted for publication (Dec. 2021)

Assessing the Impact of Urban Microclimate on Building Energy Demand by Coupling CFD and Building Performance Simulation

J Brozovsky[a,*], J Radivojevic[b], A Simonsen[c]

[a] Department of Architecture and Technology, Faculty for Architecture and Design, NTNU – Norwegian University of Science and Technology, Høgskoleringen 1, 7491 Trondheim, Norway

[b] Spesialfag Bygg, Rambøll Norge AS, Postboks 9420 Torgarden, 7493 Trondheim, Norway

[c] Process Technology, SINTEF Industry, S.P. Andersens veg 15B, 7031 Trondheim, Norway

ABSTRACT

To quantify the effect of different compositions of the urban surface on the urban microclimate, building energy demand, and summerly overheating of a selected 13-floor office high-rise building in Trondheim, Norway, a validated Computational Fluid Dynamics model is coupled with Building Performance Simulation. In total, four scenarios were investigated in three one-week periods in summer (15.06.20 – 21.06.20), autumn (16.09.20 – 22.09.20), and winter (21.12.20 – 27.12.20). The scenarios were: (1) *base case* or current situation; (2) *no vegetation* in the entire domain with no trees and grass surfaces being substituted with concrete; (3) *all vegetation* with all concrete, asphalt, and pavements replaced by grass; and (4) the base case situation with highly improved insulation levels of surrounding buildings. The results demonstrate clear benefits from urban greening during a one-week heat wave as the *no vegetation* scenario increased the cooling energy demand by 28.5 %. The positive effect of evapotranspiration from grass surfaces was noticeable especially on the lowest two floors, where cooling energy demands were halved. During the simulated weeks in autumn and winter, the *no vegetation* scenario resulted in respectively 3.5 % and 0.9 % lower heating energy demands. At the investigated building, improving the insulation properties of all modeled surrounding buildings led to 0.1 °C higher average air temperatures during summer, and 0.1 °C lower during winter, while they remained unchanged in autumn. However, the energy demands were 0.8 %, 0.9 %, and 0.8 % higher compared to the *base case* for summer, autumn, and winter, respectively.

Keywords: Urban microclimate; Computational Fluid Dynamics; Building Performance Simulation; Cold climate; Urban physics; Materials

Abbreviations

AT	Air temperature
AUT	Autumn simulation period (16.09.20 00:00:00 – 22.09.20 23:59:59)
BC	Boundary conditions
BPS	Building Performance Simulation
CFD	Computational Fluid Dynamics
CHTC	Convective heat transfer coefficient
COP	Coefficient of Performance
Cp	Pressure coefficient

* = corresponding author details, johannes.brozovsky@ntnu.no

EW	External wall
F-HVAC	Heat flux from Heating, Ventilation, and Air-Conditioning equipment
F-SL	Latent soil heat flux
GFA	Gross floor area
GR	Ground reflectance
HPN	High-performance neighborhood
HVAC	Heating, Ventilation, and Air-Conditioning
IAT	Indoor air temperature
LCZ	Local climate zone
LiDAR	Light detection and ranging
MRM	Mass-rate of moisture
MS	Microclimate scenario
MS-AllVeg	Microclimate scenario with all ground surfaces covered with grass
MS-Base	Microclimate scenario of the current situation
MS-HPN	Microclimate scenario with all explicitly modeled surrounding building envelopes well-insulated
MS-NoVeg	Microclimate scenario with all ground surfaces concrete and asphalt
NTNU	Norwegian University of Science and Technology
R-AV	Absorbed radiation in vegetation
R_{diff}	Diffuse solar radiation
R_{dir}	Direct solar radiation
RH	Relative humidity
R-LW	Longwave radiation
R-SW	Shortwave radiation
RWS	Reference weather station
SB1	Sentralbygg 1 (investigated building)
SH	Specific humidity
SP	Simulation period
ST	Surface temperature
SUM	Summer simulation period (15.06.20 00:00:00 – 21.06.20 23:59:59)
TT	Tree transmittance
UHI	Urban heat island
VF	View factor
WD	Wind direction
WIN	Winter simulation period (21.12.20 00:00:00 – 27.12.20 23:59:59)
WS	Wind speed

1 Introduction

Climate change, ongoing urbanization, population growth, and their associated environmental consequences are among the major challenges that humanity faces in the 21st century [1,2]. In these challenges, the building and construction sector, as well as cities, hold a central role. Between 67 and 76 % of global energy use and 71 to 76 % of carbon dioxide emissions from global final energy use come from urban areas [1]. In 2018, the building and construction sector was responsible for 36 % of final energy use and 39 % of energy process-related carbon dioxide emissions [3]. Accordingly, *Sustainable Cities and Communities* is one of the 17 Sustainable Development Goals proclaimed in the 2030 Agenda for Sustainable Development by the United Nations [4]. The goal is to create and transform cities into climate-resilient, safe, healthy, and livable environments for their citizens. Especially with globally rising temperatures and more frequent occurrences of heat waves [5–7], the adverse effects of urban climate and especially the urban heat island (UHI) effect on human health and energy use in cities have received increased attention from researchers, authorities and the general public.

The UHI is defined as the characteristic warmth of a city, often approximated by the temperature difference between a city and its rural surroundings [8]. Adverse effects of the UHI can be for instance thermal discomfort for urban dwellers [9,10], excess mortality [11–13], and increased building cooling demands [13–15]. They were reported not only in warm or temperate but also in cold and polar climate zones [16–18]. Even in Scandinavia, where summers tend to be relatively mild, two studies illustrated heat wave-related health risks and mortality for the case of Oslo [19] and several municipalities in Sweden [20]. Compared to a share of about 90 % in the USA or nearly 60 % in China, less than 10 % of households in the European Union have air conditioning installed to counteract excessive heat [21]. The share in Scandinavia can be expected to be far lower. On the other hand, the UHI was found to contribute to a net decrease of building energy use through larger heating energy savings than cooling energy increases in the north of the USA [22,23], Russia [24], or in Northeast China [25,26]. Additionally, inner-city climatic conditions were found to shield people from extreme cold stress during winter in the Russian Far East.

The major causes of the UHI phenomenon are for instance the lack of evapotranspiration from vegetation and unsealed surfaces, a high share of heavy materials with a low surface albedo that store significant amounts of energy from incoming solar irradiation, and anthropogenic heat release from buildings, fuel combustion in vehicles, or industrial processes [27,28]. The individual contributing shares of the afore-mentioned causes to the UHI, however, are strongly dependent on the specific characteristics of a city. Given the causes and impacts of the urban climate, the structure of the surface and climatic conditions in urban areas need to be given a more dominant role in urban planning, architecture, and building engineering to protect vulnerable population groups and reduce the energy use in buildings.

Steadily rising computational power and decreasing computational costs have led to the development and increased application of numerical tools to study the urban climate since the early 2000s [29–31]. As opposed to field measurements, numerical tools can be used to easily investigate different scenarios and provide the climate variables for every location in the investigated area instead of only a few measurement points. The typical scale to study outdoor thermal comfort or the impact of the urban

climate on building energy use is the meteorological microscale (horizontal extension between 2 m and 2 km) [32]. The local climatic conditions in this scale are usually referred to as *microclimate*.

In the literature, Computational Fluid Dynamics (CFD) has been used in a wide range of numerical studies to investigate the urban microclimate. The applications of CFD include for instance pedestrian wind comfort [33–37], pollutant dispersal [38–41], wind-driven rain [42–44], or outdoor thermal comfort [45–55]. A powerful way to investigate the impact of urban microclimate on building energy use is to couple CFD with building performance simulation (BPS). This can be done either to supply the CFD side with more detailed boundary conditions (BC) from BPS-output (type A), to use CFD-generated data as BC in BPS software (type B), or both (type C). While types A and B are one-way coupling techniques which means that data is exchanged only in one direction, type C is a two-way coupling approach. The advantage of two-way coupling is generally a higher accuracy, as it involves several iterations of data exchange between the models. Consequently, they influence each other's results until acceptable accuracy is reached before moving to the next time step in a dynamic simulation. On the other hand, one-way coupling is computationally less expensive than two-way coupling [56]. Moreover, it can be distinguished between the coupling of BPS with building-interior [57–63] and exterior CFD. In Table 1, an overview of published scientific articles coupling exterior CFD with BPS is presented.

From the 31 listed articles (excluding this study) in Table 1, most studies (13 articles, 41.9 %) are of one-way coupling type B, i.e., supplying BPS software with BCs from CFD simulations. Ten studies (32.3 %) used a two-way coupling approach (type C) and in eight cases (25.8 %), BPS results were used for more accurate BCs in CFD (type A). Most commonly, surface temperature (ST) was exchanged between the tools (18 articles, 58.1 %), followed by air temperature (AT) in 14 studies (45.2 %) and wind speed (WS) in 12 articles (38.7 %). A clear majority of 19 articles (61.3 %) considered generic urban environments as opposed to ten (32.3 %) for real cities. In two articles, both real and generic environments were studied [64,65]. In both cases, the real environment served as a validation case study for the following investigation of a generic urban layout. About half of the studies (51.6 %) used weather data from European cities for their analysis with Zürich in Switzerland representing the most-used study location (six times). It is also evident that the open-source tools *OpenFOAM* (http://www.openfoam.org/) and *EnergyPlus* [66] were the most popular among the selected articles in Table 1, as they were used 10 (32.3 %) and 17 (54.8 %) times, respectively.

Due to the high computational cost, coupling exterior CFD and BPS is a relatively new approach which is documented by several articles that propose new methodologies, frameworks, or tools. Bouyer et al. [67] for instance, presented a building thermal sub-model for *SOLENE* which they coupled with *ANSYS Fluent* to investigate the influence of microclimate on building energy demand in Lyon, France. *SOLENE* was in the following extended with a CFD code to *SOLENE-Microclimate* and used in several other studies [68–71]. Zhang et al. [72] and Zhang and Mirzaei [73,74] propose different, complex type C frameworks for coupling *ANSYS Fluent* and in one case *ANSYS CFX* with *EnergyPlus*. Most studies addressed the building energy performance [68–87]. Others addressed the impact of the built environment on microclimatic conditions [88–92], the efficiency of cooling systems [64,65,93], or methods to include and distribute BC in CFD [94,95].

In this article, CFD simulations of the urban microclimate for the *Gløshaugen* campus of the *Norwegian University of Science and Technology* (NTNU) in Trondheim, Norway, are carried out. This is done for different seasons of the year (summer, autumn, and winter) and four different compositions of the urban surface. These include (1) *base case* or current situation; (2) *no vegetation* in the entire domain with grass surfaces being substituted with concrete; (3) *all vegetation* with all concrete, asphalt, and pavements replaced by grass surfaces; and (4) the base case situation but with improved insulation properties of the building envelopes. The resulting microclimatic conditions around a 13-floor office high-rise building on site are captured and used as climate input for BPS simulations in order to quantify their impact on the building's energy use and summerly overheating. The office building is representative of the major part of buildings at the study site and was selected due to its construction type and year. Section 2 of this article presents the study area, local climate conditions, and the CFD-BPS coupling methodology. In sections 3 and 4, the settings and boundary conditions which were used for the CFD and BPS tool, respectively, are presented. Following the results in section 5 and the discussion in section 6 respectively, section 7 concludes this article.

Table 1: Overview of published articles on the coupling between exterior CFD and BPS.

Authors	Year	Ref.	City (country)[1]	Type of environment	Research focus	Tools used		Exchanged variables[2]	Type[3]
						CFD	BPS		
Bouyer et al.	2011	[67]	Lyon (FR)	Real	Presenting a CFD-thermoradiative coupled simulation tool	*ANSYS Fluent*	*SOLENE*	AT, MRM, CHTC, ST, R-AV, F-SL	C
Yang et al.	2012	[75]	Guangzhou (CN) Frankfurt (DE)	Generic	Quantitative analysis of building energy performance in the urban context	*ENVI-Met*	*EnergyPlus*	AT, ST, WS, GR, TT, SH	B
Allegrini et al.	2013	[88]	Zürich (CH)	Generic	Effect of an urban neighborhood on local microclimatic conditions	*OpenFOAM*	*CitySim*	ST	A
Yi and Feng	2013	[76]	-	Generic	Propose a coupling methodology between BPS and CFD in order to investigate microclimate impact on building performance	*ANSYS Fluent*	*EnergyPlus*	ST, CHTC	C
Allegrini et al.	2015	[89]	Zürich (CH)	Generic	Investigation of urban heat fluxes for different urban morphologies	*OpenFOAM*	*CitySim*	ST	A
Allegrini et al.	2015	[90]	Zürich (CH)	Generic	Effect of different urban morphologies on the urban microclimate	*OpenFOAM*	*CitySim*	ST	A
Gracik et al.	2015	[64]	State College, PA (US)	Real and Generic	Quantification of the influence of the urban neighborhood on the degradation of building cooling system COP	*OpenFOAM*	*EnergyPlus*	ST, CHTC	C
Liu et al.	2015	[77]	Philadelphia, PA (US)	Generic	Local weather data impact on building energy demand	*PHOENICS*	*EnergyPlus*	AT, ST, WS	C
Malys et al.	2015	[68]	Nantes (FR)	Real	Effect of microclimate on winter energy consumption and summer indoor temperatures in insulated and non-insulated buildings	*SOLENE-microclimate (SATURNE)*	*SOLENE*	AT, ST, WS	C
Gros et al.	2016	[69]	La Rochelle (FR)	Real	Comparing two building densities and their impacts on radiation, wind, indoor temperatures, and energy demand	*SOLENE-microclimate (SATURNE)*	*EnviBatE*	ST, WS, R-SW, VF, IAT	B
Morille et al.	2016	[70]	Nantes (FR)	Generic	Impact of urban greenery on building energy consumption in a street canyon	*SOLENE-microclimate (SATURNE)*	*SOLENE*	CHTC	B
Skehorn et al.	2016	[78]	Manchester (GB)	Generic	Impact of UHI and vegetation on cooling energy use	*ENVI-Met*	*IES-VE*	AT, WS, RH	B
Allegrini and Carmeliet	2017	[91]	Zürich (CH)	Generic	Influence of surface temperatures from BPS, urban form, and buoyancy on air temperatures	*OpenFOAM*	*CitySim*	ST	A
Gobakis and Kolokotsa	2017	[79]	Chania (GR)	Real	Coupling CFD and BPS to improve accuracy for energy performance calculations	*ENVI-Met*	*ESP-r*	AT, WS, WD, R-SW, RH	B
Huang and Li	2017	[80]	Taipei (TW)	Generic	Impact of street canyon topology on a building's peak cooling energy demand	*ENVI-Met*	*EnergyPlus*	AT, WS, WD, RH	B
Merlier et al.	2017	[71]	Lyon (FR)	Generic	Microclimatic effects on the building energy behavior	*SOLENE-microclimate (SATURNE)*	*BuildSysPro*	AT, R-SW, R-LW, AP	B
Allegrini and Carmeliet	2018	[92]	Zürich (CH)	Real	Effect of new buildings on the local microclimate	*OpenFOAM*	*CitySim*	ST	A

Toparlar et al.	2018	[87]	Antwerp (BE)	Real	Impact of urban microclimate and cooling energy demand	*ANSYS Fluent*	*EnergyPlus*	AT, WS, WD	B
Zhang et al.	2018	[72]	Los Angeles, CA (US)	Generic	Coupling CFD and BES tools to enhance the modeling of CHTCs in urban neighborhoods	*ANSYS Fluent*	*EnergyPlus*	ST, CHTC	C
Javanroodi and Nik	2019	[81]	Stockholm (SE)	Generic	Impact of microclimate in typical and extreme climate conditions on the energy performance of an office building	*AutodeskCFD*	*EnergyPlus*	AT, WS, AP, RH	B
Liu et al.	2019	[82]	College Park, MD (US)	Real	Microclimate impact on energy consumption of an academic building	*OpenFOAM*	*EnergyPlus*	AT, WS	B
Natanian et al.	2019	[83]	Tel Aviv (IL)	Generic	Interrelation between form, energy, and urban microclimatic conditions	*ENVI-Met*	*Honeybee (EnergyPlus)*	AT, RH	B
Shirzadi et al.	2019	[84]	Rasht (IR)	Generic	Framework development for improving BPS with urban microclimate interaction	*ANSYS CFX*	*EnergyPlus*	Cp, CHTC, WS	B
Chen et al.	2020	[95]	Guangzhou (CN)	Generic	Comparison of urban airflow between a solar-induced thermal wall and uniform wall temperature BCs	-	*CitySim*	ST	A
Mosteiro-Romero et al.	2020	[85]	Zürich (CH)	Real	Quantitative analysis of building energy demand at district scale considering local microclimatic conditions	*ENVI-Met*	*City Energy Analyst*	AT, WS, RH	B
Shen and Wang	2020	[86]	Chicago, IL (USA)	Generic	Influence of neighborhood form on building energy use in winter design conditions	*ANSYS Fluent*	*EnergyPlus*	CHTC, ST	C
Hadavi and Pasdarshahri	2021	[93]	Tehran (IR)	Real	Thermal and aerodynamic effects of urban buildings on microclimate and cooling system performance	*OpenFOAM*	*EnergyPlus*	ST	A
Hadavi and Pasdarshahri	2021	[65]	Tehran (IR)	Real and Generic	Propose a coupling algorithm between CFD and BPS for the accurate simulation of near-building microclimate	*OpenFOAM*	*EnergyPlus*	ST	A
Wong et al.	2021	[94]	Singapore (SG)	Real	Method of distributing BCs from meso- to microscale	*OpenFOAM*	*EnergyPlus*	ST, CHTC, F-HVAC	C
Zhang and Mirzaei	2021	[73]	Los Angeles, CA (US)	Generic	Novel framework for the integration of high-resolution CFD into a coupled model of low-resolution CFD with BPS	*ANSYS CFX* *ANSYS Fluent*	*EnergyPlus*	ST, CHTC	C
Zhang and Mirzaei	2021	[74]	Los Angeles, CA (US)	Generic	Novel framework of virtual dynamic BES-CFD-artificial intelligence coupling	*ANSYS Fluent*	*EnergyPlus*	CHTC	C
This study	-	-	Trondheim (NO)	Real	Influence of different microclimate scenarios on energy use in buildings during different seasons	*ANSYS Fluent*	*IDA ICE*	AT, WS, WD, Cp	B

Abbreviations: Absorbed radiation in vegetation (R-AV), Air pressure (AP), Air temperature (AT), Boundary condition (BC), Building Performance Simulation (BPS), Coefficient of Performance (COP), Computational Fluid Dynamics (CFD), Convective Heat Transfer Coefficient (CHTC), Ground reflectance (GR), Heating Ventilation and Air Conditioning (HVAC), Heat flux from HVAC equipment (F-HVAC), Indoor air temperature (IAT), Latent soil heat flux (F-SL), Longwave radiation (R-LW), Mass rate of moisture (MRM), Pressure coefficient (Cp), Shortwave radiation (R-SW), Specific humidity (SH), Surface temperature (ST), Tree transmittance (TT), Wind direction (WD), Wind speed (WS), View factor (VF)

[1] Location of the (real) urban area or climate data

[2] Variables generated in one software environment and used as input in the other

[3] Type A: BPS provides BCs for CFD, Type B: CFD provides BCs for BPS, Type C: CFD and BPS provide BCs to each other (two-way coupling, mostly in an iterative approach)

2 Methodology

2.1 Study area and local climate

The area of interest in this study is the NTNU campus (*Gløshaugen*) in Trondheim, Norway. Located in Central Norway and with an urbanized area of about 70.6 km^2 and 208,000 inhabitants [96], the city lies at a latitude of 63.4° N. The investigated part of NTNU's campus is approximately 0.26 km^2 in size and is situated ca. 1.5 km south of the city center at an altitude between 38 and 49 m a.s.l. Trondheim is embedded in complex terrain to the east, west, and south, and borders a fjord to the north. Referring to Stewart and Oke's [97] classification of urban landscape types, called *Local Climate Zone* (LCZ), the city is mainly characterized by a mix of open, low-rise (LCZ 6), and midrise (LCZ 5) built-up areas, as well as park-like areas (LCZ 9/LCZ B). The built-up areas are frequently traversed by patches of forests (LCZ A) and the meandering *Nidelva* river. The city center can be categorized as *dense midrise* (LCZ 2). The campus itself might be categorized as a mixture of *dense midrise* (LCZ 2) and *open midrise* (LCZ 5). Another essential feature of the city is the large water body of the *Trondheim Fjord* to the north of the city center (LCZ G, see Figure 1). In total, almost 1.6 km^2 of the domain are covered by water which corresponds to 8.6 % of the domain's ground surface area.

Furthermore, Figure 1 shows a map of the NTNU campus with the different building categories and surface materials, and the building of interest in the center of the campus area (the high-rise of *Sentralbygg 1*, SB1). This building is considered to be a representative building of the study area due to its construction type and year. In this study, it will be used to evaluate the impact of different urban microclimates at the campus on building energy demand and summerly overheating.

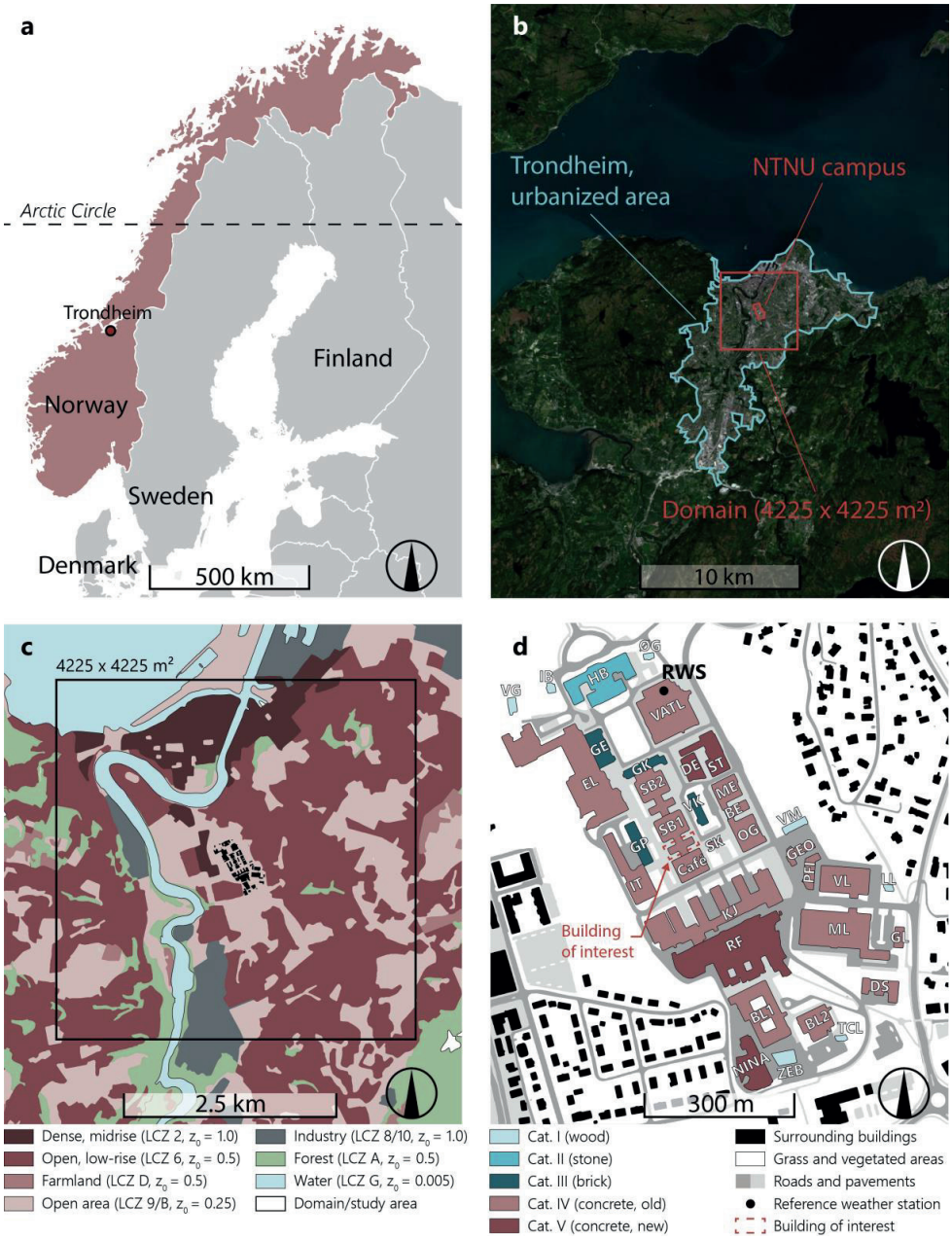

Figure 1: (a) Location of Trondheim within Norway and Fennoscandia. (b) Satellite image of Trondheim's built-up area (from the Norwegian Mapping Authority, www.kartverket.no). (c) Surrounding of the NTNU campus with Local Climate Zones (LCZ) from Stewart and Oke [97], and aerodynamic roughness length z_0 from Wieringa [98] (data from the Norwegian Mapping Authority). (d) Site plan of the NTNU campus with building categories, surface types, and the highlighted building of interest.

Trondheim's climate is categorized as *oceanic* (Dfb) by the Köppen-Geiger climate classification system [99], but closely borders continental, subpolar, and subarctic climates [100]. From November to March, moderate snowfall with periods of milder weather patterns and rain is common. Summers are relatively short and mild, winters long and cool. In the period between 1961 and 1990, the annual mean

temperature was 4.8 °C in Trondheim, but due to climate change, temperatures have been rising during the last decades. With an annual mean temperature of 5.8 °C, the most recent norm period from 1991 to 2020 was 1.0 °C higher (5.8 °C) than the previous between 1961 and 1990 [101].

Considering their latitudes, Norway's coastal cities experience a rather mild climate. This is caused by the distinct warming effect from the Gulf Stream [102]. However, the solar elevation angles are generally quite low which results in very limited daylight hours during winter. In summer, on the other hand, the contrary is the case (see Table 2). The low solar altitude during winter in combination with complex, hilly terrain and the urban landscape results in significant shading at the pedestrian level and the lower floors of buildings.

Table 2: Sun elevation angles and daylight hours for different dates in 2020 for Trondheim, Norway.

Date	Max. sun elevation angle	Time of sunrise	Time of sunset	Length of day
20.03. (vernal equinox)	26.7°	06:18	18:34	12.3 h
20.06. (summer solstice)	50.0°	03:02	23:37	20.6 h
22.09. (autumnal equinox)	26.6°	07:02	19:17	12.3 h
21.12. (winter solstice)	3.3°	10:01	14:31	4.5 h

The NTNU Gløshaugen campus features a rather heterogeneous mix of buildings. The oldest dates back to ca. 1850, the newest was finished in 2021, but about half of the gross floor area at the campus was constructed in the 1950s and 1960s (ca. 150,000 m^2). The building heights range from around 6–45 m. While for the smaller buildings, the main construction and façade surface material is wood, the building surfaces of the campus are dominated by heavy materials like stone, brick, and particularly concrete with about 99 % of the built gross floor area (GFA).

2.2 CFD-BPS coupling

In this study, a CFD (*ANSYS Fluent 2020 R1*) and BPS tool (*IDA ICE 4.8 SP2*) are coupled to study the influence of different compositions of the urban surface on building energy demand during different times of the year. *ANSYS Fluent* is a widely used CFD simulation and physical modeling software with a wide range of applications. It has been applied in many previous studies of the urban microclimate [103,104] and the coupling with BPS (see Table 1). *IDA ICE*, on the other hand, is a dynamic multi-zone simulation software for studying the thermal indoor climate as well as the energy demand of a building [105,106]. It has been validated with respect to several standards [107–109] and can be used to model for instance double-skin façades [110,111], boreholes [112], or advanced control strategies of heat pumps [113,114], among other things. The coupling strategy, according to the terminology used in section 1 in this article, is a one-way coupling of type B. Consequently, the results from the CFD simulations are used as input for BPS (Figure 2). Additional climate variables that are required for BPS are taken from the reference weather station (RWS) at the campus. The following microclimate scenarios (MS) are investigated in CFD:

1. *Base case (MS-Base)*: actual situation.
2. *No vegetation (MS-NoVeg)*: no trees, all vegetated ground surfaces substituted with concrete.

3. *All vegetation (MS-AllVeg)*: all ground surfaces substituted with grass.
4. *"High-Performance Neighborhood" (MS-HPN)*: All explicitly modeled buildings surrounding the building of interest (SB1) with high-performance building envelope (0.3 m insulation and exterior charred wood cladding).

The four MSs are simulated for three 168-hour (1 week) simulation periods (SP) in different seasons of the year, namely summer, autumn, and winter. The terminology used in the remainder of this article and the dates of these SPs are SUM (June 15 00:00:00 – June 21 23:59:59), AUT (September 16 00:00:00 – September 22 23:59:59), and WIN (December 21 00:00:00 – December 27 23:59:59) for summer, autumn, and winter 2020, respectively (see also Figure 2). From BPS, the heating energy demands during AUT and WIN are obtained. For SUM, the cooling energy demand and the number of hours in which the operative temperature (T_{op}) in the zones exceeds 26 °C ($N_{T_{op}>26\,°C}$) are compared.

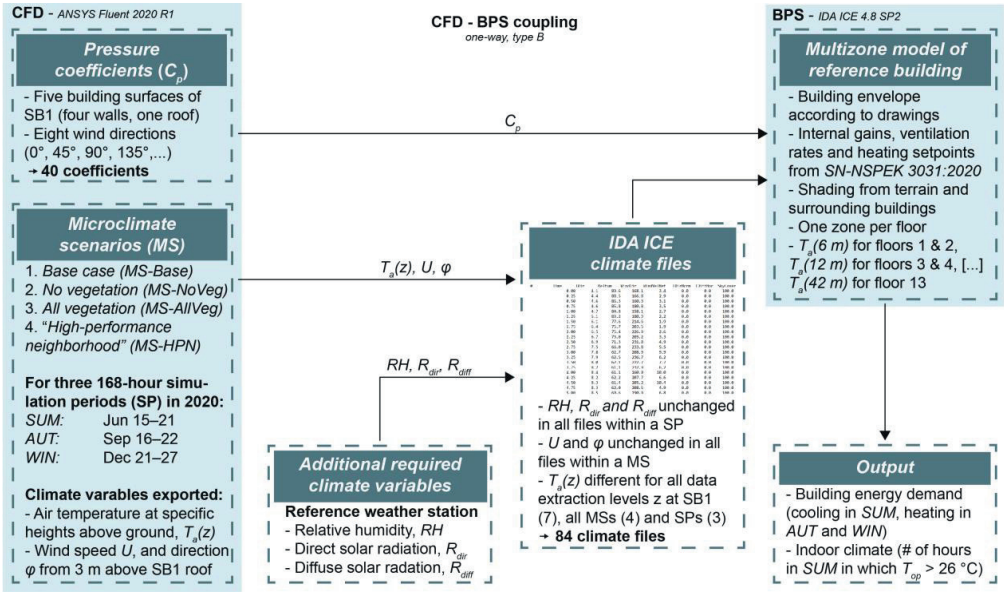

Figure 2: Coupling methodology between CFD and BPS in this study.

Although *MS-HPN* addresses the microclimatic situation with a district-wide high-performance building envelope, the building envelope of the building of interest (SB1) is not changed to ensure comparability between the scenarios. The microclimatic conditions in these scenarios are logged in *ANSYS Fluent* in close vicinity to SB1 at overall 43 logging points (Figure 3a). Always seven of these logging points are lined up vertically in front of each building façade to log air temperature. The spacing between the measurement points is 6 m (two stories), the distance between the points and the building surface is 2 m. Due to the oblong shape of the building, the façades towards the northwest and southeast have two lines with points in front of them. A 43rd point, centrally located 3 m above the roof of the building is used to log wind speed and wind direction. The collected data are used to create the weather files for BPS. It is accounted for a changing air temperature $T_a(z)$ over the height of the building, where z is the height above ground. For that, separate weather files with an air temperature calculated as a mean of all data extraction points with the same z (6 m, 12 m, etc.) are created and assigned to always two building floors at about the same height. A more detailed description of the procedure is outlined in section 4.2.

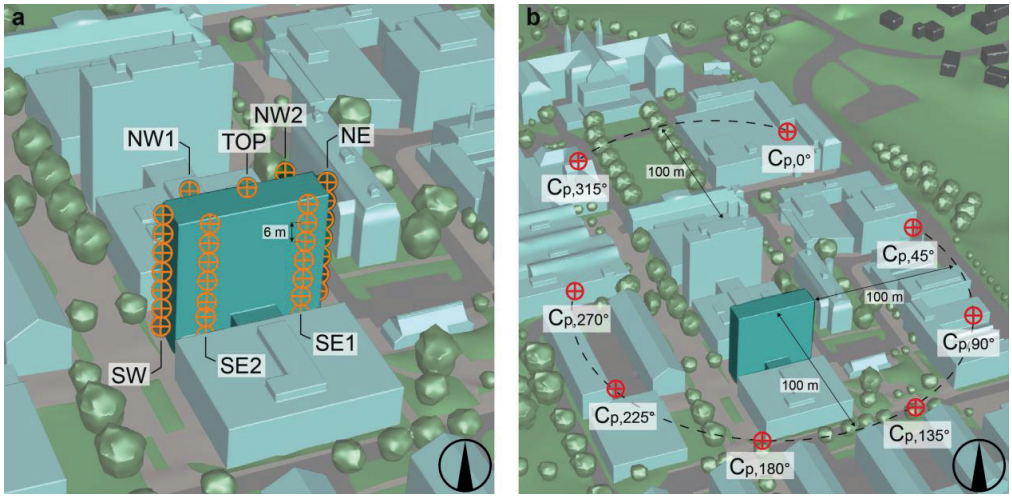

Figure 3: Location of data logging points in ANSYS Fluent with the building of interest (SB1) highlighted within the central campus area, viewed from the south. (a) shows the temperature logging points (orange markers) with a 2 m horizontal distance from the respective façades and a 6 m vertical spacing between the single points. "TOP" is the data logging point for wind speed and direction, centrally located 3 m above SB1. (b) shows the freestream reference points (red markers) for each wind direction at 100 m distance from SB1. The northern and northwestern reference points are placed at 100 m distance from the neighboring SB2, as this building evokes an upstream wind-blocking effect that disturbs the freestream.

Furthermore, the CFD model is used to determine the pressure coefficients C_p [-] on each façade of the investigated building which are then exported to the BPS tool (see Figure 2). Eq. 1 shows the calculation procedure for C_p, where P_x [Pa] is the static pressure at a specific point on the building façade, P_0 [Pa] is the freestream static reference pressure, and P_d [Pa] is the dynamic pressure at freestream which is calculated from $P_d = \rho U^2/2$. There, ρ [kg m^{-3}] is the density of air, and U [m s^{-1}] is the wind speed, often at building roof level in the upstream undisturbed flow. Pressure coefficients are determined for the eight standard wind directions for every surface of the building envelope. In this study, the data extraction points for the freestream flow variables P_0 and P_d are stipulated at 100 m distance from the building of interest in the respective wind direction (Figure 3b). A rather large distance to the building was chosen in order to capture the freestream flow variables that are not affected by the upstream wind-blocking effect [115–117].

$$C_p = \frac{P_x - P_0}{P_d} \tag{1}$$

The standard procedure in BPS tools, such as *IDA ICE*, is usually to use generic pressure coefficients from the AIVC database, based on a specified wind profile and building density of the surrounding environment [118,119]. Local effects from close buildings and vegetation, however, are not included in this standard procedure. Considering the vicinity of the SB2 high-rise building to the northwest these effects are important and require a closer examination, for instance by using CFD. The resulting façade-specific pressure coefficients for each wind direction are then entered into the pressure coefficient table of BPS tool.

3 CFD model design and settings

3.1 Measurement campaign for CFD model validation

From September 23 to October 21, 2019, a measurement campaign was conducted to record the microclimatic conditions at the campus. A network of five mobile weather stations (Figure 4) that recorded air temperature, relative humidity, wind speed, and direction in 0.1 Hz intervals at a height of 3 m was used. Additionally, a fixed weather station, 10 m above the roof of the VATL building (28 m above the ground, see Figure 1) was used as the RWS for calibration. There, global horizontal radiation was measured in addition to the previously mentioned climate variables. The recorded climate variables from the RWS served as a basis for the input at the domain boundaries in the CFD simulations.

The validation was carried out for two 48-hour periods during the measurement campaign which were September 27–28 and October 19–20. In general, both periods featured a strong variability in meteorological conditions regarding wind speed, wind direction, air temperature, and global horizontal radiation. The goal of selecting these dates was to investigate the CFD model's performance under variable and fluctuating conditions. Further information about the measurement campaign, as well as the CFD model's performance can be found in a separate study entirely dedicated to the CFD model validation process [120].

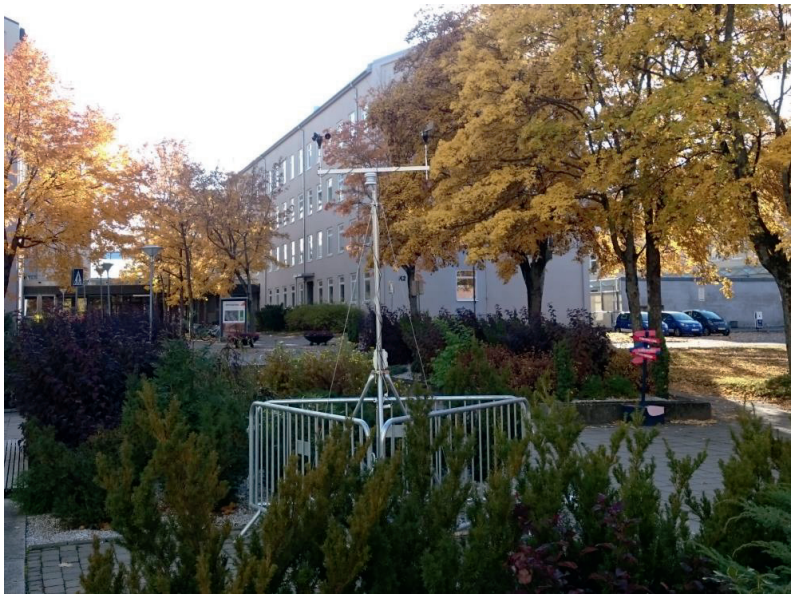

Figure 4: A mobile weather station at NTNU's Gløshaugen campus in October 2019.

3.2 Computational domain

This section presents the key information about designing the computational domain, as a detailed description can be found in a separate article by Brozovsky et al. [120].

The computational domain of the study area features regions of three different types of geometrical modeling (Figure 5a): (a) where buildings and trees are represented explicitly with a rather high level of details (NTNU campus), (b) the area around the NTNU campus, where only buildings and no vegetation are represented explicitly yet with a lower degree of detail (representation of buildings as simple boxes), and (c) the wider surroundings of the area of interest which are only represented implicitly by assigning an aerodynamic roughness length z_0 according to the Davenport-Wieringa roughness classification [98].

There are two main sources of geometrical data for the terrain and buildings in this study. (1) A freely available 3D geometrical city model from Trondheim Municipality and (2) Light Detection And Ranging (LiDAR) data created at NTNU. These two sources of geometrical information were joined and post-processed in the 3D computer-aided design software *Rhinoceros 5*. In the whole domain, elements such as street signs, bus stops, lamp posts, curbs, vehicles, small monuments, garden sheds, dog houses, etc. are omitted. Due to the creation date of the geometrical data sources, three newer buildings (ZEB, TCL, and LL, see Figure 1) at the campus were not included. Therefore, they were designed in *Trimble SketchUp* according to their technical drawings. Both the *Rhinoceros* file containing the modified data from Trondheim Municipality and the *SketchUp* file of the campus buildings were imported into *ANSYS SpaceClaim 2020.R1* and merged. In *SpaceClaim*, the dimensioning of the domain, positioning of the tree geometries according to on-site visits and satellite images was performed.

The computational domain is designed following the CFD best practice guidelines by Franke et al. [121] and Tominaga et al. [122]. Consequently, all buildings within a distance of at least 250 m (at least one street block) around the campus buildings are explicitly modeled. The height of the highest building in the domain is 73 m and is located about 300 m southwest of the campus. The surrounding terrain is quite complex and ranges in elevation from 0 to 172 m a.s.l., causing obstructions to the wind flow much higher than the modeled buildings. To avoid unwanted blockage from the terrain, the domain's bottom boundary is copied to the top, so that they largely have the same shape (the only difference is the lower grid resolution at the top) and all lateral boundaries have the same surface area (see Figure 5a). The maximum blockage ratio of all buildings and trees is 1.1 % and the resulting domain size is 4,225 × 4,225 × 1,550 m³.

The domain is discretized into a poly-hexcore grid that consists of 9,123,834 cells (see Figure 5b and c) with *ANSYS Fluent 2020.R1* in meshing mode. The grid is based on a grid-convergence analysis and was compared to a coarser grid with 4,371,409 cells, and a fine grid with 23,566,616 cells. The main difference between the three grids is the sizing of the surface mesh in the area of interest, mainly consisting of the geometrically explicitly modeled buildings and trees. All three grids are following the best practice guidelines [121,122]. More detailed information about the grid convergence study and the results can be found in a separate article by Brozovsky et al. [120].

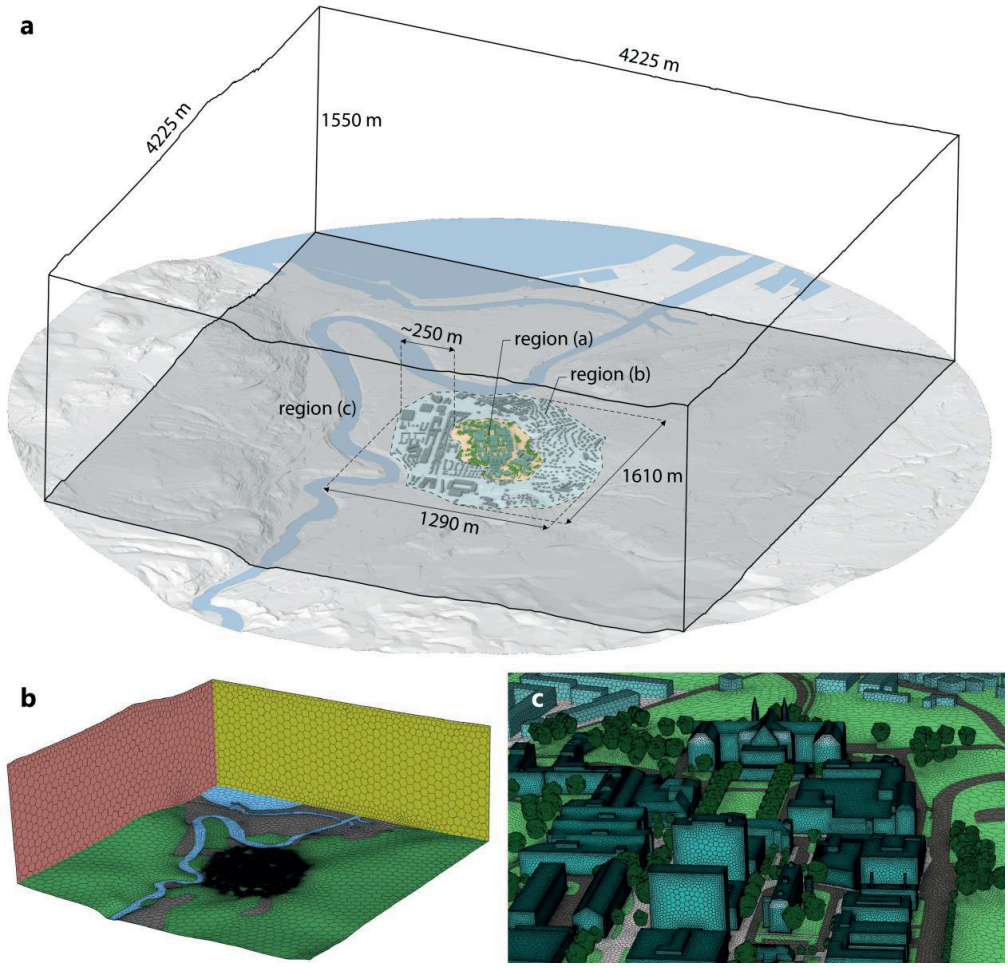

Figure 5: Computational domain (4,225 × 4,225 × 1,550 m³) with 9,123,834 cells; (a) Domain boundaries viewed from the south-east with different geometrical modeling regions and dimensions; (b) Meshed domain with different surface types: water (blue), primarily green spaces (green), densely built-up or industrial areas (grey), northern (yellow) and western (red) boundary; asphalt (dark grey), concrete/pavement (light grey); (c) Close-up view of the NTNU campus buildings and trees and different surface types: asphalt (dark grey), concrete/pavement (light grey) and green spaces (green).

3.3 Computational settings and boundary conditions

The 3D unsteady Reynolds Averaged Navier Stokes (URANS) equations are solved for which the realizable k-ε turbulence model [123] provides closure. This turbulence model was reported to have good performance for wind flow around buildings [35,116,124] and has been successfully applied in many validated CFD studies of the urban microclimate [87,91,92,103,125]. The Boussinesq approximation is used to account for natural convection. *ANSYS Fluent*'s Solar Calculator determines the sun's position for each time step. The model developed by Skartveit and Olseth [126] is applied to divide measured global horizontal radiation (at the reference station) into its direct and diffuse fractions which are updated for each time step. The exchange of long-wave radiation is included by employing the Discrete Ordinates radiation model [127,128]. This model's angular discretization settings are kept

at the standard value of 2 for the number of theta and phi divisions, and 1 for the number of theta and phi pixels. The SIMPLEC [129] algorithm is employed for the pressure-velocity coupling and schemes of second-order only are used for the spatial discretization.

In the implicitly modeled areas of the domain, an aerodynamic roughness length z_0 [m] for different surface types as given by Wieringa [98] is applied (Table 3). *ANSYS Fluent*, however, only allows for the input of sand grain roughness height k_s [m]. Therefore, the correlation $k_s = 9.793\ z_0\ C_s^{-1}$ is used where C_s [-] is a roughness constant kept at its default value of 0.5 in this study [130]. For the explicitly modeled surfaces in the domain, the sand grain roughness was entered directly. It was k_s = 0.05 m for asphalt, concrete, and pavement surfaces, and k_s = 0.1 m for grass and building surfaces to account for irregularities and protrusions. Fluid-wall interactions are treated with the standard wall functions by Launder and Spalding [131].

Table 3: Surface roughness settings in the computational domain.

Modeling type	Surface	z_0 [m]	k_s [m]	C_s [-]	LCZ[1]
Explicit	Building surfaces	-	0.10	0.5	-
	Asphalt	-	0.05	0.5	-
	Concrete	-	0.05	0.5	-
	Grass-covered earth	-	0.10	0.5	-
Implicit	Urban cityscape	1.0	19.59	0.5	5
	Industry	1.0	19.59	0.5	8
	Other[2]	0.5	9.79	0.5	6, A

[1] Local climate zone according to Stewart and Oke [97].

[2] Combining the surface types *Dense low-rise*, *Farmland*, *Open area*, and *Forest* (see Figure 1) into one BC type.

The effects of heat storage in the urban surface and buildings are accounted for with shell conduction in *ANSYS Fluent* for which the urban surface and all buildings were modeled according to the material layers of the structures. This sub-model considers heat transfer in both the normal and planar directions of the domain's walls. The buildings on campus are grouped into five categories according to their construction types and assigned a constant indoor temperature of 21 °C. All ground surfaces were modeled with a thickness of 10 m. At this depth, a constant temperature according to groundwater temperature measurements near the study site. The assigned ground temperatures at 10 m depth are 4.2 °C, 5.0 °C, and 5.8 °C for SUM, AUT, and WIN, respectively. There is a strong seasonal shift of approximately 6 months between maximum air temperature and groundwater temperatures which results in higher ground temperatures in the winter months than in summer.

The water-covered areas, namely the river *Nidelva* and *Trondheim Fjord* are not modeled as a fluid but as a "thin wall" with surface water temperatures obtained from Sea and Land Surface Temperature Radiometry onboard the European Space Agency's Copernicus Earth monitoring system of the Sentinel-3 satellites. These satellite images have a resolution of 1 km^2 and provide the input at the simulated times of the year. The temperatures used as BC are 18.5 °C for SUM, 11.4 °C for AUT, and 4.8 °C for WIN. The material layers of the building categories and the urban surface are listed in Table 4. Table 5 lists the optical and thermal properties of the surface materials that are used in the model. In *MS-HPN*, the envelope insulation properties of all explicitly modeled buildings surrounding SB1 were improved. SB1 on the other hand remained unchanged. In this scenario, buildings which in the base case scenario

were not modeled with an insulation layer, such as categories II, III, IV, and the surrounding buildings were equipped with 0.3 m of insulation and a 0.05 m charred wood cladding to the exterior of the building, adjacent to the fluid cells of the domain. In the remaining building categories I and V, the existing insulation layer was increased to 0.3 m, and a 0.05 m charred wood cladding is added to the outside of the building, adjacent to the fluid cells of the domain. In building category I, the existing wood cladding is replaced by charred wood.

Table 4: Wall structure of buildings and the urban surface for the CFD simulations.

Building categories/ Urban surface	Layer 1 (adjacent to fluid cells)		Layer 2		Layer 3 (domain's exterior)	
	Material	d [m]	Material	d [m]	Material	d [m]
I (Wood)	Wood: spruce	0.05	Insulation	0.25	Wood: spruce	0.05
II (Stone)	Granite	0.2	Brick	0.2	–	–
III (Brick)	Brick	0.36	–	–	–	–
IV (Concrete, old)	Concrete	0.36	–	–	–	–
V (Concrete, new)	Plaster	0.02	Insulation	0.2	Concrete	0.2
Surrounding buildings	Brick	0.3	-	-	-	-
Roads	Asphalt	0.3	Granite	1.0	Earth	8.7
Pavement	Concrete	0.3	Granite	1.0	Earth	8.7
Grass	Earth	0.01	Earth	0.49	Earth	9.5

Symbols: Material layer thickness (d)

Table 5: Selected optical and thermal properties of the surface materials on campus [8,132–134].

Surface	α [–]	ε [–]	c [kJ kg^{-1} K^{-1}]	δ [kg m^{-3}]	λ [W m^{-1} K^{-1}]
Wood: spruce	0.75	0.90	2310	700	0.17
Wood: spruce (charred)	0.93	0.95	2310	700	0.17
Asphalt	0.70	0.95	800	2400	0.75
Concrete	0.66	0.95	1000	2300	1.60
Plaster	0.66	0.95	1000	1800	1.00
Insulation (not a surface material)	-	-	840	50	0.05
Granite	0.70	0.95	790	2800	3.00
Earth (covered with grass)	0.77	0.95	1000	1400	1.80
Brick	0.66	0.95	900	2050	0.80

Symbols: Absorptivity (α), emissivity (ε), heat capacity (c), density (δ), thermal conductivity (λ)

Special attention was given to grass surfaces which were divided into three layers of earth with a top layer thickness of only 0.01 m where the evapotranspirational cooling flux E [W m^{-2}] from the grass canopy is applied. As this heat flux is applied in the center of the respective layer in *Fluent*, a thickness of 0.01 m ensures this cooling flux is close to the surface facing the fluid cells. E is determined by the Penman-Monteith equation [134–137] (Eq. 2) where $(R_n - G)$ is the available energy with the net radiation R_n [W m^{-2}], the soil heat flux G [W m^{-2}], the vapor pressure deficit of the air D [Pa], and the (bulk) surface and aerodynamic resistance r_s and r_a [s m^{-1}]. λ is the latent heat of water vaporization [J kg^{-1}], γ is the psychrometric constant [Pa K^{-1}], and c_p is the specific heat capacity of air [J kg^{-1} K^{-1}]. Finally, Δ represents the slope of the vapor pressure curve [Pa K^{-1}]. In this study, the soil heat flux G is estimated to be negligible, as it approaches a relatively small value for dense grass canopies. A more

detailed description of how the Penman-Monteith equation was applied in this CFD model can be found in Brozovsky et al. [120].

$$E = \frac{\Delta\,(R_n - G) + \rho\, c_p \frac{D}{r_a}}{\Delta + \gamma\,\left(1 + \frac{r_s}{r_a}\right)} \tag{2}$$

Furthermore, the evapotranspirational cooling from the trees was taken into account in the CFD model. They were modeled as volumetric porous zones in a spherical shape. For the cells of these porous zones, source/sink terms for the momentum S_{u_i} [Pa m^{-1}] for the velocity components u_i with $i = x, y, z$ (Eq. 3, from [138,139]), turbulent kinetic energy S_k [kg m^{-1} s^{-3}] (Eq. 4, from [139]), turbulent dissipation rate S_ε [kg m^{-1} s^{-4}] (Eq. 5, from [140]) and volumetric heat transfer from evapotranspiration P_c [W m^{-3}] (Eq. 6, from [125,141,142]) are added:

$$S_{u_i} = -\rho\, LAD\, C_d\, U\, u_i \tag{3}$$

$$S_k = \rho\, LAD\, C_d\, \left(\beta_p\, U^3 - \beta_d\, U\, k\right) \tag{4}$$

$$S_\varepsilon = \rho\, LAD\, C_d \left(C_{\varepsilon 4}\, \beta_p \frac{\varepsilon}{k} U^3 - C_{\varepsilon 5}\, \beta_d\, U\, \varepsilon\right) \tag{5}$$

$$P_{c,trees} = (0.0252\, T_a - 0.078)\, R_h\, LAD \tag{6}$$

In equations 3–6, ρ is the density of air [kg m^{-3}], LAD the Leaf Area Density [m^{-1}], C_d the sectional drag for vegetation [-], $\left(\beta_p, \beta_d, C_{\varepsilon 4}, C_{\varepsilon 5}\right)$ = (1.0, 4.0, 0.9, 0.9) are model coefficients [-], U the wind speed (across all directions) [m s^{-1}], T_a the air temperature [K], R_h the incoming global solar radiation [W m^{-2}] [143]. The Leaf Area Density of the trees is set to 1.5 m^{-1} for SUM, 1.0 m^{-1} for AUT, and 0.2 m^{-1} for WIN. The latter value is not set to 0, although the trees have no leaves during this SP. However, with a value of 0.2 m^{-1}, the aerodynamic effect especially of the trees' branches is approximated. The energy sink term (Eq. 6) was set to zero during WIN.

Always two of the lateral domain boundaries are set as inlets and the other two as outlets, depending on the wind direction. At the inlets, the profiles for the air velocity $U(z)$ [m s^{-1}] (Eq. 7), turbulent kinetic energy $k(z)$ [m^2 s^{-2}] (Eq. 8), and turbulence dissipation rate $\varepsilon(z)$ [m^2 s^{-3}] (Eq. 9) are taken from Richards and Hoxey [144]. In these relationships, u^*_{ABL} [m s^{-1}] (Eq. 10) is the Atmospheric Boundary Layer friction velocity [m s^{-1}], κ is the von Karman constant [-] (= 0.42), z is the height coordinate [m], and C_μ is a constant [-] (= 0.09). For determining u^*_{ABL}, the wind speed at the boundaries u_b [m s^{-1}] is needed, for which no measurements are available during the SPs. Therefore, Wieringa's [145] logarithmic transformation equation (Eq. 11) is used to calculate u_b based on the wind speed measured at the RWS u_{RWS} [m s^{-1}], the surface roughness at the RWS $z_{0,RWS}$ [m], the target height of the transformation h_b [m] and a blending height h_{bh} [m]. Depending on the wind direction, different surface roughness lengths $z_{0,b}$ [m] at the inlet boundaries are used to determine the shape of the profile. Due to the coastal location of Trondheim, the northern boundary is bordering the sea, for which a different $z_{0,b}$ is used than for the other three boundaries that are located on land. It is estimated that between 65 and 310° from north, $z_{0,b}$ = 0.25 m. For the remaining directions, $z_{0,b}$ is set to a lower value of 0.1 m. Reference wind speed and

direction are taken from the RWS at h_{RWS} = 28 m height (10 m above the VATL building, see Figure 1d). The blending height h_{bh} defines the height at which the influence of the ground gets negligible and is assumed to be 200 m due to the complex terrain in the area of the computational domain.

$$U(z) = \frac{u^*_{ABL}}{\kappa} \ln\left(\frac{z + z_{0,b}}{z_{0,b}}\right) \tag{7}$$

$$k(z) = \frac{{u^*_{ABL}}^2}{\sqrt{C_\mu}} \tag{8}$$

$$\varepsilon(z) = \frac{{u^*_{ABL}}^3}{\kappa\,(z + z_{0,b})} \tag{9}$$

$$u^*_{ABL} = \frac{\kappa\, u_b}{\ln\left(\frac{h_b + z_{0,b}}{z_{0,b}}\right)} \tag{10}$$

$$u_b = u_{RWS}\left[\frac{\ln\left(\frac{h_{bh}}{z_{0,RWS}}\right)\ln\left(\frac{h_b}{z_{0,b}}\right)}{\ln\left(\frac{h_{RWS}}{z_{0,RWS}}\right)\ln\left(\frac{h_{bh}}{z_{0,b}}\right)}\right] \tag{11}$$

The shear condition at the domain top is set to zero normal gradients for all flow variables (free-slip condition). To account for longwave radiation losses to the sky, the domain's inlets, outlets, and top boundary are assigned a temperature T_{sky} according to Swinbank's [146] simplified correlation (Eq. 12). As a basis, the air temperature measured at the RWS $T_{a,C,ref}$ [°C] is used.

$$T_{sky} = 0.0552\, T_{a,C,ref}^{1.5} \tag{12}$$

In this study, three 168-hour periods are simulated with 1-hour time steps and 400 iterations per time step except for the first one, for which 800 iterations were performed to provide better convergence. As a consequence, in total 168 time steps with 67,600 iterations are carried out for each of the three 168-hour periods. On average, the following scaled residuals are reached at the end of each time step: 2.1×10^{-5} for continuity, 1.8×10^{-4} for x-velocity, 2.2×10^{-4} for y-velocity, 1.6×10^{-4} for z-velocity, 5.8×10^{-4} for k, 1.6×10^{-3} for ε, 9.6×10^{-8} for energy, and 1.1×10^{-6} for radiation.

4 BPS model design and settings

4.1 Building specifications

The building of interest, an office high-rise, is part of the *Sentralbygg* (English: *Central Building*) complex, in the middle of the NTNU campus. This building complex comprises two high-rises and three low-rise buildings (see Figure 3 and Figure 6). SB1 is axially aligned with the main Gløshaugen development which is rotated ca. 335° from the north. SB1 was constructed in 1961 with a concrete skeleton as the bearing structure and is 40 m high. It has a GFA of ca. 6,000 m^2 and the ceiling height

is 3.0 m, with exception of the 1st and 2nd floors which are 3.2 m high. The exterior walls show a regular window grid, consisting of 29 window columns, each between load-bearing columns on the south-eastern façade. To the northwestern side, the same grid applies, with exception of the building core which consists of two staircases, an elevator shaft, restrooms, and other technical rooms (see Figure 7). Besides the roof, the insulating materials are located on the inside of the bearing structure. There are three types of external walls (EW): (EW1) prefabricated wall panels with 10 cm interior rock wool insulation between the columns (on the south-eastern and the northwestern façade apart from the building core), (EW2) a thick concrete wall with 5 cm of internal cork insulation (building core between the staircases), and (EW3) the gable walls with 15 cm aerated concrete blocks on the inside (see Table 6). Moreover, the building features two different types of windows. On the northwestern side of the building, triple-glazing insulating windows are installed (U-value incl. frame: 0.93 W m^{-2} K^{-1}; g-value: 0.60), while on the south-eastern side, double-glazing windows with integrated Venetian blinds and a protecting third glass pane on the outside are mounted (U-value incl. frame: 1.30 W m^{-2} K^{-1}; g-value: 0.52). As mentioned in the methodology section, the same BPS model is used for all investigated scenarios.

Table 6: Wall structures used for SB1 from the inside (layer 1) to the outside (layer 4) in the BPS simulations.

Envelope surface	Layer 1 (inside)		Layer 2		Layer 3		Layer 4 (outside)		U-value
	Material	*d* [m]	Material	*d* [m]	Material	*d* [m]	Material	*d* [m]	[W m^{-2} K^{-1}]
EW1	Gypsum	0.013	Rockwool	0.1	Concrete	0.05	Render	0.025	0.36
EW2	Plaster	0.015	Cork	0.05	Concrete	0.4	Render	0.025	0.73
EW3	Render	0.015	Aerated concrete	0.15	Concrete	0.18	Render	0.025	0.73
Roof	Render	0.015	Concrete	0.16	Rockwool	0.14	Ventilated air cavity[1]		0.27

Symbols: Material layer thickness (*d*)

[1] Thermally not relevant

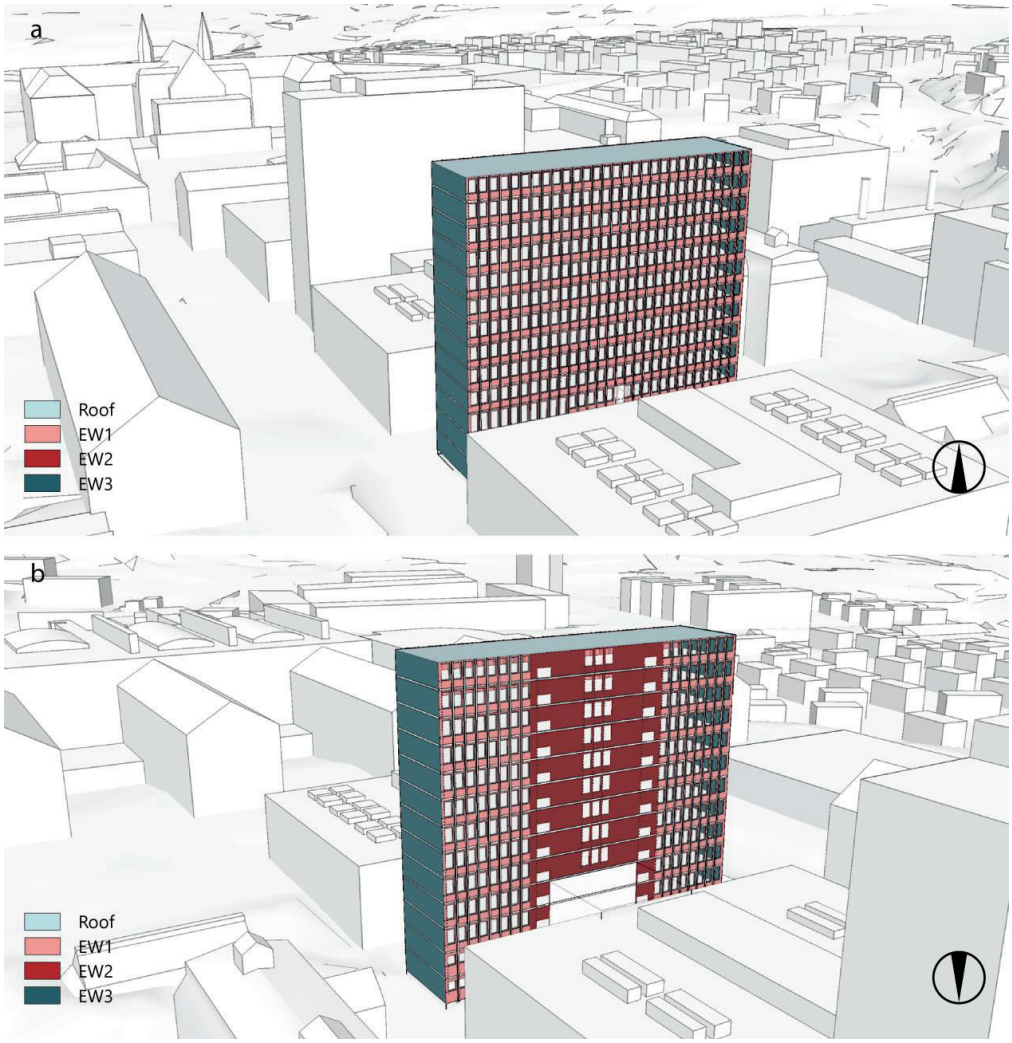

Figure 6: Different constructions used in the IDA ICE BPS model. (a) View of SB1 from the south; (b) View of SB1 from the north.

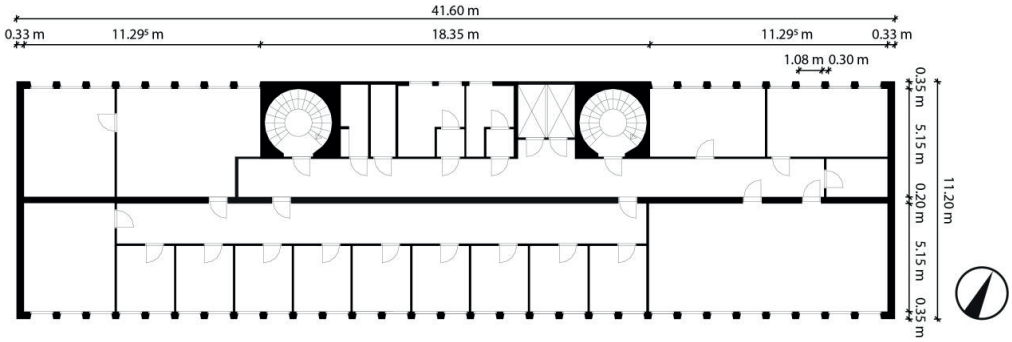

Figure 7: Typical floor plan and dimensions of SB1.

4.2 Other BPS settings

The operating schedules and internal loads for the BPS are taken from the Norwegian standard SN-NSPEK 3031:2020 [147] for the building category *Office building* (Figure 8). In accordance with NS 3031:2014 [148], the operation times for mechanical ventilation and room heating are from 07:00 – 19:00 during the weekdays. For room heating, the setpoints are 21 °C and 19 °C during and outside of the operational hours, respectively. The mechanical ventilation system (constant air volume) supplies the zones with 7 m^3 m^{-2} h^{-1} and 2 m^3 m^{-2} h^{-1} during and outside of the operational hours, respectively [147]. From the ventilation system, in which a rotary heat recovery unit with 70 % efficiency pre-conditions the incoming air, the zones are supplied with air a constant 19 °C. With only a heating and no cooling coil installed, the supply air temperature can get higher in summer when the outdoor air temperature exceeds 19 °C. The interior insulation and poor prevention of thermal bridges cause a normalized thermal bridge factor of ca. 0.20 W m^{-2} K^{-1}. It needs to be pointed out that this factor is based on the gross internal area of buildings in Norway, not the envelope area. The infiltration rate is assumed to be 3.0 h^{-1} at 50 Pa pressure difference [149]. In the simulation model, a control strategy is added for the operation of the window-integrated Venetian blinds. Following NS 3031:2014 [148], it is modeled so that the blinds are pulled down when solar irradiation on the outside of the window exceeds 100 W m^{-2} in WIN, and 250 W m^{-2} in SUM and AUT. No window opening control strategy is implemented as the building has a mechanical ventilation system to ensure the required ventilation rates and user behavior related to operating windows in buildings is very complex [150]. Equally important, the Norwegian standards that are used for the calculation of a building's energy performance do not provide for windows to be opened. Domestic hot water is not considered in this study.

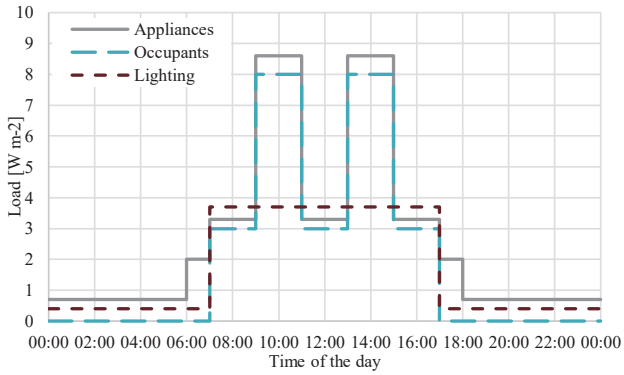

Figure 8: Internal gains on weekdays for an office building according to SN-NSPEK 3031:2020 [147].

Furthermore, every floor was modeled as a single zone. Because the used standards require using the same internal loads irrespective of the specific usage of a room (e.g. office, hallway, meeting room), a finer segmentation of zones would not increase the accuracy of the simulation model but prolong simulation times. To determine the energy demand, an ideal heating element that is capable of providing enough thermal energy to reach the desired heating setpoints at any time is placed in every zone. In this way, the obtained demand is independent of the system type and comparability is facilitated. The SUM simulations were carried out in two different ways: (1) with ideal cooling elements to be able to compare hypothetical cooling loads, and (2) no ideal cooling elements in the zones, as the real building does not have a cooling system installed. While in case 1, the energy demand for cooling in kWh is compared, case 2 shows a comparison of the number of hours in which the T_{op} in the zones exceeds 26 °C ($N_{T_{op}>26\,°C}$). The latter is a metric used for documenting the quality of indoor thermal comfort for summer periods according to the Norwegian building code [151].

Furniture, internal walls, and structures such as the building core and staircases are considered as thermal mass in every zone. Because the influence of the microclimatic conditions on the building's basement is negligible, it is not taken into consideration in this study. Therefore, the BC of the floor towards the basement is set to adiabatic.

The pressure coefficients are determined from CFD simulations and used in the BPS (see section 5.1). However, *IDA ICE* requires the specification of an exponential wind profile (see Eq. 13) which is applied to the wind speed from the climate file. From that, the wind speed at any height $U(z)$ [m s^{-1}] is determined. In this equation, $U_{ref,CFD}$ [m s^{-1}] and $z_{ref,CFD}$ [m] are the wind speed and height at which the wind speed was extracted from the CFD simulations. There, $z_{ref,CFD}$ is 45 m and a_0 [-] and a_{exp} [-] are assumed to be 0.67 and 0.25, respectively, based on Liddament's guide on air infiltration calculation techniques [118] for the terrain category *urban, industrial, or forest areas*.

$$U(z) = U_{ref,CFD}\, a_0 \left(\frac{z}{z_{ref,CFD}}\right)^{a_{exp}} \tag{13}$$

For the simulations, the standard settings in *IDA ICE* regarding the time step size are kept. Correspondingly, the solver selects the time step size dynamically. As a consequence, the time steps are not equidistant on the one hand, but on the other hand, it allows the solver to proceed in smaller time steps if large gradients are detected to improve stability. A two-week startup period, using recorded climate data from the RWS, ensures that the impact of the initial value at the start of a simulation is minimized.

In BPS, normally one global outdoor air temperature which is taken from the weather file is used for the simulations, but as shown in Figure 3a, outdoor air temperatures in this study have been extracted from CFD around and over the entire height of the building of interest in 6 m steps. Thus, the BPS model has been modified to account for a changing air temperature over height $T_a(z)$. Floors 1 and 2 have been assigned the average of all extracted outdoor air temperatures from CFD at 6 m height, floors 3 and 4 that of 12 m, etc. Finally, the 13th floor is assigned the extracted outdoor air temperature at 42 m. The change of outdoor air temperature was only considered in a vertical direction. Although data for the different temperatures at the individual façades of SB1 was available, no further segmentation of climatic BC was undertaken. The additional modeling necessary for façade-specific, temperature BC is extremely time-consuming and does not improve accuracy if all lateral building surfaces are adjacent to the same zone as in the present study.

5 Results

5.1 Pressure coefficients

The distribution of pressure coefficients C_p on each of the investigated building's envelope surfaces is presented in Figure 9. The situation is shown for wind from the south, as during the three investigated weeks it was the most common wind direction (44.0 % of the time or 222 h in total). In 21.6 % of the time (109 h in total), the wind was coming from Trondheim's prevailing wind direction southwest. As visible in Figure 9, the pressure distribution on the building envelope surfaces is quite heterogenic, presenting large gradients especially at the corners of the building. The pressure coefficients ranged from -1.20 at the southern edges of the roof to 1.30 at the upper left corner of the southeastern facade. Particularly at the roof, the northeastern and southwestern façade, the respective minimum values occur at the edges that are shared with the southeastern façade. In these locations, flow separation is observed which evokes large gradients, visualized by narrow contour lines at the edges.

In this study, the standard approach using façade-averaged pressure coefficients was employed. To obtain a finer raster and higher accuracy in the calculations, subdividing the building façades into smaller surfaces and determining their average pressure coefficients in *ANSYS Fluent* as well as entering them in *IDA ICE* is generally possible, but requires excessive modeling work. This level of detail was deemed unnecessary for the comparative analysis done in this study. The façade-averaged pressure coefficients for each of the eight investigated wind directions are listed in Table 7.

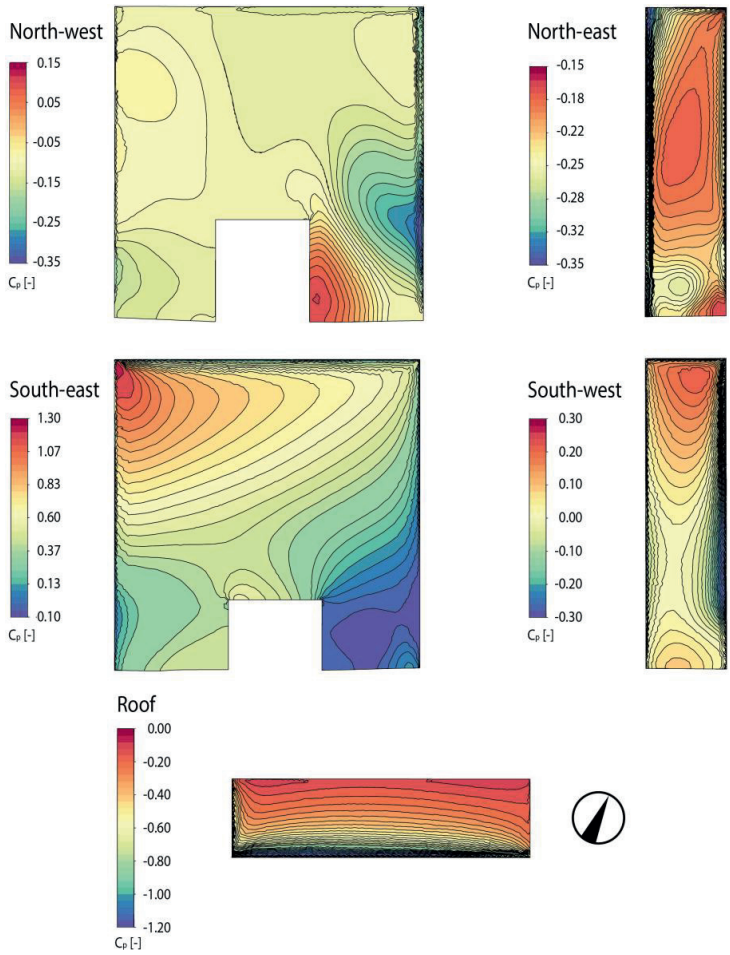

Figure 9: Pressure coefficients C_p on the building envelope surfaces of the building of interest (SB1) at southerly wind.

Table 7: Façade-averaged pressure coefficients C_p for the eight investigated wind directions. The relative frequency of each wind direction at the RWS during the three investigated weeks in % is given in brackets below the wind direction.

	Wind direction [°] (relative frequency [%])							
Façade (azimuth)	0° (3.4%)	45° (0.2%)	90° (0.2%)	135° (4.8%)	180° (44.0%)	225° (21.6%)	270° (7.3%)	315° (18.5%)
North-east (65°)	-0.09	0.23	0.35	-0.09	-0.22	-0.18	-0.14	-0.16
South-east (155°)	-0.21	-0.30	0.02	0.51	0.42	-0.09	-0.18	-0.11
South-west (245°)	-0.28	-0.25	-0.23	-0.20	0.01	0.36	0.21	0.02
North-west (335 °)	0.14	-0.09	-0.31	-0.07	-0.12	-0.27	0.06	0.17
Roof (-)	-0.44	-0.39	-0.43	-0.40	-0.43	-0.37	-0.28	-0.24

5.2 CFD microclimate simulations

Since the used CFD model has been validated in detail and found suitable to be used for microclimate studies in a separate study by Brozovsky et al. [120], no further validation process will be reported at

this point. However, comparing the results from the simulated base case scenario (*MS-Base*) to the measurements at the RWS in the respective SPs, similar model accuracies were obtained as in the article dedicated to the model validation.

In the remainder of this article, the average air temperature from the 42 logging points around the building of interest (SB1) will be simply referred to as *air temperature at SB1*, as opposed to the *air temperature at the RWS* which is logged at the location of the RWS, 10 m above the VATL building.

In Figure 10, the air temperatures at SB1 for the different MSs during SUM, AUT, and WIN are presented. Furthermore, the differences in air temperature $\Delta T_{MS-Base}$ at SB1 of *MS-NoVeg*, *MS-AllVeg*, and *MS-HPN* compared to *MS-Base* are illustrated. While in SUM quite pronounced differences between the MSs can be observed, particularly with regard to *MS-NoVeg*, the investigated MSs have a fairly small impact on air temperature during AUT and WIN. This tendency can be explained by the seasonal availability and intensity of solar radiation onto the urban surface. While during SUM, the solar elevation angle is rather high and days are long, the urban surface is able to absorb a lot of energy from solar radiation. Towards WIN, the situation reverts.

In all three SPs, *MS-NoVeg* shows the largest variation of microclimatic conditions with an air temperature that almost continuously surpasses that of *MS-Base*. During SUM, when the daily temperature maxima in *MS-Base* are reached (typically around 18:00–20:00), the differences are most pronounced. It is worth highlighting that the maxima of the air temperature at SB1 are postponed between two and three hours when compared to the temperature curves obtained at the RWS. This was observed for all MSs during SUM and can be explained by the large, exposed façade of SB1 which provides a nearly optimal angle of attack for the comparatively low solar elevation angle (ca. 10°) but still strong solar radiation from the west at these times of the day.

Because of lower solar irradiation levels, this behavior was not observed during AUT and WIN where a smaller elevation angle hides the sun behind the large hill in the west of the computational domain. Other metrics and key figures of the three SPs, such as minimum, maximum, and average air temperatures, air temperature differences, and the respective times of occurrence, are given in Table 8. From the data in this table, it can be seen that the simulated air temperatures at SB1 for *MS-NoVeg* are on average 1.0 °C, 0.2 °C, and 0.1 °C warmer than in *MS-Base* in SUM, AUT, and WIN, respectively. On the other hand, *MS-AllVeg* is on average 0.1 °C cooler than in *MS-Base* in both SUM and AUT. In WIN, the average temperature remained close to unchanged. While *MS-HPN* is 0.1 °C warmer than *MS-Base* during SUM, there is only a marginal influence on air temperature at SB1 during AUT and WIN on average. In *MS-NoVeg*, up to 2.4 °C higher air temperatures are obtained in SUM, while the maximum difference is 0.4 °C in AUT and 0.3 °C in WIN. In *MS-AllVeg*, the additional greening led to a maximum decrease in air temperature of 0.6 °C during SUM and 0.3 °C during AUT, while in WIN, it was 0.1 °C.

It is important to remember that Trondheim is a city with a significant share of greening and that the NTNU campus is surrounded by a green belt with numerous trees and expansive green areas. Consequently, the differences between *MS-AllVeg* and the base case are not as pronounced as between *MS-NoVeg* and the base case. There, the degree of modification of the urban surface is distinctly higher than in *MS-AllVeg*.

MS-HPN on the one hand led to relatively large reductions of air temperature at certain points in time with a maximum of 0.6 °C during SUM and AUT, and 0.2 during WIN, but also caused significant air temperature increases at other times. These maximum increases were 1.0 °C and 0.6 °C during SUM and AUT, respectively. It is furthermore noticeable that there is a strong diurnal variation in air temperature differences between *MS-HPN* and *MS-Base*. While during the day, this difference first begins to decrease and eventually becomes negative during the morning, it becomes positive again during the late afternoon until the next morning.

Table 8: Key figures of the air temperatures at SB1 from the CFD simulations and time of occurrence where applicable.

SP	MS	T_{min}		T_{max}		T_{avg}	ΔT_{low}		ΔT_{high}		ΔT_{avg}
		[°C]	time	[°C]	time	[°C]	[°C]	time	[°C]	time	[°C]
SUM	*Base*	13.9	19.06. 04:00	30.5	20.06. 18:00	20.7	-	-	-	-	-
	NoVeg	14.4	19.06. 04:00	31.9	20.06. 15:00	21.7	0.1	15.06. 01:00	2.4	17.06. 15:00	1.0
	AllVeg	13.8	19.06. 05:00	30.3	20.06. 18:00	20.6	-0.6	19.06. 22:00	0.5	17.06. 06:00	-0.1
	HPN	13.7	19.06. 05:00	30.8	20.06. 18:00	20.8	-0.6	17.06. 18:00	1.0	19.06. 00:00	0.1
AUT	*Base*	5.4	17.09. 06:00	14.4	21.09. 17:00	9.2	-	-	-	-	-
	NoVeg	5.5	17.09. 06:00	14.8	21.09. 17:00	9.4	0.0	20.09. 12:00	0.4	18.09. 22:00	0.2
	AllVeg	5.3	17.09. 06:00	14.4	21.09. 17:00	9.2	-0.3	22.09. 02:00	0.1	16.09. 12:00	-0.1
	HPN	5.3	17.09. 06:00	14.6	21.09. 17:00	9.2	-0.6	19.09. 10:00	0.6	21.09. 19:00	0.0
WIN	*Base*	-0.7	25.12. 17:00	8.7	21.12. 01:00	3.2	-	-	-	-	-
	NoVeg	-0.7	25.12. 17:00	8.7	21.12. 01:00	3.3	0.0	26.12. 22:00	0.3	24.12. 12:00	0.1
	AllVeg	-0.8	25.12. 23:00	8.7	21.12. 01:00	3.1	-0.1	24.12. 13:00	0.0	21.12. 01:00	0.0
	HPN	-0.9	25.12. 23:00	8.7	21.12. 01:00	3.1	-0.2	24.12. 13:00	0.0	21.12. 04:00	-0.1

Symbols: Minimum air temperature (T_{min}), maximum air temperature (T_{max}), average air temperature (T_{avg}), largest lower deviation to *MS-Base* (ΔT_{low}), largest higher deviation to *MS-Base* (ΔT_{high}), and average deviation to *MS-Base* (ΔT_{avg}).

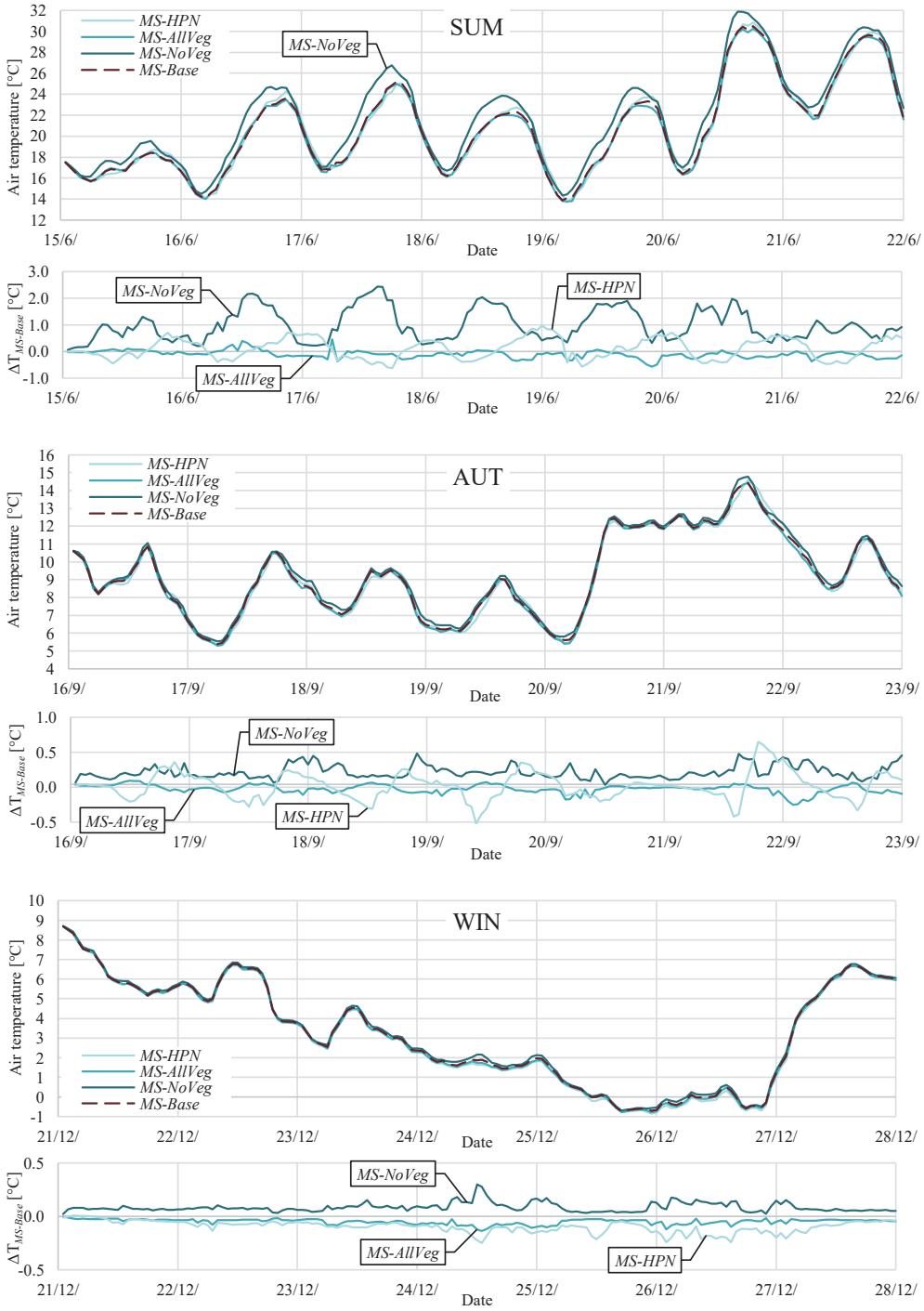

Figure 10: Air temperature of the different MSs and air temperature difference of MS-NoVeg, MS-AllVeg, and MS-HPN compared to MS-Base during SUM, AUT, and WIN as an average of the 42 logging points around the building of interest (SB1).

Figure 11 shows the air temperature at SB1 for the different MSs at selected points in time, averaged and plotted with respect to the logging points' height above the ground. It can be seen that the differences between the temperature profiles are larger close to the ground and that they converge with increasing height. Having in mind that the differences between the MSs are related to the materials of the urban surface (at the bottom of the domain) and that all MSs of an SP are assigned the same inlet air temperature profile over time, it is plausible that the profiles get more and more uniform at increasing heights. It is also noticeable that with the transition from summer to winter, the differences between the MSs of an SP get smaller. The temperature profiles for SUM present the situation at the point in time where the air temperature at SB1 reaches its maximum in *MS-Base* (20.06. 18:00). In *MS-Base*, the temperature profile shows the least variation over the height of SB1 with a mean of 30.5 °C. Large differences can be identified especially with regard to *MS-NoVeg* and *MS-AllVeg*. At 6 m height, *MS-NoVeg* is on average 1.0 °C warmer than *MS-Base* but this difference is steadily decreasing towards 0.4 °C at roof level. The opposite relationship is found in *MS-AllVeg* where the low-level air temperature at 6 m height is 0.4 °C cooler than in *MS-Base*. Moving further up towards roof level, air temperature in *MS-AllVeg* approximates that of *MS-Base*. The notch in all scenarios but *MS-NoVeg* at 12 m height can be attributed to trees close by at this height. Depending on the wind direction, this indentation is sometimes more, sometimes less pronounced.

During AUT, the minimum air temperature of *MS-Base* is obtained on 17.09. at 06:00. At this point in time, the difference between all scenarios is rather small. Across all scenarios, the air temperature closest to the ground is the highest. However, the air temperature of *MS-NoVeg* is constantly above that of *MS-Base*, by about 0.2 °C. Both the air temperature in *MS-AllVeg* and *MS-HPN* are about 0.1 °C lower than in *MS-Base*. Only at the lowest level, the air temperature of *MS-HPN* is slightly higher than that of *MS-AllVeg*, as it approaches the value from *MS-Base*.

On Dec 25, at 17:00, the coldest point in time during WIN and of all SPs, it can be seen that *MS-HPN* has the lowest air temperatures at SB1. The better insulation of the building envelopes leads to fewer heat losses which are particularly noticeable close to the buildings. Additionally, very little solar radiation during WIN leads to a generally smaller influence from the materials of the urban surface. Similar to SUM and AUT, *MS-NoVeg* shows a warmer temperature than *MS-Base*, over the whole height of SB1. However, in general, the temperature differences between the four scenarios are very small, with a maximum of less than 0.2 °C.

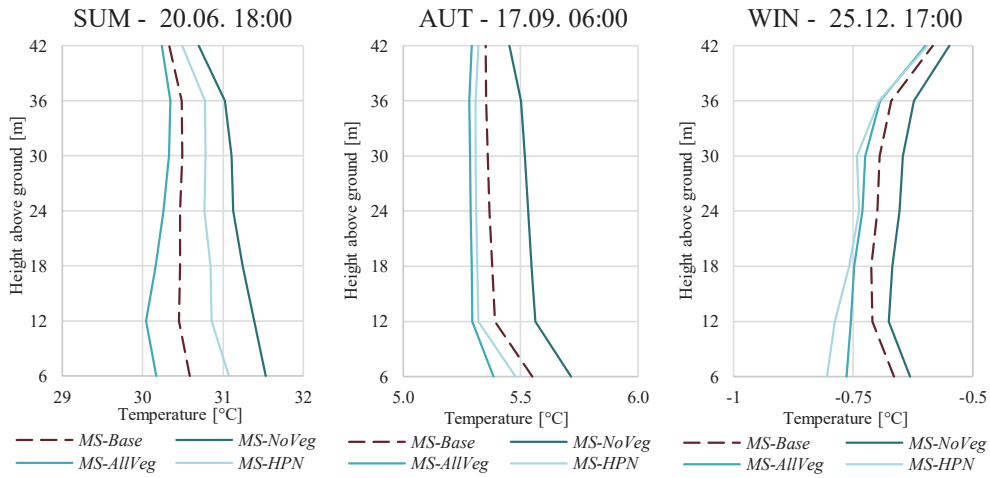

Figure 11: Temperature profiles showing the air temperature averages according to the logging point heights around SB1 for all MSs at selected times of the day during SUM (20.06. at 18:00), AUT (17.09. at 06:00), and WIN (25.12. at 17:00).

5.3 Building performance simulations

The influence of the local microclimate conditions on building energy demand is strongly in line with the results from the CFD simulations where the differences were largest in SUM and smallest in WIN. Figure 12 shows the total heating/cooling energy demand of the four MSs in every SP. Resulting from the large temperature differences between *MS-NoVeg* and *MS-Base* in the CFD simulations during SUM, the absence of green infrastructure as in *MS-NoVeg* in Trondheim during the simulated week in June 2020 would have increased the cooling energy demand in SB1 by 26.6 %. At the same time, an entirely greened urban surface as in *MS-AllVeg* would have reduced the cooling energy demand by 1.5 % compared to the current situation. Improving the insulation level of the buildings surrounding SB1 in *MS-HPN* led to a slight increase of cooling energy demand by 0.8 %. In this scenario, a lower albedo of the building envelopes leads to more absorbed radiation and thus higher surface temperatures. Consequently, due to higher convective heat exchange with the environment, higher outdoor air temperatures are observed.

On the other hand, in both AUT and WIN, *MS-NoVeg* represents the scenario with the lowest energy demand. As in both SPs, outdoor temperatures require the building to be actively heated, slightly higher outdoor temperatures from an urban surface without greening result in reduced heating demands. These reductions add up to 2.5 % and 0.5 % in AUT and WIN, respectively. Conversely, as more vegetation leads to lower outdoor temperatures, heating energy demands are slightly higher than in the base case. Accordingly, *MS-AllVeg* causes increases in heating energy demands by 1.0 % and 0.4 % in AUT and WIN, respectively. In *MS-HPN*, however, the tendency of increased energy demands found in SUM also persists in AUT and WIN, amounting to 0.9 % and 0.8 %, respectively. An explanation for that is the better insulation levels of the buildings' envelopes which lead to less *urban self-heating* and consequently slightly lower air temperatures [152].

Overall, the level of the energy demands is highest in WIN with about 13,400 kWh of heating energy for the whole building during the simulated week. In SUM, the cooling energy demand of SB1 amounts

to between about 6,400 kWh in *MS-AllVeg* to 8,250 kWh in *MS-NoVeg*. As the temperature differences between the indoor setpoints to outdoor conditions are smallest in AUT, the total energy demand during this period is lower than in SUM and WIN, amounting to about 5,200 kWh. The specific energy demands per square meter GFA [kWh m^{-2}_{GFA}] of *MS-Base* in SUM, AUT, and WIN are 1.1 kWh m^{-2}_{GFA}, 0.9 kWh m^{-2}_{GFA}, and 2.2 kWh m^{-2}_{GFA}, respectively.

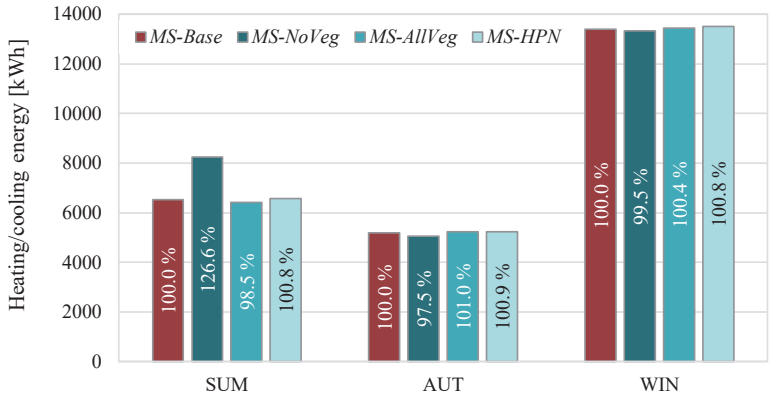

Figure 12: Total heating (AUT and WIN) and cooling (SUM) energy demand of SB1 during the investigated SPs.

When looking at the simulated energy demands per floor, large differences can be noticed (see Figure 13). From Figure 13a, especially the differences between the lower two floors to the upper nine are apparent in SUM. While in *MS-Base*, *MS-AllVeg*, and *MS-HPN* floors 5–13 have an energy demand between 138 % and 188 % higher than in the respective scenario on the first two floors, the differences are smaller within *MS-NoVeg* (58 % to 63 %) where the energy demand is generally higher. As the lower floors (1–4) have adjacent buildings on the northwest and southeast façade, the area exposed to the ambient conditions becomes lower. Furthermore, shading levels from surrounding buildings and terrain are higher on lower floors. Especially during SUM, this can lead to significant reductions in solar heat gains and thus cooling energy demands.

The situation in AUT and WIN (Figure 13b and c) on the other hand is very different. In AUT, the heating energy demands of floors 1–12 are fairly similar, while floor 13 shows demands about 2.4 times as high. In WIN, the differences are slightly less pronounced and the heating energy demand of all investigated scenarios on floor 13 is about 71 % higher than in floors 5–12, the difference to floors 1 and 2 is ca. 104 %. The main reason for this is the additional envelope area of the roof where significant amounts of energy are lost through heat transmission but also infiltration during the heating period.

Certainly, influenced by 22 % less wall surface area, floors 1 and 2 show overall the best energy performance throughout all seasons. In WIN, where the differences in air temperatures at SB1 between the investigated MSs were fairly small and solar heat gains are almost negligible, this difference resulted in about 20 % lower heating energy demands on the 1st floor, compared to the average of floors 5–12. During AUT, however, the 4th floor shows the lowest heating energy demands, mainly because of two reasons. First, it is less shaded towards the south than its lower floors, providing higher solar heat gains. And second, because there is an adjacent building on a part of the northwestern façade, its exposed surface area to ambient conditions is effectively reduced. In SUM, on the other hand, where the

differences in microclimatic conditions between the investigated MSs are significant, the distribution of energy demand among the floors cannot be solely explained by a lower external wall surface of the lower floors. There, the cooling energy is primarily dependent on the microclimatic conditions which showed the largest differences near the ground level.

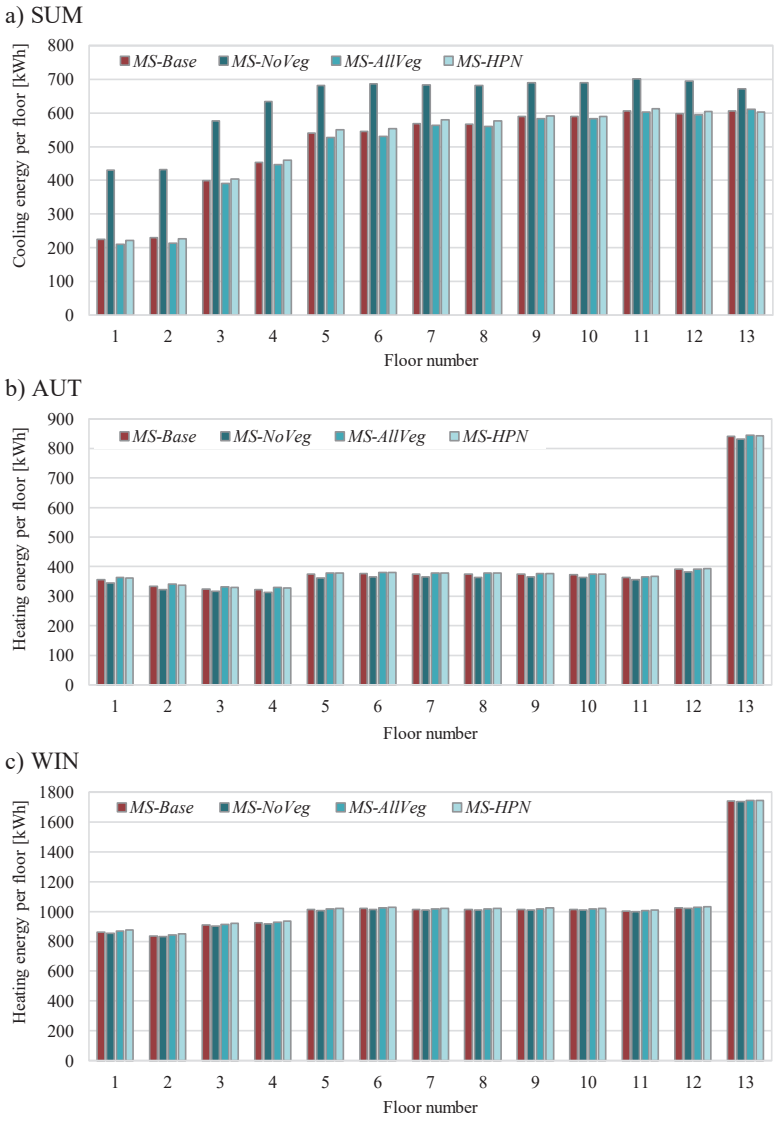

Figure 13: Energy demands of the simulated scenarios in the SPs per floor. a) cooling energy demand in SUM; b) heating energy demand in AUT; c) heating energy demand in WIN.

When simulating SB1 in SUM without an active cooling system, the investigated scenarios can be compared in terms of $N_{T_{op}>26\,°C}$ (see Figure 14), a threshold that is regulated in the Norwegian building code [151]. Similar to the distribution of cooling energy demands, the lowest floors also have the lowest $N_{T_{op}>26\,°C}$. Across all floors and scenarios, values range from 6.8 h on the first floor in *MS-AllVeg*, to 48.8 h on floor 11 in *MS-NoVeg*. While the differences among the investigated scenarios are rather small from floors 5–13 (from 17 % to 40 % between the highest and lowest value on each floor), especially

on the first four floors, *MS-NoVeg* exceeds *MS-AllVeg* by 160 % to 171 %. Floor 13 benefits from the additional envelope area from the roof to cool down during the night which also has a positive effect on the floor below. On both floors, the thermal inertia of the building delays re-exceeding 26 °C during the day when they were effectively cooled down the night before. The mean values of $N_{T_{op}>26\,°C}$ across all floors are 31.5 h, 41.6 h, 29.7 h, and 30.8 h for *MS-Base*, *MS-NoVeg*, *MS-AllVeg*, and *MS-HPN*, respectively.

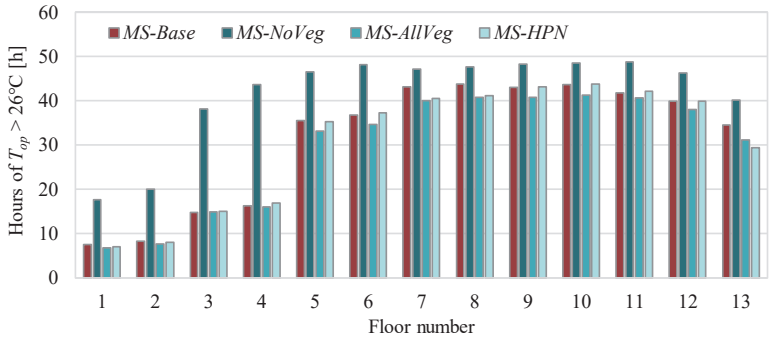

Figure 14: Number of hours above 26 °C for the single floors during SUM, when SB1 is simulated without cooling.

6 Discussion

6.1 Interpretation of results

The presented results show a distinct effect of the urban surface on urban microclimatic conditions and consequently on building energy demands. This effect, however, is inherently linked to the seasonal cycle of meteorological conditions. Especially in the polar and subpolar regions, the shift in meteorological conditions over the year is most significant particularly with regard to the sun, the most dominant source of energy on the Earth's surface. As a consequence, this study showed that the impact of different material compositions of the urban surface on the microclimate is fairly small in winter, even with large-scale modifications like in *MS-NoVeg* or *MS-AllVeg*. The resulting differences in heating energy demand between *MS-Base* and the other three investigated MSs during the simulated week in December were in the range of -0.5 % to +0.8 %. After all, the main difference between concrete and earth with grass as surface materials is the evapotranspiration ability of grass depending on the amount of solar irradiance. Thus, in the absence of solar irradiation, both materials have comparable properties as both concrete and earth (with grass) are relatively heavy, have a similar heat conductivity, and specific heat capacity.

In summer on the other hand, close to the ground surface, the largest differences between the investigated microclimate scenarios occurred. While *MS-AllVeg* might seem to have little effect on reducing the summerly cooling demands or $N_{T_{op}>26\,°C}$, it must be remembered that the city of Trondheim has considerable amounts of green spaces already in the base case scenario. Moreover, the NTNU campus with the investigated building SB1 is surrounded by a green belt with numerous trees

and expansive green areas. Rather than the difference to the base case, the differences between scenarios *MS-NoVeg* and *MS-AllVeg* should be considered. During heat waves such as in SUM in this study, proximity to green spaces which provide significant amounts of evapotranspiration proved to be an effective means to reduce the energy demand for cooling or improve indoor thermal comfort when no cooling system is available. On the 1st floor, an urban surface made of concrete instead of grass doubled cooling energy demands and increased $N_{T_{op}>26\,°C}$ by 160 %. It must be kept in mind that the BPS results in this study are obtained from simulating an office building where internal heat loads are generally rather high. However, the microclimatic conditions resulting from the investigated MSs in the CFD simulations are equally marked and valid for any type of building. Considering the negative impacts on health from cold and heat stress that have been reported even in Scandinavia [19,20,153], accommodations for vulnerable population groups should be preferably on the lower floors of buildings surrounded by expansive green areas. As shown, heat waves will be mitigated while the thermal effects in autumn and winter are relatively small. Nevertheless, especially in the transitional seasons, access to solar radiation can effectively reduce heating demands as unobstructed, south-oriented windows can be net-energy gainers throughout the year [154,155]. However, ensuring solar access on the lower floors of a building in a dense neighborhood in Scandinavia is often challenging outside of the summer months.

Arguably, because summers in Trondheim are relatively short and mild, the investigated week in June 2020 cannot be regarded as typical, nor representative for the season. On the other hand, the investigated summer conditions are more common in South Norway. At the same time, as global temperatures are rising, also Scandinavia will experience periods of extensive heat more and more frequently in the future. Unlike in countries with warmer climates, neither the people nor buildings are adequately prepared for such a development. It is a known problem that well-insulated office buildings suffer from increased cooling demands because heat from internal sources gets trapped inside [87,156]. However, it needs to be kept in mind that only very few buildings in Norway are equipped with cooling systems. Furthermore, opening the windows for natural ventilation purposes is often not an option due to noise from the outside, air pollution from nearby roads, allergies, etc. The generally well-insulated building stock in the Nordic countries is therefore particularly susceptible to overheating. Additionally, it needs to be kept in mind that the simulations in this study were carried out for a rather poorly insulated building. For well-insulated and airtight buildings, even higher cooling energy demands and a more distinct increase of $N_{T_{op}>26\,°C}$ can be expected. At the same time, well-insulated buildings will generally have less benefit from slightly higher outdoor temperatures during the heating season [157]. In other words, the heating energy savings potential for modern, well-insulated, and airtight buildings during the heating season due to slightly warmer microclimatic conditions can be reasonably expected to be even smaller than reported in this study.

An aspect often overlooked is the benefit of greening on mental health and the reduction of stress which has been reported in many studies [158–160]. Particularly in Japan, the concept of *shinrin-yoku* which might be translated as *taking in the forest atmosphere or forest bathing* is a well and long-known method for stress-reduction and relaxation [161,162]. Even from within buildings, briefly viewing natural features like green spaces, trees, birds, etc. through the windows allow people opportunities for so-called *micro-restorative* experiences [163].

Just as important to consider is urban stormwater management. The steadily progressing sealing of the urban surface puts increasing pressure on the public sewage systems as water runoff increases [164,165]. In Norway, not only temperatures are expected to rise due to climate change, but also precipitation levels by about 18 % [166]. Several studies underlined the efficacy of urban green areas to reduce peak runoff levels in urban environments [167,168]. Even the trees themselves contribute to stormwater retention by temporarily withholding a portion of the rainfall in the crowns and directing it down the trunk into the soil and their root network [169,170].

Regarding the investigated *MS-HPN* scenario, improving the envelope insulation properties of the explicitly modeled buildings surrounding SB1 had a noticeable effect both on the air temperature at SB1 and its energy demands. Considering that only a very small fraction of all buildings in Trondheim's urbanized area were taken into account here, the effects of a city-wide building envelope upgrade are expected to be even more apparent. To ensure comparability with the other scenarios, the building envelope of the building of interest was not modified in *MS-HPN*.

6.2 Limitations

The simulations and results presented in this study are subject to several limitations that are important to have in mind. With respect to the CFD simulations, three main limitations apply. First, the CFD model was not validated for the specific simulation periods investigated in this study. However, from its performance in a previous study [120], it can be reasonably assumed that the microclimatic conditions in the present work are predicted with similar accuracy.

Second, no snow, or water runoff/retention properties of the urban surface were considered, as water vapor transfer and evaporation were only indirectly considered (only the thermal effects). For that, the Penman-Monteith equation was applied at grass surfaces and source/sink terms at the trees. Even though it was found that this approach slightly overestimates the cooling flux from grass [120], the effects on the reported cooling energy savings are estimated to be rather small. In the winter SP, the selected week did not feature a snow-covered urban surface which is not generally representative for winter in Trondheim. The latent energy needed for freezing and thawing, as well as its thermal insulation properties, are expected to have considerable influence on the microclimatic conditions which should be investigated in future studies.

Third, geometrical simplifications apply. Trees are only considered in the NTNU campus area and small elements of the urban environment such as bus stops, etc. are omitted. In this study, on the other hand, the flow conditions at the roof level of SB1 are assumed to be only minorly affected by this simplification. Furthermore, all modeled buildings were roughly grouped according to their wall constructions. While in reality, every building has its own characteristic features, including them in a study like the present is an almost impossible task as such data is difficult to acquire. This is especially the case for the privately-owned buildings around the campus. Other limitations of the CFD simulations, for instance regarding the used turbulence model, inlet boundary conditions, etc. can be found in a separate article [120].

At the same time, some limitations apply to the BPS. First of all, only one zone per floor was modeled. Mainly, this decision was governed by the way the Norwegian standards for the dynamic assessment of

indoor climate and energy demand using BPS are defined. The loads and occupancy schedules in the standards might not be realistic in the case of the investigated building, however, no measured data from SB1 was available to be used instead. On the other hand, for the present comparative study, this simplification is not considered to be critical.

Furthermore, the windows were modeled in a way so that they are not opened for natural ventilation because the Norwegian standards do not contain guidelines for it. In reality, opening windows is an easy and fast measure to deal with overheating in buildings. Also, it is questionable how representative the deployed automatic control for the window blinds is. In reality, the blinds are drawn manually and do not follow a rule-based strategy. However, such user behavior is difficult to model and it was not regarded as critical for the purpose of this study.

Lastly, the pressure coefficients were determined as an average value per building façade. As was shown in Figure 9, the distribution of pressure coefficients across a façade is very heterogeneous. Subdividing the single façades into several smaller surfaces would better represent the pressure conditions on the building envelope but also require considerably more modeling work. However, as it is the standard procedure in BPS, it was deemed sufficient not to depart from common practice and façade-averaged pressure coefficients were used in this study.

Finally, there are two general limitations to this study. First, only three one-week periods were simulated which limits the extent to which the actual influence of different urban surface compositions on the microclimate and building energy demands can be estimated over an entire year. Certainly, a whole-year simulation using representative climate data as meteorological input would deliver more conclusive results. But considering the computational expense necessary for annual, dynamic CFD simulations made such an approach in the context of this study unfeasible.

Second, this study pursued a one-way coupling approach of type B. Consequently, no BPS results were fed back to CFD for an iteratively updated solution using more precise input data on the heat fluxes through the building envelope of the investigated building. Again, implementing such a coupling mechanism and interface between the two simulation tools would have required extensive additional modeling work which was not realizable in the context of this study.

7 Conclusion

In this study, unsteady Reynolds-averaged Navier-Stokes CFD simulations with a validated model of the urban area around the NTNU campus in Trondheim, Norway, were carried out for four different compositions of the urban surface and in three different seasons. The specific microclimatic conditions around an office high-rise building at the NTNU campus were extracted from these simulations and used for BPS of the building of interest. The exported variables were air temperature, wind speed, and wind direction. Moreover, façade-averaged pressure coefficients were determined from the CFD simulations and used in BPS.

In summary, the presented results are evidence of the benefits from vast urban greening in Norwegian, coastal climate conditions during a summerly heat wave. A concrete-sealed urban surface led to 28.5 %

higher cooling energy demands compared to an entirely greened urban surface. Especially at the lower floors, the positive effect of evapotranspiration from grass surfaces and trees was noticeable, leading for instance to 51 % savings in cooling energy demand on the 1st floor. The savings potential decreases with increasing floor number but still amounts to 9 % on the 13th floor. During the simulated weeks in autumn and winter, on the other hand, an urban surface entirely composed of concrete surfaces resulted in 3.5 % and 0.9 % lower energy demands for heating in the investigated building compared to intense urban greening. Considering the long winters in Trondheim and probably most of Scandinavia, a few percent of heating energy reduction are expected to add up to higher total energy savings over the year, than high reductions in cooling energy demand during relatively short heat waves.

It was also found that improving the envelope insulation properties of the explicitly modeled buildings surrounding SB1 in the CFD simulations had a noticeable effect both on the air temperature at SB1 and its energy demands in BPS. The simulated energy demands were higher than in the base case scenario by 0.8 %, 0.9 %, and 0.8 % for summer, autumn, and winter, respectively.

The present study underlines the importance of a multi-perspective and interdisciplinary approach in city planning and emphasizes the benefits of urban green for both the built environment and urban dwellers. One-dimensional approaches to create future city districts or redevelop existing neighborhoods do not meet the complex requirements that people inherently pose to an urban environment. The CFD-BPS coupling approach presented in this work only touches upon this complexity by highlighting the far-reaching interactions between the urban fabric, urban microclimate, and building energy demand.

This study demonstrates that the common approach in BPS to use weather data from far-away airports does not consider the extremely important effects of the local urban surface on the location-specific climate data. Particularly considering the vast and open concrete surfaces at an airport, the validity of using such weather files must be fundamentally questioned if used in entirely different settings. However, high-quality and statistically representative annual weather datasets including all relevant climate variables are rarely available for the exact location of interest, and the common time and financial budgets in ordinary building projects do not allow for applying a CFD-BPS coupling strategy as presented in this study due to its complexity. While it might not be realistic that this approach will be used in general practice soon, it is extremely important to spread knowledge about local climatic effects on the building energy performance and equally important both indoor and outdoor thermal comfort for urban dwellers. Furthermore, studies like the present are important for understanding observed effects and developing new, simpler, and quicker analysis methods. Future studies should consider longer simulation periods, improved coupling strategies, and above all implement water vapor transfer and snow-covered surfaces into the CFD simulations where the climatic circumstances of the investigated location demand it.

8 Acknowledgments

This paper has been written within the Research Centre on Zero Emission Neighbourhoods in Smart Cities (FME ZEN). The authors gratefully acknowledge the support from the ZEN partners and the Research Council of Norway. The simulations were performed on resources provided by UNINETT

Sigma2 - the National Infrastructure for High Performance Computing and Data Storage in Norway. The sea surface temperature data of the Sentinel-3 Sea and Land Surface Temperature Radiometer was provided by EUMETSAT in the Sentinel-3 Marine Copernicus Online Data Access (CODA) Web Service (https://coda.eumetsat.int/). Images from ANSYS Fluent used courtesy of ANSYS, Inc. The first author of this paper gratefully acknowledges the valuable discussions with Christoph Nickl and the useful inputs he provided.

9 References

[1] Edenhofer O (ed.). Climate change 2014: Mitigation of climate change Working Group III contribution to the Fifth Assessment Report of the Intergovernmental Panel on Climate Change. New York (USA): Cambridge University Press; 2014.

[2] United Nations, Department of Economic and Social Affairs, Population Division. World Urbanization Prospects: The 2018 Revision. Online Edition. New York, USA; 2018.

[3] Global Alliance for Buildings and Construction, International Energy Agency, United Nations Environment Programme. 2019 Global Status Report for Buildings and Construction: Towards a zero-emissions, efficient and resilient buildings and construction sector; 2019.

[4] United Nations. Transforming Our World: The 2030 Agenda For Sustainable Development; 2015.

[5] Barriopedro D, Fischer EM, Luterbacher J, Trigo RM, Garcia-Herrera R. The Hot Summer of 2010: Redrawing the Temperature Record Map of Europe. Science 2011;332(6026):220–4. https://doi.org/10.1126/science.1201045.

[6] Meehl GA, Tebaldi C. More intense, more frequent, and longer lasting heat waves in the 21st century. Science 2004;305(5686):994–7. https://doi.org/10.1126/science.1098704.

[7] Perkins-Kirkpatrick SE, Gibson PB. Changes in regional heatwave characteristics as a function of increasing global temperature. Sci Rep 2017;7(1):12256. https://doi.org/10.1038/s41598-017-12520-2.

[8] Oke TR, Mills G, Christen A, Voogt JA. Urban climates. Cambridge: Cambridge University Press; 2017.

[9] Steeneveld GJ, Koopmans S, Heusinkveld BG, van Hove LWA, Holtslag AAM. Quantifying urban heat island effects and human comfort for cities of variable size and urban morphology in the Netherlands. J Geophys Res 2011;116(D20):94. https://doi.org/10.1029/2011JD015988.

[10] Watkins R, Palmer J, Kolokotroni M. Increased Temperature and Intensification of the Urban Heat Island: Implications for Human Comfort and Urban Design. Built Environ 2007;33(1):85–96. https://doi.org/10.2148/benv.33.1.85.

[11] Urban A, Davídkovová H, Kyselý J. Heat- and cold-stress effects on cardiovascular mortality and morbidity among urban and rural populations in the Czech Republic. Int J Biometeorol 2014;58(6):1057–68. https://doi.org/10.1007/s00484-013-0693-4.

[12] D'Ippoliti D, Michelozzi P, Marino C, de'Donato F, Menne B, Katsouyanni K et al. The impact of heat waves on mortality in 9 European cities: results from the EuroHEAT project. Environ Health 2010;9:37. https://doi.org/10.1186/1476-069X-9-37.

[13] Davies M, Steadman P, Oreszczyn T. Strategies for the modification of the urban climate and the consequent impact on building energy use. Energy Policy 2008;36(12):4548–51. https://doi.org/10.1016/j.enpol.2008.09.013.
[14] Kolokotroni M, Giannitsaris I, Watkins R. The effect of the London urban heat island on building summer cooling demand and night ventilation strategies. Sol Energy 2006;80(4):383–92. https://doi.org/10.1016/j.solener.2005.03.010.
[15] Vardoulakis E, Karamanis D, Fotiadi A, Mihalakakou G. The urban heat island effect in a small Mediterranean city of high summer temperatures and cooling energy demands. Solar Energy 2013;94:128–44. https://doi.org/10.1016/j.solener.2013.04.016.
[16] Brozovsky J, Gaitani N, Gustavsen A. A systematic review of urban microclimate in cold and polar climate regions. Renew Sustain Energy Rev 2021;138. https://doi.org/10.1016/j.rser.2020.110551.
[17] Miles V, Esau I. Surface urban heat islands in 57 cities across different climates in northern Fennoscandia. Urban Clim 2020;31:100575. https://doi.org/10.1016/j.uclim.2019.100575.
[18] Esau I, Miles V, Soromotin A, Sizov O, Varentsov M, Konstantinov P. Urban heat islands in the Arctic cities: an updated compilation of in situ and remote-sensing estimations. Adv. Sci. Res. 2021;18:51–7. https://doi.org/10.5194/asr-18-51-2021.
[19] Venter ZS, Krog NH, Barton DN. Linking green infrastructure to urban heat and human health risk mitigation in Oslo, Norway. Sci Total Environ 2020;709:136193. https://doi.org/10.1016/j.scitotenv.2019.136193.
[20] Oudin Åström D, Åström C, Forsberg B, Vicedo-Cabrera AM, Gasparrini A, Oudin A et al. Heat wave-related mortality in Sweden: A case-crossover study investigating effect modification by neighbourhood deprivation. Scand J Public Health 2020;48(4):428–35. https://doi.org/10.1177/1403494818801615.
[21] IEA - International Energy Agency. The Future of Cooling; 2018.
[22] Lowe SA. An energy and mortality impact assessment of the urban heat island in the US. Environ Impact Assess Rev 2016;56:139–44. https://doi.org/10.1016/j.eiar.2015.10.004.
[23] Yang J, Bou-Zeid E. Should Cities Embrace Their Heat Islands as Shields from Extreme Cold? J Appl Meteorol Climatol 2018;57(6):1309–20. https://doi.org/10.1175/JAMC-D-17-0265.1.
[24] Klimenko VV, Ginzburg AS, Demchenko PF, Tereshin AG, Belova IN, Kasilova EV. Impact of urbanization and climate warming on energy consumption in large cities. Dokl Phys 2016;61(10):521–5. https://doi.org/10.1134/S1028335816100050.
[25] Meng F, Guo J, Ren G, Zhang L, Zhang R. Impact of urban heat island on the variation of heating loads in residential and office buildings in Tianjin. Energy and Buildings 2020;226:110357. https://doi.org/10.1016/j.enbuild.2020.110357.
[26] Ding F, Pang H, Guo W. Impact of the urban heat island on residents' energy consumption: a case study of Qingdao. IOP Conf. Ser.: Earth Environ. Sci. 2018;121:32026. https://doi.org/10.1088/1755-1315/121/3/032026.
[27] Mohajerani A, Bakaric J, Jeffrey-Bailey T. The urban heat island effect, its causes, and mitigation, with reference to the thermal properties of asphalt concrete. J Environ Manage 2017;197:522–38. https://doi.org/10.1016/j.jenvman.2017.03.095.
[28] Oke TR. The energetic basis of the urban heat island. Q J Roy Meteorol Soc 1982;108(455):1–24. https://doi.org/10.1002/qj.49710845502.

[29] Mills G. Urban climatology: History, status and prospects. Urban Clim 2014;10:479–89. https://doi.org/10.1016/j.uclim.2014.06.004.
[30] Toparlar Y, Blocken B, Maiheu B, van Heijst G. A review on the CFD analysis of urban microclimate. Renew Sustain Energy Rev 2017;80:1613–40. https://doi.org/10.1016/j.rser.2017.05.248.
[31] Mirzaei PA, Haghighat F. Approaches to study Urban Heat Island – Abilities and limitations. Build Environ 2010;45(10):2192–201. https://doi.org/10.1016/j.buildenv.2010.04.001.
[32] Orlanski I. A Rational Subdivision of Scales for Atmospheric Processes. Bull Amer Meteor Soc 1975;56(5):527–30.
[33] Blocken B, Janssen WD, van Hooff T. CFD simulation for pedestrian wind comfort and wind safety in urban areas: General decision framework and case study for the Eindhoven University campus. Environ Model Softw 2012;30:15–34. https://doi.org/10.1016/j.envsoft.2011.11.009.
[34] Blocken B, Persoon J. Pedestrian wind comfort around a large football stadium in an urban environment: CFD simulation, validation and application of the new Dutch wind nuisance standard. J Wind Eng Ind Aerodyn 2009;97(5-6):255–70. https://doi.org/10.1016/j.jweia.2009.06.007.
[35] Blocken B, Roels S, Carmeliet J. Modification of pedestrian wind comfort in the Silvertop Tower passages by an automatic control system. J Wind Eng Ind Aerodyn 2004;92(10):849–73. https://doi.org/10.1016/j.jweia.2004.04.004.
[36] Janssen WD, Blocken B, van Hooff T. Pedestrian wind comfort around buildings: Comparison of wind comfort criteria based on whole-flow field data for a complex case study. Build Environ 2013;59:547–62. https://doi.org/10.1016/j.buildenv.2012.10.012.
[37] Fadl MS, Karadelis J. CFD Simulation for Wind Comfort and Safety in Urban Area: A Case Study of Coventry University Central Campus. Int J Archit Eng Constr 2013;2(2):131–43. https://doi.org/10.7492/IJAEC.2013.013.
[38] Gromke C, Blocken B. Influence of avenue-trees on air quality at the urban neighborhood scale. Part I: quality assurance studies and turbulent Schmidt number analysis for RANS CFD simulations. Environ Pollut 2015;196:214–23. https://doi.org/10.1016/j.envpol.2014.10.016.
[39] Gromke C, Blocken B. Influence of avenue-trees on air quality at the urban neighborhood scale. Part II: traffic pollutant concentrations at pedestrian level. Environ Pollut 2015;196:176–84. https://doi.org/10.1016/j.envpol.2014.10.015.
[40] Amorim JH, Rodrigues V, Tavares R, Valente J, Borrego C. CFD modelling of the aerodynamic effect of trees on urban air pollution dispersion. Sci Total Environ 2013;461-462:541–51. https://doi.org/10.1016/j.scitotenv.2013.05.031.
[41] Gousseau P, Blocken B, Stathopoulos T, van Heijst G. CFD simulation of near-field pollutant dispersion on a high-resolution grid: A case study by LES and RANS for a building group in downtown Montreal. Atmos Environ 2011;45(2):428–38. https://doi.org/10.1016/j.atmosenv.2010.09.065.
[42] Blocken B, Carmeliet J. The influence of the wind-blocking effect by a building on its wind-driven rain exposure. J Wind Eng Ind Aerodyn 2006;94(2):101–27. https://doi.org/10.1016/j.jweia.2005.11.001.

[43] Blocken B, Carmeliet J. Validation of CFD simulations of wind-driven rain on a low-rise building facade. Build Environ 2007;42(7):2530–48. https://doi.org/10.1016/j.buildenv.2006.07.032.
[44] van Hooff T, Blocken B, van Harten M. 3D CFD simulations of wind flow and wind-driven rain shelter in sports stadia: Influence of stadium geometry. Build Environ 2011;46(1):22–37. https://doi.org/10.1016/j.buildenv.2010.06.013.
[45] Chen H, Ooka R, Harayama K, Kato S, Li X. Study on outdoor thermal environment of apartment block in Shenzhen, China with coupled simulation of convection, radiation and conduction. Energy Build 2004;36(12):1247–58. https://doi.org/10.1016/j.enbuild.2003.07.003.
[46] Ma J, Li X, Zhu Y. A simplified method to predict the outdoor thermal environment in residential district. Build. Simul. 2012;5(2):157–67. https://doi.org/10.1007/s12273-012-0079-2.
[47] Targhi MZ, van Dessel S. Potential Contribution of Urban Developments to Outdoor Thermal Comfort Conditions: The Influence of Urban Geometry and Form in Worcester, Massachusetts, USA. Proc Eng 2015;118:1153–61. https://doi.org/10.1016/j.proeng.2015.08.457.
[48] Karakounos I, Dimoudi A, Zoras S. The influence of bioclimatic urban redevelopment on outdoor thermal comfort. Energy Build 2018;158:1266–74. https://doi.org/10.1016/j.enbuild.2017.11.035.
[49] Taleghani M, Berardi U. The effect of pavement characteristics on pedestrians' thermal comfort in Toronto. Urban Clim 2018;24:449–59. https://doi.org/10.1016/j.uclim.2017.05.007.
[50] Ghaffarianhoseini A, Berardi U, Ghaffarianhoseini A, Al-Obaidi K. Analyzing the thermal comfort conditions of outdoor spaces in a university campus in Kuala Lumpur, Malaysia. Sci Total Environ 2019;666:1327–45. https://doi.org/10.1016/j.scitotenv.2019.01.284.
[51] Huang H, Ooka R, Kato S. Urban thermal environment measurements and numerical simulation for an actual complex urban area covering a large district heating and cooling system in summer. Atmos Environ 2005;39(34):6362–75. https://doi.org/10.1016/j.atmosenv.2005.07.018.
[52] Lee H, Mayer H, Chen L. Contribution of trees and grasslands to the mitigation of human heat stress in a residential district of Freiburg, Southwest Germany. Landsc Urban Plan 2016;148:37–50. https://doi.org/10.1016/j.landurbplan.2015.12.004.
[53] Qaid A, Bin Lamit H, Ossen DR, Raja Shahminan RN. Urban heat island and thermal comfort conditions at micro-climate scale in a tropical planned city. Energy Build 2016;133:577–95. https://doi.org/10.1016/j.enbuild.2016.10.006.
[54] Salata F, Golasi I, Vollaro AdL, Vollaro RdL. How high albedo and traditional buildings' materials and vegetation affect the quality of urban microclimate. A case study. Energy Build 2015;99:32–49. https://doi.org/10.1016/j.enbuild.2015.04.010.
[55] Brozovsky J, Corio S, Gaitani N, Gustavsen A. Evaluation of sustainable strategies and design solutions at high-latitude urban settlements to enhance outdoor thermal comfort. Energy Build 2021;244(12):111037. https://doi.org/10.1016/j.enbuild.2021.111037.
[56] Benra F-K, Dohmen HJ, Pei J, Schuster S, Wan B. A Comparison of One-Way and Two-Way Coupling Methods for Numerical Analysis of Fluid-Structure Interactions. Journal of Applied Mathematics 2011;2011(6):1–16. https://doi.org/10.1155/2011/853560.
[57] Djunaedy E, Hensen J, Loomans M. External Coupling between CFD and Energy Simulation: Implementation and Validation. ASHRAE Transactions 2005;111(1):612–24.

[58] Zhai ZJ, Chen QY. Performance of coupled building energy and CFD simulations. Energy Build 2005;37(4):333–44. https://doi.org/10.1016/j.enbuild.2004.07.001.

[59] Kong Q, Feng J, Yang C, Miao Z, He X. Numerical Simulation of a Radiant Floor Cooling Office Based on CFD-BES Coupling and FEM. Energy Procedia 2017;105(1):3577–83. https://doi.org/10.1016/j.egypro.2017.03.825.

[60] Barbason M, Reiter S. Coupling building energy simulation and computational fluid dynamics: Application to a two-storey house in a temperate climate. Build Environ 2014;75:30–9. https://doi.org/10.1016/j.buildenv.2014.01.012.

[61] Fan Y, Ito K. Optimization of indoor environmental quality and ventilation load in office space by multilevel coupling of building energy simulation and computational fluid dynamics. Build. Simul. 2014;7(6):649–59. https://doi.org/10.1007/s12273-014-0178-3.

[62] Tian W, Han X, Zuo W, Sohn MD. Building energy simulation coupled with CFD for indoor environment: A critical review and recent applications. Energy Build 2018;165:184–99. https://doi.org/10.1016/j.enbuild.2018.01.046.

[63] Shan X, Luo N, Sun K, Hong T, Lee Y-K, Lu W-Z. Coupling CFD and building energy modelling to optimize the operation of a large open office space for occupant comfort. Sustainable Cities and Society 2020;60(3):102257. https://doi.org/10.1016/j.scs.2020.102257.

[64] Gracik S, Heidarinejad M, Liu J, Srebric J. Effect of urban neighborhoods on the performance of building cooling systems. Building and Environment 2015;90(1–2):15–29. https://doi.org/10.1016/j.buildenv.2015.02.037.

[65] Hadavi M, Pasdarshahri H. Investigating effects of urban configuration and density on urban climate and building systems energy consumption. J Build Eng 2021. https://doi.org/10.1016/j.jobe.2021.102710.

[66] U.S. Department of Energy. EnergyPlus Version 9.5.0 Documentation: Engineering Reference; 2021.

[67] Bouyer J, Inard C, Musy M. Microclimatic coupling as a solution to improve building energy simulation in an urban context. Energy Build 2011;43(7):1549–59. https://doi.org/10.1016/j.enbuild.2011.02.010.

[68] Malys L, Musy M, Inard C. Microclimate and building energy consumption: study of different coupling methods. Advances in Building Energy Research 2015;9(2):151–74. https://doi.org/10.1080/17512549.2015.1043643.

[69] Gros A, Bozonnet E, Inard C, Musy M. Simulation tools to assess microclimate and building energy – A case study on the design of a new district. Energy Build 2016;114(4):112–22. https://doi.org/10.1016/j.enbuild.2015.06.032.

[70] Morille B, Musy M, Malys L. Preliminary study of the impact of urban greenery types on energy consumption of building at a district scale: Academic study on a canyon street in Nantes (France) weather conditions. Energy Build 2016;114(7):275–82. https://doi.org/10.1016/j.enbuild.2015.06.030.

[71] Merlier L, Frayssinet L, Kuznik F, Rusaouën G, Johannes K, Hubert J-L et al. Analysis of the (urban) microclimate effects on the building energy behaviour. Proc. 13th Int. Build. Perform. Simul. Assoc. (Chambéry, France) (Proceedings of BS2017: 11th Conference of International Building Performance Simulation Association in San Francisco, USA, Aug 7-19) 2017.

[72] Zhang R, Mirzaei PA, Jones B. Development of a dynamic external CFD and BES coupling framework for application of urban neighbourhoods energy modelling. Build Environ 2018;146:37–49. https://doi.org/10.1016/j.buildenv.2018.09.006.
[73] Zhang R, Mirzaei PA. Fast and dynamic urban neighbourhood energy simulation using CFDf-CFDc-BES coupling method. Sustainable Cities and Society 2021;66(9):102545. https://doi.org/10.1016/j.scs.2020.102545.
[74] Zhang R, Mirzaei PA. Virtual dynamic coupling of computational fluid dynamics-building energy simulation-artificial intelligence: Case study of urban neighbourhood effect on buildings' energy demand. Building and Environment 2021;195(8–9):107728. https://doi.org/10.1016/j.buildenv.2021.107728.
[75] Yang X, Zhao L, Bruse M, Meng Q. An integrated simulation method for building energy performance assessment in urban environments. Energy Build 2012;54:243–51. https://doi.org/10.1016/j.enbuild.2012.07.042.
[76] Yi YK, Feng N. Dynamic integration between building energy simulation (BES) and computational fluid dynamics (CFD) simulation for building exterior surface. Build. Simul. 2013;6(3):297–308. https://doi.org/10.1007/s12273-013-0116-9.
[77] Liu J, Heidarinejad M, Guo M, Srebric J. Numerical Evaluation of the Local Weather Data Impacts on Cooling Energy Use of Buildings in an Urban Area. Procedia Engineering 2015;121:381–8. https://doi.org/10.1016/j.proeng.2015.08.1082.
[78] Skelhorn CP, Levermore G, Lindley SJ. Impacts on cooling energy consumption due to the UHI and vegetation changes in Manchester, UK. Energy Build 2016;122:150–9. https://doi.org/10.1016/j.enbuild.2016.01.035.
[79] Gobakis K, Kolokotsa D. Coupling building energy simulation software with microclimatic simulation for the evaluation of the impact of urban outdoor conditions on the energy consumption and indoor environmental quality. Energy Build 2017;157(54):101–15. https://doi.org/10.1016/j.enbuild.2017.02.020.
[80] Huang K-T, Li Y-J. Impact of street canyon typology on building's peak cooling energy demand: A parametric analysis using orthogonal experiment. Energy Build 2017;154(6):448–64. https://doi.org/10.1016/j.enbuild.2017.08.054.
[81] Javanroodi K, Nik VM. Impacts of Microclimate Conditions on the Energy Performance of Buildings in Urban Areas. Buildings 2019;9(8):189. https://doi.org/10.3390/buildings9080189.
[82] Liu J, Heidarinejad M, Nikkho SK, Mattise NW, Srebric J. Quantifying Impacts of Urban Microclimate on a Building Energy Consumption—A Case Study. Sustainability 2019;11(18):4921. https://doi.org/10.3390/su11184921.
[83] Natanian J, Maiullari D, Yezioro A, Auer T. Synergetic urban microclimate and energy simulation parametric workflow. J. Phys.: Conf. Ser. 2019;1343:12006. https://doi.org/10.1088/1742-6596/1343/1/012006.
[84] Shirzadi M, Naghashzadegan M, Mirzaei PA. Developing a framework for improvement of building thermal performance modeling under urban microclimate interactions. Sustainable Cities and Society 2019;44:27–39. https://doi.org/10.1016/j.scs.2018.09.016.
[85] Mosteiro-Romero M, Maiullari D, Pijpers-van Esch M, Schlueter A. An Integrated Microclimate-Energy Demand Simulation Method for the Assessment of Urban Districts. Front. Built Environ. 2020;6:94. https://doi.org/10.3389/fbuil.2020.553946.

[86] Shen P, Wang Z. How neighborhood form influences building energy use in winter design condition: Case study of Chicago using CFD coupled simulation. Journal of Cleaner Production 2020;261(12):121094. https://doi.org/10.1016/j.jclepro.2020.121094.
[87] Toparlar Y, Blocken B, Maiheu B, van Heijst G. Impact of urban microclimate on summertime building cooling demand: A parametric analysis for Antwerp, Belgium. Appl Energy 2018;228:852–72. https://doi.org/10.1016/j.apenergy.2018.06.110.
[88] Allegrini J, Kämpf J, Dorer V, Carmeliet J. Modelling the urban microclimate and its influence on building energy demands of an urban neighbourhood. Proceedings of CISBAT 2013 Vol. II: International Conference Cleantech for Smart Cities & Buildings from Nano to Urban Scale in Lausanne, Switzerland, September 4-6 2013:867–72.
[89] Allegrini J, Dorer V, Carmeliet J. Coupled CFD, radiation and building energy model for studying heat fluxes in an urban environment with generic building configurations. Sustainable Cities and Society 2015;19(2):385–94. https://doi.org/10.1016/j.scs.2015.07.009.
[90] Allegrini J, Dorer V, Carmeliet J. Influence of morphologies on the microclimate in urban neighbourhoods. J Wind Eng Ind Aerodyn 2015;144:108–17. https://doi.org/10.1016/j.jweia.2015.03.024.
[91] Allegrini J, Carmeliet J. Coupled CFD and building energy simulations for studying the impacts of building height topology and buoyancy on local urban microclimates. Urban Climate 2017;21(2):278–305. https://doi.org/10.1016/j.uclim.2017.07.005.
[92] Allegrini J, Carmeliet J. Simulations of local heat islands in Zürich with coupled CFD and building energy models. Urban Clim 2018;24:340–59. https://doi.org/10.1016/j.uclim.2017.02.003.
[93] Hadavi M, Pasdarshahri H. Impacts of urban buildings on microclimate and cooling systems efficiency: Coupled CFD and BES simulations. Sustainable Cities and Society 2021;67(7):102740. https://doi.org/10.1016/j.scs.2021.102740.
[94] Wong NH, He Y, Nguyen NS, Raghavan SV, Martin M, Hii DJC et al. An integrated multiscale urban microclimate model for the urban thermal environment. Urban Climate 2021;35(4):100730. https://doi.org/10.1016/j.uclim.2020.100730.
[95] Chen G, Rong L, Zhang G. Comparison of urban airflow between solar-induced thermal wall and uniform wall temperature boundary conditions by coupling CitySim and CFD. Build Environ 2020;172. https://doi.org/10.1016/j.buildenv.2020.106732.
[96] Statistisk sentralbyrå. Kommunefakta Trondheim; Available from: https://www.ssb.no/kommunefakta/trondheim.
[97] Stewart ID, Oke TR. Local Climate Zones for Urban Temperature Studies. Bull Amer Meteor Soc 2012;93(12):1879–900. https://doi.org/10.1175/BAMS-D-11-00019.1.
[98] Wieringa J. Updating the Davenport roughness classification. J Wind Eng Ind Aerodyn 1992;41(1-3):357–68. https://doi.org/10.1016/0167-6105(92)90434-C.
[99] Peel MC, Finlayson BL, McMahon TA. Updated world map of the Köppen-Geiger climate classification. Hydrol Earth Syst Sci Discuss 2007;4(2):439–73. https://doi.org/10.5194/hessd-4-439-2007.
[100] Lundstad E, Tveito OE. Homogenization of daily mean temperature in Norway; 2016.
[101] Meteorologisk Institutt. eKlima: Free access to weather- and climate data from Norwegian Meteorological Institute from historical data to real time observations. Normals; Available from:

http://sharki.oslo.dnmi.no/portal/page?_pageid=73,39035,73_39049&_dad=portal&_schema=PORTAL.

[102] Palter JB. The role of the Gulf Stream in European climate. Ann Rev Mar Sci 2015;7:113–37. https://doi.org/10.1146/annurev-marine-010814-015656.

[103] Antoniou N, Montazeri H, Neophytou M, Blocken B. CFD simulation of urban microclimate: Validation using high-resolution field measurements. Sci Total Environ 2019;695:133743. https://doi.org/10.1016/j.scitotenv.2019.133743.

[104] Toparlar Y, Blocken B, Vos PEJ, van Heijst G, Janssen WD, van Hooff T et al. CFD simulation and validation of urban microclimate: A case study for Bergpolder Zuid, Rotterdam. Build Environ 2015;83:79–90. https://doi.org/10.1016/j.buildenv.2014.08.004.

[105] Bring A, Sahlin P, Vuolle M. Models for Building Indoor Climate and Energy Simulation: A Report of IEA SHC Task 22: Building Energy Analysis Tools, Subtask B: Model Documentation; 1999.

[106] Björsell N, Bring A, Eriksson L, Grozman P, Lindgren M, Sahlin P et al. IDA Indoor Climate and Energy. Proceedings of the 6th International IBPSA Conference in Kyoto, Japan 1999.

[107] Equa Simulation AB. Validation of IDA Indoor Climate and Energy 4.0 build 4 with respect to ANSI/ASHRAE Standard 140-2004; 2010.

[108] Equa Simulation AB, Equa Simulation Finland Oy. Validation of IDA Indoor Climate and Energy 4.0 with respect to CEN Standards EN 15255-2007 and EN 15265-2007; 2010.

[109] Moosberger S. IDA ICE CIBSE-Validation: Test of IDA Indoor Climate and Energy version 4.0 according to CIBSE TM33, issue 3; 2007.

[110] Catto Lucchino E, Gelesz A, Skeie K, Gennaro G, Reith A, Serra V et al. Modelling double skin façades (DSFs) in whole-building energy simulation tools: Validation and inter-software comparison of a mechanically ventilated single-story DSF. Build Environ 2021;199:107906. https://doi.org/10.1016/j.buildenv.2021.107906.

[111] Gelesz A, Catto Lucchino E, Goia F, Serra V, Reith A. Characteristics that matter in a climate façade: A sensitivity analysis with building energy simulation tools. Energy and Buildings 2020;229:110467. https://doi.org/10.1016/j.enbuild.2020.110467.

[112] Nilsson E, Rohdin P. Empirical Validation and Numerical Predictions of an Industrial Borehole Thermal Energy Storage System. Energies 2019;12(12):2263. https://doi.org/10.3390/en12122263.

[113] Clauß J, Stinner S, Sartori I, Georges L. Predictive rule-based control to activate the energy flexibility of Norwegian residential buildings: Case of an air-source heat pump and direct electric heating. Appl Energy 2019;237:500–18. https://doi.org/10.1016/j.apenergy.2018.12.074.

[114] Clauß J, Georges L. Model complexity of heat pump systems to investigate the building energy flexibility and guidelines for model implementation. Appl Energy 2019;255:113847. https://doi.org/10.1016/j.apenergy.2019.113847.

[115] Blocken B, Carmeliet J, Stathopoulos T. CFD evaluation of wind speed conditions in passages between parallel buildings—effect of wall-function roughness modifications for the atmospheric boundary layer flow. J Wind Eng Ind Aerodyn 2007;95(9-11):941–62. https://doi.org/10.1016/j.jweia.2007.01.013.

[116] Blocken B, Moonen P, Stathopoulos T, Carmeliet J. Numerical Study on the Existence of the Venturi Effect in Passages between Perpendicular Buildings. J Eng Mech 2008;134(12):1021–8.

[117] Blocken B, Stathopoulos T, Carmeliet J. Wind Environmental Conditions in Passages between Two Long Narrow Perpendicular Buildings. J. Aerosp. Eng. 2008;21(4):280–7. https://doi.org/10.1061/(ASCE)0893-1321(2008)21:4(280).

[118] Liddament MW. Air Infiltration Calculation Techniques - An application guide. Coventry (UK); 1986.

[119] Cóstola D, Blocken B, Hensen J. Overview of pressure coefficient data in building energy simulation and airflow network programs. Build Environ 2009;44(10):2027–36. https://doi.org/10.1016/j.buildenv.2009.02.006.

[120] Brozovsky J, Simonsen A, Gaitani N. Validation of a CFD model for the evaluation of urban microclimate at high latitudes: A case study in Trondheim, Norway. Build Environ 2021;205:108175. https://doi.org/10.1016/j.buildenv.2021.108175.

[121] Franke J, Hirsch C, Jensen AG, Krüs HW, Schatzmann M, Westbury PS et al. Recommendations on the Use of CFD in Wind Engineering. Proc. Int. Conf. Urban Wind Engineering and Building Aerodynamics. COST Action C14, Impact of Wind and Storm on City Life Built Environment, von Karman Institute, Sint-Genesius-Rode, Belgium May 5-7 2004.

[122] Tominaga Y, Mochida A, Yoshie R, Kataoka H, Nozu T, Yoshikawa M et al. AIJ guidelines for practical applications of CFD to pedestrian wind environment around buildings. J Wind Eng Ind Aerodyn 2008;96(10-11):1749–61. https://doi.org/10.1016/j.jweia.2008.02.058.

[123] Shih T-H, Liou WW, Shabbir A, Yang Z, Zhu J. A New k-ε Viscosity Model For High Reynolds Number Turbulent Flows. Comput. Fluids (Computers & Fluids) 1995;24(3):227–38. https://doi.org/10.1016/0045-7930(94)00032-T.

[124] Ntinas GK, Shen X, Wang Y, Zhang G. Evaluation of CFD turbulence models for simulating external airflow around varied building roof with wind tunnel experiment. Build. Simul. 2018;11(1):115–23. https://doi.org/10.1007/s12273-017-0369-9.

[125] Toparlar Y, Blocken B, Maiheu B, van Heijst GJF. The effect of an urban park on the microclimate in its vicinity: a case study for Antwerp, Belgium. Int J Climatol 2018;38(2):e303-e322. https://doi.org/10.1002/joc.5371.

[126] Skartveit A, Olseth JA. A Model for the Diffuse Fraction of Hourly Global Radiation. Sol Energy 1987;38(4):271–4.

[127] ANSYS Inc. ANSYS Fluent Theory Guide: Release 2020 R1 January 2020. Canonsburg, PA; 2020.

[128] ANSYS Inc. Fluent User's Guide: Release 2020 R1 January 2020. Canonsburg, PA; 2020.

[129] van Doormaal JP, Raithby GD. Enhancements of the SIMPLE Method for Predicting Incompressible Fluid Flows. Numer Heat Transf 1984;7(2):147–63. https://doi.org/10.1080/01495728408961817.

[130] Blocken B, Stathopoulos T, Carmeliet J. CFD simulation of the atmospheric boundary layer: wall function problems. Atmos Environ 2007;41(2):238–52. https://doi.org/10.1016/j.atmosenv.2006.08.019.

[131] Launder BE, Spalding DB. The Numerical Computation of Turbulent Flows. Comput Meth Appl Mech Eng 1974;3(2):269–89. https://doi.org/10.1016/0045-7825(74)90029-2.

[132] Santamouris M (ed.). Environmental design of urban buildings: An integrated approach. London: Earthscan; 2006.

[133] Goris A, Schneider K-J, Albert A (eds.). Bautabellen für Ingenieure: Mit Berechnungshinweisen und Beispielen. 19th ed. Neuwied, Köln: Werner; Wolters Kluwer; 2010.
[134] Jones HG. Plants and Microclimate: A Quantitative Approach to Environmental Plant Physiology. 3rd ed. Cambridge: Cambridge University Press; 2013.
[135] Penman HL. The Physical Bases of Irrigation Control. Report of the 13th International Horticultural Congress 1953:1–13.
[136] Monteith JL. Evaporation and environment. Symp Soc Exp Biol 1965;19:205–34.
[137] Food and Agriculture Organisation of the United Nations. Crop evapotranspiration: Guidelines for computing crop water requirements. FAO Irrigation and drainage paper 56. [December 10, 2020]; Available from: http://www.fao.org/3/X0490E/x0490e00.htm#Contents.
[138] Green SR. Modelling turbulent air flow in stand of widely-spaced trees. Phoenics J. 1992;5:294–312.
[139] Liu J, Chen J, Black TA, Novak MD. E-ε Modelling of Turbulent Air Flow Downwind of a Model Forest Edge. Bound-Layer Meteorol. 1996;77(1):21–44.
[140] Sanz C. A Note on k-ε Modelling of Vegetation Canopy Air-Flows. Bound-Layer Meteorol. 2003;108:191–7. https://doi.org/10.1023/A:1023066012766.
[141] Jensen ME, Haise HR. Estimating Evapotranspiration from Solar Radiation. Proceedings of the American Society of Civil Engineers, Journal of the Irrigation and Drainage Division 1963;89:15–41.
[142] Huang YJ, Akbari H, Taha H, Rosenfeld A. The Potential of Vegetation in Reducing Summer Cooling Loads in Residential Buildings. J. Clim. Adv. Meteorol. 1987;26(9):1103–16. https://doi.org/10.1175/1520-0450(1987)026<1103:TPOVIR>2.0.CO;2.
[143] Buccolieri R, Santiago J-L, Rivas E, Sanchez B. Review on urban tree modelling in CFD simulations: Aerodynamic, deposition and thermal effects. Urban For Urban Green 2018;31:212–20. https://doi.org/10.1016/j.ufug.2018.03.003.
[144] Richards PJ, Hoxey RP. Appropriate boundary conditions for computational wind engineering models using the k-ε turbulence model. J Wind Eng Ind Aerodyn 1993;46 & 47:145–53.
[145] Wieringa J. Roughness-dependent geographical interpolation of surface wind speed averages. Q J Roy Meteorol Soc 1986;112:867–89.
[146] Swinbank WC. Long-wave radiation from clear skies. Q J Roy Meteorol Soc 1963;89(381):339–48.
[147] SN-NSPEK 3031:2020. Energy performance of buildings: Calculation of energy needs and energy supply;01.040.91; 91.120.10: Standard Norge.
[148] NS 3031:2014. Calculation of energy performance of buildings: Method and data;01.040.91; 91.120.10: Standard Norge. [October 25, 2021].
[149] Skeie K. Sustainable Facade Renovation [Master's thesis]: Norwegian University of Science and Technology (NTNU); 2013.
[150] Fabi V, Andersen RV, Corgnati S, Olesen BW. Occupants' window opening behaviour: A literature review of factors influencing occupant behaviour and models. Build Environ 2012;58:188–98. https://doi.org/10.1016/j.buildenv.2012.07.009.
[151] Norwegian Building Authority. Regulations on technical requirements for construction works; 2017.

[152] Yang J, Tham KW, Lee SE, Santamouris M, Sekhar C, Cheong DKW. Anthropogenic heat reduction through retrofitting strategies of campus buildings. Energy and Buildings 2017;152:813–22. https://doi.org/10.1016/j.enbuild.2016.11.051.

[153] Nafstad P, Skrondal, Anders, Bjertness, Espen. Mortality and temperature in Oslo, Norway, 1990-1995. Eur J Epidemiol 2001;17(7):621–7.

[154] Grynning S, Gustavsen A, Time B, Jelle BP. Windows in the buildings of tomorrow: Energy losers or energy gainers? Energy Build 2013;61:185–92. https://doi.org/10.1016/j.enbuild.2013.02.029.

[155] Brozovsky J, Gaitani N, Gustavsen A. Characterisation of Heat Losses in Zero Emission Buildings (ZEB) in Cold Climate. Proceedings of the 16th IBPSA Conference, Rome, Italy, Sept 2-4, 2019 2019:343–50. https://doi.org/10.26868/25222708.2019.210560.

[156] Boyano A, Hernandez P, Wolf O. Energy demands and potential savings in European office buildings: Case studies based on EnergyPlus simulations. Energy and Buildings 2013;65:19–28. https://doi.org/10.1016/j.enbuild.2013.05.039.

[157] Wang R, Lu S, Zhai X, Feng W. The energy performance and passive survivability of high thermal insulation buildings in future climate scenarios. Build. Simul. 2021. https://doi.org/10.1007/s12273-021-0818-3.

[158] Grahn P, Stigsdotter UA. Landscape planning and stress. Urban For Urban Green 2003;2(1):1–18. https://doi.org/10.1078/1618-8667-00019.

[159] O'Brien L, Williams K, Stewart A. Urban health and health inequalities and the role of urban forestry in Britain: A review; 2010.

[160] Barton J, Rogerson M. The importance of greenspace for mental health. Br J Psychiatry Int 2017;14(4):79–81.

[161] Park BJ, Tsunetsugu Y, Kasetani T, Kagawa T, Miyazaki Y. The physiological effects of Shinrin-yoku (taking in the forest atmosphere or forest bathing): evidence from field experiments in 24 forests across Japan. Environ Health Prev Med 2010;15(1):18–26. https://doi.org/10.1007/s12199-009-0086-9.

[162] Tsunetsugu Y, Park B-J, Miyazaki Y. Trends in research related to "Shinrin-yoku" (taking in the forest atmosphere or forest bathing) in Japan. Environ Health Prev Med 2010;15(1):27–37.

[163] Kaplan R. The role of nature in the context of the workplace. Landsc Urban Plan 1993;26(1-4):193–201. https://doi.org/10.1016/0169-2046(93)90016-7.

[164] Galderisi A, Treccozzi E. Green Strategies for Flood Resilient Cities: The Benevento Case Study. Proc Environ Sci 2017;37:655–66. https://doi.org/10.1016/j.proenv.2017.03.052.

[165] Pistocchi A, Calzolari C, Malucelli F, Ungaro F. Soil sealing and flood risks in the plains of Emilia-Romagna, Italy. J Hydrol Reg Stud 2015;4:398–409. https://doi.org/10.1016/j.ejrh.2015.06.021.

[166] Norsk Klima Service Senter. Klima i Norge 2100 [Climate in Norway 2100]; 2016.

[167] Thorolfsson ST. A new direction in the urban runoff and pollution management in the city of Bergen, Norway. Water Sci Tech 1998;38(10):123–30.

[168] Bai T, Mayer AL, Shuster WD, Tian G. The Hydrologic Role of Urban Green Space in Mitigating Flooding (Luohe, China). Sustainability 2018;10(10):1–3584. https://doi.org/10.3390/su10103584.

[169] Xiao Q, McPherson EG. Rainfall interception by Santa Monica's municipal urban forest. Urban Ecosyst 2002;6(4):291–302. https://doi.org/10.1023/B:UECO.0000004828.05143.67.

[170] Xiao Q, McPherson EG, Ustin SL, Grismer ME, Simpson JR. Winter rainfall interception by two mature open-grown trees in Davis, California. Hydrol. Process. 2000;14(4):763–84. https://doi.org/10.1002/(SICI)1099-1085(200003)14:4<763:AID-HYP971>3.0.CO;2-7.

Supplementary papers

Supplementary paper I

Microclimate analysis of a university campus in Norway

J. Brozovsky, S. Corio, N. Gaitani, A. Gustavsen

Published in *IOP Conference Series: Earth and Environmental Science 352* (2019), 012015

https://doi.org/10.1088/1755-1315/352/1/012015

IOP Conf. Series: Earth and Environmental Science **352** (2019) 012015 doi:10.1088/1755-1315/352/1/012015

Microclimate analysis of a university campus in Norway

Johannes Brozovsky[1], Sara Corio[2], Niki Gaitani[1], Arild Gustavsen[1]

[1] Department of Architecture and Technology, Norwegian University of Science and Technology – NTNU, 7034 Trondheim, Norway
[2] Department of Civil, Chemical and Environmental Engineering (DICCA), University of Genoa, 16145 Genoa, Italy

Corresponding email: johannes.brozovsky@ntnu.no

Abstract. Climate responsive urban design that makes use of passive heating and cooling strategies and enhances pedestrian comfort is a key element to a sustainable society. Knowing the impact of different materials, building typologies and arrangements and a building's sensitivity to microclimatic conditions, the energy balance can be enhanced. This study aims to evaluate the microclimatic conditions at the campus of the Norwegian University of Science and Technology, located in Trondheim, Norway. A numerical model was used and validated with punctual measurements on site. The results for air temperature showed a considerable seasonal variation with highest spatial temperature differences in summer and lowest in winter. Regarding the analysis of the wind field, east-west passages were identified as problematic. The influence of the seasonal changing leaf area density of the vegetation had a visible but minor influence on the wind field. The calibrated model will be used for further research on the influence of new building bodies on microclimate and thus building energy demand and pedestrian comfort.

1. Introduction

Ongoing urbanisation, population growth and a steadily warming climate put enormous pressure on cities worldwide. Environmental conditions and anthropogenic pollution of the air, soil and water pose an increasing threat not only to the ecological equilibrium but also to people's health [1]. Through their fabric, consumption of resources, emissions, shape and pattern, urban areas are a massive interference with nature. They are able to significantly change meteorological conditions at the microscale (< 2 km; microclimate) and mesoscale (< 200 km; mesoclimate) [2]. One of the most well-known phenomena of human-induced modification of climate is the urban heat island effect (UHI). It describes the distinct warmth of an urban area compared to its rural surroundings [3]. Many scientific publications have reported the UHI across virtually all climate zones and settlement sizes [4]. Urban-rural temperature differences (UHI magnitude) typically range from 1–3 K. Occasionally, UHI magnitudes of 10–14 K were reported during anticyclonic conditions [5, 6].

The summer heat wave of 2003 in Europe is an alarming example of how devastating climatic conditions can affect our lives. In France alone, 15 000 excess deaths were registered during only three weeks in August [7]. Seven years later, a heat wave struck Moscow with close to 11 000 excess deaths during the 44-day heat wave period [8]. Therefore, and because of increasing city populations, the evaluation of the urban environment has drawn ever-increasing attention in the past decades to make cities more resilient to elevated temperatures. Especially with the advancement of computational power, numerical tools are increasingly used for microclimate analyses [9]. They allow for instance investigating the impact of new building projects within the development of urban districts on local

microclimatic conditions [10], the effectiveness of mitigating measures for the urban heat island UHI [11], or the evaluation of outdoor comfort [12].

However, not only temperate or warm-climate regions are affected by climate change and rising temperatures. In 2018, for the first time since the beginning of the recordings in 1920, the arctic city of Tromsø in northern Norway experienced a "tropical night" where temperatures did not drop below 20 °C. Additionally, only two out of the last 30 years had a lower mean annual temperature than the mean of the norm period from 1961 to 1990 in Norway [13]. Studying urban microclimate thus also gains interest in cold climate countries where summers are usually cooler. While numerical studies on urban microclimate are quite common especially since the beginning of the 2000s, in high latitude locations close to the Arctic Circle they are scarce [9].

The 0.26 km² Gløshaugen university campus in Trondheim (Norwegian University of Science and Technology, NTNU), Norway (63.4° N, 10.4° E) is currently in the early stages of redevelopment. About 90 000 m² of gross floor area are planned to be added to the current building stock until 2027. This study aims to investigate the current microclimatic conditions of a part of the campus (see Figure 1 and 2).

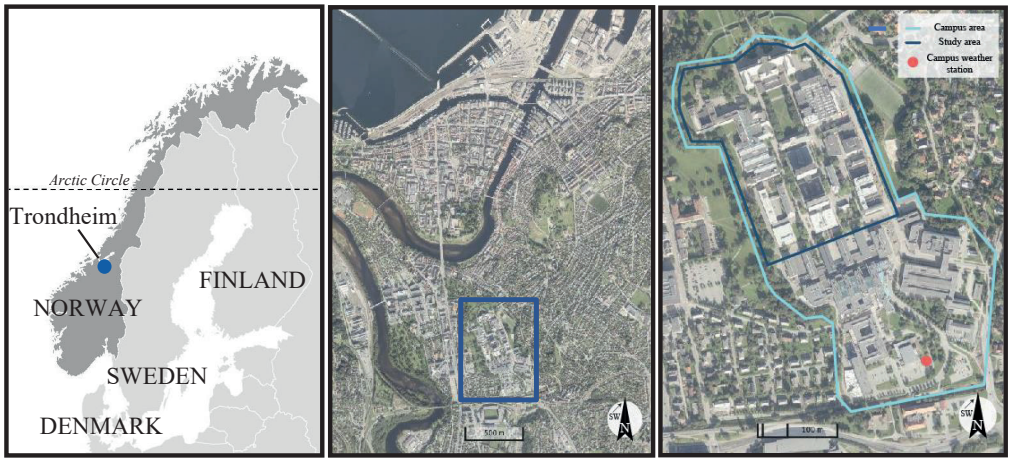

Figure 1. Location of the study area of NTNU campus within Norway and Trondheim (aerial photographs from the Norwegian Mapping Authority www.kartverket.no).

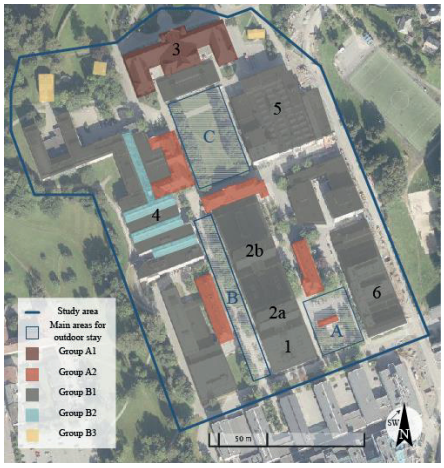

Figure 2. The study area with the building categories and the location of the main areas of outdoor stay: a small grass area (*A*) between the cafeteria (*1*) and the *Berg*-building (*6*) with seating possibilities; a pedestrian zone (*B*) west of the central buildings 1 and 2 (*2a* and *2b*) with several seating possibilities close to the cafeteria; a grass area (*C*) behind the main building (3), east of the *Elektro* building (*4*) and west of the VATL (*5*) with deckchairs during the summer.

2. Methodology

In this paper, two methods are being applied: field measurements and numerical simulations. The measurements are used to record the punctual microclimate conditions and to validate the simulation model of the current campus layout. Validation is defined as the process of determining if a computational simulation represents the real world and how accurately the computational results compare with experimental data [14, 15]. For the numerical simulation, the widely applied three-dimensional non-hydrostatic model for surface-plant-air interaction ENVI-met v. 4.4 is used [16].

2.1. Field measurements

The on-site field survey consisted of two parts: continuous meteorological measurements at a weather station and mobile infrared (IR) thermography. The meteorological measurements are obtained from a weather station which is located on the roof of the ZEB Test Cell Laboratory (TCL), south of the study area, see Figure 1. The weather station records air temperature, relative humidity, global horizontal radiation, wind speed and wind direction in one-minute intervals. The data is then compiled into one-hour averages to serve as validation input in the simulation model.

Surface temperature measurements were derived using an infrared camera (FLIR E60). The IR measurements were taken during calm, clear-sky conditions on the morning of 11 April 2019. The ambient temperature that day ranged from a low -1 °C to a high +3 °C. The IR camera is able to operate in a temperature range between -20 °C to +120 °C and has an accuracy of ±2 °C or ±2 % of reading for an ambient temperature between 10 °C and 35 °C [17]. The surface temperature of the most representative buildings for each category (see Table 1) and ground surface temperatures have been measured (see Figure 3). For the validation process, the five groups of buildings (*A1, A2, B1, B2, B3*) were sub-categorised based on the main characteristics such as the main orientation, the surroundings, the presence of trees, and the closeness and size of the plants. For each sub-category, a reference building was chosen to be analysed specifically (see Figure 4).

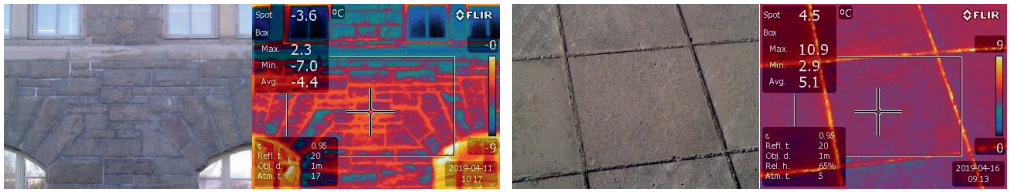

Figure 3. IR measurements of a building surface with granite stone (left) and concrete pavement (right).

2.2. Study area

Trondheim is Norway's third largest city by population with close to 200 000 inhabitants and is located at a 130 km long and 10–20 km wide fjord in Central Norway. The location's climate is subarctic (Dfc) according to the Köppen-Geiger classification system [18]. The 0.23 km² Gløshaugen campus of NTNU is located about 2 km south of Trondheim's city centre on a hill plateau (see Figure 1). In order to reduce the simulation time, a smaller portion of the campus (0.10 km²) was selected. This decision is supported by the fact that the main areas for people are also located in this smaller subarea (see Figure 2). This part has a relatively uniform elevation of about 47 m above mean sea level.

The mean annual temperature of Trondheim's official weather station in Voll is 4.8 °C. The average annual precipitation is 855 mm and the prevailing wind direction is south west (225°). As the official weather station is not in the vicinity of the campus, meteorological recordings from the ZEB TCL, located 400 m south of the study area, are used (see Figure 1 and Figure 2).

2.3. Model and computational domain

Aerial photographs from the Norwegian Mapping Authority (www.kartverket.no) were used to determine the positions of the different surface and vegetation cover types in the 3D model. Figure 4

shows the ENVI-met simulation model with view from the south. On-site inspections on the measurement date provided specific characteristics of the buildings, materials, and vegetation (including species) and confirmed that the information from the aerial photographs was up to date.

The grid of the calculation domain has dimensions of 416(x)_400(y)_94.5(z) metres and consists of 104_100_32 cells at each axis respectively. The lowest grid cell is split into five sub-cells with 0.6 m height each. Concerning the interference coming from boundaries to the flow and for the flow to develop, the distance between the objects and the domain boundaries was arranged based on ENVI-met specifications. For that, the height of the domain was modelled more than two times the highest building (Central Buildings' height: 45 m) and the horizontal distance to the model boundaries was at least equal to the closest building's height. In addition, four nesting grids were added around the core of the 3D model. For turbulence closure, ENVI-met uses the Mellor-Yamada turbulence model from 1982 [19].

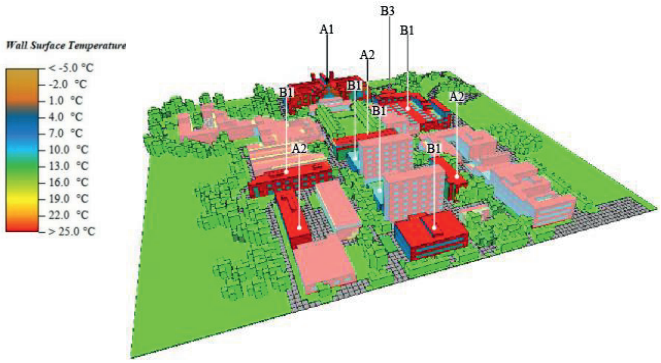

Figure 4. View of the ENVI-met simulation model from the south. The reference buildings for each category are indicated in brighter colours and are representative of sub-categories based on different conditions of orientation and surroundings.

2.3.1. Soils and surfaces. Three different surface types predominate in the area of interest. This includes the basic soil type and sealed surfaces like streets and pavements. Soil maps of the region showed that the model area's soil is mainly characterised by its clay content [20]. The remaining areas of the domain which are not covered by vegetation or buildings are impermeable surfaces. They were modelled based on the ENVI-met standard library values (surface albedo, aerodynamic roughness length, emissivity) for *Asphalt Road* and *Pavement (Concrete), used/dirty* [21].

2.3.2. Vegetation. Gløshaugen campus is embedded within a park-like environment and features green spaces and a great number of trees, shrubs and hedges throughout the area. For simplification purposes, vegetation types were limited to six different types of trees (of only three species), two hedge types, and one grass type. The existing vegetation from the program database has been scaled to fit the plant sizes on campus. Following tree species were modelled: *Norway Maple* (10, 15 and 20 m), *Larch* (20 m) and *Scots Pine* (5 and 10 m). The two hedge-types were 1 m high (one modelled as a conifer, one as deciduous) and the grass height was set to 0.1 m. The deciduous trees were assigned an annual schedule to regulate the leaf area density (LAD) according to the seasonality of foliation.

2.3.3. Buildings. The buildings at the campus were grouped into five categories (see Figure 2; Table 1) according to the wall's outermost thermally relevant material layer: stone, brick, concrete, glass and wood. Most of the buildings were built with concrete as an external wall material, followed by brick and wood. It is worth noting that the wooden buildings are rather small and situated on the north-eastern and north-western side of the campus. Moreover, for some of the buildings, glass is the main material for both walls and roofs (*Elektro* buildings). The roof materials were identified for each category. The properties of the materials used in the ENVI-met model are the default ones for concrete and glass, while for granite stone, solid brick and wood, new material database entries were created. All the materials have an emissivity of 0.90 except for the wood (0.86).

Table 1. Categories of the buildings in the ENVI-met model.

Category	Year of construction	Wall material	Roof Material
A1	1900-1950	Stone: granite	Wood: spruce
A2	1900-1950	Solid brick	Wood: spruce
B1	1951-2000	Concrete: filled blocks	Concrete: default
B2	1951-2000	Glass: clear float	Glass: clear float
B3	1951-2000	Wood: spruce	Wood: spruce

2.4. Boundary conditions

For the evaluation of the microclimatic conditions, simulations were performed for four days: 21 March (vernal equinox), 21 June (summer solstice), 23 September (autumnal equinox) and 21 December (winter solstice). The boundary conditions of the model are based on the records of the year 2018 from the weather station on campus. The hourly values of air temperature and relative humidity, the mean daily wind speed and the prevailing SW (225°) wind direction for Trondheim, were applied (Table 2). As the program does not allow for incorporating snow covered surfaces, freezing or thawing of water, the same surface properties and physical conditions for all simulated dates were used [22].

Table 2. Boundary conditions and statistical meteorological values of the simulated days during simulation time (T_{min}, T_{max} = temperature min./max. and time of occurrence in local standard time (LST); $\bar{v}_w$ = mean wind speed; $\bar{\phi}$ = mean relative humidity; t_{sr} = LST of sunrise; t_{ss} = LST of sunset; $t_{sim,s}$ = LST of simulation start; $t_{sim,e}$ = LST of simulation end; $t_{sim,tot}$ = total time of simulation).

	T_{min} (LST) [°C]	T_{max} (LST) [°C]	$\bar{v}_w$ [m/s]	$\bar{\phi}$ [%]	t_{sr} (LST)	t_{ss} (LST)	$t_{sim,s}$ (LST)	$t_{sim,e}$ (LST)	$t_{sim,tot}$ [h]
21.03.	2.6 (05:00)	4.2 (16:00)	1.7	85.1	6:17	18:35	6:00	19:00	13.0
21.06.	8.3 (06:00)	12.2 (18:00)	1.8	73.5	03:02	23:37	03:00	24:00	21.0
23.09.	5.5 (19:00)	8.0 (15:00)	2.5	77.7	07:03	19:16	07:00	20:00	13.0
21.12.	0.2 (06:00)	0.9 (12:00)	2.6	55.0	10:01	14:31	06:00	15:00	9.0

3. Results and discussion

3.1. Validation

The obtained data from the field measurements of the reference buildings were used to validate the results derived from the ENVI-met simulation from 10 April at 20:00 to 11 April at 13:00. The average difference between measured and simulated surface temperatures of the thirty measurement points was 4.9 K. However, ENVI-met presents a tendency to overestimate the surface temperature values, where IR-measured values were below or close to 0 °C (see Figure 5, eight values in total). For those values, the simulations surpassed the IR measurements by 7.9 K on average. The average deviation from the measurements of all other validation points was 2.8 K.

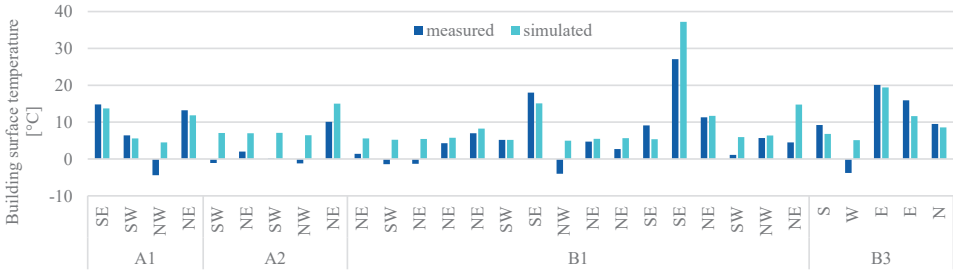

Figure 5. Measured (IR) and simulated building surface temperatures of the building categories on 11 April for different orientations.

Apart from the larger deviations at low temperatures, the magnitude of error is scattered arbitrary across the measurement points. Therefore, no systematic error for example regarding orientation, surface material, closeness to vegetation or point in time could be identified.

3.2. Microclimate analysis

Figure 6 illustrates the simulated air temperature field at 1.5 m height (pedestrian level). The unshaded south and west-facing surfaces get heated up by the exposure to solar radiation the most. Therefore, areas close to those surfaces show the highest air temperatures at pedestrian level. Especially the inner corner in the north west of the campus, where wind speeds are particularly low, represents a hot spot throughout the year, except for winter. The simulated values of air temperature correlate to the different surface types (albedo, emissivity) together with the wind field pattern and solar access. The materials with high heat storage capacity (i.e. asphalt, concrete pavement) present higher air temperatures than the vegetated areas.

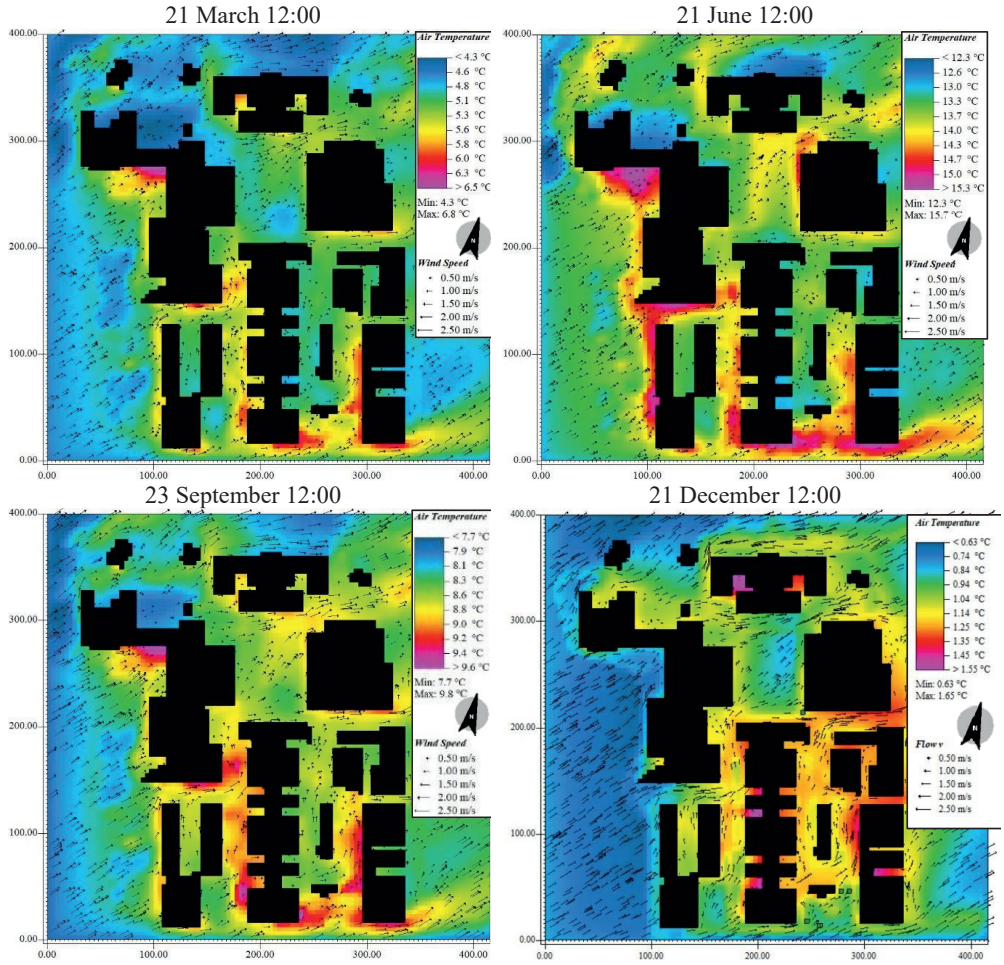

Figure 6. Air temperature and wind field at 12:00 at pedestrian level (1.5 m above ground) for the four simulated days.

In the colour map of 21 December, the grassed areas behind the main building (*C*), east of the cafeteria (*A*) and the smaller patch west of the cafeteria are recognisable in terms of contrasting colour. On the contrary, the paved and asphalted surfaces around the central buildings (*2a, 2b*), and south of the VATL (*5*) show the highest temperatures. The cooler patches east of the central buildings are the areas where hedges and trees lead to lower air temperatures. The grassed areas surrounding the campus are generally cooler all year round and with exception of 21 December, the asphalted areas north of the main building (*3*) and north of the *Elektro* building represent the cold spots.

The highest absolute temperature difference (ATD) within the study area was simulated on 21 June with 3.4 K between the coolest and warmest spot. On 21 December on the other hand, it is lowest with only 1.2 K. The vernal and autumnal equinoxes have an ATD of 2.5 K and 2.1 K respectively. It is supposed that the ATD is mainly influenced by the amount of solar radiation reaching the surfaces.

Regarding the wind field, the input data for the wind speed varied between the simulated dates. However, the prevailing wind direction (225°) was kept the same. Thus, in this study, the proportional relation of local wind speeds to the undisturbed reference inflow at the same height level is of higher interest than absolute values. The resulting so-called wind speed change (WSC) showed only minor differences between the simulated dates. The maximum value for the WSC was lowest for the vernal equinox (138.0 %) and highest for the winter solstice (157.1 %). Summer solstice and autumnal equinox had a maximum WSC of 140.5 % and 152.0 % respectively.

On all the simulated dates, the south east corner of the campus (*Berg*-building) showed the highest WSC values. The southern part of the study area is close to the boundaries of the model, so even if it is an equally densely built-up area, the simulated results for this location present higher values due to the fact that the model considers there an undisturbed approaching flow. Furthermore, the simulation results indicate windy conditions at east-west passages. Those areas are for example the passage east of central building 2 (*2b*), south of the VATL (*5*), and between the main building (*3*) and the VATL. Additionally, the passage between the main building (*3*) and the small wooden building in the north west exhibits a high WSC with values close to the maximum on all simulated dates. The influence of the seasonal changing LAD of the vegetation had a visible but minor influence on WSC, especially in the tree-lined patch of grass behind the main building (*C*). The lowest wind speeds occurred in the wake of the larger buildings and especially in the small backyards south of the main building (*3*) and east of the central buildings (*2a, 2b*).

4. Conclusion

In this study, the simulation tool ENVI-met was used for analysing the microclimatic conditions at a university campus in Trondheim, Norway. The analysis focused particularly on local air temperatures and the wind field at pedestrian level. The validation revealed an average difference of 4.9 K between the measured and the simulated building surface temperatures. However, ENVI-met tended to overestimate the low surface temperatures, especially where IR-measured values were below or very close to 0 °C.

The simulated values of air temperature correlate to the different surface types (albedo, emissivity) together with the wind field pattern and solar access. The materials with high heat storage capacity (i.e. asphalt, concrete pavement) present higher air temperatures than the vegetated areas.

The areas in front of south-facing and sunlit surfaces presented elevated local air temperature values. On 21 December, when almost no solar radiation is reaching the area due to very short days and low solar angles, the influence of the surface materials becomes more evident. At this time of the year, vegetated surfaces cause lower air temperatures at pedestrian level compared to heavier materials like concrete and asphalt. The highest ATD occurred on 21 June with 3.4 K between the warmest and coolest spot, the lowest on 21 December with 1.2 K.

The analysis of wind speed change identified east-west passages on campus as problematic. There, local wind speeds exceeded the reference wind speed at the inlet by up to 57.1 %. On the other hand, the lowest wind speed values occurred in the wake of the larger buildings and in particular in the small backyards south of the main building and on the east side of the central buildings.

The model has limitations as to the coarse grid resolution and the uniform discretisation, as the software does not allow refinements. Notably, the regular grid structure that does not admit of transverse, sloped or curved geometries, resulting in inaccuracies of simulated air flows. Additionally, the program does not allow for considering snow covered surfaces [22], which especially in December and March can have significant influence on physical properties and thus the microclimatic conditions [23]. However, the model can be of advantage and informative at the early stage of microclimate assessments.

In the future, a more comprehensive study will be conducted by using sophisticated computational fluid dynamics programs that allow a finer and more demand-actuated discretisation. The results of this study, in combination with a specific validation process for the air flows, will further deepen the knowledge of the microclimatic situation on the NTNU campus. This knowledge can then be applied in the planning of the campus' redevelopment, for instance to decide on where to plant new vegetation, which surface materials to use or where new buildings decrease the potential for natural ventilation.

5. Acknowledgements

This paper has been written within the Research Centre on Zero Emission Neighbourhoods in Smart Cities (FME ZEN). The authors gratefully acknowledge the support from the ZEN partners and the Research Council of Norway.

References

[1] Rhind S M 2009 *Philosophical transactions of the Royal Society of London. Series B, Biological sciences* **364** 3391–401
[2] Orlanski I 1975 *Bull. Amer. Meteor. Soc.* **56** 527–30
[3] Oke T R, Mills G, Christen A and Voogt J A 2017 *Urban climates* (Cambridge: Cambridge University Press)
[4] Stewart I D and Oke T R 2012 *Bull. Amer. Meteor. Soc.* **93** 1879–900
[5] Kłysik K and Fortuniak K 1999 *Atmos. Environ.* **33** 3885–95
[6] Bowling S A and Benson C S 1978 *Study of the Subarctic Heat Island at Fairbanks, Alaska (Environmental Monitoring Report* EPA-600/4-78-027*)* (United States Environmental Protection Agency)
[7] Fouillet A, Rey G, Laurent F, Pavillon G, Bellec S, Guihenneuc-Jouyaux C, Clavel J, Jougla E and Hémon D 2006 *Int. Arch. Occup. Environ. Health* **80** 16–24
[8] Shaposhnikov D *et al* 2014 *Epidemiology (Cambridge, Mass.)* **25** 359–64
[9] Toparlar Y, Blocken B, Maiheu B and van Heijst GJF 2017 *Renewable and Sustainable Energy Reviews* **80** 1613–40
[10] Berardi U and Wang Y 2016 *Sustainability* **8** 822
[11] Wang Y and Akbari H 2016 *Sustainable Cities and Society* **26** 438–46
[12] Chokhachian A, Santucci D and Auer T 2017 *Buildings* **7** 113
[13] Meteorologisk Institutt 2017 *Klima siste 150 år [Climate in the last 150 years]* https://www.met.no/vaer-og-klima/klima-siste-150-ar (accessed 18 Apr 2019)
[14] Oberkampf W L and Trucano T G 2002 *Progress in Aerospace Sciences* **38** 209–72
[15] American Institute of Aeronautics and Astronautics 1998 *AIAA guide for the verification and validation of computational fluid dynamics simulations* (Reston, VA: American Institute of Aeronautics and Astronautics)
[16] Bruse M and Fleer H 1998 *Environ. Model. Softw.* **13** 373–84
[17] FLIR Systems I 2016 *User's manual Flir Exx series*
[18] Peel M C, Finlayson B L and McMahon T A 2007 *Hydrol. Earth Syst. Sci. Discuss.* **4** 439–73
[19] Mellor G L and Yamada T 1982 *Rev. Geophys. Space. Phys.* **20** 851–75
[20] Sigmond E M O 1985 *Nasjonalatlas for Norge: National atlas of Norway* (Oslo: Statens kartverk)
[21] ENVI_MET GmbH 2019 *ENVI_MET V4.4.2: Winter1819* (Essen, Germany)
[22] ENVI_MET GmbH 2019 *Under Zero Temperature* personal email communication
[23] Malevich S B and Klink K 2011 *J. Appl. Meteor. Climatol.* **50** 1884–94

Supplementary paper II

Zero emission neighbourhoods and positive energy districts – A state-of-the-art review

J. Brozovsky, A. Gustavsen, N. Gaitani

Published in *Sustainable Cities and Society 72* (2021), 103013

https://doi.org/10.1016/j.scs.2021.103013

Sustainable Cities and Society 72 (2021) 103013

Contents lists available at ScienceDirect

Sustainable Cities and Society

journal homepage: www.elsevier.com/locate/scs

Zero emission neighbourhoods and positive energy districts – A state-of-the-art review

Johannes Brozovsky *, Arild Gustavsen, Niki Gaitani

Department of Architecture and Technology, Faculty for Architecture and Design, NTNU – Norwegian University of Science and Technology, 7491, Trondheim, Norway

ARTICLE INFO

Keywords:
Zero emission
Zero energy
Positive energy
Neighbourhoods
Districts
Blocks
Systematic review

ABSTRACT

Urban areas are critical in accomplishing the clean energy transition and meeting the climate goals in the Paris Agreement. The first part of this paper presents a systematic review of scientific publications on zero emission neighbourhoods, positive energy districts and similar concepts of climate friendly neighbourhoods (CFN). The second lists a selection of CFN definitions of public initiatives and research projects. The aim is to identify focus areas, research gaps and future research possibilities. In the systematic review, 144 papers were categorised and analysed according to their concept terminology, topic, location, used methodology, publication type, year, citations and keywords. The results document the growing but thematically and geographically unbalanced attention given to CFNs. Most research (31.9 %) was connected to the energy system, whereas social aspects (4.2 %) and the microclimate (3.5 %) were least researched. Within the analysed literature, 35 different terminologies for CFNs were used which highlights the lack of clear definitions and arbitrary use of terminologies. This issue is also reflected in the significant differences of CFN definitions from public initiatives and research projects. This article stresses the need for clear, comprehensible and structured definitions, including KPIs, system boundaries, as well as definitions of the spatial scales.

1. Introduction

Despite improvements in energy efficiency and various efforts to limit the building sector's impact on the environment, global emissions from buildings increased by about 2% for the second consecutive year from 2017 to 2018 (see Fig. 1). These increases were mainly driven by continuously rising building floor area and global population growth. Overall, the building and construction sector was responsible for 36 % of final energy use and 39 % of energy process-related carbon dioxide (CO_2) emissions in 2018 (Global Alliance for Buildings and Construction et al., 2019). Thus, buildings hold a critical role for a clean energy transition (IEA, 2019). Responding to the Paris Agreement in 2015 (United Nations Framework Convention on Climate Change, 2015), the European Union (EU) has set an ambitious target to reduce greenhouse gas (GHG) emissions by at least 40 % below 1990-levels until 2030 (European Commission, 2014b). Moreover, the EU has adopted a wide

Abbreviations: BAU, Outdoor area; BRA, Heated floor area; CFN, Climate-friendly neighbourhood; CO_2, Carbon dioxide; DOE, Department of Energy; EBC, Energy in Buildings and Communities Programme; EIP-SSC, European Innovation Partnership on Smart Cities and Communities; EPBD, Energy Performane of Buildings Directive; EPN, Energy Positive Neighbourhood; ES, Energy system; EU, European Union; FME, ZEB Research Centre on Zero Emission Buildings; FME, ZEN Research Centre on Zero Emission Neighbourhoods in Smart Cities; GHG, Greenhouse gas; HPD, High Performance District; ICT, Information and communication technology; IT, Information technology; IEA, International Energy Agency; Int/Que/Exp, Interview/questionnaire/experiment; JPI, Joint Programming Initiative; LCA, Life cycle assessment; LCD, Low Carbon District; LCDH, Low Carbon District Heating; LCN, Low Carbon Neighbourhood; LED, Low Energy District; LEED, Leadership in Energy and Environmental Design; LEN, Low Energy Neighbourhood; M/FW/Tool, Methodology/framework/tool presentation; MC, Microclimate; MILP, Mixed-integer linear programming; UM, Urban morphology; MPC, Model predictive control; NMM, Numerical/mathematical modelling; NOK, Norwegian Kroner; NTNU, Norwegian University of Science and Technology; NZEHC, Net Zero Energy Housing Community; nZEB, Nearly Zero Energy Building; nZED, Nearly Zero Energy District; NZED, Net Zero Energy District; NZEN, Net Zero Energy Neighbourhood; nZEN, Nearly Zero Energy Neighbourhood; PEB, Positive Energy Block; PED, Positive Energy District; pED, Plus Energy District; POSE, Project organisation and stakeholder engagement; PV, Photovoltaics; Rev, Review; SA, Social Aspects; SHC, Solar Heating and Cooling Programme; SET, Strategic Energy Technology; SPEN, Sustainable Plus Energy Neighbourhoods; TEA/FS, Techno-economic analysis/feasibility study; Trans, Transition to a climate-friendly neighbourhood; UK, United Kingdom; ZED, Zero Energy District; ZEDA, Zero Energy Districts Accelerator; ZEN, Zero Energy Neighbourhood; ZEN*, Zero Emission Neighbourhood.

* Corresponding author.
E-mail addresses: johannes.brozovsky@ntnu.no (J. Brozovsky), arild.gustavsen@ntnu.no (A. Gustavsen), niki.gaitani@ntnu.no (N. Gaitani).

https://doi.org/10.1016/j.scs.2021.103013
Received 24 February 2021; Received in revised form 21 April 2021; Accepted 10 May 2021
Available online 15 May 2021

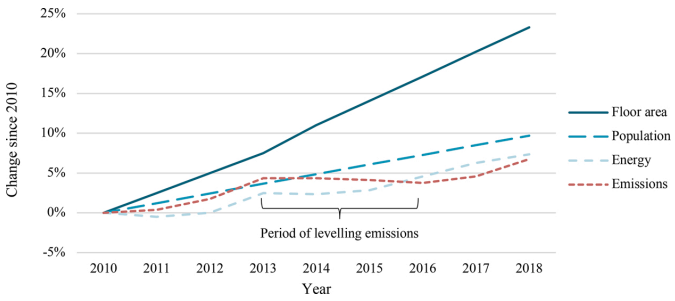

Fig. 1. Changes in floor area, population, buildings sector energy use and energy-related emissions globally since 2010, modified from Global Alliance for Buildings and Construction et al. (2019).

set of policies to become the first climate-neutral continent by 2050 with the introduction of the European Green Deal in December 2019, by moving to a clean, circular and sustainable economy (European Commission, 2019b). As a part of the Green Deal, the Renovation Wave (European Commission, 2020b) aims at not less than double the annual energy renovation rate of residential and non-residential buildings and to reach 35 million building units renovated by 2030. The legislative framework to reach the EU's climate goals is called "Clean Energy for All Europeans" which particularly highlights the importance of improving the energy and emission performance in the building sector (European Commission Directorate-General for Energy, 2019). Within the context of this framework, the recast Renewable Energy Directive (European Parliament & Council of the European Union, 2018a) entered into force in 2018, promoting the use of energy from renewable sources, especially in buildings.

A major stepping stone in this direction was the passage of the Energy Performance of Buildings Directive (EPBD) with its adaption to the EU Member States in 2010 and its recast in 2018 to transform Europe's building stock to be "highly energy efficient and decarbonised […] by 2050, facilitating the cost-effective transformation of existing buildings into nearly zero-energy buildings" (European Parliament & Council of the European Union, 2010, 2018b). The aim of the EPBD is mainly to provide a common basis for calculating the energy performance of buildings and to establish minimum requirements for the energy performance of new and existing buildings. It is furthermore specified that after 2020 all new buildings must be nearly zero energy buildings (nZEB).

Continuing the success of Horizon 2020 (European Commission, 2014a), an €80 billion EU research and innovation programme which funded a large number of research projects on these topics from 2014 to 2020, its successor Horizon Europe (European Commission, 2019a) will invest €100 billion to pursue its targets between 2021 and 2027. For that, five mission areas have been identified. Two of them are highly relevant in the context of sustainable urban development: (i) A climate-resilient Europe – Prepare Europe for climate disruptions and accelerate the transformation in a climate-resilient and just Europe by 2030 (Directorate-General for Research & Innovation, 2020b) and (ii) 100 Climate-neutral Cities by 2030 – by and for the Citizens (Directorate-General for Research & Innovation, 2020a). These missions highlight not only the EU's ambitions to tackle climate change and reduce the environmental impact from the building sector, but also underline the absolute necessity for more research in these domains.

Over the years, a considerable number of different and coexisting definitions and standards for low-, nearly or zero energy/carbon buildings have been developed (Kibert & Fard, 2012; Marszal et al., 2011; Williams et al., 2016). Commonly, to reduce GHG emissions and energy use in the building stock and new constructions, such standards and national building codes provide minimum requirements for the energy performance and airtightness of the building envelope, or the use of renewables-based technology and energy sources (Magrini et al., 2020; Williams et al., 2016). As electricity use in buildings has increased five times faster since 2000 than improvements in the carbon intensity of the power sector, renewable on-site electricity production is seen as a key element of achieving such building standards (IEA, 2019). However, the problem of variability in renewable energy production demands a high degree of demand-side flexibility, storage capabilities and optimised energy management strategies in the so-called "prosumer" buildings (PROducer and conSUMER of energy) to maximise self-consumption and minimise purchasing power from the public grid (Engeland et al., 2017; Velik & Nicolay, 2016).

To take advantage of more diverse load profiles, production and storage capabilities, and the possibility of sharing costs and resources, literature suggests taking the zero energy objective from the building to the district level (Amaral et al., 2018; Saheb et al., 2018). Moreover, *positive* energy neighbourhoods/districts/blocks are able to utilize in an efficient and flexible way the renewable energy generation and energy storage potential of the community. In respect of the environmental impact of urban areas, accommodating about 67 % of the world's population and accounting for approximately 70 % of global energy use and CO_2 emissions, their importance in the ongoing transition towards renewable energies and low-emission technologies is undisputed and actions are urgently required (Edenhofer, 2014; International Energy Agency, 2016; United Nations et al., 2018). Accordingly, the EU launched the "Positive Energy Districts and Neighbourhoods for Sustainable Urban Development" programme in the framework of the Strategic Energy Technology (SET) Plan Action 3.2 "Smart Cities and Communities" in 2018. The programme aims to support the planning, deployment and replication of 100 Positive Energy Districts (PED) by 2025 for sustainable urbanisation (European Commission Joint Research Centre, 2018). As of February 2020, there were 29 PED projects (most of them in the implementation stage) and 32 projects not declared as a PED but presenting "interesting features for the PED programme" registered by the Joint Programming Initiative (JPI) Urban Europe (Bossi et al., 2020; Gollner et al., 2020). Regulatory stimuli and public funding of research projects have led to a considerable amount of dissemination in this domain, as documented in the research paper from the International Energy Agency's Energy in Buildings and Communities Programme (IEA EBC) Annex 83 on Positive Energy Districts (Hedman et al., 2021). While several reviews have been published on (nearly/net) zero energy concepts at the building scale (Belussi et al., 2019; Deng et al., 2014; Feng et al., 2019; Li et al., 2013; Marszal et al., 2011; Panagiotidou & Fuller, 2013; Wells et al., 2018), and the district scale of performance aspects (Amaral et al., 2018), and sustainable approaches and assessment tools (Koutra et al., 2018), to the best of our knowledge, there hasn't been published a systematic review of low-, nearly zero, zero and positive energy/emission/carbon neighbourhoods/districts/-blocks yet. This article fills this gap and provides important information about existing literature to assist researchers in this field to

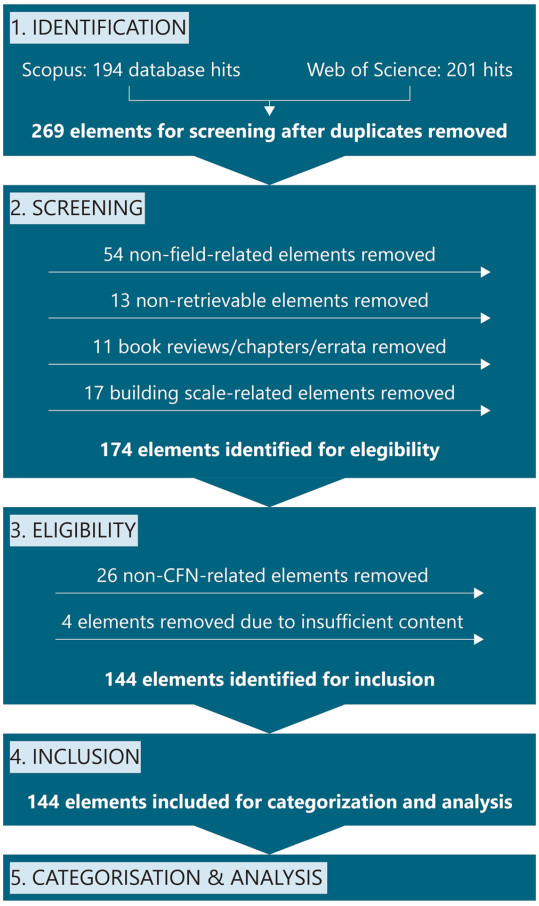

Fig. 2. Flow chart of the applied methodology in this research. Phases 1–4 represent the model for article inclusion according to Moher et al. (2010).

contextualize their work within global research activities, identify focus areas, research gaps and future research possibilities. Thus, this work will aid the global research community in speeding up the transition to a more sustainable built environment.

Assessing the environmental impact at neighbourhood/district/block scale is a vital step towards sustainable cities as neighbourhoods are their building blocks and usually represent the scale at which cities are expanded, redeveloped or transformed by urban planners and municipalities. Therefore, by addressing low-, nearly zero, zero and positive energy/emission/carbon concepts at the neighbourhood/district/block scale, this article aims to pave the way and provide important knowledge towards environmentally sustainable and resilient cities from a multi-disciplinary perspective.

The first part of this paper presents a systematic analysis of articles published in scientific journals and conferences in this context (chapter 3). In the second part, definitions of such concepts from selected research projects and public initiatives will be presented (chapter 4).

2. Method

For the first part of this article, the systematic review, relevant literature is identified by using a structured and reproducible search procedure. Although mainly used in medicine and health science, this reviewing approach has been increasingly adopted in other disciplines as well. In the centre of a systematic review is a structured question formulation that assures the reproducibility of the work. In this article, the four-phase approach described by Moher, Liberati, Tetzlaff, and Altman (2010) was applied and extended with an additional phase, the *Categorisation and Analysis*. In each of the first four phases, articles that do not fit into the scope of the review or that have been identified twice are removed. As the flow chart in Fig. 2 shows, the reasons for excluding articles from the review are outlined as well. After that, included articles are categorised and analysed based on different attributes (see chapter 3). Note that the fifth phase is not explicitly outlined in Moher et al.'s systematic review methodology. However, it represents one of the core elements of the applied methodology in this research. Therefore, extending Moher et al.'s approach with this phase was considered necessary.

It should be noted that by using this method, a subset of all relevant literature will be identified. The extent of search hits is not only dependent on the databases themselves and their content but to a considerable degree on the search terms and question formulation. The ultimately deployed search phrase is often a trade-off between several other possible search phrases, either resulting in too many results to be screened and analysed within a reasonable amount of time or yielding too few elements to represent a meaningful subset of the literature of interest. However, by doing so, many relevant publications and reports may be missed, if they do not specifically mention the search terms in their title, abstract or keywords or have not been published in form of a peer-reviewed article. This is, for instance, the case with many research projects, institutions or public authorities who do not always publish their reports in academic journals or conference proceedings.

Therefore, the second part of this review article (chapter 4) presents an overview of relevant definitions from selected public initiatives and nationally or EU-funded research projects and critically discusses differences among these. The analysis in the results section (chapter 3) of this article, however, includes only the publications that were identified by the following methodology.

2.1. Article identification and inclusion in the systematic review

There is a vast number of different terminologies regarding concepts aiming for reduced or minimised carbon emissions or energy use in a cluster of buildings. In this article, *Climate Friendly Neighbourhood* (CFN) will be used as a collective term for all the different expressions to generally and neutrally address the whole spectrum of terms.

Following the practice in other studies (Brozovsky et al., 2021; Bustami et al., 2018; Mavrigiannaki & Ampatzi, 2016), the electronic databases *Scopus* and *Web of Science* were used which require a slightly different syntax due to different search algorithms. To take account of the vast number of different CFN terms, the following search phrases were created:

Scopus: ((low OR "net zero" OR zero PRE/2 carbon) OR (plus OR positive OR "net zero" OR zero PRE/2 energy) OR ("net zero" OR zero PRE/2 emission)) PRE/2 (district OR neighbourhood OR block).

Web of Science: (((low OR "net zero" OR zero) NEAR/2 carbon) OR ((plus OR positive OR "net zero" OR zero) NEAR/2 energy) OR (("net zero" OR zero) NEAR/2 emission)) NEAR/2 (district OR neighbourhood OR block).

In Scopus, the search was conducted within the search fields *Article Title, Abstract and Keywords*. Analogously, in Web of Science, the search field was chosen to be Topic, which means *Title, Abstract, Author keywords* and *Keywords Plus®*. Both databases account for the different English spellings and apply word stemming. In other words, the databases will search for both British and American English spelling as well as different grammatical forms of the words in the search phrases given above. The search was performed on April 12, 2021.

Of the 395 identified elements, only 144 were included in the analysis in the end. A total of 126 elements were removed in the

Table 1
Abbreviations and descriptions of categories for topics and methods.

Topics		Method	
Abbreviation	Description	Abbreviation	Description
ES	Energy system	NMM	Numerical/ mathematical modelling
Trans	Transition to CFN	TEA/FS	Techno-economic analysis and feasibility study
ICT	Information and communication technology	Int/Que/Exp	Interview/ questionnaire/ experiment
POSE	Project organization and stakeholder engagement	M/FW/Tool	Methodology/ framework/tool presentation
UM	Urban morphology		
LCA	Life cycle assessment	Rev	Review
SA	Social aspects	Other	Methods not captured by previous categories
MC	Microclimate		
Other	Research not captured by previous categories		

identification stage where the element titles were used to sort out duplicates. In the screening stage, 95 articles were excluded. 54 of them had to be excluded as they did not cover the intended research domain and were mostly associated with chemistry or material science. 13 titles could not be downloaded due to missing licensing and other accessibility issues. Furthermore, 17 articles related only to the building scale and 11 book reviews, chapters, and article errata were excluded, as solely peer-reviewed scientific articles covering clusters of buildings were to be included in the analysis. Finally, in the eligibility stage, the remaining articles' contents and methods were examined. 26 of them did not specifically cover ecological concepts at the neighbourhood scale, and four elements were not regarded to be of sufficient quality to be included in the analysis of this systematic review.

2.2. Categorisation

After determining the elements to be included in this article's analysis, they were carefully examined and sorted into categories, according to their thematic focus and in the best judgement of this article's authors:

1 *Energy system*: Focusing mainly on the energy system of a building cluster, the management or integration of renewable energy sources etc.
2 *Transition to CFN*: Transforming existing clusters of buildings into a CFN.
3 *Information and communication technology*: Studies on information and communication technology and data management.
4 *Project organisation and stakeholder engagement*: Articles on the management, stakeholders and other organisational aspects of projects.
5 *Urban morphology*: Related to the arrangement of buildings in, and shape of, a CFN.
6 *Life cycle assessment*: Focusing on GHG emissions in CFN from a life cycle point of view.
7 *Social aspects*: Impact of CFN on humans and interactions between CFNs and people.
8 *Microclimate*: Mainly addressing microclimatic aspects in CFNs.
9 *Other*: Research not falling under the previous categories, for example with focus on economic evaluations, the assessment of indicator systems, monitoring results, position papers etc.

Furthermore, the included articles were grouped according to their methodological approaches: Numerical/mathematical modelling, Techno-economic analysis/feasibility study, Interview/questionnaire/ experiment, Methodology/framework/tool presentation, Review, and Others not captured by the previous five methods. Table 1 gives an overview of the abbreviations and descriptions of the topic and methodology categories.

3. Results

Following the aforementioned methodology, of the initially identified 395 scientific articles, 144 were included in this study. In the following section, the included research was thoroughly analysed based on different attributes such as (i) the nomenclature used in the articles, (ii) usage and location of case studies, (iii) the main topic of the articles, (iv) the methodological approaches, (v) the publication channels, years, and citations, and (vi) the author keywords. This analysis aims to determine the structure, the focus areas and the gaps in the literature related to CFNs.

3.1. Terminology

As previously mentioned, there is a large number of different terms used for strategies aimed at reducing the energy use or GHG emissions in clusters of buildings. Fig. 3 shows the terminologies that were used by at the minimum three studies. In total, there were 35 different terminologies, of which 21 were used two times or less (note that "neighbourhood" also includes the corresponding American spelling). Sometimes authors addressed more than one CFN concept in their articles, others used different terms as synonyms for addressing the same CFN concept or case study. Especially regarding the spatial scale, there seems to be disagreement or at least ambiguity about when to call a cluster of buildings "neighbourhood", "district", "block", "community",

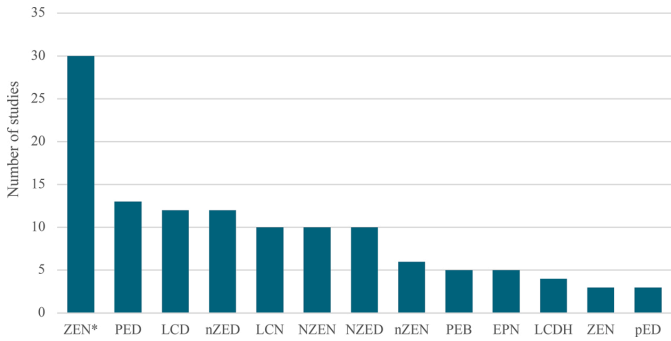

Fig. 3. Terminology of CFNs used in at least three studies.

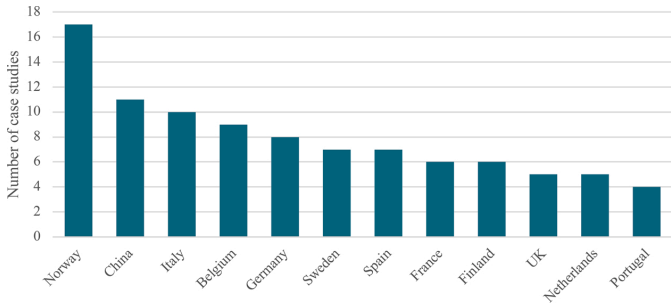

Fig. 4. Country of case study locations if used at least two times.

"settlement" or "precinct".

In the included subset of literature, *Zero Emission Neighbourhood* (ZEN*) was by far the most frequently used CFN concept with a count of 30 studies (20.8 %). *Positive Energy District* (PED) was used in 13 (9.0 %), *Low Carbon District* (LCD) and *Nearly Zero Energy District* (nZED) each in 12 (8.3 %), and *Low Carbon Neighbourhood* (LCN), *Net Zero Energy Neighbourhood* (NZEN) and *Net Zero Energy District* (NZED) each in 10 research papers (6.9 %). Other terminologies used were:

- *Nearly Zero Energy Neighbourhood* (nZEN),
- *Positive Energy Block* (PEB),
- *Energy Positive Neighbourhood* (EPN),
- *Low Carbon District Heating* (LCDH),
- *Zero Energy Neighbourhood* (ZEN),
- *Plus Energy District* (pED),
- *Zero Energy District* (ZED),
- *Positive Energy Precinct,*
- *Zero Carbon District,*
- *Zero Carbon Neighbourhood,*
- *Smart City Eco District,*
- *Zero Energy Emission District,*
- *Zero Non-Renewable Energy Neighbourhood,*
- *Plus Energy Neighbourhood,*
- *Nearly Zero Energy Settlement,*
- *Net Zero Exergy District,*
- *Net Zero Carbon Emission District,*
- *Low or Zero Emission District Heating,*
- *Low Carbon Energy District,*
- *Low Carbon Local Energy Community,*
- *Net Positive Energy Neighbourhood,*
- *Energy Positive District,*
- *Smart Energy Community,*
- *Net Zero Energy Block,*
- *Nearly Zero Carbon Neighbourhood,*
- *Net Zero Energy Settlement,*
- *Net Zero Energy Campus,* and
- *Net Zero Energy Community.*

The outweighing part of articles (70) used "neighbourhood" as an expression for the spatial boundary, which corresponds to 48.6 %. 60 studies (41.6 %) used "district" and 8 (5.6 %) "block". However, when just focusing on the spectrum of terminologies, "district" (15 out of 35) was used more often than "neighbourhood" (11 out of 35). The most used word in the CFN concept terminologies was "energy" (23 out of 35).

While most of the more frequently used terminologies are more or less defined, regarding their energy or emission balance ("zero", "plus", "positive" over a certain accounting period), *Low Carbon* is fairly vague. In the included subset of literature, this term was often used to describe any form of carbon reduction.

Table 2
Most-used case studies among included articles.

Name	Type	Status (04/2021)	Location	References
Ydalir	ZEN*	Under construction	Elverum, Norway	(Hamdan & Boer, 2019; Lausselet et al., 2021; Lausselet, Ellingsen et al., 2020; Lund et al., 2019; Nielsen et al., 2019; Yttersian et al., 2019)
Campus Evenstad	ZEN*	Completed	Evenstad, Norway	(Askeland et al., 2019; Nielsen et al., 2019; Pinel et al., 2020, 2021; Woods & Berker, 2019)
Wüstenrot	pED	Completed	Wüstenrot, Germany	(Brennenstuhl et al., 2019; Ge et al., 2019; Pietruschka et al., 2015; Romero Rodríguez et al., 2019)
Milano4You	nZED	At planning stage	Milano, Italy	(Aste et al., 2017, 2020; Del Pero et al., 2021)
Zero Village Bergen	ZEN*	At planning stage	Bergen, Norway	(Lausselet et al., 2019; Nielsen et al., 2018, 2019)

3.2. Case studies

More than half (87 or 60.4 %) of the 144 reviewed studies applied their research to case studies. Here, the term case study does not include generic and fictional, but only real neighbourhoods that either already

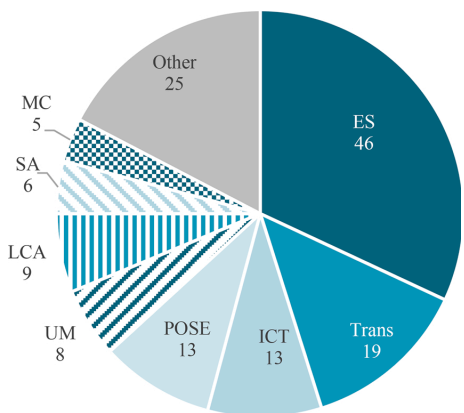

Fig. 5. Distribution of topics of included articles.

exist or are at the planning or construction stage. Fig. 4 shows the countries that had at least four case studies in the reviewed articles. However, the included subset of literature covers case studies from all continents, although the global distribution is quite unbalanced. As can be seen, 17 case studies were located in Norway and 11 in China, followed by Italy with 10, Belgium with 9, Germany with 8, and Sweden and Spain with 7. Note that when an article had more than one case study from the same country, the country was only counted once.

The most-used case studies are listed in Table 2. Note that Ydalir, Campus Evenstad and Zero Village Bergen are three of the nine pilot projects in the Research Centre on Zero Emission Neighbourhoods in Smart Cities (ZEN Research Centre, FME ZEN) (Bremvåg et al., 2018, 2020; Kvellheim et al., 2021; Woods et al., 2019).

3.3. Topics

This section analyses the primary topics of the included articles, as some of the articles covered more than one topic. During a careful examination of the included articles, their thematic focus was identified to the best of the authors' knowledge and judgement, which can be seen in Fig. 5.

3.3.1. Energy system

Most of the publications (46 articles or 31.9 %) focused on the energy system (ES) of a CFN. Traditionally accounting for the largest share of energy use (Fay et al., 2000; Koezjakov et al., 2018) and GHG emissions (Georges et al., 2015; Passer et al., 2012) in buildings, the energy supply during the use phase represents a key element for reaching a CFN, whatever the target unit or concept is. Although grouped within the same category, articles were dealing with a great range of aspects regarding the ES. The integration of multiple, and most importantly renewable energy sources in the energy supply system of a CFN is of central importance for reducing the share of fossil energy carriers and consequently GHG emissions. Therefore, a large part of the reviewed articles addressed multi-energy systems and the management of several energy sources (Bartolini et al., 2018; Capuder & Mancarella, 2016; Cheng et al., 2020; Comodi et al., 2019; Del Pero et al., 2021; Gabaldón Moreno et al., 2021; Garau et al., 2017; Ge et al., 2019; Hachem-Vermette & Singh, 2020; Heendeniya et al., 2020; Kim et al., 2019; Koutra et al., 2016; Morales Gonzalez et al., 2012; Pietruschka et al., 2015; Pinel et al., 2019; Pinel et al., 2020; Wang et al., 2015). It was common to evaluate different scenarios of energy production (Aste et al., 2015, 2017; Garau et al., 2017; Kılkış, 2014; Kim et al., 2019; Morales Gonzalez et al., 2012; Rezaei et al., 2021; Zwickl-Bernhard & Auer, 2021) or the inclusion of storage systems, with some articles focusing on thermal (Kim et al., 2019; Renaldi et al., 2017; Roccamena et al., 2019; Sameti & Haghighat, 2018), some on electrical (Sameti & Haghighat, 2018; Shafiullah et al., 2018; Shaw-Williams et al., 2020) storages. Frequently, mixed-integer linear programming (MILP) (Bartolini et al., 2018; Capuder & Mancarella, 2016; Iturriaga et al., 2021; Pinel, 2020; Pinel et al., 2020; Sameti & Haghighat, 2018; Shafiullah et al., 2018; Zwickl-Bernhard & Auer, 2021) was used, and in one case, model predictive control (MPC) (Pietruschka et al., 2015). Cortés, Auladell-León, Muñuzuri, and Onieva (2020) and Hachem-Vermette and Singh (2020) used a non-linear model to simulate the distributed energy resources in a CFN and its connection to the public grid. Other studies elaborated on the role of a CFN in a bigger context, for example, the larger power system (Askeland et al., 2019; Backe et al., 2018; Klebow et al., 2013; Romero Rodríguez et al., 2019) or grid tariffs (Askeland et al., 2019; Pinel et al., 2019; Pinel et al., 2021). In three articles, the problem of overvoltage, or voltage rise/drop in the grid due to photovoltaics (PV) production was addressed (Baetens et al., 2011; Coninck et al., 2014; Shaw-Williams et al., 2020). Boccalatte, Fossa, and Ménézo (2020) discussed the optimal arrangement of building-integrated PV surfaces in existing districts in order to reach Nearly Zero Energy standard. Kılkış published two studies on a Net Zero Exergy District, where the goal is to produce as much energy at the same grade or quality as it is consumed on an annual basis (Kılkış, 2014, 2015). Lowering the environmental impact through efficient district heating systems was the topic of research in four articles (Di Lucia & Ericsson, 2014; Finney et al., 2013; Hirvonen & Kosonen, 2020; Jadwiszczak, 2017). Yang, Chi, Wu, and Quan (2018) presented a multidisciplinary geodesign method to integrate systems of "renewable energy production, energy consumption, stormwater management, as well as a measurement of human experiences in cities". Koch, Girard, and McKoen (2012) examined load matching between a building's electrical and thermal needs and its distributed generation. Walker, Labeodan, Maassen, and Zeiler (2017) reviewed research on energy hubs for EPN.

3.3.2. Transition to CFN

19 of the included articles (13.2 %) addressed the transition (Trans) of an existing neighbourhood to a CFN. This category was dominated by articles proposing novel methodologies, frameworks or performance indicators to support implementing CFNs (Ala-Juusela et al., 2016; Blumberga et al., 2019; Clemente et al., 2019; García-Fuentes et al., 2018; Keough & Ghitter, 2020; Koutra et al., 2019; Koutra, Becue, Griffon et al., 2017; Koutra, Becue, & Ioakimidis, 2017; Marique & Reiter, 2014; Torre et al., 2021), mostly by using multi-criteria approaches (Blumberga et al., 2019; Koutra, Becue, Ioakimidis et al., 2017; García-Fuentes et al., 2018; Koutra et al., 2019). Commonly, the possibility of transformation to a CFN was evaluated through case studies (Ala-Juusela et al., 2016; Blumberga et al., 2020; Delmastro et al., 2017; García-Fuentes et al., 2018; Haneef et al., 2020; Janzadeh & Zandieh, 2021; Keough & Ghitter, 2020; Koutra et al., 2019; Koutra, Becue, Griffon et al., 2017; Leal et al., 2015; Leibold et al., 2020; Marique & Reiter, 2014; Nematchoua, 2020; Yamaguchi et al., 2013). In a paper by Ala-Juusela et al. (2016) KPIs for EPNs are given along with a decision support tool called AtLas. Such decision making support methodologies were also developed or applied in other papers of this category (Blumberga et al., 2019; García-Fuentes et al., 2018; Koutra et al., 2019).

3.3.3. Project organisation and stakeholder engagement (POSE)

This category contains 13 articles (9.0 %) that address a broad spectrum of different aspects, ranging for example from a critical discourse analysis in an LCN project in the UK (Genus & Theobald, 2016), over the role of utility companies in municipal planning of a Smart Energy Community (Nielsen et al., 2018), innovative public procurement (Hamdan & Boer, 2019), the roles of university researchers in CFN projects (Genus & Theobald, 2015), citizen engagement (Fatima et al., 2021), public-private collaboration (Ekambaram et al., 2020) to the visualisation of key performance indicators (KPI) for improved stakeholder participation by using virtual reality (Wiberg et al., 2019). Freeman and Yearworth (2017) discussed problem structuring methods in complex multiorganizational collaboration projects in the context of a project aiming to develop energy master plans for three city districts. Nielsen, Baer, and Lindkvist (2019) Klicken oder tippen Sie hier, um Text einzugeben.investigate exploitative and explorative innovation models and how they are applied by using Norwegian case study projects. Two articles analysed the practices of district energy planning in China in order to achieve a low carbon target (Xu et al., 2014; Xu et al., 2015). Two papers reported the experiences from EU Horizon 2020 projects and discussed an implementation framework for energy flexibility (Maas et al., 2020) and the challenges and barriers for the implementation of positive energy communities and districts (Uspenskaia et al., 2021).

3.3.4. Information and communication technology

A term that is frequently used in the CFN context is "smart". Smart City, Smart Grid, Smart Homes, Smart Appliances, etc. The basis for such smart systems is an information and communication technology (ICT) infrastructure for data management and sharing, a topic which was covered in 13 of the included articles (9.0 %). In the majority of cases,

management architectures for data (Sinaeepourfard, Krogstie, & Petersen, 2018; Sinaeepourfard, Krogstie, Petersen et al., 2018; Sinaeepourfard, Krogstie, Petersen, & Ahlers, 2019; Sinaeepourfard & Petersen, 2019; Soltvedt et al., 2020), smart technology (Sinaeepourfard, Krogstie, & Petersen, 2019; Sinaeepourfard, Petersen. & Ahlers, 2019) or software (Sinaeepourfard, Petersen, et al., 2019) in the ZEN* context were proposed. Other publications in this category addressed, for instance, the energy management (Bourdeau et al., 2013; Redmond et al., 2015), presented an in-house monitoring and control network (Carreiro et al., 2011) or an enterprise architecture framework for cities to create value-added services for its citizens (Petersen et al., 2019). One paper discusses IT-centred challenges that lie in designing a "flexible, open, transferable, and replicable smart city" architecture (Ahlers, Wienhofen et al., 2019). In another study by Petersen, Petersen, and Ahcin (2020), a mobile app to increase citizens' awareness of their carbon footprint is discussed.

3.3.5. Urban morphology

The arrangement of buildings within a cluster has been addressed in 8 studies (5.6 %). Most commonly, the relationship between urban shape and mobility was investigated (Hou et al., 2019; Lima et al., 2016; Zhou et al., 2019). In a study by Lima et al. (2016), an algorithmic approach was presented to support city planning with effective sustainable methods towards better urban mobility. Amaral et al. (2018) conducted a review of the relevant aspects that influence energy performance, such as climatic and morphological, in nZED.

Guarino et al. (2016) optimised solar energy gains in the Mediterranean context with a parametric analysis of building shapes, building mutual distances, road shape, building orientation, and PV area available. Based on urban morphology, Wang, Zhao, He, Wang, and Peng (2016) proposed planning technologies and an indicator system for LCN design. Another Chinese study investigated the relationship between land use data and urban indicators, such as density, land use mix, accessibility to public transport etc., and household carbon emissions in Beijing (Qin & Han, 2013). Li, Quan, and Yang (2016) proposed a GIS-based simulation model to assess the influence of urban form and building typology on the energy performance and carbon emissions of two districts in Macau, China.

3.3.6. Life cycle assessment

In this category, 9 articles (6.3 %) were collected. 8 of them addressed ZEN*s, where the concept focuses on GHG of a neighbourhood over its life cycle. In three studies, a modular LCA model for ZEN*s was proposed (Lausselet et al., 2019; Lausselet et al., 2021; Lausselet et al., 2020), Lausselet, Urrego, Resch, and Brattebø (2020) developed a dynamic material flow analysis LCA model. Lund, Lausselet, and Brattebø (2019) applied the model from Lausselet et al. (2019) to a Norwegian case study. Several studies (Lausselet et al., 2019; Lausselet, Ellingsen et al., 2020; Lund et al., 2019) highlight the significant contribution from mobility and transportation to the total emissions which is supported by Yttersian, Fuglseth, Lausselet, and Brattebø (2019), who developed an LCA tool, called OmrådeLCA (Norwegian for AreaLCA). Skaar, Solli, and Vevatne (2019) explored the system boundaries and ambition levels for a ZEN* campus based on key design choices. Skaar, Labonnote, and Gradeci (2018) conducted a mapping review to "analyse how parametric LCA and algorithms have been used to address neighbourhoods, buildings, and construction materials". The only non-ZEN*-related study presented a comparison of the life cycle performance of two different urban energy systems in Calgary, Canada (Guarino et al., 2020).

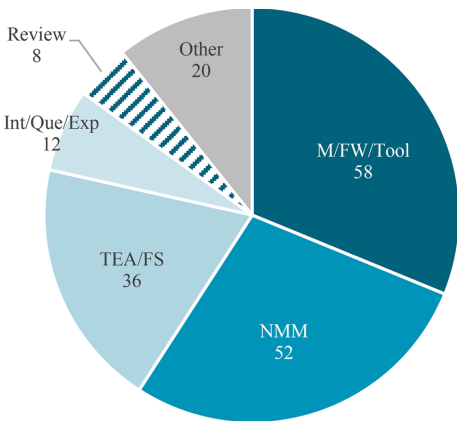

Fig. 6. Distribution of research methods used in the included studies.

3.3.7. Social aspects

A comparatively small number of articles (6 or 4.2 %) addressed social aspects. In two articles, the low-carbon behaviours of neighbourhood residents were investigated based on a survey (Peng, Wang, & Guo, 2018; Peng, Wang, Zhao, & Wang, 2018). Tironi (2020) reports on a public experiment in form of an urban laboratory in Santiago de Chile where a neighbourhood was temporarily transformed through design intervention. It included the introduction of bike lanes which replaced car lanes and sensor kits to measure air pollution and local climate conditions. Woods and Berker (2019) discussed the limitations and potentials associated with the concept of living labs in the ZEN* context and, in another study, present results from a survey conducted in a Norwegian case study (Woods & Berker, 2020). Soutullo, Aelenei, Nielsen, Ferrer, and Gonçalves (2020) present results from an empirical study using the testing facilities from the members of the Joint Program on Smart Cities of the European Energy Research Alliance.

3.3.8. Microclimate

Only 5 articles (3.5 %) are included in the category *Microclimate*. Two of which addressed urban heat island mitigation strategies (Castaldo et al., 2018; Lehmann, 2014). Gros, Bozonnet, Inard, and Musy (2016) presented the capabilities of two microclimatic and building energy simulation tools, EnviBatE and SOLENE-Microclimate, through a case study. Natanian and Auer (2020) proposed a holistic microclimatic energy and environmental quality evaluation workflow for Grasshopper to evaluate the impacts of building and urban design parameters on energy performance and environmental quality. Piselli, Di Grazia, and Pisello (2020) looked into the effect of outdoor microclimatic boundary conditions on air conditioning system efficiency and building energy demand.

3.3.9. Other

The 25 studies in this category, which represent 17.4 % of the included articles, addressed a variety of aspects of CFNs. Covered topics were for instance the design of buildings in a CFN (Acre & Wyckmans, 2015; Taveres-Cachat et al., 2019; Yang & Zhang, 2016), evaluating the economic benefits from CFNs (Becchio et al., 2018; Kalaycıoğlu & Yılmaz, 2017), or reporting the monitoring results from case studies (Guyot et al., 2020; Himpe, Janssens et al., 2015; Himpe, van de Putte et al., 2015). In some articles, indicator tools and systems were presented, e.g. Wiik, Fufa, Andresen, Brattebø, and Gustavsen (2019) for ZEN*s or Zhao, Yu, He, and Tu (2019) for the evaluation of rural LCN. Koutra et al. (2018) reviewed such assessment tools and sustainable approaches towards the development of NZED, while Zhang et al. (2019) reviewed green neighbourhood rating systems. Clerici Maestosi, Andreucci, and Civiero (2021) discussed frameworks and funding opportunities in Europe to drive the transition to PEDs and climate-neutral cities. Komninos, Kakderi, Mora, Panori, and Sefertzi (2021) addressed the knowledge gap about developing cross-sector, high-impact smart city systems and looked for a universal architecture, incorporating multiple

Table 3
Journals and Conferences (disregarding the journal volume or conference edition) that published three or more of the included articles.

Journals		Conferences	
Applied Energy	8	*Nordic Conference on Zero Emission and Plus Energy Buildings* (Nordic ZEB+)	9
Energies	7	*Conference on Smart Cities* (IEEE Smart Cities)	3
Building and Environment	6		
Energy	5		
Sustainability	5		
Buildings	5		
Sustainable Cities and Society	4		
Energy and Buildings	4		

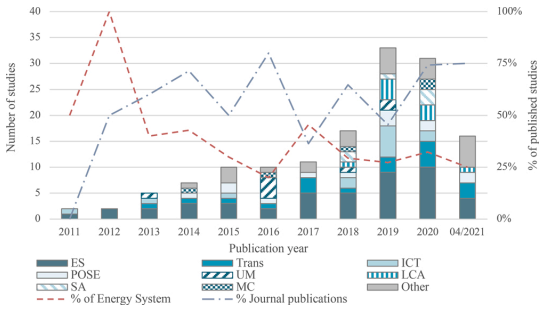

Fig. 7. Publication history of included articles according to the publication year.

dimensions of the smart city, including safety, transportation and energy. Other papers addressed solar shading in nZENs (Verbruggen et al., 2020), reviewed literature on net zero energy buildings to analyse the possibility to move to the neighbourhood scale (Nematchoua et al., 2021), or provided definitions of different PED types and a survey of the renewable energy market circumstances in the EU (Lindholm et al., 2021). Hedman et al. (2021) discussed challenges related to PEDs and provides an overview of the organization and tasks of IEA EBC Annex 83 Positive Energy Districts. The remaining articles in this category are given in the References (Ahlers, Driscoll et al., 2019; Good, Martínez Ceseña, Mancarella et al., 2017; Pinna et al., 2018; Scognamiglio et al., 2014).

3.4. Methods

Fig. 6 shows how often a specific research method has been used in the included literature. Many articles used more than one method and most commonly (in 58 publications or 40.3 %), the articles presented a new method, framework or tool (M/FW/Tool) which illustrates that the field is still quite new and a lot of methodological groundwork is carried out. The second most frequently used method (in 52 articles or 36.1 %) was numerical and mathematical Modelling (NMM), often in connection with M/FW/Tool (14 times). In 36 publications (25.0 %), a techno-economic analysis or feasibility study (TEA/FS) was carried out. In 12 studies (8.3 %), a survey in form of interviews or a questionnaire, or an experiment (Int/Que/Exp) was conducted. An experiment in this context means for example studies using a living laboratory. 8 of the studies (5.6 %) conducted a review (Rev). Studies marked as *Other* comprise for instance position papers, project reports and other kinds of analyses that are not captured by the previously mentioned research methods.

3.5. Publication channels, timeline and citations

In this section, the type of publication will be examined closer. 90 of the 144 (62.5 %) included elements were published as journal papers, 54 (37.5 %) as conference papers. As shown in chapter 2.1, book chapters, editorials, errata and all other kinds of publications were excluded from this analysis. Table 3 shows the journals and conferences (disregarding the journal volume/issue or conference edition) that published at least 3 of the included articles. *Applied Energy* published a total of 8 articles, followed by *Energies* with 7, *Building and Environment* with 6 and *Energy, Sustainability,* and *Buildings* with each 5. *Sustainable Cities and Society* and *Energy and Buildings* have 4 publications each.

By far the most conference papers (9) were published at the *Nordic Conference on Zero Emission and Plus Energy Buildings* (Nordic ZEB+), albeit the conference's name suggests a focus on the buildings rather than the neighbourhood scale. At the *Conference on Smart Cities* (IEEE Smart Cities), three of the included articles were published.

Fig. 7 shows the distribution of article topics and type according to the year of publication. 2011 marks the first year in which scientific articles related to CFNs were published. In that year, two conference articles with a focus on the ES and ICT were published. In the following, the number of published articles per year has been surpassing or has at least been equal to the number of published articles from the previous year until 2020, where three articles less than 2019 were published. As of April 2021, the time of literature identification, 16 articles were

Table 4
The 10 most cited articles of the included literature according to Web of Science.

Rank	Times cited	Title	Authors	Publ. channel	Category
1.	71	A simplified framework to assess the feasibility of zero-energy at the neighbourhood/community scale	(Marique & Reiter, 2014)	Energy Research & Social Science	*Trans*
2.	62	Low-carbon district heating in Sweden – Examining a successful energy transition	(Di Lucia & Ericsson, 2014)	Energy and Buildings	*ES*
3.	55	An optimisation framework for thermal energy storage integration in a residential heat pump heating system	(Renaldi et al., 2017)	Applied Energy	*ES*
4.	42	Energy system analysis of a pilot net-zero exergy district	(Kılkış, 2014)	Energy Conversion and Management	*ES*
4.	42	Low carbon districts: Mitigating the urban heat island with green roof infrastructure	(Lehmann, 2014)	City, Culture and Society	*MC*
6.	38	Integration of distributed energy storage into net-zero energy district systems: Optimum design and operation	(Sameti & Haghighat, 2018)	Energy	*ES*
7.	32	Rule-based demand-side management of domestic hot water production with heat pumps in zero energy neighbourhoods	(Coninck et al., 2014)	Habitat International	*ES*
7.	32	Planning parameters and household carbon emission: Evidence from high- and low-carbon neighborhoods in Beijing	(Qin & Han, 2013)	Journal of Building Performance Simulation	*UM*
9.	29	Simulation tools to assess microclimate and building energy – A case study on the design of a new district	(Gros et al., 2016)	Energy and Buildings	*MC*
10.	27	Ten questions concerning smart districts	(Good et al., 2017)	Building and Environment	*Other*

Table 5
The 10 most used author keywords in the included studies.

Rank	Keyword	No. of times used
1.	Smart city/Smart cities	19
2.	Positive Energy District(s)/PED	10
3.	Optimisation/Optimization	9
4.	Multi-energy carriers/Multi energy carrier systems/Multi energy systems	8
4.	District/District scale	8
4.	Zero emission neighbo(u)rhoods/ZEN	8
4.	(Local) renewable energy (integration)	8
5.	Photovoltaics/Photovoltaic energy/Photovoltaic systems	7
5.	Life cycle assessment (LCA)/LCA	7
5.	Energy efficiency	7

published. From 2012 onwards, the share of journal articles of the total number of publications has been at least 40 %, except for 2017 where it was 36 %. Unlike all other categories, *ES* studies have been published every year, with the highest percentage reached in 2012 (100 %). Over the last decade, there has been a declining trend in the share of *ES* publications. In 2021, so far 25 % of the published articles have been categorised as *ES*, the second-lowest value after 2016 with 20 %. Studies in the categories *SA* and *LCA* emerged as recently as 2018, while the earliest year of publication in the category *Trans* and *UM* was 2013, and in *POSE* and *MC* 2014.

The popularity of studies about the ES is also reflected by the list of the most cited (according to *Web of Science*) articles of included literature (see also Table 4). Half of the 10 most cited articles, as well as one of the two articles with the highest citation score, are assigned to category *ES*. The articles in category *ES* received 394 citations in total which are far more than in the other categories. The second most cited category is *Other* with 157, followed by *Trans* with 130, and *Urban morphology* with 113 citations. The category with the lowest citation count is *SA* with 5 citations. All 10 most cited articles were published in journals, the most cited conference paper, a review study of the concept and current research on energy hubs in energy positive neighbourhoods, received 12 citations (Walker et al., 2017). The citation analysis is biased towards the fact that more recent articles generally received fewer citations, simply because they might not be known to an equally large audience yet than articles from earlier publication years.

3.6. Author keyword analysis

The analysis of author keywords showed that *Smart city/Smart cities* were utilised the most among the included articles with a count of 19 (see also Table 5). Following the recent developments on a European scale, *Positive Energy District()s/PED* takes second place with being used 10 times. After that, *Optimization/Optimisation comes in with a count of 9 and Multi-energy carriers/Multi-energy carrier systems/Multi-energy systems, District/District scale, Zero emission neighbo(u)rhoods/ZEN, and (Local) renewable energy (integration)* take a shared third place having been used 8 times each. The fourth most used keywords, used 7 times, were *Photovoltaics/Photovoltaic energy/Photovoltaic systems*, *Life cycle assessment (LCA)/LCA,* and *Energy efficiency*.

4. Definitions of climate friendly neighbourhoods

As mentioned earlier, there are numerous concepts for CFNs which is illustrated by the great number of terms for CFNs from the systematic review (see Section 3.1). However, there aren't always clear definitions for every term and sometimes slightly differing definitions for the same term exist. Additionally, clear definitions of CFN concepts are rarely included in scientific articles. In the following, frequently used and well-defined CFN concepts mostly from EU-projects (see also Appendix A) and other literature are presented to complement the systematic review. The included projects are based on an ordinary web search and, in the case of the EU-funded projects, the cordis database (https://cordis.europa.eu/). Here, no structured approach was followed. This section provides an overview of some selected, existing definitions and projects that apply them. It is not intended to be exhaustive but to provide the reader with an overview of KPIs, targets, boundaries, assessment criteria and the most important references to the respective definitions.

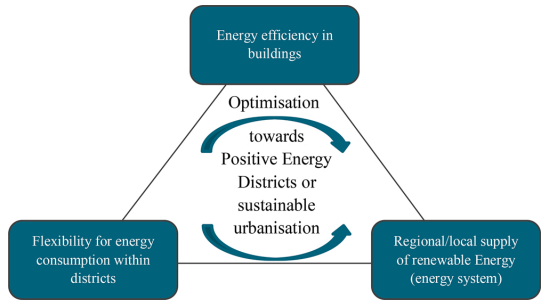

Fig. 8. Definition of Positive Energy Districts, modified from (European Commission Joint Research Centre, 2018).

4.1. Positive energy district

The PED concept is a common objective in many ongoing EU research projects, like for instance *SPARCS, POCITYF, ATELIER, +CityxChange*, and *Making City* (see also Appendix A). It is defined in the European SET Plan Action 3.2 Smart Cities and Communities Implementation Plan as "a district with annual net zero energy import, and net zero CO_2 emission working towards an annual local surplus production of renewable energy" (European Commission Joint Research Centre, 2018). PEDs are part of an urban and regional energy system to ensure security and flexibility of supply and storage. The key to a PED is to keep annual local energy use below the amount of locally produced renewable energy. PEDs also promote charging capabilities for electric vehicles and make use of advanced materials, local renewable energy sources, local storage, smart energy grids, demand response, energy management, user interaction and involvement, and ICT (see Fig. 8). At the same time, affordability for the inhabitants is highlighted in the implementation plan (European Commission Joint Research Centre, 2018).

In the *White Paper on the Reference Framework for Positive Energy Districts and Neighbourhoods* by Hinterberger, Gollner, Noll, Meyer, and Schwarz (2020) an essentially similar definition can be found. In their paper, however, PEDs and Positive Energy Neighbourhoods (PEN) are used sometimes interchangeably.

"Positive Energy Districts are energy-efficient and energy-flexible urban areas or groups of connected buildings which produce net zero greenhouse gas emissions and actively manage an annual local or regional surplus production of renewable energy. They require integration of different systems and infrastructures and interaction between buildings, the users and the regional energy, mobility and ICT systems while securing the energy supply and a good life for all in line with social, economic and environmental sustainability".

As to the size of a PED/PEN, no clear definition is given due to varying national conditions. Hinterberger et al. (2020) write that a definition at the national level might be appropriate and add that PEDs/PENs comprise a "group of connected buildings (respectively, more than one building)". An overview of 61 PEDs and projects that did not declare a PED ambition but are interesting for the PED program at different project stages is given by Gollner et al. (2020).

Although largely concurrent with the previously mentioned definitions, in IEA EBC Annex 83, the description of a PED is given without the clear focus on net zero GHG emissions. It is merely stated that PEDs are

"intended to shape cities into carbon neutral communities in the near future" and use low-carbon energy production (IEA EBC Annex 83, 2020). The whole definition is:

"[A]n area within the city boundaries, capable of generating more energy than is used, and agile/flexible enough to respond to respond to energy market variations. Rather than simply achieving an annual net energy surplus, it should also support minimizing impacts on the connected centralized energy networks by offering options for increasing onsite load-matching and self-use of energy, technologies for short- and long-term energy storage, and providing energy flexibility with smart control. PEDs can include all types of buildings present in the urban environment and they are not isolated from the energy grid. Within the research community, the PED is an emerging concept intended to shape cities into carbon neutral communities in the near future. Reaching the goal of a PED requires firstly improving energy efficiency, secondly cascading local energy flows by making use of any surpluses, and thirdly using low-carbon energy production to cover the remaining energy use. Smart control and energy flexibility are needed to match demand with production locally as far as practical, and also to minimize the burdens and maximize the usefulness of PEDs on the grid at large."

4.2. Positive energy block

The European Commission Smart Cities Marketplace: Positive energy blocks, 2021 defines a Positive Energy Block (PEB) as a "group of at least three connected neighbouring buildings producing on a yearly basis more primary energy than what they use" (Cartuyvels et al., 2018; European Commission Smart Cities Marketplace: Positive energy blocks, 2021). To utilise advantages from complementary consumption curves and local renewable energy production, consumption and storage, this group of buildings must be mixed-use. An important aspect of PEBs is the focus on energy. Embodied emissions are not included in its definition. The first PEB in operation in Europe is HIKARI in Lyon Confluence, France (European Commission Smart Cities Marketplace: Positive energy blocks, 2021). This project was also a case study in a paper by Roccamena et al. (Roccamena et al., 2019) which has been included in this article's review. However, in their paper, Roccamena et al. did not use the term block but district.

The European Commission uses PEB and PED interchangeably in their definition for the Horizon 2020 Work Programme 2018–2020 and do not mention the three-building-minimum but use the term "several buildings" which can be new, retro-fitted or both (European Commission, 2020a). Similar to the SET Plan Action 3.2 definition of a PED (European Commission Joint Research Centre, 2018), local renewable energy production and storage, as well as advanced materials, smart energy grids, demand-response, energy management and user interaction/involvement are the basis for PEB/PED (European Commission, 2020a). EU research projects that included PEBs in their objectives are for example *SPARCS* and *+CityxChange* (see also Appendix A).

4.3. Nearly zero energy neighbourhood

The definition of the *Nearly Zero Energy Neighbourhood research project (ZenN)* for a Nearly Zero Energy Neighbourhood (NZEN) is focussing on residential building clusters (Sørnes et al., 2014). The energy demand in such a cluster is to be low and partly met by renewable energy self-produced within the neighbourhood. The balance boundary for NZENs includes heating, cooling, ventilation, and domestic hot water. Lighting is only included in two non-residential demo case buildings in the project. Appliances were a priori excluded. The physical boundary includes the sites of renewable energy production besides the buildings themselves.

4.4. Zero emission neighbourhood

ZEN* is a term primarily coined by the Research Centre on Zero Emission Neighbourhoods and Smart Cities (FME ZEN) (Bremvåg et al., 2018, 2020; Kvellheim et al., 2021; Woods et al., 2019). Continuing the work from the Research Centre on Zero Emission Buildings (FME ZEB) (Hestnes & Eik-Nes, 2017) that was active from 2009 to 2017, it lifts the zero emission concept from the building to the neighbourhood scale.

In FME ZEN, a neighbourhood is defined as a group of interconnected buildings (new, existing, retrofitted or a combination) in a confined geographical area with associated infrastructure like for instance pavements, roads, grids, technologies for supply, generation, storage, and export of electricity and heat, and may also include grids and technologies for water, sewage, waste, mobility and ICT. The area needs to have a defined physical boundary to external grids. This physical boundary does not necessarily need to be the same as the boundary for analysis of energy facilities serving the neighbourhood.

In a ZEN*, depending on the chosen ambition level, different life cycle modules and building and infrastructure elements are included in its aim to reduce its direct and indirect GHG emissions towards zero over the analysis period. For buildings, normally a period of 60 years, for infrastructure 100 years are assumed. The definition underlines that a ZEN* should focus on the following (Wiik, Fufa, Baer et al., 2018; Wiik, Fufa, Krogstie et al., 2018):

- Plan, design and operate buildings and associated infrastructure components towards zero life cycle GHG emissions.

Table 6
ZEN* assessment criteria and KPIs covered in the ZEN* definition guideline (Wiik, Fufa, Baer et al., 2018; Wiik, Fufa, Krogstie et al., 2018).

Category	Assessment criteria	KPI
GHG emission	Total GHG emissions	Total GHG emissions in $tCO_{2eq}/m^2BRA/a$; $kgCO_{2eq}/m^2BAU/a$; tCO_{2eq}/capita
	GHG emission reduction	% reduction compared to the base case
Energy	Energy efficiency in buildings	Net energy need in $kWh/m^2BRA/a$; Gross energy need in $kWh/m^2BRA/a$; Total energy need in $kWh/m^2BRA/a$
	Energy carriers	Energy use in kWh/a; Energy generation in kWh/a; Delivered energy in kWh/a; Exported energy in kWh/a; Self-consumption in %; Self-generation in %; Colour coded carpet plot in kWh/a
Power/Load	Power/load performance	Net load early profile in kW; Net load duration curve in kW; Peak load in kW; Peak export in kW; Utilisation factor in %
	Power/load flexibility	Daily net load profile in kW
Mobility	Mode of transport	% share
	Access to public transportation	Meters; Frequency
Economy	Life cycle cost (LCC)	NOK; $NOK/m^2BRA/a$; $NOK/m^2BAU/a$; NOK/capita
Spatial qualities	Demographic needs and consultation plan	Qualitative
	Delivery and proximity to amenities	Number of amenities; Meters (distance from buildings)
	Public space	Qualitative
Innovation[1]	–	–

Abbreviations: Heated floor area (BRA); Outdoor space (BAU); Norwegian Kroner (NOK)[1]Assessment criteria and KPIs not yet decided upon.

Table 7
Categories, subcategories and KPIs defined in the syn.ikia evaluation framework (Salom & Tamm, 2020).

Category	Assessment criteria	KPI
Energy and Environmental Performance	Overall performance	Non-renewable primary energy balance, Renewable energy ratio
	Matching factors	Grid purchase factor, Load cover factor/Self-generation, Supply cover factor/Self-consumption
	Grid interaction factors	Net energy/Net power, Peak delivered/Peak exported power, Connection capacity credit
	Environmental balance	Total greenhouse gas emissions
Economic Performance	Capital costs	Investment costs, Share of investments covered by grants
	Operational costs	Maintenance-related costs, Requirement-related costs, Operation-related costs, Other costs
	Overall performance	Net Present Value, Internal Rate of Return, Economic Value Added, Payback Period, nZEB Cost Comparison
Indoor Environmental Quality	Indoor air quality	CO_2
	Thermal comfort	Predicted Mean Vote (PMV), Predicted Percentage Dissatisfied (PPD), Temperature, Relative Humidity
	Lighting and visual comfort	Illuminance, Daylight factor
	Acoustics comfort	Sound Pressure Level
Social Performance	Equity	Access to amenities, Access to services, Affordability of energy, Affordability of housing, Democratic legitimacy, Living conditions, Sustainable mobility, Universal design
	Community	Demographic composition, Diverse community, Social cohesion
	People	Personal safety, Energy consciousness, Healthy community
Smartness and Flexibility	Flexibility	Flexiblity index
	Smartness	Smartness Readiness Indicater (SRI)

- Become highly energy efficient and powered by a high share of new renewable energy in the neighbourhood energy supply system.
- Manage energy flows (within and between buildings) and exchanges with the surrounding energy system in a smart and flexible way.
- Promote sustainable transport patterns and smart mobility systems.
- Plan, design and operate with respect to economic sustainability, by minimising total life cycle costs.
- Plan and locate amenities in the neighbourhood to provide good spatial qualities and stimulate sustainable behaviour.
- Development of the area is characterised by innovative processes based on new forms of cooperation between the involved partners leading to innovative solutions.

Consequently, the ZEN* definition includes the following seven categories: GHG emissions, energy, power/load, mobility, economy, spatial qualities, and innovation. These categories each contain several assessment criteria and for each of those a set of KPIs. The ZEN* assessment criteria and KPIs that are covered in the ZEN* definition guideline are listed in Table 6.

4.5. Sustainable plus energy neighbourhood

The EU research project *syn.ikia* focuses on Sustainable Plus Energy Neighbourhoods (SPEN). The definition of a SPEN is closely aligned with the PED concept and describes a group of interconnected buildings with associated infrastructure, located within both a confined geographical area and a virtual boundary (Salom & Tamm, 2020). It aims to reduce its direct and indirect annual energy use towards zero and increased use and production of renewable energy. There is also a strong focus on cost efficiency, indoor environmental quality, occupant satisfaction, social factors (co-use, shared services and infrastructure) and power performance (peak shaving, flexibility, self-consumption). The following are the key aspects of a SPEN, according to (Salom & Tamm, 2020):

- Embedded in an urban and regional energy system and driven by renewable energy to provide optimized security and flexibility of supply
- Based on a high level of energy efficiency in order to keep annual local energy consumption lower than the amount of locally produced renewable energy
- Enables increased use of renewable energy within the local and regional energy system by offering optimized flexibility and by managing consumption and storage capacities according to demand
- Couples the built environment with sustainable energy production, consumption, and mobility (e.g. EV charging) to create added value and incentives for the consumers and the society
- Makes optimal use of advanced materials, local renewable energy supply, and other low carbon solutions (i.e. local storage, smart energy grids, demand-response, cutting-edge energy management systems, user interaction, and ICT).
- Offers affordable living, improved indoor environment, and well-being for the inhabitants

syn.ikia also addresses the common issue of where to draw the system boundaries for the evaluation of a SPEN. Three different boundary types are defined (Salom & Tamm, 2020):

- *Geographical boundary*: where the spatial-physical limits of the building portfolio, sites and infrastructures may be contiguous or in a configuration of detached patches
- *Functional boundary:* where the limits are with regard to the energy grids
- *Virtual boundary:* where the limits are in terms of contractual boundaries, e.g. including an energy production infrastructure owned by the occupants but situated outside the normal geographical boundaries.

"[T]he net positive yearly energy balance of a SPEN will be assessed within the virtual and/or geographical boundaries. Thus, a SPEN is able to achieve a net positive yearly energy balance and dynamic exchanges within the geographical/functional boundaries, but in addition, it will provide a connection between buildings within the virtual boundaries of the neighbourhood. In a SPEN, buildings are digitally connected via digital cloud hub […], common ICT infrastructure and Energy Management Systems. Dynamic exchanges with the hinterland may be provided to compensate for momentary surpluses and shortages according to the assessment boundary methods." Reference (Salom & Tamm, 2020) also provides a list of KPIs in the syn.ikia evaluation framework (see Table 7).

4.6. Near zero energy retrofit district

In transition track 1 of the EU research project *IRIS,* several terms for CFNs are used. While the name of this track is "Renewable and energy positive districts" the designation of the integrated solution relevant in the context of a CFN is "Near zero energy districts". In the deliverables, however, the term "Near zero energy retrofit district" (nZERD) is used for this solution and KPIs have been developed for it (see Table 8)

Table 8
Categories and KPIs defined in the IRIS research project (Tryferidis et al., 2019).

Category	KPI
Technical	Energy demand and consumption, Energy savings, Degree of energetic self-supply by renewable energy sources, Maximum Hourly Deficit, Technical compatibility, Improved interoperability
Environmental	CO_2 Emission Reduction, Increase in Local Renewable Energy Generation, Reduction in annual final energy consumption
Economic	Total investments, Grants, Total annual costs, Payback, Return on Investment, Fuel poverty, CO_2 reduction cost efficiency, Financial benefit for the end user, Reduction of energy cost, Stimulating an innovative environment
Social	Professional stakeholder involvement, Advantages for end-users, Increased environmental awareness, Increased consciousness of citizenship, Increased participation of vulnerable groups, Ease of use for end users of the solution, People reached, Advantages for stakeholders, Social compatibility, Consumers engagement
ICT	Reliability, Increased system flexibility for energy players
Legal	Change in rules and regulations, Green Building self-consumption Legal Framework Compatibility

(Tryferidis et al., 2018, 2019). Energy consumption is to be reduced and renewable production to be increased which will lead to more stable and lower housing bills in combination with higher comfort/less draught and humidity in homes for the citizens. Within the *IRIS* framework, the following nZERD solutions are expected to be demonstrated (Tryferidis et al., 2018):

- Near zero energy building retrofit in the social housing sector
- Smart street lighting
- Smart hybrid heat pumps
- Energy efficient deep retrofitting
- District heating optimization
- Citizen Utilities Savings through awareness
- House with integrated technologies in façade and roof
- Geothermal energy for preheating incoming ventilation

4.7. Low energy district

In the recently finished projects *REMO Urban* and *GrowSmarter*, Low Energy Districts (LED) were to be developed. Neither of the two projects gives a detailed definition of what constitutes an LED, but list actions connected to them. In *REMO Urban*, monitoring tools for energy, district scale retrofitting, renewable heating and cooling, electricity distributed generation, and advanced building energy management systems are specified. Furthermore, "[a] 50 % reduction of the building energy consumption will be achieved through retrofitting interventions, but also by improving lighting and equipment efficiency. Low carbon solutions for thermal energy supply and optimized electric facilities by means of decentralized electricity generation and smart grid management will be deployed in order to achieve near zero energy and zero emission districts". Again, several CFN terms are used in the same context without clearly differentiating between the single concepts or defining a clear goal.

In *GrowSmarter*, the LED action area focuses on reducing the energy use, environmental impact, and carbon footprint by implementing affordable and sustainable retrofit solutions at a large scale. The solutions that were applied in the participating demo cities were energy efficient refurbishments, smart energy management systems, sometimes also including photovoltaics and energy storage at the building and district level (Sanmarti & Sola, 2019).

4.8. Zero energy community

Quite early on, Carlisle, van Geet, and Pless (2009) from the National Renewable Energy Laboratory presented a report in which the definition of a Zero Energy Community (ZEC) is included. The terminology used in this document comprises Zero Energy Community, Net-Zero Energy Community and Zero Net Energy Community. It is not made clear why these different terms were used or if they are supposed to be used as synonyms. Generally, the definition is based on the work by Torcellini, Pless, Deru, and Crawley (2006) who focused on the building scale. Carlisle et al. (2009) write a ZEC is "one that has greatly reduced energy needs through efficiency gains such that the balance of energy for vehicles, thermal, and electrical energy within the community is met by renewable energy". They further specify that if the community produces at least 75 % of its required energy through the use of on-site renewable energy, it is considered a near-zero community. In Table 9, the classification system where ZECs are rated according to different energy supply options from Carlisle et al. (2009) is presented.

Table 9
ZEC classification system according to different energy supply options from Carlisle et al. (2009).

ZEC classification	Renewable energy supply option
A	1 Energy efficiency opportunities maximized 2 100 % energy load met by renewables in the built environment and unbuildable brownfield sites within the community
B	1 Energy-efficiency opportunities maximized 2 A fraction of the energy load met by renewables in the built environment and unbuildable brownfield sites within the community 3 A fraction of the energy load met by renewable generation on community greenfield sites or from off-site renewables used on site
C	1 Energy-efficiency opportunities maximized 2 A fraction of the energy load met by renewables in the built environment and unbuildable brownfield sites within the community 3 A fraction of the energy load met by renewable generation on community resources or from off-site renewables used on site 4 A fraction of the energy load met through RECs[1] that add new grid generation capacity
D	1 Energy efficiency opportunities maximized 2 The remainder of the load is met through RECs that add new grid generation capacity

[1] RECs represent the attributes of electricity generated from renewable energy. These attributes can be unbundled from the electricity and bought and sold separately.

4.9. Other concepts

In *Sharing Cities*, the significant benefits of smart city concepts and solutions are demonstrated by focusing on the needs of Low Energy Neighbourhoods. Specifically, retrofitting buildings, installing integrated energy management systems and smart lamp posts, as well as introducing electric mobility services are named. However, no set of KPIs or further explanation of the term is given.

In the *MAtchUP* project, high-performance districts (HPD) are aimed at through building energy efficiency improvements, integrating high shares of renewables in the energy supply, and implementing advanced energy management systems in combination with innovative storage systems. Specific focus is put on reducing the grid impact of the urban energy infrastructure. A list of targets, KPIs or assessment criteria of

Table 10
KPIs and targets as defined by the Zero-Plus research project (Zero-Plus, 2020b).

KPI	Target
Net regulated energy consumption (kWh/m^2/year)	< 20 kW h/m^2/year
Renewable Energy production (kWh/m^2/year)	> 50 kW h/m^2/year
Cost reduction	16 % reduction compared to the reference case

Table 11
Key energy-related elements to address in the Zero Energy District (ZED) master plan structure based on the DOE's experience with the ZEDA partners (Pless et al., 2018).

General energy strategy	Definitions of energy-related metrics being considered/used (e.g., zero energy) Energy modelling/analysis approach for different district design scenarios - Existing consumption/benchmarking/minimum code scenario - Alternative design scenarios Building and energy systems retrofit/construction phasing strategy Design guidelines and design advisory board Utility interconnection technical considerations
Building-scale energy requirements	Building types and areas, including structured parking Building efficiency levels for both new construction and existing building upgrades - Relevant efficiency codes and targeted percentage reductions relative to code - Energy use intensity targets - Labeling/certification/recognition options • Residential: Home Energy Rating System, DOE Zero Energy Ready Home, ENERGY STAR® Certified Homes, LEED, Passive House, Home Energy Score, Home Performance with ENERGY STAR, etc. • Commercial: LEED, ENERGY STAR, International Living Future Building Institute Living Building Challenge, New Buildings Institute, etc. Building systems to interface with district systems Solar access - Available roof area maximization - Solar-ready design guidelines Batteries/load control for demand management and microgrids
District-scale energy strategies	Energy-efficiency characteristics of nonbuilding infrastructure - Site and surface parking lighting District thermal systems - Load diversity and shared heat opportunities - Centralized waste heat recovery opportunities • Data centres, sewer lines, shared ground wells Large solar - Parking canopy, community solar Microgrids/batteries/load control at distribution/utility scale Electric vehicle charging infrastructure and anticipated loads Other sustainability strategies (e.g., water efficiency, waste reduction) and how they interact with energy strategy

HPDs, however, is missing.

Net Zero Energy Settlements (NZES) were the targeted CFN concept in *Zero-Plus*. The KPIs and targets for NZES within the *Zero-Plus* research project are listed in Table 10.

But also outside of Europe, governments have taken action and supported projects to address the zero energy objective at the district scale. In the United States, for instance, the Department of Energy (DOE) launched the *Zero Energy Districts Accelerator* (ZEDA) in late 2016. ZEDA was a three-year effort that provided a platform for districts, researchers, experts, and related national organizations to explore and address issues facing the implementation of ZEDs. The aim was to help partners further develop their projects and find solutions while identifying and refining promising practices with each other and the market (Better Buildings, 2021; Pless et al., 2018). Pless et al. (2018) report a ZED master plan structure with key energy strategies of a ZED to help guide each district through the energy planning process. These strategies are divided into a general energy strategy, building-scale efficiency requirements, and district-scale energy strategies (see Table 11). The ZED master plan structure also contains other key sections, including District Description and Vision/Goals, Stakeholders/Community Engagement, Utility Engagement, Financial Strategy, and Operations. Unfortunately, no KPIs or targets are reported.

In Canada, the *Net Zero Homes* project is funded by Natural Resources Canada under the ecoENERGY Innovation Initiative and in-kind contributions of the building industry with over $4 million (Net Zero Homes, 2015). Founded in 2013, the objective of the project is to demonstrate the feasibility of building Net Zero Energy Housing Communities (NZEHC) in Ontario, Quebec, Nova Scotia, and Alberta, to address challenges to NZEHC specific to production housing, and to act as a platform for the broader application of NZEHC across the country. To the best of our knowledge, a definition of the NZEHC concept, however, is not available.

5. Discussion

5.1. Systematic review

As can be seen in the results of this work's systematic review, there is a large variety of topics addressed in scientific publications on CFNs. The interest in the scientific community has been growing continuously over the years with the earliest included studies dating back one decade (2011). Similar to the situation of the low, net/nearly zero energy/emission concept at the building scale (Kibert & Fard, 2012; Marszal et al., 2011; Williams et al., 2016), a great number of different and coexisting terminologies have been introduced over the years. In the 144 included articles of the systematic review, more than 35 different terminologies were used. This proliferation of terms causes not only confusion among the authors of scientific papers but makes it unnecessarily difficult for non-expert readers to follow. It furthermore complicates comparing methodologies or projects with each other as at the same time targets are often not defined. This issue has also been identified by Saheb et al. (2018). Interestingly, even the same case study projects have been addressed with different terminologies for its CFN concept. A more consistent and uniform description of targets, key performance indicators, system boundaries, and scales would not only facilitate but foster the adaption of CFN concepts in municipalities and local initiatives that are interested in becoming more sustainable.

The review has shown that there is a distinct imbalance in the number of articles in each category. While most of the studies were focussing on the energy system in building clusters, there is a clear lack of articles dealing for instance with embodied energy/emissions and LCA, the microclimate or the social aspects in CFNs. It is also visible from the results that transforming existing neighbourhoods into a CFN, one of the main research areas of the EU does not receive the same level of attention in published scientific articles. Although representing the second-largest category, only a quite small percentage of included articles (13.2 %) addressed this topic. The reviewed articles still focus

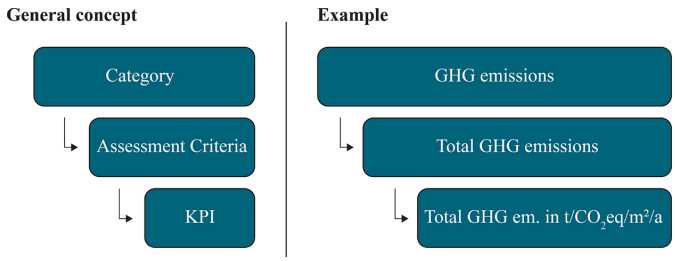

Fig. 9. System of category, assessment criteria and KPIs (general concept to the left and an example to the right).

predominantly on building-related issues, while little attention is paid to other important dimensions of a neighbourhood/district/block etc. It is important to realise that neighbourhoods/districts/blocks etc. do not only encompass buildings but also the air-filled space between them, as well as infrastructure and people with their associated activities (like mobility). Hallman (1984) definition of a neighbourhood particularly puts weight on the social aspect, describing it as "[…] a limited territory within a larger urban area, where people inhabit dwellings and interact socially". More research on how a neighbourhood/district/block can promote peoples' interaction with each other, their environment and technology to support sustainable awareness and behaviour is critical. Furthermore, microclimatic effects have only rarely been addressed in the reviewed studies. With the climate changing, especially the spatial quality and wellbeing (incl. thermal comfort) in outdoor spaces are aspects with increasing importance in urban planning which should not be neglected in the context of CFNs (Wu, 2014).

The novelty of this research domain explains the large fraction of articles proposing new methodologies, frameworks or tools, as its theoretical foundation has not yet fully been laid. This is also partly illustrated by the already mentioned variety of terminologies that are often used interchangeably. The novelty of this field might also explain, why the most-discussed topic among the literature subset has been the energy system, as it is responsible for the largest fraction of emissions or energy use, thus beyond doubt the most important element in reaching a CFN target. The overall attention has therefore been concentrated on this central aspect of a CFN, while the more secondary aspects like social, microclimatic, economic considerations etc. have received less attention. Because of that, research in these areas has the potential to fill wide research gaps.

As shown in this review, in more than half of the included articles, case studies have been used to apply research. Although case studies from all continents have been used in the included subset of literature, the global distribution is quite unbalanced. Certainly fueled by the ambitions and consequently public funding of research and demonstration projects in the EU, Europe is a hotspot for case studies (Joint Programming Initiative (JPI) Urban Europe (2021). Also, China hosts a number of case studies. There, however, the vaguely defined low carbon concept is dominant. More research outside of Europe and China is needed to cover a broader spectrum of climates and facilitate the application of CFNs in a wider geographical context, especially where the main increase of global population is expected to take place.

5.2. Definitions of climate friendly neighbourhoods

When looking at existing definitions for CFN concepts, initiatives at the European level, as well as nationally and EU-funded research projects play an important role. In several of these projects, definitions for CFNs have been developed and/or applied. Most commonly, the PED concept is targeted, as defined by the European SET Plan Action 3.2 Smart Cities and Communities Implementation Plan (European Commission Joint Research Centre, 2018). Another frequently applied concept is the PEB (Cartuyvels et al., 2018; European Commission Smart Cities Marketplace: Positive energy blocks, 2021). Other quite detailed definitions that also include a list of categories and KPIs were developed for example by *FME ZEN* for ZEN* (Wiik, Fufa, Baer et al., 2018; Wiik, Fufa, Krogstie et al., 2018), *syn.ikia* for SPEN (Salom & Tamm, 2020), and *IRIS* for nZERD (Tryferidis et al., 2018, 2019). In some research projects, rather vaguely defined concepts are targeted, like the LED or LEN.

However, there is an ongoing discussion on whether to include mobility in the CFN definitions and consequently allocate this "burden" to the buildings or not, as urban form undoubtedly has a significant influence on energy use and emissions from mobility. While in some of the definitions, mobility is explicitly mentioned, in others it is left out. In some research projects, mobility is not part of the CFN concept but represents an own action area, like for example in the projects *REMO Urban, MAtchUP* and *GrowSmarter*. Generally, where to draw the boundaries is a common problem among such definitions and therefore needs to be stated clearly. In *syn.ikia's* SPEN concept, different boundaries are defined which can be used as an example for other definitions as well.

KPIs are often listed as third level after categories and assessment criteria or subcategories (see Fig. 9). This way, the concept-specific priorities can be grasped quickly. A more standardized set of KPIs, however, would facilitate comparing case studies of different CFN types.

As shown, there are various international efforts and collaborations dedicated to paving the way to a cleaner, healthier and more resilient built environment in the future. Still, there are many barriers, namely political/regulatory, economic, social, and technological, as identified by Good, Martínez Ceseña, Mancarella, Monti et al. (2017) that need to be overcome before CFNs can find a broad application.

6. Conclusion

During the last years, there has been considerable research activities and thus dissemination in the field of Climate Friendly Neighbourhoods (CFN). This paper presented a systematic review of scientific literature from the databases *Scopus* and *Web of Science*. The results of this study help researchers to contextualize their research, as well as to identify focus areas, research gaps, future research possibilities, and similar studies within their research domain. The databases were searched by using a pre-defined syntax. In total, 144 articles have been found eligible, categorised and analysed according to the terminology used, their publication year, topic, method, location of case studies (if

applicable), keywords (where specified), citations, and publication channels. The main findings were:

- In the literature subset of 144 articles, a total of 35 different terminologies were used. There is a lack of common definitions, targets and key performance indicators which makes it unnecessarily difficult for academics and especially non-expert readers to follow or to compare different projects using the same terms.
- The first publication in the included literature dates back one decade (2011). Since then, the yearly number of publications has been rising continuously with exception of 2020. Whereas in 2011, two of the included articles were published, in 2019 it was 33. As of April 2021, when the literature identification has been carried out, so far 16 publications were registered for this year. In total, 90 publications (62.5 %) were published in academic journals, the remaining ones as conference papers. The most used keyword among the articles was *Smart city/Smart cities*, being used 19 times.
- A distinct imbalance has been identified regarding the number of articles in each topic category. While most of the studies were focussing on the energy system in building clusters, there is a clear lack of articles dealing for instance with embodied energy/emissions and LCA, the microclimate or the social interdependencies in CFNs. The reviewed articles still focus predominantly on building-related issues, while little attention is paid to other important dimensions of a neighbourhood/district/block like social and spatial aspects (microclimate, outdoor thermal comfort etc.). More research is needed to fill this gap.
- A considerable part of the included articles presented new methodologies, frameworks or tools (58 publications or 40.3 %) which illustrates that the field is still quite new and a lot of methodological groundwork is carried out. The second most frequently used method (52 articles or 36.1 %) was numerical and mathematical modelling, often in connection with presenting a new methodology, framework or tool (14 times).
- More than half (87 or 60.4 %) of the 144 reviewed studies applied their research to case studies. 17 case studies were located in Norway and 11 in China, followed by Italy with 10, Belgium with 9, Germany with 8, and Sweden and Spain with 7.

Finally, some selected CFN definitions from research projects, mainly in Europe, are shown. This paper stresses the need for clear definitions and a more structured approach in developing them. The levels of detail of CFN definitions vary widely and range from a few describing sentences to detailed descriptions of system boundaries, KPIs and targets. However, most existing definitions of CFNs are not yet methodologically sound, meaning that key performance indicators, system boundaries and targets are not always clearly defined. This makes it hard for policymakers, researchers and planning professionals to carry out an independent assessment of reported CFN performances. Especially in large, publicly funded research projects, clear definitions are needed to facilitate the comparability of case studies (also of different CFN types) and increase transparency. A standard set of categories, KPIs, system boundary types, and clear definitions of the spatial scales could help to systematically develop CFN base definitions that still offer the possibility for customization, as every case study presents individual features and circumstances. Research in the future should, therefore, focus on clear common definition guidelines.

7. Limitations

As mentioned earlier, there are some limitations in this study that need to be kept in mind. First of all, the identification of articles is strongly dependent on the content of the searched databases and the used search phrases. The ultimately deployed search phrase is often a trade-off between several other possible search phrases, either resulting in too many results to be screened and analysed within a reasonable amount of time or yielding too few elements to represent a meaningful subset of the literature of interest. However, by doing that, many relevant publications and reports may be missed, if they do not specifically mention the search terms in their title, abstract or keywords or have not been published in form of a peer-reviewed article. Moreover, there have been articles that were not accessible due to licensing restrictions but might be highly relevant.

During the screening and eligibility phase of the applied methodology, many articles have been sorted out due to their content or poor quality. While this has been done to the best of the authors' judgement, it is highly subjective and a different group of authors might have come to a different subset of literature. The same applies to the categorisation of the included articles.

In the second part of this article, selected definitions of frequently used or well-defined CFN concepts and projects were shown. This selection is not complete as it does not include research projects and initiatives for example from Asia, South America, Oceania or Africa. Moreover, it was not possible to list all the relevant information connected to the CFN definitions within the scope of this article. For more information, it is recommended to visit the respective project websites, or referenced publications in this section.

Declaration of Competing Interest

The authors declare that they have no known competing financial interests or personal relationships that could have appeared to influence the work reported in this paper.

Acknowledgements

This paper has been written within the Research Centre on Zero Emission Neighbourhoods in Smart Cities (FME ZEN). The authors gratefully acknowledge the support from the ZEN partners and the Research Council of Norway.

Appendix A

In line with Europe's ambition to be a global role model in energy transition and reducing its carbon footprint, the EU funded a number of projects with a focus on sustainability, the reduction of energy use, and GHG emissions at the neighbourhood/district/block scale (Joint Programming Initiative (JPI) Urban Europe (2021). They are funded by Horizon 2020, the biggest EU research and innovation programme so far with a budget of almost €80 billion over 7 years (2014–2020) in addition to private and national public investments (European Commission, 2014a). Within the 6th and 7th EU Framework Programmes of the EU, a number of projects have been funded under the CONCERTO initiative (https://smartcities-infosystem.eu/sites-projects/projects). Table A1 lists a selection of ongoing and recently finished projects focusing on CFNs. More Horizon 2020 funded projects can be found at https://cordis.europa.eu/en. At this point, also the research activities of the International Energy Agency, namely IEA EBC Annex 83 (https://annex83.iea-ebc.org/) on *Positive Energy Districts* (2020–2024) and Task 63 in the IEA Solar Heating and Cooling Programme (SHC) (https://task63.iea-shc.org/) about Solar Neighbourhood Planning (2019–2023) are worth mentioning.

Table A1
List of selected EU-funded projects.

Project name and ID	CFN type	Website and project period	Participating cities	Additional References
REMO Urban ID: 646511	LED	http://www.remourban.eu/ 01/2015–12/2019	Valladolid (ESP) Nottingham (GBR) Tepebaşi (TUR) Seraing (BEL) Miskolc (HUN)	(REMO Urban, 2020)
GrowSmarter ID: 646456	LED	https://grow-smarter.eu/ 01/2015–12/2019	Stockholm (SWE) Cologne (DEU) Barcelona (ESP) Graz (AUT) Porto (PRT) Suceava (ROU) Cork (IRL) Valletta (MLT)	(Pejstrup et al., 2019; Sanmarti & Sola, 2019)
Sharing Cities ID: 691895	LEN	http://www.sharingcities.eu/ 01/2016–12/2020	London (GBR) Lisbon (PRT) Milan (ITA) Warsaw (POL) Bordeaux (FRA) Burgas (BGR)	(Eurocities, 2017)
SPARCS ID: 864242	PEB/PED	https://www.sparcs.info/ 10/2019–09/2024	Espoo (FIN) Leipzig (DEU) Reykjavik (ISL) Maia (PRT) Kladno (CZE) Lviv (UKR) Kifissia (GRC)	
POCITYF ID: 864400	PED	https://pocityf.eu 10/2019–09/2024	Alkmaar (NLD) Évora (PRT) Bari (ITA) Celje (SVN) Granada (ESP) Hvidovre (DNK) Ioánnina (GRC) Újpest (HUN)	
ATELIER ID: 864374	PED	https://smartcity-atelier.eu/ 11/2019–10/2024	Amsterdam (NLD) Bilbao (ESP) Bratislava (SVK) Budapest (HUN) Copenhagen (DNK) Krakow (POL) Matosinhos (PRT) Riga (LVA)	
+CityxChange ID: 824260	PEB/PED	https://cityxchange.eu/ 11/2018–10/2023	Trondheim (NOR) Limerick (IRL) Sestao (ESP) Alba Iulia (ROU) Písek (CZE) Võru (EST) Smolyan (BGR)	(Ahlers, Driscoll et al., 2019)
Making-City ID: 824418	PED	http://makingcity.eu/ 12/2018–11/2023	Groningen (NLD) Oulu (FIN) Bassano Del Grappa (ITA) León (ESP) Trenčín (SVK) Kadiköy (TUR) Lublin (POL) Vidin (BGR)	(Alpagut et al., 2019)
IRIS ID: 774199	nZERD	https://www.irissmartcities.eu/ 10/2017–09/2022	Utrecht (NLD) Nice (FRA) Gothenburg (SWE) Vaasa (FIN) Alexandroupolis (GRC) Santa Cruz de Tenerife (ESP) Foscani (ROU)	(Tryferidis et al., 2018, 2019)
Zero-Plus ID: 678407	NZES	http://www.zeroplus.org/ 10/2015-09/2019	Case studies in: York (GBR) Granarolo dell'Emilia (ITA) Nicosia (CYP) Voreppe (FRA)	(Zero-Plus, 2017, 2018, 2020a, 2020b)
syn.ikia ID: 869918	SpEN	https://synikia.eu 01/2020–06/2024	Demo neighbourhoods in: Oslo (NOR) Uden (NLD) Salzburg (AUT) Santa Coloma de Gramenet (ESP)	(Salom & Tamm, 2020)

(*continued on next page*)

Table A1 (*continued*)

Project name and ID	CFN type	Website and project period	Participating cities	Additional References
RESPONSE ID: 957751	PED	https://h2020response.eu/ 10/2020–09/2025	Turku (FIN) Dijon (FRA) Brussels (BEL) Zaragoza (ESP) Botosani (ROU) Ptolemaida (GRC) Gabrovo (BGR) Severodonetsk (UKR)	
MatchUP ID: 774477	HPD	https://www.matchup-project.eu/ 10/2017–09/2022	Valencia (ESP) Dresden (DEU) Antalya (TUR) Herzliya (Israel) Kerava (FIN) Ostend (BEL) Skopje (MKD)	

References

Acre, F., & Wyckmans, A. (2015). The impact of dwelling renovation on spatial quality. *Smart and Sustainable Built Environment, 4*(3), 268–309. https://doi.org/10.1108/SASBE-05-2015-0008

Ahlers, D., Driscoll, P., Wibe, H., & Wyckmans, A. (2019). Co-creation of positive energy blocks. In *IOP Conference Series: Earth and Environmental Science, 352* p. 12060). https://doi.org/10.1088/1755-1315/352/1/012060

Ahlers, D., Wienhofen, L. W. M., Petersen, S. A., & Anvaari, M. (2019). A smart City ecosystem enabling Open innovation. In K.-H. Lüke, G. Eichler, C. Erfurth, & G. Fahrnberger (Eds.), *Communications in Computer and Information Science. INNOVATIONS FOR COMMUNITY SERVICES: 19th International Conference, i4cs, 1041* pp. 109–122). https://doi.org/10.1007/978-3-030-22482-0_9. SPRINGER NATURE.

Ala-Juusela, M., Crosbie, T., & Hukkalainen, M. (2016). Defining and operationalising the concept of an energy positive neighbourhood. *Energy Conversion and Management, 125*, 133–140. https://doi.org/10.1016/j.enconman.2016.05.052

Alpagut, B., Akyürek, Ö., & Mitre, E. M. (2019). Positive energy districts methodology and its replication potential. *Proceedings, 20*(1), 8. https://doi.org/10.3390/proceedings2019020008

Amaral, A. R., Rodrigues, E., Rodrigues Gaspar, A., & Gomes, Á. (2018). Review on performance aspects of nearly zero-energy districts. *Sustainable Cities and Society, 43*, 406–420. https://doi.org/10.1016/j.scs.2018.08.039

Askeland, M., Backe, S., & Lindberg, K. B. (2019). Zero energy at the neighbourhood scale: Regulatory challenges regarding billing practices in Norway. In *IOP Conference Series: Earth and Environmental Science, 352* p. 12006). https://doi.org/10.1088/1755-1315/352/1/012006

Aste, N., Adhikari, R. S., Caputo, P., Del Pero, C., Buzzetti, M., & Leonforte, F. (2017). In *Smart-Grid and Smart-Districts: Case-Study and Techno-Economic Analysis*.

Aste, N., Caputo, P., Del Pero, C., Ferla, G., Huerto-Cardenas, H. E., Leonforte, F., et al. (2020). A renewable energy scenario for a new low carbon settlement in northern Italy: Biomass district heating coupled with heat pump and solar photovoltaic system. *Energy, 206*, 118091. https://doi.org/10.1016/j.energy.2020.118091

Backe, S., Pinel, D., del Granado, P. C., Tomasgard, A., Korpås, M., & Lindberg, K. B. (2018). Towards zero emission neighbourhoods: Implications for the power system. In *15th International Conference on the European Energy Market (EEM)*. https://doi.org/10.1109/EEM.2018.8469976

Baetens, R., Coninck, R., Helsen, L., & Saelens, D. (2011). Integrated dynamic electric and thermal simulations for a residential neighborhood: Sensitivity to time resolution of boundary conditions. In *Proceedings of Building Simulation 2011: 12th Conference of International Building Performance Simulation Association* (pp. 1745–1752).

Bartolini, A., Carducci, F., Giovannelli, A., & Comodi, G. (2018). In *Conference Proceedings 2018 IEEE International Conference on Environment and Electrical Engineering and 2018 IEEE Industrial and Commercial Power Systems Europe (EEEIC/I & CPS Europe)*.

Becchio, C., Bottero, M. C., Corgnati, S. P., & Dell'Anna, F. (2018). Decision making for sustainable urban energy planning: An integrated evaluation framework of alternative solutions for a NZED (Net Zero-Energy District) in Turin. *Land Use Policy, 78*, 803–817. https://doi.org/10.1016/j.landusepol.2018.06.048

Belussi, L., Barozzi, B., Bellazzi, A., Danza, L., Devitofrancesco, A., Fanciulli, C., et al. (2019). A review of performance of zero energy buildings and energy efficiency solutions. *Journal of Building Engineering, 25*, 100772. https://doi.org/10.1016/j.jobe.2019.100772

Better Buildings. (2021). *Zero Energy Districts - Completed*. U.S. Department of Energy. https://betterbuildingssolutioncenter.energy.gov/accelerators/zero-energy-district.

Blumberga, A., Vanaga, R., Antuzs, J., Freimanis, R., Bondars, E., & Treija, S. (2019). Is the High Quality Baukultur a Monkey Wrench in the Global Climate Challenges? *Environmental and Climate Technologies, 23*(3), 230–244. https://doi.org/10.2478/rtuect-2019-0092

Blumberga, A., Vanaga, R., Freimanis, R., Blumberga, D., Antužs, J., Krastiņš, A., et al. (2020). Transition from traditional historic urban block to positive energy block. *Energy, 202*, 117485. https://doi.org/10.1016/j.energy.2020.117485

Boccalatte, A., Fossa, M., & Ménézo, C. (2020). Best arrangement of BIPV surfaces for future NZEB districts while considering urban heat island effects and the reduction of reflected radiation from solar façades. *Renewable Energy, 160*, 686–697. https://doi.org/10.1016/j.renene.2020.07.057

Bossi, S., Gollner, C., & Theierling, S. (2020). Towards 100 positive energy districts in Europe: Preliminary data analysis of 61 European cases. *Energies, 13*(22), 6083. https://doi.org/10.3390/en13226083

Bourdeau, M., Riederer, P., Rezgui, Y., & Desmedt, J. (2013). An ICT framework for coupling renewables and energy storage in low carbon districts and cities. In G. F. Issa (Ed.), *2013 1st International Conference & Exhibition on the Applications of Information Technology to Renewable Energy Processes and Systems (IT-DREPS): Date: 29-31 May 2013 (Pp. 133–138)*.. https://doi.org/10.1109/IT-DREPS.2013.6588169

Bremvåg, A., Gustavsen, A., & Hestnes, A. G. (Eds.). (2018). ZEN Research Centre on Zero Emission Neighbourhoods in Smart Cities: Annual Report 2017.

Bremvåg, A., Hestnes, A. G., & Gustavsen, A. (Eds.). (2020). ZEN Research Centre on Zero Emission Neighbourhoods in Smart Cities: Annual Report 2019.

Brennenstuhl, M., Zeh, R., Otto, R., Pesch, R., Stockinger, V., & Pietruschka, D. (2019). Report on a plus-energy district with low-temperature DHC network, novel agrothermal heat source, and applied demand response. *Applied Sciences, 9*(23), 5059. https://doi.org/10.3390/app9235059

Brozovsky, J., Gaitani, N., & Gustavsen, A. (2021). A systematic review of urban microclimate in cold climate conditions. *Renewable and Sustainable Energy Reviews, 138*(5). https://doi.org/10.1016/j.rser.2020.110551

Bustami, R. A., Belusko, M., Ward, J., & Beecham, S. (2018). Vertical greenery systems: A systematic review of research trends. *Building and Environment, 146*, 226–237. https://doi.org/10.1016/j.buildenv.2018.09.045

Capuder, T., & Mancarella, P. (2016). Assessing the benefits of coordinated operation of aggregated distributed multi-energy generation. In *19th Power Systems Computation Conference: Pscc 2016 Genova : June 20-24, 2016*. https://doi.org/10.1109/PSCC.2016.7540829

Carlisle, N., van Geet, O., & Pless, S. (2009). *Definition of a "Zero net energy" community (Technical report NREL/TP-7A2-46065)*. Golden, CO: National Renewable Energy Laboratory.

Carreiro, A. M., Lopez, G. L., Moura, P. S., Moreno, J. I., Almeida, A., de, T., et al. (2011). In-house monitoring and control network for the Smart Grid of the future. In *2nd IEEE PES International Conference and Exhibition on Innovative Smart Grid Technologies (ISGT Europe)*. https://doi.org/10.1109/ISGTEurope.2011.6162736

Cartuyvels, P., Mautone, O., & Colazza, D. (2018). Sustainable districts and built environment: Positive energy blocks. *European innovation partnership on smart cities and communities*. https://eu-smartcities.eu/sites/eu-smartcities.eu/files/2018-06/EIP_infographics_PositiveEnergyBlocks.pdf.

Castaldo, V. L., Pisello, A. L., Piselli, C., Fabiani, C., Cotana, F., & Santamouris, M. (2018). How outdoor microclimate mitigation affects building thermal-energy performance: A new design-stage method for energy saving in residential near-zero energy settlements in Italy. *Renewable Energy, 127*, 920–935. https://doi.org/10.1016/j.renene.2018.04.090

Cheng, Y., Zhang, N., Kirschen, D. S., Huang, W., & Kang, C. (2020). Planning multiple energy systems for low-carbon districts with high penetration of renewable energy: An empirical study in China. *Applied Energy, 261*, 114390. https://doi.org/10.1016/j.apenergy.2019.114390

Clemente, C., Civiero, P., & Cellurale, M. (2019). Solutions and services for smart sustainable district: An innovative approach in KPI to support transition. Advance online publication. *International Journal of Sustainable Energy Planning and Management, 24*. https://doi.org/10.5278/IJSEPM.3350, 2019.

Clerici Maestosi, P., Andreucci, M. B., & Civiero, P. (2021). Sustainable urban areas for 2030 in a Post-COVID-19 scenario: Focus on innovative research and funding frameworks to boost transition towards 100 positive energy districts and 100 climate-neutral cities. *Energies, 14*(1), 216. https://doi.org/10.3390/en14010216

Comodi, G., Bartolini, A., Carducci, F., Nagaranjan, B., & Romagnoli, A. (2019). Achieving low carbon local energy communities in hot climates by exploiting networks synergies in multi energy systems. *Applied Energy, 256*, 113901. https://doi.org/10.1016/j.apenergy.2019.113901

Coninck, R., Baetens, R., Saelens, D., Woyte, A., & Helsen, L. (2014). Rule-based demand-side management of domestic hot water production with heat pumps in zero energy neighbourhoods. *Journal of Building Performance Simulation, 7*(4), 271–288. https://doi.org/10.1080/19401493.2013.801518

Cortés, P., Auladell-León, P., Muñuzuri, J., & Onieva, L. (2020). Near-optimal operation of the distributed energy resources in a smart microgrid district. *Journal of Cleaner Production, 252*, 119772. https://doi.org/10.1016/j.jclepro.2019.119772

Del Pero, C., Leonforte, F., Lombardi, F., Stevanato, N., Barbieri, J., Aste, N., et al. (2021). *Modelling of an integrated multi-energy system for a nearly zero energy smart district*.

Delmastro, C., Martinsson, F., Mutani, G., & Corgnati, S. P. (2017). Modeling building energy demand profiles and district heating networks for low carbon urban areas. *Procedia Engineering, 198*, 386–397. https://doi.org/10.1016/j.proeng.2017.07.094

Deng, S., Wang, R. Z., & Dai, Y. J. (2014). How to evaluate performance of net zero energy building – A literature research. *Energy, 71*, 1–16. https://doi.org/10.1016/j.energy.2014.05.007

Di Lucia, L., & Ericsson, K. (2014). Low-carbon district heating in Sweden – Examining a successful energy transition. *Energy Research & Social Science, 4*, 10–20. https://doi.org/10.1016/j.erss.2014.08.005

Directorate-General for Research and Innovation. (2020a). 100 climate-neutral cities by 2030 - By and for the citizens. *Report of the mission board for adaption to climate change, including societal transformation*. Brussels, Belgium: European Commission. https://op.europa.eu/en/publication-detail/-/publication/bc7e46c2-fed6-11ea-b44f-01aa75ed71a1/language-en/format-PDF/source-160480388.

Directorate-General for Research and Innovation. (2020b). A climate resilient Europe: Prepare Europe for climate disruptions and accelerate the transformation to a climate resilient and just Europe by 2030. *Report of the mission board for adaption to climate change, including societal transformation*. Brussels, Belgium: European Commission. https://op.europa.eu/en/publication-detail/-/publication/2bac8dae-fc85-11ea-b44f-01aa75ed71a1.

Edenhofer, O. (Ed.). (2014). *Climate change 2014: Mitigation of climate change working group III contribution to the fifth assessment report of the intergovernmental panel on climate change*. Cambridge University Press.

Ekambaram, A., Kvellheim, A. K., & de Boer, L. (2020). Public private collaboration and the role of learning in developing zero-emission neighbourhoods. *ECKM 2020 PROCEEDINGS OF THE 21ST EUROPEAN CONFERENCE ON KNOWLEDGE*. https://doi.org/10.34190/EKM.20.254. ACPIL.

Engeland, K., Borga, M., Creutin, J.-D., François, B., Ramos, M.-H., & Vidal, J.-P. (2017). Space-time variability of climate variables and intermittent renewable electricity production – A review. *Renewable and Sustainable Energy Reviews, 79*, 600–617. https://doi.org/10.1016/j.rser.2017.05.046

Eurocities. (2017). *Smart city baseline report: Lisbon, London, Milan, Bordeaux, Burgas, Warsaw*. http://nws.eurocities.eu/MediaShell/media/Sixcitybaselinereports.pdf.

European Commission. (2014a). *Horizon 2020 in brief: The EU framework programme for research & innovation (KI-02-13-413-EN-C)*. Luxembourg: European Commission. https://ec.europa.eu/programmes/horizon2020/sites/horizon2020/files/H2020_inBrief_EN_FinalBAT.pdf.

European Commission. (2014b). Communication from the commission to the European Parliament, the council. *The European Economic an Social Committee and the Committee of the Regions: A policy framework for climate and energy in the period from 2020 to 2030*. Brussels, Belgium.

European Commission. (2019a). *Horizon Europe*. https://ec.europa.eu/info/sites/info/files/research_and_innovation/knowledge_publications_tools_and_data/documents/ec_rtd_factsheet-horizon-europe_2019.pdf.

European Commission. (2019b). *The European Green Deal sets out how to make Europe the first climate-neutral continent by 2050, boosting the economy, improving people's health and quality of life, caring for nature, and leaving no one behind [Press release]*. Brussels, Belgium https://ec.europa.eu/commission/presscorner/detail/e%20n/ip_19_6691.

European Commission. (2020a). *Horizon 2020 Work Programme 2018-2020: 10. Secure, clean and efficient energy*. European Commission.

European Commission. (2020b). *Communication from the Commission to the European Parliament, the Council, the European Economic and Social Committee and the Committee of the Regions: A Renovation Wave for Europe - greening our buildings, creating jobs, improving lives*. Brussels, Belgium: European Commission.

European Commission Directorate-General for Energy. (2019). *Clean energy for all Europeans*. Publications Office of the European Union.

European Commission Joint Research Centre. (2018). *SET-Plan ACTION no 3.2 Implementation Plan: Europe to become a global role model in integrated, innovative solutions for the planning, deployment, and replication of Positive Energy Districts*. Brussels, Belgium.

European Commission Smart Cities Marketplace: Positive energy blocks https://smart-cities-marketplace.ec.europa.eu/action-clusters-and-initiatives/action-clusters/sustainable-districts-and-built-environment-0.

European Parliament, & Council of the European Union. (2010). Directive 2010/31/EU of the European Parliament and of the council of 19 May 2010 on the energy performance of buildings. *Official Journal of the European Union, 53*(L 153), 13–35.

European Parliament, & Council of the European Union. (2018a). Directive (EU) 2018/2001 of the European Parliament and of the council of 11 December 2018 on the promotion of the use of energy from renewable sources. *Official Journal of the European Union, 61*(L 328), 82–209.

European Parliament, & Council of the European Union. (2018b). Directive (EU) 2018/844 of the European Parliament and of the council of 30 May 2018 amending Directive 2010/31/EU on the energy performance of buildings and Directive 2012/27/EU on energy efficiency. *Official Journal of the European Union, 61*(L 156), 75–91.

Fatima, Z., Pollmer, U., Santala, S.-S., Kontu, K., & Ticklen, M. (2021). Citizens and positive energy districts: are Espoo and Leipzig ready for PEDs? *Buildings, 11*(3), 102. https://doi.org/10.3390/buildings11030102

Fay, R., Treloar, G., & Iyer-Raniga, U. (2000). Life-cycle energy analysis of buildings: A case study. *Building Research & Information, 28*(1), 31–41. https://doi.org/10.1080/096132100369073

Feng, W., Zhang, Q., Ji, H., Wang, R., Zhou, N., Ye, Q., et al. (2019). A review of net zero energy buildings in hot and humid climates: Experience learned from 34 case study buildings. *Renewable and Sustainable Energy Reviews, 114*, 109303. https://doi.org/10.1016/j.rser.2019.109303

Finney, K. N., Zhou, J., Chen, Q., Zhang, X., Chan, C., Sharifi, V. N., et al. (2013). Modelling and mapping sustainable heating for cities. *Applied Thermal Engineering, 53*(2), 246–255. https://doi.org/10.1016/j.applthermaleng.2012.04.009

Freeman, R., & Yearworth, M. (2017). Climate change and cities: Problem structuring methods and critical perspectives on low-carbon districts. *Energy Research & Social Science, 25*, 48–64. https://doi.org/10.1016/j.erss.2016.11.009

Gabaldón Moreno, A., Vélez, F., Alpagut, B., Hernández, P., & Sanz Montalvillo, C. (2021). How to achieve positive energy districts for sustainable cities: A proposed calculation methodology. *Sustainability, 13*(2), 710. https://doi.org/10.3390/su13020710

Garau, M., Ghiani, E., Celli, G., & Pilo, F. (2017). Tecno-economic and environmental assessment of a full electric smart city eco-district. In *2017 AEIT International Annual Conference*.

García-Fuentes, M.Á., García-Pajares, R., Sanz, C., & Meiss, A. (2018). Novel design support methodology based on a multi-criteria decision analysis approach for energy efficient district retrofitting projects. *Energies, 11*(9), 2368. https://doi.org/10.3390/en11092368

Ge, X., Kremers, E., Yadack, M., & Eicker, U. (2019). Simulation-supported quantification of flexibility: Assessing the potential for blocks of buildings to participate in demand response markets. In *16th International Conference on the European Energy Market (EEM): 18-20 September 2019*.

Genus, A., & Theobald, K. (2015). Roles for university researchers in urban sustainability initiatives: The UK Newcastle Low Carbon Neighbourhoods project. *Journal of Cleaner Production, 106*, 119–126. https://doi.org/10.1016/j.jclepro.2014.08.063

Genus, A., & Theobald, K. (2016). Creating low-carbon neighbourhoods: A critical discourse analysis. *European Urban and Regional Studies, 23*(4), 782–797. https://doi.org/10.1177/0969776414546243

Georges, L., Haase, M., Houlihan Wiberg, A., Kristjansdottir, T., & Risholt, B. (2015). Life cycle emissions analysis of two nZEB concepts. *Building Research & Information, 43*(1), 82–93. https://doi.org/10.1080/09613218.2015.955755

Global Alliance for Buildings and Construction, International Energy Agency, & United Nations Environment Programe. (2019). *2019 Global Status Report for Buildings and Construction: Towards a zero-emissions, efficient and resilient buildings and construction sector*. International Energy Agency. https://www.iea.org/reports/global-status-report-for-buildings-and-construction-2019.

Gollner, C., Hinterberger, R., Bossi, S., Theierling, S., Noll, M., Meyer, S., et al. (2020). *Europe towards Positive Energy Districts: A compilation of projects towards sustainable urbanization and the energy transition*.

Good, N., Martínez Ceseña, E. A., & Mancarella, P. (2017). Ten questions concerning smart districts. *Building and Environment, 118*, 362–376. https://doi.org/10.1016/j.buildenv.2017.03.037

Good, N., Martínez Ceseña, E. A., Mancarella, P., Monti, A., Pesch, D., & Ellis, K. A. (2017). Barriers, challenges, and recommendations related to development of energy positive neighborhoods and smart energy districts. In A. Monti, D. Pesch, K. A. Ellis, & P. Mancarella (Eds.), *Energy positive neighborhoods and smart energy districts: Methods, tools, and experiences from the field* (pp. 251–274). Academic Press. https://doi.org/10.1016/B978-0-12-809951-3.00008-9.

Gros, A., Bozonnet, E., Inard, C., & Musy, M. (2016). Simulation tools to assess microclimate and building energy – A case study on the design of a new district. *Energy and Buildings, 114*, 112–122. https://doi.org/10.1016/j.enbuild.2015.06.032

Guarino, F., Longo, S., Hachem Vermette, C., Cellura, M., & La Rocca, V. (2020). Life cycle assessment of solar communities. *Solar Energy, 207*, 209–217. https://doi.org/10.1016/j.solener.2020.06.089

Guarino, F., Tumminia, G., Longo, S., Mistretta, M., Bilotta, R., & Cellura, M. (2016). Energy planning methodology of net-zero energy solar neighborhoods in the Mediterranean basin. *Science and Technology for the Built Environment, 22*(7), 928–938. https://doi.org/10.1080/23744731.2016.1195656

Guyot, D., Giraud, F., Simon, F., Corgier, D., Marvillet, C., & Tremeac, B. (2020). Detailed monitoring as an essential tool for achieving energy performance targets in operation conditions: The HIKARI case study. In *E3S Web of Conferences, 172* p. 22006). https://doi.org/10.1051/e3sconf/202017222006

Hachem-Vermette, C., & Singh, K. (2020). Developing an optimization methodology for urban energy resources mix. *Applied Energy, 269*, 115066. https://doi.org/10.1016/j.apenergy.2020.115066

Hallman, H. W. (1984). *Neighborhoods [Neighbourhoods]: Their place in urban life*. Sage library of social research: v. 154. Sage Publications.

Hamdan, H. A. M., & de Boer, L. (2019). Innovative public procurement (IPP) – Implications and potential for zero-emission neighborhood (ZEN) projects?. In *IOP Conference Series: Earth and Environmental Science, 352* p. 12013). https://doi.org/10.1088/1755-1315/352/1/012013

Haneef, F., Battini, F., Pernigotto, G., & Gasparella, A. (2020). A CitySim urban energy simulation for the development of retrofit scenarios for a neighbourhood in Bolzano, Italy. *Proceedings of BSA 2019: 4th IBPSA-Italy Conference on Building Simulation Applications*, 59–66.

Hedman, Å., Rehman, H. U., Gabaldón, A., Bisello, A., Albert-Seifried, V., Zhang, X., et al. (2021). IEA EBC Annex83 positive energy districts. *Buildings, 11*(3), 130. https://doi.org/10.3390/buildings11030130

Heendeniya, C. B., Sumper, A., & Eicker, U. (2020). The multi-energy system co-planning of nearly zero-energy districts – Status-quo and future research potential. *Applied Energy, 267*, 114953. https://doi.org/10.1016/j.apenergy.2020.114953

Hestnes, A. G., & Eik-Nes, N. L. (Eds.). (2017). Zero emission building. Fagbokforlaget.

Himpe, E., Janssens, A., & Rebollar, J. E. V. (2015). Energy and comfort performance assessment of monitored low energy buildings connected to low-temperature district heating. *Energy Procedia, 78*, 3465–3470. https://doi.org/10.1016/j.egypro.2015.12.331

Himpe, E., van de Putte, S., Laverge, J., & Janssens, A. (2015). Operational performance of passive multi-family buildings: Commissioning with regard to ventilation and indoor climate. *Energy Procedia, 78*, 2983–2988. https://doi.org/10.1016/j.egypro.2015.11.699

Hinterberger, R., Gollner, C., Noll, M., Meyer, S., & Schwarz, H.-G. (2020). *White paper on PED reference framework for positive energy districts and neighbourhoods*. https://jpi-urbaneurope.eu/ped/.

Hirvonen, J., & Kosonen, R. (2020). Waste incineration heat and seasonal thermal energy storage for promoting economically optimal net-zero energy districts in Finland. *Buildings, 10*(11), 205. https://doi.org/10.3390/buildings10110205

Hou, Q., Zhang, X., Li, B., Zhang, X., & Wang, W. (2019). Identification of low-carbon travel block based on GIS hotspot analysis using spatial distribution learning algorithm. *Neural Computing & Applications, 31*(9), 4703–4713. https://doi.org/10.1007/s00521-018-3447-8

IEA. (2019). *Perspectives for the clean energy transition: The critical role of buildings*. France: International Energy Agency. https://www.iea.org/reports/the-critical-role-of-buildings.

IEA EBC Annex 83. (2020). Positive energy districts. *International Energy Agency (IEA) Energy in Buildings and Communities (EBC) technology collaboration programme*. https://annex83.iea-ebc.org/Data/publications/EBC_Annex83_Factsheet.pdf.

International Energy Agency. (2016). *Energy technology perspectives 2016: Towards sustainable urban energy systems*. OECD/IEA.

Iturriaga, E., Campos-Celador, Á., Terés-Zubiaga, J., Aldasoro, U., & Álvarez-Sanz, M. (2021). A MILP optimization method for energy renovation of residential urban areas: Towards Zero Energy Districts. *Sustainable Cities and Society, 68*, 102787. https://doi.org/10.1016/j.scs.2021.102787

Jadwiszczak, P. (2017). Heat pumps as a way to Low or zero emission district heating systems. In *E3S Web of Conferences, 17* p. 32). https://doi.org/10.1051/e3sconf/20171700032

Janzadeh, A., & Zandieh, M. (2021). Design feasibility of a net-zero energy neighborhood in Qazvin. *Energy Efficiency, 14*(1), 336. https://doi.org/10.1007/s12053-020-09909-w

Joint Programming Initiative (JPI) Urban Europe. (2021). *Positive Energy Districts (PED)*. https://jpi-urbaneurope.eu/ped/.

Kalaycıoğlu, E., & Yılmaz, A. Z. (2017). A new approach for the application of nearly zero energy concept at district level to reach EPBD recast requirements through a case study in Turkey. *Energy and Buildings, 152*, 680–700. https://doi.org/10.1016/j.enbuild.2017.07.040

Keough, N., & Ghitter, G. (2020). Pathways to sustainable low-carbon transitions in an auto-dependent Canadian city. *Sustainability Science, 15*(1), 203–217. https://doi.org/10.1007/s11625-019-00698-5

Kibert, C. J., & Fard, M. M. (2012). Differentiating among low-energy, low-carbon and net-zero-energy building strategies for policy formulation. *Building Research & Information, 40*(5), 625–637. https://doi.org/10.1080/09613218.2012.703489

Kılkış, Ş. (2014). Energy system analysis of a pilot net-zero exergy district. *Energy Conversion and Management, 87*, 1077–1092. https://doi.org/10.1016/j.enconman.2014.05.014

Kılkış, Ş. (2015). Exergy transition planning for net-zero districts. *Energy, 92*, 515–531. https://doi.org/10.1016/j.energy.2015.02.009

Kim, M.-H., Kim, D., Heo, J., & Lee, D.-W. (2019). Techno-economic analysis of hybrid renewable energy system with solar district heating for net zero energy community. *Energy, 187*, 115916. https://doi.org/10.1016/j.energy.2019.115916

Klebow, B., Purvins, A., Piira, K., Lappalainen, V., & Judex, F. (2013). Eepos automation and energy management system for neighbourhoods with high penetration of distributed renewable energy sources: A concept. In T. Strasser (Ed.), *2013 IEEE International Workshop on Intelligent Energy Systems (IWIES)* (pp. 89–94). https://doi.org/10.1109/IWIES.2013.6698567. IEEE.

Koch, A., Girard, S., & McKoen, K. (2012). Towards a neighbourhood scale for low- or zero-carbon building projects. *Building Research & Information, 40*(4), 527–537. https://doi.org/10.1080/09613218.2012.683241

Koezjakov, A., Urge-Vorsatz, D., Crijns-Graus, W., & van den Broek, M. (2018). The relationship between operational energy demand and embodied energy in Dutch residential buildings. *Energy and Buildings, 165*, 233–245. https://doi.org/10.1016/j.enbuild.2018.01.036

Komninos, N., Kakderi, C., Mora, L., Panori, A., & Sefertzi, E. (2021). Towards high impact smart cities: A universal architecture based on connected intelligence spaces. *Journal of the Knowledge Economy, 24*(6), 838. https://doi.org/10.1007/s13132-021-00767-0

Koutra, S., Becue, V., Gallas, M.-A., & Ioakimidis, C. S. (2018). Towards the development of a net-zero energy district evaluation approach: A review of sustainable approaches and assessment tools. *Sustainable Cities and Society, 39*, 784–800. https://doi.org/10.1016/j.scs.2018.03.011

Koutra, S., Becue, V., & Ioakimidis, C. S. (2016). From the 'Smart Ground' to the 'Smart City'. In , *Smartgreens 2016: Proceedings of the 5th International Conference on Smart Cities and Green ICT Systems : Rome, Italy* (Vol. 47, pp. 95–106). https://doi.org/10.1016/j.cities.2015.05.004. April 23-25, 2016.

Koutra, S., Pagnoule, C., Galatoulas, N.-F., Bagheri, A., Waroux, T., Becue, V., et al. (2019). The zero-energy idea in districts: Application of a methodological approach to a case study of Epinlieu (Mons). *Sustainability, 11*(17), 4814. https://doi.org/10.3390/su11174814

Koutra, S., Becue, V., Griffon, J.-B., & Ioakimidis, C. S. (2017). Towards a net-zero energy district transformation in a mono-criterion scenario analysis - The case of Bo01, Malmö District. In M. Helfert, C. Klein, & B. Donnellan (Eds.), *Smartgreens 2017: Proceedings of the 6th International Conference on Smart Cities and Green ICT Systems : Porto, Portugal* (pp. 180–187). https://doi.org/10.5220/0006301901800187. April 22-24, 2017.

Koutra, S., Becue, V., & Ioakimidis, C. S. (2017). A simplified methodological approach towards the net zero energy district. In , *Communications in Computer and Information Science: Vol. 738. Smart Cities, Green Technologies, and Intelligent Transport Systems: 5th International Conference, SMARTGREENS 2016 and Second International Conference, VEHITS 2016, 738* pp. 207–224). https://doi.org/10.1007/978-3-319-63712-9_12. Rome, Italy, April 23-25, 2016, revised selected papers.

Kvellheim, A. K., Danielsen, S. M., Hestnes, A. G., & Gustavsen, A. (2021). *ZEN Research Centre on zero emission neighbourhoods in smart cities: Annual report 2020*. Trondheim, Norway: Norwegian University of Science and Technology (NTNU); SINTEF Community.

Lausselet, C., Lund, K. M., & Brattebø, H. (2021). LCA and scenario analysis of a Norwegian net-zero GHG emission neighbourhood: The importance of mobility and surplus energy from PV technologies. *Building and Environment, 189*(10), 107528. https://doi.org/10.1016/j.buildenv.2020.107528

Lausselet, C., Borgnes, V., & Brattebø, H. (2019). LCA modelling for Zero Emission Neighbourhoods in early stage planning. *Building and Environment, 149*, 379–389. https://doi.org/10.1016/j.buildenv.2018.12.034

Lausselet, C., Ellingsen, L. A.-W., Strømman, A. H., & Brattebø, H. (2020). A life-cycle assessment model for zero emission neighborhoods. *Journal of Industrial Ecology, 24*(3), 500–516. https://doi.org/10.1111/jiec.12960

Lausselet, C., Urrego, J. P. F., Resch, E., & Brattebø, H. (2020). Temporal analysis of the material flows and embodied greenhouse gas emissions of a neighborhood building stock. *Journal of Industrial Ecology*. https://doi.org/10.1111/jiec.13049. Advance online publication.

Leal, V. M. S., Granadeiro, V., Azevedo, I., & Boemi, S.-N. (2015). Energy and economic analysis of building retrofit and energy offset scenarios for Net Zero Energy Buildings. *Advances in Building Energy Research, 9*(1), 120–139. https://doi.org/10.1080/17512549.2014.944567

Lehmann, S. (2014). Low carbon districts: Mitigating the urban heat island with green roof infrastructure. *City Culture and Society, 5*(1), 1–8. https://doi.org/10.1016/j.ccs.2014.02.002

Leibold, J., Schneider, S., Tabakovic, M., Zelger, T., Bell, D., Schöfmann, P., Bartlmä, N., et al. (2020). 'Zukunftsquartier'—On the path to plus energy neighbourhoods in Vienna. In J. Littlewood, R. J. Howlett, A. Capozzoli, & L. C. Jain (Eds.), *Smart innovation, systems and technologies: volume 163. Sustainability in energy and buildings* (Vol. 163, pp. 199–209). Springer. https://doi.org/10.1007/978-981-32-9868-2_17. Proceedings of SEB 2019.

Li, D. H. W., Yang, L., & Lam, J. C. (2013). Zero energy buildings and sustainable development implications – A review. *Energy, 54*, 1–10. https://doi.org/10.1016/j.energy.2013.01.070

Li, Z., Quan, S. J., & Yang, P. P.-J. (2016). Energy performance simulation for planning a low carbon neighborhood urban district: A case study in the city of Macau. *Habitat International, 53*, 206–214. https://doi.org/10.1016/j.habitatint.2015.11.010

Lima, F. T., Kos, J. R., & Paraizo, R. C. (2016). Algorithmic approach toward Transit-Oriented Development neighborhoods: (Para)metric tools for evaluating and proposing rapid transit-based districts. *International Journal of Architectural Computing, 14*(2), 131–146. https://doi.org/10.1177/1478077116638925

Lindholm, O., Rehman, H. U., & Reda, F. (2021). Positioning positive energy districts in European cities. *Buildings, 11*(1), 19. https://doi.org/10.3390/buildings11010019

Lund, K. M., Lausselet, C., & Brattebø, H. (2019). LCA of the zero emission neighbourhood Ydalir. In *IOP Conference Series: Earth and Environmental Science, 352* p. 12009). https://doi.org/10.1088/1755-1315/352/1/012009

Maas, N., Georgiadou, V., Roelofs, S., Amaral Lopes, R., Pronto, A., & Martins, J. (2020). Implementation framework for energy flexibility technologies in Alkmaar and évora. *Energies, 13*, Article 5811. https://doi.org/10.3390/en13215811

Magrini, A., Lentini, G., Cuman, S., Bodrato, A., & Marenco, L. (2020). From nearly zero energy buildings (NZEB) to positive energy buildings (PEB): The next challenge - the most recent European trends with some notes on the energy analysis of a forerunner PEB example. *Developments in the Built Environment, 3*, 100019. https://doi.org/10.1016/j.dibe.2020.100019

Marique, A.-F., & Reiter, S. (2014). A simplified framework to assess the feasibility of zero-energy at the neighbourhood/community scale. *Energy and Buildings, 82*, 114–122. https://doi.org/10.1016/j.enbuild.2014.07.006

Marszal, A. J., Heiselberg, P., Bourrelle, J. S., Musall, E., Voss, K., Sartori, I., et al. (2011). Zero Energy Building – A review of definitions and calculation methodologies. *Energy and Buildings, 43*(4), 971–979. https://doi.org/10.1016/j.enbuild.2010.12.022

Mavrigiannaki, A., & Ampatzi, E. (2016). Latent heat storage in building elements: A systematic review on properties and contextual performance factors. *Renewable and Sustainable Energy Reviews, 60*, 852–866. https://doi.org/10.1016/j.rser.2016.01.115

Moher, D., Liberati, A., Tetzlaff, J., & Altman, D. G. (2010). Preferred reporting items for systematic reviews and meta-analyses: The PRISMA statement. *International Journal*

of Surgery (London, England), 8(5), 336–341. https://doi.org/10.1016/j.ijsu.2010.02.007

Morales Gonzalez, R., Asare-Bediako, B., Cobben, J. F. G., Kling, W. L., Scharrenberg, G., & Dijkstra, D. (2012). Distributed energy resources for a zero-energy neighborhood. In *3rd IEEE PES International Conference and Exhibition on Innovative Smart Grid Technologies (ISGT Europe)*. https://doi.org/10.1109/ISGTEurope.2012.6465820, 2012: 14-17 Oct. 2012 (pp. 1–8).

Natanian, J., & Auer, T. (2020). Beyond nearly zero energy urban design: A holistic microclimatic energy and environmental quality evaluation workflow. *Sustainable Cities and Society, 56*, 102094. https://doi.org/10.1016/j.scs.2020.102094

Nematchoua, M. K. (2020). From existing neighbourhoods to net-zero energy and nearly zero carbon neighbourhoods in the tropical regions. *Solar Energy, 211*(November), 244–257. https://doi.org/10.1016/j.solener.2020.09.062

Nematchoua, M. K., Marie-Reine Nishimwe, A., & Reiter, S. (2021). Towards nearly zero-energy residential neighbourhoods in the European Union: A case study. *Renewable and Sustainable Energy Reviews, 135*(3), 110198. https://doi.org/10.1016/j.rser.2020.110198

Net Zero Homes. (2015). *Project objective*. https://www.zeroenergy.ca/project-objective/.

Nielsen, B. F., Baer, D., & Lindkvist, C. (2019). Identifying and supporting exploratory and exploitative models of innovation in municipal urban planning; key challenges from seven Norwegian energy ambitious neighborhood pilots. *Technological Forecasting and Social Change, 142*, 142–153. https://doi.org/10.1016/j.techfore.2018.11.007

Nielsen, B. F., Resch, E., & Andresen, I. (2018). The role of utility companies in municipal planning of smart energy communities. *International Journal of Sustainable Development and Planning, 13*(04), 695–706. https://doi.org/10.2495/SDP-V13-N4-695-706

Panagiotidou, M., & Fuller, R. J. (2013). Progress in ZEBs—A review of definitions, policies and construction activity. *Energy Policy, 62*, 196–206. https://doi.org/10.1016/j.enpol.2013.06.099

Passer, A., Kreiner, H., & Maydl, P. (2012). Assessment of the environmental performance of buildings: A critical evaluation of the influence of technical building equipment on residential buildings. *The International Journal of Life Cycle Assessment, 17*(9), 1116–1130. https://doi.org/10.1007/s11367-012-0435-6

Pejstrup, E., Sola Saura, A., & Sanmarti, M. (2019). *Factsheets low energy districts*. https://grow-smarter.eu/fileadmin/editor-upload/Smart/Action_Area_1-compressed.pdf.

Peng, W., Wang, X., & Guo, L. (2018). An exploration of neighborhood residents' cognition of and participation in low-carbon behaviors in Wuhan, China. *Advances in Civil Engineering, 2018*(1), 1–9. https://doi.org/10.1155/2018/8764801

Peng, W. J., Wang, X. M., Zhao, G. C., & Wang, X. (2018). An investigation into neighborhood residents' cognition of and participation in low-carbon behavior: a case study in Chengyang district of Qingdao, China. *International Journal of Sustainable Development and Planning, 13*(05), 818–837. https://doi.org/10.2495/SDP-V13-N5-818-837

Petersen, S. A., Petersen, I., & Ahcin, P. (2020). Smiling earth—raising awareness among citizens for behaviour change to reduce carbon footprint. *Energies, 13*(22), 5932. https://doi.org/10.3390/en13225932

Petersen, S. A., Pourzolfaghar, Z., Alloush, I., Ahlers, D., Krogstie, J., & Helfert, M. (2019). Value-added services, virtual enterprises and data spaces inspired Enterprise architecture for smart cities. In Camarinha-Matos, & Birukou (Eds.), *IFIP advances in information and communication technology. Collaborative networks and digital transformation* (1st ed.,, *568* pp. 393–402). Springer International Publishing. https://doi.org/10.1007/978-3-030-28464-0_34.

Pietruschka, D., Brennenstuhl, M., Matthiss, B., & Binder, J. (2015). Decentralised heat pumps and small electricity storages as active components in a virtual power plant for smart grid services. In *2015 IEEE 15th International Conference on Environment and Electrical Engineering (EEEIC): 10-13 June 2015* (pp. 737–741). https://doi.org/10.1109/EEEIC.2015.7165256. IEEE.

Pinel, D. (2020). Clustering methods assessment for investment in zero emission neighborhoods' energy system. *International Journal of Electrical Power & Energy Systems, 121*. https://doi.org/10.1016/j.ijepes.2020.106088, 106088.

Pinel, D., Bjarghov, S., & Korpås, M. (2019). *Impact of grid tariffs design on the zero emission neighborhoods energy system investments*.

Pinel, D., Korpås, M., & B. Lindberg, K. (2021). Impact of the CO2 factor of electricity and the external CO2 compensation price on zero emission neighborhoods' energy system design. *Building and Environment, 187*(2), 107418. https://doi.org/10.1016/j.buildenv.2020.107418

Pinel, D., Korpås, M., & Lindberg, K. B. (2020). Cost optimal design of zero emission neighborhoods' (ZENs) energy system. In , *Trends in Mathematics. Advances in Energy System Optimization: Proceedings of the 2nd International Symposium on Energy System Optimization, 127* pp. 145–163). https://doi.org/10.1007/978-3-030-32157-4_9

Piselli, C., Di Grazia, M., & Pisello, A. L. (2020). Combined effect of outdoor microclimate boundary conditions on air conditioning system's efficiency and building energy demand in net zero energy settlements. *Sustainability, 12*(15), 6056. https://doi.org/10.3390/su12156056

Pless, S., Polly, B., & Zaleski, S. (2018). Communities of the future: Accelerating zero energy district master planning: Preprint. *Proceedings of 2018 ACEEE Summer Study: 20th ACEEE Conference on Energy Efficiency in Buildings*. Article NREL/CP-5500-71841 https://www.nrel.gov/docs/fy18osti/71841.pdf.

Qin, B., & Han, S. S. (2013). Planning parameters and household carbon emission: Evidence from high- and low-carbon neighborhoods in Beijing. *Habitat International, 37*, 52–60. https://doi.org/10.1016/j.habitatint.2011.12.017

Redmond, A., Fies, B., & Zarli, A. (2015). Developing an integrated Cloud platform for enabling 'Holistic energy management' in urban areas. In A. Mahdavi, & B. Martens (Eds.), *Ework and eBusiness in Architecture, Engineering and Construction: Proceedings of 10th European Conference on Product and Process Modelling (ECPPM 2014)*.

REMO Urban. (2020). *REgeneration MOdel for smart URBAN transformation*. http://www.remourban.eu/kdocs/1948018/REMOURBAN_Final_brochure_WEB.pdf.

Renaldi, R., Kiprakis, A., & Friedrich, D. (2017). An optimisation framework for thermal energy storage integration in a residential heat pump heating system. *Applied Energy, 186*, 520–529. https://doi.org/10.1016/j.apenergy.2016.02.067

Rezaei, A., Samadzadegan, B., Rasoulian, H., Ranjbar, S., Samareh Abolhassani, S., Sanei, A., et al. (2021). A new modeling approach for low-carbon district energy system planning. *Energies, 14*(5), 1383. https://doi.org/10.3390/en14051383

Roccamena, L., El Mankibi, M., & Stathopoulos, N. (2019). Development and validation of the numerical model of an innovative PCM based thermal storage system. *Journal of Energy Storage, 24*, 100740. https://doi.org/10.1016/j.est.2019.04.014

Romero Rodríguez, L., Brennenstuhl, M., Yadack, M., Boch, P., & Eicker, U. (2019). Heuristic optimization of clusters of heat pumps: A simulation and case study of residential frequency reserve. *Applied Energy, 233-234*, 943–958. https://doi.org/10.1016/j.apenergy.2018.09.103

Saheb, Y., Shnapp, S., & Johnson, C. (2018). The Zero Energy concept: Making the whole greater than the sum of the parts to meet the Paris Climate Agreement's objectives. *Current Opinion in Environmental Sustainability, 30*, 138–150. https://doi.org/10.1016/j.cosust.2018.04.014

Salom, J., & Tamm, M. (2020). *WP3 technology integration in smart managed plus energy buildings and neighbourhoods: D3.1 methodology framework for plus energy buildings and neighbourhoods*.

Sameti, M., & Haghighat, F. (2018). Integration of distributed energy storage into net-zero energy district systems: Optimum design and operation. *Energy, 153*, 575–591. https://doi.org/10.1016/j.energy.2018.04.064

Sanmarti, M., & Sola, A. (2019). *Implementing low energy districts in European cities - conclusions from GrowSmarter*. https://grow-smarter.eu/fileadmin/editor-upload/Reports/GrowSmarter_Concluding_Report_WP2.pdf.

Shafiullah, D. S., Vo, T. H., & Nguyen, P. H. (2018). A heuristic search approach for sizing battery storage of a neighbourhood including nearly Zero Energy Buildings (nZEB): Sarajevo, Bosnia and Herzegovina. October 21-25, 2018 *Proceedings. IEEE*.

Shaw-Williams, D., Susilawati, C., Walker, G., & Varendorff, J. (2020). Towards net-zero energy neighbourhoods utilising high rates of residential photovoltaics with battery storage: A techno-economic analysis. *International Journal of Sustainable Energy, 39*(2), 190–206. https://doi.org/10.1080/14786451.2019.1668394

Sinaeepourfard, A., & Petersen, S. A. (2019). Distributed-to-centralized data management through data LifeCycle models for zero emission neighborhoods. In L. Grandinetti, S. L. Mirtaheri, & R. Shahbazian (Eds.), *Communications in computer and information science: Vol. 891. High-performance computing and big data analysis: Second International congress* (Vol. 891, pp. 132–142). Springer. https://doi.org/10.1007/978-3-030-33495-6_11. TopHPC 2019, Tehran, Iran, April 23-25, 2019, Revised selected papers.

Sinaeepourfard, A., Krogstie, J., Petersen, S. A., & Ahlers, D. (2019). F2c2C-DM: A fog-to-cloudlet-to-cloud data management architecture in smart City. In *IEEE 5th World Forum on Internet of Things: 15-18 April 2019, Limerick, Ireland : Conference Proceedings*.

Sinaeepourfard, A., Krogstie, J., & Petersen, S. A. (2019). A distributed-to-centralized smart technology management (D2C-STM) model for smart cities: A use case in the zero emission neighborhoods. In *5th IEEE International Smart Cities Conference (ISC2)*.

Sinaeepourfard, A., Krogstie, J., & Petersen, S. A. (2018). A big data management architecture for smart cities based on fog-to-cloud data management architecture-6November.Docm. In O. Ozgobek, J. A. Gulla, R. D. Svendsen, & C. G. Linden Chairs (Eds.), *4th Norwegian Bid Data Symposium (NOBIDS 2018)*.

Sinaeepourfard, A., Krogstie, J., Petersen, S. A., & Gustavsen, A. (2018). A zero emission neighbourhoods data management architecture for smart city scenarios: Discussions toward 6Vs challenges. In *ICTC 2018 The 9th International Conference on ICT Convergence*.

Sinaeepourfard, A., Petersen, S. A., & Ahlers, D. (2019). D2C-SM: Designing a distributed-to-centralized software management architecture for smart cities. In , *Lecture Notes in Computer Science: Vol. 11701. Digital Transformation for a Sustainable Society in the 21st Century: 18th IFIP WG 6.11 Conference on e-Business, e-Services, and e-Society, I3E 2019, 11701* pp. 329–341). https://doi.org/10.1007/978-3-030-29374-1_27. Springer.

Skaar, C., Labonnote, N., & Gradeci, K. (2018). From zero emission buildings (ZEB) to zero emission neighbourhoods (ZEN): A mapping review of algorithm-based LCA. *Sustainability, 10*(7), 2405. https://doi.org/10.3390/su10072405

Skaar, C., Solli, C., & Vevatne, J. (2019). Designing a ZEN campus: An exploration of ambition levels and system boundaries. In *IOP Conference Series: Earth and Environmental Science, 352* p. 12025). https://doi.org/10.1088/1755-1315/352/1/012025

Sørnes, K., Sartori, I., Fredriksen, E., Martinsson, F., Romero, A., Rodriguez, F., et al. (2014). *ZenN nearly zero energy neighborhoods final report on common definition for nZEB renovation: D.1.2 report*.

Soltvedt, T. K., Sinaeepourfard, A., & Ahlers, D. (2020). A cost model for data discovery in large-scale IoT networks of smart cities. In D. Skoutas, & S. Yin (Eds.), *2020 21st IEEE International Conference on Mobile Data Management: MDM 2020* (pp. 348–353). https://doi.org/10.1109/MDM48529.2020.00076. IEEE.

Soutullo, S., Aelenei, L., Nielsen, P. S., Ferrer, J. A., & Gonçalves, H. (2020). Testing platforms as drivers for positive-energy living laboratories. *Energies, 13*(21), 5621. https://doi.org/10.3390/en13215621

Taveres-Cachat, E., Grynning, S., Thomsen, J., & Selkowitz, S. (2019). Responsive building envelope concepts in zero emission neighborhoods and smart cities - A roadmap to implementation. *Building and Environment, 149*, 446–457. https://doi.org/10.1016/j.buildenv.2018.12.045

Tironi, M. (2020). Prototyping public friction: Exploring the political effects of design testing in urban space. *The British Journal of Sociology, 71*(3), 503–519. https://doi.org/10.1111/1468-4446.12718

Torcellini, P., Pless, S., Deru, M., & Crawley, D. (2006). *Zero energy buildings: A critical look at the definition: Preprint (Conference paper NREL/CP-550-39833)*. Pacific Grove, CA: National Renewable Energy Laboratory. https://www.nrel.gov/docs/fy06osti/39833.pdf.

Torre, C., Antolín, J., García-Fuentes, M.Á., Gómez-Tribiño, J., Cubillo, J., Mirantes, M. L., & Tome, I. (2021). REMOURBAN: Evaluation results after the implementation of actions for improving the energy efficiency in a District in Valladolid (Spain). In S. Nesmachnow, & L. Hernández Callejo (Eds.), *Communications in computer and information science: Vol. 1359. Smart cities: Third Ibero-American congress, ICSC-cities 2020, San José, Costa Rica, November 9-11, 2020, 1359* pp. 30–41). Springer. https://doi.org/10.1007/978-3-030-69136-3_3. Revised selected papers.

Tryferidis, A., Pramangioulis, D., Kakaras, E., Tsarchopoulos, P., Nikolopoulos, N., Salanova, J. M., et al. (2019). *IRIS D1.1: Report on the list of selected KPIs for each transition track*. https://irissmartcities.eu/system/files/private/irissmartcities/d1.1_report_on_the_list_of_selected_kpis_for_each_transition_track_v1.2.pdf.

Tryferidis, A., Tsarchopoulos, P., Noula, A., Prekas, M., Harmelink, M., Broekman, M., Caccavelli, D., Keim, C., Maillard, P., Régis, M., Pavic, E., Westling, B., Giovanakis, T., Lymperopoulos, K., Pertti, O., Pieskä, M., Minciuc, E., Vasile, E., Nicola, N., Stanculea, A., & Brook Hijar, D. (2018). *Deliverable 1.2: User, business and technical requirements of transition track #1 solutions*. https://irissmartcities.eu/sites/default/files/documents/d1.2_user_business_and_technical_requirements_of_transition_track_1_solutions.pdf.

United Nations, Department of Economic and Social Affairs, & Population Division. (2018). World urbanization prospects: The 2018 revision. Online edition. New York, USA. *Population division of the United Nations department of economic and social affairs*.

United Nations Framework Convention on Climate Change. (2015). *Adoption of the Paris agreement: Proposal by the president*. Paris, France https://unfccc.int/files/essential_background/convention/application/pdf/english_paris_agreement.pdf.

Uspenskaia, D., Specht, K., Kondziella, H., & Bruckner, T. (2021). Challenges and Barriers for Net-Zero/Positive Energy Buildings and Districts—Empirical Evidence from the Smart City Project SPARCS. *Buildings, 11*(2), 78. https://doi.org/10.3390/buildings11020078

Velik, R., & Nicolay, P. (2016). Energy management in storage-augmented, grid-connected prosumer buildings and neighborhoods using a modified simulated annealing optimization. *Computers & Operations Research, 66*, 248–257. https://doi.org/10.1016/j.cor.2015.03.002

Verbruggen, S., Hertoge, J., Delghust, M., Laverge, J., & Janssens, A. (2020). The use of solar shading in a nearly zero-energy neighbourhood. In *E3S Web of Conferences, 172* p. 19003). https://doi.org/10.1051/e3sconf/202017219003

Walker, S., Labeodan, T., Maassen, W., & Zeiler, W. (2017). A review study of the current research on energy hub for energy positive neighborhoods. *Energy Procedia, 122*, 727–732. https://doi.org/10.1016/j.egypro.2017.07.387

Wang, C., Martinac, I., & Magny, A. (2015). Multi-objective robust optimization of energy systems for a sustainable District in Stockholm. In *Proceedings of Building Simulation 2015: 14th Conference of International Building Performance Simulation Association*.

Wang, X., Zhao, G., He, C., Wang, X., & Peng, W. (2016). Low-carbon neighborhood planning technology and indicator system. *Renewable and Sustainable Energy Reviews, 57*, 1066–1076. https://doi.org/10.1016/j.rser.2015.12.076

Wells, L., Rismanchi, B., & Aye, L. (2018). A review of Net Zero Energy Buildings with reflections on the Australian context. *Energy and Buildings, 158*, 616–628. https://doi.org/10.1016/j.enbuild.2017.10.055

Wiberg, A. H., Løvhaug, S., Mathisen, M., Tschoerner, B., Resch, E., Erdt, M., et al. (2019). Visualisation of KPIs in zero emission neighbourhoods for improved stakeholder participation using virtual reality. In *IOP Conference Series: Earth and Environmental Science, 323* p. 12074). https://doi.org/10.1088/1755-1315/323/1/012074

Wiik, M. K., Fufa, S. M., Andresen, I., Brattebø, H., & Gustavsen, A. (2019). A Norwegian zero emission neighbourhood (ZEN) definition and a ZEN key performance indicator (KPI) tool. In *IOP Conference Series: Earth and Environmental Science, 352* p. 12030). https://doi.org/10.1088/1755-1315/352/1/012030

Wiik, M. K., Fufa, S. M., Baer, D., Sartori, I., & Andresen, I. (2018). *The ZEN definition - a guideline for the ZEN pilot areas: Version 1.0 (ZEN REPORT No. 11)*. *Norwegian university of science and technology (NTNU)*. SINTEF Building and Infrastructure.

Wiik, M. K., Fufa, S. M., Krogstie, J., Ahlers, D., Wyckmans, A., Driscoll, P., et al. (2018). *Zero emission neighbourhoods in smart cities: Definition, key performance indicators and assessment criteria: Version 1.0 bilingual version (ZEN REPORT No. 7)*. Norwegian University of Science and Technology (NTNU); SINTEF Building and Infrastructure.

Williams, J., Mitchell, R., Raicic, V., Vellei, M., Mustard, G., Wismayer, A., et al. (2016). Less is more: A review of low energy standards and the urgent need for an international universal zero energy standard. *Journal of Building Engineering, 6*, 65–74. https://doi.org/10.1016/j.jobe.2016.02.007

Woods, R., & Berker, T. (2019). Living labs in a zero emission neighbourhood context. In *IOP Conference Series: Earth and Environmental Science, 352* p. 12004). https://doi.org/10.1088/1755-1315/352/1/012004

Woods, R., & Berker, T. (2020). Citizen participation in Steinkjer: Stories about the "old NRK building at Lø". In *IOP Conference Series: Earth and Environmental Science, 588* p. 32016). https://doi.org/10.1088/1755-1315/588/3/032016

Woods, R., Sætersdal Remøe, K., Hestnes, A. G., & Gustavsen, A. (Eds.). (2019). ZEN Research Centre on Zero Emission Neighbourhoods in Smart Cities: Annual Report 2018.

Wu, J. (2014). Urban ecology and sustainability: The state-of-the-science and future directions. *Landscape and Urban Planning, 125*, 209–221. https://doi.org/10.1016/j.landurbplan.2014.01.018

Xu, B., Zhou, S., & Hao, L. (2015). Approach and practices of district energy planning to achieve low carbon outcomes in China. *Energy Policy, 83*, 109–122. https://doi.org/10.1016/j.enpol.2015.04.008

Xu, B., Zhu, C., & Xu, W. (2014). Approach and practice of District energy planning under low-carbon emission background. Lecture Notes in Electrical Engineering: Vol. 262. In , *Proceedings of the 8th International Symposium on Heating, Ventilation and Air Conditioning: ISHVAC 2013; Held in Xi'an, China from October 19 to 21, 2013* (Vol. 262, pp. 37–45). https://doi.org/10.1007/978-3-642-39581-9_4.

Yamaguchi, Y., Shimoda, Y., & Kitano, T. (2013). Reduction potential of operational carbon dioxide emission of Nakanoshima business/cultural area as a model for low-carbon districts in warm climates. *Building and Environment, 59*, 187–202. https://doi.org/10.1016/j.buildenv.2012.08.019

Yang, P. P.-J., Chi, C. S.-F., Wu, Y., & Quan, S. J. (2018). A geodesign method of human-energy-water interactive systems for urban infrastructure design: 10KM2 near-zero district project in Shanghai. *Engineering, 4*(2), 182–189. https://doi.org/10.1016/j.eng.2018.03.014

Yang, T., & Zhang, X. (2016). Benchmarking the building energy consumption and solar energy trade-offs of residential neighborhoods on Chongming Eco-Island, China. *Applied Energy, 180*, 792–799. https://doi.org/10.1016/j.apenergy.2016.08.039

Yttersian, V. L., Fuglseth, M., Lausselet, C., & Brattebø, H. (2019). OmrådeLCA, assessment of area development: Case study of the zero-emission neighbourhood Ydalir. In *IOP Conference Series: Earth and Environmental Science, 352* p. 12041). https://doi.org/10.1088/1755-1315/352/1/012041

Zero-Plus. (2017). *Achieving near zero and positive energy settelement in Europe using advanced energy technology*. http://www.zeroplus.org/pdf/ZERO-PLUS_Booklet.pdf.

Zero-Plus. (2018). *Achieving near zero and positive energy settelement in Europe using advanced energy technology*. http://www.zeroplus.org/pdf/ZERO-PLUS_Booklet2.pdf.

Zero-Plus. (2020a). *Achieving near zero and positive energy settelement in Europe using advanced energy technology*. http://www.zeroplus.org/pdf/ZERO-PLUS_BOOKLET3.pdf.

Zero-Plus. (2020b). *Designing net zero energy (NZE) settlements: Guidebook*. http://www.zeroplus.org/pdf/ZERO%20PLUS%20GUIDEBOOK%20FINAL.pdf.

Zhang, C., Cui, C., Zhang, Y., Yuan, J., Luo, Y., & Gang, W. (2019). A review of renewable energy assessment methods in green building and green neighborhood rating systems. *Energy and Buildings, 195*, 68–81. https://doi.org/10.1016/j.enbuild.2019.04.040

Zhao, G., Yu, X., He, C., & Tu, F. (2019). Low-carbon evaluation of rural neighborhood: A case study of Yanhe Village, Hubei Province, China. *Growth and Change, 50*(1), 247–265. https://doi.org/10.1111/grow.12273

Zhou, Y., Ji, H., Zhang, S., Qian, C., & Wei, Z. (2019). Empirical study on the boundary space form of residential blocks oriented toward low-carbon travel. *Sustainability, 11*(10), 2812. https://doi.org/10.3390/su11102812

Zwickl-Bernhard, S., & Auer, H. (2021). Open-source modeling of a low-carbon urban neighborhood with high shares of local renewable generation. *Applied Energy, 282*(2–3), 116166. https://doi.org/10.1016/j.apenergy.2020.116166

ISBN 978-82-326-5192-4 (printed ver.)
ISBN 978-82-326-6886-1 (electronic ver.)
ISSN 1503-8181 (printed ver.)
ISSN 2703-8084 (online ver.)

NTNU

Norwegian University of
Science and Technology